frontiers | Research Topics

Association between oral microbiota dysbiosis and the development of systemic conditions

Edited by
Zuomin Wang, Dong Xia, Jian Zhou and Zheng Zhang

Published in
Frontiers in Cellular and Infection Microbiology

ISSN 1664-8714
ISBN 978-2-8325-2324-7
DOI 10.3389/978-2-8325-2324-7

About Frontiers

Frontiers is more than just an open access publisher of scholarly articles: it is a pioneering approach to the world of academia, radically improving the way scholarly research is managed. The grand vision of Frontiers is a world where all people have an equal opportunity to seek, share and generate knowledge. Frontiers provides immediate and permanent online open access to all its publications, but this alone is not enough to realize our grand goals.

Frontiers journal series

The Frontiers journal series is a multi-tier and interdisciplinary set of open-access, online journals, promising a paradigm shift from the current review, selection and dissemination processes in academic publishing. All Frontiers journals are driven by researchers for researchers; therefore, they constitute a service to the scholarly community. At the same time, the *Frontiers journal series* operates on a revolutionary invention, the tiered publishing system, initially addressing specific communities of scholars, and gradually climbing up to broader public understanding, thus serving the interests of the lay society, too.

Dedication to quality

Each Frontiers article is a landmark of the highest quality, thanks to genuinely collaborative interactions between authors and review editors, who include some of the world's best academicians. Research must be certified by peers before entering a stream of knowledge that may eventually reach the public - and shape society; therefore, Frontiers only applies the most rigorous and unbiased reviews. Frontiers revolutionizes research publishing by freely delivering the most outstanding research, evaluated with no bias from both the academic and social point of view. By applying the most advanced information technologies, Frontiers is catapulting scholarly publishing into a new generation.

What are Frontiers Research Topics?

Frontiers Research Topics are very popular trademarks of the *Frontiers journals series*: they are collections of at least ten articles, all centered on a particular subject. With their unique mix of varied contributions from Original Research to Review Articles, Frontiers Research Topics unify the most influential researchers, the latest key findings and historical advances in a hot research area.

Find out more on how to host your own Frontiers Research Topic or contribute to one as an author by contacting the Frontiers editorial office: frontiersin.org/about/contact

Association between oral microbiota dysbiosis and the development of systemic conditions

Topic editors

Zuomin Wang — Capital Medical University, China
Dong Xia — Royal Veterinary College (RVC), United Kingdom
Jian Zhou — Capital Medical University, China
Zheng Zhang — Nankai University, China

Citation

Wang, Z., Xia, D., Zhou, J., Zhang, Z., eds. (2023). *Association between oral microbiota dysbiosis and the development of systemic conditions*. Lausanne: Frontiers Media SA. doi: 10.3389/978-2-8325-2324-7

Table of contents

frontiers | Frontiers in Cellular and Infection Microbiology

TYPE Editorial
PUBLISHED 18 April 2023
DOI 10.3389/fcimb.2023.1204103

OPEN ACCESS

EDITED AND REVIEWED BY
Xin Xu,
Sichuan University, China

*CORRESPONDENCE
Zuomin Wang
wzuomin@sina.cn
Dong Xia
dxia@rvc.ac.uk
Zheng Zhang
zhangzheng@nankai.edu.cn

†These authors have contributed equally to this work

SPECIALTY SECTION
This article was submitted to Microbiome in Health and Disease, a section of the journal Frontiers in Cellular and Infection Microbiology

RECEIVED 11 April 2023
ACCEPTED 13 April 2023
PUBLISHED 18 April 2023

CITATION
Zhang Z, Zhou J, Xia D and Wang Z (2023) Editorial: Association between oral microbiota dysbiosis and the development of systemic conditions.
Front. Cell. Infect. Microbiol. 13:1204103.
doi: 10.3389/fcimb.2023.1204103

Editorial: Association between oral microbiota dysbiosis and the development of systemic conditions

Zheng Zhang[1,2*†], Jian Zhou[3†], Dong Xia[4*] and Zuomin Wang[5*]

[1]Tianjin Stomatological Hospital, School of Medicine, Nankai University, Tianjin, China, [2]Tianjin Key Laboratory of Oral and Maxillofacial Function Reconstruction, Tianjin, China, [3]The School and Hospital of Stomatology, Capital Medical University, Beijing, China, [4]Royal Veterinary College, University of London, London, United Kingdom, [5]Department of Stomatology, Beijing Chao-Yang Hospital, Capital Medical University, Beijing, China

KEYWORDS

oral microbiota, dysbiosis, systemic diseases, inflammatory, mechanisms

Editorial on the Research Topic
Association between oral microbiota dysbiosis and the development of systemic conditions

Human oral cavity harbors a complex ecosystem of numerous microorganisms, including bacteria, fungi, viruses, and bacteriophages, referred to as the oral microbiota (Peng et al., 2022). In a healthy state, the oral microbiota is composed of commensals. The mutual commensal oral microbiota plays a crucial role in promoting not only oral, but also systemic health (Han et al., 2022). However, in a diseased state, host-microbial networks lead to dysbiosis. The influence of oral microbiota dysbiosis can extend beyond the oral cavity, and some systemic conditions are also associated with the oral microbiota (Peng et al., 2022). A mechanistic understanding for such associations may arise from the ability of many oral microorganisms to alter the inflammatory microenvironment and to interfere with host signaling pathways that control cell viability, proliferation and differentiation.

Furthermore, there is likely to be an alteration in oral microbial composition or bacterial pathogenicity in systemic pathologic conditions (Graves et al., 2019). Therefore, there may be a bidirectional relationship between the oral microbiota and systemic diseases. The abundance of oral microbiota specifically associated with systemic diseases appears to be a clinical biomarker to some extent, although further exploration is still necessary. If this clinical phenomenon is confirmed, early prediction of systemic diseases using microbial detection might be a crucial breakthrough. In the present research topic, we aim to assemble original research articles and reviews discussing recent advancements in understanding the association between oral microbiota dysbiosis and the development of systemic conditions.

Alteration in oral microbial composition in systemic pathologic conditions

Oral microbiomes are closely related to the health status of the body. Oral squamous cell carcinoma (OSCC), one of the most common malignant tumors of the head and neck, is closely associated with the dysbiosis of the oral microbiome. Nie et al. analyzed microbial samples collected from six oral niches, including OSCC tumor tissue, adjacent normal tissue, cancer surface tissue, anatomically matched contralateral normal mucosa, saliva, and tongue coat. They found significant differences in microbial composition and function among the six different oral niches, and most of the genera significantly enriched in tumor tissue samples were those that have been associated with periodontal diseases. Nasopharyngeal carcinoma (NPC) is another common head and neck cancer. Hao et al. established a non-invasive and low-cost NPC risk screening model based on the oral and nasopharyngeal microbiome. The oral microbiome accuracy rate for NPC risk screening was reported to reach 77.2%.

Significant increases in circulating levels of estrogen and progesterone are thought to have a significant effect on the periodontium throughout pregnancy (Wu et al., 2015). The study by Zhang et al. compared the microbial community characteristics of supragingival plaque in 30 pregnant and 10 non-pregnant women, and indicated a trend toward increased oral microbial diversity during pregnancy. The imbalance of local and systemic immunity and metabolism in HIV-infected/AIDS patients can cause an imbalance in oral ecology (Tappuni and Sufiawati, 2020). Cao et al. demonstrated that highly active antiretroviral therapy (HAART), the most effective therapy for HIV infection, has a key role in the balance of salivary microecology in AIDS patients. However, there are still some systemic diseases that do not result in significant changes in oral microbiomes. Lu et al. explored the impact of diabetes on periodontitis-related microorganisms in the saliva, and showed that diabetes did not affect the diversity of salivary microbiota in the context of periodontitis.

Effects of oral microorganisms on systemic diseases

The detrimental effects of oral microorganisms are not confined to the oral cavity, they can also contribute to systemic disorders, such as type 2 diabetes mellitus, cardiovascular disease, and inflammatory bowel disease (IBD) (Hajishengallis and Chavakis, 2021). The study by Kang et al. evaluated the influence of periodontal organism on glucose metabolism disorder in mice. After 22 weeks of periodontal pathogen infection, significant differences were observed at 30 and 60 min for the glucose tolerance test (GTT) and at 15 min for the insulin tolerance test (ITT). In the review by Li et al. the authors provided a comprehensive overview on the influence of periodontitis and the effect of periodontal therapy on vascular endothelial function, and the molecular mechanisms involved. In the article by Chen et al. the influence of periodontal pathogen infection on gut mycobiome was explored. The authors demonstrated the first evidence of gut fungal dysbiosis with periodontal pathogen administration. Wang et al. further reported that periodontitis salivary microbiota gavage could exacerbate intestinal inflammation, and aggravate long bone loss through the oral-gut axis in ovariectomized (OVX) rats.

Pathogenic mechanism of oral microorganisms

The presence of integrin β6 (ITGB6), an epithelial-specific receptor, is essential for periodontal health, as its low expression in the gingival epithelium is related to the development of periodontal diseases (Ghannad et al., 2008). An interesting research paper contributed by Xu et al. showed that the interaction of the transcription factors forkhead box protein O1 (FOXO1) and signal transducer and activator of transcription 3 (STAT3) mediated oral bacterial biofilm components induced ITGB6 downregulation in human epithelial cells, and speculated that targeting the FOXO1–STAT3 signaling axis might be an effective method for treating periodontal diseases. Previous research has confirmed that potassium ion is associated with enhanced virulence of the plaque community *in vitro* (Yost et al., 2017). The study by Zou et al. deciphered the role of TrkA, the regulatory subunit of the potassium uptake system Trk in periodontal pathogen-*Porphyromonas gingivalis* (*P.gingivalis*). The authors found that TrkA is required for the virulence of *P.gingivalis in vivo*.

It has been concluded that *P.gingivalis* or its virulence factors can induce memory impairment and Alzheimer's disease (AD)-related pathologies (Jiang et al., 2021; Tang et al., 2021). Outer membrane vesicles (OMVs), secreted by Gram-negative bacteria, could carry bacterial LPS, protease, membrane receptor, DNA, RNA, and so forth, and act as long-distance weapons and cause systemic disease (Toyofuku et al., 2019). In the study by Gong et al. the authors demonstrated the relationship between *P.gingivalis* OMVs and AD-like phenotypes for the first time. This study indicated that oral gavage of *P.gingivalis* OMVs could induce AD-like phenotypes, including memory dysfunction, neuroinflammation, and tau phosphorylation, and NLRP3 inflammasome activation was a possible mechanism.

Conclusion

In summary, the articles presented in this research topic provide readers with updated data on the association of oral microbiota dysbiosis with systemic conditions. We hope that the knowledge from these published articles will be useful for initiating new studies

in this exciting area where the detailed or acquired molecular mechanisms remain unexplored.

Author contributions

All authors listed have made a substantial, direct and intellectual contribution to the work, and approved it for publication.

Acknowledgments

The editorial team thanks all of the contributors to this Research Topic.

Conflict of interest

The authors declare that the research was conducted in the absence of any commercial or financial relationships that could be construed as a potential conflict of interest.

Publisher's note

All claims expressed in this article are solely those of the authors and do not necessarily represent those of their affiliated organizations, or those of the publisher, the editors and the reviewers. Any product that may be evaluated in this article, or claim that may be made by its manufacturer, is not guaranteed or endorsed by the publisher.

References

Ghannad, F., Nica, D., Fulle, M. I., Grenier, D., Putnins, E. E., Johnston, S., et al. (2008). Absence of alphavbeta6 integrin is linked to initiation and progression of periodontal disease. *Am. J. Pathol.* 172, 1271–1286. doi: 10.2353/ajpath.2008.071068

Graves, D. T., Correa, J. D., and Silva, T. A. (2019). The oral microbiota is modified by systemic diseases. *J. Dent. Res.* 98, 148–156. doi: 10.1177/0022034518805739

Hajishengallis, G., and Chavakis, T. (2021). Local and systemic mechanisms linking periodontal disease and inflammatory comorbidities. *Nat. Rev. Immunol.* 21, 426–440. doi: 10.1038/s41577-020-00488-6

Han, Y., Wang, B., Gao, H., He, C., Hua, R., Liang, C., et al. (2022). Insight into the relationship between oral microbiota and the inflammatory bowel disease. *Microorganisms* 10 (9), 1868. doi: 10.3390/microorganisms10091868

Jiang, M., Zhang, X., Yan, X., Mizutani, S., Kashiwazaki, H., Ni, J., et al. (2021). GSK3beta is involved in promoting alzheimer's disease pathologies following chronic systemic exposure to porphyromonas gingivalis lipopolysaccharide in amyloid precursor protein(NL-F/NL-F) knock-in mice. *Brain Behav. Immun.* 98, 1–12. doi: 10.1016/j.bbi.2021.08.213

Peng, X., Cheng, L., You, Y., Tang, C., Ren, B., Li, Y., et al. (2022). Oral microbiota in human systematic diseases. *Int. J. Oral. Sci.* 14, 14. doi: 10.1038/s41368-022-00163-7

Tang, Z., Liang, D., Cheng, M., Su, X., Liu, R., Zhang, Y., et al. (2021). Effects of porphyromonas gingivalis and its underlying mechanisms on Alzheimer-like tau hyperphosphorylation in sprague-dawley rats. *J. Mol. Neurosci.* 71, 89–100. doi: 10.1007/s12031-020-01629-1

Tappuni, A. R., and Sufiawati, I. (2020). The Bali declaration on oral health in HIV/AIDS. *Oral. Dis.* 26 Suppl 1, 172. doi: 10.1111/odi.13404

Toyofuku, M., Nomura, N., and Eberl, L. (2019). Types and origins of bacterial membrane vesicles. *Nat. Rev. Microbiol.* 17, 13–24. doi: 10.1038/s41579-018-0112-2

Wu, M., Chen, S. W., and Jiang, S. Y. (2015). Relationship between gingival inflammation and pregnancy. *Mediators Inflamm.* 2015, 623427. doi: 10.1155/2015/623427

Yost, S., Duran-Pinedo, A. E., Krishnan, K., and Frias-Lopez, J. (2017). Potassium is a key signal in host-microbiome dysbiosis in periodontitis. *PloS Pathog.* 13, e1006457. doi: 10.1371/journal.ppat.1006457

frontiers | Frontiers in Cellular and Infection Microbiology

ORIGINAL RESEARCH
published: 29 June 2022
doi: 10.3389/fcimb.2022.937039

Clinical Oral Condition Analysis and the Influence of Highly Active Antiretroviral Therapy on Human Salivary Microbial Community Diversity in HIV-Infected/AIDS Patients

Peilin Cao[1†], Yifan Zhang[2,3,4†], Guangyan Dong[2], Hongkun Wu[2], Yuxiang Yang[5] and Yi Liu[1*]*

[1] Department of Stomatology, Sichuan Provincial People's Hospital, University of Electronic Science and Technology of China, Chengdu, China, [2] State Key Laboratory of Oral Diseases, National Clinical Research Center for Oral Diseases, West China Hospital of Stomatology, Sichuan University, Chengdu, China, [3] Department of Stomatology, Hangzhou Dental Hospital Group, Hangzhou, China, [4] Division of Advanced Prosthetic Dentistry, Tohoku University Graduate School of Dentistry, Sendai, Japan, [5] Department of Radiology, West China School of Public Health and West China Fourth Hospital, Sichuan University, Chengdu, China

OPEN ACCESS

Edited by:
Zheng Zhang,
Nankai University, China

Reviewed by:
Pingping Bao,
Affiliated Stomatological Hospital of Nankai University, China
A. Thirumal Raj,
Sri Venkateswara Dental College, India

***Correspondence:**
Yuxiang Yang
simonbv937@gmail.com
Yi Liu
liuyikq@med.uestc.edu.cn

[†]These authors have contributed equally to this work

Specialty section:
This article was submitted to Microbiome in Health and Disease, a section of the journal Frontiers in Cellular and Infection Microbiology

Received: 05 May 2022
Accepted: 01 June 2022
Published: 29 June 2022

Citation:
Cao P, Zhang Y, Dong G, Wu H, Yang Y and Liu Y (2022) Clinical Oral Condition Analysis and the Influence of Highly Active Antiretroviral Therapy on Human Salivary Microbial Community Diversity in HIV-Infected/AIDS Patients. Front. Cell. Infect. Microbiol. 12:937039. doi: 10.3389/fcimb.2022.937039

The purpose of this study was to assess the clinical oral status and investigate the effect of highly active antiretroviral therapy (HAART) on oral flora diversity in human immunodeficiency virus (HIV)-infected/acquired immune deficiency syndrome (AIDS) patients. We first recorded and analyzed the demographic indicators of 108 HIV-infected patients and assessed their periodontal health, dental health and oral lesion status by oral examination. Besides, we compared the changes in salivary microbial communities of healthy controls, before and after treatment of HAART-processed AIDS patients by Roche 454 sequencing and RT-qPCR. In HIV-infected/AIDS patients, age, sex, marital status, income level, smoking and oral health behaviors had an effect on periodontal clinical indicators; age and marital status were correlated with dental clinical indicators; most of them were accompanied by oral manifestations, mainly including candidiasis albicans, salivary gland disease, AIDS-associated periodontitis, and oral ulcers. Besides, a total of 487 species were detected in the saliva of AIDS patients. The microbial communities of HAART-unprocessed AIDS patients significantly differed from those processed patients, with 112 unique microbial species. More importantly, a large number of conditioned pathogens were also detected in the saliva samples of AIDS patients, which may be associated with opportunistic infections. Therefore, HAART might have a crucial role in salivary microecological balance in AIDS patients. And these patients should pay attention to the maintenance of oral health, and the early initiation of HAART may be important for the development of oral lesions.

Keywords: acquired immune deficiency syndrome, oral characterization, oral microbiota, roche 454 sequencing, highly active antiretroviral therapy

INTRODUCTION

Acquired immune deficiency syndrome (AIDS) is caused by infection with the human immunodeficiency virus (HIV) (Upreti et al., 2020; Chen and Wang, 2022). HIV can attack and disrupt the immune system microbalance, producing a range of signs and symptoms (Bbosa et al., 2019). Patients with AIDS are highly susceptible to various bacterial or viral infections due to their severely compromised immune function (Meer, 2019). Besides, HIV infection can be combined with various opportunistic infections and rare tumors, leading to death (Cilliers et al., 2019; Chen and Wang, 2022). In recent years, the number of HIV infections worldwide is increasing and has become an increasingly serious social problem (Lapointe and Harrigan, 2020). It has been reported that 30% of HIV patients first present with oral symptoms, which will cause oral and maxillofacial infections after immune compromise (Hulgan and Samuels, 2021). Within 1-4 years prior to the onset of AIDS, patients may present with various typical oral lesions (Peacock et al., 2017). This has also become a key symptom for the early detection and diagnosis of AIDS. Currently, the international medical community attaches great importance to the oral manifestations of HIV. Therefore, it is of scientific importance to further investigate the oral representation of AIDS and its potential treatment strategies.

Highly active antiretroviral therapy (HAART) is the most effective therapy for HIV infection (Lu et al., 2018). And the effective implementation of HAART therapy can greatly reduce the opportunistic infections in AIDS patients, and decrease the morbidity and mortality of HIV-infected patients (Andrade et al., 2017). A decreasing trend has been reported in the incidence of HIV/AIDS-related oral diseases after the introduction of HAART (Oliva-Moreno and Trapero-Bertran, 2018). Research also testified that HIV/AIDS-related oral disease can be applied as one of the indicators to evaluate the efficacy of HAART (Shekatkar et al., 2021). Additionally, studies confirmed that the development of oral diseases is relevant to the oral microbial community (Graves et al., 2019; Mosaddad et al., 2019). The oral cavity is inhabited by vast commensal and pathogenic microorganisms (Gao et al., 2018). Dysbiosis of ecological balance is the initiating factor in the progression of oral infectious diseases (Zhang et al., 2018). The imbalance of local and systemic immunity and metabolism in HIV-infected/AIDS patients can cause an imbalance in oral ecology, which often result in multiple infectious diseases (Tappuni and Sufiawati, 2020). However, the alteration of the oral microbial community in AIDS patients after HAART is not completely clear. Therefore, it is crucial to explore the changes and characteristics of oral microorganisms in AIDS patients during HAART for the evaluation of HAART efficacy.

Currently, 454 pyrophosphate sequencing can enable deep sequencing of microorganisms in the oral environment, which also can identify the changes in the structure of the oral microbiome (Keijser et al., 2008; Yan et al., 2016). This has an essential role in exploring the dynamic relationship between oral microorganisms and changes in the oral environment and systemic health status. The Roche 454 GS FLX+ is the latest upgraded high-throughput sequencing system from 454 Life Science (Forgetta et al., 2013). And its maximum read length can reach 1000bp, and the sequencing accuracy reaches 99.997% (Allali et al., 2017). This technique has been successfully applied to study the microbiome of oral samples, such as saliva, plaque, pulp infections, etc (Keijser et al., 2008; Nasidze et al., 2009; Lazarevic et al., 2010; Li et al., 2010; Ling et al., 2010).

Above all, we collected the demographic characteristics of HIV-infected patients through questionnaires and conducted detailed oral examinations of these patients, thereby assessing the relationship between patient demographic risk factors and periodontal or dental health status. Besides, we also adopted the Roche 454 GS FLX+ sequencing platform to compare the differences in salivary microbial communities among normal controls, before and after treatment of HAART-processed AIDS patient. Furthermore, we investigate the oral health and oral microbalance in HIV-infected patients. Therefore, the study will be clinically important for the disease control of HIV-infected patients and the efficacy monitoring of HARRT treatment. This will also have key clinical implications for monitoring the efficacy of HARRT treatment in AIDS patients.

MATERIALS AND METHODS

Patient Samples

108 HIV-infected patients were obtained from the Public Health Clinical Medical Center (Chengdu, Sichuan, China). The informed consent forms were signed by all patients. Inclusion criteria included being 18 years of age and older, having the ability to express themselves, and meeting the diagnostic criteria for HIV-infected patients and AIDS patients (Volberding et al., 2012). Exclusion criteria included co-infection with serious opportunistic infections; co-infection with other serious or unstable chronic diseases; inability to move autonomously; and women during pregnancy. All study subjects completed an epidemiological questionnaire before undergoing clinical examination. This study also received the approval of the ethics committee in West China Hospital of Stomatology, Sichuan University (WCHSIRB-D-2015-004).

Clinical Assessment of Periodontal Health

All enrolled patients underwent a comprehensive periodontal examination using Hu-Friedy William Probe and disposable mouth mirror. Periodontal clinical examination was performed by 4 dentists based on the Carranza's Clinical Periodontology method (Newman et al., 2011). And the examination indexes contain probing Depth (PD), clinical attachment loss (CAL), CAL > 3 mm, and CAL > 5 mm, PD > 4 mm, and bleeding on probing (BOP). For PD and CAL, six locis (Proximal mid-buccal loci, buccal loci, distal mid-buccal loci, distal mid lingual loci, lingual loci and proximal mid-lingual loci) of each tooth were evaluated using a periodontal probe (Williams probe; Hu-Friedy; Hu-Friedy, Chicago, IL, USA). For BOP: a total of 4 locis in distal mid-buccal, median, proximal mid and lingual locis were examined. 0 = no bleeding, 1 = bleeding.

Clinical Assessment of Dental Health

The dental examination method was consistent with periodontal examination. In line with the World Health Organization (WHO) method of oral health survey (Newman et al., 2011), natural teeth were counted as 28 teeth, excluding upper and lower third molars, and missing teeth were recorded as missing. Non-carious teeth: complete teeth without fillings and without filling treatment. Caries: sulcus or smooth surface of the tooth with a softened lesion at the base, and potential damage to the enamel or softening of the sulcus wall (Liu et al., 2020). The dental examination included number of permanent sound teeth, number of missing teeth from oral disease, number of decayed, missing, filled teeth (DMFT), and Number of decayed, missing, filled surfaces (DMFS).

Oral Mucosa Examination

Fungal culture was performed in oral mucosal scrapings from the included patients. The examination was uniformly conducted using the WHO-recommended CPI probe and planar mouth mirror. Oral mucosal disease is diagnosed by referring to the criteria developed by the WHO collaborating centre for oral manifestations of HIV infection (Pinna et al., 2019; Indrastiti et al., 2020).

Experimental Grouping

The study population was randomly divided into healthy control group (H, n = 78), AIDS group (before treatment of HAART-processed AIDS patients (UT), n = 64), and HAART treatment group (after treatment of HAART-processed AIDS patients (T), n = 62). Healthy controls were age-sex matched healthy people, which were chosen at random. And inclusion criteria for healthy controls included 18 years of age or older, HIV antibody test was negative, having the ability to express themselves, informed consent, voluntary participation. Exclusion criteria included combination of fatal opportunistic infections, combination of various malignancies, combined with cranial infection, unconsciousness, inability to move on their own, women during pregnancy.

Bacterial Total Genomic DNA Extraction

Referring to the method described in previous study, 5 mL of non-stimulated saliva samples were collected and stored in a -80°C refrigerator (Wong, 2009). Based on the kit instruction and previous research (Tian et al., 2010), the collected saliva samples were subjected to extraction of total bacterial genomic DNAs through the MasterPure™ DNA Purification Kit (Epicentre, Madison, USA) after optimizing the conditions. Briefly, an equal volume of saliva was mixed with PBS, centrifuged, and the supernatant was collected. The supernatant was centrifuged at 14,000 × g for 10 min at 4°C and the precipitate was retained. The precipitate was added to 299 μL of cell lysate and 1 μL of 50 μg proteinase K in a 65°C water bath for 40 min. The sample was cooled to 37°C, and added with 1.5 μL of RNase A in a 37°C water bath for 30 min. After 3 min on ice, 175 μL of MPC Protein Precipitation Reagent was added to the sample and centrifuged at 14,000 × g for 10 min at 4°C. the precipitate was added to 500 μL of isopropanol and centrifuged. The precipitate was washed with 75% alcohol and the DNA was lysed with 20 μL TE buffer.

Roche 454 Sequencing

Each group contained 5 samples were collected for Roche 454 sequencing. The bacterial genomic DNA was first amplified using multiple pairs primers. And we selected the universal primer 347F/803R for the V3-V5 region of the bacterial 16S rDNA gene (Nossa et al., 2010). Roche 454 universal junction primers (454 A and B), multiplex identifier (MID) and target amplification primers were integrated as fusion primers. Then genomic DNA was amplified by multiplex PCR through the FastStart High Fidelity PCR System (Roche Applied Science, Mannheim, Germany). The amplification product is the amplicon library. Next, the libraries were purified using Agencourt AMPure XP PCR (Agencourt Bioscience, MA, USA). The libraries were assayed for fragmentation and concentration using LabChip GX (Caliper Life Sciences, MA, USA). Libraries were emulsified with GS FLX Titanium emPCR Kit (454 Life Sciences, CT, USA). And the library was sent to the GS FLX Titanium sequencing platform (454 Life Sciences, CT, USA) for pyrosequencing.

Quantitative Real-Time PCR Analysis

Quantitative real-time PCR (RT-qPCR) assays were performed using the 16S rRNA gene as the target and using PCR amplification primers and hydrolysis-probe detection on the Light Cycler 96 (Roche, Basel, Switzerland). Each microbial DNA RT-qPCR array plate analyzed one sample for 93 species (NCBI Tax ID)/gene at a time. Overall bacterial load and host genomic DNA were measured as internal reference (Korona-Glowniak et al., 2021).

Composition and Abundance Analysis of Operation Taxonomy Unit in Microbial Community

The sequences of 16S rDNA V3-V5 region were sequenced to obtain the raw sequence data, which were then processed using Mothur (Version 1.32.1, http://www.mothur.org/) to acquire Unique Reads. And then the operation taxonomy unit (OUT) with species were annotated (Schloss et al., 2009). The VennDiagram package in R language was applied to produce the Venn diagram (Chen and Boutros, 2011). The heat map was produced using R language (v2.15.3, http://www.r-project.org/index.html). Phylogenetic trees were constructed and plotted using QIIME (Version 1.50, http://qiime.org/index.html) and R language.

Diversity Analysis

α-diversity analysis refers to the analysis of species diversity in individual samples (Kemp and Aller, 2004). The α-diversity of samples was calculated using mothur (Schloss et al., 2009). Differences in α-diversity indices between groups were compared using R language and the corresponding dilution curves were plotted. The β-diversity can reflect the differences

in species diversity of different samples, which was analyzed with QIIME (Crawford et al., 2009).

Cluster Analysis of Species Composition

Using QIIME software, 75% of the reads were randomly chosen for calculation in each sample, and the final clustering tree was obtained after 100 iterations of comprehensive statistics, which was plotted using R language. Significant differences in microbial composition between groups were analyzed using Metastats software, and p-values were corrected for the Benjamini-Hochberg method using the R language (Crawford et al., 2009).

Statistical Analysis

The clinical data was compared using non-parametric Kruskal Wallis test with SPSS 23.0 software (Inc., Chicago, IL). For α-diversity analysis, the Wilcoxon Rank-Sun test was applied for the comparison of two samples; the Kruskal-Wallis test was applied for the comparison of multiple samples. $P < 0.05$ signified that the difference was significant.

RESULTS

Relationship Between Demographic Variables and Periodontal Clinical Indicators in HIV-Infected Patients

By analyzing the relationship between demographic variables and clinical indicators of periodontal health, we found that age was associated with probing depth, CAL, PD > 4 mm, CAL > 3 mm, and CAL > 5 mm in the study population ($P < 0.01$). Sex was relevant to probing depth and CAL only ($P < 0.05$), with the female group being higher than the male group. There was no statistically significant difference between ethnicity and periodontal clinical indicators. Marital status was related to probing depth, CAL, PD > 4 mm, and CAL > 5 mm ($P < 0.05$, $P < 0.01$), and all three indicators were lower in the unmarried group than in the other groups. Education and income per year were associated with probing depth, CAL, CAL > 3 mm and CAL > 5 mm ($P < 0.05$, $P < 0.01$). Residence had an effect on CAL only ($P < 0.05$) and was higher in the rural group than in the urban group. BMI was correlated with BOP-positive sites and probing depth ($P < 0.05$), and both indicators were also higher in the higher BMI group (**Table 1**). Besides, we found that alcohol consumption was relevant to CAL > 3 mm ($P = 0.044$), while the smoking population was statistically associated with probing depth, CAL, PD > 4 mm, CAL > 3 mm, and CAL > 5 mm. Moreover, we discovered that in the target population, frequency of tooth was only associated with BOP-positive sites ($P = 0.035$); Dental flossing was statistically associated with BOP-positive sites and CAL > 5 mm ($P < 0.05$). Dental visit experience was negatively associated with BOP-positive sites, PD, PD > 4 mm, CAL > 3 mm, and CAL > 5 mm ($P < 0.05$) (**Table 2**).

Oral Lesions in HIV-Infected Patients

Among the 108 HIV-infected patients, oral manifestations were higher in candidiasis albicans (47.23%), salivary gland disease (7.41%), AIDS-associated periodontitis (19.44%), and oral ulcers (20.37%), and low in oral hairy leukoplakia (1.85%) and herpes

TABLE 1 | Comparison of demographic variables with periodontal health status in HIV-infected patients, n = 108.

Variables	N	BOP (%)	Mean Probing Depth (mm)	Mean CAL (mm)	PD > 4 mm (%)	CAL>3mm (%)	CAL > 5 mm (%)
Age (years)	108						
13~24	26	36.47	1.58	0.59	3.40	7.02	2.66
25~44	32	33.29	2.75	2.46	14.43	31.40	9.94
45~64	29	34.74	4.28	4.11	24.62	41.74	13.49
≥65	21	29.84	3.88	3.88	17.36	39.06	12.38
	p value	0.275	**0.000****	**0.000****	**0.000****	**0.000****	**0.000****
Sex	108						
Male	50	33.92	2.95	2.59	15.43	28.05	9.207
Female	58	32.73	3.75	3.36	13.71	37.33	11.41
	p	0.587	0.021*	0.046*	0.554	0.088	0.145
Ethnic	108						
Han	97	33.94	3.16	2.81	15.34	29.96	9.86
Minority	11	30.50	2.46	2.03	11.86	29.85	7.23
	p value	0.508	0.202	0.258	0.362	0.919	0.209
Marital status	108						
Single	19	31.94	2.23	1.50	8.42	19.16	3.95
Married	45	35.68	3.12	2.90	14.23	31.59	10.59
Divorced	25	33.58	3.68	3.47	18.63	35.02	11.61
Widowed	19	30.63	3.24	2.68	20.31	31.13	11.67
	p value	0.497	**0.004****	**0.001****	**0.038***	0.088	**0.001****
Education (years)	108						
<9	43	33.09	3.57	3.35	18.18	36.02	11.50
9~12	46	34.92	3.031	2.61	14.12	27.83	8.98
>12	19	31.41	2.03	1.43	9.16	19.04	6.47

(Continued)

TABLE 1 | Continued

Variables	N	BOP (%)	Mean Probing Depth (mm)	Mean CAL (mm)	PD > 4 mm (%)	CAL>3mm (%)	CAL > 5 mm (%)
	p value	0.463	**0.000****	**0.000****	0.077	**0.000****	**0.012***
Income per year (RMB)	108						
<12000	12	30.06	4.03	3.42	19.36	38.77	10.76
12000~36000	62	33.91	3.30	3.12	16.18	32.12	10.80
>36000	34	34.61	2.45	1.85	11.61	22.95	7.28
	p value	0.612	**0.004****	**0.001****	0.090	**0.015***	**0.038***
Residence	108						
Urban	38	33.14	2.79	2.27	14.41	25.40	8.46
Rural area	70	33.62	3.31	3.03	15.55	32.40	10.28
	p value	0.931	0.127	**0.031***	0.560	0.070	0.183
BMI (kg/m^2)	108						
<18.5	25	27.81	3.88	3.30	17.73	35.16	10.90
18.5~24	78	34.37	2.83	2.51	14.71	28.08	9.29
24~28	5	52.75	3.95	3.79	7.56	34.40	9.35
	p value	**0.024***	**0.006****	0.072	0.196	0.254	0.762

*Non-parametric Kruskal Wallis test. *, P < 0.05; **, P < 0.01. BOP, Bleeding on probing; CAL, Clinical attachment loss; PD, Probing depth. Bold values means p < 0.05.*

simplex stomatitis (3.70%). Lymphadenitis, Kaposi's sarcoma, and non-Hodgkin's lymphoma were not found (**Table 3**).

Overall Characteristics of Roche 454 Sequencing in the Oral Flora in AIDS Patients After HAART

Further, we adopted Roche 454 sequencing to investigate the impacts of HAART on the diversity of salivary microbial communities in 5 healthy controls, 5 HAART processed AIDS patients, and 5 HAART unprocessed AIDS patients. We obtained 150,342 valid 16s rDNA gene sequences. After the raw sequences were optimized and filtered, 81,182 high quality valid sequences were applied for data analysis. And the effective length of the sequences was around 241 bp after removing primer and Barcode (**Figure 1**).

Diversity Analysis of Microecological Communities in the Saliva Samples of AIDS Patients After HAART

We first applied the rarefaction curve to evaluate the diversity of the original community. When the curve flattens out or reaches a plateau, the sequencing depth has largely covered all species in the sample. Our data displayed that the sequencing level has reached a good depth at the 0.03 cut off level. With the increase of sequencing volume, the shannon index curve gradually became flat. Therefore, our sequencing volume can basically reflect the diversity of oral flora in each group (**Figure 2A**). The α-diversity reflects the species diversity of individual samples and mainly includes: Shannon index and Chao1 index. The Shannon index was adopted to estimate the level of community diversity, and the higher the shannon value, the higher the community diversity.

TABLE 2 | Effect of oral health care behaviors on periodontal clinical indicators in HIV-infected patients, n = 108.

Variables	N	BOP (%)	Probing Depth (Mean, mm)	Mean CAL (mm)	PD > 4 mm Sites (%)	CAL > 3 mm Sites (%)	CAL > 5 mm Sites (%)
Frequency of tooth brushing	108						
Twice a day	23	26.60	2.87	2.42	15.70	24.79	8.21
Once a day	76	35.07	3.11	2.80	15.00	30.88	9.89
Seldom/Never	9	45.05	4.43	3.55	13.29	39.63	12.88
	P value	**0.035***	0.246	0.406	0.988	0.310	0.390
Dental flossing	108						
Once a day	14	27.47	2.58	2.17	10.10	22.54	5.62
Seldom/Never	94	34.78	3.21	2.85	15.96	31.26	10.38
	p value	**0.034***	0.062	0.173	0.173	0.136	**0.028***
Dental prophylaxis	108						
Once a year	4	11.5	2.10	1.77	5.82	22.90	3.97
Dentists' advice	39	34.56	2.75	2.21	14.06	23.55	7.80
Never	65	34.33	3.39	3.12	16.20	34.21	11.09
	p value	**0.025***	**0.034***	0.058	0.207	**0.026***	**0.016***
Dental visit	108						
Less than a year	4	25.73	3.30	3.29	30.87	37.10	13.80
1~2 years ago	39	37.00	2.87	2.34	10.41	24.37	8.87
3~5 years ago	31	31.37	3.07	2.94	14.84	30.42	6.37
>5 years ago	34	32.98	3.36	2.95	18.47	34.48	10.89
	p value	0.503	0.408	0.529	**0.042***	0.267	0.584

*Non-parametric Kruskal Wallis test. *, P < 0.05. BOP, Bleeding on probing; CAL, Clinical attachment loss; PD, Probing depth. Bold values means p < 0.05.*

TABLE 3 | Oral lesions in HIV-infected patients.

Lesion type	Cases	Percentage
Candidiasis albicans	51	47.23%
Salivary gland disease (xerostomia)	8	7.41%
Oral hairy leukoplakia	2	1.85%
Herpes simplex stomatitis	4	3.70%
AIDS-associated periodontitis	21	19.44%
Oral ulcers	22	20.37%

The chao1 index can assess the number of OUTs contained in the community by calculating the colony abundance, which responds to the total number of species. Our results denoted that the *P* values corresponding to shannon and Chao indices were less than 0.05, indicating the significant differences in community diversity from each group (**Figures 2B, C**). Besides, β-diversity can be applied to compare the differences between multiple groups of samples. And we compared the salivary microbial community diversity of AIDS patients using the UniFrac weighting algorithm to plot Heat map. Vertical clustering signifies the similarity of all species in samples, and horizontal clustering signifies the similarity in abundance of the species in samples. Based on the UniFrac clustering analysis of β-diversity of salivary microecological communities, we found that samples from healthy controls, samples from before treatment of HAART-processed AIDS patients, and samples from after treatment of HAART-processed AIDS patients were clustered together respectively (**Figure 2D**). Therefore, the microecological communities in the saliva of the three groups of patients had their own characteristics.

Species Composition and Distribution of Flora in Saliva Samples From AIDS Patients After HAART at the Genus Level

Additionally, based on the sequencing alignment results, we discovered that there are 10 phyla of bacteria at the level of taxonomic "phylum" of biological species. Among them, *Firmicutes*, *Bacteroidetes*, *Proteobacteria*, *Fusobacteria*, and *Actinobacteria* accounted for more than 90% of the total bacterial phyla. And the differences between the three groups of samples were not statistically significant at this level of classification (**Table 4**). Moreover, at the "genus" level, we detected a total of 105 genera. And three of these genera (*Streptococcus, Synergistetes*, and *Veillonella*), were detectable in all three sets of saliva samples. The distribution of *Solobacterium*, *Gemella*, *Rothia, Neisseria*, *Leptotrichia*, *Parvimonas, and Haemophilus* was not significantly different in the three groups of samples. *Kingella*, *Slackia*, *Capnocytophaga*, *Peptostreptococcaceae*, *Atopobium*, *Porphyromonas*, and *Lactobacillus* were only present in the healthy control group. And some genera, such as *Fusobacterium*, *Selenomonas*, *Campylobacter*, *Capnocytophaga*, *Prevotella*, and *Granulicatella* were significantly increased in the samples from after treatment of HAART-processed AIDS patients compared with samples from before treatment of HAART-processed AIDS patients (**Figure 3**).

Distribution of Saliva Sample Flora Species in AIDS Patients After HAART

Furthermore, we also analyzed the distribution of flora species at the species level in three groups of saliva samples. As exhibited in **Figure 4A**, at the level of "species", a total of 91 species were annotated in the saliva of healthy controls, 185 species in saliva samples from before treatment of HAART-processed AIDS patients, and 136 species in saliva samples of after treatment of HAART-processed AIDS patients. In the Venn diagram, we more intuitively understand the common presence of 93 OTUs in the three groups with significant diversity variation; there were 216 unique OTUs in the HAART unprocessed group, and these species might be associated with opportunistic infections (**Figure 4B**).

Distribution of Different Genera of Bacteria in Saliva Samples of AIDS Patients After HAART Treatment

Based on the sequencing alignment results, RT-qPCR was performed to confirm the distribution of different genera of bacteria in saliva samples of AIDS patients after HAART treatment. As shown in **Table 5**, the positive samples of *Kingella*, *Slackia*, *Capnocytophaga*, *Peptostreptococcaceae*,

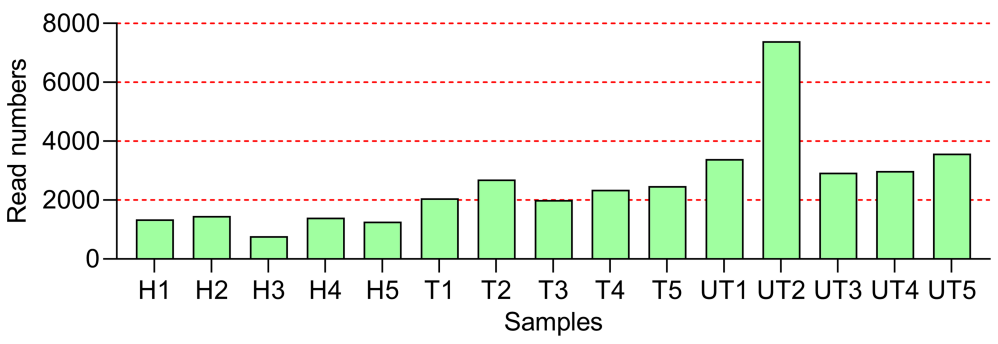

FIGURE 1 | Overall characteristics of Roche 454 sequencing in the oral flora in HIV-infected/AIDS patients after HAART. The statistics of Read Number for each sample. H, Normal control; UT, HIV-infected/AIDS patients not processed with HAART; T, HIV-infected/AIDS patients processed with HAART.

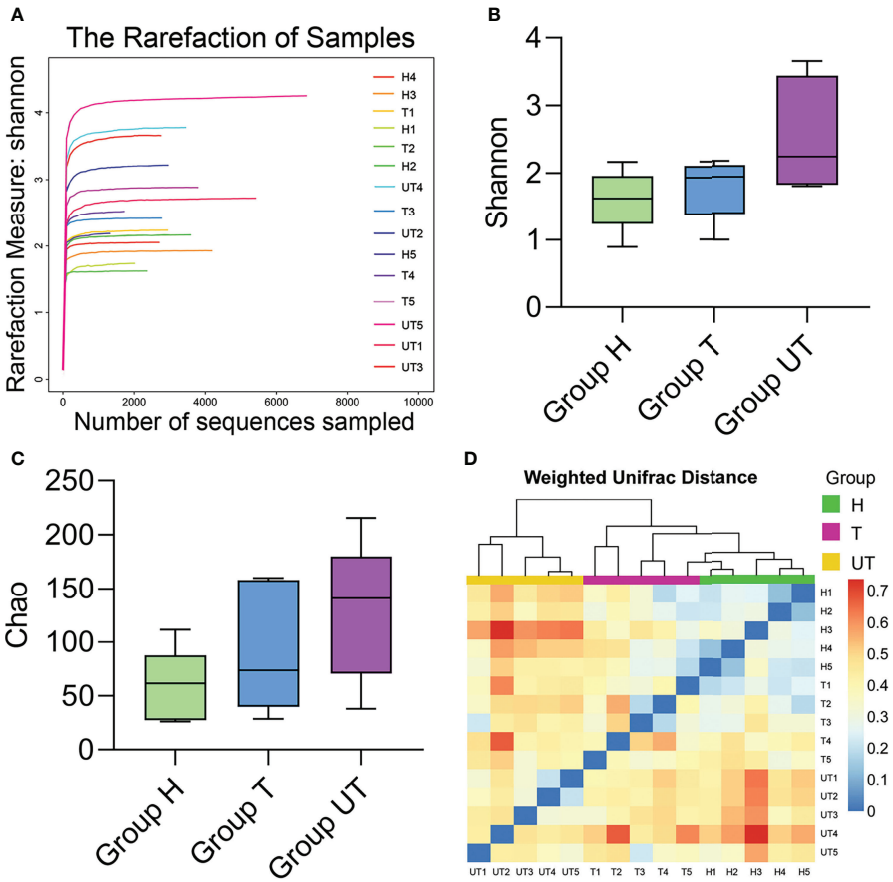

FIGURE 2 | Diversity analysis of microecological communities in the saliva samples of HIV-infected/AIDS patients after HAART. **(A)** Rarefaction curve of Shannon index in the flora of saliva samples in different groups. **(B)** Comparison of Shannon index in HAART processed or unprocessed HIV-infected/AIDS patients. **(C)** Comparison of Chao1 index in HAART processed or unprocessed HIV-infected/AIDS patients. **(D)** Heat map of β-diversity the flora of saliva samples in different groups.

Atopobium, *Porphyromonas*, and *Lactobacillus* were significantly lower in AIDS patients compared with healthy control group, meanwhile which were increased after HAART treatment. Furthermore, the contributions of *Fusobacterium*, *Campylobacter*, *Prevotella*, *Capnocytophaga*, *Selenomonas*, and *Granulicatella* in AIDS samples were significantly decreased in AIDS patients compared with healthy control group, meanwhile which were increased after HAART treatment (**Table 6**). The RT-qPCR results were consistent with the Roche 454 sequencing alignment results.

TABLE 4 | Relative abundance of microbial diversity in saliva samples at the phylum level for different subgroups.

Phylum	Relative Distribution %		
	Group H	Group T	Group UT
Actinobacteria	8.98	9.01	8.09
Bacteroidetes	12.81	12.82	11.89
Deinococcus-Thermus	0	0.21	0
Fusobacteria	6.68	4.24	5.05
Proteobacteria	10.12	11.12	10.97
Spirochaetes	2.86	1.73	3.87
Tenericutes	0	0.12	0.21
Firmicutes	58.44	58.81	58.91
Other	0.11	0.96	1.01
SR1	0	0.98	0

Group H, Healthy control; Group T, After treatment of HAART-processed AIDS patients; Group UT, Before treatment of HAART-processed AIDS patients; HAART, Highly active antiretroviral therapy.

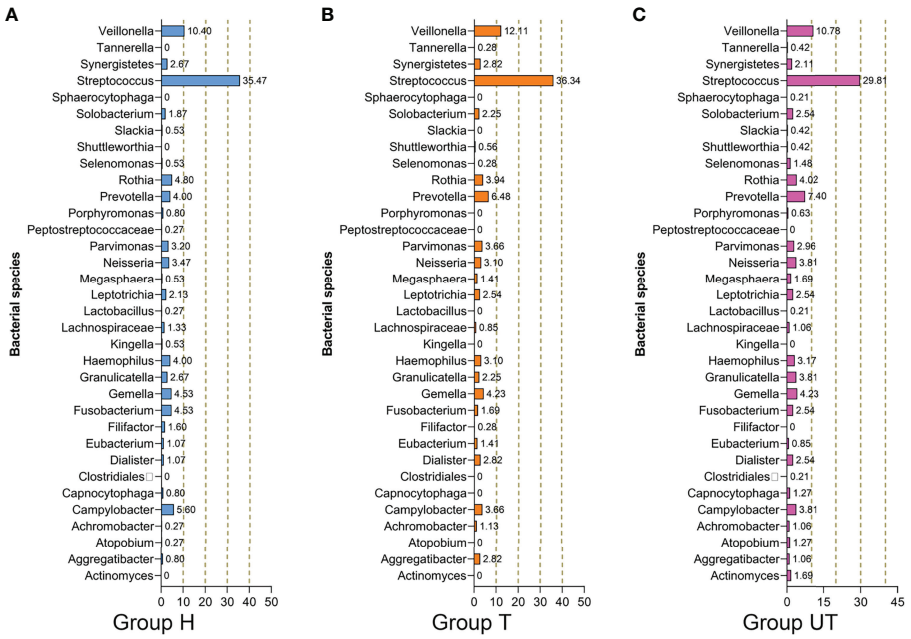

FIGURE 3 | Species composition and distribution of flora in saliva samples from HIV-infected/AIDS patients after HAART at the genus level. Proportional distribution of major bacterial genus in the healthy control, HAART unprocessed, and HAART groups. **(A)** Bacterial species in Group H. **(B)** Bacterial species in Group T. **(C)** Bacterial species in Group UT. Group H, Healthy control; Group T, After treatment of HAART-processed AIDS patients; Group UT, Before treatment of HAART-processed AIDS patients.

DISCUSSION

Different opportunistic infections can invade different tissues and organs of the body (Duff, 2019). And the oral cavity is a common infection site for AIDS opportunistic infections (Peacock et al., 2017). AIDS-related oral lesions are considered the key indications for the detection and diagnosis of HIV infection (Keijser et al., 2008; Nasidze et al., 2009; Lazarevic et al., 2010; Li et al., 2010; Ling et al., 2010). Periodontal disease is a group of periodontal support tissue infections caused by oral

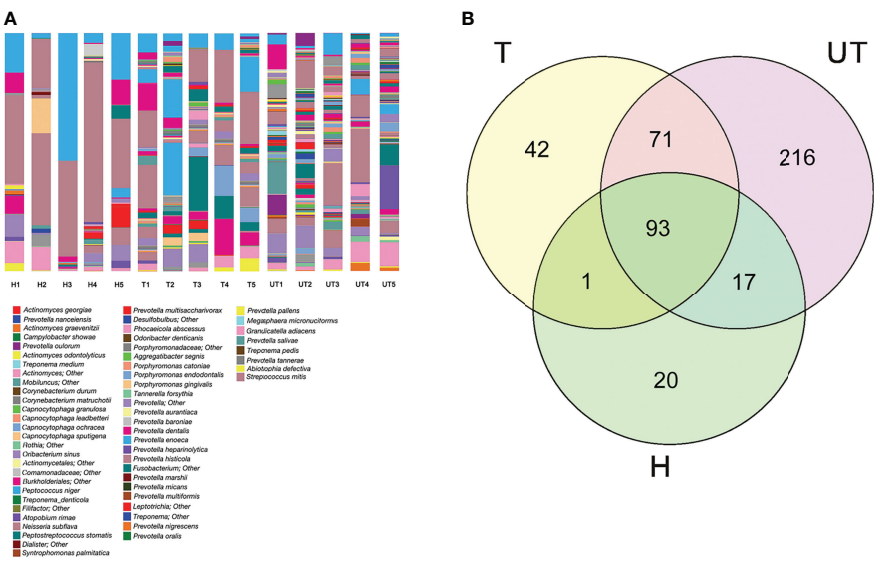

FIGURE 4 | Distribution of saliva sample flora species in HIV-infected/AIDS patients after HAART. **(A)** The proportion of different species was displayed using the species profiling in each sample. **(B)** Venn diagram showed the overlap and differences in the composition of salivary microecological communities of different groups.

TABLE 5 | Different genera of bacteria in saliva samples of AIDS patients after HAART treatment.

Genura	Positive		
	Group H (n = 78)	Group UT (n = 64)	Group T (n = 62)
Capnocytophaga	68 (87.18%)	8 (12.50%)**	51 (82.26%)##
Slackia	67 (85.90%)	12 (18.75%)**	48 (77.41%)##
Porphyromonas	72 (92.31%)	7 (10.94%)**	43 (69.35%)##
Kingella	74 (94.87%)	15 (23.44%)**	49 (79.03%)##
Peptostreptococcaceae	71 (91.03%)	14 (21.88%)**	51 (82.26%)##
Lactobacillus	69 (88.46%)	13 (20.31%)**	48 (77.42%)##
Atopobium	73 (93.59%)	10 (15.63%)**	42 (67.74%)##

*Group H, Healthy control; Group T, After treatment of HAART-processed AIDS patients; Group UT, Before treatment of HAART-processed AIDS patients; HAART, Highly active antiretroviral therapy. **P < 0.01 vs Group H; ##P < 0.01 vs Group T.*

bacteria and is the most frequent microbial infectious disease (Carrizales-Sepúlveda et al., 2018). Studies demonstrated a correlation between the occurrence of periodontal lesions and HIV infection, reflecting a close relationship between oral and systemic status (Patton et al., 2000; Paster et al., 2002; Vernon et al., 2009; Vernon et al., 2011).

In our study, we performed statistics on the relationship between periodontal and dental health indicators and demographic variables of HIV-infected/AIDS patients. The data displayed that age, sex, and marital status were associated with several periodontal health indicators. Although study has concluded that there is no statistical relationship between marital status and periodontal health status (Persson et al., 2004) a series of events such as family relationship breakups and financial pressures leading to increased mental stress in HIV-infected individuals may have had an impact on periodontal disease (Leserman et al., 1999; Ketchen et al., 2009; Dalmida et al., 2013; Warren et al., 2014). Meanwhile, socioeconomic variables such as income, education level, and residence were correlated with PD and CAL. And these results are consistent with the published literatures (Ababneh et al., 2012; Soares et al., 2013; Soares et al., 2014). Besides, our data revealed the percentage of BOP positive loci was lower in the group with lower BMI, probably because of the poorer systemic nutritional status of this group of patients. Researches confirmed that smoking can greatly increase the risk of periodontal destruction (Johnson, 2017); alcohol consumption is also a risk factor for developing periodontitis (Ryder et al., 2019). Our data further reveal an association between smoking and alcohol consumption and periodontal health of HIV-infected patients. Also, HIV-infected patients with good oral hygiene behaviors had better periodontal health. Additionally, our data also manifested that age, marital status and BMI were associated with dental health. And mouth rinsing frequency was also\ associated with number of permanent sound teeth and DMFT. Our present study also found that the most common oral lesion among HIV-infected patients was oral candidiasis, as previously reported (Suryana et al., 2020). And oral ulcers are the second most frequent oral lesion after oral candidiasis. Other study also proved that ulcers in people with HIV/AIDS are larger, deeper and longer lasting than those in HIV recessive patients (Tappuni, 2020). Dry mouth was also found in some patients in this study, but no enlargement of the salivary glands was detected. Therefore, oral hygiene behaviors are key for maintaining periodontal health in HIV-infected patients.

Oral microbiomes, as a complex and abundant microbiota, play a vital role in maintaining a normal oral physiological environment (Gao et al., 2018). In the human body, oral microbiomes can interact with the body to affect oral health and some systemic diseases (Graves et al., 2019). HIV-infected/AIDS patients are in a state of chronic immune system compromise, which has a significant impact on the overall oral flora (Hegde et al., 2014). The widespread application of HAART has been reported to improve oral representations (Fidel et al., 2021). However, the effect of HAART on the oral flora of AIDS patients has not been clearly elucidated. In our study, we adopted Roche 454 sequencing to analyze the salivary microbial diversity of healthy controls, before and after treatment of HAART-processed AIDS patient. Our data suggested that salivary microbial diversity can be reduced in AIDS patients processed

TABLE 6 | Different genera of bacteria in different saliva samples.

Genura	Contribution (%)		
	Group H (n = 78)	Group UT (n = 64)	Group T (n = 62)
Fusobacterium	6.27 ± 0.74	1.49 ± 0.41**	2.83 ± 0.47##
Campylobacter	8.62 ± 0.58	3.27 ± 0.65**	5.34 ± 0.46##
Prevotella	4.26 ± 0.41	2.32 ± 0.34**	3.86 ± 0.37##
Capnocytophaga	1.24 ± 0.21	0.24 ± 0.11**	0.12 ± 0.17##
Selenomonas	0.76 ± 0.13	0.26 ± 0.08**	0.57 ± 0.12##
Granulicatella	3.58 ± 0.52	1.38 ± 0.47**	2.86 ± 0.33##

*Group H, Healthy control; Group T, After treatment of HAART-processed AIDS patients; Group UT, Before treatment of HAART-processed AIDS patients; HAART, Highly active antiretroviral therapy. **P < 0.01 vs Group H; ##P < 0.01 vs Group T.*

with HARRT. This may be related to the increase of *Candida* and other genera including *Dialister*, *Aggregatibacter*, *Atopobium*, *Actinomyces*, etc. Besides, we detected 105 genera in the three groups of samples. Of these, *Streptococcus* and *Veillonella* were the dominant groups. Although these two genera are oral commensals, they contain many vital species that may cause human infections (Moussa et al., 2021; Yuan et al., 2021). Interestingly, seven genera were present only in the healthy control group. Five genera notably increased in the AIDS group; Six genera including *Aggregatibacter* prominently increased in the HAART-processed group, and *Aggregatibacter* dramatically decreased in the HAART-processed group. At the "species" level, we identified 319 strains. 7% of the strains only appeared in healthy control group and 24% of the strains appeared only in the AIDS group. Some strains exhibited significant differences among the three groups of samples, covering *Atopobium spp*, *Actinomyces gerencseriae*, and *Aggregatibacter segnis*.

In this study, the 108 HIV-infected patients have poor periodontal and dental health, mostly with oral lesions, and the severity of which is related to age, gender, BMI, and degree of immunodeficiency. Salivary microflora species were increased in HIV-infected patients relative to healthy controls. And HARRT treatment can obviously reduce salivary microbial diversity in AIDS patients. Therefore, the maintenance of oral health and oral ecosystem balance in HIV-infected/AIDS patients are of great importance. And HAART has a key role in the balance of salivary microecology in AIDS patients. Early HAART has an irreplaceable role in improving the oral health status of AIDS patients, reducing oral lesions and prolonging the survival of AIDS. Although HAART treatment has a beneficial effect on salivary microecological balance in AIDS patients, its possible mechanism of action is not clear and needs further study. Besides, we will also further collect more information about HAART-treated patients for examining and comparing the periodontal or dental health of patients before and after treatment. The small sample size of patients included in the Roche 454 sequencing is also a potential limitation of the current study, and we will expand the sample size in future studies to focus on the diversity of salivary microbial communities in HIV-infected/AIDS patients.

DATA AVAILABILITY STATEMENT

The datasets presented in this study can be found in online repositories. The name of the repository and accession number can be found below: NCBI; PRJNA844037.

ETHICS STATEMENT

The studies involving human participants were reviewed and approved by This study also received the approval of the ethics committee in West China Hospital of Stomatology, Sichuan University (WCHSIRB-D-2015-004). The patients/participants provided their written informed consent to participate in this study.

AUTHOR CONTRIBUTIONS

YL and YY conceived and designed the study and provided administrative support. PC, YZ and GD performed the experiments and analyzed data. PC, YZ and HW analyzed and interpreted the data. YL, GD and YY wrote the manuscript. All authors read and approved the final manuscript.

FUNDING

This study was supported by Science and Technology Foundation of Chengdu, China (2021-YF05-00442-SN), Science and Technology Foundation of Sichuan Province, China (2022YFS0116).

REFERENCES

Ababneh, K. T., Abu Hwaij, Z. M., and Khader, Y. S. (2012). Prevalence and Risk Indicators of Gingivitis and Periodontitis in a Multi-Centre Study in North Jordan: A Cross Sectional Study. *BMC Oral. Health* 12, 1. doi: 10.1186/1472-6831-12-1

Allali, I., Arnold, J. W., Roach, J., Cadenas, M. B., Butz, N., Hassan, H. M., et al. (2017). A Comparison of Sequencing Platforms and Bioinformatics Pipelines for Compositional Analysis of the Gut Microbiome. *BMC Microbiol.* 17 (1), 194. doi: 10.1186/s12866-017-1101-8

Andrade, H. B., Shinotsuka, C. R., da Silva, I. R. F., Donini, C. S., Yeh Li, H., de Carvalho, F. B., et al. (2017). Highly Active Antiretroviral Therapy for Critically Ill HIV Patients: A Systematic Review and Meta-Analysis. *PloS One* 12 (10), e0186968. doi: 10.1371/journal.pone.0186968

Bbosa, N., Kaleebu, P., and Ssemwanga, D. (2019). HIV Subtype Diversity Worldwide. *Curr. Opin. HIV AIDS* 14 (3), 153–160. doi: 10.1097/COH.0000000000000534

Carrizales-Sepúlveda, E. F., Ordaz-Farías, A., Vera-Pineda, R., and Flores-Ramírez, R. (2018). Periodontal Disease, Systemic Inflammation and the Risk of Cardiovascular Disease. *Heart Lung Circ.* 27 (11), 1327–1334. doi: 10.1016/j.hlc.2018.05.102

Chen, H., and Boutros, P. C. (2011). VennDiagram: A Package for the Generation of Highly-Customizable Venn and Euler Diagrams in R. *BMC Bioinf.* 12, 35. doi: 10.1186/1471-2105-12-35

Chen, W.-Y., and Wang, J. (2022). Primary Syphilitic Proctitis Associated With Human Immunodeficiency Virus Infection in a Male Patient Who Had Sex With Men: A Case Report. *JOMH* 18 (2):30. doi: 10.31083/jomh.2021.086

Cilliers, K., Muller, C. J. F., and Page, B. J. (2019). Human Immunodeficiency Virus in Cadavers: A Review. *Clin. Anat* 32 (4), 603–610. doi: 10.1002/ca.23358

Crawford, P. A., Crowley, J. R., Sambandam, N., Muegge, B. D., Costello, E. K., Hamady, M., et al. (2009). Regulation of Myocardial Ketone Body Metabolism by the Gut Microbiota During Nutrient Deprivation. *Proc. Natl. Acad. Sci. U. S. A.* 106 (27), 11276–11281. doi: 10.1073/pnas.0902366106

Dalmida, S. G., Koenig, H. G., Holstad, M. M., and Wirani, M. M. (2013). The Psychological Well-Being of People Living With HIV/AIDS and the Role of Religious Coping and Social Support. *Int. J. Psychiatry Med.* 46 (1), 57–83. doi: 10.2190/PM.46.1.e

Duff, P. (2019). Prevention of Opportunistic Infections in Women With HIV Infection. *Clin. Obstet. Gynecol.* 62 (4), 816–822. doi: 10.1097/GRF.0000000000000483

Fidel, P. L.Jr., Thompson, Z. A., Lilly, E. A., Granada, C., Treas, K., Dubois, K. R.3rd, et al. (2021). Effect of HIV/HAART and Other Clinical Variables on the Oral Mycobiome Using Multivariate Analyses. *mBio* 12 (2). doi: 10.1128/mBio.00294-21

Forgetta, V., Leveque, G., Dias, J., Grove, D., Lyons, R.Jr., Genik, S., et al. (2013). Sequencing of the Dutch Elm Disease Fungus Genome Using the Roche/454 GS-FLX Titanium System in a Comparison of Multiple Genomics Core Facilities. *J. Biomol Tech.* 24 (1), 39–49. doi: 10.7171/jbt.12-2401-005

Gao, L., Xu, T., Huang, G., Jiang, S., Gu, Y., and Chen, F. (2018). Oral Microbiomes: More and More Importance in Oral Cavity and Whole Body. *Protein Cell.* 9 (5), 488–500. doi: 10.1007/s13238-018-0548-1

Graves, D. T., Corrêa, J. D., and Silva, T. A. (2019). The Oral Microbiota Is Modified by Systemic Diseases. *J. Dent. Res.* 98 (2), 148–156. doi: 10.1177/0022034518805739

Hegde, M. C., Kumar, A., Bhat, G., and Sreedharan, S. (2014). Oral Microflora: A Comparative Study in HIV and Normal Patients. *Indian J. Otolaryngol Head Neck Surg.* 66 (Suppl 1), 126–132. doi: 10.1007/s12070-011-0370-z

Hulgan, T., and Samuels, D. C. (2021). Mitochondria and Human Immunodeficiency Virus: A Troubled Relationship Enters Its Fourth Decade. *Clin. Infect. Dis.* 73 (2), e474–e4e6. doi: 10.1093/cid/ciaa983

Indrastiti, R. K., Wardhany, I. I., and Soegyanto, A. I. (2020). Oral Manifestations of HIV: Can They be an Indicator of Disease Severity? (A Systematic Review). *Oral. Dis.* 26 Suppl 1, 133–136. doi: 10.1111/odi.13394

Keijser, B. J., Zaura, E., Huse, S. M., van der Vossen, J. M., Schuren, F. H., Montijn, R. C., et al. (2008). Pyrosequencing Analysis of the Oral Microflora of Healthy Adults. *J. Dent. Res.* 87 (11), 1016–1020. doi: 10.1177/154405910808701104

Kemp, P. F., and Aller, J. Y. (2004). Bacterial Diversity in Aquatic and Other Environments: What 16S rDNA Libraries Can Tell Us. *FEMS Microbiol. ecology.* 47 (2), 161–177. doi: 10.1016/S0168-6496(03)00257-5

Ketchen, B., Armistead, L., and Cook, S. (2009). HIV Infection, Stressful Life Events, and Intimate Relationship Power: The Moderating Role of Community Resources for Black South African Women. *Women Health* 49 (2-3), 197–214. doi: 10.1080/03630240902963648

Korona-Glowniak, I., Piatek, D., Fornal, E., Lukowiak, A., Gerasymchuk, Y., Kedziora, A., et al. (2021). Patterns of Oral Microbiota in Patients With Apical Periodontitis. *J. Clin. Med.* 10 (12), 2707. doi: 10.3390/jcm10122707

Lapointe, H. R., and Harrigan, P. R. (2020). Human Immunodeficiency Virus Phylogenetics in the United States-And Elsewhere. *J. Infect. Dis.* 222 (12), 1939–1940. doi: 10.1093/infdis/jiaa108

Lazarevic, V., Whiteson, K., Hernandez, D., Francois, P., and Schrenzel, J. (2010). Study of Inter- and Intra-Individual Variations in the Salivary Microbiota. *BMC Genomics* 11, 523. doi: 10.1186/1471-2164-11-523

Leserman, J., Jackson, E. D., Petitto, J. M., Golden, R. N., Silva, S. G., Perkins, D. O., et al. (1999). Progression to AIDS: The Effects of Stress, Depressive Symptoms, and Social Support. *Psychosomatic Med.* 61 (3), 397–406. doi: 10.1097/00006842-199905000-00021

Li, L., Hsiao, W. W., Nandakumar, R., Barbuto, S. M., Mongodin, E. F., Paster, B. J., et al. (2010). Analyzing Endodontic Infections by Deep Coverage Pyrosequencing. *J. Dent. Res.* 89 (9), 980–984. doi: 10.1177/0022034510370026

Ling, Z., Kong, J., Jia, P., Wei, C., Wang, Y., Pan, Z., et al. (2010). Analysis of Oral Microbiota in Children With Dental Caries by PCR-DGGE and Barcoded Pyrosequencing. *Microbial ecology.* 60 (3), 677–690. doi: 10.1007/s00248-010-9712-8

Liu, L., Wu, W., Zhang, S. Y., Zhang, K. Q., Li, J., Liu, Y., et al. (2020). Dental Caries Prediction Based on a Survey of the Oral Health Epidemiology Among the Geriatric Residents of Liaoning, China. *BioMed. Res. Int.* 2020, 5348730. doi: 10.1155/2020/5348730

Lu, D. Y., Wu, H. Y., Yarla, N. S., Xu, B., Ding, J., and Lu, T. R. (2018). HAART in HIV/AIDS Treatments: Future Trends. *Infect. Disord. Drug Targets* 18 (1), 15–22. doi: 10.2174/1871526517666170505122800

Meer, S. (2019). Human Immunodeficiency Virus and Salivary Gland Pathology: An Update. *Oral. Surg. Oral. Med. Oral. Pathol. Oral. Radiol.* 128 (1), 52–59. doi: 10.1016/j.oooo.2019.01.001

Mosaddad, S. A., Tahmasebi, E., Yazdanian, A., Rezvani, M. B., Seifalian, A., Yazdanian, M., et al. (2019). Oral Microbial Biofilms: An Update. *Eur. J. Clin. Microbiol. Infect. Dis.* 38 (11), 2005–2019. doi: 10.1007/s10096-019-03641-9

Moussa, H. A., Wasfi, R., Abdeltawab, N. F., and Megahed, S. A. (2021). High Counts and Anthracene Degradation Ability of Streptococcus Mutans and Veillonella Parvula Isolated From the Oral Cavity of Cigarette Smokers and Non-Smokers. *Front. Microbiol.* 12, 661509. doi: 10.3389/fmicb.2021.661509

Nasidze, I., Li, J., Quinque, D., Tang, K., and Stoneking, M. (2009). Global Diversity in the Human Salivary Microbiome. *Genome Res.* 19 (4), 636–643. doi: 10.1101/gr.084616.108

Newman, M. G., Takei, H., Klokkevold, P. R., and Carranza, F. A. (2011). *Carranza's Clinical Periodontology* (Philadelphia, USA: Elsevier, Saunders).

Nossa, C. W., Oberdorf, W. E., Yang, L., Aas, J. A., Paster, B. J., Desantis, T. Z., et al. (2010). Design of 16S rRNA Gene Primers for 454 Pyrosequencing of the Human Foregut Microbiome. *World J. Gastroenterol. WJG* 16 (33), 4135–4144. doi: 10.3748/wjg.v16.i33.4135

Oliva-Moreno, J., and Trapero-Bertran, M. (2018). Economic Impact of HIV in the Highly Active Antiretroviral Therapy Era - Reflections Looking Forward. *AIDS Rev.* 20 (4), 226–235. doi: 10.24875/AIDSRev.M17000011

Paster, B. J., Russell, M. K., Alpagot, T., Lee, A. M., Boches, S. K., Galvin, J. L., et al. (2002). Bacterial Diversity in Necrotizing Ulcerative Periodontitis in HIV-Positive Subjects. *Ann. Periodontology / Am. Acad. Periodontology* 7 (1), 8–16. doi: 10.1902/annals.2002.7.1.8

Patton, L. L., McKaig, R., Strauss, R., Rogers, D., and Eron, J. J.Jr. (2000). Changing Prevalence of Oral Manifestations of Human Immuno-Deficiency Virus in the Era of Protease Inhibitor Therapy. *Oral Surg. Oral Med Oral Patho. Oral Padiol. Endodontics* 89 (3), 299–304. doi: 10.1016/S1079-2104(00)70092-8

Peacock, M. E., Arce, R. M., and Cutler, C. W. (2017). Periodontal and Other Oral Manifestations of Immunodeficiency Diseases. *Oral. Dis.* 23 (7), 866–888. doi: 10.1111/odi.12584

Persson, G. R., Persson, R. E., Hollender, L. G., and Kiyak, H. A. (2004). The Impact of Ethnicity, Gender, and Marital Status on Periodontal and Systemic Health of Older Subjects in the Trials to Enhance Elders' Teeth and Oral Health (TEETH). *J. Periodontology* 75 (6), 817–823. doi: 10.1902/jop.2004.75.6.817

Pinna, R., Cocco, F., Campus, G., Conti, G., Milia, E., Sardella, A., et al. (2019). Genetic and Developmental Disorders of the Oral Mucosa: Epidemiology; Molecular Mechanisms; Diagnostic Criteria; Management. *Periodontol 2000.* 80 (1), 12–27. doi: 10.1111/prd.12261

Ryder, M. I., Couch, E. T., and Chaffee, B. W. (2018). Personalized Periodontal Treatment for the Tobacco-and Alcohol-Using Patient. *Periodontology* 78 (1), 30-46. doi: 10.1111/prd.12229

Schloss, P. D., Westcott, S. L., Ryabin, T., Hall, J. R., Hartmann, M., Hollister, E. B., et al. (2009). Introducing Mothur: Open-Source, Platform-Independent, Community-Supported Software for Describing and Comparing Microbial Communities. *Appl. Environ. Microbiol.* 75 (23), 7537–7541. doi: 10.1128/AEM.01541-09

Shekatkar, M., Kheur, S., Gupta, A. A., Arora, A., Raj, A. T., Patil, S., et al. (2021). Oral Candidiasis in Human Immunodeficiency Virus-Infected Patients Under Highly Active Antiretroviral Therapy. *Dis. Mon.* 67 (9), 101169. doi: 10.1016/j.disamonth.2021.101169

Soares, G. B., Garbin, C. A., Moimaz, S. A., and Garbin, A. J. (2013). Oral Health Status of People Living With HIV/AIDS Attending a Specialized Service in Brazil. *Special Care Dentistry* 34, 176–184. doi: 10.1111/scd.12056

Soares, G. B., Garbin, C. A., Rovida, T. A., and Garbin, A. J. (2014). Oral Health Associated With Quality of Life of People Living With HIV/AIDS in Brazil. *Health Qual. Life Outcomes* 12, 28. doi: 10.1186/1477-7525-12-28

Suryana, K., Suharsono, H., and Antara, I. (2020). Factors Associated With Oral Candidiasis in People Living With HIV/AIDS: A Case Control Study. *HIV AIDS (Auckl)* 12, 33–39. doi: 10.2147/HIV.S236304

Tappuni, A. R. (2020). The Global Changing Pattern of the Oral Manifestations of HIV. *Oral. Dis.* 26 Suppl 1, 22–27. doi: 10.1111/odi.13469

Tappuni, A. R., and Sufiawati, I. (2020). The Bali Declaration on Oral Health in HIV/AIDS. *Oral. Dis.* 26 Suppl 1, 172. doi: 10.1111/odi.13404

Tian, Y., He, X., Torralba, M., Yooseph, S., Nelson, K. E., Lux, R., et al. (2010). Using DGGE Profiling to Develop a Novel Culture Medium Suitable for Oral Microbial Communities. *Mol. Oral. Microbiol.* 25 (5), 357–367. doi: 10.1111/j.2041-1014.2010.00585.x

Upreti, R., Oli, U., Bhattarai, S., Baral, D., and Sharma Poudel, I. (2020). Family Planning Practice Among People Living With Human Immuno Deficiency Virus/Acquired Immune Deficiency Syndrome. *J. Nepal Health Res. Counc* 18 (1), 10–15. doi: 10.33314/jnhrc.v18i1.1775

Vernon, L. T., Babineau, D. C., Demko, C. A., Lederman, M. M., Wang, X., Toossi, Z., et al. (2011). A Prospective Cohort Study of Periodontal Disease Measures and Cardiovascular Disease Markers in HIV-Infected Adults. *AIDS Res. Hum. Retroviruses* 27 (11), 1157–1166. doi: 10.1089/aid.2010.0320

Vernon, L. T., Demko, C. A., Whalen, C. C., Lederman, M. M., Toossi, Z., Wu, M., et al. (2009). Characterizing Traditionally Defined Periodontal Disease in HIV+ Adults. *Community dentistry Oral. Epidemiol.* 37 (5), 427–437. doi: 10.1111/j.1600-0528.2009.00485.x

Volberding, P., Lange, J. M. A., Greene, W. C., and Sewankambo, N. (2012). *Sande's HIV/AIDS Medicine: Medical Management of AIDS 2012* (Philadelphia, USA: Elsevier Saunders).

Warren, K. R., Postolache, T. T., Groer, M. E., Pinjari, O., Kelly, D. L., and Reynolds, M. A. (2014). Role of Chronic Stress and Depression in Periodontal Diseases. *Periodontology 2000.* 64 (1), 127–138. doi: 10.1111/prd.12036

Wong, D. (2009). *Salivary Diagnostics* (New Jersey, USA: Wiley-Blackwell).

Yan, X., Feng, B., Li, P., Tang, Z., and Wang, L. (2016). Microflora Disturbance During Progression of Glucose Intolerance and Effect of Sitagliptin: An Animal Study. *J. Diabetes Res.* 2016, 2093171. doi: 10.1155/2016/2093171

Yuan, H., Qiu, J., Zhang, T., Wu, X., Zhou, J., and Park, S. (2021). Quantitative Changes of Veillonella, Streptococcus, and Neisseria in the Oral Cavity of Patients With Recurrent Aphthous Stomatitis: A Systematic Review and Meta-Analysis. *Arch. Oral. Biol.* 129, 105198. doi: 10.1016/j.archoralbio.2021.105198

Zhang, J., Yu, J., Dou, J., Hu, P., and Guo, Q. (2017). The Impact of Smoking on Subgingival Plaque and the Development of Periodontitis: A Literature Review. *Frontiers Oral Health* 2, 751099. doi: 10.3389/froh.2021.751099

Zhang, Y., Wang, X., Li, H., Ni, C., Du, Z., and Yan, F. (2018). Human Oral Microbiota and its Modulation for Oral Health. *BioMed. Pharmacother* 99, 883–893. doi: 10.1016/j.biopha.2018.01.146

Conflict of Interest: The authors declare that the research was conducted in the absence of any commercial or financial relationships that could be construed as a potential conflict of interest.

Publisher's Note: All claims expressed in this article are solely those of the authors and do not necessarily represent those of their affiliated organizations, or those of the publisher, the editors and the reviewers. Any product that may be evaluated in this article, or claim that may be made by its manufacturer, is not guaranteed or endorsed by the publisher.

frontiers | Frontiers in Cellular and Infection Microbiology

ORIGINAL RESEARCH
published: 01 August 2022
doi: 10.3389/fcimb.2022.933833

Salivary Microbiome Profile of Diabetes and Periodontitis in a Chinese Population

Chunting Lu[1†], Qingtong Zhao[2†], Jianwen Deng[3†], Kexiao Chen[3], Xinrong Jiang[3], Fengyu Ma[3], Shuyuan Ma[4] and Zejian Li[4,5]*

[1] Science and Education Office, The First Affiliated Hospital, Jinan University, Guangzhou, China, [2] Department of Stomatology, The Sixth Affiliated Hospital of Jinan University, Dongguan, China, [3] School of Stomatology, Jinan University, Guangzhou, China, [4] Medical Center of Stomatology, The First Affiliated Hospital, Jinan University, Guangzhou, China, [5] Chaoshan Hospital, The First Affiliated Hospital of Jinan University, Chaozhou City, China

OPEN ACCESS

Edited by:
Zheng Zhang,
Nankai University, China

Reviewed by:
Shu Deng,
Boston University, United States
Ke Deng,
Shanghai Jiao Tong University, China
Ying An,
Fourth Military Medical University, China
Yalin Zhan,
Peking University Hospital of Stomatology, China

***Correspondence:**
Zejian Li
tlizejian@jnu.edu.cn

[†]These authors have contributed equally to this work

Specialty section:
This article was submitted to Microbiome in Health and Disease, a section of the journal Frontiers in Cellular and Infection Microbiology

Received: 01 May 2022
Accepted: 06 June 2022
Published: 01 August 2022

Citation:
Lu C, Zhao Q, Deng J, Chen K, Jiang X, Ma F, Ma S and Li Z (2022) Salivary Microbiome Profile of Diabetes and Periodontitis in a Chinese Population. Front. Cell. Infect. Microbiol. 12:933833. doi: 10.3389/fcimb.2022.933833

Aim: There is a bidirectional association between diabetes and periodontitis. However, the effect of diabetes on the periodontitis salivary microbiota has not been elucidated. The aim of this study was to determine the effect of the presence of diabetes on the microbiota among Chinese patients with periodontitis.

Materials and Methods: Unstimulated whole saliva samples were collected from the periodontitis with diabetes group (TC), chronic periodontitis group (CP), and periodontally healthy and systemically healthy group (H) by spitting method. Bacterial genomic DNA was PCR-amplified at the V4 variable region of 16S rRNA gene. The library was constructed according to the obtained sequence results, and biological analysis and statistical analysis were carried out. Functional prediction of three groups of microbial communities was performed by the PICRUSt algorithm.

Results: There was no significant difference in bacterial diversity between the TC and CP groups. Compared with the H group, the TC group and CP group presented a higher diversity of salivary flora. *Firmicutes*, *Streptococcus*, *Haemophilus*, *Veillonella*, and *Haemophilus parainfluenzae* dominated the H group. *Corynebacterium*, *Leptotrichia*, *Dialister*, *Comamonas*, *Capnocytophaga*, *Catonella*, *Filifactor*, *Campylobacter*, *Treponema*, *Campylobacter concisus*, *Prevotella oralis*, and *Porphyromonas gingivalis* were significantly enriched in the TC and CP groups. Among them, *Treponema* and *P. oralis* were the most abundant in the TC group. The PICRUSt results showed that many pathways related to cell motility and functional metabolism of the salivary microbial flora changed in the TC group and the CP group.

Conclusions: Diabetes was not the main factor causing the altered diversity of salivary microbiota in patients with periodontitis; however, the presence of diabetes altered the abundance of some microbiota in saliva.

Keywords: diabetes, periodontitis, saliva, 16S rDNA, microbiota

INTRODUCTION

Diabetes mellitus is a common metabolic disorder characterized by chronic hyperglycemia. The latest epidemiological studies have shown that more than 440 million people worldwide suffer from diabetes (Lovic et al., 2020), mainly in countries in the Asia-Pacific region. According to statistics, China has the largest number of diabetic patients in the world (Ma, 2018). Therefore, diabetes is an unresolved public health problem in China and throughout the world.

Periodontitis is the sixth most common complication in people with diabetes (Löe, 1993). Current epidemiological investigations have demonstrated a bidirectional relationship between diabetes and periodontitis. Type 2 diabetes mellitus (T2DM) is the most common type of diabetes, and its age of onset is more similar to periodontitis. Considering the different etiologies of type 1 diabetes (T1DM) and T2DM, and the potential differences in the pathobiology of these two diseases, it is more beneficial to explore their effects on periodontitis separately to explain their relationship with periodontitis. Systemic effects associated with T2DM and periodontitis may act synergistically to produce more severe periodontal disease progression than T1DM (Novak et al., 2008). Increased severity of periodontal disease in T2DM may reflect the altered pathogenic potential of periodontal bacteria and/or altered host inflammatory response characteristics, which may lead to a breakdown of periodontal homeostasis (Naguib et al., 2004). However, studies on the effect of T2DM on the periodontitis microbiota have yielded conflicting results (Polak and Shapira, 2018). This may be due to factors such as different regions, ethnic differences, and age (Taylor et al., 2013). Therefore, it is necessary to conduct in-depth research on the differences in the microbiota structure of periodontitis patients with or without diabetes among different populations.

In the Chinese population, the impact of diabetes on periodontitis salivary flora is relatively unknown. In the study of inflammatory mediators and microbiota in periodontitis and systemic diseases, saliva has been proven to be a viable substitute for serum and gingival crevicular fluid (Deepa and Thirrunavukkarasu, 2010), which helps to solve some problems inherent to gingival crevicular fluid sampling (Ghallab, 2018), such as time consumption, multiple sampling, and blood contamination. With the loss of periodontal attachment and the appearance of deep periodontal pockets, many serum-like fluids and microorganisms in gingival crevicular fluid infiltrate into saliva; thus, most periodontal pathogens and inflammatory mediators can be detected in saliva (Kim et al., 2018). Therefore, this study used a Chinese population as the research object to explore the impact of diabetes on periodontitis-related microorganisms in the saliva, in order to provide a theoretical basis for further research on the microbial mechanism of diabetes on periodontitis.

METHODS

Study Population

The subjects of the study were patients who visited the Department of Stomatology and Endocrinology of the First Affiliated Hospital of Jinan University from January 2021 to January 2022. Thirty volunteers were recruited by convenience sampling and divided into the periodontitis with diabetes group (TC group, n = 10), chronic periodontitis group (CP group, n = 10), and healthy group (H group, n = 10).

Periodontitis was defined by the presence of alveolar bone resorption in at least 30% of sites and more than 4 sites with probing depth (PD) ≥4 mm and clinical attachment loss (CAL) ≥2 mm (Zhou et al., 2013). T2DM was defined as glycated hemoglobin (HbA_1C) ≥6.5% and fasting blood glucose (FBG) ≥7.0 mmol/L (Maboudi et al., 2019). Individuals who were diagnosed with periodontitis and had no history of diabetes, self-reported systemic health, or blood tests with normal HbA_1C were included in the CP group. Patients newly diagnosed with T2DM in the endocrinology department and periodontitis diagnosed in the stomatology department were included in the TC group. Individuals without periodontitis and self-reported systemic health were included in the H group.

The following patients were excluded from our study: 1) any patient diagnosed with metabolic disease other than diabetes and systemic disease that may have affected the progression of the periodontitis, such as hyperthyroidism or cancer; 2) prior to the experimental history of special medication, such as antibiotics or hormones, within 6 months; 3) received periodontal treatment, such as scaling, within 6 months; 4) pregnant or breastfeeding; 5) current smokers (Becker et al., 2014); 6) remaining tooth with root caries. All participants signed a written informed consent form and agreed to use their own saliva samples for this study. This study was approved by the Medical Ethics Committee of the First Affiliated Hospital of Jinan University in China (Approval Number Kyk-2022-014) and strictly followed the Declaration of Helsinki.

Saliva Collection and DNA Extraction

Before the periodontal assessment, unstimulated whole saliva samples were collected by spitting. All research subjects were asked to fast for at least 8 h and to avoid eating, rinsing, brushing their teeth, and performing other oral exercises for at least 2 h before sampling. Then, 2 ml of saliva was collected between 9:00 am and 11:00 am and immediately stored in a −80°C refrigerator. The genomic DNA of the samples was extracted by the conventional cetyl trimethylammonium bromide method (CTAB), and the purity and concentration of the DNA were then detected by agarose gel electrophoresis.

High-Throughput Sequencing

With the use of the diluted genomic DNA as a template and specific primers with Barcode, PCR amplification was performed on the 16S rRNA gene V4 variable region. The forward primer sequence was 515F (5′-GTGCCAGCMGCCGCGCTAA-3′), and the reverse primer sequence was 806R (5′-GGAC TACHVGGGTTWTCTAAT-3′). The TruSeq® DNA PCR-Free Sample Preparation Kit (Illumina, San Diego, CA, USA) was used for library construction. The library quality was assessed on the Qubit@ 2.0 Fluorometer (Thermo Scientific, Waltham, MA, USA) and Agilent Bioanalyzer 2100 system (Agilent Technologies, Santa Clara, CA, USA). After the library was

qualified, the Illumina NovaSeq 6000 platform was used for on-machine sequencing.

Biological Analysis and Statistical Analysis

The original sequence was spliced and filtered to obtain clean data (effective tags). Then, Uparse software (Uparse v7.0.1001, http://www.drive5.com/uparse/) was used to perform operational taxonomic unit (OTU) clustering on the effective tags of all samples. Species annotation taxonomic analysis was performed using the Silva database (http://www.arb-silva.de/) based on the Mothur algorithm. Differences in dominant species between groups were compared using MUSCLE software (version 3.8.31, http://www.drive5.com/muscle/). After the data were normalized, alpha diversity analysis and beta diversity analysis were performed using QIIME software (Version 1.9.1) and R software (Version 2.15.3). With the use of R software (Version 2.15.3), statistical analysis methods, such as T-test, MetaStat, and analysis of similarity (ANOSIM), were used to test the significance of differences in the species composition and community structure of the grouped samples. PICRUSt predicted microbial function, and a T-test was used to detect functional differences between groups. Statistical analysis was performed on the baseline data of the study population using ANOVA or Tukey's test and the chi-square test in GraphPad Prism software.

RESULTS

Sociodemographic Characteristics and Clinical Examination

As shown in **Table 1**, there was no significant difference in age or sex among the TC group, CP group, and H group ($p > 0.05$). There were significant differences in CAL and PD between the CP group, TC group, and H group ($p < 0.05$), but there were no significant differences in CAL or PD between the CP group and TC group ($p > 0.05$). The average levels of HbA_1C and FBG in the TC group were 8.54% ± 1.38% and 12.03 ± 2.63 mmol/L.

Operational Taxonomic Unit and Sequencing Depth Analysis

To study the bacterial community composition of each sample, OTUs were clustered with 97% consistency for the effective tags of all samples, and species annotation was then performed on the sequences of OTUs. In total, 2,471 OTUs were identified in this study, from which 22 phylum-, 277 genus-, and 264 species-level taxa were detected. As shown in **Figure 1A**, 711 OTUs overlapped in the three sets of samples. The CP group had 1,094 OTUs, the TC group had 1,045 OTUs, and the H group had 1,952 OTUs. The CP group had 224 unique OTUs, the TC group had 188 unique OTUs, and the H group had 1,150 unique OTUs. The sparsity curve among the three groups was flat (**Figure 1B**), indicating that the sequencing sampling of the study was reasonable and that more data volumes would yield only a small number of new species.

Microbial Diversity Analysis

The alpha diversity among the three groups is shown in **Figures 2A, B**. From the Beeswarm of the observed species (**Figure 2A**), there was no significant difference in species abundance among the three groups ($p > 0.05$). The Beeswarm of Shannon indicated (**Figure 2B**) that the diversity of the TC group and the CP group was significantly increased compared with that of the H group. However, there was no significant difference in species abundance or diversity between the TC group and the CP group.

The beta diversity among the three groups is shown in **Figure 2C**. The principal coordinate analysis (PCoA) based on the weighted UniFrac distance showed that the samples in the TC group and the CP group were closer in distance, indicating that the degree of bacterial evolution of the samples between the two groups was similar, and the bacterial community structure between the two groups was similar. The distance between the H group and the TC and CP groups was farther, indicating that the bacterial community structures of the disease study group (TC and CP groups) and the H group were significantly different. ANOSIM further showed that there was no significant difference in the flora structure between the TC group and the CP group ($R^2 = 0.008$, $p > 0.05$). The bacterial community structure between the CP group and the H group ($R^2 = 0.162$, $p < 0.001$) and the TC group and the H group ($R^2 = 0.204$, $p < 0.001$) were statistically significant.

Differences in Bacterial Community Structure Between Groups at the Phylum Level

As shown in **Figure 3A**, at the phylum level, the three groups of samples were dominated by Proteobacteria, Bacteroidota,

TABLE 1 | Social demographic characteristics and clinical parameters among TC, CP, and H groups.

Variable	TC (mean ± SD)	CP (mean ± SD)	H (mean ± SD)	P-value
Age (years)	36.10 ± 2.60	32.40 ± 6.26	32.70 ± 3.56	$p > 0.05^a$
Sex (male/female)	5/5	6/4	5/5	$p > 0.05^b$
PD (mm)	$4.51 \pm 0.53^{\#c}$	$4.09 \pm 0.38^{\#c}$	1.65 ± 0.29	$p < 0.05^a$
CAL (mm)	$2.27 \pm 0.98^{\#c}$	$1.78 \pm 0.51^{\#c}$	0.00 ± 0.00	$p < 0.05^a$
HbA_1C (%)	8.54 ± 1.38	–	–	–
FBG (mmol/L)	12.03 ± 2.63	–	–	–

PD, pocket depth; CAL, clinical attachment loss; HbA_1C, glycosylated hemoglobin; FBG, fasting blood glucose. $p < 0.05$ is statistically significant.

[#] *$p > 0.05$ between TC and CP groups.*

[a] *ANOVA.*

[b] *Chi-square test.*

[c] *Turkey test.*

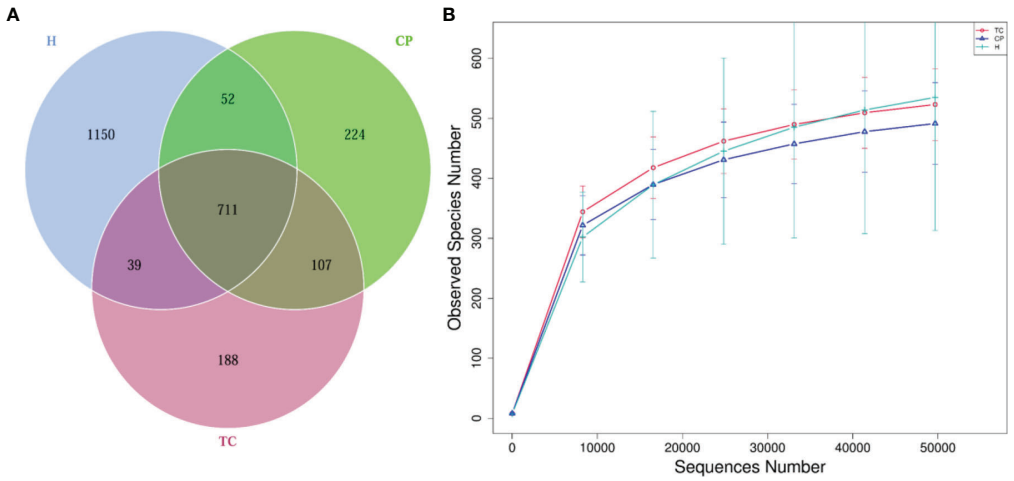

FIGURE 1 | Venn diagram and rarefaction curve diagram. **(A)** Venn diagram. Each circle in the figure represents a group, the numbers in the overlapping parts of the circles and the circles represent the number of operational taxonomic units (OTUs) shared among the samples (groups), and the numbers without overlapping parts represent the unique OTUs of the groups. **(B)** Rarefaction curve diagram. The abscissa is the number of sequencing strips randomly selected from a sample, and the ordinate is the number of OTUs that can be constructed based on the number of sequencing strips. Different groups are represented by curves with different colors.

Firmicutes, Fusobacteriota, and Actinobacteria. The MetaStat and T-test results (**Figure 4** and **Supplementary Figure S1**) showed that the phyla Fusobacteriota, Cyanobacteria, and Spirochaetota in the TC group were higher than those in the H group, and the phylum Gracilibacteria was lower than that in the H group; the phyla Fusobacteriota, Campylobacterota, Spirochaetota, and Cyanobacteria in the CP group were higher than those in the H group, while Firmicutes was lower than that in the H group; Spirochaetota was higher in the TC group than in the CP group.

Differences in Bacterial Community Structure Between Groups at the Genus Level

As shown in **Figure 3B**, the genus-level distribution among the three groups of samples was in the order of *Neisseria*, *Prevotella*, *Haemophilus*, *Streptococcus*, *Veillonella*, and *Porphyromonas*. The MetaStat and T-test results (**Figure 5** and **Supplementary Figure S2**) showed that the *Leptotrichia*, *Selenomonas*, *Campylobacter*, *Catonella*, *Treponema*, *Corynebacterium*, *Capnocytophaga*, *Dialister*, *Comamonas*, and *Filifactor* genera were higher in the TC group than in the H group; *Haemophilus* was lower than that in the H group; the *Neisseria*, *Leptotrichia*, *Campylobacter*, *Catonella*, *Treponema*, *Corynebacterium*, *Capnocytophaga*, *Dialister*, and *Filifactor* genera were higher in the CP group than in the H group, and *Haemophilus*, *Streptococcus*, and *Veillonella* were lower than those in the H group; the *Treponema* genus was higher in the TC group than the CP group.

Differences in Bacterial Community Structure Between Groups at the Species Level

The MetaStat and T-test results (**Figure 6** and **Supplementary Figure S3**) showed that, at the species level, *Campylobacter concisus*, *Prevotella oris*, *Porphyromonas gingivalis*, and *Prevotella intermedia* were higher in the CP group and TC group than in the H group and that *Haemophilus parainfluenzae* was lower than that in the H group. The relative abundances of *P. intermedia* were higher in the TC group, compared with the CP group (**Supplementary Figure S3**).

Predictive Analysis of Salivary Microbial Community Function

Using the PICRUSt algorithm, we performed functional predictions based on the Kyoto Encyclopedia of Genes and Genomes (KEGG) database for the three groups of microbial communities. As shown in **Supplementary Figures S4A, B**, at level 1, there were significant differences in the genetic information processing and the functions of cellular processes between the TC group, the CP group, and the H group ($p < 0.05$). As shown in **Supplementary Figures S4C, D**, **S5**, and **S6**, at level 2 and level 3, the TC group exhibited significantly enriched cellular processes (bacterial motility proteins, flagellar assembly, and bacterial chemotaxis), signaling (two-component system), basal energy (oxidative phosphorylation), and amino acid metabolism (aspartate metabolism, glutamate metabolism, histidine metabolism, tyrosine metabolism, tryptophan metabolism, etc.); the CP group showed significantly enriched amino acid metabolism (alanine, aspartic acid, glutamine, lysine, histidine, tyrosine, tryptophan, phenylalanine, etc.), cellular processes (cell motility, bacterial motility proteins, flagellar assembly, and bacterial chemotaxis), membrane transport (secretory system), basal energy (energy metabolism and oxidative phosphorylation), and other functions; group H showed significantly enriched replication and repair, translation, nucleotide metabolism (purine metabolism, pyrimidine metabolism) and other functions.

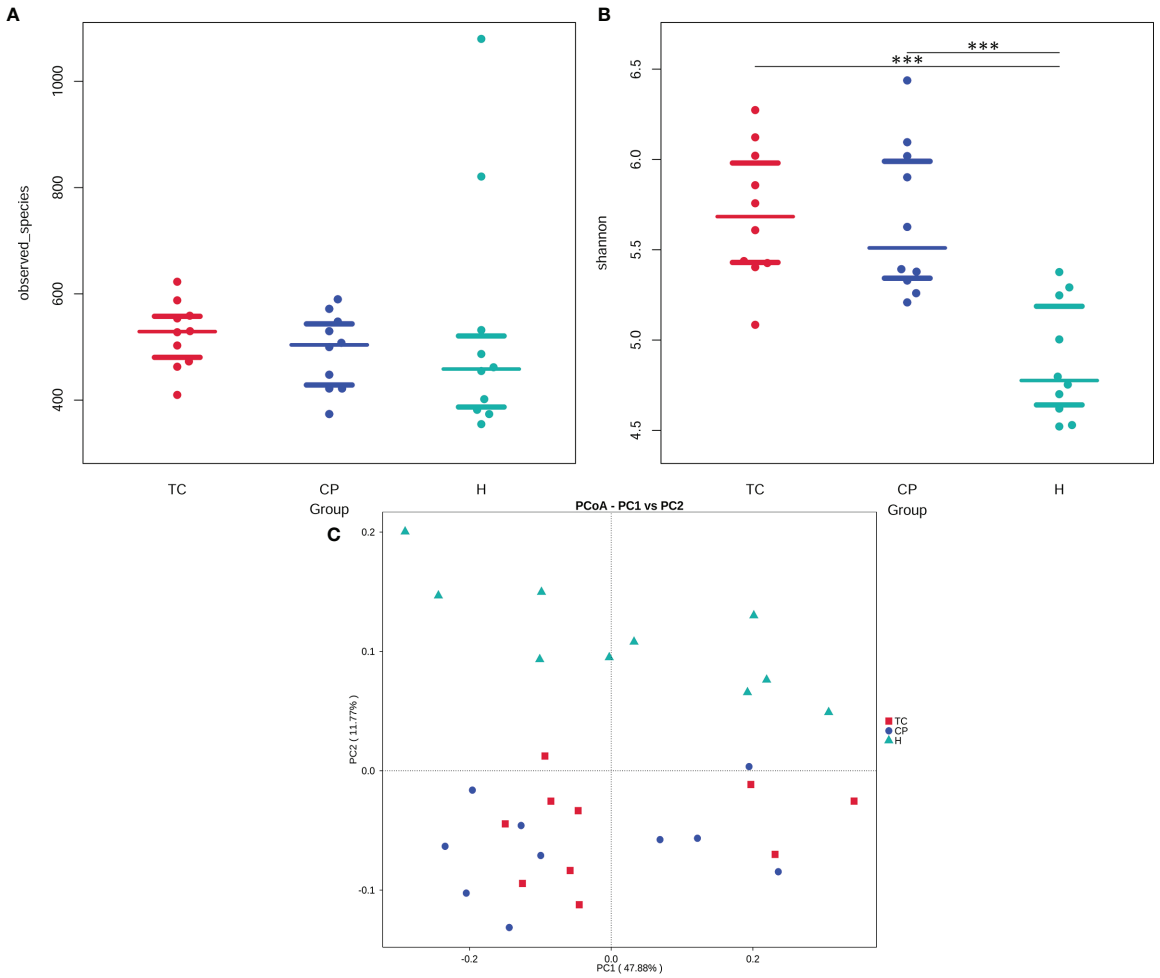

FIGURE 2 | Diversity analysis plot. **(A)** Beeswarm of the observed species index. **(B)** Beeswarm of the Shannon index. **(C)** Principal coordinate analysis (PCoA) plot. The samples of the same group in the figure are represented by the same color, each point represents a sample, and the distance between the points represents the degree of difference.

DISCUSSION

Periodontitis is an inflammatory disease that is thought to be associated with a variety of microbial disturbances (Darveau, 2010). Considering the bidirectional relationship between diabetes and periodontitis, in the context of diabetes, the bacterial community structure and diversity of periodontitis may be altered, thereby exacerbating periodontal bone loss. In recent years, many countries have carried out research on the impact of diabetes on periodontitis-related flora. However, the findings of these studies are not necessarily applicable to the Chinese population. Therefore, based on the Chinese population, we explored the influence of the presence or absence of diabetes on the salivary flora of periodontitis patients.

Similar to our findings, Liu (Liu et al., 2021) and Farina (Farina et al., 2019) et al. showed that diabetes did not affect the diversity of salivary microbiota in the context of periodontitis disease. Previous studies have shown that the presence of diabetes alone does not affect the structure of the salivary flora. This is further supported by studies by Almeida-Santos (Almeida-Santos et al., 2021) and Shi et al. (2020) In the study by Sun et al., periodontitis patients with and without T2DM had an increased diversity of salivary flora compared with healthy controls, while there was no significant difference between T2DM and periodontitis with T2DM patients after active blood sugar control (Sun et al., 2020). Therefore, they believe that periodontitis-related parameters are the main factors affecting the composition of salivary microbes, and the combined effect of T2DM and periodontitis on changes in the salivary microbiome is significantly greater than that of T2DM alone.

Compared with the H group or the CP group, the TC group showed an increasing trend in the flora biodiversity. This is similar to that reported by Balmasova (Balmasova et al., 2021) and Chen (Chen et al., 2020). However, Sabharwal (Sabharwal et al., 2019) and Saeb et al. (2019) believed that the presence of

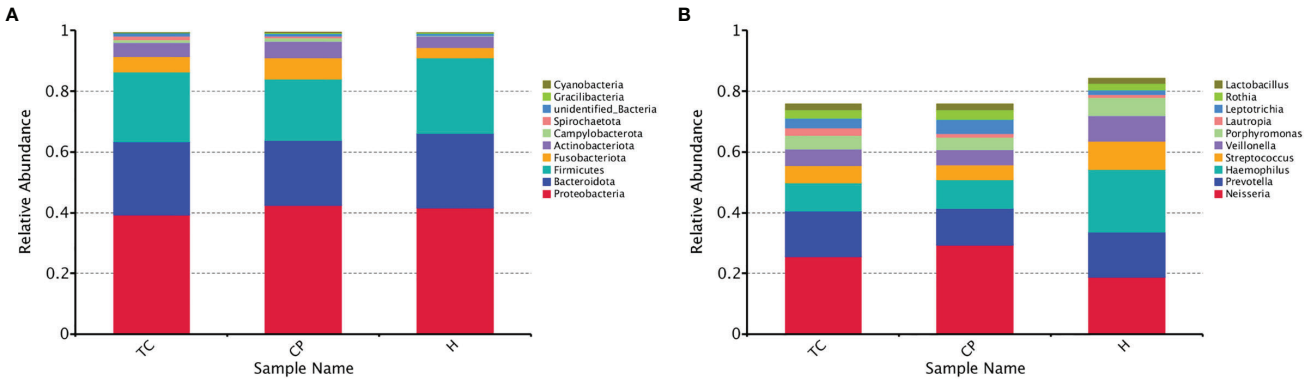

FIGURE 3 | Species relative abundance column chart. **(A)** Phylum level. **(B)** Genus level.

diabetes reduces the diversity of periodontitis salivary flora. These studies have different viewpoints, which may be attributed to the following reasons: 1) the sample size of each study was different, and small sample sizes may lead to a limited detection rate of flora related to the background of periodontitis. 2) Salivary flora may be affected by blood sugar status and different stages of periodontal disease, but many studies have not strictly distinguished whether the differential changes in salivary flora are caused by hyperglycemia or periodontal disease. 3) Studies have shown that the microbiota of stimulated saliva samples and unstimulated saliva samples is different (Gomar-Vercher et al., 2018); thus, the different ways of collecting saliva samples in each study may have affected the microbiota analysis results.

The dominant bacterial phyla in saliva were mainly Firmicutes, Bacteroidota, Proteobacteria, Actinobacteria, and Fusobacteriota (Lazarevic et al., 2010; Wade, 2013), among which Firmicutes were mainly enriched in healthy people (Griffen et al., 2012; Esparbès et al., 2021). This is largely consistent with the findings of this study. The statistical analysis of the differences in community structure at the phylum level showed that the common dominant bacterial phyla in the TC and CP groups were Fusobacteriota, Spirochaetota, and Campylobacterota, and Spirochaetota was more significantly enriched in the TC group. The Spirochaetota phylum is mainly composed of the genus *Treponema*. At the genus level, differential expression of this genus was observed in the TC group. It has been reported that the Spirochaetota flora accounts for 50% of the subgingival microbial population in periodontitis and less than 1% in healthy individuals (Chan and McLaughlin, 2000). They were found to be significantly higher in relative abundance in moderate-to-severe periodontitis (Listgarten and Levin, 1981; Armitage et al., 1982). The results of Marotz et al. confirmed that

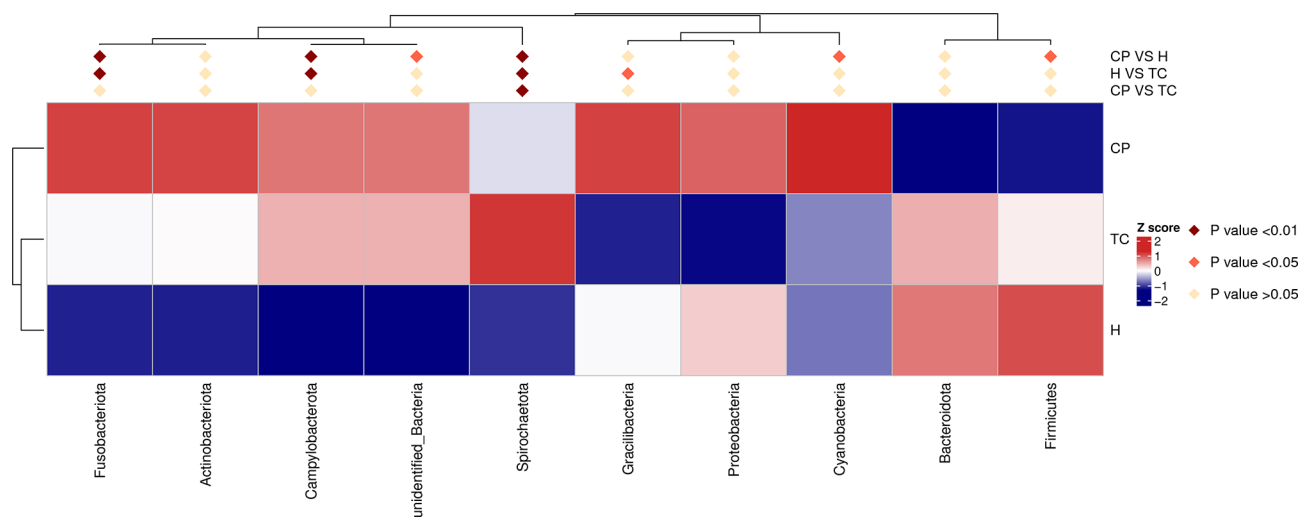

FIGURE 4 | MetaStat analysis; phylum annotation heatmap. Different colors in the heatmap represent the values obtained after the Z score of the relative content of differential metabolites is standardized, reflecting the level of their relative content (red represents high content, and blue represents low content).

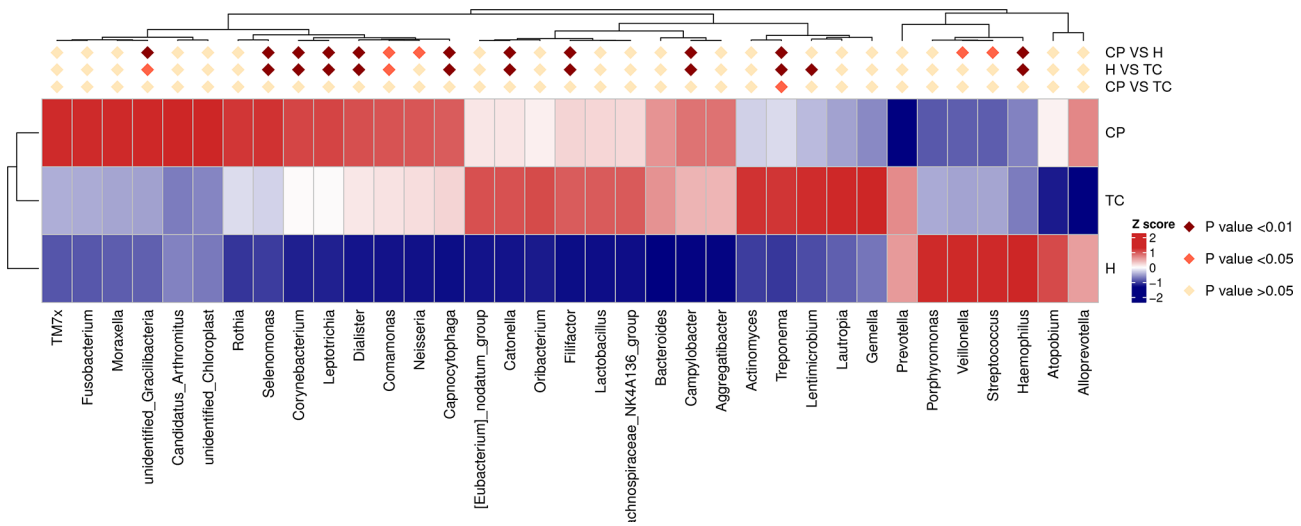

FIGURE 5 | MetaStat analysis; genus annotation heatmap. Different colors in the heatmap represent the values obtained after the Z score of the relative content of differential metabolites is standardized, reflecting the level of their relative content (red represents high content, and blue represents low content).

the log ratio of *Treponema* and *Corynebacterium* is a novel microbial indicator of periodontitis, and the increase in the detection rate of *Treponema* predicts the trend of periodontitis (Marotz et al., 2022). Diabetes has been reported to significantly increase the expression levels of these genera in the oral cavity (Sabharwal et al., 2019; Sun et al., 2020; Balmasova et al., 2021). A potential reason for the selective increase in this microbiota in periodontitis with diabetes may be the altered microenvironment due to differences in blood glucose, leading to the preferential proliferation of microorganisms with different growth requirements in specific oral niches.

At the genus level, the three groups of saliva samples were dominated by *Neisseria*, *Prevotella*, and *Haemophilus* species. The relative relationship between *Corynebacterium*, *Leptotrichia*, *Dialister*, *Comamonas*, *Capnocytophaga*, *Catonella*, *Filifactor*, *Campylobacter*, and *Treponema* in the TC and CP groups was higher than that in the H group, while *Haemophilus*, *Veillonella*, and *Streptococcus* were more abundant in the H group. In the process of plaque formation, *Streptococcus*, *Haemophilus*, *Veillonella*, *Actinomyces*, and *Fusobacterium* are the main flora in the early stage of bacterial colonization (Marsh, 2010). Periodontal disease-associated flora was observed to increase in

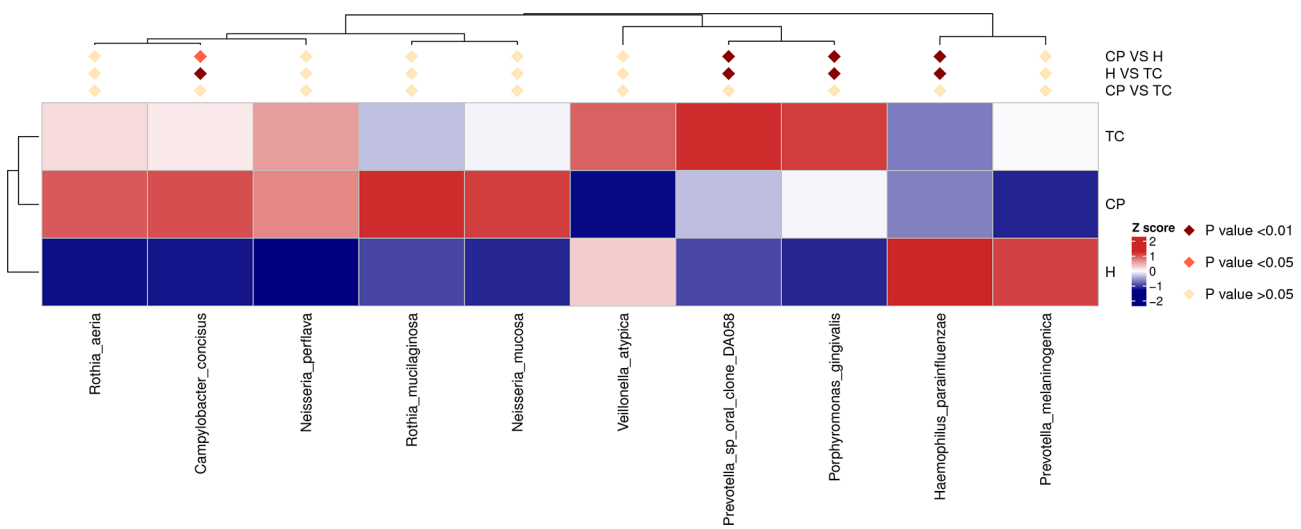

FIGURE 6 | MetaStat analysis; species annotation heatmap. Different colors in the heatmap represent the values obtained after the Z score of the relative content of differential metabolites is standardized, reflecting the level of their relative content (red represents high content, and blue represents low content).

abundance within the plaque as the plaque matured (Borisy and Valm, 2021). Belstrøm et al. suggested that *Streptococcus* gradually decreased in the late stage of oral plaque formation, while the abundance of some periodontal disease-related genera, such as *Leptotrichia* and *Prevotella*, gradually increased (Belstrøm et al., 2018). Therefore, the differences in the composition of microflora in saliva may indirectly reflect different stages of plaque formation and different stages of periodontitis. At the genus level, oral *Streptococcus* was confirmed to be the most abundant genus in healthy populations. However, *Haemophilus*, *Veillonella*, *Prevotella*, *Leptotrichia*, *Campylobacter*, *Neisseria*, and *Capnocytophaga* were not only expressed in periodontitis but also enriched in the periodontally healthy (Cao et al., 2018; Chen et al., 2018; Abusleme et al., 2021). This may be due to differences in the pathogenic potential of bacteria of the same genus.

At the species level, the dominant floras of the TC group and CP group were *C. concisus*, *Prevotella oralis*, and *P. gingivalis*, while the dominant flora of the H group was *H. parainfluenzae*. The presence of diabetes increased the expression of *P. intermedia* in saliva. These two bacteria belong to a core group closely associated with periodontitis and were confirmed to be positively associated with the subgingival plaque flora (Sakamoto et al., 2000; Belstrøm et al., 2017). Therefore, we speculate that patients with T2DM are more susceptible to the dysbiosis of oral flora, which in turn increases the risk and severity of periodontitis. In fact, the role of *P. gingivalis* and *Prevotella* (e.g., *P. intermedia*) in periodontitis has been extensively studied, while research on *C. concisus* in periodontitis is still limited. Studies have reported that the abundance of *C. concisus* is associated with increased levels of attachment loss in subjects with periodontitis (Haffajee et al., 1984). Henne et al. suggested that periodontitis does not affect changes in the absolute abundance of periodontitis and does not affect absolute changes in the abundance of *C. concisus* in the oral cavity, but the proportion of different species within *Campylobacter* may reflect microbial community changes as periodontitis progresses (Henne et al., 2014). The role of *Campylobacter* in periodontitis still needs further research in the future.

This study used the PICRUSt algorithm to predict the biological functions of differential enrichment of salivary microbiota in different groups. It is worth noting that cell motility, bacterial motility proteins, flagellar assembly, and bacterial chemotaxis were significantly enriched in the TC and CP groups. These biological functions related to the microbial virulence system can promote the adhesion and invasion of pathogenic microorganisms in periodontal tissue and then play an important role in the pathological process of periodontitis (Cai et al., 2021). In addition, similar to previous studies (Ikeda et al., 2020), we observed upregulation of pathways related to the metabolism of amino acids, such as aspartate, glutamate, tyrosine, tryptophan, and phenylalanine, in the TC group and the CP group. Although the underlying mechanism of amino acids in diabetes and periodontitis is not clear, amino acid metabolism (e.g., phenylalanine, tryptophan, and tyrosine) has been associated with the risk of diabetes and periodontitis in previous studies (Chen et al., 2016; Liebsch et al., 2019). Increases in certain amino acid catabolism-derived metabolites may induce disruption of host homeostasis, which in turn promotes the progression of periodontal inflammation (Kim, 2011).

It is worth noting that the small sample size of this study may have limited the detection rate of microbiota. In addition, we did not consider the effect of different periodontitis states on the expression of salivary flora. Therefore, the findings of this study need to be interpreted with caution. Nonetheless, we detected differential expression of some microbiota in periodontitis saliva in the presence of diabetes, and these results may inform future studies of these two common diseases.

CONCLUSIONS

Diabetes was not the main factor causing the altered diversity of salivary microbiota in patients with periodontitis, but the presence of diabetes altered the expression abundance of some microbiota in saliva.

DATA AVAILABILITY STATEMENT

The datasets presented in this study can be found in online repositories. The name of the repository and accession number can be found below: NCBI; PRJNA843376.

ETHICS STATEMENT

The studies involving human participants were reviewed and approved by The Ethics Committee of the First Affiliated Hospital of Jinan University, China. The patients/participants provided their written informed consent to participate in this study.

AUTHOR CONTRIBUTIONS

ZL designed the research project. CL, QZ and JD conducted experiments and contributed significantly to analysis and manuscript preparation. KC and XJ performed the data analyses and wrote the manuscript. FM and SM helped perform the analysis with constructive discussions. All the authors discussed and analyzed the experimental data, and wrote and revised the manuscript. All authors have reviewed the manuscript.

FUNDING

This work was partly supported by the National Nature Science Foundation (grant No. 81804153), Guangzhou Science and Technology Plan Foundation and Application Foundation

Research Project (grant No. 202102020020), Guangdong Foundation for Basic and Applied Basic Research (grant No. 2019A1515110161), Fundamental Research for the Central Universities (grant No. 21621410), Scientific Research Project of Guangdong Provincial Administration of Traditional Chinese Medicine (grant No. 20201107), and Starting fund for doctoral research of the Sixth Affiliated Hospital of Jinan University (grant No. JDLY2022001).

SUPPLEMENTARY MATERIAL

The Supplementary Material for this article can be found online at: https://www.frontiersin.org/articles/10.3389/fcimb.2022.933833/full#supplementary-material

Supplementary Figure S1 | T test analysis of species differences at the phylum level between groups. **(A)** TC and H groups. **(B)** CP and H groups. **(C)** TC and CP groups. The left picture shows the difference in species abundance between groups, and each bar in the figure represents the mean value of species with significant differences in abundance between groups in each group.

Supplementary Figure S2 | T test analysis of species differences at the genus level between groups. **(A)** TC and H groups. **(B)** CP and H groups. **(C)** TC and CP groups. The left picture shows the difference in species abundance between groups, and each bar in the figure represents the mean value of species with significant differences in abundance between groups in each group.

Supplementary Figure S3 | T test analysis of species differences at the species level between groups. **(A)** TC and H groups. **(B)** CP and H groups. **(C)** TC and CP groups. The left picture shows the difference in species abundance between groups, and each bar in the figure represents the mean value of species with significant differences in abundance between groups in each group.

Supplementary Figure S4 | PICRUSt predictions of the functional composition of the saliva microbiome. **(A)** KEGG pathway at level 1 between the TC and the H groups; **(B)** KEGG pathway at level 1 between the CP and the H groups; **(C)** KEGG pathway at level 2 between the TC and the H groups; **(D)** KEGG pathway at level 2 between the CP and the H groups. The left picture shows the difference in species abundance between groups, and each bar in the figure represents the mean value of species with significant differences in abundance between groups in each group.

Supplementary Figure S5 | PICRUSt predictions of the functional composition of saliva microbiome at level 3 between TC and H group. The left picture shows the difference in species abundance between groups, and each bar in the figure represents the mean value of species with significant differences in abundance between groups in each group.

Supplementary Figure S6 | PICRUSt predictions of the functional composition of saliva microbiome at level 3 between CP and H group. The left picture shows the difference in species abundance between groups, and each bar in the figure represents the mean value of species with significant differences in abundance between groups in each group.

REFERENCES

Abusleme, L., Hoare, A., Hong, B. Y., and Diaz, P. I. (2021). Microbial Signatures of Health, Gingivitis, and Periodontitis. *Periodontol. 2000* 86 (1), 57–78. doi: 10.1111/prd.12362

Almeida-Santos, A., Martins-Mendes, D., Gayà-Vidal, M., Pérez-Pardal, L., and Beja-Pereira, A. (2021). Characterization of the Oral Microbiome of Medicated Type-2 Diabetes Patients. *Front. Microbiol.* 12. doi: 10.3389/fmicb.2021.610370

Armitage, G., Dickinson, W., Jenderseck, R., Levine, S., and Chambers, D. (1982). Relationship Between the Percentage of Subgingival Spirochetes and the Severity of Periodontal Disease. *J. Periodontol.* 53 (9), 550–556. doi: 10.1902/jop.1982.53.9.550

Balmasova, I. P., Olekhnovich, E. I., Klimina, K. M., Korenkova, A. A., Vakhitova, M. T., Babaev, E. A., et al. (2021). Drift of the Subgingival Periodontal Microbiome During Chronic Periodontitis in Type 2 Diabetes Mellitus Patients. *Pathogens* 10 (5), 504. doi: 10.3390/pathogens10050504

Becker, S. T., Beck-Broichsitter, B. E., Graetz, C., Dörfer, C. E., Wiltfang, J., and Häsler, R. (2014). Peri-Implantitis Versus Periodontitis: Functional Differences Indicated by Transcriptome Profiling. *Clin. Implant Dent. Relat. Res.* 16 (3), 401–411. doi: 10.1111/cid.12001

Belstrøm, D., Sembler-Møller, M. L., Grande, M. A., et al. (2017). Microbial Profile Comparisons of Saliva, Pooled and Site-Specific Subgingival Samples in Periodontitis Patients. *PloS One* 12 (8), e0182992. doi: 10.1371/journal.pone.0182992

Belstrøm, D., Sembler-Møller, M., Grande, M., Kirkby, N., Cotton, S. L., Paster, B. J, et al. (2018). Impact of Oral Hygiene Discontinuation on Supragingival and Salivary Microbiomes. *JDR Clin. Trans. Res.* 3 (1), 57–64. doi; 10.1177/2380084417723625

Borisy, G. G., and Valm, A. M. (2021). Spatial Scale in Analysis of the Dental Plaque Microbiome. *Periodontol. 2000* 86 (1), 97–112. doi: 10.1111/prd.12364

Cai, Z., Lin, S., Hu, S., and Zhao, L. (2021). Structure and Function of Oral Microbial Community in Periodontitis Based on Integrated Data. *Front. Cell. Infect. Microbiol.* 11. doi: 10.3389/fcimb.2021.663756

Cao, Y., Qiao, M., Tian, Z., Yu, Y., Xu, B., Lao, W., et al. (2018). Comparative Analyses of Subgingival Microbiome in Chronic Periodontitis Patients With and Without IgA Nephropathy by High Throughput 16S rRNA Sequencing. *Cell Physiol. Biochem.* 47 (2), 774–783. doi: 10.1159/000490029

Chan, E., and McLaughlin, R. (2000). Taxonomy and Virulence of Oral Spirochetes. *Oral. Microbiol. Immunol.: Mini Rev* 15 (1), 1–9. doi: 10.1034/j.1399-302x.2000.150101.x

Chen, W.-P., Chang, S.-H., Tang, C.-Y., Liou, M.-L., Tsai, S.-J. J., and Lin, Y.-L. (2018). Composition Analysis and Feature Selection of the Oral Microbiota Associated With Periodontal Disease. *BioMed. Res. Int.* 2018, 3130607. doi: 10.1155/2018/3130607

Chen, T., Ni, Y., Ma, X., Bao, Y., Liu, J., Huang, F, et al. (2016). Branched-Chain and Aromatic Amino Acid Profiles and Diabetes Risk in Chinese Populations. *Sci. Rep.* 6 (1), 1–8. doi: 10.1038/srep20594

Chen, B., Wang, Z., Wang, J., Su, X., Yang, J., Zhang, Q., et al. (2020). The Oral Microbiome Profile and Biomarker in Chinese Type 2 Diabetes Mellitus Patients. *Endocrine* 68 (3), 564–572. doi: 10.1007/s12020-020-02269-6

Darveau, R. P. (2010). Periodontitis: A Polymicrobial Disruption of Host Homeostasis. *Nat. Rev. Microbiol.* 8 (7), 481–490. doi: 10.1038/nrmicro2337

Deepa, T., and Thirrunavukkarasu, N. (2010). Saliva as a Potential Diagnostic Tool. *Indian J. Med. Sci.* 64 (7), 293–306. doi: 10.4103/0019-5359.99854

Esparbès, P., Legrand, A., Bandiaky, O. N., Carpentier, M., Martin, H., Montassier, E., et al. (2021). Subgingival Microbiota and Cytokines Profile Changes in Patients With Periodontitis: A Pilot Study Comparing Healthy and Diseased Sites in the Same Oral Cavities. *Microorganisms* 9 (11), 2364. doi: 10.3390/microorganisms9112364

Farina, R., Severi, M., Carrieri, A., Miotto, E., Sabbioni, S., Trombelli, L., et al. (2019). Whole Metagenomic Shotgun Sequencing of the Subgingival Microbiome of Diabetics and Non-Diabetics With Different Periodontal Conditions. *Arch. Oral. Biol.* 104, 13–23. doi: 10.1016/j.archoralbio.2019.05.025

Ghallab, N. A. (2018). Diagnostic Potential and Future Directions of Biomarkers in Gingival Crevicular Fluid and Saliva of Periodontal Diseases: Review of the Current Evidence. *Arch. Oral. Biol.* 87, 115–124. doi: 10.1016/j.archoralbio.2017.12.022

Gomar-Vercher, S., Simón-Soro, A., Montiel-Company, J. M., Almerich-Silla, J. M., and Mira, A. (2018). Stimulated and Unstimulated Saliva Samples Have Significantly Different Bacterial Profiles. *PloS One* 13 (6), e0198021. doi: 10.1371/journal.pone.0198021

Griffen, A. L., Beall, C. J., Campbell, J. H., Firestone, N. D., Kumar, P. S., Yang, Z. K., et al. (2012). Distinct and Complex Bacterial Profiles in Human

Periodontitis and Health Revealed by 16S Pyrosequencing. *ISME J.* 6 (6), 1176–1185. doi: 10.1038/ismej.2011.191

Haffajee, A., Socransky, S., Ebersole, J., and Smith, D. (1984). Clinical, Microbiological and Immunological Features Associated With the Treatment of Active Periodontosis Lesions. *J. Clin. Periodontol.* 11 (9), 600–618. doi: 10.1111/j.1600-051X.1984.tb00913.x

Henne, K., Fuchs, F., Kruth, S., Horz, H.-P., and Conrads, G. (2014). Shifts in Campylobacter Species Abundance may Reflect General Microbial Community Shifts in Periodontitis Progression. *J. Oral. Microbiol.* 6 (1), 25874. doi: 10.3402/jom.v6.25874

Ikeda, E., Shiba, T., Ikeda, Y., Suda, W., Nakasato, A., Takeuchi, Y., et al. (2020). Japanese Subgingival Microbiota in Health vs Disease and Their Roles in Predicted Functions Associated With Periodontitis. *Odontology* 108 (2), 280–291. doi: 10.1007/s10266-019-00452-4

Kim, H. (2011). Glutamine as an Immunonutrient. *Yonsei Med. J.* 52 (6), 892–897. doi: 10.3349/ymj.2011.52.6.892

Kim, E.-H., Joo, J.-Y., Lee, Y. J., Koh, J. K., Choi, J. H., Shin, Y., et al. (2018). Grading System for Periodontitis by Analyzing Levels of Periodontal Pathogens in Saliva. *PloS One* 13 (11), e0200900. doi: 10.1371/journal.pone.0200900

Lazarevic, V., Whiteson, K., Hernandez, D., François, P., and Schrenzel, J. (2010). Study of Inter-and Intra-Individual Variations in the Salivary Microbiota. *BMC Genomics* 11 (1), 1–11. doi: 10.1186/1471-2164-11-523

Liebsch, C., Pitchika, V., Pink, C., Samietz, S., Kastenmüller, G., Artati, A., et al. (2019). The Saliva Metabolome in Association to Oral Health Status. *J. Dent. Res.* 98 (6), 642–651. doi: 10.1177/0022034519842853

Listgarten, M., and Levin, S. (1981). Positive Correlation Between the Proportions of Subgingival Spirochetes and Motile Bacteria and Susceptibility of Human Subjects to Periodontal Deterioration. *J. Clin. Periodontol.* 8 (2), 122–138. doi: 10.1111/j.1600-051X.1981.tb02352.x

Liu, Y.-K., Chen, V., He, J.-Z., Zheng, X., Xu, X., and Zhou, X.-D. (2021). A Salivary Microbiome-Based Auxiliary Diagnostic Model for Type 2 Diabetes Mellitus. *Arch. Oral. Biol.* 126, 105118. doi: 10.1016/j.archoralbio.2021.105118

Löe, H. (1993). Periodontal Disease: The Sixth Complication of Diabetes Mellitus. *Diabetes Care* 16 (1), 329–334. doi: 10.2337/diacare.16.1.329

Lovic, D., Piperidou, A., Zografou, I., Grassos, H., Pittaras, A., and Manolis, A. (2020). The Growing Epidemic of Diabetes Mellitus. *Curr. Vasc. Pharmacol.* 18 (2), 104–109. doi: 10.2174/1570161117666190405165911

Ma, R. C. (2018). Epidemiology of Diabetes and Diabetic Complications in China. *Diabetologia* 61 (6), 1249–1260. doi: 10.1007/s00125-018-4557-7

Maboudi, A., Eghbalian-Nouzanizadeh, A., Seifi, H., Bahar, A., Mohadese, M., Ali Mohammadpour, R., et al. (2019). Serum Levels of Interleukin-23 and 35 in Patients With and Without Type 2 Diabetes Mellitus and Chronic Periodontitis. *Caspian J. Internal Med.* 10 (3), 295–302. doi: 10.22088/cjim.10.3.295

Marotz, C., Molinsky, R., Martino, C., Bohn, B., Roy, S., Rosenbaum, M, et al. (2022). Early Microbial Markers of Periodontal and Cardiometabolic Diseases in ORIGINS. *NPJ Biofilms Microbiomes* 8 (1), 1–10. doi: 10.1038/s41522-022-00289-w

Marsh, P. D. (2010). Microbiology of Dental Plaque Biofilms and Their Role in Oral Health and Caries. *Dental Clinics* 54 (3), 441–454. doi: 10.1016/j.cden.2010.03.002

Naguib, G., Al-Mashat, H., Desta, T., and Graves, D. T. (2004). Diabetes Prolongs the Inflammatory Response to a Bacterial Stimulus Through Cytokine Dysregulation. *J. Invest. Dermatol.* 123 (1), 87–92. doi: 10.1111/j.0022-202X.2004.22711.x

Novak, M. J., Potter, R. M., Blodgett, J., and Ebersole, J. L. (2008). Periodontal Disease in Hispanic Americans With Type 2 Diabetes. *J. Periodontol.* 79 (4), 629–636. doi: 10.1902/jop.2008.070442

Polak, D., and Shapira, L. (2018). An Update on the Evidence for Pathogenic Mechanisms That may Link Periodontitis and Diabetes. *J. Clin. Periodontol.* 45 (2), 150–166. doi: 10.1111/jcpe.12803

Sabharwal, A., Ganley, K., Miecznikowski, J. C., Haase, E. M., Barnes, V., and Scannapieco, F. A. (2019). The Salivary Microbiome of Diabetic and non-Diabetic Adults With Periodontal Disease. *J. Periodontol.* 90 (1), 26–34. doi: 10.1002/JPER.18-0167

Saeb, A. T., Al-Rubeaan, K. A., Aldosary, K., Udaya Raja, G. K., Mani, B., Abouelhoda, M., et al. (2019). Relative Reduction of Biological and Phylogenetic Diversity of the Oral Microbiota of Diabetes and Pre-Diabetes Patients. *Microb. Pathog.* 128, 215–229. doi: 10.1016/j.micpath.2019.01.009

Sakamoto, M., Umeda, M., Ishikawa, I., and Benno, Y. (2000). Comparison of the Oral Bacterial Flora in Saliva From a Healthy Subject and Two Periodontitis Patients by Sequence Analysis of 16S rDNA Libraries. *Microbiol. Immunol.* 44 (8), 643–652. doi: 10.1111/j.1348-0421.2000.tb02545.x

Shi, B., Lux, R., Klokkevold, P., Chang, M., Barnard, E., Haake, S., et al. (2020). The Subgingival Microbiome Associated With Periodontitis in Type 2 Diabetes Mellitus. *ISME J.* 14 (2), 519–530. doi: 10.1038/s41396-019-0544-3

Sun, X., Li, M., Xia, L., Fang, Z., Yu, S., Gao, J., et al. (2020). Alteration of Salivary Microbiome in Periodontitis With or Without Type-2 Diabetes Mellitus and Metformin Treatment. *Sci. Rep.* 10 (1), 1–14. doi: 10.1038/s41598-020-72035-1

Taylor, J. J., Preshaw, P. M., and Lalla, E. (2013). A Review of the Evidence for Pathogenic Mechanisms That may Link Periodontitis and Diabetes. *J. Clin. Periodontol.* 40, S113–S134. doi: 10.1111/jcpe.12059

Wade, W. G. (2013). The Oral Microbiome in Health and Disease. *Pharmacol. Res.* 69 (1), 137–143. doi: 10.1016/j.phrs.2012.11.006

Zhou, M., Rong, R., Munro, D., Zhu, C., Gao, X., Zhang, Q., et al. (2013). Investigation of the Effect of Type 2 Diabetes Mellitus on Subgingival Plaque Microbiota by High-Throughput 16S rDNA Pyrosequencing. *PloS One* 8 (4), e61516. doi: 10.1371/journal.pone.0061516

Conflict of Interest: The authors declare that the research was conducted in the absence of any commercial or financial relationships that could be construed as a potential conflict of interest.

Publisher's Note: All claims expressed in this article are solely those of the authors and do not necessarily represent those of their affiliated organizations, or those of the publisher, the editors and the reviewers. Any product that may be evaluated in this article, or claim that may be made by its manufacturer, is not guaranteed or endorsed by the publisher.

frontiers | Frontiers in Cellular and Infection Microbiology

TYPE Original Research
PUBLISHED 09 August 2022
DOI 10.3389/fcimb.2022.925435

OPEN ACCESS

EDITED BY
Zheng Zhang,
Nankai University, China

REVIEWED BY
Shu Deng,
Boston University, United States
Sasanka Chukkapalli,
Texas A&M University College Station, United States

*CORRESPONDENCE
Deqin Yang
yangdeqin@hospital.cqmu.edu.cn

SPECIALTY SECTION
This article was submitted to Microbiome in Health and Disease, a section of the journal Frontiers in Cellular and Infection Microbiology

RECEIVED 21 April 2022
ACCEPTED 01 July 2022
PUBLISHED 09 August 2022

CITATION
Gong T, Chen Q, Mao H, Zhang Y, Ren H, Xu M, Chen H and Yang D (2022) Outer membrane vesicles of *porphyromonas gingivalis* trigger nlrp3 inflammasome and induce neuroinflammation, tau phosphorylation, and memory dysfunction in mice.
Front. Cell. Infect. Microbiol. 12:925435.
doi: 10.3389/fcimb.2022.925435

Outer membrane vesicles of *Porphyromonas gingivalis* trigger NLRP3 inflammasome and induce neuroinflammation, tau phosphorylation, and memory dysfunction in mice

Ting Gong[1,2,3], Qi Chen[1,2,3], Hongchen Mao[1,2,3], Yao Zhang[1,2,3], Huan Ren[1,2,3], Mengmeng Xu[1,2,3], Hong Chen[1,2,3] and Deqin Yang[1,2,3]*

[1]Department of Endodontics, Stomatological Hospital of Chongqing Medical University, Chongqing, China, [2]Chongqing Key Laboratory of Oral Diseases and Biomedical Sciences, Chongqing Medical University, Chongqing, China, [3]Chongqing Municipal Key Laboratory of Oral Biomedical Engineering of Higher Education, Chongqing Medical University, Chongqing, China

Background: *Porphyromonas gingivalis* (Pg), the keystone pathogen in chronic periodontitis, is reported to initiate Alzheimer's disease pathologies in preclinical studies. However, the specific mechanisms and signaling pathways acting on the brain still need to be further explored. Outer membrane vesicles are derived from Gram-negative bacteria and contain many virulence factors of bacteria. We hypothesized that outer membrane vesicles are an important weapon of *Porphyromonas gingivalis* to initiate Alzheimer's disease pathologies.

Methods: The outer membrane vesicles of *Porphyromonas gingivalis* (Pg OMVs, 4 mg/kg) or saline were delivered to 14-month-old mice by oral gavage every other day for eight weeks. Behavioral alterations were assessed by the open field test, Morris water maze, and Y-maze test. Blood–brain barrier permeability, neuroinflammation, tau phosphorylation, and NLRP3 inflammasome-related protein were analyzed.

Results: Pg OMVs impaired memory and learning ability of mice and decreased tight junction–related gene expression ZO-1, occludin, claudin-5, and occludin protein expression in the hippocampus. Pg OMVs could be detected in the hippocampus and cortex three days after oral gavage. Furthermore, Pg OMVs activated both astrocytes and microglia and elevated IL-1β, tau phosphorylation on the Thr231 site, and NLRP3 inflammasome–

related protein expression in the hippocampus. In *in vitro* studies, Pg OMV (5 μg/ml) stimulation increased the mRNA and immunofluorescence of NLRP3 in BV2 microglia, which were significantly inhibited by the NLRP3 inhibitor MCC950. In contrast, the tau phosphorylation in N2a neurons was enhanced after treatment with conditioned media from Pg OMV-stimulated microglia, which was attenuated after pretreatment with MCC950.

Conclusions: These results indicate that Pg OMVs prompt memory dysfunction, neuroinflammation, and tau phosphorylation and trigger NLRP3 inflammasome in the brain of middle-aged mice. We propose that Pg OMVs play an important role in activating neuroinflammation in the AD-like pathology triggered by *Porphyromonas gingivalis*, and NLRP3 inflammasome activation is a possible mechanism.

KEYWORDS

***porphyromonas gingivalis*, outer membrane vesicles, inflammasome, neuroinflammation, Alzheimer's disease, tau**

1 Introduction

Alzheimer's disease (AD) is the main cause of dementia and represents an enormous burden for the health economies. β-amyloid (Aβ) and tau phosphorylation, the main components of senile plaque and neurofibrillary tangles (NFTs), respectively, in the brain, are characteristic pathological hallmarks of AD (Braak and Braak, 1991).

Epidemiological studies propose that periodontal disease is a risk factor for AD (Sparks et al., 2012; Noble et al., 2014; Ryder, 2020). *Porphyromonas gingivalis* (Pg) is a Gram-negative bacterium known as a major pathogen of periodontal disease (Darveau et al., 2012). Many experimental studies conclude that Pg or its virulence factors could induce memory impairment and AD-related pathologies (Wu et al., 2017; Ding et al., 2018; Ilievski et al., 2018; Zhang et al., 2018; Dominy et al., 2019; Hayashi et al., 2019; Nie et al., 2019; Gu et al., 2020; Hu et al., 2020; Chi et al., 2021; Hao et al., 2022 Jiang et al., 2021; Qian et al., 2021; Su et al., 2021; Tang et al., 2021). Gingipains are toxic proteases secreted by Pg, it is reported that gingipains are neurotoxic *in vivo* and *in vitro*, causing detrimental effects on tau, a protein needed for normal neuronal function (Dominy et al., 2019), and gingipains could degrade tight junction proteins of human cerebral microvascular endothelial cells *in vitro* (Nonaka et al., 2022), suggesting that gingipains may be responsible for blood–brain barrier (BBB) damage. Lipopolysaccharide (LPS) is another virulence factor of Pg; Pg LPS can induce neuronal inflammation through the TLR4/NF-κB pathway (Zhang et al., 2018) and intracellular Aβ accumulation in neurons in a cathepsin B–dependent manner (Wu et al., 2017). However, the specific virulence factors, mechanisms, and signaling pathways acting on the brain still need to be further explored.

Outer membrane vesicles (OMVs) are gaining researchers' attention. OMVs are secreted by Gram-negative bacteria; range from 20 to 250 nm in diameter; and carry bacterial LPS, protease, membrane receptor, DNA, RNA, and so forth (Toyofuku et al., 2019). It is suggested that OMVs could act as long-distance weapons and cause systemic disease, including AD (Amano et al., 2010; Schertzer and Whiteley, 2013; Singhrao and Olsen, 2018; Seyama et al., 2020; Wei et al., 2020; Nara et al., 2021). In fact, the majority of Pg gingipains are packaged and associated with Pg OMVs (Nara et al., 2021), and Pg OMVs could increase BBB permeability and degrade tight junction proteins in a human *in vitro* model (Pritchard et al., 2022). Thus, we aimed to explore the effect of Pg OMVs on AD pathologies.

Neuroinflammation is suggested to play a critical role in AD onset and progression (Heneka et al., 2015). IL-1β are elevated in brains of AD patients and can be associated with the onset and progression of AD (Alvarez et al., 1996; Griffin et al., 2000; Oprica et al., 2007; Deniz-Naranjo et al., 2008). The nucleotide-binding oligomerization domain-like receptor family, pyrin domain containing 3 (NLRP3), is an intracellular signaling molecule that senses many pathogen-, environmental-, and host-derived factors (Wen et al., 2013). Upon activation, NLRP3 binds to an apoptosis-associated speck-like protein containing a CARD (ASC), and ASC, in turn, interacts with

procaspase-1, forming a complex termed the inflammasome. This results in the formation of the active caspase-1 p10/p20 tetramer, which then processes cytokine proforms, such as IL-1β and IL-18, to generate active molecules and mediates a type of inflammatory cell death known as pyroptosis (Schroder and Tschopp, 2010). The NLRP3 inflammasome is found to play an important role in microglial activation (Tan et al., 2013), and inhibition or knock-out of the NLRP3 inflammasome could reduce Aβ and tau phosphorylation *in vitro* and *in vivo* (Heneka et al., 2013; Ising et al., 2019; Beyer et al., 2020).

Given that the NLRP3 inflammasome is important in AD progression, it has become the focus of research, which may help to uncover the mechanism of AD. Recently Pg OMVs were reported to activate the NLRP3 inflammasome and induce IL-1β production in macrophages and monocytes (Cecil et al., 2017; Fleetwood et al., 2017).

The aim of this study was to explore whether Pg OMVs can trigger the NLRP3 inflammasome and neuroinflammation in the hippocampus, thus potentially inducing behavioral cognitive changes.

2 Materials and methods

2.1 Bacterial cultures and preparation of OMVs

Pg strain ATCC 33277 was cultured on anaerobic agar plates supplemented with defibrillated sheep blood, brain-heart infusion (OXOID, Britain), hemin (0.5 mg/mL), and menadione (10 mg/mL) in an anaerobic system (Gene Science, America) with 10% CO_2, 10% H_2, and 80% N_2. OMVs were isolated by an established protocol (Seyama et al., 2020). Briefly, when Pg cells were grown to the late exponential phase, the bacterial culture medium was collected and centrifuged at 2800 ×g for 15 minutes at 4°C to remove bacterial cells. The supernatant was filtered with a 0.22-μm syringe filter. The supernatant was concentrated to <1 mL by using an Ultra-15 Centrifugal Filter Device for nominal molecular weight limit (NMWL) 100,000 (Amicon, Merck, USA). The concentrate was mixed with Total Exosome Isolation Reagent (Invitrogen) and incubated overnight at 4°C. Afterward, the sample was centrifuged at 10,000 ×g for 60 minutes at 4°C. The OMV fractions were eluted with phosphate buffered saline (PBS) and quantified by protein concentrations using a BCA protein assay kit (Pierce, Rockford, IL, USA). Characterization of Pg OMVs utilized nanoparticle-tracking analysis (NTA) and transmission electron microscopy (TEM). To characterize the proteins of Pg OMVs, the same amount of Pg and OMVs (10 μg of total protein) were separated by sodium dodecyl sulfate (SDS)-poly-acrylamide gel electrophoresis (PAGE) and stained with Coomassie blue for one hour, washed in PBS overnight, and images were taken.

2.2 Animals

Fourteen-month-old male C57BL/6 mice were obtained from the Dashuo company. All animal studies were conducted following the guidelines approved by the Institutional Animal Care and Use Committee of the Stomatological Hospital of Chongqing Medical University. All mice were housed in groups of two to four mice per cage in biosafety barriers with a controlled light cycle and given sterile food and water ad libitum. The light–dark cycle was 1:1 with lights on at 7:00 a.m. Room temperature was 18°C ± 2°C, and humidity was 55% ± 10%. After one week of habituation, mice were treated with Pg OMVs or PBS by oral gavage using feeding needles (n = 12 in each group). The experimental group received Pg OMVs (4 mg/kg) diluted in PBS every other day for a consecutive eight weeks. The control group received an equivalent volume of PBS. The dosage of Pg OMVs were deduced from a previous study (Ho et al., 2016).

2.3 Mouse behavioral tests

A battery of behavioral tests comprising the Morris water maze (MWM), Y-maze, and open field tests were conducted to assess behavioral performance of mice.

2.3.1 Morris water maze test

The MWM was conducted in a circular pool that was 120 cm in diameter, and it was filled with opaque water stained with milk and surrounded by a set of spatial cues. The tank was imaginarily divided into four quadrants. A platform that was 9 cm in diameter was submerged 1 cm under the water surface in a quadrant. The MWM test consisted of three platform trials per day for five consecutive days, followed by a probe trial. In the platform trial, the mouse navigated in the pool to locate the platform and was then able to escape. If the mouse failed to locate the platform within 60 seconds, it was directed to the platform. The mouse was allowed to remain on the platform for 60 seconds once it escaped onto the platform. The escape latency was measured to test spatial learning ability. In the probe trial, the platform was withdrawn. The mouse navigated freely in the pool for one minute. The time spent in each quadrant and the number of annulus crossings were recorded to assess memory consolidation.

2.3.2 Y-maze test

A novel arm exploration test was performed in the Y-maze. One arm was blocked (defined as the novel arm), and the mice were allowed to explore the other two arms (home arm and familiar arm) for five minutes. After a one-hour interval, the mice were allowed to freely explore all three arms for five

minutes. The number of novel arm entries and time spent in the novel arm were recorded.

2.3.3 Open-field test

The mice were placed in the center of the open field apparatus for five minutes. The paths were tracked, and the distance travelled was recorded.

2.4 RNA isolation, reverse transcription, and quantitative real-time PCR

Total RNA was isolated by using the Trizol reagent (Takara, Japan), and it was subjected to reverse transcription by using the cDNA Reverse Transcription Kit (Takara, Japan). The quantitative real-time PCR analyses were carried out in the ABI Prism 7500 Real-Time PCR System (Applied Biosystems, Foster City, CA) with the SYBR Green PCR master mix reagent (Takara, Japan). PCR primer sequences are detailed in the supplementary data. The $2^{-\Delta\Delta Ct}$ value was used to calculate the relative gene expression normalized by the expression level of GAPDH.

2.5 Western blot assay

The hippocampus was homogenized and sonicated. The protein concentration was determined with a BCA protein assay reagent (Pierce, Rockford, IL, USA) according to the manufacturer's instructions. The same amount of protein samples (30 μg) from each tube was boiled in 5 × loading buffer for 10 minutes at 95°C. The sample was then separated on 10% tris-glycine SDS-PAGE gels and transferred onto immobilon PTM polyvinylidene fluoride (PVDF) membranes. To block nonspecific background, the membranes were incubated in 5% nonfat milk in Tris-buffered saline containing 0.1% Tween-20 (TBST) at 37°C for one hour. The target proteins were immunoblotted with primary antibody overnight at 4°C (see the supplemental information for details) followed by incubation with a secondary antibody (1:1000; Cell signaling technology) at room temperature for one hour. The blots were imaged by the Bio-Rad Imager using ECL Western blotting substrate (Beyotime Technology). The relative level of target protein is expressed as the percentage between the intensity of the target protein and that of the marker protein, GAPDH. The band intensity of each protein was quantified by ImageJ software.

2.6 Brain sampling

The mice were killed by transcardial perfusion with saline after anesthetization. The left hemispheres were fixed in 4% paraformaldehyde (pH 7.4) for 24 hours, followed by incubation with 30% sucrose for 24 hours, and coronal sections were cut at 30 μm thickness for histological analysis. The right hemispheres were snap frozen in liquid nitrogen and stored at −80°C for Western blots and real-time PCR.

2.7 Immunofluorescence

Tissue sections were washed with PBS, penetrated with 0.5% Triton-100 for 20 minutes, blocked with normal serum, and incubated with primary antibodies (detailed in the supplemental information) at 4°C overnight. After PBS washing, anti-rabbit 488 (1:1000; Beyotime Technology) and anti-mouse 555(1:1000; Beyotime Technology) were added at 37°C for two hours. Then, the sections were incubated with DAPI (1:200; Beyotime Technology) and mounted in antifading medium (Beyotime technology), and images were acquired by confocal microscopy.

2.8 Tracking Pg OMVs in the brain

The OMVs (100 μg/mice) and the same volume of PBS were labeled with DiO (Beyotime Company, China) for 20 minutes at 37°C, fetal bovine serum was used to neutralize excessive dye, ultracentrifugation at 150,000 × g for one hour at 4°C was used to recollect labeled Pg OMVs, and then mice were treated with Pg OMVs or PBS by oral gavage. After three days, the mice were killed by transcardial perfusion with saline, and the brains were fixed in 4% paraformaldehyde for 24 hours, followed by incubation with 30% sucrose for 24 hours, and coronal sections were cut at 50-μm thickness, stained with DAPI, and viewed by confocal microscopy.

2.9 Cellular experiment

BV2 microglia cells and mouse neuroblastoma cell line N2a (kindly gifted by Dr. Zhifang Dong from Children's Hospital of Chongqing Medical University) were maintained in high glucose Dulbecco's modified Eagle's medium (DMEM) supplemented with 10% fetal bovine serum, 100 units/ml penicillin, and 100 mg/ml streptomycin. For the vesicle uptake experiment, BV2 cells ($1.5*10^{4}$/well) were seeded on glass cover slides and cultured in 12-well plates overnight. Pg OMVs (10 μg/ml) and saline were stained with PKH26 (Merck, USA) and then were added to the cultures and incubated for 30 minutes. After fixing with 4% paraformaldehyde at room temperature for 10 minutes and penetration with 0.1% Triton-100 for 10 minutes, the nuclear

was stained with DAPI, and images were acquired by confocal microscopy. For BV2 and N2a stimulation experiments, the BV2 were stimulated with different concentrations of *Pg* OMVs, and 5 μg/ml was chosen for the rest of the *in vitro* experiments. BV2 were stimulated with Pg OMVs or pretreated with MCC950 (NLRP3 inhibitor; 20 μM; AbMole) for one hour. After six hours of Pg OMV stimulation, the medium was changed to fresh medium, and the BV2 conditioned medium was harvested 24 hours later. The N2a was treated with the BV2 conditioned medium and harvested 24 hours later.

2.10 Statistical analyses

Two-way repeated measures ANOVA was used for escape latency in MWM measurements. The statistical analyses were performed by Student's *t*-test and one-way ANOVA using the GraphPad Prism software package (GraphPad Software, California, USA). Data were expressed as means ± SEM, and a value of p <.05 was considered to indicate statistical significance.

3 Results

3.1 Characterization of Pg OMVs

Pg OMVs were characterized by TEM, which revealed that Pg OMVs are spherical bilayered cell portions (Figure 1A), and NTA showed the average diameter of Pg OMVs was 115.7 ± 4.1 nm (Figure 1B), which is the typical OMV diameter of Gram-negative bacteria. To analyze the protein contents of Pg OMVs,

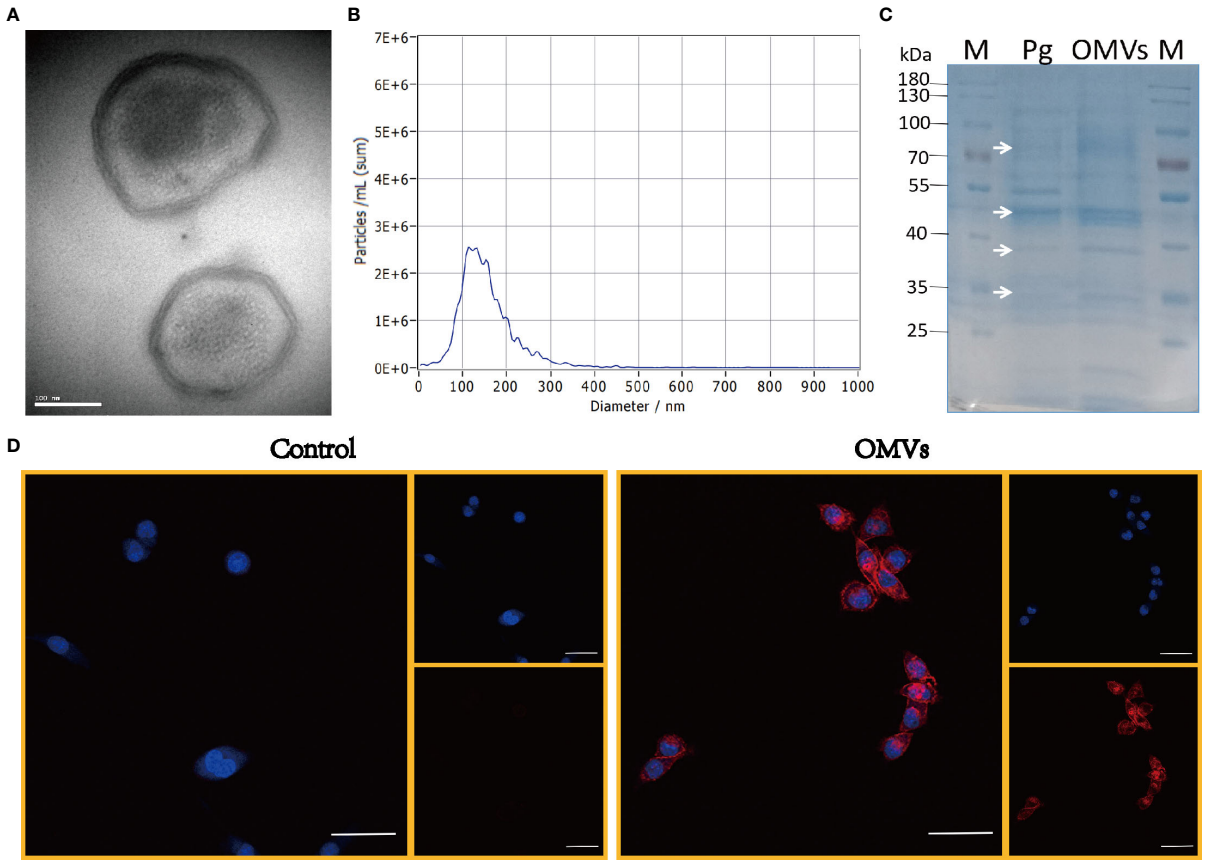

FIGURE 1
Characterization of Pg OMVs. **(A)** Pg OMVs observed by TEM. Scale bar = 100 nm. **(B)** NTA measured the diameter of Pg OMVs. **(C)** SDS-PAGE gel showed cargo proteins of Pg OMVs. White arrows indicate the bands in Pg OMVs samples (Pg OMVs) that correspond to Pg bacterial cell proteins (Pg). **(D)** Confocal images of Pg OMVs uptake by BV2 cells within 30 minutes, Nuclei (blue) were labeled with DAPI, Pg OMVs or PBS were labeled with PKH26 (red). Scale bar = 50 μm. TEM, transmission electron microscopy; NTA, nanoparticle-tracking analysis.

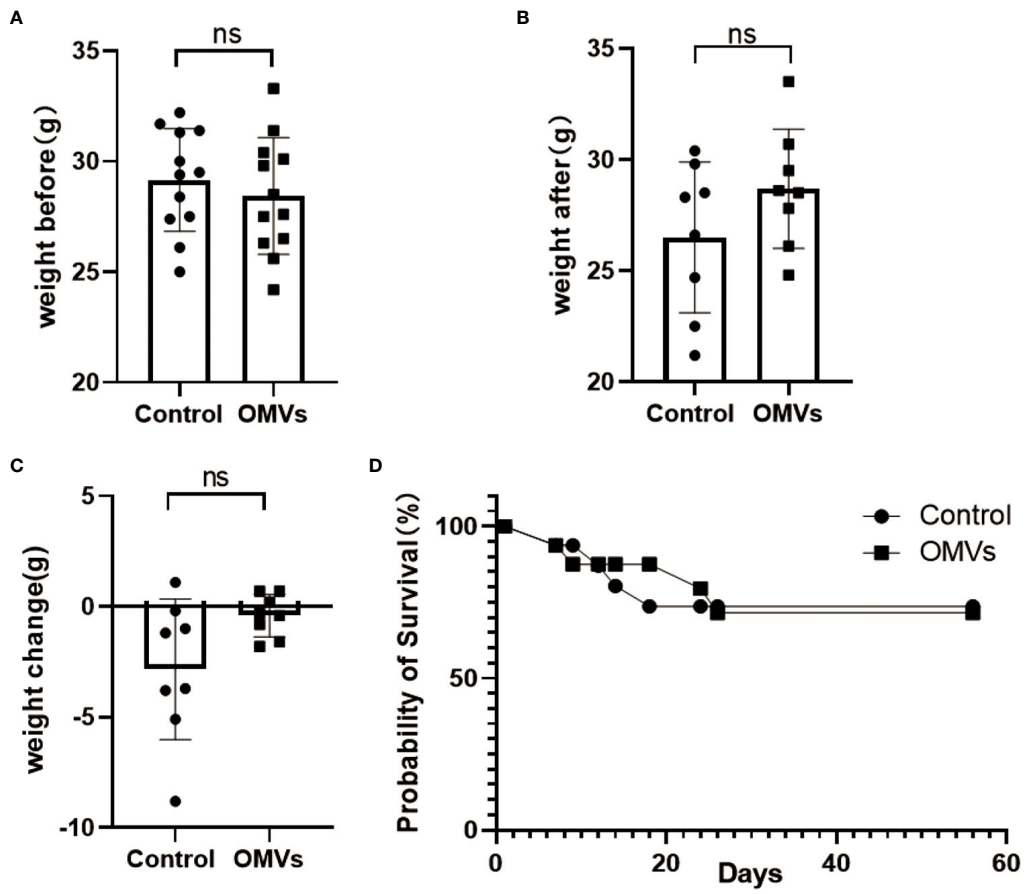

FIGURE 2
Pg OMVs did not affect body weight or survival rate. The mice were weighed before **(A)** and after **(B)** treatment, and the weight change **(C)** is shown. **(D)** Kaplan–Meier survival plots of mice. Data are presented as mean ± SEM. (ns: $P > .05$).

Pg OMVs and Pg fractions were separated by SDS-PAGE and visualized by Coomassie blue. We found that some Pg OMV protein bands corresponded to those of the Pg bacterial cell, suggesting that Pg proteins were present in the OMVs (Figure 1C). The Pg OMVs could be internalized by BV2 microglia cells within 30 minutes (Figure 1D).

3.2 Effect of Pg OMVs on body weight and survival

Twenty-four normal C57BL/6 mice, 14 months of age, were randomly divided into two groups: Pg OMVs and control. The mice were weighed before and after the eight-week treatment, and the results were analyzed. There was no significant difference in the weight change (Figures 2A–C) or survival rates (Figure 2D) among the two groups before and after treatment.

3.3 Pg OMVs cross blood–brain barrier of mice and decrease tight junction–related gene and protein expression in the hippocampus of mice

To determine whether Pg OMVs could cross the blood–brain barrier, Pg OMVs labeled with DiO were applied to mice by oral gavage, and labeled Pg OMVs were clearly detected in the hippocampus and cortex after three days (Figure 3). To test whether Pg OMVs changed BBB permeability, we performed Western blot analysis and RT-qPCR to detect tight junction–related protein and gene expression after eight weeks oral gavage. Claudin-5, ZO-1, and occludin are important proteins for the tight junctions between capillary endothelial cells. RT-qPCR showed that claudin-5, ZO-1, and occludin gene expression were decreased in the hippocampus of Pg OMV–treated mice (Figures 4A-C). The Western blot indicated that

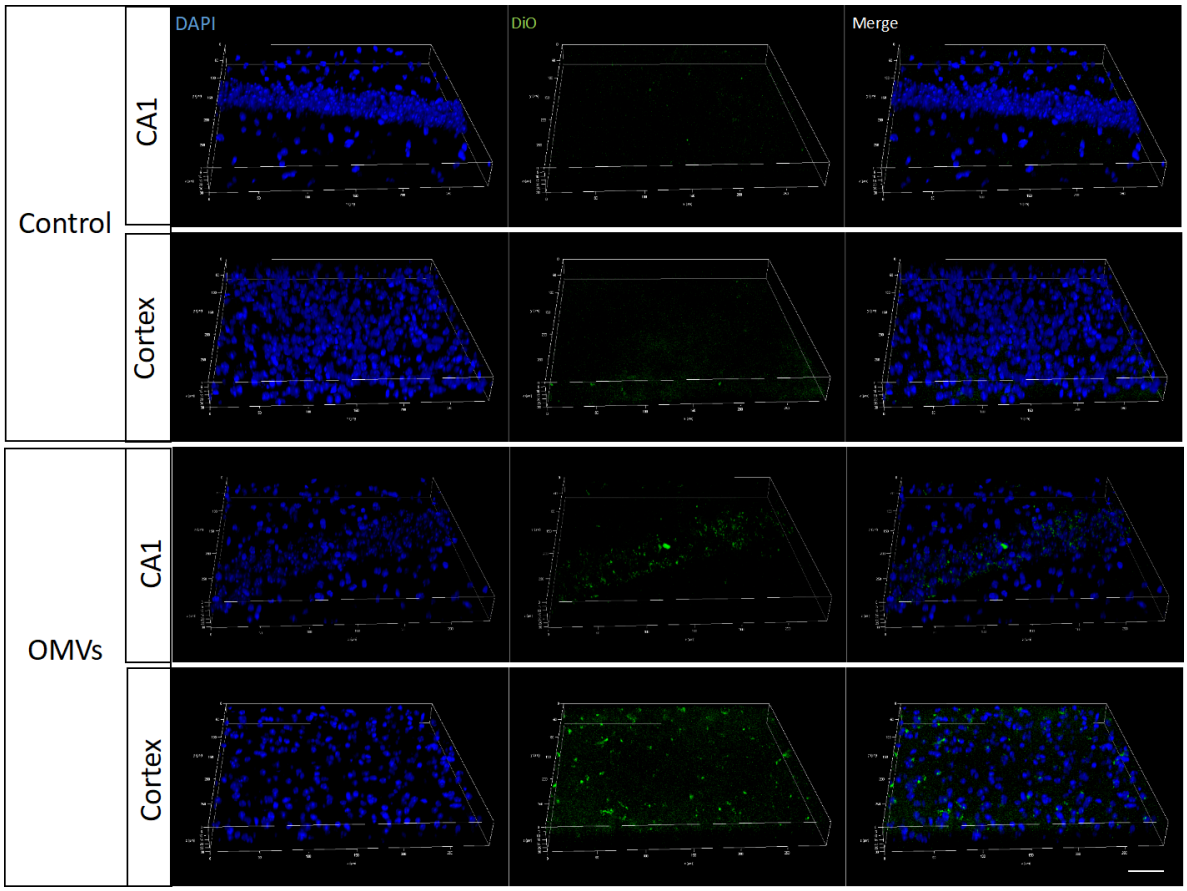

FIGURE 3
Pg OMVs enter the brain. Pg OMVs labeled with DiO (green) were applied by oral gavage for three days and were detected by confocal microscopy in the hippocampus and cortex of mice. Scale bar = 50 μm.

occludin was significantly decreased in the hippocampus of Pg OMV–treated mice (Figures 4D, E).

3.4 Oral gavage of Pg OMVs impairs learning and memory ability in mice

Sickness may reduce local motor activity, which may affect mouse behavior in the MWM and Y-maze tests. To exclude the effects of sickness symptoms on mouse behavior, the open field test was performed. In open field test, there was no significant difference in traveling distance or velocity between the two groups (Figures 5A, B), suggesting that Pg OMVs did not impair the locomotor activity of mice. To test whether Pg OMVs had an effect on memory and learning ability, we performed the MWM and Y-maze tests. In the MWM test, Pg OMVs impaired learning and spatial reference memory in mice as reflected by an increase in the escape latency in the five-day platform trial (Figure 5C). In the probe trial on the sixth day, the Pg OMV–treated mice showed worse memory consolidation as reflected by a lower number of platform area crossings and less time spent in the target quadrant compared with controls (Figures 5D, E) representative tracing graphs of Morris water maze on the sixth day were shown in Figures 5F, G. In the Y-maze test, the Pg OMV–treated mice showed a significantly decreased number of entries and time spent in the novel arm (Figures 5H–K).

3.5 Oral gavage of Pg OMVs increases tau phosphorylation in the brain of mice

Tau phosphorylation is one of the hallmark pathologies in AD and is closely related to memory consolidation. Immunofluorescent images showed that the Thr231-site

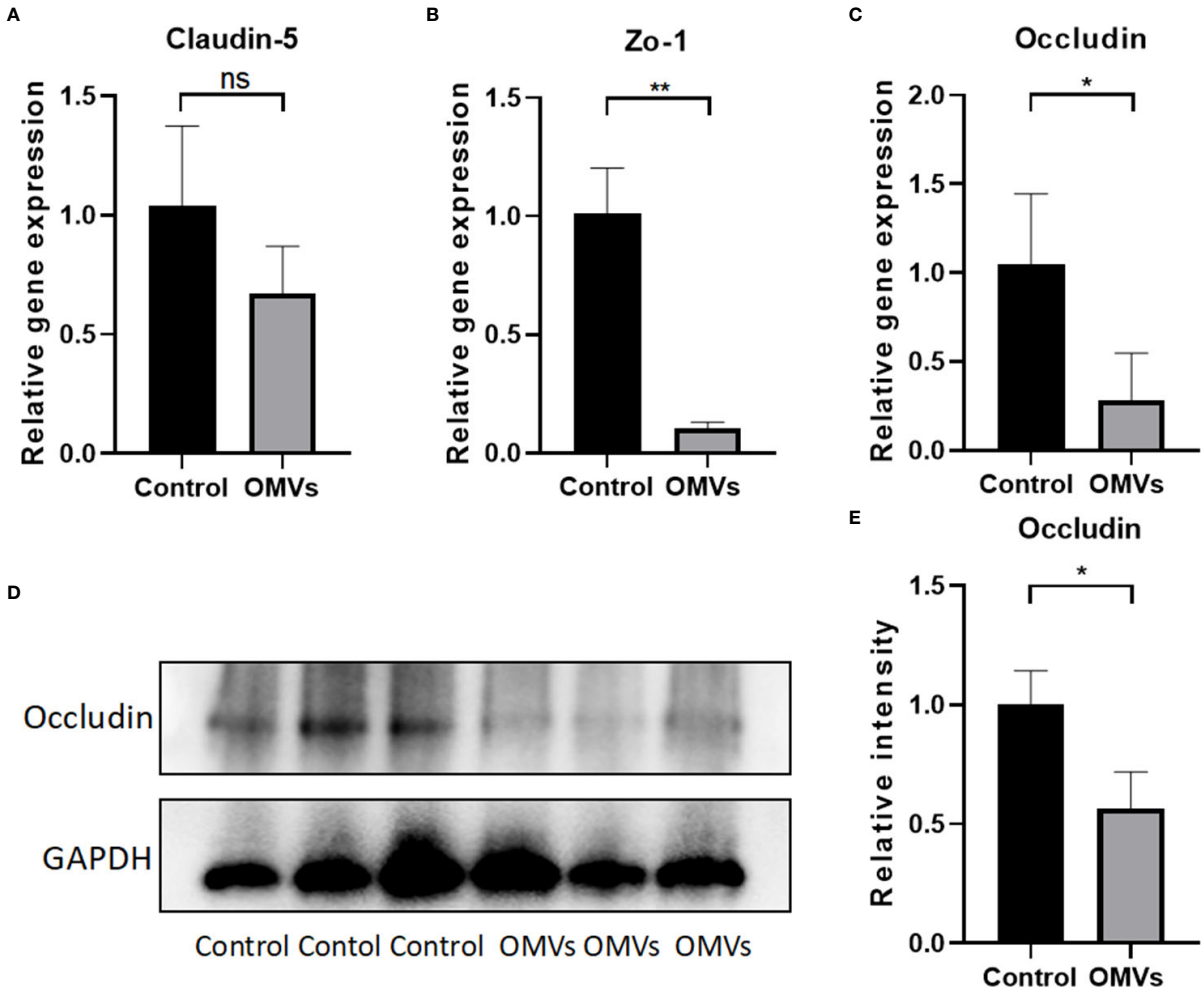

FIGURE 4
Oral gavage of Pg OMVs decreases tight junction–related gene and protein expression in the brain. **(A–C)** Gene expression of claudin-5, occluding, and zo-1 in the brain. **(D)** Occludin protein expression was measured by Western blot analysis. **(E)** The quantitative analysis of occludin immunoblots in (D). Values are expressed as the mean ± SEM. OMVs, outer membrane vesicle; SEM, standard error of the mean. (n = 3, ns: P >.05, *p <.05, **p <.01).

phosphorylation in the hippocampus was significantly increased in the experimental group (Figures 6A, B), and the mean degree of tau phosphorylation on the Thr231 site was increased significantly in the hippocampus of mice in the experimental group (Figures 6C, D).

3.6 Oral gavage of Pg OMVs induces neuroinflammation

To clarify whether Pg OMVs could induce neuroinflammation, we detected microglia, astrocytes, and IL-1β by immunofluorescence. Microglia are resident macrophage-like cells in the brain, which would be overactivated and release proinflammatory cytokines in response to microbial infection. The immunofluorescent images showed that a number of Iba1-positive microglia were significantly increased in the experimental group (Figures 7A, B). Astrocytes are known to function in biochemical support of endothelial cells that form the BBB. An increased number of astrocytes can be induced by infection. We then examined whether astrocytes in the hippocampus were activated by using a GFAP antibody. There was a significantly higher number of astrocytes in the experimental group compared with controls (Figures 7A, C). IL-1β played a central role in neuroinflammation, and the number of IL-1β positive cells were significantly increased in the experimental group (Figures 7A, D).

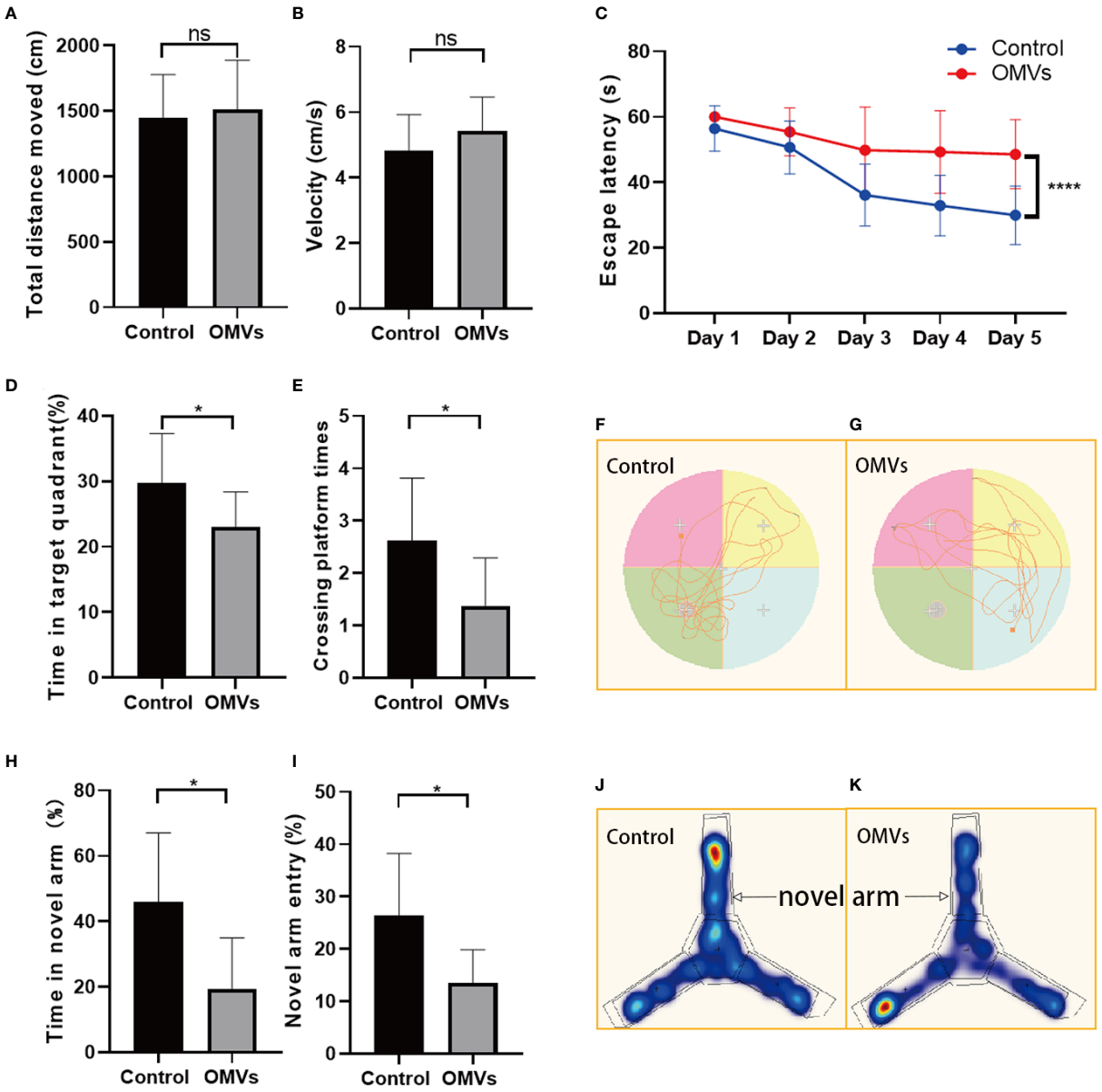

FIGURE 5
Oral gavage of Pg OMVs impairs memory and spatial learning of mice. **(A, B)** Distance and velocity traveled in the open-field test. **(C)** Latency to find the platform during the acquisition phase of the MWM test. **(D, E)** Crossing platform times and time in the target quadrant on the sixth day when the platform was removed. **(F, G)** Representative tracing graphs of Morris water maze on the sixth day. **(H, I)** Novel arm entry and time spent in the novel arm in the Y-maze test. **(J, K)** Representative hot spot graphs. (n = 8, ns: P >.05, *p <.05, ****p <.0001).

3.7 Oral gavage of Pg OMVs activates the NLRP3 inflammasome in the hippocampus of mice

Since the NLRP3 inflammasome is reported to drive microglia activation and tau pathology (Ising et al., 2019; Lempriere, 2020), we next explored whether the NLRP3 inflammasome was activated. Proteins of NLRP3, ASC, and caspase-1 were elevated significantly in the hippocampus of the experimental group (Figures 8A–D). Immunofluorescence double staining showed that ASC co-localized mainly with microglia (Figure 8E; Figures S1, 2). Immunofluorescent

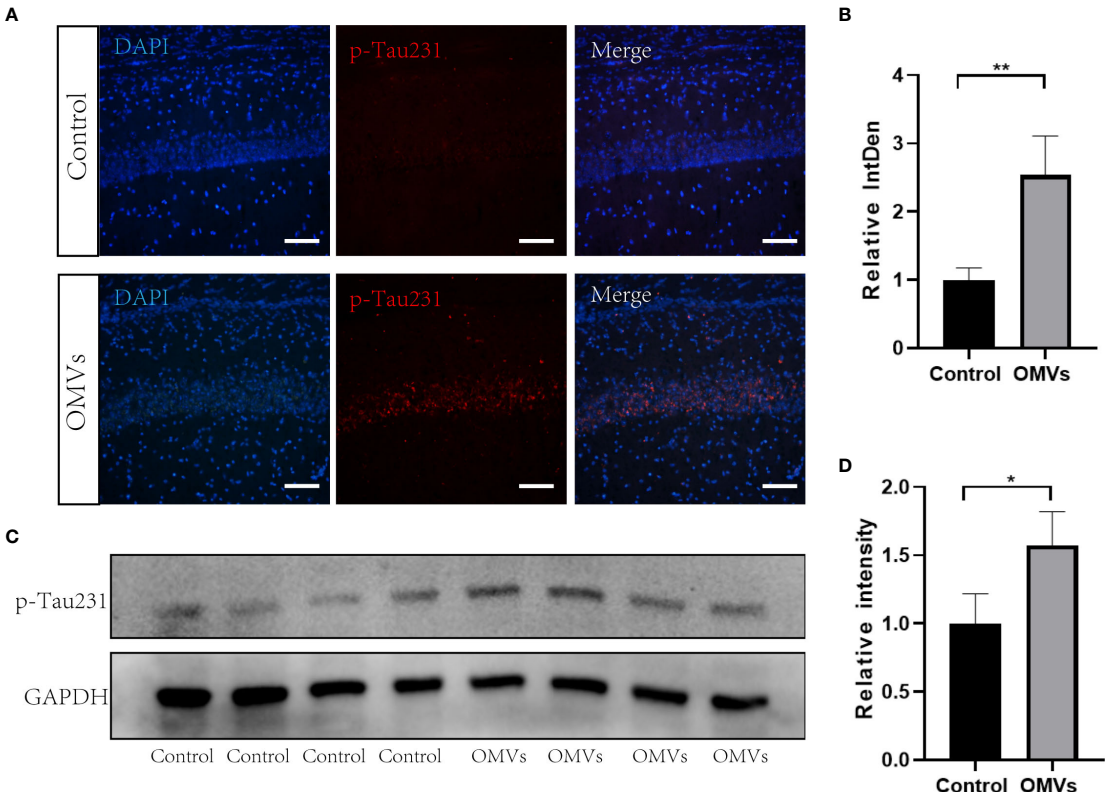

FIGURE 6
Oral gavage of Pg OMVs increases tau phosphorylation in the hippocampus of mice. **(A)** Immunofluorescent images of p-Tau231 (red) in the hippocampus of mice. Scale bar = 50 μm. **(B)** Mean relative fluorescence intensity (relative integrated density) of p-Tau231 in image **(A)** (n = 3, $^{**}p$ <.01, Student's t-test). **(C)** The Western blots showing p-Tau231 in the hippocampus of mice. **(D)** The quantitative analyses of the ratio of p-Tau231 immunoblots in the image **(C)** (n = 4, $^{*}p$ <.05).

images showed that the fluorescent intensity of ASC and NLRP3 were significantly increased in the experimental group in the hippocampus (Figures 8F–H), and intracellular and extracellular ASC specks were significantly increased in the experimental group (Figures 8I–K).

3.8 Pg OMVs activate the NLRP3 inflammasome in cultured microglia and contributes to tau hyperphosphorylation in cultured neurons

To test whether Pg OMVs activate the NLRP3 inflammasome and promote tau phosphorylation *in vitro*, we first measured extracellular ASC specks of BV2 cells with Pg OMV stimulation. The result showed that the extracellular ASC specks increased in a Pg OMV–dosage manner (Figures 9A, B), the 5 μg/ml dosage of Pg OMVs was chosen in the rest of the *in vitro* experiments. The expression of NLRP3 was increased with Pg OMV stimulation and decreased when pretreated with the NLRP3 inhibitor MCC950 (Figures 9C, D). To clarify whether the effects of Pg OMVs on tau phosphorylation in neurons are exerted indirectly *via* microglial activation, we treated N2a neurons with microglia-conditioned medium (MCM). Compared with MCM from control, a significantly increased mean degree of phosphorylated tau at Thr231 (Figures 10A–C) was observed in the N2a neurons following incubation with MCM stimulated by Pg OMVs. In contrast, the expression of phosphorylated tau at Thr231 was significantly decreased in the N2a neurons following incubation with NLRP3 inhibitor–pretreated and Pg OMV–treated MCM.

4 Discussion

The present study indicates that chronic infection by oral gavage of Pg OMVs induced AD-like phenotypes, including learning and memory deficiency, microglia-mediated neuroinflammation, and intracellular tau phosphorylation.

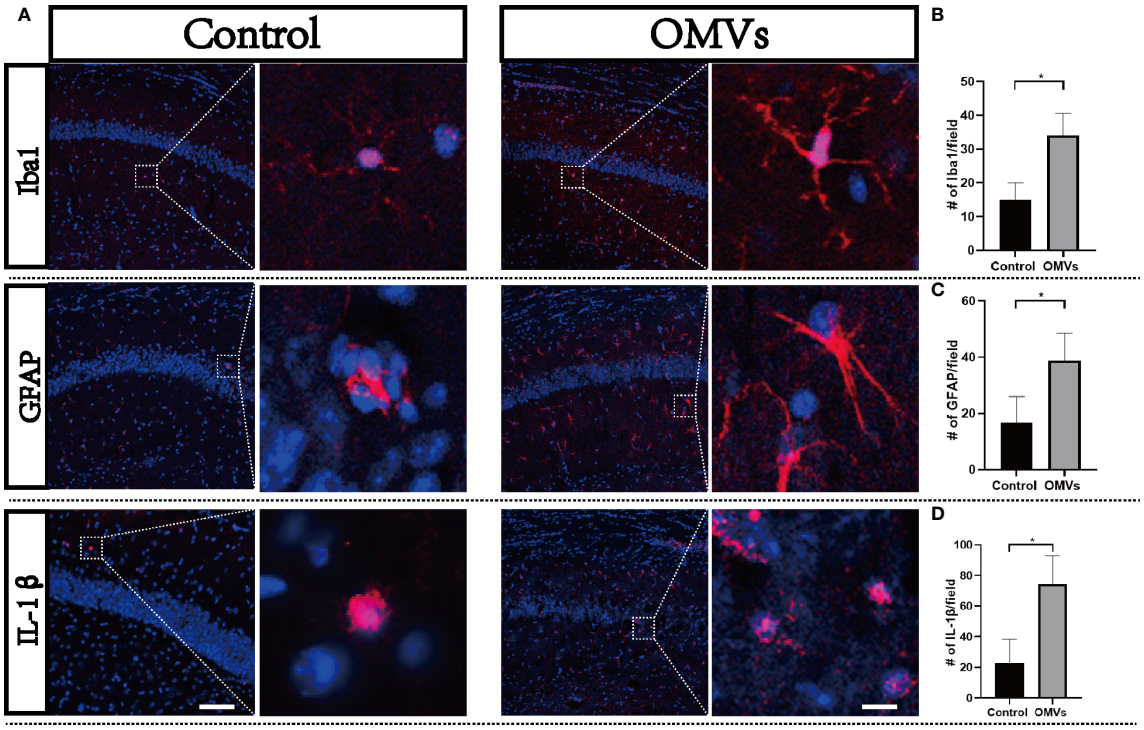

FIGURE 7
Oral gavage of Pg OMVs induces neuroinflammation. **(A)** Activation of microglia (Iba1 marker, red) and astrocytes (GFAP marker, red) and expression of IL-1β (red) in the hippocampus of mice. Scale bar left = 50 µm, scale bar right = 5 µm. **(B)** Number of microglia (Iba1 positive) counted in the hippocampus from five slides for each mouse and are means ± SEM; *n* = 3 mice/group. **(C)** Number of astrocytes (GFAP positive) in the hippocampus counted from five slides for each mouse and are means ± SEM; *n* = 3 mice/group. **(D)** Number of IL-1βpositive cells in the hippocampus counted from five slides for each mouse and are means ± SEM; *n* = 3 mice/group. **p* <.05.

NLRP3 inflammasome activation is involved in this process. To the best of our knowledge, this study, for the first time, demonstrates the relationship between Pg OMVs and AD-like phenotypes.

There are studies showing Pg LPS (Poole et al., 2013) and Pg DNA (Emery et al., 2017; Dominy et al., 2019) in autopsy specimens from brains of AD patients. Gingipains, the toxic protease of Pg, was also detected in the brain of AD patients, and levels correlated with tau pathology (Dominy et al., 2019). *In vivo* studies identified gingipains in the neuron, microglia, and astrocytes after oral application of Pg for 22 weeks in mice (Ilievski et al., 2018). However, none of these studies recovered Pg in the brains of AD patients or in the brains of mice, leaving the question of whether live Pg or just its virulence factors entered the brain. We focused on Pg OMVs because Pg OMVs contain LPS, DNA, and gingipains that were detected in the brain of AD patients. Compared with Pg, Pg OMVs have advantages to enter the brain. First, they are greater in quantity. The number of Pg OMVs is about 2000 times of the number of Pg (Fleetwood et al., 2017). Second, they are smaller in size; the diameter of Pg OMVs is about 80 nm on average, whereas the diameter of Pg is about 600 nm (Gui et al., 2016), which is seven times larger than that of Pg OMVs. Third, Pg OMVs contain gingipains and LPS, which are reported to cause pathological changes related to AD. Compared with the same protein amount of Pg, Pg OMVs are reported to contain three to five times the gingipains compared with that of Pg (Mantri et al., 2015). Last but not least, Pg OMVs invade epithelial cells more efficiently than Pg (Ho et al., 2015). Thus, we speculate that Pg OMVs are important virulence factors of Pg in the relationship between Pg and AD.

The first question is whether Pg OMVs can cross the BBB and enter the brain. We detected Pg OMVs in the cortex and hippocampus of mice three days after oral gavage. This is in agreement with Lee et al. In their study, five days after oral gavage of extracellular vesicles of Paenalcaligenes hominis, a member of the *Proteobacteria* in the gut, the extracellular vesicles could be detected in the hippocampus of mice, and

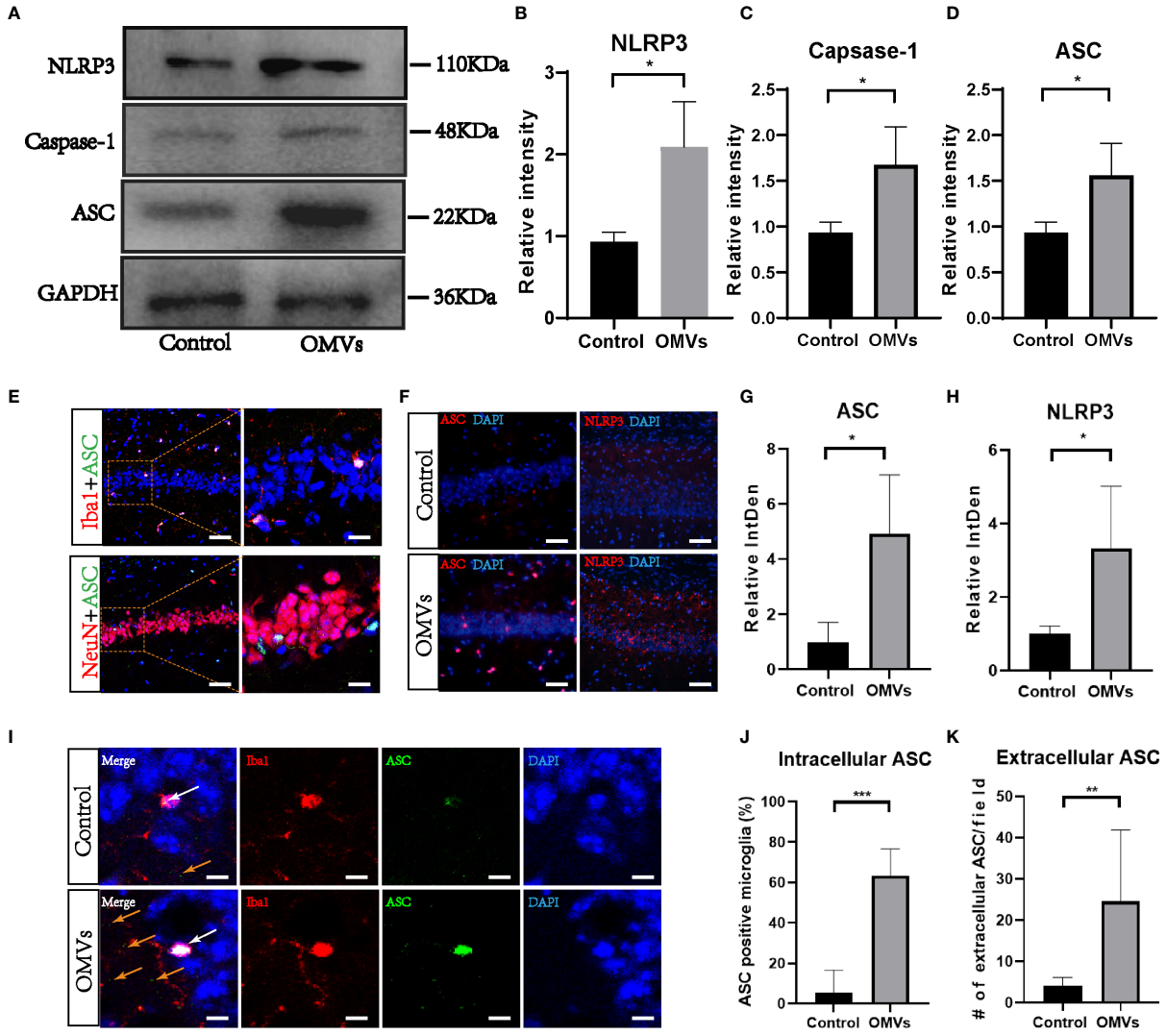

FIGURE 8
Oral gavage of Pg OMVs triggers NLRP3 inflammasome in the hippocampus of mice. **(A)** The Western blots showed NLRP3, caspase-1, and ASC in the hippocampus of mice. **(B–D)** The quantitative analyses of immunoblots in image **(A)** (n = 3, *p <.05). **(E)** Co-localization of ASC with neuronal cell marker (NeuN) and microglia marker (Iba1) revealed expression of ASC in microglia but not in neurons, scale bar left = 50 μm, scale bar right = 20 μm. **(F)** Immunofluorescent images showed ASC (red) and NLRP3 (red) expression in hippocampus of mice, scale bar = 50 μm. **(G, H)** The quantitative analyses of immunoblots in image **(F)** (n = 3, *p <.05) **(I)** Immunofluorescent images showed intracellular ASC (white arrow) and extracellular ASC (yellow arrows) in hippocampus of mice. Scale bar = 5 μm. **(J)** The percentage of intracellular ASC positive microglia in hippocampus of mice, counted from five slides per mouse and expressed as means ± SEM; n = 4 mice/group. (n = 4, ***p <.001) **(K)** Number of extracellular ASC per field in hippocampus of mice. (n = 4, **p <.01).

vagotomy inhibited the accumulation of Paenalcaligenes hominis extracellular vesicles in the hippocampus (Lee et al., 2020). OMVs of *Aggregatibacter actinomycetemcomitans*, a well-known periodontal pathogen, can cross BBB and be detected in the brain 24 hours after cardiac injection (Han et al., 2019) or intravenous injection (Ha et al., 2020). OMVs of gut microbiota could be detected in the hippocampus 12 hours after intravenous injection (Wei et al., 2020). Bittel et al. found that OMVs of *Escherichia coli* could be detected in the brain after oral gavage of *Escherichia coli*, but *Escherichia coli* could not be detected in the brain. This is the first proof-of-principle study visualizing that OMVs, but not the parental bacteria could transport to the brain from the gut (Bittel et al., 2021).

The BBB forms an effective barrier between the central nervous system and the blood to maintain homeostasis of the brain microenvironment (Keaney and Campbell, 2015). A

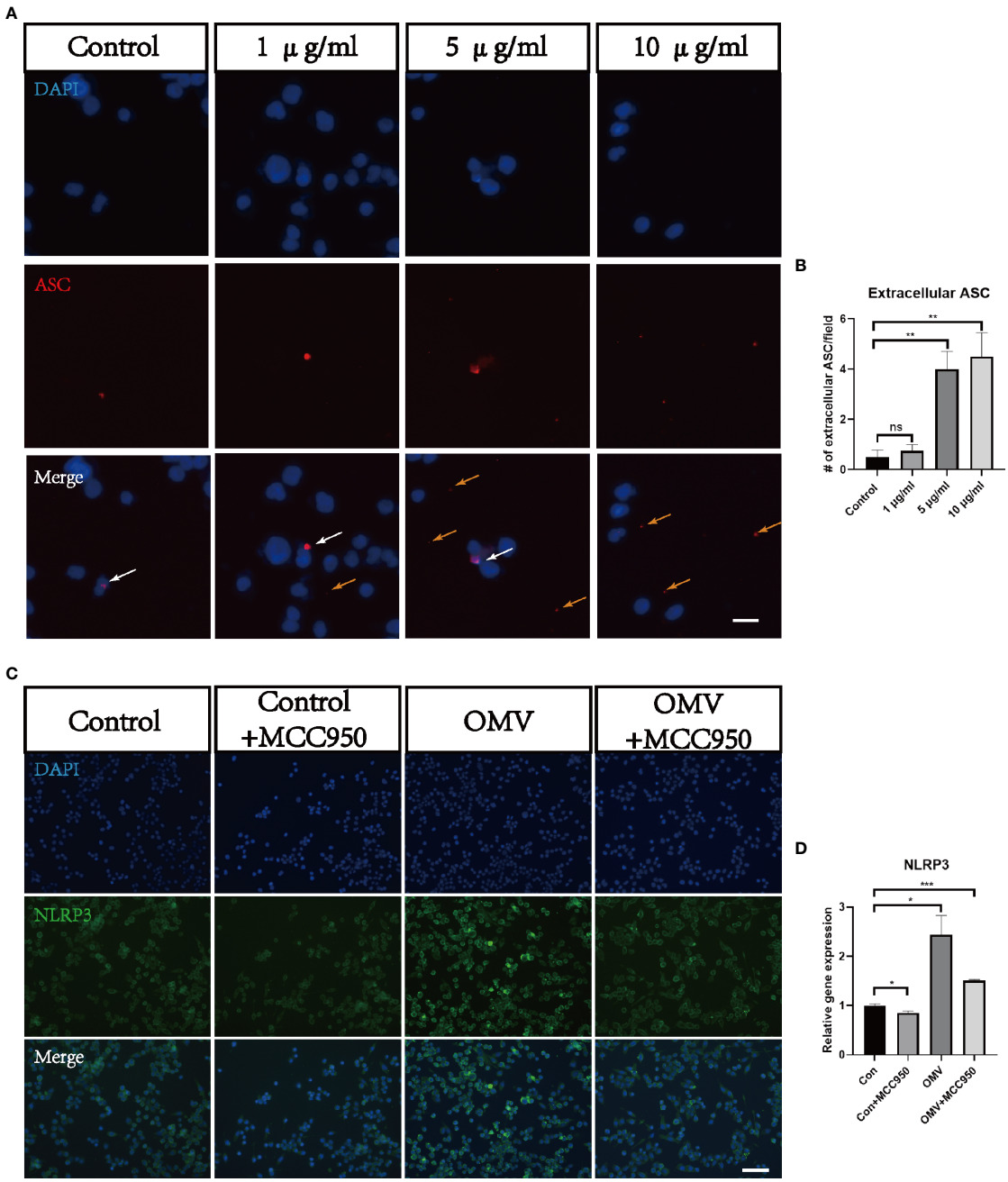

FIGURE 9
Pg OMVs triggers NLRP3 inflammasome in microglia *in vitro*. **(A)** Immunofluorescent images showed intracellular ASC (white arrow) and extracellular ASC (yellow arrows) of BV2 cells stimulated with different concentrations of Pg OMVs. Scale bar = 10 μm. **(B)** Number of extracellular ASC per field. (n =4, ns, not significant, $^{**}p$ <.01). **(C)** Immunofluorescent images showed NLRP3 staining of BV2 cells stimulated by Pg OMVs. MCC950 (20 μM) were used for pretreatment for one hour. **(D)** The mRNA expression of NLRP3 in BV2 cells stimulated by Pg OMVs. MCC950 (20 μM) were used for pretreatment for one hour. (n=3, *p <0.05).

correlation between BBB dysfunction and tau pathology is reported (Cai et al., 2018). Tight junctions, consisting of cytoplasmic proteins (ZOs), transmembrane proteins (occludin and claudins), and cytoskeleton proteins, play a critical role in maintaining the integrity and permeability of the BBB (Zihni et al., 2016). We found that Pg OMVs decreased ZO-1 and occludin gene expression and also decreased occludin protein expression, suggesting that Pg OMVs caused disruption of the

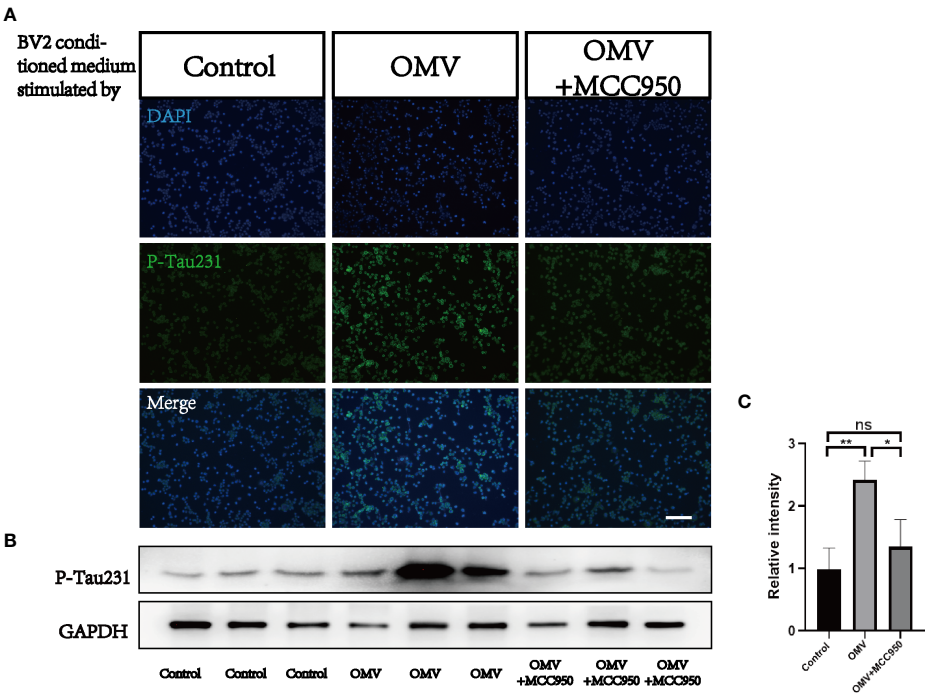

FIGURE 10
Microglia-conditioned medium (MCM) stimulated by Pg OMVs contributes to tau hyperphosphorylation in cultured neurons. **(A)** Immunofluorescent images of P-Tau231 in N2a cells treated with MCM from control, Pg OMV–primed MCM, or Pg OMV–primed MCM pretreated with NLRP3 inhibitor for 24 hours. **(B)** The Western blot images of P-Tau231 in N2a cells treated with MCM from control, Pg OMV–primed MCM, or Pg OMV–primed MCM pretreated with NLRP3 inhibitor for 24 hours, samples from three independent experiments are shown. **(C)** The quantitative analyses of immunoblots in image **(B)** (n = 3, *p <.05, **p <.01). (ns: p >.05).

BBB, which would facilitate Pg OMVs and other harmful compounds in the blood to enter the brain. OMVs of gut microbiota were also reported to decrease tight junctions of the BBB (Wei et al., 2020). *In vitro*, Pg OMVs could induce degradation of ZO-1 and occludin in human cerebral microvascular endothelial cell lines, and gingipains in Pg OMVs played a critical role in tight junction degradation (Nonaka et al., 2022).

In our study, chronic oral gavage of Pg OMVs did not influence body weight or locomotion, suggesting that Pg OMV–induced learning and memory impairment was not associated with sickness behaviors. Tau pathology is closely linked to learning and memory functions in AD pathology (van der Kant et al., 2020). Tau phosphorylation on the Thr231 site is shown to be significantly increased in the early stage of AD (Neddens et al., 2018). We show that Pg OMVs could increase tau phosphorylation on the Thr231 site in the hippocampus of mice, which may be caused by gingipains of Pg OMVs. The abundance of gingipains correlates with the tau protein load in AD brain autopsies (Dominy et al., 2019), and gingipains can cleave tau *in vitro* (Dominy et al., 2019), an activity that might contribute to aberrant tau phosphorylation and accumulation of insoluble tau forms in AD (Kovacech and Novak, 2010). Other studies also demonstrate that Pg or Pg LPS can elevate tau phosphorylation. Tang et al. intravenously injected Pg for 12 weeks and found that tau phosphorylation on the Thr231 and Thr181 sites were increased in the hippocampus of rats (Tang et al., 2021), and Jiang et al. peritoneally injected Pg LPS for three weeks in $APP^{NL\text{-}F/NL\text{-}F}$ mice and found that tau phosphorylation on the Ser202, Thr231, and Ser396 sites were elevated in the cortex of mice (Jiang et al., 2021). Ilievski et al. orally applied Pg for 22 weeks in mice and detected that tau phosphorylation on the Ser396 site was increased in the hippocampus of mice (Ilievski et al., 2018).

Microglia-mediated neuroinflammation is a key factor involved in regulating AD pathogenesis, and IL-1β is associated with the progression and onset of AD (Alvarez et al., 1996; Oprica et al., 2007; Deniz-Naranjo et al., 2008). Since Pg OMVs could activate the NLRP3 inflammasome and induce IL-1β in macrophages (Cecil et al., 2017), we speculate

that NLRP3 inflammasome activation is involved in the process. We found that NLRP3 and ASC were significantly elevated in the hippocampus of mice. ASC mainly co-localized with microglia, and few co-localized with neurons (Figure S1), which is in accordance with other studies (Lei et al., 2017; Reimers et al., 2021). ASC specks were reported to be principally in the nuclei of microglia with a small amount in microglia processes (Reimers et al., 2021). Since inflammasome activation results in the activation of highly pro-inflammatory cytokines and the death of the activated cell, ASCs specks could be found in the extracellular space after cell death. In fact, extracellular ASC specks were reported to have prionoid activities and further promote IL-1β maturation (Franklin et al., 2014). We found that both intracellular and extracellular ASC specks were increased in the experimental group, which suggested an inflammatory state. Overexpression of IL-1β exacerbates tau phosphorylation and tangle formation (Sheng et al., 2000; Kitazawa et al., 2011), which affects synaptic plasticity, inhibiting long-term potentiation and, subsequently, learning and memory (Pickering and O'Connor, 2007).

Oral gavage of Pg OMVs was applied in this study. Ding et al. applied Pg by oral gavage to middle-aged mice and induced AD-like pathologies (Ding et al., 2018). We speculate that oral gavage of Pg OMVs would change gastrointestinal microbiota and, thus, indirectly influence AD-like pathologies since gastrointestinal microbiota were reported to be related to AD (Pistollato et al., 2016, Doulberis et al., 2019, Papaefthymiou et al., 2019, Giovannini et al., 2021). In fact, according to a quantitative analysis, it was estimated that patients with severe periodontitis swallowed approximately 10^{12}~10^{13} Pg per day (Boutaga et al., 2007; Saygun et al., 2011; He et al., 2012), oral gavage of Pg once or for five weeks in mice have been reported to change gut microbiota with Bacteroidetes increased and Firmicutes decreased, indicating an inflammatory state (Nakajima et al., 2015; Kato et al., 2018). Ligature-induced periodontitis is reported to change gut microbiota and associated with memory decline in mice, and tight junctions of the gut and brain were decreased (Xue et al., 2020).

The current study is beset with certain limitations. First, the dosage and duration of Pg OMVs treatment should be investigated in further study. Second, oral gavage of Pg OMVs may not fully simulate the pathology of periodontitis. Last, the effect of Pg OMVs compared with Pg in inducing AD-like pathology is not explored in this study. Our group is conducting relevant studies now to further deduce the effect of Pg OMVs in Pg related to AD. However, this study is a novel attempt, and we believe that OMVs are important weapon of bacteria and expect the current study to draw readers' attention to OMVs.

In conclusion, we reveal for the first time that Pg OMVs promote the activation of astrocytes and microglia, activate NLRP3 inflammasome, elevate IL-1β and tau phosphorylation, which further impairs the cognitive function (Figure 11).

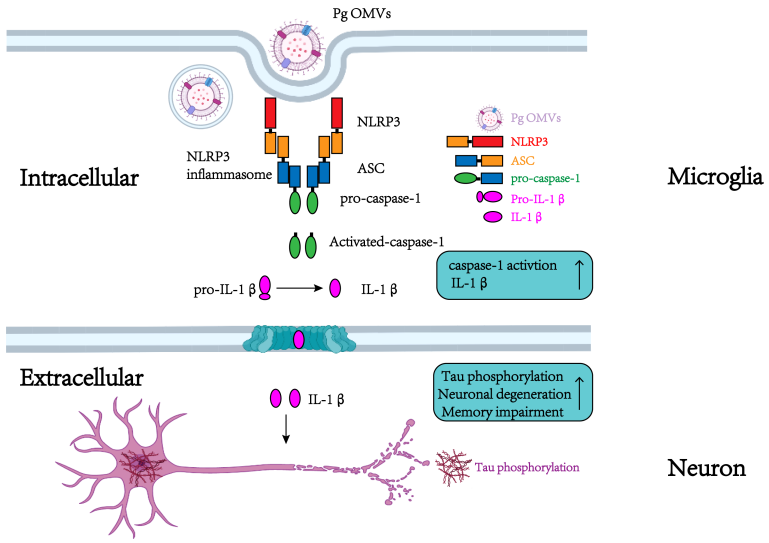

FIGURE 11
Schematic to show the roles of Pg OMVs on microglia and neurons. In microglia, Pg OMV induce IL-1β production though the activation of the NLRP3 inflammasome. In neurons, the microglia-released IL-1β is involved in tau phosphorylation, neuronal degeneration, and memory impairment. Created with BioRender.com.

Data availability statement

The original contributions presented in the study are included in the article/Supplementary Files, further inquiries can be directed to the corresponding author/s.

Ethics statement

The animal study was reviewed and approved by the Institutional Animal Care and Use Committee of the Stomatological Hospital of Chongqing Medical University.

Author contributions

TG wrote the main manuscript text. DY critically revised Manuscript. TG, QC, HM, YZ, HR, MX and HC performed the research. TG, QC, HM, YZ, HR, MX, HC and DY analyzed the data. TG and DY designed the main research study and provided the necessary guidance on the performance of all the experiment. TG, HC and DY contributed the essential reagents or tools. All authors read and approved the final manuscript.

Funding

This work was sponsored by Program for Youth Innovation in Future Medicine, Chongqing Medical University (No.W0060 to DY), Program for Top talent Distinguished Professor from Chongqing Medical university (No.[2021]215 to DY), Natural Science Foundation of Chongqing, China (No.cstc2021jcyj-bshX0176 to TG), Chongqing Special Postdoctoral Science Foundation (No. 2010010005994583 to HC).

Conflict of interest

The authors declare that the research was conducted in the absence of any commercial or financial relationships that could be construed as a potential conflict of interest.

Publisher's note

All claims expressed in this article are solely those of the authors and do not necessarily represent those of their affiliated organizations, or those of the publisher, the editors and the reviewers. Any product that may be evaluated in this article, or claim that may be made by its manufacturer, is not guaranteed or endorsed by the publisher.

Supplementary material

The Supplementary Material for this article can be found online at: https://www.frontiersin.org/articles/10.3389/fcimb.2022.925435/full#supplementary-material

References

Alvarez, X. A., Franco, A., Fernandez-Novoa, L., and Cacabelos, R. (1996). Blood levels of histamine, IL-1 beta, and TNF-alpha in patients with mild to moderate Alzheimer disease. *Mol. Chem. Neuropathol.* 29, 2-3, 237–252. doi: 10.1007/BF02815005

Amano, A., Takeuchi, H., and Furuta, N. (2010). Outer membrane vesicles function as offensive weapons in host-parasite interactions. *Microbes Infect.* 12, 791–798. doi: 10.1016/j.micinf.2010.05.008

Beyer, M. M. S., Lonnemann, N., Remus, A., Latz, E., Heneka, M. T., and Korte, M. (2020). Enduring changes in neuronal function upon systemic inflammation are NLRP3 inflammasome dependent. *J. Neurosci.* 40, 5480–5494. doi: 10.1523/JNEUROSCI.0200-20.2020

Bittel, M., Reichert, P., Sarfati, I., Dressel, A., Leikam, S., Uderhardt, S., et al. (2021). Visualizing transfer of microbial biomolecules by outer membrane vesicles in microbe-host-communication *in vivo*. *J. Extracell Vesicles.* 10, e12159. doi: 10.1002/jev2.12159

Boutaga, K., Savelkoul, P. H., Winkel, E. G., and van Winkelhoff, A. J. (2007). Comparison of subgingival bacterial sampling with oral lavage for detection and quantification of periodontal pathogens by real-time polymerase chain reaction. *J. Periodontol.* 78, 9–86. doi: 10.1902/jop.2007.060078

Braak, H., and Braak, E. (1991). Neuropathological stageing of Alzheimer-related changes. *Acta Neuropathol.* 82, 239–259. doi: 10.1007/BF00308809

Cai, Z., Qiao, P. F., Wan, C. Q., Cai, M., Zhou, N. K., and Li, Q. (2018). Role of blood-brain barrier in alzheimer's disease. *J. Alzheimers Dis.* 63, 1223–1234. doi: 10.3233/JAD-180098

Cecil, J. D., O'Brien-Simpson, N. M., Lenzo, J. C., Holden, J. A., Singleton, W., Perez-Gonzalez, A., et al. (2017). Outer membrane vesicles prime and activate macrophage inflammasomes and cytokine secretion *In vitro* and *In vivo*. *Front. Immunol.* 8. doi: 10.3389/fimmu.2017.01017

Chi, L., Cheng, X., Lin, L., Yang, T., Sun, J., Feng, Y., et al. (2021). *Porphyromonas gingivalis* induced cognitive impairment is associated with gut dysbiosis, neuroinflammation, and glymphatic dysfunction. *Front. Cell Infect. Microbiol.* 11. doi: 10.3389/fcimb.2021.755925

Darveau, R. P., Hajishengallis, G., and Curtis, M. A. (2012). *Porphyromonas gingivalis* as a potential community activist for disease. *J. Dent. Res.* 91,9, 816–820. doi: 10.1177/0022034512453589

Deniz-Naranjo, M. C., Munoz-Fernandez, C., Alemany-Rodriguez, M. J., Perez-Vieitez, M. C., Aladro-Benito, Y., Irurita-Latasa, J., et al. (2008). Cytokine IL-1 beta but not IL-1 alpha promoter polymorphism is associated with Alzheimer disease in a population from the canary islands, Spain. *Eur. J. Neurol.* 15, 1080–1084. doi: 10.1111/j.1468-1331.2008.02252.x

Ding, Y., Ren, J., Yu, H., Yu, W., and Zhou, Y. (2018). *Porphyromonas gingivalis*, a periodontitis causing bacterium, induces memory impairment and age-dependent neuroinflammation in mice. *Immun. Ageing.* 15, 6. doi: 10.1186/s12979-017-0110-7

Dominy, S. S., Lynch, C., Ermini, F., Benedyk, M., Marczyk, A., Konradi, A., et al. (2019). *Porphyromonas gingivalis* in alzheimer's disease brains: Evidence for disease causation and treatment with small-molecule inhibitors. *Sci. Adv.* 5, eaau3333. doi: 10.1126/sciadv.aau3333

Doulberis, M., Papaefthymiou, A., Polyzos, S. A., Boziki, M., Deretzi, G., Giartza-Taxidou, E., et al. (2019). Microbes and alzheimer' disease: lessons from h. pylori and GUT microbiota. *Eur. Rev. Med. Pharmacol. Sci.* 23, 1845–1846. doi: 10.26355/eurrev_201903_17218

Emery, D. C., Shoemark, D. K., Batstone, T. E., Waterfall, C. M., Coghill, J. A., Cerajewska, T. L., et al. (2017). 16S rRNA next generation sequencing analysis shows bacteria in alzheimer's post-mortem brain. *Front. Aging Neurosci.* 9. doi: 10.3389/fnagi.2017.00195

Fleetwood, A. J., Lee, M. K. S., Singleton, W., Achuthan, A., Lee, M. C., O'Brien-Simpson, N. M., et al. (2017). Metabolic remodeling, inflammasome activation, and pyroptosis in macrophages stimulated by *Porphyromonas gingivalis* and its outer membrane vesicles. *Front. Cell Infect. Microbiol.* 7. doi: 10.3389/fcimb.2017.00351

Franklin, B. S., Bossaller, L., De Nardo, D., Ratter, J. M., Stutz, A., Engels, G., et al. (2014). The adaptor ASC has extracellular and 'prionoid' activities that propagate inflammation. *Nat. Immunol.* 15, 727–737. doi: 10.1038/ni.2913

Giovannini, M. G., Lana, D., Traini, C., and Vannucchi, M. G. (2021). The microbiota-Gut-Brain axis and Alzheimer disease. from dysbiosis to neurodegeneration: Focus on the central nervous system glial cells. *J. Clin. Med.* 10, 2358. doi: 10.3390/jcm10112358

Griffin, W. S., Nicoll, J. A., Grimaldi, L. M., Sheng, J. G., and Mrak, R. E. (2000). The pervasiveness of interleukin-1 in alzheimer pathogenesis: a role for specific polymorphisms in disease risk. *Exp. Gerontol.* 35, 481–487. doi: 10.1016/s0531-5565(00)00110-8

Gui, M. J., Dashper, S. G., Slakeski, N., Chen, Y. Y., and Reynolds, E. C. (2016). Spheres of influence: *Porphyromonas gingivalis* outer membrane vesicles. *Mol. Oral. Microbiol.* 31, 365–378. doi: 10.1111/omi.12134

Gu, Y., Wu, Z., Zeng, F., Jiang, M., Teeling, J. L., Ni, J., et al. (2020). Systemic exposure to lipopolysaccharide from *Porphyromonas gingivalis* induces bone loss-correlated alzheimer's disease-like pathologies in middle-aged mice. *J. Alzheimers Dis.* 78, 61–74. doi: 10.3233/JAD-200689

Ha, J. Y., Choi, S. Y., Lee, J. H., Hong, S. H., and Lee, H. J. (2020). Delivery of periodontopathogenic extracellular vesicles to brain monocytes and microglial IL-6 promotion by RNA cargo. *Front. Mol. Biosci.* 7. doi: 10.3389/fmolb.2020.596366

Han, E. C., Choi, S. Y., Lee, Y., Park, J. W., Hong, S. H., and Lee, H. J. (2019). Extracellular RNAs in periodontopathogenic outer membrane vesicles promote TNF-alpha production in human macrophages and cross the blood-brain barrier in mice. *FASEB J.* 33, 13412–13422. doi: 10.1096/fj.201901575R

Hao, X., Li, Z., Li, W., Katz, J., Michalek, S. M., Barnum, S. R., et al. (2022). Periodontal infection aggravates C1q-mediated microglial activation and synapse pruning in alzheimer's mice. *Front. Immunol.* 13. doi: 10.3389/fimmu.2022.816640

Hayashi, K., Hasegawa, Y., Takemoto, Y., Cao, C., Takeya, H., Komohara, Y., et al. (2019). Continuous intracerebroventricular injection of *Porphyromonas gingivalis* lipopolysaccharide induces systemic organ dysfunction in a mouse model of alzheimer's disease. *Exp. Gerontol.* 120, 1–5. doi: 10.1016/j.exger.2019.02.007

He, J., Huang, W., Pan, Z., Cui, H., Qi, G., Zhou, X., et al. (2012). Quantitative analysis of microbiota in saliva, supragingival, and subgingival plaque of Chinese adults with chronic periodontitis. *Clin. Oral. Investig.* 16, 1579–1588. doi: 10.1007/s00784-011-0654-4

Heneka, M. T., Carson, M. J., El Khoury, J., Landreth, G. E., Brosseron, F., Feinstein, D. L., et al. (2015). Neuroinflammation in alzheimer's disease. *Lancet Neurol.* 14, 388–405. doi: 10.1016/S1474-4422(15)70016-5

Heneka, M. T., Kummer, M. P., Stutz, A., Delekate, A., Schwartz, S., Vieira-Saecker, A., et al. (2013). NLRP3 is activated in alzheimer's disease and contributes to pathology in APP/PS1 mice. *Nature* 493, 674–678. doi: 10.1038/nature11729

Ho, M. H., Chen, C. H., Goodwin, J. S., Wang, B. Y., and Xie, H. (2015). Functional advantages of *Porphyromonas gingivalis* vesicles. *PloS One* 10, e0123448. doi: 10.1371/journal.pone.0123448

Ho, M. H., Guo, Z. M., Chunga, J., Goodwin, J. S., and Xie, H. (2016). Characterization of innate immune responses of human endothelial cells induced by *Porphyromonas gingivalis* and their derived outer membrane vesicles. *Front. Cell Infect. Microbiol.* 6. doi: 10.3389/fcimb.2016.00139

Hu, Y., Li, H., Zhang, J., Zhang, X., Xia, X., Qiu, C., et al. (2020). Periodontitis induced by p. gingivalis-LPS is associated with neuroinflammation and learning and memory impairment in sprague-dawley rats. *Front. Neurosci.* 14. doi: 10.3389/fnins.2020.00658

Ilievski, V., Zuchowska, P. K., Green, S. J., Toth, P. T., Ragozzino, M. E., Le, K., et al. (2018). Chronic oral application of a periodontal pathogen results in brain inflammation, neurodegeneration and amyloid beta production in wild type mice. *PloS One* 13, e0204941. doi: 10.1371/journal.pone.0204941

Ising, C., Venegas, C., Zhang, S., Scheiblich, H., Schmidt, S. V., Vieira-Saecker, A., et al. (2019). NLRP3 inflammasome activation drives tau pathology. *Nature* 575, 669–673. doi: 10.1038/s41586-019-1769-z

Jiang, M., Zhang, X., Yan, X., Mizutani, S., Kashiwazaki, H., Ni, J., et al. (2021). GSK3beta is involved in promoting alzheimer's disease pathologies following chronic systemic exposure to *Porphyromonas gingivalis* lipopolysaccharide in amyloid precursor protein(NL-F/NL-F) knock-in mice. *Brain Behav. Immun.* 98, 1–12. doi: 10.1016/j.bbi.2021.08.213

Kato, T., Yamazaki, K., Nakajima, M., Date, Y., Kikuchi, J., Hase, K., et al. (2018). Oral administration of *Porphyromonas gingivalis* alters the gut microbiome and serum metabolome. *mSphere* 3, e00460–18. doi: 10.1128/mSphere.00460-18

Keaney, J., and Campbell, M. (2015). The dynamic blood-brain barrier. *FEBS J.* 282, 4067–4079. doi: 10.1111/febs.13412

Kitazawa, M., Cheng, D., Tsukamoto, M. R., Koike, M. A., Wes, P. D., Vasilevko, V., et al. (2011). Blocking IL-1 signaling rescues cognition, attenuates tau pathology, and restores neuronal beta-catenin pathway function in an alzheimer's disease model. *J. Immunol.* 187, 6539–6549. doi: 10.4049/jimmunol.1100620

Kovacech, B., and Novak, M. (2010). Tau truncation is a productive posttranslational modification of neurofibrillary degeneration in alzheimer's disease. *Curr. Alzheimer Res.* 7, 708–716. doi: 10.2174/156720510793611556

Lee, K. E., Kim, J. K., Han, S. K., Lee, D. Y., Lee, H. J., Yim, S. V., et al. (2020). The extracellular vesicle of gut microbial paenalcaligenes hominis is a risk factor for vagus nerve-mediated cognitive impairment. *Microbiome* 8, 107. doi: 10.1186/s40168-020-00881-2

Lei, Y., Chen, C. J., Yan, X. X., Li, Z., and Deng, X. H. (2017). Early-life lipopolysaccharide exposure potentiates forebrain expression of NLRP3 inflammasome proteins and anxiety-like behavior in adolescent rats. *Brain Res.* 1671, 43–54. doi: 10.1016/j.brainres.2017.06.014

Lempriere, S. (2020). NEURODEGENERATIVE DISEASE NLRP3 inflammasome activation implicated in tau pathology. *Nat. Rev. Neurol.* 16, 4. doi: 10.1038/s41582-019-0299-5

Mantri, C. K., Chen, C. H., Dong, X., Goodwin, J. S., Pratap, S., Paromov, V., et al. (2015). Fimbriae-mediated outer membrane vesicle production and invasion of *Porphyromonas gingivalis*. *Microbiologyopen* 4, 53–65. doi: 10.1002/mbo3.221

Nakajima, M., Arimatsu, K., Kato, T., Matsuda, Y., Minagawa, T., Takahashi, N., et al. (2015). Oral administration of p. gingivalis induces dysbiosis of gut microbiota and impaired barrier function leading to dissemination of enterobacteria to the liver. *PloS One* 10, e0134234. doi: 10.1371/journal.pone.0134234

Nara, P. L., Sindelar, D., Penn, M. S., Potempa, J., and Griffin, W. S. T. (2021). *Porphyromonas gingivalis* outer membrane vesicles as the major driver of and explanation for neuropathogenesis, the cholinergic hypothesis, iron dyshomeostasis, and salivary lactoferrin in alzheimer's disease. *J. Alzheimers Dis.* 82, 1417–1450. doi: 10.3233/JAD-210448

Neddens, J., Temmel, M., Flunkert, S., Kerschbaumer, B., Hoeller, C., Loeffler, T., et al. (2018). Phosphorylation of different tau sites during progression of alzheimer's disease. *Acta Neuropathol. Commun.* 6, 52. doi: 10.1186/s40478-018-0557-6

Nie, R., Wu, Z., Ni, J., Zeng, F., Yu, W., Zhang, Y., et al. (2019). *Porphyromonas gingivalis* infection induces amyloid-beta accumulation in Monocytes/Macrophages. *J. Alzheimers Dis.* 72, 479–494. doi: 10.3233/JAD-190298

Noble, J. M., Scarmeas, N., Celenti, R. S., Elkind, M. S., Wright, C. B., Schupf, N., et al. (2014). Serum IgG antibody levels to periodontal microbiota are associated with incident Alzheimer disease. *PloS One* 9, e114959. doi: 10.1371/journal.pone.0114959

Nonaka, S., Kadowaki, T., and Nakanishi, H. (2022). Secreted gingipains from *Porphyromonas gingivalis* increase permeability in human cerebral microvascular endothelial cells through intracellular degradation of tight junction proteins. *Neurochem. Int.* 154, 105282. doi: 10.1016/j.neuint.2022.105282

Oprica, M., Hjorth, E., Spulber, S., Popescu, B. O., Ankarcrona, M., Winblad, B., et al. (2007). Studies on brain volume, Alzheimer-related proteins and cytokines in mice with chronic overexpression of IL-1 receptor antagonist. *J. Cell Mol. Med.* 11, 810–825. doi: 10.1111/j.1582-4934.2007.00074.x

Pickering, M., and O'Connor, J. J. (2007). Pro-inflammatory cytokines and their effects in the dentate gyrus. *Dentate. Gyrus.: A Comphrehens. Guide. To. Struct. Function. Clin. Implicat.* 163, 339–354. doi: 10.1016/S0079-6123(07)63020-9

Pistollato, F., Sumalla Cano, S., Elio, I., Masias Vergara, M., Giampieri, F., and Battino, M. (2016). Role of gut microbiota and nutrients in amyloid formation and pathogenesis of Alzheimer disease. *Nutr. Rev.* 74, 624–634. doi: 10.1093/nutrit/nuw023

Poole, S., Singhrao, S. K., Kesavalu, L., Curtis, M. A., and Crean, S. (2013). Determining the presence of periodontopathic virulence factors in short-term postmortem alzheimer's disease brain tissue. *J. Alzheimers Dis.* 36, 665–677. doi: 10.3233/JAD-121918

Pritchard, A. B., Fabian, Z., Lawrence, C. L., Morton, G., Crean, S., and Alder, J. E. (2022). An investigation into the effects of outer membrane vesicles and lipopolysaccharide of *Porphyromonas gingivalis* on blood-brain barrier integrity, permeability, and disruption of scaffolding proteins in a human *in vitro* model. *J. Alzheimers Dis.* 86, 343–364. doi: 10.3233/JAD-215054

Qian, X., Zhang, S., Duan, L., Yang, F., Zhang, K., Yan, F., et al. (2021). Periodontitis deteriorates cognitive function and impairs neurons and glia in a

mouse model of alzheimer's disease. *J. Alzheimers Dis.* 79, 1785–1800. doi: 10.3233/JAD-201007

Reimers, D., Vallejo-Munoz, M., Casarejos, M. J., Jimenez-Escrig, A., Gonzalo-Gobernado, R., and Bazan, E. (2021). Immunohistochemical study of ASC expression and distribution in the hippocampus of an aged murine model of alzheimer's disease. *Int. J. Mol. Sci.* 22, 8697. doi: 10.3390/ijms22168697

Ryder, M. I. (2020). *Porphyromonas gingivalis* and Alzheimer disease: Recent findings and potential therapies. *J. Periodontol.* 91 Suppl 1, S45–S49. doi: 10.1002/JPER.20-0104

Saygun, I., Nizam, N., Keskiner, I., Bal, V., Kubar, A., Acikel, C., et al. (2011). Salivary infectious agents and periodontal disease status. *J. Periodontal. Res.* 46, 235–239. doi: 10.1111/j.1600-0765.2010.01335.x

Schertzer, J. W., and Whiteley, M. (2013). Bacterial outer membrane vesicles in trafficking, communication and the host-pathogen interaction. *J. Mol. Microbiol. Biotechnol.* 23, 118–130. doi: 10.1159/000346770

Schroder, K., and Tschopp, J. (2010). The inflammasomes. *Cell* 140, 821–832. doi: 10.1016/j.cell.2010.01.040

Seyama, M., Yoshida, K., Yoshida, K., Fujiwara, N., Ono, K., Eguchi, T., et al. (2020). Outer membrane vesicles of *Porphyromonas gingivalis* attenuate insulin sensitivity by delivering gingipains to the liver. *Biochim. Biophys. Acta Mol. Bas. Dis.* 1866, 165731. doi: 10.1016/j.bbadis.2020.165731

Sheng, J. G., Zhu, S. G., Jones, R. A., Griffin, W. S., and Mrak, R. E. (2000). Interleukin-1 promotes expression and phosphorylation of neurofilament and tau proteins *in vivo*. *Exp. Neurol.* 163, 388–391. doi: 10.1006/exnr.2000.7393

Singhrao, S. K., and Olsen, I. (2018). Are *Porphyromonas gingivalis* outer membrane vesicles microbullets for sporadic alzheimer's disease manifestation? *J. Alzheimers Dis. Rep.* 2, 219–228. doi: 10.3233/adr-180080

Sparks Stein, P., Steffen, M. J., Smith, C., Jicha, G., Ebersole, J. L., Abner, E., et al. (2012). Serum antibodies to periodontal pathogens are a risk factor for alzheimer's disease. *Alzheimers Dement.* 8, 196–203. doi: 10.1016/j.jalz.2011.04.006

Su, X. Y., Tang, Z. Q., Lu, Z. Y., Liu, Y. Q., He, W. Z., Jiang, J. P., et al. (2021). Oral treponema denticola infection induces a beta(1-40) and a beta(1-42) accumulation in the hippocampus of C57BL/6 mice. *J. Mol. Neurosci.* 71, 1506–1514. doi: 10.1007/s12031-021-01827-5

Tang, Z., Liang, D., Cheng, M., Su, X., Liu, R., Zhang, Y., et al. (2021). Effects of *Porphyromonas gingivalis* and its underlying mechanisms on Alzheimer-like tau hyperphosphorylation in sprague-dawley rats. *J. Mol. Neurosci.* 71, 89–100. doi: 10.1007/s12031-020-01629-1

Tan, M. S., Yu, J. T., Jiang, T., Zhu, X. C., and Tan, L. (2013). The NLRP3 inflammasome in alzheimer's disease. *Mol. Neurobiol.* 48, 875–882. doi: 10.1007/s12035-013-8475-x

Toyofuku, M., Nomura, N., and Eberl, L. (2019). Types and origins of bacterial membrane vesicles. *Nat. Rev. Microbiol.* 17, 13–24. doi: 10.1038/s41579-018-0112-2

van der Kant, R., Goldstein, L. S. B., and Ossenkoppele, R. (2020). Amyloid-beta-independent regulators of tau pathology in Alzheimer disease. *Nat. Rev. Neurosci.* 21, 21–35. doi: 10.1038/s41583-019-0240-3

Wei, S., Peng, W., Mai, Y., Li, K., Wei, W., Hu, L., et al. (2020). Outer membrane vesicles enhance tau phosphorylation and contribute to cognitive impairment. *J. Cell Physiol.* 235, 4843–4855. doi: 10.1002/jcp.29362

Wen, H., Miao, E. A., and Ting, J. P. (2013). Mechanisms of NOD-like receptor-associated inflammasome activation. *Immunity* 39, 432–441. doi: 10.1016/j.immuni.2013.08.037

Wu, Z., Ni, J., Liu, Y., Teeling, J. L., Takayama, F., Collcutt, A., et al. (2017). Cathepsin b plays a critical role in inducing alzheimer's disease-like phenotypes following chronic systemic exposure to lipopolysaccharide from *Porphyromonas gingivalis* in mice. *Brain Behav. Immun.* 65, 350–361. doi: 10.1016/j.bbi.2017.06.002

Xue, L., Zou, X., Yang, X. Q., Peng, F., Yu, D. K., and Du, J. R. (2020). Chronic periodontitis induces microbiota-gut-brain axis disorders and cognitive impairment in mice. *Exp. Neurol.* 326, 113176. doi: 10.1016/j.expneurol.2020.113176

Zhang, J., Yu, C., Zhang, X., Chen, H., Dong, J., Lu, W., et al. (2018). *Porphyromonas gingivalis* lipopolysaccharide induces cognitive dysfunction, mediated by neuronal inflammation *via* activation of the TLR4 signaling pathway in C57BL/6 mice. *J. Neuroinflammat.* 15, 37. doi: 10.1186/s12974-017-1052-x

Zihni, C., Mills, C., Matter, K., and Balda, M. S. (2016). Tight junctions: from simple barriers to multifunctional molecular gates. *Nat. Rev. Mol. Cell Biol.* 17, 564–580. doi: 10.1038/nrm.2016.80

frontiers | Frontiers in Cellular and Infection Microbiology

TYPE Original Research
PUBLISHED 11 August 2022
DOI 10.3389/fcimb.2022.989188

OPEN ACCESS

EDITED BY
Zuomin Wang,
Capital Medical University, China

REVIEWED BY
Li Lin,
China Medical University, China
Shu Deng,
Boston University, United States

*CORRESPONDENCE
Ning Ma
maningbsh76@sina.com
Li Zhang
2239003764@qq.com

†These authors have contributed equally to this work and share first authorship

SPECIALTY SECTION
This article was submitted to Extra-intestinal Microbiome, a section of the journal Frontiers in Cellular and Infection Microbiology

RECEIVED 08 July 2022
ACCEPTED 21 July 2022
PUBLISHED 11 August 2022

CITATION
Jiao J, Zheng Y, Zhang Q, Xia D, Zhang L and Ma N (2022) Saliva microbiome changes in thyroid cancer and thyroid nodules patients. *Front. Cell. Infect. Microbiol.* 12:989188. doi: 10.3389/fcimb.2022.989188

Saliva microbiome changes in thyroid cancer and thyroid nodules patients

Junjun Jiao[1†], Youli Zheng[2†], Qingyu Zhang[1], Degeng Xia[1], Li Zhang[1*] and Ning Ma[1*]

[1]Hospital of Stomatology, Jilin University, Changchun, China, [2]The School and Hospital of Stomatology, Tianjin Medical University, Tianjin, China

Objective: Thyroid disease has been reported to associate with gut microbiota, but the effects of thyroid cancer and thyroid nodules on the oral microbiota are still largely unknown. This study aimed to identify the variation in salivary microbiota and their potential association with thyroid cancer and thyroid nodules.

Methods: We used 16S rRNA high-throughput sequencing to examine the salivary microbiota of thyroid cancer patients (n = 14), thyroid nodules patients (n = 9), and healthy controls (n = 15).

Results: The alpha-diversity indices Chao1 and ACE were found to be relatively higher in patients with thyroid cancer and thyroid nodules compared to healthy controls. The beta diversity in both the thyroid cancer and thyroid nodules groups was divergent from the healthy control group. The genera Alloprevotella, Anaeroglobus, Acinetobacter, unclassified Bacteroidales, and unclassified Cyanobacteriales were significantly enriched in the thyroid cancer group compared with the healthy control group. In contrast, the microbiome of the healthy controls was mainly composed of the genera Haemophilus, Lautropia, Allorhizobium Neorhizobium Pararhizobium Rhizobium, Escherichia Shigella, and unclassified Rhodobacteraceae. The thyroid nodules group was dominated by genre uncultured Candidatus Saccharibacteria bacterium, unclassified Clostridiales bacterium feline oral taxon 148, Treponema, unclassified Prevotellaceae, Mobiluncus, and Acholeplasma. In contrast, the genera unclassified Rhodobacteraceae and Aggregatibacter dominated the healthy control group. The study also found that clinical indicators were correlated with the saliva microbiome.

Conclusion: The salivary microbiota variation may be connected with thyroid cancer and thyroid nodules.

KEYWORDS

thyroid cancer, thyroid nodules, microbiota, 16S rRNA sequencing, oral, clinical index

Introduction

Thyroid nodules are common in clinical practice, with approximately 60% of adults harboring one or more thyroid nodules, and the majority of them are benign. Palpable thyroid nodules occur in about 4-7% of the population, but only about 8% to 16% of thyroid nodules harbor thyroid cancer (Burman and Wartofsky, 2015). Thyroid cancer is the most common endocrine malignancy and is responsible for 586000 cancer cases worldwide, with a higher global incidence rate in women (Ferlay et al., 2015; Sung et al., 2021). Over the past 3 decades, the global incidence rate of thyroid cancer has rapidly increased by 300%, but the mortality rate remains much lower and comparatively stable (Kitahara and Sosa, 2016; Lortet-Tieulent et al., 2019; Sung et al., 2021). As a result, though better-prognosis thyroid cancer may seem like a "good cancer," previous studies have shown that thyroid cancer survivors with a better prognosis have a poorer quality of life than normal people and other worse-prognosis cancer survivors (Singer et al., 2012; Goswami et al., 2018; Chan et al., 2021). Some risk factors, such as familial influences, sex, obesity, hormonal exposure, smoking, and environmental risk factors, may increase the risk of thyroid cancer, but the etiology of thyroid cancer remains poorly understood to date (Kim et al., 2020). Interestingly, some studies have suggested that thyroid cancer and thyroid nodules may have a relationship with microbiota, and the risk factors of thyroid diseases such as hormones and obesity are also linked to the composition and diversity of microbiota, implicating the microbiota perhaps play a role in thyroid cancer and thyroid nodules (Maruvada et al., 2017; Stefura et al., 2021; Dong et al., 2021).

It is known that the relationship between oral microbiota and cancer has been extensively studied. Several oral taxa have been shown to promote cancer development through different mechanisms such as inhibiting apoptosis, activating cell proliferation, promoting cell invasion, inducing chronic inflammation, and directly producing carcinogens (Irfan et al., 2020; Tuominen and Rautava, 2021). Indeed, a growing number of studies have shown associations between changes in the oral microbiota and a wide variety of cancer types such as colorectal cancer, esophageal cancer, throat cancer, liver cancer, and lung cancer (Peters et al., 2017; Yang et al., 2018; Wang et al., 2019; Li et al., 2020; Uchino et al., 2021). These studies suggest that the oral microbiota may provide a potential biomarker for some cancer diagnoses. Additionally, a study reported that salivary microbial profiles change with increasing serum TSH (thyroid-stimulating hormone), which is reflected in increased taxa diversity, changes in community structure, and species composition (Dong et al., 2021). And there is evidence that serum TSH at presentation is an independent predictor of differentiated thyroid cancer (DTC) and the thyroid nodules are at increased risk for malignancy with elevated serum TSH concentrations within the normal range (Haymart et al., 2008). Another study suggests that sex hormones affect the change of oral microbiota, while estrogen has been proven to play an essential role in thyroid nodules (Kim et al., 2010; Lin et al., 2018). Moreover, recent evidence has revealed that thyroid cancer and thyroids nodules are associated with gut microbiota (Feng et al., 2019; Zhang et al., 2019; Li et al., 2021). Oral-to-gut and gut-to-oral microbial transmission can modulate the pathogenesis of various human diseases, suggesting the potential interaction between thyroid diseases and oral microbiota despite the paucity of studies on the role of the oral microbiota in thyroid cancer (Kitamoto et al., 2020; Park et al., 2021).

Therefore, we compared the microbiota in human saliva from healthy controls and patients with thyroid cancer and thyroid nodules using 16s rRNA gene sequencing to identify the potential relationship between the oral microbiota and thyroid cancer and thyroid nodules.

Materials and method

Participant recruitment

This study enrolled patients with thyroid cancer and thyroid nodules from March 2022 to May 2022 in North China and recruited healthy people as controls from the resident community in Qingdao, China. The inclusion criteria for patients with thyroid disease were as follows: (1) clinically diagnosed with thyroid nodules by ultrasound; (2) Some high-grade thyroid nodules such as TI-RADS level 4a and thyroid cancer identified by pathological examination. The healthy controls were frequently matched with the thyroid cancer and thyroid nodules patients for age, gender, and body mass index (BMI); no healthy controls had thyroid lesions. The following exclusion criteria were applied to all groups: pregnancy; lactation; cigarette smoking; alcohol addiction; hypertension; diabetes mellitus; kidney disease; BMI < 18.5; BMI > 30.3; recent (< 3 months prior) use of antibiotics, probiotics, prebiotics, symbiotics, hormonal medication; known history of disease with an autoimmune component; and history of malignancy; unwilling to sign the informed consent.

This study followed the Declaration of Helsinki on medical protocols and ethics and obtained approval from the Regional Ethical Review Board of the Hospital of stomatology, Jilin University. All participants have been informed of the intention of the sample collection and signed written informed consent.

Anthropometric, biochemical measurements, and group definition

Demographic information, including height, gender, and body mass index (BMI), was obtained during subject recruitment. The clinical indicators were obtained from the participants who were required to fast for 8 hours. Two independent ultrasonography clinicians verified the description of the thyroid nodules and classified them according to the Kwak-TIRADS criteria (Kwak et al., 2011). At least two pathologists confirmed the diagnosis of thyroid cancer.

We recruited 14 thyroid cancer patients, 9 thyroid nodules patients, and 15 healthy controls. All the thyroid cancer patients we recruited were papillary thyroid cancer (PTC). All the thyroid nodules patients were not malignant. All participants live in the northern coastal provinces of CHINA, where the typical diet includes steamed bread, meat, seafood, vegetables, and fruits.

Sample collection

Saliva samples were obtained from recruited patients before brushing their teeth and eating breakfast. Subjects started by rinsing the mouth with stroke-physiological saline solution before sampling. Then, 2 to 5 ml saliva was collected in a 10ml sterile Eppendorf tube, transferred to the laboratory immediately in an ice box, and stored at -80℃ until sequencing.

DNA extraction, amplification, and high-throughput sequences

The genomic DNA was extracted from saliva samples with a QIAamp DNA Mini Kit (Qiagen, Valencia, CA, USA) according to the manufacturer's instruction and then quantified using a spectrophotometer and 1% agarose gel electrophoresis.

The V3-V4 variable regions were high-throughput sequenced by Biomarker Technologies Co, Ltd. (Beijing, China) using an Illumina NovaSeq6000 platform according to established protocol. A sample-unique 8-base barcode was contained in each forward primer. The V3-V4 region of the bacterial 16S rRNA gene was amplified using the universal forward primer 338F: 5′-ACTCCTACGGGAGGCAGCA-3′ and reverse primer 806R: 5′-GGACTACHVGGGTWTCTAAT-3′. The PCR program was as follows: 95°C, 5 min; 25 cycles of 30 s at 95°C, 30 s at 50°C, and 40 s at 72°C; and a final extension of 72°C for 7 min. PCRs were performed with a 10μL reaction mixture containing 5 μL of KOD FX Neo Buffer, 2 μL of 2mMDNTPS, 0.3 μL of each primer (10μm), 0.2 U of KOD FX Neo, and 15 ng of template DNA.

1.8% agarose gel electrophoresis separated the PCR products. Purified amplicons from different samples were pooled in equimolar and sequenced in the Illumina NovaSeq6000 platform.

Data processing

Merging the paired-end reads used FLASH v1.2.7 (Yang et al., 2020). According to the default settings, the minimum overlap length and maximum mismatch ratio of merged paired-end reads were 10bp and 0.2, respectively. Simultaneously, the tags with more than six mismatches were eliminated. Quality control was performed using Trimmomatic (version 0.33) to determine the merged tags with an average quality score < 20 in a 50bp sliding window and remove those shorter than 350bps (Sheng et al., 2019). Denoising and removing the chimeras in dada2 *via* QIME2 2020.6 and obtaining amplicon sequence variations (ASVs) feature sequences (Callahan et al., 2016; Bolyen et al., 2019).

Statistical analysis

Data analyses were undertaken using SPSS (version 25.0) and R software (version 4.20). P values < 0.05 were considered statistically significant. For continuous variables with normal distributions and equal variance, including BMI (body mass index), WBC (white blood cell), RBC (red blood cell), PLT (platelet), TP (total protein), and GLU (glucose), analysis of variance (ANOVA) was carried out for group comparisons. Continuous variables conforming to normal distribution but with unequal variance included AST (aspartate transaminase) and FT3 (free triiodothyronine), which were analyzed by the ANOVA after Welch correction. Wilcoxon rank-sum test was utilized to detect the continuous variable without normality, including age, ALT (alanine aminotransferase), TBIL (total bilirubin), TG (triglyceride), CHOL (total cholesterol), HDL (high-density lipoprotein), LDL (low-density lipoprotein), FT4 (free thyroxine), TSH (thyroid-stimulating hormone), TGAb (antithyroglobulin antibody), TPOAb (antithyroperoxidase antibody), and PTH (parathyroid hormone). The Fisher exact test was assessed for the data of categorical variables of gender.

We drew a Venn diagram to depict the unique or shared ASVs in three groups (Figure 1) (Chen and Boutros, 2011). Alpha diversity was calculated on the basis of the gene profile for each sample, based on the Simpson, Chao1, and ACE index. Alpha-diversity estimates were computed using QIIME2 2020.6 software (Figure 2) (Bolyen et al., 2019). The ANOVA method was used to examine the differences between the three groups.

The β-diversity index comparisons were used to compare differences in microbial diversity among the three groups using principal coordinate analysis (PCoA) based on the unweighted UniFrac analysis. The weighted UniFrac used to calculate the Phylogenetic distances of the system took the evolutionary

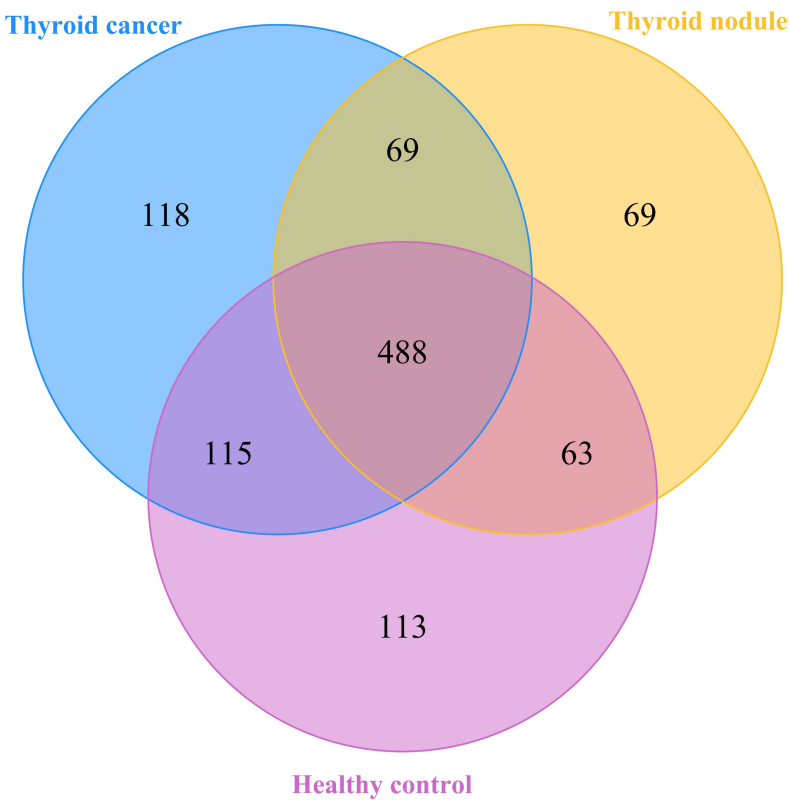

FIGURE 1
A Veen diagram comparing the distribution of amplicon sequence variations (ASVs) among the thyroid cancer, thyroid nodules, and healthy control groups. The different colors represent different groups. The overlap represents shared bacteria.

distance between the species into account to compare the microbial diversity differences (Lozupone and Knight, 2005). Permutational multivariate analysis of variance (PERMANOVA) was used to test the significance of the differences among the three groups.

LEfSe (Linear discriminant analysis Effect Size) can be used to analyze the differences between groups and look for biomarkers with statistical differences between groups.

First, Kruskal-Wallis (KW) was used to detect features with significant differences in abundance between different groups, and significance was set to 0.05; Subsequently, a set of pairwise tests among subclasses was performed to use the Wilcoxon rank-sum test, with significance set at 0.5; At last, linear discriminant analysis (LDA) was used to downscale the data and assess the influence of species with significant differences. Lefse was performed to identify the most discriminating taxa in groups from phylum to genus, and taxa with an LDA score > 2.0 were considered the most discriminating species (Segata et al., 2011). Correlations between the clinical parameters and different microbiota were quantitatively evaluated using the Pearson correlation coefficient, and the correlation was presented using a heatmap.

Result

Study population

To establish the salivary microbiota characteristics of patients with thyroid cancer and thyroid nodules, we analyzed 38 saliva samples from 38 participants (14 patients with thyroid cancer, 9 patients with thyroid nodules, and 15 healthy controls) using 16S rRNA gene sequencing. No significant differences were noticed in the clinical parameters ($p > 0.05$) among the three groups. The demographic and biochemical variables of patients with thyroid cancer and thyroid nodules were summarized in Table 1.

Bacterial composition in saliva in patients with thyroid cancer and patients with thyroid nodules and HCs

After filtering poor-quality reads, we collected an average of 79,817 clean reads per sample and 1035 ASVs in total. Among the 1035 ASVs found in the 38 samples, 488 were shared among

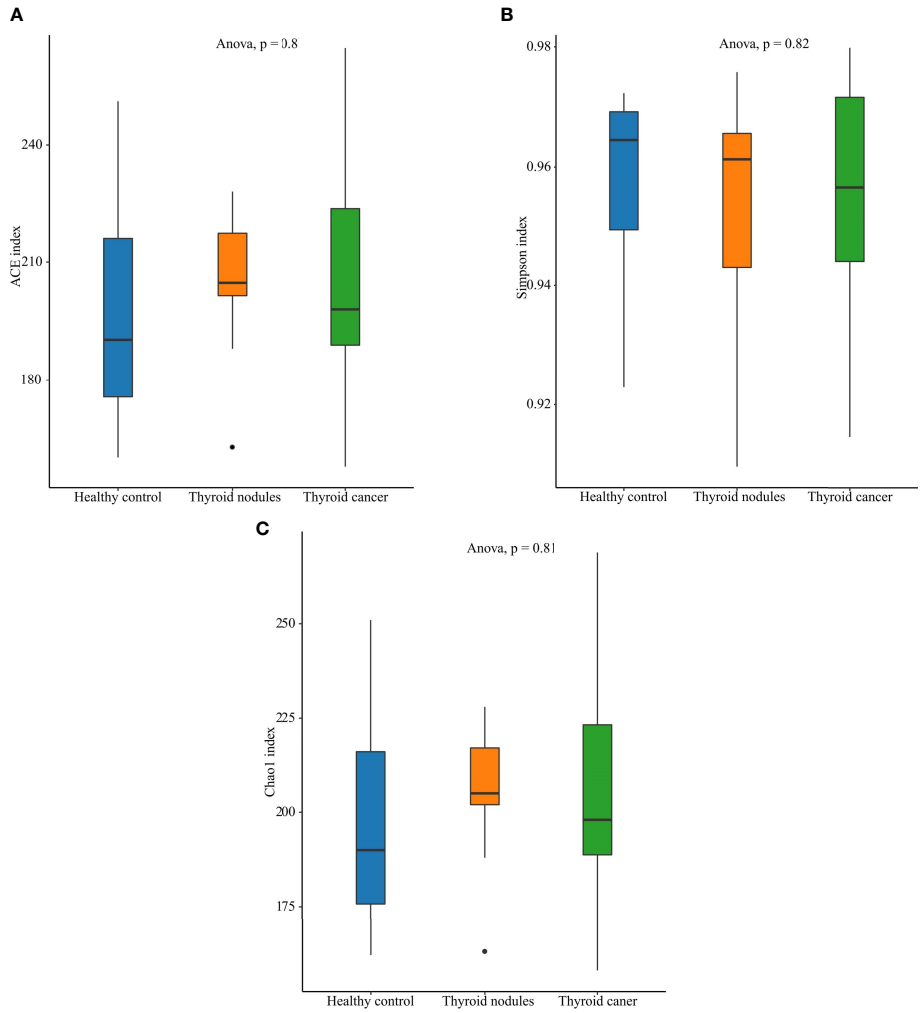

FIGURE 2
Alpha diversity of the saliva microbiome in thyroid cancer patients, thyroid nodules patients, and healthy controls. **(A)** Richness of saliva microbiota assessed by ACE. **(B)** Simpson is a diversity index. **(C)** Richness of saliva microbiota assessed by Chao1.

all three groups. We identified 790 ASVs, 689 ASVs, and 779 ASVs in the thyroid cancer, thyroid nodules, and healthy control groups, respectively (Figure 1). Additionally, 118 ASVs were found only in thyroid cancer group, 69 were observed only in the thyroid nodules group, and 113 unique were observed in the healthy control group. Sixty-nine ASVs were shared by patients with thyroid cancer and those with thyroid nodules, 63 were found in the thyroid nodules group and healthy control group, and 115 were observed in patients with thyroid cancer and healthy controls.

Alpha-diversity in three groups

An increase in abundance (CHAO1, ACE) was observed in the thyroid cancer group and thyroid nodules group compared with the normal control group, though the differences showed little statistical significance among the three groups (ANOVA, $p > 0.05$). Also, the Shannon index, which reflects community abundance and evenness, did not show significant differences among the three groups (ANOVA, $p > 0.05$). Hence, there was no significant difference in the alpha diversity among the three groups (Figure 2).

Salivary microbiota composition and abundance in thyroid cancer and thyroid nodules patients, and healthy controls

The dominant abundance of bacterial species at the genus and phylum levels was shown in Figure 3. The dominant phyla among the thyroid cancer, thyroid nodules, and healthy control

TABLE 1 Basic characteristics of participants.

Variables	Thyroid cancer	Thyrois nodules	Healthy control	P- value
Gender (M: F)	11:3	9:0	12:3	0.40
Age (years)	54.50 (41.30, 58.80)	54.00 (49.00, 57.00)	55.00 (36.50, 59.50)	0.91
BMI (kg/m^2)	24.20 ± 3.380	23.70 ± 2.88	23.20 ± 2.65	0.71
WBC ($10^9/L$)	5.52 ± 1.10	5.84 ± 1.31	5.63 ± 1.16	0.82
RBC ($10^{12}/L$)	4.59 ± 0.33	4.48 ± 0.39	4.48 ± 0.47	0.72
PLT ($10^9/L$)	239.71 ± 58.01	221.44 ± 66.97	226.00 ± 40.89	0.69
ALT (U/L)	18.00 (13.30, 26.80)	17.00 (15.00, 18.00)	18.00 (17.00, 21.50)	0.55
AST (U/L)	22.00 ± 6.88	18.89 ± 1.83	17.13 ± 6.40	0.19
TP (g/L)	71.11 ± 6.42	71.22 ± 7.41	70.67 ± 3.92	0.95
TBIL (umol/L)	10.60 (9.44, 14.40)	12.00 (8.57, 14.70)	11.00 (9.00, 12.50)	0.88
GLU (mmol/L)	5.15 ± 0.57	5.42 ± 0.66	5.19 ± 0.48	0.55
TG (mmol/L)	1.03 (0.74, 0.81)	1.10 (1.01, 1.21)	0.98 (0.81, 1.20)	0.25
CHOL (mmol/L)	4.38 (4.08, 4.78)	4.39 (4.35, 4.77)	4.29 (4.04, 4.52)	0.14
HDL (mmol/L)	1.31 (1.20, 1.38)	1.04 (0.97, 1.49)	1.32 (1.21, 1.38)	0.40
LDL (mmol/L)	2.96 (2.80, 3.47)	2.78 (2.72, 3.36)	2.91 (2.80, 3.21)	0.59
FT3 (Pmol/L)	5.14 ± 1.48	4.90 ± 0.44	NA	0.58
FT4 (Pmol/L)	15.20 (14.00, 19.40)	17.10 (15.20, 18.80)	NA	0.55
TSH (uIU/ml)	1.940 (1.43, 4.35)	2.27 (1.17, 2.39)	NA	0.61
TG-Ab (IU/ml)	16.50 (15.00, 17.80)	16.40 (14.60, 20.10)	NA	0.90
TPO-Ab (IU/ml)	9.50 (9.00, 10.20)	10.00 (9.00, 10.30)	NA	0.41
PTH (pg/ml)	37.30 (29.70, 47.70)	38.90 (36.00, 41.70)	NA	0.66

The analysis of variance (ANOVA) was carried out to compare BMI, WBC, RBC, PLT, TP, and GLU. The ANOVA analyzed AST and FT3 after Welch correction. Wilcoxon rank-sum test was used to detect age, ALT, TBIL, TG, CHOL, HDL, LDL, FT4, TSH, TGAb, TPOAb, and PTH. The Fisher exact test was assessed for the data of categorical variables of gender.

group were Firmicutes, Proteobacteria, Bacteroidata, Actinobacteriota, and Fusobacteriota. We found that the above bacteria ranked differently in various groups. The Firmicutes accounted for 42.63%, 44.53%, and 36.38% in thyroid cancer, thyroid nodules, and healthy control group, respectively. The proteobacteria accounted for 19.21%, 19.80% and 27.52% in three groups respectively, the Bacteroidata accounted for 22.35%, 20.34%, and 18.31%, the Actinobacteriota accounted

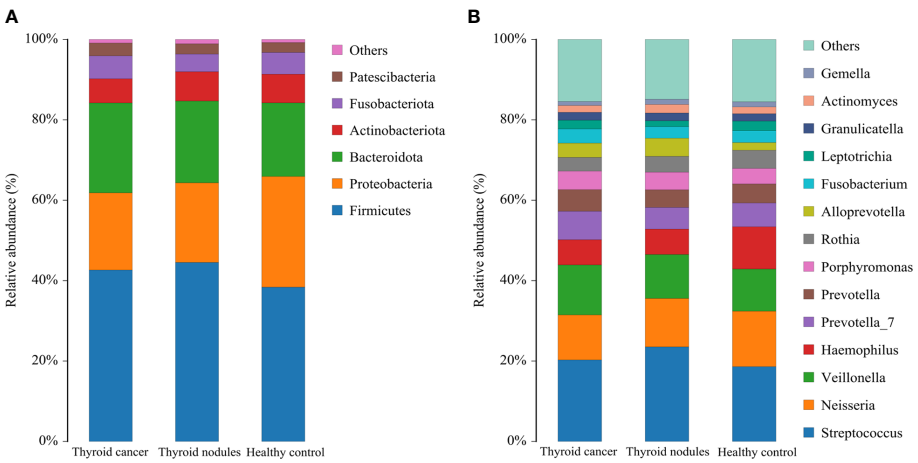

FIGURE 3
Relative abundance of dominant species in patients with thyroid cancer, patients with thyroid nodules, and healthy controls. **(A, B)** shows the relative abundance of the major phylum and genus, respectively. Each column of the bar graph represents a group, and each patch represents the proportion of a class of microbes in that group.

for 5.99%, 7.29%, and 7.12%, and the Fusobacteriota accounted for 5.70%, 4.39%, and 5.42%. In addition, the most prevalent genera were Streptococcus, Neisseria, Veillonella, Haemophilus, Prevotella 7, Prevotella, and Porphyromonas.

In conclusion, Firmicutes was the most prevalent phylum in all three groups. However, Proteobacteria only ranked second in the healthy control group, and Bacteroidata was more abundant in the thyroid cancer and thyroid nodules group than in the healthy control group.

Variation in the composition and diversity of community of thyroid cancer, thyroid nodules, and healthy control group

Beta-diversity analyses based on principal coordinates (PCoA) analysis suggested the differences in the composition and abundance of salivary microbiota of thyroid cancer, thyroid nodules, and healthy control groups. The differences between the three groups assessed by PERMANOVA based on unweighted UniFrac distance matrices were significant ($p < 0.05$, Figure 4). In a PCoA analysis, the closer the two samples were, the greater the similarity in community composition. The two circles for the thyroid cancer group and thyroid nodules group overlapped each other on the map, which indicated that the bacterial composition of the thyroid cancer group is similar to that of the thyroid nodules group. Moreover, the circle for the healthy control group was far from the other groups, suggesting that the saliva microbiota of the patients with thyroid cancer and thyroid nodules differed from healthy controls.

Bacterial taxa differences in the salivary microbiota among the three groups

To further compare the structure of the salivary microbiota in the thyroid cancer group, thyroid nodules group, and healthy controls, we used a combination of linear discriminant effect size (LEfSe) and linear discriminant analysis discriminant effect size (LDA value of 2.0).

In total, 34 taxa differed between the thyroid cancer and healthy controls; 15 taxa were significantly enriched in the thyroid cancer group (Kruskal-Wallis test, $P < 0.05$). One phylum Cyanobacteria, one class Cyanobacteria, one order (Cyanobacteriales), two families (unclassified Bacteroidales, unclassified Cyanobacteriales), and five genera (including Alloprevotella, Anaeroglobus, Acinetobacter, unclassified Bacteroidales, unclassified Cyanobacteriales) were significantly enriched in the thyroid cancer group compared with the healthy control group. In contrast, the microbiome of the healthy controls was mainly composed of the genera Haemophilus, Lautropia, Allorhizobium Neorhizobium Pararhizobium Rhizobium, Escherichia Shigella, and unclassified Rhodobacteraceae (Figure 5). Moreover, 36 taxa were siseven

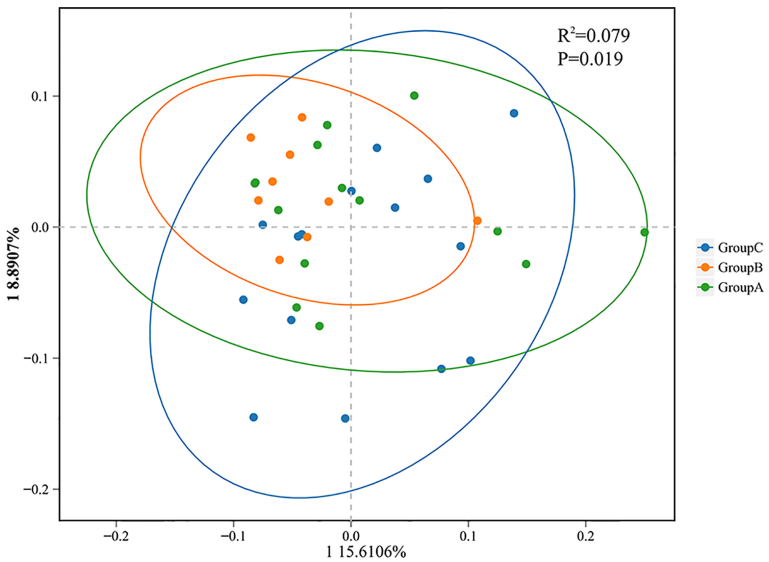

FIGURE 4
Principal coordinate analysis (PCoA) showing bacterial differences among groups. PCoA analysis is based on unweighted UniFrac distance matrices, and each symbol represents a sample. Blue rounds show samples from healthy controls (Group **C**), green rounds represent patients with thyroid cancer (Group **A**), and orange rounds represent patients with thyroid nodules (Group **B**). The healthy control group is separated from the others.

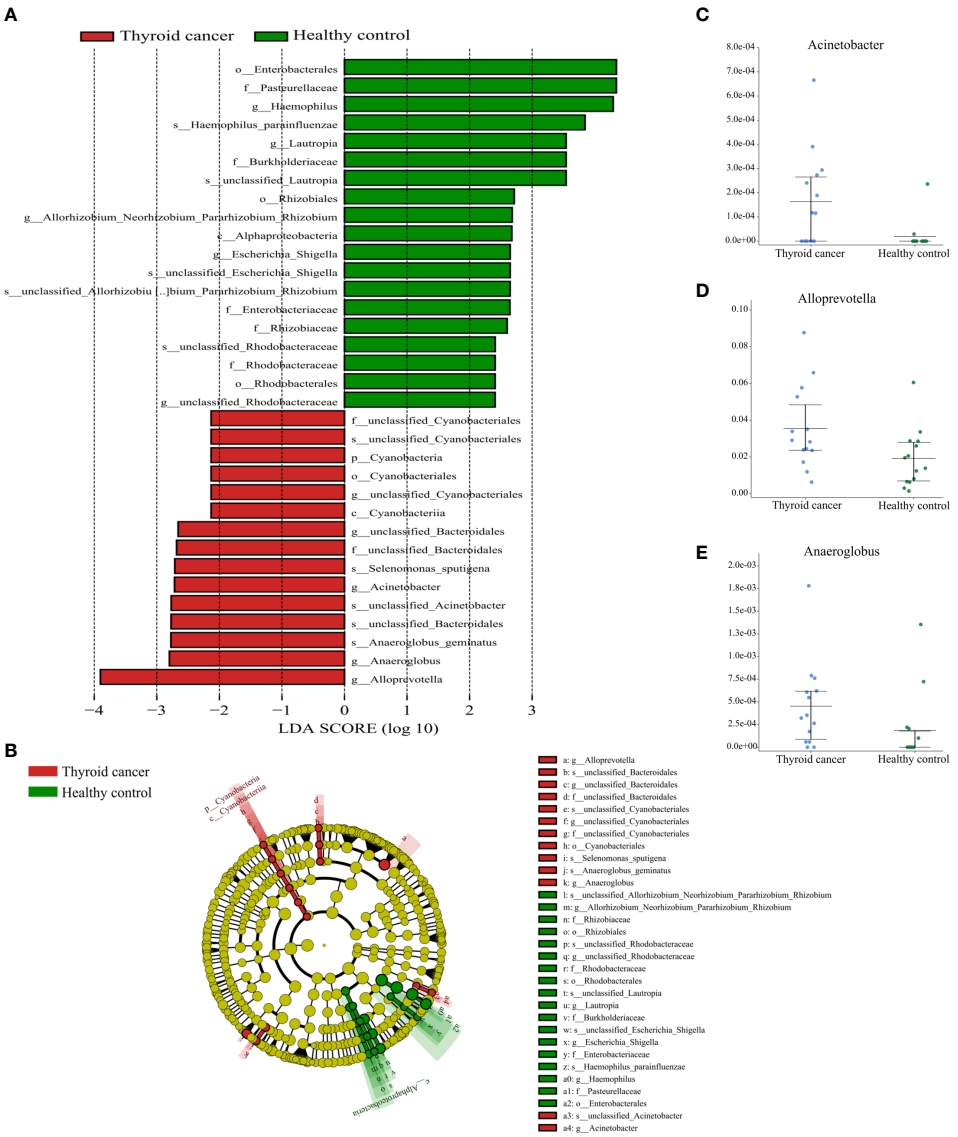

FIGURE 5
Partial bacterial taxa that differed significantly between healthy control and thyroid cancer groups. **(A)** Shows differentially abundant taxa in thyroid cancer and healthy control groups based on the linear discriminant analysis coupled with effect size (LEfSe). Taxa in this graph were both statistically significant ($P < 0.05$) and had LDA score above 2, which is considered a significant effect size. **(B)** A cladogram of the differential bacteria based on LEfSe. Circles from inside to outside represent species taxonomic levels from phylum to genera. The diameters of the circles represent the relative abundance. Red and green indicate enrichment in samples from the thyroid cancer patients and healthy controls, respectively. Yellow indicates no significant difference. **(C–E)** Relative abundance of taxonomy between thyroid cancer and healthy control groups was compared ($P < 0.05$).

gnificantly different between the thyroid nodules group and healthy controls (Kruskal-Wallis test, $P < 0.05$). The thyroid nodules group was dominated by genre uncultured Candidatus Saccharibacteria bacterium, unclassified Clostridiales bacterium feline oral taxon 148, Treponema, unclassified Prevotellaceae, Mobiluncus, and Acholeplasma, whereas the genera unclassified Rhodobacteraceae and Aggregatibacter dominated the healthy control group (Figure 6).

Associations between clinical indices and salivary microbiome

To explore the correlation between the relative abundance of saliva microbiota and clinical indices of patients with thyroid disease, we used Pearson's correlation coefficient ($p < 0.05$, $|\text{correlation coefficient}| > 0.4$). The clinical parameters including TSH (thyroid-stimulating hormone), FT3 (Freetriiodothyronine),

10.3389/fcimb.2022.989188

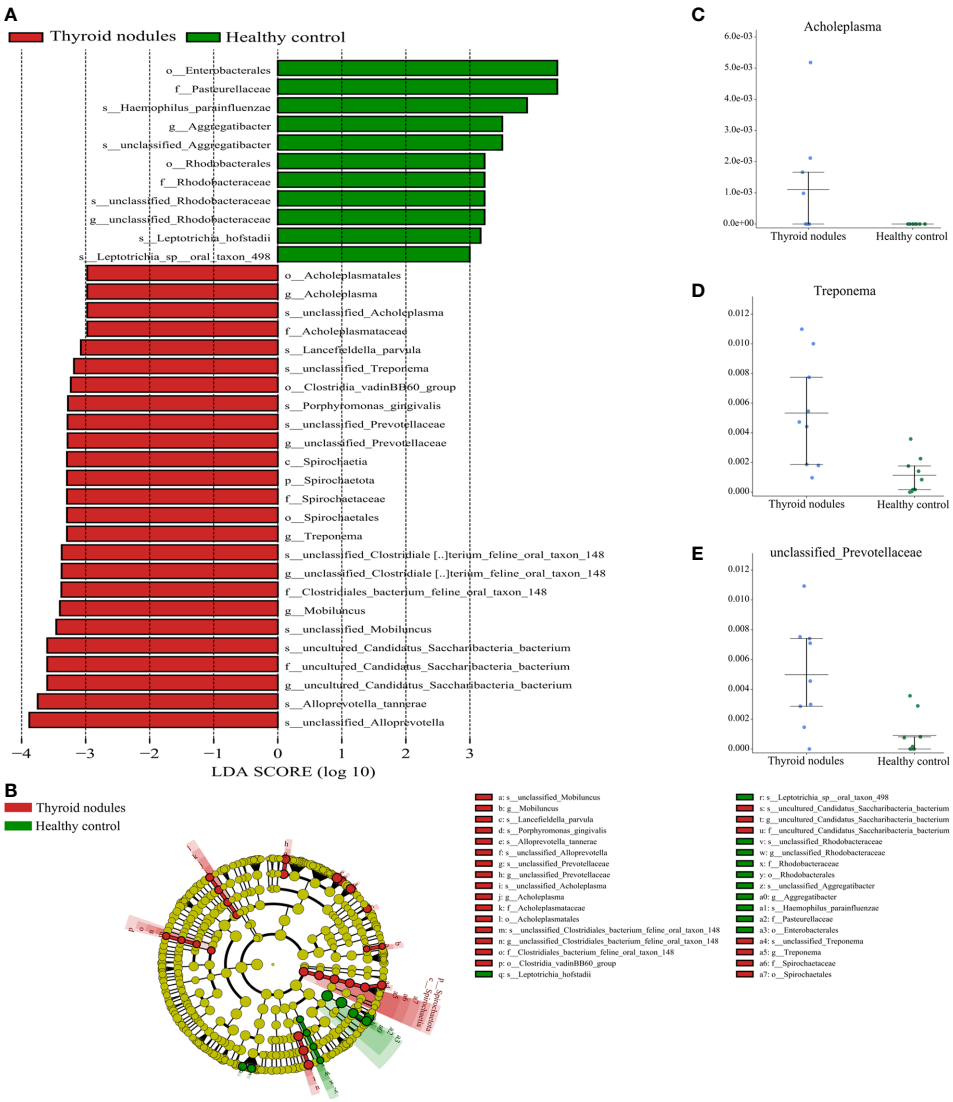

FIGURE 6
Partial bacterial taxa that differed significantly between healthy control and thyroid nodules groups. **(A)** Shows differentially abundant taxa in thyroid nodules and healthy control groups based on the linear discriminant analysis coupled with effect size (LEfSe). Taxa in this graph were both statistically significant ($P < 0.05$) and had LDA score above 2, which is considered a significant effect size. **(B)** A cladogram of the differential bacteria based on LEfSe. Circles from inside to outside represent species taxonomic levels from phylum to genera. The diameters of the circles represent the relative abundance. Red and green indicate enrichment in samples from the thyroid nodules patients and healthy controls, respectively. Yellow indicates no significant difference. **(C–E)** Relative abundance of taxonomy between thyroid nodules and healthy control groups was compared ($P < 0.05$).

FT4 (Freetetraiodothyronine), TgAb (Thyroglobulin antibody), TPOAb (Thyroid peroxidase antibody), and PTH (Parathyroid hormone) and the genera with abundance ratios above 0.01 were visualized with a heatmap (Figure 7). TPOAb exhibited a positive correlation with the genera Treponema, Comamonas, Abiotrophia, unclassified Clostridia vadinBB60 group, unclassified Candidatus Saccharibacteria bacterium UB2523, Acholeplasma, Kingella, Gemella, and unclassified Saccharimonadaceae and showed a negative association with genera Solobacterium, Alloprevotella, Family XIII UCG 001, [Eubacterium] nodatum group, Prevotella 7, Butyrivibrio, unclassified Clostridia UCG 014, and unclassified Lachnospiraceae. The TGAb was negatively correlated with the genera Parvimonas, Peptococcus, and unclassified Bacteria. In addition, FT4 showed a positive connection with the genera unclassified Clostridia UCG 014 and unclassified Clostridia vadinBB60 group, but genera Actinobacillus was positively correlated with FT4 level. What's more, a positive association

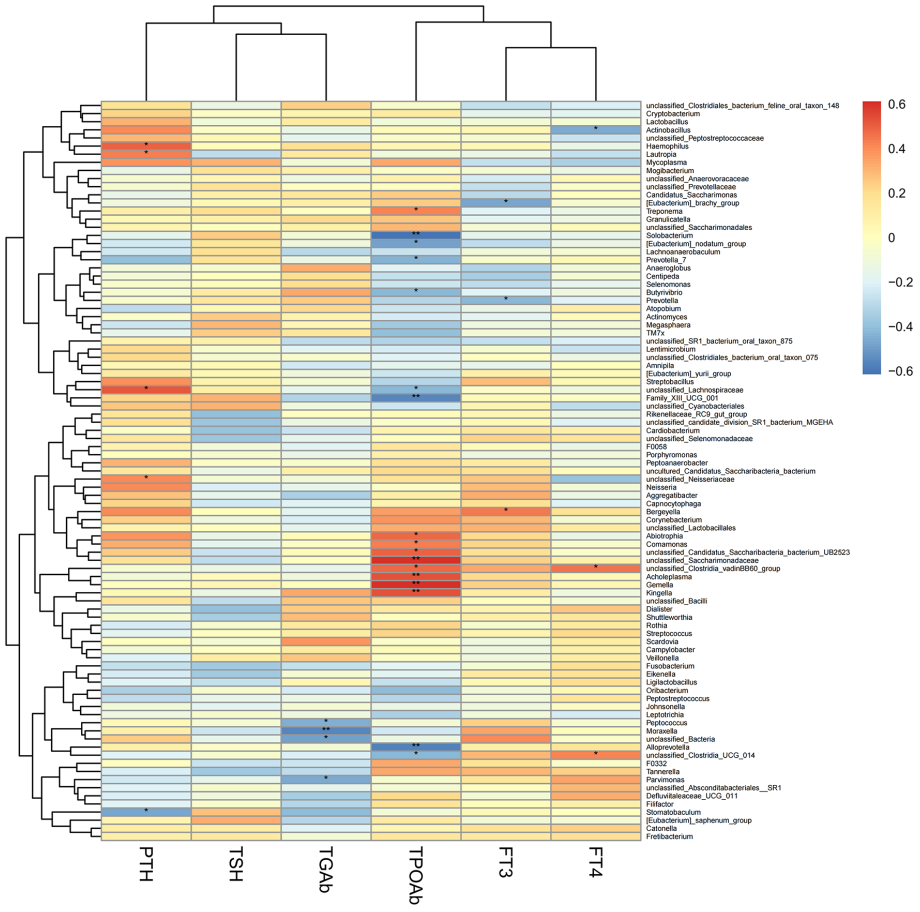

FIGURE 7
Heatmap of Pearson's correlation analysis between the saliva microbiota at the genera levels of thyroid cancer and thyroid nodules and clinical variables. R value shows in different colors, red indicates positive correlation while blue indicates negative correlation. The darker the color, the greater the correlation coefficient. Species clustering trees were presented on the left side of the heat map. *P < 0.05; **P < 0.01.

can be observed between the genera Bergeyella and FT3. However, FT3 exhibited a negative correlation with genera Prevotella and [Eubacterium] brachy group. Additionally, the correlation between the genera Lautropia, unclassified Lachnospiraceae, and Stomatobaculum and the level of PTH was positive, but PTH was negatively correlated with unclassified Neisseriaceae and Haemophilus. At the same time, we observed that the genera Alloprevotella enriched in thyroid cancer was positively correlated with TPOAb levels. Similarly, the microbiota enriched in thyroid nodules, including genera Treponema and Acholeplasma, family Spirochaetaceae and Acholeplasmataceae, all exhibited a strong positive correlation with TPOAb ($p < 0.05$, Figures 7, 8).

Discussion

In this study, we characterized the richness and abundance of salivary microbiota of patients with thyroid cancer and thyroid nodules by 16S rRNA gene sequencing of saliva samples from patients with thyroid cancer and thyroid nodules, and healthy controls. The study demonstrated that the richness of saliva microbiota of the patients with thyroid cancer and thyroid nodules was higher than healthy controls, although the difference showed little significance. Several studies have investigated the relationship between the saliva microbiota and cancer (Galloway-Peña et al., 2017; Wang et al., 2019; Zhao et al., 2020). According to our data, the microbial richness was relatively higher in patients with thyroid cancer and thyroid nodules than in healthy controls, though there is no significant difference. Increased saliva microbiota richness has been documented in cancer cases and is believed to be one of the manifestations of oral microbial dysbiosis (Zhang et al., 2019; Wei et al., 2020). Notably, increasing evidence indicates a strong correlation between gut microbes and oral microbes (Arimatsu et al., 2014; Qin et al., 2014; Olsen and Yamazaki, 2019; Maki et al., 2020). There were some studies has reported

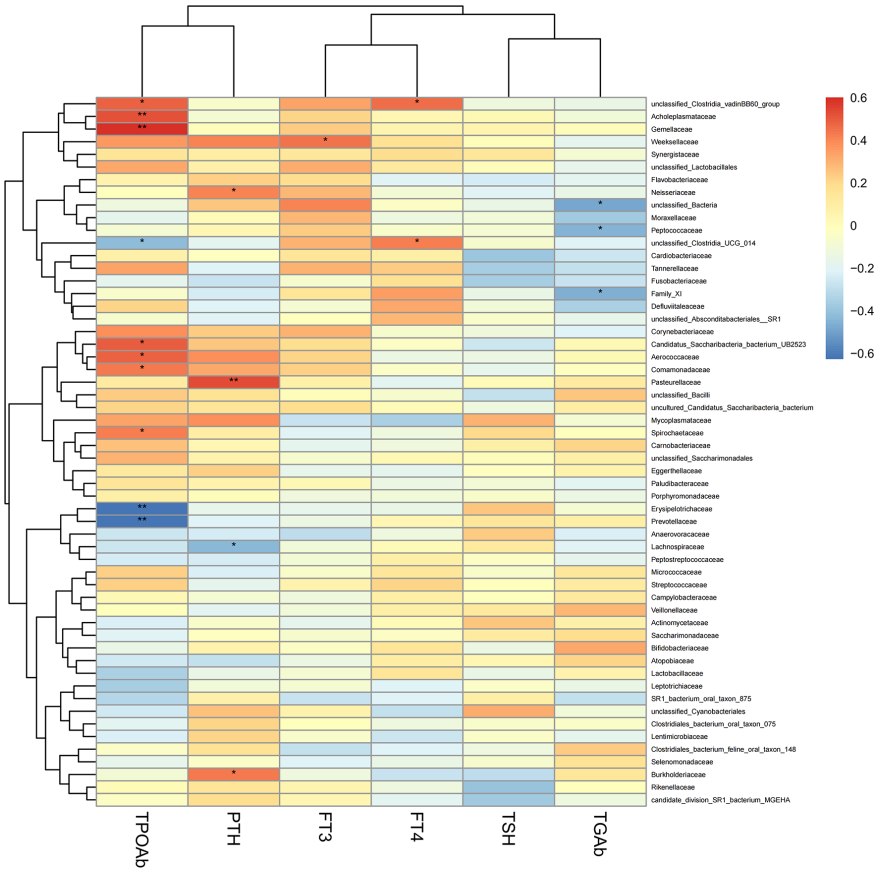

FIGURE 8
Heatmap of Pearson's correlation analysis between the saliva microbiota at the family levels of thyroid cancer and thyroid nodules and clinical variables. R value shows in different colors, red indicates positive correlation while blue indicates negative correlation. The darker the color, the greater the correlation coefficient. Species clustering trees were presented on the left side of the heat map. *P < 0.05; **P < 0.01.

the relationship between gut microbiota and patients with thyroid cancer and thyroid nodules, and some of our findings are consistent with the previous result. In 2018, Zhang et al. found an increase in the richness of the gut microbiota in patients with thyroid cancer and thyroid nodules by the Chao indices (Zhang et al., 2019). In the same year, another study indicated that patients with thyroid cancer show more extraordinary richness and diversity (α-diversity) of gut microbiota compared to healthy controls, as estimated by the Shannon and Chao induces (Feng et al., 2019). However, one opposite result was recently found in patients with thyroid cancer. Xia et al. found that the richness and diversity (α-diversity) of gut microbiota in thyroid cancer patients are significantly increased, as estimated by the Ace and Shannon index. The difference in the results may be related to the sampling area, time, and dietary habits of the patients. Still, most of the above results for the gut microbiota variation in thyroid cancer are consistent with our study.

In addition to changes in richness and diversity, we found a significant difference in the composition of salivary microbiota. The relative abundance of genera Alloprevotella, Anaeroglobus, Acinetobacter, unclassified Bacteroidales, and unclassified Cyanobacteriales was significantly higher in thyroid cancer patients. Genera Alloprevotella inhabits the human oral cavity and is related to but different from genera Prevotella (Downes et al., 2013). Previous studies evaluating the differences in saliva microbiota between patients with pancreatic adenocarcinoma (PDAC) and healthy people observed a significantly increased abundance of Alloprevotella among the patients with bloating in PDAC (Wei et al., 2020). Wu et al. found that the genera Alloprevotella was associated with a higher risk of cardia cancer (Wu et al., 2018). Zhang et al. reported that oral carcinoma showed a significantly higher abundance of genera Alloprevotella (Zhang et al., 2019). Additionally, a prior study indicated that the abundance of genera Alloprevotella as one of the periodontal pathogens has progressively increased along

with the order of controls-PML (premalignant lesions)-OC-SCC (oral cavity squamous cell cancer) and contributed to enriched the variety of proinflammatory genes, which suggests a strong association between Alloprevotella spp. and cancer (Ganly et al., 2019). These studies suggest an increased abundance of Alloprevotella is associated with certain cancers. Additionally, recent studies indicate a strong relationship between the genera Alloprevotella and chromosomal aberrations, which have been shown to be related to the pathogenesis of anaplastic thyroid cancer and impact cancer incidence (Zitzelsberger et al., 2010; Saini et al., 2019; Druzhinin et al., 2020; Farkas et al., 2021). Based on these findings, we conclude that the increased abundance of Alloprevotella in the saliva is associated with thyroid cancer.

A study has demonstrated that the species Anaeroglobus geminatus are associated with the four lipid mediators in human periodontitis (Lee et al., 2021). To the best of our knowledge, inflammation is a hallmark of cancer, and the level of lipid mediators has a relationship with different cancers such as oral cancer, gastric cancer, melanomas, pancreatic cancer, colon cancer, liver cancer, and lung cancer (Sulciner et al., 2018; Biswas et al., 2022). Therefore, we hypothesized that variation in the species Anaeroglobus geminatus might have a relationship with cancer through lipid mediator levels.

Our study found the genera Acinetobacter was enriched in the saliva microbiota of patients with thyroid cancer. A 16s rRNA gene sequencing analysis of thyroid cancer tumor tissues and matched peritumor tissues reveals that the abundance of genus Acinetobacter is significantly enhanced in the tumor tissue. This result accords with our observation which suggested that the genera Acinetobacter could be strongly related to thyroid cancer patients. Besides, the genera Acinetobacter is confirmed to be the potential biomarkers of White-thin coating of GC (gastric cancer) patients using 16S and 18S rRNA high-throughput sequencing (Xu et al., 2019). A 16s rRNA gene sequencing analysis of saliva microbiota found that the genera Acinetobacter shows lower abundance in patients with lung cancer (Yang et al., 2018). The above studies indicate that the genus Acinetobacter plays a vital role in the carcinogenesis of different malignancies.

Regarding the changes in the salivary microbiota of patients with thyroid nodules, our study found that the abundance of Treponema and unclassified Prevotellaceae was significantly increased compared to the healthy population. In reviewing the literature, the genera Treponema shows potential pathogenic importance in autoimmune thyroid disease by molecular mimicry (Benvenga and Guarneri, 2016). Also, the prevalence and abundance of Treponema denticola evaluated by the real-time polymerase chain reaction of dental plaque in patients with esophageal cancer are higher than in healthy people (Kawasaki et al., 2021). The potential mechanisms for Treponema denticola contributing to carcinoma are associated with Treponema denticola chymotrypsin-like proteinase (Nieminen et al., 2018). Therefore, the virulence factor chymotrypsin-like proteinase of the Treponema genera enriched in thyroid nodules may affect the thyroid glands. Both unclassified Prevotellaceae and Prevotella are in the family prevotellaceae. Two studies indicate that the abundance of prevotellaceae is enriched in healthy people compared with thyroid cancer patients using a 16S rRNA analysis of the stool samples (Feng et al., 2019; Ishaq et al., 2022). In our study, we observed that the genera unclassified Prevotellaceae were enriched in salivary microbiota of thyroid nodules patients compared to healthy controls, which is somewhat different from the results of the two studies mentioned above. According to reports, the abundance levels of Prevotella are 11.56% in the microbiota of the throat, palatine tonsils, tongue dorsum, and saliva, and 3.16% in the fecal sample, which has the potential to explain the above opposite results (Segata et al., 2012). The reverse results may be related to the different effects of thyroid cancer and thyroid nodules on the body's microbiota and, more likely, to the differences in the oral and gut microbiota. A previous study that evaluated the shifts of oral microbiota related to pregnancy has indicated that the abundance of genera Treponema spp and Prevotella spp is positively correlated with sex hormones (Lin et al., 2018). Moreover, some studies have suggested that estrogen might play a key role in thyroid nodules (Kim et al., 2010). The above studies show that the genera Treponema and unclassified Prevotellaceae may promote the progress of thyroid nodules.

In our study, we discovered that the genera Alloprevotella enriched in the thyroid cancer group showed a significant negative correlation with the level of TPOAb. Moreover, the genera Treponema ($p < 0.05$, $r = 0.42$) and genera Acholeplasma ($p < 0.01$, $r = 0.53$) enriched in thyroid nodules were positively correlated with TPOAb ($p < 0.05$). The family Spirochaetaceae ($p < 0.05$, $r = 0.42$) and Acholeplasmataceae ($p < 0.01$, $r = 0.53$) enriched in thyroid nodules patients were also significantly associated with the level of TPOAb. Hence, these results suggest that TPOAb is positively associated with parts of oral microbiota enriched in patients with thyroid nodules. However, current studies suggest that the relative role of TPOAb in thyroid nodules and thyroid cancer is unclear and remains to be further elucidated (Boi et al., 2017). Azizi et al. indicated that papillary thyroid carcinoma had a significant association with TSH levels and serum TgAb except for TPOAb in a prospective cytological study (Azizi et al., 2014).

In summary, our results indicated that the composition of saliva microbiota in patients with thyroid decrease is different from healthy controls, especially in some periodontal pathogenic bacteria. However, the mechanism is still not precise. While past studies have focused on changes in gut microbes in patients with thyroid cancer and thyroid nodules, our study presents the first

characterization of salivary microbes in patients with thyroid cancer and thyroid nodules. However, the present study has several limitations that require further investigation. First, this study did not assess the function of bacterial and bacterial metabolites, and the mechanism is uncertain. Second, due to the limited conditions at the sampling time, we did not have a specialist to determine the patient's periodontal condition, and the patient was unaware of any history of periodontal disease. Third, we included a relatively small sample size and did not validate across regions and time. Forth, the detection method is 16S gene sequencing. However, there are still many tentative names and unknown and unclassified bacteria in the database; hence further exploration of multiple groups such as macrogenes is recommended. Fifth, we were unable to observe changes in the microbiota after cancer or nodules development due to the experimental design. Last but not least, our findings should be validated with animal models.

Conclusion

We identified the variation of salivary microbiota is connected with thyroid cancer and thyroid nodules. Based on our preliminary findings, the potential pathogens in thyroid cancer and thyroid nodules are active. However, it is still unknown whether thyroid disease causes dysbiosis of the oral microbiota or dysbiosis of the oral microbiota causes thyroid disease. These findings point the way forward for future research using modelled organisms to scrutinize the underlying mechanisms of the relationship between the salivary microbiome and thyroid disease.

Data availability statement

The data presented in the study was deposited in NCBI Sequence Read Archive (SRA), accession number PRJNA863466.

Ethics statement

The studies involving human participants were reviewed and approved by Medical Ethics Committee of Hospital of Stomatology, Jilin University. The patients/participants provided their written informed consent to participate in this study.

Author contributions

NM, LZ, and JJ designed the study. JJ and YZ interpreted the data and wrote the paper. JJ gathered clinical data. JJ, YZ, DX, and QZ conducted analysis. All authors contributed to the article and approved the submitted version.

Funding

This study was supported by Science and Technology Research Project of Jilin Provincial Education Department (JJKH20221095KJ).

Conflict of interest

The authors declare that the research was conducted in the absence of any commercial or financial relationships that could be construed as a potential conflict of interest.

Publisher's note

All claims expressed in this article are solely those of the authors and do not necessarily represent those of their affiliated organizations, or those of the publisher, the editors and the reviewers. Any product that may be evaluated in this article, or claim that may be made by its manufacturer, is not guaranteed or endorsed by the publisher.

References

Arimatsu, K., Yamada, H., Miyazawa, H., Minagawa, T., Nakajima, M., Ryder, M. I., et al. (2014). Oral pathobiont induces systemic inflammation and metabolic changes associated with alteration of gut microbiota. *Sci. Rep.* 4, 4828–4828. doi: 10.1038/srep04828

Azizi, G., Keller, J. M., Lewis, M., Piper, K., Puett, D., Rivenbark, K. M., et al. (2014). Association of hashimoto's thyroiditis with thyroid cancer. *Endocr. Relat. Cancer* 21 (6), 845–852. doi: 10.1530/ERC-14-0258

Benvenga, S., and Guarneri, F. (2016). Molecular mimicry and autoimmune thyroid disease. *Rev. Endocr. Metab. Disord.* 17 (4), 485–498. doi: 10.1007/s11154-016-9363-2

Biswas, P., Datta, C., Rathi, P., and Bhattacharjee, A. (2022). Fatty acids and their lipid mediators in the induction of cellular apoptosis in cancer cells. *Prostaglandins Other Lipid Mediat* 160, 106637. doi: 10.1016/j.prostaglandins.2022.106637

Boi, F., Pani, F., and Mariotti, S. (2017). Thyroid autoimmunity and thyroid cancer: Review focused on cytological studies. *Eur. Thyroid J.* 6 (4), 178–186. doi: 10.1159/000468928

Bolyen, E., Rideout, J.R., Dillon, M.R., Bokulich, N. A., Abnet, C. C., Al-Ghalith, G. A., et al. (2019). Reproducible, interactive, scalable and extensible microbiome data science using QIIME 2. *Nat. Biotechnol.* 37 (8), 852–857. doi: 10.1038/s41587-019-0209-9

Burman, K. D., and Wartofsky, L. (2015). CLINICAL PRACTICE. thyroid nodules. *N Engl. J. Med.* 373 (24), 2347–2356. doi: 10.1056/NEJMcp1415786

Callahan, B. J., McMurdie, P. J., Rosen, M. J., Han, A. W., Johnson, A. J., Holmes, S. P., et al. (2016). DADA2: High-resolution sample inference from illumina amplicon data. *Nat. Methods* 13 (7), 581–583. doi: 10.1038/nmeth.3869

Chan, W. L., Choi, H. C., Lang, B., Wong, K. P., Yuen, K. K., Lam, K. O., et al. (2021). Health-related quality of life in Asian differentiated thyroid cancer survivors. *Cancer Control* 28, 10732748211029726. doi: 10.1177/10732748211029726

Chen, H., and Boutros, P. C. (2011). VennDiagram: a package for the generation of highly-customizable Venn and Euler diagrams in r. *BMC Bioinf.* 12 (1), 35. doi: 10.1186/1471-2105-12-35

Dong, T., Zhao, F., Yuan, K., Zhu, X., Wang, N., Xia, F., et al. (2021). Association between serum thyroid-stimulating hormone levels and salivary microbiome shifts. *Front. Cell Infect. Microbiol.* 11, 603291. doi: 10.3389/fcimb.2021.603291

Downes, J., Dewhirst, F. E., Tanner, A. C. R., and Wade, W. G. (2013). *Description of alloprevotella rava gen. nov.*, sp. nov., isolated from the human oral cavity, and reclassification of prevotella tannerae Moore et al. 1994 as alloprevotella tannerae gen. nov., comb. nov. *Int. J. Systematic Evolutionary Microbiol.* 63 (Pt 4), 1214–1218. doi: 10.1099/ijs.0.041376-0

Druzhinin, V. G., Matskova, L. V., Demenkov, P. S., Baranova, E. D., Volobaev, V. P., Minina, V. I., et al. (2020). Taxonomic diversity of sputum microbiome in lung cancer patients and its relationship with chromosomal aberrations in blood lymphocytes. *Sci. Rep.* 10 (1), 9681. doi: 10.1038/s41598-020-66654-x

Farkas, G., Kocsis, Z. S., Szekely, G., Dobozi, M., Kenessey, I., Polgar, C., et al. (2021). Smoking, chromosomal aberrations, and cancer incidence in healthy subjects. *Mutat. Res. Genet. Toxicol. Environ. Mutagen* 867, 503373. doi: 10.1016/j.mrgentox.2021.503373

Feng, J., Zhao, F., Sun, J., Lin, B., Zhao, L., Liu, Y., et al. (2019). Alterations in the gut microbiota and metabolite profiles of thyroid carcinoma patients. *Int. J. Cancer* 144 (11), 2728–2745. doi: 10.1002/ijc.32007

Ferlay, J., Soerjomataram, I., Dikshit, R., Eser, S., Mathers, C., Rebelo, M., et al. (2015). Cancer incidence and mortality worldwide: sources, methods and major patterns in GLOBOCAN 2012. *Int. J. Cancer* 136 (5), E359–E386. doi: 10.1002/ijc.29210

Galloway-Peña, J. R., Smith, D. P., Sahasrabhojane, P., Wadsworth, W. D., Fellman, B. M., Ajami, N. J., et al. (2017). Characterization of oral and gut microbiome temporal variability in hospitalized cancer patients. *Genome Med.* 9 (1), 21. doi: 10.1186/s13073-017-0409-1

Ganly, I., Yang, L., Giese, R. A., Hao, Y., Nossa, C. W., Morris, L. G. T., et al. (2019). Periodontal pathogens are a risk factor of oral cavity squamous cell carcinoma, independent of tobacco and alcohol and human papillomavirus. *Int. J. Cancer* 145 (3), 775–784. doi: 10.1002/ijc.32152

Goswami, S., Mongelli, M., Peipert, B. J., Helenowski, I., Yount, S. E., and Sturgeon, C. (2018). Benchmarking health-related quality of life in thyroid cancer versus other cancers and united states normative data. *Surgery* 164 (5), 986–992. doi: 10.1016/j.surg.2018.06.042

Haymart, M. R., Repplinger, D. J., Leverson, G. E., Elson, D. F., Sippel, R. S., Jaume, J. C., et al. (2008). Higher serum thyroid stimulating hormone level in thyroid nodule patients is associated with greater risks of differentiated thyroid cancer and advanced tumor stage. *J. Clin. Endocrinol. Metab.* 93 (3), 809–814. doi: 10.1210/jc.2007-2215

Irfan, M., Delgado, R. Z. R., and Frias-Lopez, J. (2020). The oral microbiome and cancer. *Front. Immunol.* 11, 591088. doi: 10.3389/fimmu.2020.591088

Ishaq, H. M., Mohammad, I. S., Hussain, R., Parveen, R., Shirazi, J. H., Fan, Y., et al. (2022). Gut-thyroid axis: How gut microbial dysbiosis associated with euthyroid thyroid cancer. *J. Cancer* 13 (6), 2014–2028. doi: 10.7150/jca.66816

Kawasaki, M., Ikeda, Y., Ikeda, E., Takahashi, M., Tanaka, D., Nakajima, Y., et al. (2021). Oral infectious bacteria in dental plaque and saliva as risk factors in patients with esophageal cancer. *Cancer* 127 (4), 512–519. doi: 10.1002/cncr.33316

Kim, M. H., Park, Y. R., Lim, D. J., Yoon, K. H., Kang, M. I., Cha, B. Y., et al. (2010). The relationship between thyroid nodules and uterine fibroids. *Endocr. J.* 57 (7), 615–621. doi: 10.1507/endocrj.K10E-024

Kim, J., Gosnell, J. E., and Roman, S. A. (2020). Geographic influences in the global rise of thyroid cancer. *Nat. Rev. Endocrinol.* 16 (1), 17–29. doi: 10.1038/s41574-019-0263-x

Kitahara, C. M., and Sosa, J. A. (2016). The changing incidence of thyroid cancer. *Nat. Rev. Endocrinol.* 12 (11), 646–653. doi: 10.1038/nrendo.2016.110

Kitamoto, S., Nagao-Kitamoto, H., Hein, R., Schmidt, T. M., and Kamada, N. (2020). The bacterial connection between the oral cavity and the gut diseases. *J. Dent. Res.* 99 (9), 1021–1029. doi: 10.1177/0022034520924633

Kwak, J. Y., Han, K. H., Yoon, J. H., Moon, H. J., Son, E. J., Park, S. H., et al. (2011). Thyroid imaging reporting and data system for US features of nodules: a step in establishing better stratification of cancer risk. *Radiology* 260 (3), 892–899. doi: 10.1148/radiol.11110206

Lee, C. T., Li, R., Zhu, L., Tribble, G. D., Zheng, W. J., Ferguson, B., et al. (2021). Subgingival microbiome and specialized pro-resolving lipid mediator pathway profiles are correlated in periodontal inflammation. *Front. Immunol.* 12, 691216. doi: 10.3389/fimmu.2021.691216

Li, D., Xi, W., Zhang, Z., Ren, L., Deng, C., Chen, J., et al. (2020). Oral microbial community analysis of the patients in the progression of liver cancer. *Microb. Pathog.* 149, 104479. doi: 10.1016/j.micpath.2020.104479

Li, A., Li, T., Gao, X., Yan, H., Chen, J., Huang, M., et al. (2021). Gut microbiome alterations in patients with thyroid nodules. *Front. Cell Infect. Microbiol.* 11, 643968. doi: 10.3389/fcimb.2021.643968

Lin, W., Jiang, W., Hu, X., Gao, L., Ai, D., Pan, H., et al. (2018). Ecological shifts of supragingival microbiota in association with pregnancy. *Front. Cell Infect. Microbiol.* 8, 24. doi: 10.3389/fcimb.2018.00024

Lortet-Tieulent, J., Franceschi, S., Dal Maso, L., and Vaccarella, S. (2019). Thyroid cancer "epidemic" also occurs in low- and middle-income countries. *Int. J. Cancer* 144 (9), 2082–2087. doi: 10.1002/ijc.31884

Lozupone, C., and Knight, R. (2005). UniFrac: a new phylogenetic method for comparing microbial communities. *Appl. Environ. Microbiol.* 71 (12), 8228–8235. doi: 10.1128/AEM.71.12.8228-8235.2005

Maki, K. A., Kazmi, N., Barb, J. J., and Ames, N. (2020). The oral and gut bacterial microbiomes: Similarities, differences, and connections. *Biol. Res. For Nurs.* 23 (1), 7–20. doi: 10.1177/1099800420941606

Maruvada, P., Leone, V., Kaplan, L. M., and Chang, E. B. (2017). The human microbiome and obesity: Moving beyond associations. *Cell Host Microbe* 22 (5), 589–599. doi: 10.1016/j.chom.2017.10.005

Nieminen, M. T., Listyarifah, D., Hagström, J., Haglund, C., Grenier, D., Nordström, D., et al. (2018). Treponema denticola chymotrypsin-like proteinase may contribute to orodigestive carcinogenesis through immunomodulation. *Br. J. Cancer* 118 (3), 428–434. doi: 10.1038/bjc.2017.409

Olsen, I., and Yamazaki, K. (2019). Can oral bacteria affect the microbiome of the gut? *J. Oral. Microbiol.* 11 (1), 1586422. doi: 10.1080/20002297.2019.1586422

Park, S. Y., Hwang, B. O., Lim, M., Ok, S. H., Lee, S. K., Chun, K. S., et al. (2021). Oral-gut microbiome axis in gastrointestinal disease and cancer. *Cancers (Basel)* 13 (9), 2124. doi: 10.3390/cancers13092124

Peters, B. A., Wu, J., Pei, Z., Yang, L., Purdue, M. P., Freedman, N. D., et al. (2017). Oral microbiome composition reflects prospective risk for esophageal cancers. *Cancer Res.* 77 (23), 6777–6787. doi: 10.1158/0008-5472.CAN-17-1296

Qin, N., Yang, F., Li, A., Prifti, E., Chen, Y., and Shao, L. (2014). Alterations of the human gut microbiome in liver cirrhosis. *Nature* 513 (7516), 59–64.

Saini, S., Maker, A. V., Burman, K. D., and Prabhakar, B. S. (2019). Molecular aberrations and signaling cascades implicated in the pathogenesis of anaplastic thyroid cancer. *Biochim. Biophys. Acta Rev. Cancer* 1872 (2), 188262. doi: 10.1016/j.bbcan.2018.12.003

Segata, N., Izard, J., Waldron, L., Gevers, D., Miropolsky, L., Garrett, W. S., et al. (2011). Metagenomic biomarker discovery and explanation. *Genome Biol.* 12 (6), R60. doi: 10.1186/gb-2011-12-6-r60

Segata, N., Haake, S. K., Mannon, P., Lemon, K. P., Waldron, L., Gevers, D., et al. (2012). Composition of the adult digestive tract bacterial microbiome based on seven mouth surfaces, tonsils, throat and stool samples. *Genome Biol.* 13 (6), R42. doi: 10.1186/gb-2012-13-6-r42

Sheng, D., Zhao, S., Gao, L., Zheng, H., Liu, W., Hou, J., et al. (2019). BabaoDan attenuates high-fat diet-induced non-alcoholic fatty liver disease via activation of AMPK signaling. *Cell Biosci.* 9, 77. doi: 10.1186/s13578-019-0339-2

Singer, S., Lincke, T., Gamper, E., Bhaskaran, K., Schreiber, S., Hinz, A., et al. (2012). Quality of life in patients with thyroid cancer compared with the general population. *Thyroid* 22 (2), 117–124. doi: 10.1089/thy.2011.0139

Stefura, T., Zapała, B., Gosiewski, T., Skomarovska, O., Dudek, A., Pędziwiatr, M., et al. (2021). Differences in compositions of oral and fecal microbiota between patients with obesity and controls. *Medicina (Kaunas)* 57 (7), 678. doi: 10.3390/medicina57070678

Sulciner, M. L., Gartung, A., Gilligan, M. M., Serhan, C. N., and Panigrahy, D. (2018). Targeting lipid mediators in cancer biology. *Cancer Metastasis Rev.* 37 (2-3), 557–572. doi: 10.1007/s10555-018-9754-9

Sung, H., Ferlay, J., Siegel, R. L., Laversanne, M., Soerjomataram, I., Jemal, A., et al. (2021). Global cancer statistics 2020: GLOBOCAN estimates of incidence and mortality worldwide for 36 cancers in 185 countries. *CA Cancer J. Clin.* 71 (3), 209–249. doi: 10.3322/caac.21660

Tuominen, H., and Rautava, J. (2021). Oral microbiota and cancer development. *Pathobiology* 88 (2), 116–126. doi: 10.1159/000510979

Uchino, Y., Goto, Y., Konishi, Y., Tanabe, K., Toda, H., Wada, M., et al. (2021). Colorectal cancer patients have four specific bacterial species in oral and gut microbiota in common-a metagenomic comparison with healthy subjects. *Cancers (Basel)* 13 (13), 3332. doi: 10.3390/cancers13133332

Wang, L., Yin, G., Guo, Y., Zhao, Y., Zhao, M., Lai, Y., et al. (2019). Variations in oral microbiota composition are associated with a risk of throat cancer. *Front. Cell Infect. Microbiol.* 9, 205. doi: 10.3389/fcimb.2019.00205

Wei, A. L., Li, M., Li, G. Q., Wang, X., Hu, W. M., Li, Z. L., et al. (2020). Oral microbiome and pancreatic cancer. *World J. Gastroenterol.* 26 (48), 7679–7692. doi: 10.3748/wjg.v26.i48.7679

Wu, J., Xu, S., Xiang, C., Cao, Q., Li, Q., Huang, J., et al. (2018). Tongue coating microbiota community and risk effect on gastric cancer. *J. Cancer* 9 (21), 4039–4048. doi: 10.7150/jca.25280

Xu, J., Xiang, C., Zhang, C., Xu, B., Wu, J., Wang, R., et al. (2019). Microbial biomarkers of common tongue coatings in patients with gastric cancer. *Microb. Pathog.* 127, 97–105. doi: 10.1016/j.micpath.2018.11.051

Yang, J., Mu, X., Wang, Y., Zhu, D., Zhang, J., Liang, C., et al. (2018). Dysbiosis of the salivary microbiome is associated with non-smoking female lung cancer and correlated with immunocytochemistry markers. *Front. Oncol.* 8, 520. doi: 10.3389/fonc.2018.00520

Yang, C., Xu, Z., Deng, Q., Huang, Q., Wang, X., Huang, F., et al. (2020). Beneficial effects of flaxseed polysaccharides on metabolic syndrome via gut microbiota in high-fat diet fed mice. *Food Res. Int.* 131, 108994. doi: 10.1016/j.foodres.2020.108994

Zhang, J., Zhang, F., Zhao, C., Xu, Q., Liang, C., Yang, Y., et al. (2019). Dysbiosis of the gut microbiome is associated with thyroid cancer and thyroid nodules and correlated with clinical index of thyroid function. *Endocrine* 64 (3), 564–574. doi: 10.1007/s12020-018-1831-x

Zhang, W., Luo, J., Dong, X., Zhao, S., Hao, Y., Peng, C., et al. (2019). Salivary microbial dysbiosis is associated with systemic inflammatory markers and predicted oral metabolites in non-small cell lung cancer patients. *J. Cancer* 10 (7), 1651–1662. doi: 10.7150/jca.28077

Zhang, L., Liu, Y., Zheng, H. J., Zhang, C. P., et al. (2019). The oral microbiota may have influence on oral cancer. *Front. Cell Infect. Microbiol.* 9, 476. doi: 10.3389/fcimb.2019.00476

Zhao, Q., Yang, T., Yan, Y., Zhang, Y., Li, Z., Wang, Y., et al. (2020). Alterations of oral microbiota in Chinese patients with esophageal cancer. *Front. Cell. Infection Microbiol.* 10. doi: 10.3389/fcimb.2020.541144

Zitzelsberger, H., Thomas, G., and Unger, K. (2010). Chromosomal aberrations in thyroid follicular-cell neoplasia: in the search of novel oncogenes and tumour suppressor genes. *Mol. Cell Endocrinol.* 321 (1), 57–66. doi: 10.1016/j.mce.2009.11.014

frontiers | Frontiers in Cellular and Infection Microbiology

TYPE Original Research
PUBLISHED 12 August 2022
DOI 10.3389/fcimb.2022.983608

OPEN ACCESS

EDITED BY
Zheng Zhang,
Nankai University, China

REVIEWED BY
Shan Jiang,
Southern Medical University, China
Zhibin Du,
Queensland University of Technology, Australia
Li Lin,
China Medical University, China

*CORRESPONDENCE
Fuhua Yan
yanfh@nju.edu.cn
Yanfen Li
liyanfen2003@126.com

†These authors have contributed equally to this work

SPECIALTY SECTION
This article was submitted to Extra-intestinal Microbiome, a section of the journal Frontiers in Cellular and Infection Microbiology

RECEIVED 01 July 2022
ACCEPTED 15 July 2022
PUBLISHED 12 August 2022

CITATION
Wang N, Zheng L, Qian J, Wang M, Li L, Huang Y, Zhang Q, Li Y and Yan F (2022) Salivary microbiota of periodontitis aggravates bone loss in ovariectomized rats. *Front. Cell. Infect. Microbiol.* 12:983608. doi: 10.3389/fcimb.2022.983608

Salivary microbiota of periodontitis aggravates bone loss in ovariectomized rats

Nannan Wang†, Lichun Zheng†, Jun Qian, Min Wang, Lili Li, Yuezhen Huang, Qian Zhang, Yanfen Li* and Fuhua Yan*

Department of General Dentistry, Nanjing Stomatological Hospital, Medical School of Nanjing University, Nanjing, China

The mechanisms underlying the crosstalk between periodontitis and osteoporosis remain unclear. Recently, the gut microbiota has been recognized as a pivotal regulator of bone metabolism, and oral and gut mucosae are microbiologically connected. In this study, we investigated the effects of periodontitis on osteoporosis through the oral-gut axis. The salivary microbiota of patients with periodontitis was collected and then pumped into the intestine of Sprague–Dawley rats *via* intragastric administration for 2 weeks. An osteoporosis model was established using ovariectomy. Changes in the maxillae and femora were evaluated using microcomputed tomography (micro CT) and HE staining. Intestinal barrier integrity and inflammatory factors were examined using real-time quantitative polymerase chain reaction and immunofluorescence. The gut microbiota was profiled by 16S rRNA gene sequencing. Metabolome profiling of serum was performed using liquid chromatography-mass spectrometry sequencing. Micro CT and HE staining revealed osteoporotic phenotypes in the maxillae and femora of ovariectomized (OVX) rats. Our results confirmed that the salivary microbiota of patients with periodontitis aggravated femoral bone resorption in OVX rats. In addition, intestinal inflammation was exacerbated after periodontitis salivary microbiota gavage in OVX rats. Correlation analysis of microbiota and metabolomics revealed that lipolysis and tryptophan metabolism may be related to the bone loss induced by the salivary microbiota of patients with periodontitis. In conclusion, periodontitis can aggravate long bone loss through the oral-gut axis in OVX rats.

KEYWORDS

periodontitis, osteoporosis, salivary microbiota, gut microbiota, bone loss

Introduction

Periodontitis is a chronic inflammatory disease caused by dysbiosis of the periodontal microbiota, resulting in resorption of alveolar bone and destruction of the periodontal ligament. The alveolar bone is responsive to the oral microenvironment and influenced by systemic metabolism (Hathaway-Schrader and Novince, 2021). Osteoporosis is characterized by low bone mass and deterioration of the trabecular microstructure, which often occurs in elderly individuals, especially postmenopausal women. Previous studies have revealed a positive association between periodontitis and osteoporosis (Luo et al., 2014; Xu et al., 2021); however, the mechanism by which periodontitis influences systemic skeletal metabolism remains unclear.

The gut microbiota has emerged as an important regulatory factor of bone metabolism (Chen et al., 2017; Li et al., 2019; Chevalier et al., 2020) and is necessary for the pathological process of bone loss in ovariectomized (OVX) animal models (Yuan et al., 2022). A large population-based study showed that the genera *Bacteroides*, *Blautia*, *Phascolarctobacterium*, *Oscillospira*, *Ruminococcaceae* and *Actinobacillus* were elevated in osteoporosis (Ling et al., 2021). Probiotics such as *Lactobacillus reuteri* and *Lactobacillus rhamnosus* significantly decrease the intestinal permeability and prevent bone loss (Britton et al., 2014; Li et al., 2016). Furthermore, metabolites produced by the gut microbiota—such as short-chain fatty acids, amino acids, and polyamines—are related to the change of systemic bone mass (Lucas et al., 2018; Chevalier et al., 2020; Ling et al., 2021).

The oral cavity, which is the entry site into the gastrointestinal tract, harbors diverse microbial communities (Peng et al., 2022), and previous reports support the hypothesis that oral and gastrointestinal mucosae are microbiologically connected (Read et al., 2021; Bao et al., 2022). In addition, the salivary microbiota of periodontitis, which is rich in oral pathobionts, can translocate from the oral cavity to the intestine and disrupt the colonization resistance of gut-resident microbiota (Kitamoto et al., 2020). Our previous study demonstrated that treatment with the periodontitis salivary microbiota can lead to gut dysbiosis and worsen colitis (Qian et al., 2022a). Therefore, we speculate that the oral-gut axis might play a pivotal role in periodontitis affecting the systemic diseases.

Currently, studies on the salivary microbiota in periodontitis have mainly adopted the method of single-strain or *in vitro* culture. To better simulate the complex oral microbiota in periodontitis, we collected salivary microbiota from patients with periodontitis. Subsequently, we explored the effect of the periodontitis salivary microbiota on bone mass in rats with OVX-induced osteoporosis, where the potential biological pathways—including the gut barrier, microbiota, and metabolic profiling—were also explored (Supplementary Figure S1).

Materials and methods

Patient saliva collection and preparation

Patients diagnosed with periodontitis were recruited from the Nanjing Stomatological Hospital, Medical School of Nanjing University (NJSH-2021NL-93). The inclusion criteria were as follows: (1) patients diagnosed with Stage III or IV periodontitis based on the new classification proposed in the 2017 AAP and EAP World Workshop, and (2) patients over the age of 18. The exclusion criteria were set as follows: (1) patients who had received periodontal therapy in the last 12 months; (2) patients who had received medication in the last 6 months; and (3) patients with systemic disease, psychiatric disorders, pregnancy or lactation, and other oral diseases that might affect the periodontal status. All the included patients were confirmed by an experienced periodontist. A total of 18 eligible patients were recruited for the present study.

Unstimulated salivary samples were collected and analyzed using a previously described method (Atarashi et al., 2017). Briefly, saliva samples were mixed with an equal volume (w/v) of phosphate-buffered saline (PBS) containing 20% glycerol/PBS, later snap-frozen in liquid nitrogen, and then stored at −80°C until use.

Animals and experimental design

The experimental animal protocol was approved by the ethics authorities of Nanjing Agriculture University (PZW2021026). Thirty-two female Sprague-Dawley rats (9-week-old) were purchased and kept in a specific pathogen-free facility. After a 3-week adaptation period, the rats were anesthetized and either sham-operated (Sham) or bilaterally ovariectomized (OVX). At 10 weeks after the operation, the rats were gavaged with PBS or the salivary microbiota of patients with periodontitis. Before the intragastric administration, the frozen salivary samples were thawed, centrifuged at 3,300 × *g* for 10 min at 4°C, and suspended in an equal volume of PBS. The saliva samples from different patients were well mixed when used. Each rat was given 1 mL of liquid (PBS or saliva) every other day for 2 weeks. All rats were then sacrificed, and samples were collected for subsequent tests. The rats were randomly and equally allocated to the following groups:

1. ShamPBS group: sham-operated and PBS gavaged;
2. ShamSP group: sham-operated and gavaged with the salivary microbiota of patients with periodontitis;
3. OVXPBS group: ovariectomized and PBS gavaged;
4. OVXSP group: ovariectomized and gavaged with the salivary microbiota of patients with periodontitis.

Microcomputed tomography analysis

Femora and maxillae dissected from rats were fixed in 4% paraformaldehyde for 72 h and scanned using micro-computed tomography (micro-CT) with a Skyscan 1176 scanner (Bruker, Karlsruhe, Germany). Data Viewer and CTAn software were used to analyze bone parameters. Bone mineral density (BMD) was obtained using two hydroxyapatite [$Ca_{10}(PO_4)_6(OH)_2$] phantoms with BMD values of 0.250 and 0.750 g/cm^3 as a reference.

The region of interest for the femoral trabecular was set at 1.00 from the distal growth plate level, extending toward the proximal femora (112 slides). For maxillae, trabecular morphometry was measured in the furcation area of the left maxillary second molar root, as previously described, with minor modifications (Dai et al., 2014; Johnston and Ward, 2015). The trabecular parameters of bone volume versus total volume ratio (BV/TV), trabecular thickness (Tb.Th), trabecular spacing (Tb.Sp), and trabecular number (Tb.N) were measured and quantified.

Histological analysis

Femora and maxillae were decalcified and embedded in paraffin blocks. Sections were prepared for hematoxylin and eosin (HE) staining. PANNORAMIC MIDI (3DHISTECH Ltd., Budapest, Hungary) and CaseViewer software were used to scan and evaluate the sections.

Tartrate-resistant acid phosphatase staining

The number of osteoclasts was quantified using tartrate-resistant acid phosphatase (TRAP) staining of femurs. The sections were evaluated using the CaseViewer software. The osteoclast numbers were calculated by averaging each section's four different visual regions in each section.

Immunofluorescence analysis

Immunofluorescent staining was performed to determine the expression of zona occludens protein 1 (ZO-1) in the colon. Briefly, sections were incubated with rabbit anti-ZO-1 (Servicebio, Wuhan, China) overnight at 4°C and incubated with a cyanine 3-conjugated goat anti-rabbit IgG secondary antibody (Servicebio, Wuhan, China). Nuclei were then stained with 4′,6-diamidino-2-phenylindole for 10 min. A confocal laser microscope (NikonA1, Nikon Inc., Tokyo, Japan) was used to obtain the images.

Serum analysis

The levels of high-density lipoprotein cholesterol (HDL-C) (Fosun Diagnostics, Shanghai, China) and low-density lipoprotein cholesterol (LDL-C) (Fosun Diagnostics, Shanghai, China) in serum were assayed using a Siemens ADVIA 1800 Automated Chemistry Analyzer. In addition, serum levels of CTX-I (Cusabio, Wuhan, China) were measured using enzyme-linked immunosorbent assay (ELISA) according to the manufacturer's instructions.

Colonic RNA preparation and quantitative polymerase chain reaction

RNA was extracted from colonic tissues using the RNAprep Pure Tissue Kit (Tiangen, Beijing, China) and then reverse-transcribed into cDNA using the HiScript III RT SuperMix (Vazyme, Nanjing, China). An ABI ViiA 7 detection system (Thermo Fisher Scientific, Waltham, USA) was used for quantitative polymerase chain reaction (qPCR) following the manufacturer's instructions. All reactions were carried out in triplicate. Analysis was performed using the $2^{-\Delta\Delta Ct}$ method. The β-actin was set as the housekeeping gene. The primers used in this study are listed in Supplementary Table S1.

Gut microbiota analysis

Cecal samples were collected after sacrificing the rats, then snap-frozen and stored at –80°C. 16S rRNA sequencing was conducted by OeBiotech (Shanghai, China). Briefly, microbial DNA was isolated from cecum samples using MagPure Soil DNA LQ Ki (Magen, Guangzhou, China). The V3-V4 region of the 16S rRNA gene was amplified. Sequencing was performed using an Illumina NovaSeq6000 system (Illumina Inc., CA, USA). The original two-terminal sequence was dehybridized using Trimmomatic software. Clean reads were subjected to primer sequence removal and clustering to generate operational taxonomic units (OTUs) using the VSEARCH software with a threshold of 97% similarity. All representative reads were assigned to a taxon using the Ribosomal Database Project classifier (confidence threshold of 70%) against the Silva database (version 132). The α/β indices were calculated using QIIME (Version 1.8.0).

Metabolome profiling of serum

Metabolome profiling of serum was performed using chromatography-mass spectrometry (LC-MS) sequencing, as previously described (Zhang P. et al., 2021). Data were

processed using Progenesis QI V2.3 (Nonlinear). Online databases, including the Human Metabolome Database, Metlin, Electron Microscopy Data Bank, Lipidmaps (V2.3), and Protein Model DataBase, were used to qualify the data. Orthogonal partial least squares discriminant analysis (OPLS-DA) was used to identify the metabolites of different groups and obtain variable importance of projection (VIP) values. The pathways involved in the differential metabolites were annotated using the metabolic pathways in the Kyoto Encyclopedia of Genes and Genomes (KEGG) database (https://www.kegg.jp).

Statistics

The statistical analyses were carried out by GraphPad Prism 9 unless otherwise specified. Differences between two groups were evaluated using a two-tailed Student's *t*-test (parametric) or the Mann-Whitney U test (nonparametric). For more than two groups, one-way analysis of variance (ANOVA; parametric) or the Kruskal–Wallis test (nonparametric) was performed, followed by Bonferroni's multiple comparisons test. A value of $p < 0.05$ was considered significantly significant.

Results

OVX reduces bone density of alveolar bone

A schematic diagram is shown in Figure 1A. Body weight increased rapidly following OVX surgery (Figure 1B). Treatment with the periodontitis salivary microbiota alone showed no effect on the gain rates of body weight and HDL-C levels compared with PBS gavage ($p > 0.05$) (Figure 1C). LDL-C levels in the OVXSP rats were higher than those in the OVXPBS rats ($p < 0.05$). Neither HDL-C nor LDL-C showed statistically significant differences between the ShamPBS and ShamSP rats (Figure 1D).

To investigate the effects of OVX surgery and periodontitis salivary microbiota on the alveolar bone, we determined the microstructure of the trabeculae using micro-CT. The OVXPBS and OVXSP groups had a porous microarchitecture (Supplementary Figure 2), including a lower BMD (Figure 1E) and looser construction of more widely separated trabeculae than the ShamPBS and ShamSP groups (Figures 1F–I). HE staining revealed that the area of the periodontal ligament increased in the root furcation of OVX rats (Figure 1J), suggesting that the interradicular bone mass reduced as a result of OVX surgery. Furthermore, the serum CTX-I levels were significantly increased after OVX ($p < 0.05$) (Figure 1K); thus, an osteoporotic phenotype was successfully established in the alveolar bone. Nevertheless, no significant changes in alveolar bone were observed after intragastric administration of PBS or periodontitis salivary microbiota (Figures 1E–J).

Salivary microbiota of periodontitis patients aggravates long bone loss in OVX rats

Micro-CT analysis and HE staining validated an osteoporotic phenotype in the femurs of OVX rats (Figures 2A, B). Furthermore, the periodontitis salivary microbiota gavage led to a significant decrease in bone mass and impaired bone microstructure of the femurs in OVX rats, as indicated by lower BMD, BV/TV, and Tb.N, and a higher Tb.Sp, compared to the OVXPBS group; in contrast, no difference was observed between the ShamPBS and ShamSP groups (Figures 2C–G). Histological analysis showed that the trabecular bone area of the femur in the OVXSP group was markedly smaller than that in the OVXPBS group (Figure 2B). Osteoclasts were almost absent in the trabecular region, except in the growth plate, of the femur in OVX rats (Figure 2H), suggesting that the destruction of trabeculae had peaked. The largest number of osteoclasts was observed in the ShamSP group (Figures 2H, I). These results suggest that the salivary microbiota of patients with periodontitis aggravates long bone loss, particularly in OVX rats.

OVX and salivary microbiota affect intestinal inflammation

To determine whether the periodontitis salivary microbiota affects intestinal barrier integrity, the expression of tight junction (TJ) proteins was analyzed. Immunohistochemical staining showed lower ZO-1 expression in the colon of OVX rats (Figure 3A), while the transcription of ZO-1 and occludin was also downregulated in these rats (Figures 3B, C). No significant difference in ZO-1 or occludin was observed after the periodontitis salivary microbiota treatment in this experiment. The OVX rats exhibited a higher IL-1β mRNA expression; moreover, the expression of IL-1β mRNA was significantly elevated after gavage with the periodontitis salivary microbiota ($p < 0.05$) (Figure 3D). The above results indicate that OVX may impair intestinal barrier integrity; furthermore, OVX and periodontitis salivary microbiota may have a synergistic effect in promoting intestinal inflammation.

Salivary microbiota alters the microbiota composition

Previous studies have demonstrated crosstalk between the gut microbiota and bone metabolism. In order to reveal the

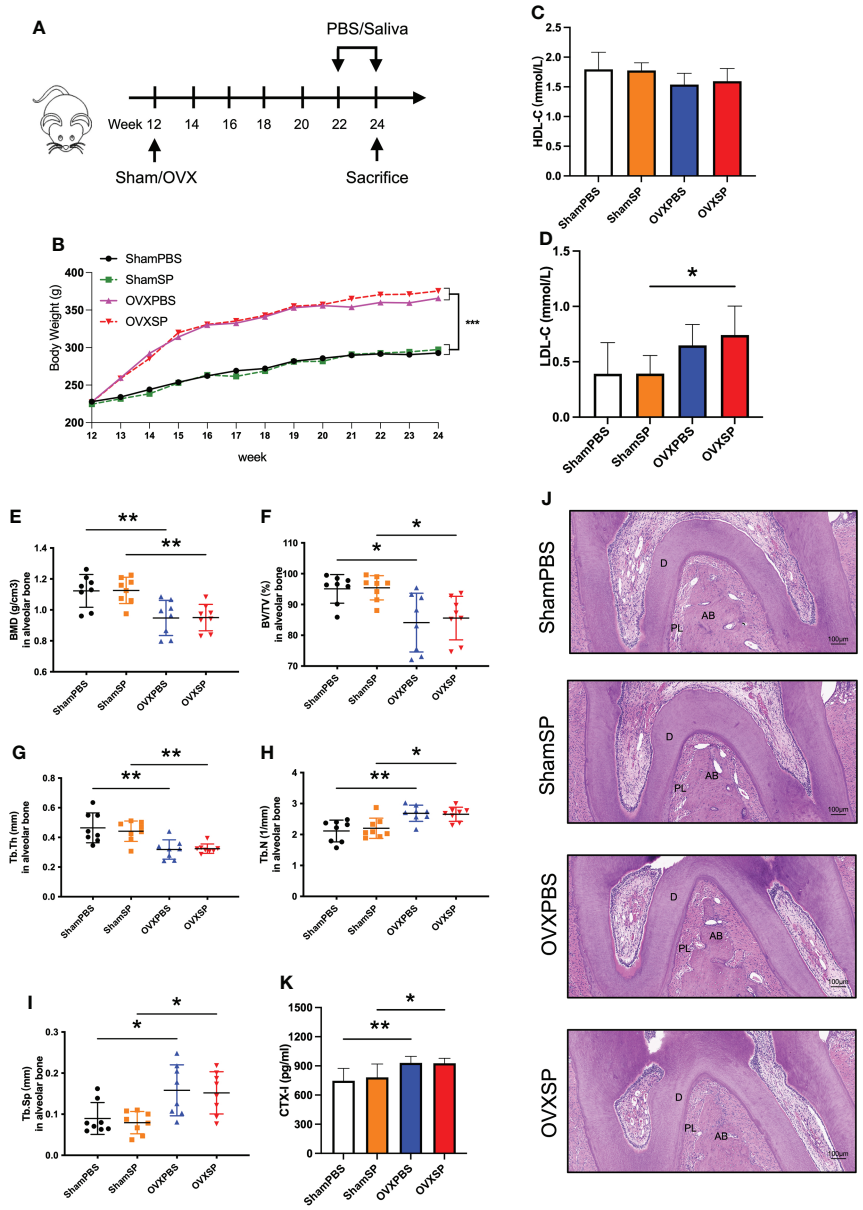

FIGURE 1
Effects of OVX and salivary microbiota treatment on alveolar bone. **(A)** Experimental schematic diagram. **(B)** Line chart of body weight change in rats. **(C)** HDL-C and **(D)** LDL-C levels in serum from the four groups. **(E–I)** Quantitative analysis of bone-related parameters. Compared to the Sham groups, the OVX groups exhibited significant trabecular bone loss at furcation area of the maxillary second molar, which showed decreased BMD **(E)**, BV/TV **(F)**, Tb.Th **(G)**, Tb.N **(H)**, and a higher Tb.Sp **(I)**. **(J)** Representative images of HE staining of alveolar bone. **(K)** Serum CTX-I levels measured using ELISA. Data are presented as the mean ± SD (n = 8/group). AB, alveolar bone; D, dentine; PL, periodontal ligament area. Scale bar = 100 μm. *$p < 0.05$ and **$p < 0.01$.

possible mechanism of the oral-gut axis in treatment with salivary microbiota of patients with periodontitis, alterations in the gut microbiota were analyzed by detecting the 16S rRNA gene. The indices of α diversity (Observed, Shannon, Chao1) in OVX rats were significantly higher than those in Sham rats ($p < 0.05$; Figure 4A). Furthermore, the salivary microbiota of periodontitis slightly reduced the observed species diversity in OVX rats but not in Sham rats, which is similar to the trabecular phenotype of the femur. Principal component analysis (PCA) revealed distinct clustering of the gut microbiota composition in the four groups (Figure 4B). The ratio of *Firmicutes* to *Bacteroidota*, a known marker of obesity, was elevated in OVX rats (Figure 4C), consistent with the changes in weight and LDL-L. At the family level, the OVXSP group possessed a significantly

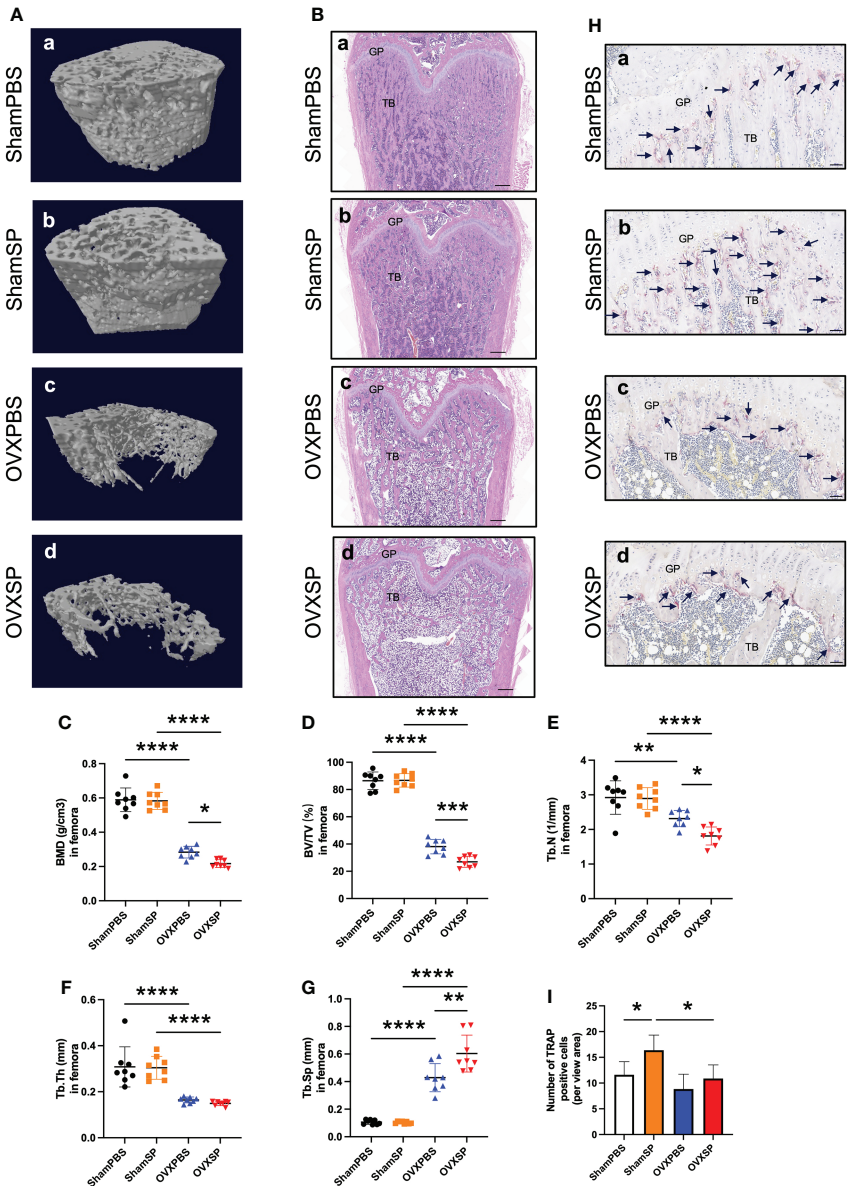

FIGURE 2
Effects of OVX and salivary microbiota treatment on the femur. **(A)** Representative reconstruction of trabeculae in the femurs used for analysis. **(B)** Representative images of the HE-stained femurs. Scale bar = 500 μm. **(C–G)** Quantitative analysis of bone-related parameters. Compared to the OVXPBS group, the OVXSP group had a significant decrease in bone mass and impaired bone microstructure; **(C)** BMD, **(D)** BV/TV, **(E)** Tb.N, **(F)** Tb.Th, and **(G)** Tb.Sp (n = 8/group). **(H, I)** Immunohistological analysis of TRAP staining (n = 6/group). Arrows indicate TRAP+ cells. Scale bar = 50 μm. Data are presented as the mean ± SD. GP, growth plate; TB, trabecular bone. *$p < 0.05$, **$p < 0.01$, ***$p < 0.001$, and ****$p < 0.0001$.

higher relative abundance of *Lactobacillaceae* than the OVXPBS group ($p < 0.05$; Figure 4D). To further identify the gut microbial composition affected by the salivary microbiota of patients with periodontitis, the relative abundance of the gut microbiota at the genus level was compared. The abundance of 77 genera (29 genera in Sham rats and 48 genera in OVX rats) significantly changed in response to treatment with periodontitis salivary microbiota (Supplementary Figures 3A, B). We then integrated the differential gut microbiota using random forest analysis (Supplementary Figures S3C, D). Specifically, after gavage with saliva, a significant increase in *Prevotella, Colidextribacter and Pygmaiobacter* abundances, as well as a decrease in that of *Lachnospiraceae_NK4A136*, were detected in the Sham rats (Figure 4E). However, the salivary microbiota exhibited a completely different effect on the gut microbiota composition in OVX rats. The OVXSP group presented higher amounts of

10.3389/fcimb.2022.983608

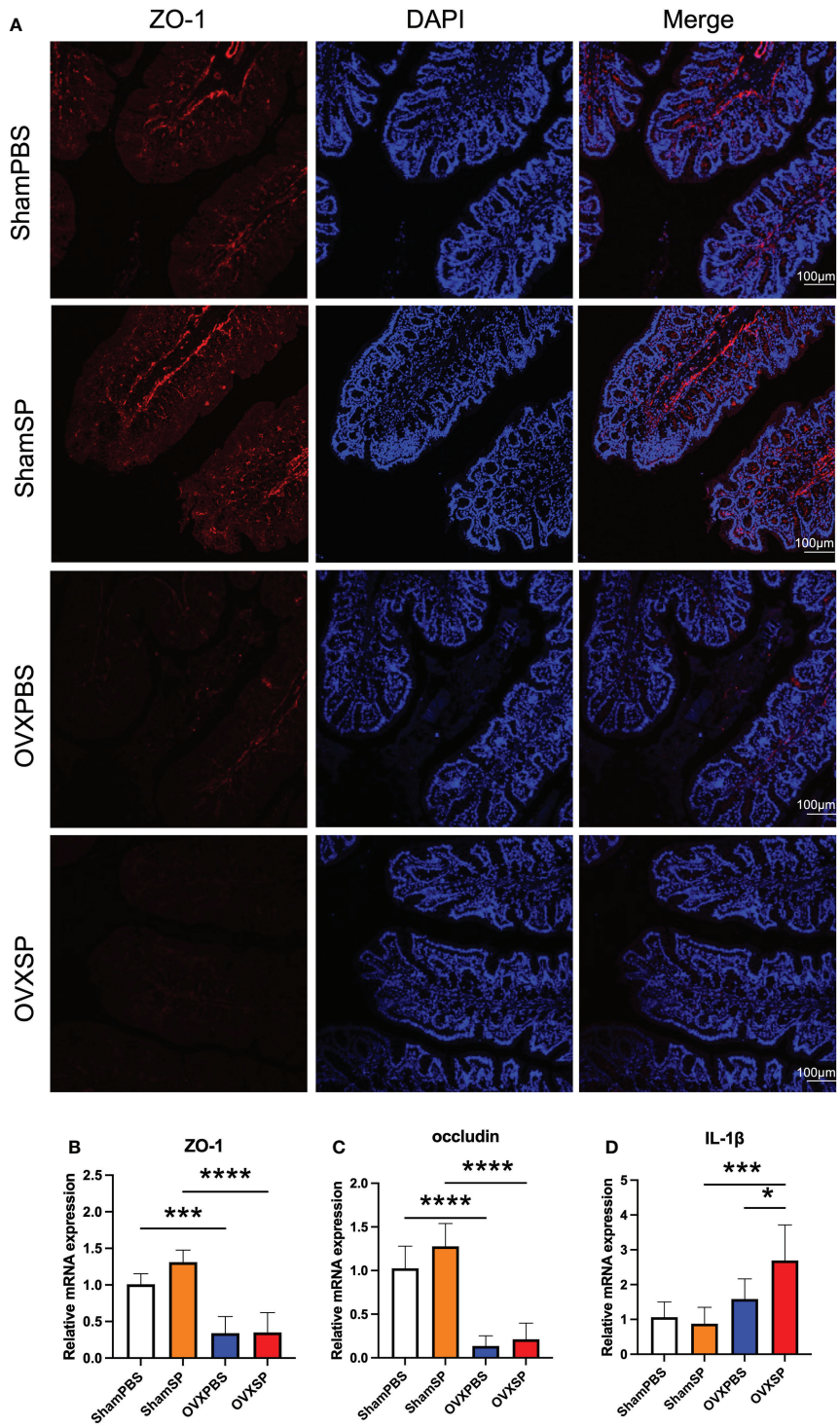

FIGURE 3
Effects of OVX and salivary microbiota treatment on intestinal permeability and inflammation. **(A)** Immunofluorescence analysis of ZO-1 expression (ZO-1, red; nucleus, blue) in colon. Scale bar = 100 μm. **(B–D)** mRNA levels of ZO-1 **(B)**, occludin **(C)**, and IL-1β **(D)** were measured using RT-qPCR. Data are presented as the mean ± SD (n = 5 to 6/group). *$p < 0.05$, ***$p < 0.001$, and ****$p < 0.0001$.

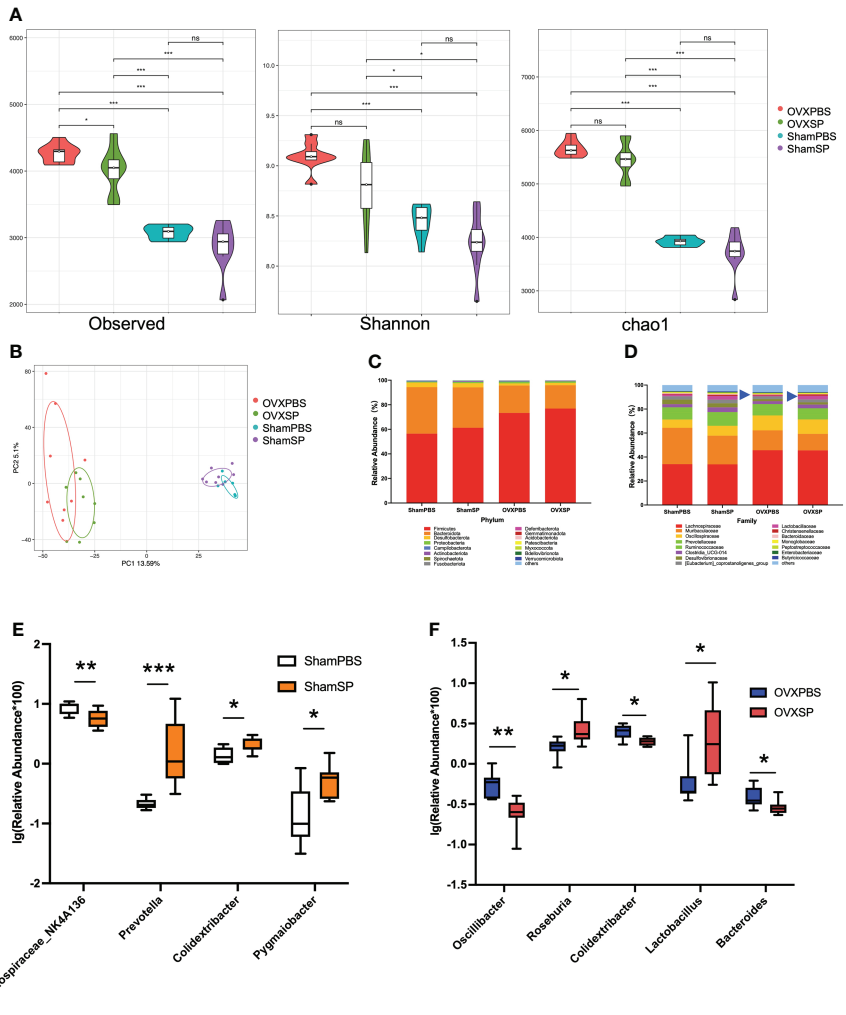

FIGURE 4
The salivary microbiota alters the gut microbiota. **(A)** Violin Plots of alpha diversity estimated by Observed, Shannon, and Chao1. **(B)** PCA of the cecum microbiota. **(C, D)** Relative abundance of gut microbiota at the phylum **(C)** and family **(D)** levels. **(E, F)** Relative abundance of the main differential gut microbiota combined with random forest at the genus level in Sham rats **(E)** and OVX rats **(F)**. The relative abundance was transformed by logarithm (log_{10}). Boxplots and whiskers show the median, quantiles, and 1.5 interquartile ranges (n = 8/group). *$p < 0.05$, **$p < 0.01$, and ***$p < 0.001$.

Roseburia and *Lactobacillus* and lower relative abundances of *Oscillibacter, Colidextribacter*, and *Bacteroides* than the OVXPBS group (Figure 4F).

Salivary microbiota affects serum metabolites

Serum metabolic profiles are shown in an OPLS-DA plot (Figure 5A) and were notably separated from each other, indicating that the salivary microbiota of patients with periodontitis has a profound effect on the serum metabolic profiles. Hierarchical clustering was conducted for differential metabolites—variables with $p < 0.05$ and VIP > 1.0. Notably, the differential metabolites influenced by the periodontitis salivary microbiota were enriched for lipids, indoles, and their derivatives (Figure 5B). The differential metabolic pathways identified by KEGG analysis are shown in Figures 5C, D. In Sham rats, serotonergic synapse, inflammatory mediator regulation of TRP channels, and the GnRH signaling pathway were the top three pathways. In OVX rats, the most different pathways between OVXPBS and OVXSP groups were choline metabolism in cancer, vascular smooth muscle contraction, and the regulation of lipolysis in adipocytes. Serotonin, indole, and derivatives are tryptophan metabolites. Given the above, these findings suggest that metabolism related to lipolysis and tryptophan might play an important role in aggravating bone loss.

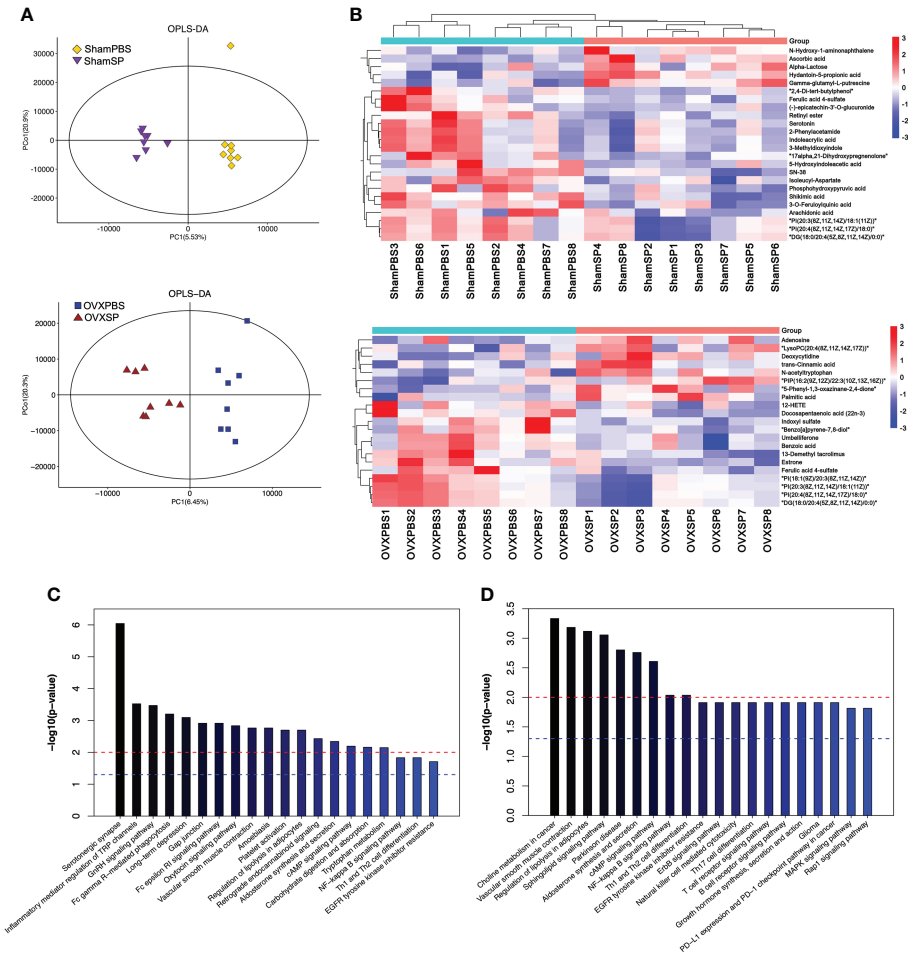

FIGURE 5
Effect of salivary microbiota on serum metabolites. **(A)** OPLS-DA plot of serum metabolites. **(B)** Heatmap showing the differential metabolites by salivary microbiota gavage. **(C, D)** Pathway analysis of the top 20 differentially enriched metabolites after gavage in Sham groups **(C)** and OVX groups **(D)**.

Correlations among parameters of bone, serum metabolites, and gut microbiota composition

As the differential metabolic profiling pointed to lipids, indole, and tryptophan metabolites, Spearman's rank correlation analysis was conducted for bone parameters (BMD, BV/TV, Tb.Th, Tb.N, and Tb.Sp) and metabolites (lipids, lipid-like molecules, indoxyl sulfate, indoles and derivatives). A total of 28 serum metabolites were identified (Figure 6A). We then explored the potential involvement of the differential gut microbiota (48 genera) in mediating the metabolites induced by the periodontitis salivary microbiota in OVX rats (Figure 6B). Indoxyl sulfate, known as tryptophan metabolite catabolism by the gut microbiota, was significantly correlated with 15 genera. Glycerophosphocholine was significantly correlated with 10 genera. PC (14:0/22:1(13Z)) was significantly correlated with 7 genera. LysoPCs, 12-HETE, linoleic acid, indoleacrylic acid, N-ethyl trans-2-cis-6-nonadienamide, and other phosphatidylcholines were significantly correlated with no more than 5 genera. A total of 7 metabolites and 10 genera were not significantly correlated with any other genera or metabolites.

Discussion

Periodontitis and osteoporosis are prevalent conditions characterized by bone resorption. The consensus report of the 2017 World Workshop concluded that postmenopausal osteoporosis can increase alveolar bone turnover leading to net bone loss (Albandar et al., 2018; Jepsen et al., 2018). To further explore the relationship between periodontitis and osteoporosis, a bilateral ovariectomy was performed in our study. We

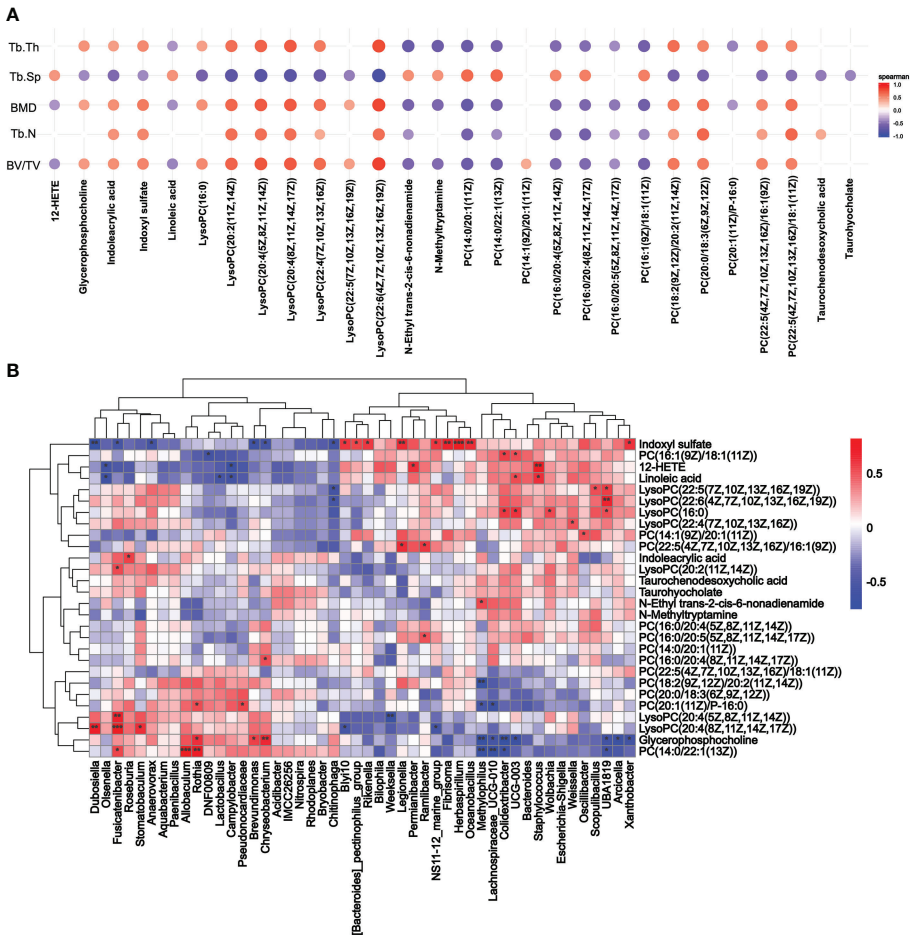

FIGURE 6
Correlation analysis of metabolites. **(A)** Spearman's rank correlation analysis of the femoral parameters (BMD, BV/TV, Tb.Th, Tb.N, and Tb.Sp) and serum metabolites (lipids, lipid-like molecules, indoxyl sulfate, indoles and derivatives). Only $p < 0.05$ and correlations with a correlation coefficient greater than 0.1 are presented. **(B)** Correlation between metabolites screened from **(A)** and changes in genus abundance of OVX rats. $^{*}p < 0.05$, $^{**}p < 0.01$, and $^{***}p < 0.001$.

successfully established a postmenopausal osteoporosis rat model, and the alveolar bone density was reduced significantly in OVX rats compared to Sham rats, consistent with our previous study (Luo et al., 2014).

The periodontal pocket provides a convenient channel for periodontal pathogens and inflammatory cytokines to enter the circulation, which is considered a major mediator of osteoporosis and periodontitis (Yu and Wang, 2022). To avoid the influence of the periodontal pocket, the rats were gavaged with the salivary microbiota of periodontitis, instead of the maxillary molar ligation. In the femoral neck, periodontal salivary microbiota led to a marked decrease in BMD and an impaired bone microstructure in OVX rats; nevertheless, no significant changes were observed in the alveolar bone. Earlier reports found that bone loss in the femur occurred 4 weeks after OVX (Li et al., 1997); however, it was not until 9 weeks after OVX that the reduced alveolar bone volume was significant (Tanaka et al., 2002; Johnston and Ward, 2015), suggesting that the alveolar bone was much more resistant to bone resorption than the femur.

The intestinal epithelium is an essential barrier for pathogen resistance. TJ proteins play crucial roles in paracellular permeability. The expression and distribution of TJ proteins can be affected by both physiological and pathological stimuli, leading to increased paracellular permeability and facilitation of pathogen colonization (Konig et al., 2016). In our study, OVX induced the disruption of TJ proteins, consistent with previous studies (Jia et al., 2019; Li et al., 2020). This finding may explain why the periodontitis salivary microbiota aggravated long bone resorption only in OVX rats. Proinflammatory cytokines, which can stimulate osteoclastogenesis and induce bone loss, also participate in regulating intestinal barrier integrity (Xu et al., 2017; Wang et al., 2021; Qiao et al., 2022). Consistent with changes in the femoral phenotype, the IL-1β

expression was significantly elevated in OVX rats after salivary gavage. Our previous study also showed that IL-1β was highly expressed in colitis mice after periodontitis salivary microbiota gavage (Qian et al., 2022b). Recent studies have shown that ectopic colonization of oral pathobionts into gut may contribute to the activation and/or expansion of memory T cells by inducing IL-1β expression (Kitamoto et al., 2020; Read et al., 2021). Moreover, the IL-1β expression of periodontitis patients was higher than healthy patients, according to previous reports (Park et al., 2014; Qian et al., 2022b). These results suggest that IL-1β is potentially involved in the bone loss induced by periodontitis salivary microbiota.

The α diversity of the gut microbiota was significantly increased in OVX rats. After salivary gavage, more differential bacteria were observed in the OVX groups than in the Sham groups, suggesting that the colonization resistance mediated by the gut microbiota was weakened in OVX rats. In our study, the proportions of genera, including *Oscillibacter, Roseburia, Colidextribacter, Lactobacillus*, and *Bacteroides*, were significantly altered; these genera are related to lipid and amino acid metabolism (Natividad et al., 2018; Liu et al., 2022; Yan et al., 2022). Interestingly, the family *Lactobacillaceae* and genus *Lactobacillus* were both increased in the OVXSP group. *Lactobacillus* is one of the most well-understood probiotics. Effector metabolites include short-chain fatty acids, tryptophan, bacteriocins, and lactic acid (Xiao et al., 2021). A previous study indicated an association between *Lactobacillaceae* and obesity (Li et al., 2013). The relative abundance of *Lactobacillus* was also increased in obesity and osteoporosis (Larsen et al., 2010; Li et al., 2013; Das et al., 2019; Huang et al., 2019). However, no significant correlation was observed between *Lactobacillus* and BMD; thus, it appears that the change in *Lactobacillus* might be due to a compensatory effect.

Excessive fat accumulation can increase intestinal permeability, which, in turn, could lead to bone metabolism disorders (Zhang Z. et al., 2021). Our study showed that nearly half of the differential metabolites between OVXPBS and OVXSP were lipids and lipid-like molecules. According to hierarchical clustering and Spearman's rank correlation analysis, 12-HETE, indoxyl sulfate, and LysoPC (20:4(8Z,11Z,14Z,17Z)) may be associated with the bone loss induced by the salivary microbiota. The level of 12-HETE, a bioactive lipid derived from arachidonic acid, significantly decreased in the OVXSP group; however, the levels of LysoPCs, which reportedly have proinflammatory activity (Xia et al., 2020), were significantly increased in the OVXSP group. In addition, indoxyl sulfate, a chronic kidney disease-specific renal osteodystrophy metabolite, was substantially reduced in the OVXSP group. Indoxyl sulfate is a product of tryptophan, which is metabolized to indole by the gut microbiota. As previously reported, indoxyl sulfate can control bone cellular processes through aryl hydrocarbon receptor signaling (Liu et al., 2018). Short-term and low-dose indoxyl sulfate leads to osteoclast differentiation, whereas long-term and high-dose indoxyl sulfate inhibit osteoclast differentiation (Liu et al., 2020). Thus, the optimal concentration and duration of metabolites remain to be studied. Considering the changes in gut microbiota, periodontitis salivary microbiota aggravates bone loss in OVX rats, possibly through lipid and amino acid metabolism generated by gut microbiota.

Our study has several limitations. First, the two-week salivary gavage period was too short to detect changes in the jaw; therefore, it is necessary to extend the treatment duration in subsequent studies. Second, the potential pathways identified in our results need to be confirmed by further *in vitro* and *in vivo* studies. Nevertheless, our study demonstrated that the contribution of the oral-gut axis to periodontitis salivary microbiota aggravates bone loss. The salivary microbiota of patients with periodontitis can alter the composition of the gut microbiota and increase intestinal inflammation, leading to changes in serum metabolites. These results suggest a novel mechanism by which periodontitis affects systemic disease.

Data availability statement

The data presented in the study are deposited in the NCBI SRA database, accession number PRJNA855534.

Ethics statement

The studies involving human participants were reviewed and approved by Ethical Committee of the Nanjing Stomatological Hospital, Medical School of Nanjing University. The patients/participants provided their written informed consent to participate in this study. The animal study was reviewed and approved by ethics authorities of Nanjing Agriculture University.

Author contributions

FY designed and supervised the study. NW performed the majority of experiments and wrote the manuscript. YL, JQ, and LZ contributed to data interpretation and revised the paper. MW, LL, YH, and LZ provided technical assistance and assisted in the animal experiment. QZ and YL assist in data analysis. All authors contributed to the article and approved the submitted version.

Funding

This project was supported by National Natural Science Foundation of China (81970939), the Nanjing Clinical Research Center for Oral Diseases (2019060009) and Nanjing Medical Science and Technology development fund (YKK21180).

Acknowledgments

We thank Heng Dong, Qiang Li, Xiaoxin Zhang and Liang Ding at the Central Laboratory of Stomatology, Nanjing Stomatological Hospital, Medical School of Nanjing University for technical assistance. We also thank BioRender for providing drawing elements, which helped visualize our research.

Conflict of interest

The authors declare that the research was conducted in the absence of any commercial or financial relationships that could be construed as a potential conflict of interest.

Publisher's note

Supplementary material

The Supplementary Material for this article can be found online at: https://www.frontiersin.org/articles/10.3389/fcimb.2022.983608/full#supplementary-material

References

Albandar, J. M., Susin, C., and Hughes, F. J. (2018). Manifestations of systemic diseases and conditions that affect the periodontal attachment apparatus: Case definitions and diagnostic considerations. *J. Periodontol.* 89 Suppl 1, S183–S203. doi: 10.1002/JPER.16-0480

Atarashi, K., Suda, W., Luo, C., Kawaguchi, T., Motoo, I., Narushima, S., et al. (2017). Ectopic colonization of oral bacteria in the intestine drives TH1 cell induction and inflammation. *Science* 358 (6361), 359–365. doi: 10.1126/science.aan4526

Bao, J., Li, L. L., Zhang, Y., Wang, M., Chen, F., Ge, S., et al. (2022). Periodontitis may induce gut microbiota dysbiosis *via* salivary microbiota. *Int. J. Oral. Sci.* 14 (1), 32. doi: 10.1038/s41368-022-00183-3

Britton, R. A., Irwin, R., Quach, D., Schaefer, L., Zhang, J., Lee, T., et al. (2014). Probiotic l. reuteri treatment prevents bone loss in a menopausal ovariectomized mouse model. *J. Cell Physiol.* 229 (11), 1822–1830. doi: 10.1002/jcp.24636

Chen, Y. C., Greenbaum, J., Shen, H., and Deng, H. W. (2017). Association between gut microbiota and bone health: Potential mechanisms and prospective. *J. Clin. Endocrinol. Metab.* 102 (10), 3635–3646. doi: 10.1210/jc.2017-00513

Chevalier, C., Kieser, S., Colakoglu, M., Hadadi, N., Brun, J., Rigo, D., et al. (2020). Warmth prevents bone loss through the gut microbiota. *Cell Metab.* 32 (4), 575–590.e7. doi: 10.1016/j.cmet.2020.08.012

Dai, Q. G., Zhang, P., Wu, Y. Q., Ma, X. H., Pang, J., Jiang, L. Y., et al. (2014). Ovariectomy induces osteoporosis in the maxillary alveolar bone: an *in vivo* micro-CT and histomorphometric analysis in rats. *Oral. Dis.* 20 (5), 514–520. doi: 10.1111/odi.12166

Das, M., Cronin, O., Keohane, D. M., Cormac, E. M., Nugent, H., Nugent, M., et al. (2019). Gut microbiota alterations associated with reduced bone mineral density in older adults. *Rheumatol. (Oxford)* 58 (12), 2295–2304. doi: 10.1093/rheumatology/kez302

Hathaway-Schrader, J. D., and Novince, C. M. (2021). Maintaining homeostatic control of periodontal bone tissue. *Periodontol* 86 (1), 157–187. doi: 10.1111/prd.12368

Huang, F., Zheng, X., Ma, X., Jiang, R., Zhou, W., Zhou, S., et al. (2019). Theabrownin from Pu-erh tea attenuates hypercholesterolemia *via* modulation of gut microbiota and bile acid metabolism. *Nat. Commun.* 10 (1), 4971. doi: 10.1038/s41467-019-12896-x

Jepsen, S., Caton, J. G., Albandar, J. M., Bissada, N. F., Bouchard, P., Cortellini, P., et al. (2018). Periodontal manifestations of systemic diseases and developmental and acquired conditions: Consensus report of workgroup 3 of the 2017 world workshop on the classification of periodontal and peri-implant diseases and conditions. *J. Periodontol.* 89 Suppl 1, S237–S248. doi: 10.1002/JPER.17-0733

Jia, X., Jia, L., Mo, L., Yuan, S., Zheng, X., He, J., et al. (2019). Berberine ameliorates periodontal bone loss by regulating gut microbiota. *J. Dent. Res.* 98 (1), 107–116. doi: 10.1177/0022034518797275

Johnston, B. D., and Ward, W. E. (2015). The ovariectomized rat as a model for studying alveolar bone loss in postmenopausal women. *BioMed. Res. Int.* 2015, 635023. doi: 10.1155/2015/635023

Kitamoto, S., Nagao-Kitamoto, H., Jiao, Y., Gillilland, M. G., Hayashi, A., Imai, J., et al. (2020). The intermucosal connection between the mouth and gut in commensal pathobiont-driven colitis. *Cell* 182 (2), 447–462.e14. doi: 10.1016/j.cell.2020.05.048

Konig, J., Wells, J., Cani, P. D., Garcia-Rodenas, C. L., MacDonald, T., Mercenier, A., et al. (2016). Human intestinal barrier function in health and disease. *Clin. Transl. Gastroenterol.* 7 (10), e196. doi: 10.1038/ctg.2016.54

Larsen, N., Vogensen, F. K., van den Berg, F. W., Nielsen, D. S., Andreasen, A. S., Pedersen, B. K., et al. (2010). Gut microbiota in human adults with type 2 diabetes differs from non-diabetic adults. *PLoS One* 5 (2), e9085. doi: 10.1371/journal.pone.0009085

Li, J. Y., Chassaing, B., Tyagi, A. M., Vaccaro, C., Luo, T., Adams, J., et al. (2016). Sex steroid deficiency-associated bone loss is microbiota dependent and prevented by probiotics. *J. Clin. Invest* 126 (6), 2049–2063. doi: 10.1172/JCI86062

Li, F., Jiang, C., Krausz, K. W., Li, Y., Albert, I., Hao, H., et al. (2013). Microbiome remodelling leads to inhibition of intestinal farnesoid X receptor signalling and decreased obesity. *Nat. Commun.* 4, 2384. doi: 10.1038/ncomms3384

Li, B., Liu, M., Wang, Y., Gong, S., Yao, W., Li, W., et al. (2020). Puerarin improves the bone micro-environment to inhibit OVX-induced osteoporosis *via* modulating SCFAs released by the gut microbiota and repairing intestinal mucosal integrity. *BioMed. Pharmacother.* 132, 110923. doi: 10.1016/j.biopha.2020.110923

Ling, C. W., Miao, Z., Xiao, M. L., Zhou, H., Jiang, Z., Fu, Y., et al. (2021). The association of gut microbiota with osteoporosis is mediated by amino acid metabolism: multiomics in a large cohort. *J. Clin. Endocrinol. Metab.* 106 (10), e3852–e3864. doi: 10.1210/clinem/dgab492

Li, L., Rao, S., Cheng, Y., Zhuo, X., Deng, C., Xu, N., et al. (2019). Microbial osteoporosis: The interplay between the gut microbiota and bones *via* host metabolism and immunity. *Microbiologyopen* 8 (8), e00810. doi: 10.1002/mbo3.810

Li, M., Shen, Y., and Wronski, T. J. (1997). Time course of femoral neck osteopenia in ovariectomized rats. *Bone* 20 (1), 55–61. doi: 10.1016/s8756-3282(96)00317-1

Liu, W. C., Shyu, J. F., Lim, P. S., Fang, T. C., Lu, C. L., Zheng, C. M., et al. (2020). Concentration and duration of indoxyl sulfate exposure affects osteoclastogenesis by regulating nfatc1 *via* aryl hydrocarbon receptor. *Int. J. Mol. Sci.* 21, (10). doi: 10.3390/ijms21103486

Liu, W. C., Tomino, Y., and Lu, K. C. (2018). Impacts of indoxyl sulfate and p-cresol sulfate on chronic kidney disease and mitigating effects of AST-120. *Toxins (Basel)* 10, (9). doi: 10.3390/toxins10090367

Liu, X., Tong, X., Zou, Y., Lin, X., Zhao, H., Tian, L., et al. (2022). Mendelian randomization analyses support causal relationships between blood metabolites and the gut microbiome. *Nat. Genet.* 54 (1), 52–61. doi: 10.1038/s41588-021-00968-y

Lucas, S., Omata, Y., Hofmann, J., Bottcher, M., Iljazovic, A., Sarter, K., et al. (2018). Short-chain fatty acids regulate systemic bone mass and protect from pathological bone loss. *Nat. Commun.* 9 (1), 55. doi: 10.1038/s41467-017-02490-4

Luo, K., Ma, S., Guo, J., Huang, Y., Yan, F., and Xiao, Y. (2014). Association between postmenopausal osteoporosis and experimental periodontitis. *BioMed. Res. Int.* 2014, 316134. doi: 10.1155/2014/316134

Natividad, J. M., Agus, A., Planchais, J., Lamas, B., Jarry, A. C., Martin, R., et al. (2018). Impaired aryl hydrocarbon receptor ligand production by the gut microbiota is a key factor in metabolic syndrome. *Cell Metab.* 28 (5), 737–749.e4. doi: 10.1016/j.cmet.2018.07.001

Park, E., Na, H. S., Song, Y. R., Shin, S. Y., Kim, Y. M., and Chung, J. (2014). Activation of NLRP3 and AIM2 inflammasomes by porphyromonas gingivalis infection. *Infect. Immun.* 82 (1), 112–123. doi: 10.1128/IAI.00862-13

Peng, X., Cheng, L., You, Y., Tang, C., Ren, B., Li, Y., et al. (2022). Oral microbiota in human systematic diseases. *Int. J. Oral. Sci.* 14 (1), 14. doi: 10.1038/s41368-022-00163-7

Qian, J., Lu, J., Huang, Y., Wang, M., Chen, B., Bao, J., et al. (2022a). Periodontitis salivary microbiota worsens colitis. *J. Dent. Res.* 101 (5), 559–568. doi: 10.1177/00220345211049781

Qian, J., Zhang, Y., Cheng, S., Wang, N., Zheng, L., Li, L., et al. (2022b). Effects of salivary microbiota on tryptophan-aryl hydrocarbon receptor signaling axis in mice with periodontitis. *Chin. J. Stomatol.* 57 (06), 595–603. doi: 10.3760/cma.j.cn112144-20220323-00126

Qiao, D., Chen, R., Li, L., Zhu, F., Zhang, Y., and Yan, F. (2022). Accelerated alveolar bone loss in a mouse model of inflammatory bowel disease and its relationship with intestinal inflammation. *J. Periodontol.* doi: 10.1002/JPER.21-0374

Read, E., Curtis, M. A., and Neves, J. F. (2021). The role of oral bacteria in inflammatory bowel disease. *Nat. Rev. Gastroenterol. Hepatol.* 18 (10), 731–742. doi: 10.1038/s41575-021-00488-4

Tanaka, M., Ejiri, S., Toyooka, E., Kohno, S., and Ozawa, H. (2002). Effects of ovariectomy on trabecular structures of rat alveolar bone. *J. Periodontal Res.* 37 (2), 161–165. doi: 10.1034/j.1600-0765.2002.01601.x

Wang, Z., Chen, K., Wu, C., Chen, J., Pan, H., Liu, Y., et al. (2021). An emerging role of prevotella histicola on estrogen deficiency-induced bone loss through the gut microbiota-bone axis in postmenopausal women and in ovariectomized mice. *Am. J. Clin. Nutr.* 114 (4), 1304–1313. doi: 10.1093/ajcn/nqab194

Xia, F., Liu, C., and Wan, J. B. (2020). Characterization of the cold and hot natures of raw and processed rehmanniae radix by integrated metabolomics and network pharmacology. *Phytomedicine* 74, 153071. doi: 10.1016/j.phymed.2019.153071

Xiao, Y., Zhai, Q., Zhang, H., Chen, W., and Hill, C. (2021). Gut colonization mechanisms of lactobacillus and bifidobacterium: An argument for personalized designs. *Annu. Rev. Food Sci. Technol.* 12, 213–233. doi: 10.1146/annurev-food-061120-014739

Xu, X., Jia, X., Mo, L., Liu, C., Zheng, L., Yuan, Q., et al. (2017). Intestinal microbiota: a potential target for the treatment of postmenopausal osteoporosis. *Bone Res.* 5, 17046. doi: 10.1038/boneres.2017.46

Xu, S., Zhang, G., Guo, J. F., and Tan, Y. H. (2021). Associations between osteoporosis and risk of periodontitis: A pooled analysis of observational studies. *Oral. Dis.* 27 (2), 357–369. doi: 10.1111/odi.13531

Yan, S., Chen, J., Zhu, L., Guo, T., Qin, D., Hu, Z., et al. (2022). Oryzanol alleviates high fat and cholesterol diet-induced hypercholesterolemia associated with the modulation of the gut microbiota in hamsters. *Food Funct.* 13 (8), 4486–4501. doi: 10.1039/d1fo03464b

Yuan, Y., Yang, J., Zhuge, A., Li, L., and Ni, S. (2022). Gut microbiota modulates osteoclast glutathione synthesis and mitochondrial biogenesis in mice subjected to ovariectomy. *Cell Prolif.* 55 (3), e13194. doi: 10.1111/cpr.13194

Yu, B., and Wang, C. Y. (2022). Osteoporosis and periodontal diseases - an update on their association and mechanistic links. *Periodontol* 89 (1), 99–113. doi: 10.1111/prd.12422

Zhang, P., Feng, Y., Li, L., Ge, W., Yu, S., Hao, Y., et al. (2021). Improvement in sperm quality and spermatogenesis following faecal microbiota transplantation from alginate oligosaccharide dosed mice. *Gut* 70 (1), 222–225. doi: 10.1136/gutjnl-2020-320992

Zhang, Z., Lin, T., Meng, Y., Hu, M., Shu, L., Jiang, H., et al. (2021). FOS/GOS attenuates high-fat diet induced bone loss *via* reversing microbiota dysbiosis, high intestinal permeability and systemic inflammation in mice. *Metabolism* 119, 154767. doi: 10.1016/j.metabol.2021.154767

frontiers | Frontiers in Cellular and Infection Microbiology

ORIGINAL RESEARCH
published: 15 August 2022
doi: 10.3389/fcimb.2022.905653

Characteristics of Microbial Distribution in Different Oral Niches of Oral Squamous Cell Carcinoma

Fujiao Nie[1,2†], Lihua Wang[1,3†], Yingying Huang[4,5], Pishan Yang[1,2], Pizhang Gong[1,2], Qiang Feng[1,3] and Chengzhe Yang[4,5*]*

[1] Department of Periodontology, School and Hospital of Stomatology, Cheeloo College of Medicine, Shandong University, Jinan, China, [2] Shandong Key Laboratory of Oral Tissue Regeneration & Shandong Engineering Laboratory for Dental Materials and Oral Tissue Regeneration, Jinan, China, [3] Department of Human Microbiome, School and Hospital of Stomatology, Cheeloo College of Medicine, Shandong University, Jinan, China, [4] Department of Oral and Maxillofacial Surgery, Qilu Hospital of Shandong University, Jinan, China, [5] Institute of Stomatology, Shandong University, Jinan, China

OPEN ACCESS

Edited by:
Zuomin Wang,
Capital Medical University, China

Reviewed by:
Yuan Liu,
Shanghai Jiao Tong University, China
Jin-hai Ye,
Nanjing Medical University, China

***Correspondence:**
Qiang Feng
fengqiang@sdu.edu.cn
Chengzhe Yang
yangchengzhe19@163.com

[†]These authors have contributed equally to this work

Specialty section:
This article was submitted to Microbiome in Health and Disease, a section of the journal Frontiers in Cellular and Infection Microbiology

Received: 27 March 2022
Accepted: 28 April 2022
Published: 15 August 2022

Citation:
Nie F, Wang L, Huang Y, Yang P, Gong P, Feng Q and Yang C (2022) Characteristics of Microbial Distribution in Different Oral Niches of Oral Squamous Cell Carcinoma. Front. Cell. Infect. Microbiol. 12:905653. doi: 10.3389/fcimb.2022.905653

Oral squamous cell carcinoma (OSCC), one of the most common malignant tumors of the head and neck, is closely associated with the presence of oral microbes. However, the microbiomes of different oral niches in OSCC patients and their association with OSCC have not been adequately characterized. In this study, 305 samples were collected from 65 OSCC patients, including tumor tissue, adjacent normal tissue (paracancerous tissue), cancer surface tissue, anatomically matched contralateral normal mucosa, saliva, and tongue coat. 16S ribosomal DNA (16S rDNA) sequencing was used to compare the microbial composition, distribution, and co-occurrence network of different oral niches. The association between the microbiome and the clinical features of OSCC was also characterized. The oral microbiome of OSCC patients showed a regular ecological distribution. Tumor and paracancerous tissues were more microbially diverse than other oral niches. Cancer surface, contralateral normal mucosa, saliva, and tongue coat showed similar microbial compositions, especially the contralateral normal mucosa and saliva. Periodontitis-associated bacteria of the genera *Fusobacterium*, *Prevotella*, *Porphyromonas*, *Campylobacter*, and *Aggregatibacter*, and anaerobic bacteria were enriched in tumor samples. The microbiome was highly correlated with tumor clinicopathological features, with several genera (*Lautropia*, *Asteroleplasma*, *Parvimonas*, *Peptostreptococcus*, *Pyramidobacter*, *Roseburia*, and *Propionibacterium*) demonstrating a relatively high diagnostic power for OSCC metastasis, potentially providing an indicator for the development of OSCC.

Keywords: oral squamous cell carcinoma, oral microbiome, distribution characteristics, oral niches, clinicopathological features

INTRODUCTION

Oral squamous cell carcinoma (OSCC), one of the most common malignant tumors of the head and neck, accounting for approximately 90% of oral cancers (Chi et al., 2015), is characterized by invasiveness, rapid development, early metastasis, and poor prognosis (Siegel et al., 2020). The incidence of OSCC has increased significantly in recent years, accounting for over 370,000 new cases and 170,000 deaths worldwide in 2020, while the five-year survival rate remained between 50% and 60% (Choi et al., 2014; Patel et al., 2016; van Dijk et al., 2016). The pathogenesis of OSCC is multifactorial, among which tobacco, alcohol, chewing betel nut and human papillomavirus (HPV) have been demonstrated as risk factors (Chi et al., 2015). Recently, chronic pathogenic infections, including Candida infection and periodontitis, have been recognized as high-risk factors for the occurrence and development of OSCC (Peres et al., 2019).

More than 700 bacterial species have been detected in the oral cavity, and the oral microbiome, which is considered highly diverse compared to other body sites, encompasses a wide variety of microorganisms from different niches, such as tongue, buccal mucosa, and saliva, reflecting site-specificity in oral species (Minarovits, 2021). Human oral microbiome composition are closely correlated with oral and systematic health (Verma et al., 2018). For example, the oral pathogen, *Fusobacterium nucleatum*, has been well studied as an oncogenic pathogen of colorectal cancer (Brennan and Garrett, 2019). Additionally, more and more oral pathogenic microbes, such as *Porphyromonas gingivalis*, *Actinobacillus actinomycetemcomitans*, *Tannerella forsythus*, and *Prevotella intermedius*, have been demonstrated to be risk factors for esophageal, gastric, and pancreatic carcinomas (Mascitti et al., 2019).

Dysbiosis of the oral microbiome has gained significant attention as a potential oncogenic factor of OSCC in recent years. Most bacterial taxa isolated from tumor tissue were periodontitis-related and saccharolytic or aciduric species in comparison to non-tumorous paracancerous mucosal tissue (Hooper et al., 2007; Zhao et al., 2017), while the abundance of *Streptococcus* progressively decreased with the progression of OSCC (Chattopadhyay et al., 2019; Ganly et al., 2019). Oral inflammatory-related bacteria (e.g., *Fusobacterium nucleatum* and *Pseudomonas aeruginosa*) are more likely to be enriched in OSCC tissue (Al-Hebshi et al., 2017b; Perera et al., 2018). Abundances of the bacteria *Porphyromonas endodontalis* and *Peptostreptococcus anaerobius* in salivary were reported to be significantly correlated with increases of inflammatory cytokines IL-6, IL-8, TNF-α, IFN-γ, and GM-CSF in OSCC patients (Rai et al., 2021).

Studies have increasingly shown that oral microorganisms are closely related to oral cancer, while the microbial compositions in different oral niches differ significantly due to the different microenvironments. However, in OSCC patients, whether there exists a substantial difference in the oral microbiome signature among intratumor and oral other niches remains scarcely reported. In this study, microbial samples of six oral niches were collected from OSCC patients. Phenotypic and functional characteristics of the oral microbiome were identified, and the association between the oral microbiome and the clinical biological behavior of OSCC was investigated.

MATERIALS AND METHODS

Participant Recruitment and Sample Collection

The study was approved by the Ethics Committee of Qilu Hospital of Shandong University (KYLL-2017-256), and conducted in accordance with the Declaration of Helsinki. All subjects gave written informed consent before participating in the study. The patients diagnosed with OSCC for the first time based on clinical symptoms and histopathological detection were eligible for this study. Prior to sampling, no patients received any treatments such as surgery, immune therapy, radio- or chemotherapy. Exclusion criteria were the use of antibiotics in the past 3 months or diseases/conditions known to modify oral microbial composition such as pregnancy, nursing, and oral mucosal diseases. Subjects with a history of any previous cancer diagnosis or any other severe systemic disorder, such as diabetes, infectious disease, HBV, syphilis, and HIV infection, autoimmune diseases, gastrointestinal and respiratory diseases were excluded from the study.

A total of 65 patients with OSCC were recruited from the Qilu Hospital of Shandong University (Shandong, China) from 2018 to 2020. Samples from six oral niches (tumor tissue, paracancerous tissue, cancer surface, anatomically matched contralateral normal mucosa, saliva, and tongue coat) were collected according to the protocols of Human Microbiome Project (HMP) (McInnes and Cutting, 2010). Participants were instructed not to eat, drink, smoke, or to brush their teeth for at least 2 hours before sample collection. For the saliva samples, participants were asked to stop swallowing for 1 minute and to spit saliva into a 50 mL collection tube, repeating the procedure several times and finally collecting approximately 5mL saliva. The samples from the cancer surface, contralateral normal mucosa, and tongue coat niches were obtained with a sterile swab by swabbing the surface of the soft tissue with pressure for 10 times in one direction, then turning the swab 180° and swabing 10 times with the opposite side. The central 1 cm^2 area of tongue dorsum, the entire buccal mucosa, and the entire cancer surface were samplings, avoiding the teeth and the internal tumor. Tumor tissue and paracancerous tissue samples were collected during the surgical resection of OSCC from the regions of the tumor lesion and from the adjoining clinically uninvolved normal tissue (paracancerous niche). Concisely, around 5 mm^3 tumor samples were excised from the deep tissue of tumor mass without involving the margin, and paired normal tissues of similar size were excised from the paracancerous region 2 cm away from the edge of tumor lesions. All operation maintained consistency in the sampling process to facilitate the repetition of experimental results.

All the samples were placed in prepared oral swab preservation solution (Tris, EDTA, and antiseptic) to prevent

DNA degradation and transported to the laboratory on ice within 20 mins of collection before being stored at −80°C until processing.

DNA Extraction

DNA was extracted from all samples using DNeasy Blood and Tissue Kit (Qiagen, Hilden, Germany) following the manufacturer's protocol. The concentration and purity of the isolated DNA were detected using 1% agarose gels electrophoresis. DNA was diluted to 1ng/μl using sterile water.

16S rDNA Amplification and Sequencing

Genome DNA from each sample was used as an amplification template. PCR targeting of the V3-V4 region of the 16S rDNA hypervariable region was conducted, using the primers 341F (5′-CCTAYGGGRBGCASCAG-3′) and 806R (5′-GGACTACNN GGGTATCTAAT -3′). PCR was performed in a total volume of 30μL reactions, composing 15μL of Phusion® High-Fidelity PCR Master Mix (New England Biolabs), 0.2μM of forward and reverse primers, and 10 ng of the template DNA. Thermal cycling was initially used to denature samples at 95°C for 10 min, followed by 30 cycles of denaturation at 95°C for 30s, then annealing at 50°C for 30s and extension at 72°C for 40s, followed finally by elongation at 72°C for 7 min.

PCR products were then purified using a 2% agarose gel electrophoresis and GeneJET Gel Extraction Kit (Thermo Scientific, USA), selecting samples with a single amplification product for further analysis. The library was sequenced on an Illumina Hiseq 2500 platform (Novogene, Beijing, China).

Sequencing Data Analysis

The microbiome bioinformatics platform QIIME2 was used to analyze the raw sequence. Usearch software (Usearch, version 11.0.667_i86linux64) was used to identify the Operational Taxonomic Units OTUs (Edgar, 2010). Sequence data were clustered into OTUs at 97% similarity by Usearch, and then taxonomic annotation of the representative sequences of OTUs was performed by the database Ribosomal Database Project (RDP) at a threshold of 0.8.

The alpha-diversity index reflected the species richness, evenness, and diversity in every group, and the beta-diversity was used to compare the degree of similarity or dissimilarity among different groups, both performed using the QIMME2 (Bolyen et al., 2019). Alpha-diversity was analyzed by comparing the Chao1 index, Faith-PD, observed OTUs, Shannon index, and Simpson diversity index. Principle Coordinate Analysis (PCoA) based on unweighted UniFrac were performed to visualize beta-diversity. ADONIS analysis was used to evaluate any statistical differences. Microbiome variations in different niches were analyzed at the phylum, genus, and species levels. The taxonomic composition and average relative abundance of microbiome were displayed using a histogram (R package: "ggplot2", version 3.3.5), and the differential microbiomes between groups at the genus and species levels were demonstrated using a heatmap (R package, pheatmap, version 1.0.12).

By following the law of power-law distribution, the SparCC network was constructed using the FastSpar to analyze the correlation and interaction between flora species, as well as to identify the key flora and related flora according to the co-occurrence network of flora-species interaction (Friedman and Alm, 2012; Watts et al., 2019).

To characterize the relationship between oral microbiome and the clinical characteristics of OSCC, tumor tissue samples were divided by tumor size, grade, stage, and metastasis. The bacteria related to the clinical indicators were screened using Maaslin2 (R, version 1.6.0) at a significance threshold of $p < 0.05$. Subsequently, the Boruta algorithm (R package version 7.0.0) was used to select the taxa exhibiting predictive power. Finally, a random forest algorithm (R package, randomForest, version 4.6-14) was performed with 500 classification trees based on leave one out cross validation (LOOCV) to establish classification models for the diagnosis of OSCC (Basu et al., 2018). The predictive performance of each classification model was assessed using the ROC curve (R package: pROC, version 1.16.2), and for each the area under the curve (AUC) was calculated.

The functional prediction of the microbial community was investigated using a phenotypic classification based on BugBase, and metabolic pathway prediction based on Tax4Fun2 (R package version 1.1.5). OTU abundance table and representative OTU sequences were aligned against the Ref99NR database using Tax4Fun2, then Kyoto Encyclopedia of Genes and Genomes (KEGG) functional classification between samples were realized by STAMP software (version 2.1.3) (Kanehisa and Goto, 2000).

RESULTS

Sociodemographic Characteristics and Statistics of the Sequencing Data

A total of 65 subjects with OSCC were recruited and 305 samples were collected from 6 different oral niches. Clinical characteristics of the study subjects were presented in the **Table 1**. 16S rDNA regions V3–V4 were amplified and sequenced successfully from each sample according to the standard process described in the Methods section. After post-processing and quality filtering, 23,451,170 reads were obtained across all samples, with 76,889 reads per sample on average. OTU detection based on the RDP database showed 2,398, 2,542, 2,030, 1,562, 1,279, 1,149 bacterial OTUs were obtained from the six niches (tumor tissue, paracancerous tissue, cancer surface, contralateral normal mucosa, saliva, and tongue coat), respectively. The rarefaction curve showed that all samples reached saturation, indicating that almost all detectable microbial species in each sample were identified.

Alpha and Beta Diversity Across Oral Niches

Alpha diversity was assessed to compare the richness, uniformity, and diversity of the microbiome. Using Chao1, Faith PD, and OTU analyses (**Figure 1A** and **Supplementary Figures 1A–C**), we identified a gross spatial trend of microbial communities with species richness being highest in the tumor and paracancerous samples, while cancer surface, contralateral normal tissue, saliva, and tongue coat samples exhibited a trend

TABLE 1 | Clinicopathological characteristics of the patients.

Variable	C (n=37)	PC (n=37)	CS (n=64)	N (n=38)	S (n=65)	T (n=64)
Age (mean ± SD)	57.9 ± 9.6	58.1 ± 9.7	59.5 ± 10.9	58.2 ± 10.3	59.5 ± 10.8	59.5 ± 10.9
Males: No. (%)	27 (73.0)	27 (73.0)	41 (64.1)	25 (65.8)	41 (63.1)	41 (64.1)
Cancer site:						
Tongue	15	14	23	17	24	23
Buccal	2	2	8	4	8	8
Floor of Mouth	7	7	10	5	10	10
Pharynx	1	1	1	1	1	1
Palate	3	3	6	4	6	6
Maxilla	2	2	4	2	4	4
gingiva	7	8	12	5	12	12

of progressively decreasing richness. The Shannon and Simpson indices suggested that the diversity and uniformity of bacteria were significantly higher in the tumor tissue than in other niches ($P < 0.001$).

Non-metric multidimensional scaling (NMDS) and principal coordinate analysis (PCoA) were conducted to measure the niche-related differences in microbial communities and their clustering relationships. The PCoA was based on unweighted UniFrac. As shown in **Figures 1B, D**, the six niches formed separate clusters, and this difference was found using ADONIS to be statistically significant. Further ADONIS analysis of the distributions of samples from different niches showed that the core regions of tumor samples and paracancerous samples were highly similar ($P > 0.05$), suggesting similar microbial diversities in those two niches, while the contralateral normal mucosa, saliva, and tongue coat were different from the tumor and paracancerous samples, but similar to each other.

Generality and Discrepancy of Microbial Composition Across Oral Niches

The generality and discrepancy of oral microbial composition was compared across niches to elucidate the microbial transitions along different oral niches. As indicated in **Figures 1C, E, F**, there were significant differences in oral microbial composition across niches. *Proteobacteria*, *Firmicutes*, *Bacteroidetes*, *Fusobacteria*, and *Actinobacteria* were the predominant microorganisms in all niches at the phylum level. Among these, *Proteobacteria*, *Firmicutes*, and *Bacteroidetes* accounted for the greatest proportion. The microbiome of contralateral normal mucosa and saliva samples showed great similarity at the phylum, genus, and species levels. Further, *Pseudomonas beteli* was the most abundant species in both tumor and paracancerous tissue samples, whereas, in the other four niches, *Streptococcus dentisani* accounted for the largest proportion, indicating a more similar community composition between tumor and paracancerous tissues, while the other four niches were more similar to each other. We propose that it is the fluidity of saliva and activity of tongue that caused microbial composition of this saliva, tongue coat, cancer surface, and contralateral normal mucosa resemble each other, especially contralateral normal mucosa and saliva (Mager et al., 2003; Li et al., 2020). This finding might facilitate selecting sampling sites for microbial composition research.

Microbiome Profiles of Tumor and Paracancerous Tissues

The tumor and paracancerous tissues were sampled from the surgically resected tumor and adjacent non-tumorous tissues, while the other four groups were sampled from liquid saliva and using swabs. This may be a major contributor to the microbial differences observed. Thus, subsequent analyses focused on the variations between tumor and paracancerous tissue samples to characterize the dysbiosis of the oral microbiome associated with OSCC.

The bacterial composition of tumor tissue was noticeably different in comparison to the paracancerous tissue in most patients, suggesting a shift in bacterial colonization. The results of phylum-level taxonomic analysis in **Figures 2A, B, E** show that *Proteobacteria* were overwhelmingly dominant in paracancerous tissue, while significantly reduced in tumor tissue, while *Firmicutes*, *Bacteroidetes*, *Fusobacteria*, and *Spirochaetes* were increased in tumor tissue. At the genus level, tumor tissue showed a greater abundance of *Fusobacterium*, *Prevotella*, *Porphyromonas*, *Campylobacter*, *Aggregatibacter*, *Treponema*, and *Peptostreptococcus*, and a lower prevalence of *Stenotrophomonas* (the most abundant in control tissue), *Neisseria*, *Sphingomonas*, and *Veillonella* (**Figures 2A, C, F**, $P < 0.05$). At the species level, *Pseudomonas beteli* accounted for the highest proportion in paracancerous tissue but was significantly reduced in tumor tissue. *Rothia mucilaginosa*, *Sphingomonas alpina*, and *Veillonella dispar* were also significantly decreased in tumor tissue. Conversely, *Porphyromonas endodontalis*, *Campylobacter gracilis*, *Peptostreptococcus stomatis*, *prevotella intermedia*, *Eubacterium vuril subsp schtika*, and *Parvimonas micra* were significantly increased in tumor tissue (**Figures 2D, G**, $P < 0.05$).

To further distinguish differences of the microbial community between cancer tissue and paracancerous tissue, differential clusters were visualized using a heatmap (see **Figure 3**). 22 genera were identified as being differentially enriched between tumor and paracancerous tissue samples. Compared to paracancerous tissue, *prevotella*, *Slackia*, *Peptostreptococcus*, *Treponema*, *Selenomonas*, *Porphyromonas*, *parvimonas*, *Peptococcus*, *Mycoplasma*, and *Bulleidia* were enriched in tumor tissue. Interestingly, these are all anaerobic or facultative anaerobes. Conversely, Actinomyces, Veillonella, Neisseria, Rothia, Delftia, Ralstonia, Stenotro phomonas, pelomonas, Proteus, Bradyrhizobium, and Serratia, were less abundant in tumor tissue. There were also differences

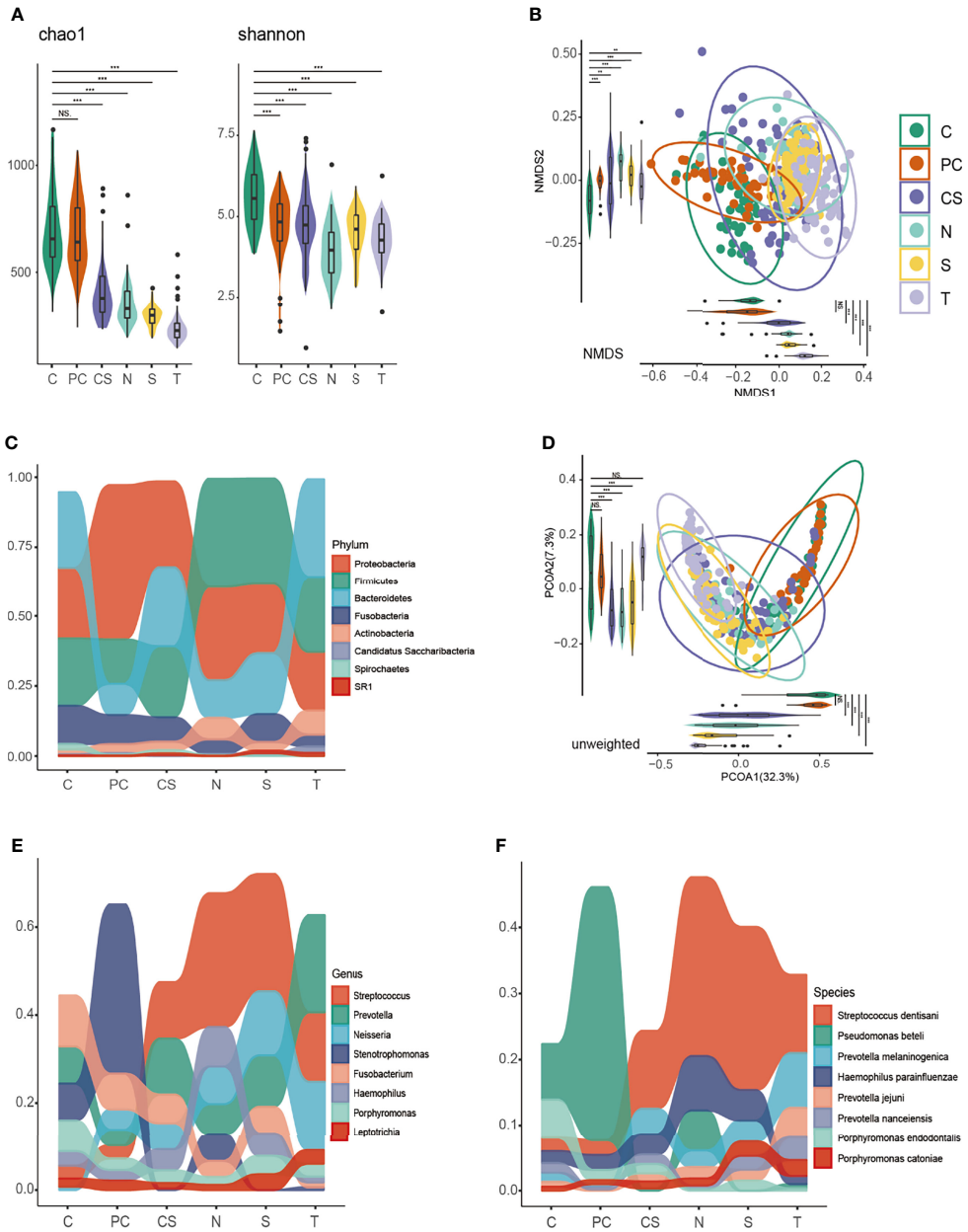

FIGURE 1 | Diversity analysis and taxonomy distribution of the oral microbiome among six niches. Bacterial richness, evenness and diversity were evaluated by **(A)** Chao 1 and Shannon index. Clusters formed by **(B)** non-metric multidimensional scaling (NMDS) and **(D)** principal coordinate analysis (PCoA) based on unweighted UniFrac. Differential taxonomy distribution at the **(C)** phylum, **(E)** genus and **(F)** species level. C, tumor tissue; PC, paracancerous tissue; CS, cancer surface; N, anatomically matched contralateral normal mucosa; S, saliva; T, tongue coat. ns, no significance; $^{**}P < 0.005$, $^{***}P < 0.001$.

in the species level cluster distributions, whereby tumor tissue exhibited increased *Porphyromonas endodontalis* and *Parvimonas micra*, and reduced *Pseudomonas beteli*, *Rothia mucilaginosa*, *Sphingomonas alpina*, and *Veillonella rogosae*.

SparCC Analysis of the Co-Occurrence Network and Core Microbiome

To describe the microbial symbiosis and the connections across different bacterial communities, the microbial co-occurrence network was constructed using SparCC analysis (**Supplementary Figure 2**). SparCC provides a novel method of sequencing data to infer correlations between species (Rai et al., 2021). The degree of microbial symbiosis in the network corresponded with the power-law distribution, indicating the ecologic characteristics of the oral microbiome in OSCC patients (**Figure 4B**). The nodes of the network represented the bacterial species, while the edges between nodes represent ecological relationships between species. The node with most edges was considered as the key species. As shown in

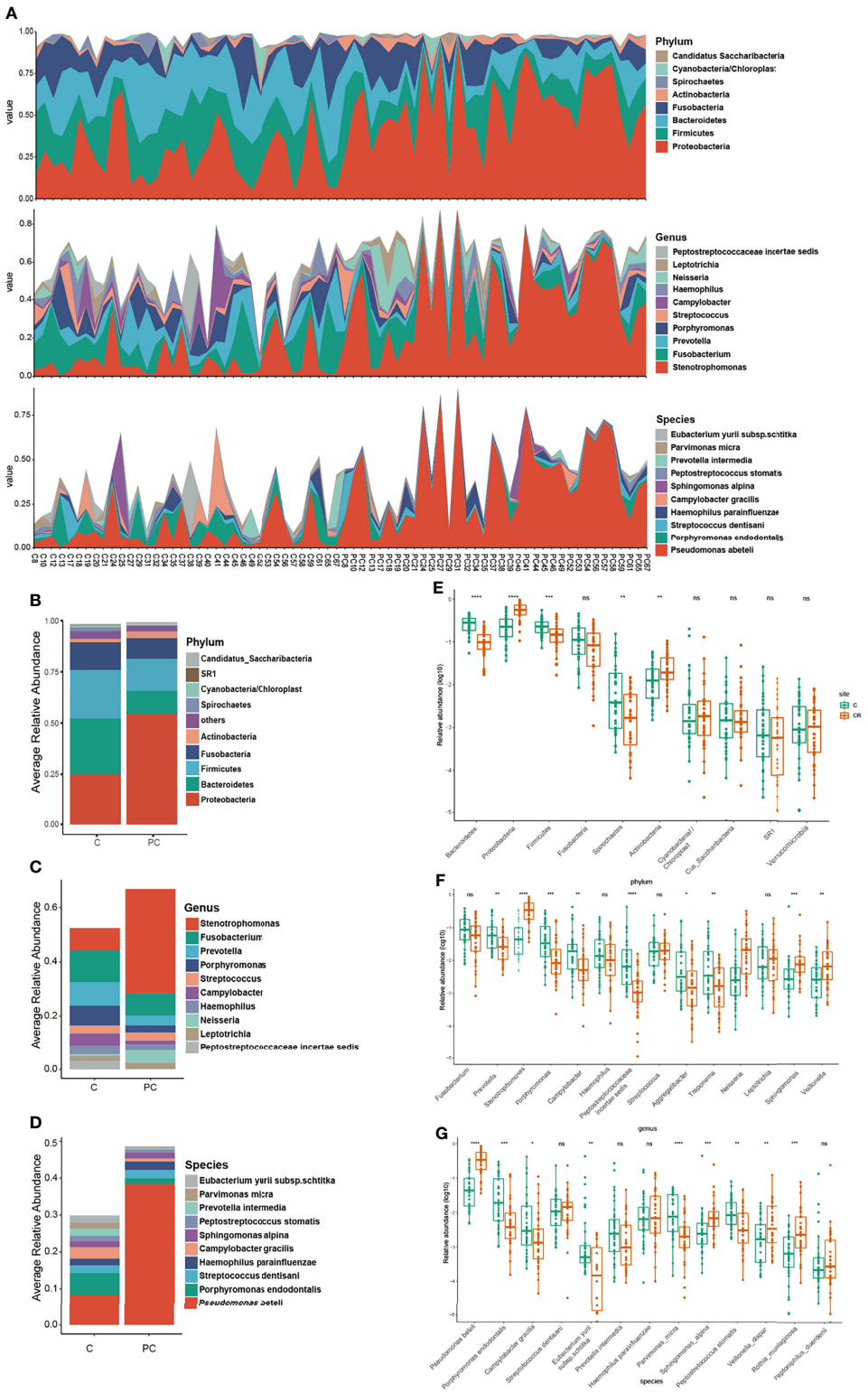

FIGURE 2 | **(A)** The comparison of taxonomic composition between tumor and paracancerous tissue samples. Distribution of relative abundance of microbiome in the tumor tissue and paracancerous tissue of each OSCC subject at the phylum, genus, and species level. Histograms described relative abundances of the **(B)** top 10 phylum, **(C)** 10 genera, and **(D)** top 10 species in the tumor tissue and paracancerous tissue. **(E–G)** Prevalence of bacterial phylum, genera and species associated with tumor and paracancerous tissue of OSCC subjects. C, tumor tissue; PC, paracancerous tissue. ns, no significance; $^{*}P < 0.05$, $^{**}P < 0.005$, $^{***}P < 0.001$, $^{****}P < 0.0001$.

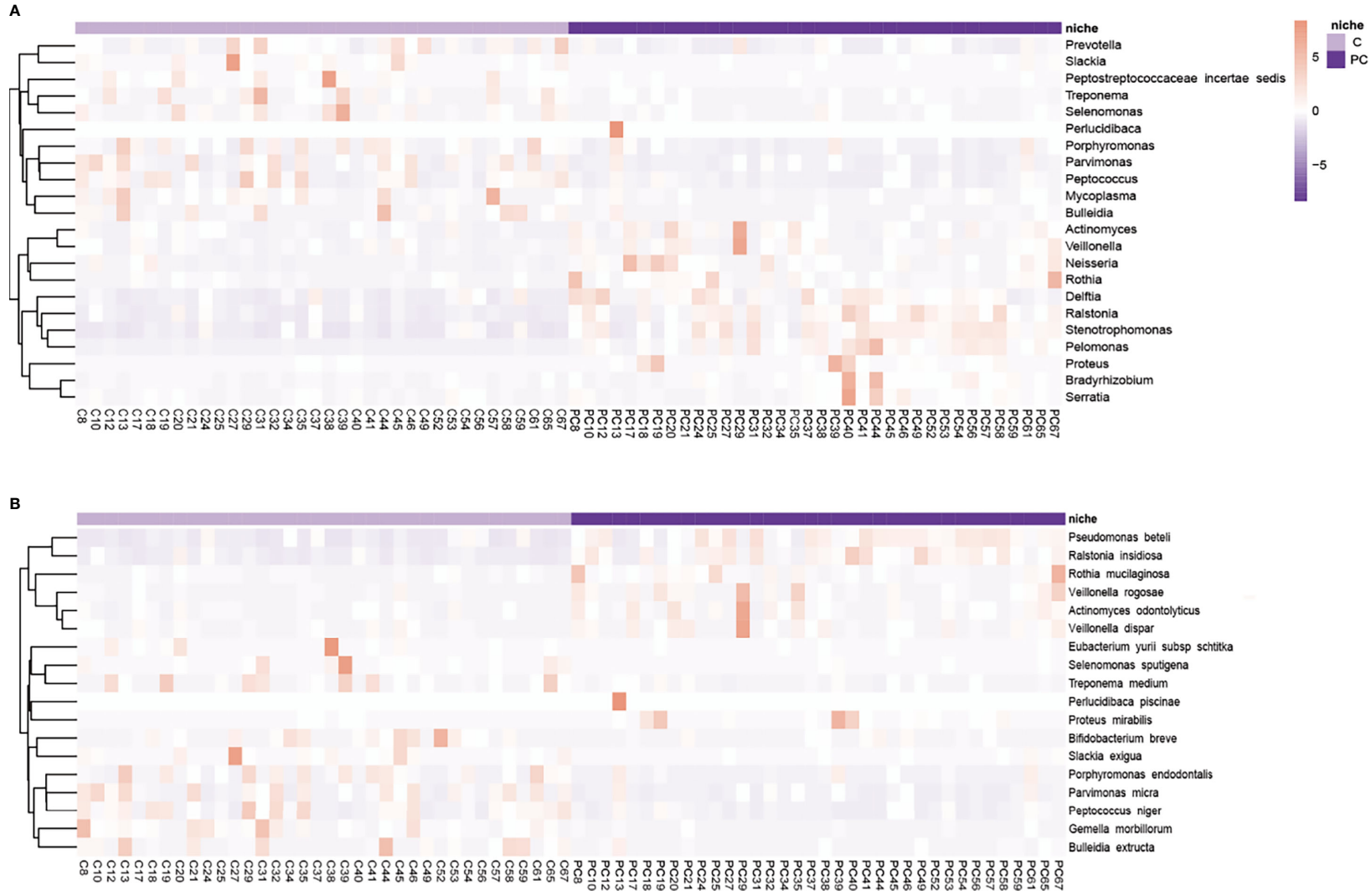

FIGURE 3 | Hierarchically clustered heatmap analysis of differential microflora. The **(A)** genera and **(B)** species level microbial community indicated the formation of two main clusters, separating tumor tissue and paracancerous tissue of each subject. Color key of heat map was shown on the right side of the figure. It shows microbes with high abundance in red, microbes with low abundance in purple. C, tumor tissue; PC, paracancerous tissue.

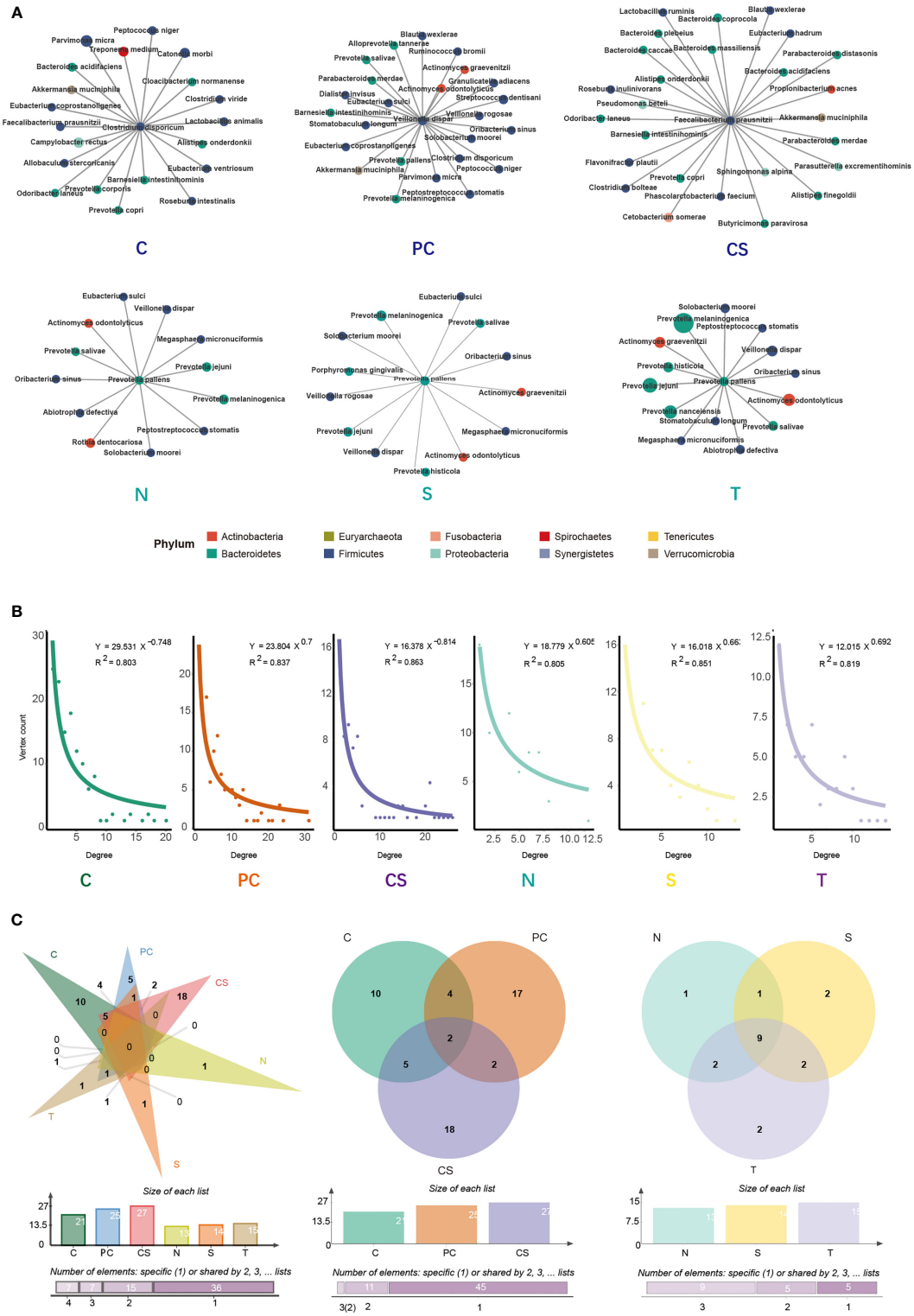

FIGURE 4 | SparCC analysis of the co-occurrence network and core microbiome. **(A)** Key species network in tumor tissue, paracancerous tissue, cancer surface, anatomically matched contralateral normal mucosa, saliva, and tongue coat. Each node represents a specie, and each edge represents a significant co-occurrence relationship. **(B)** SparCC network followed the law of power-law distribution. **(C)** Venn diagram depicts the overlap of bacterial species among the different niches. C, tumor tissue; PC, paracancerous tissue; CS, cancer surface; N, anatomically matched contralateral normal mucosa; S, saliva; T, tongue coat.

Supplementary Figure 2, tumor and paracancerous group were the two densest clusters among the six niches, indicating increased network complexity of the two groups. *Clostridium disporicum* and *Veillonella dispar*, with the most associations in the clusters, were the key species in tumor and paracancerous tissue samples, respectively (**Figure 4A**). On the cancer surface, the key species was *Faecalibacterium prausnitzi*, one of the most abundant and important commensal bacteria in the human intestinal microbiome. Contralateral normal mucosa, saliva, and tongue coat samples exhibited the same key species, *Prevotella pallens*, indicating that this species heavily participates in the bacterial ecology structure of the 3 niches, and the three niches presented relatively similar microbial community compositions.

As showcased in **Figure 4C**, the Venn diagram was generated by the bacterial species in **Figure 4A**, and it represented the overlap of species among different groups. For the species directly connected to the key species, there were no overlapping species across all six groups. Besides, 2 species overlap across the tumor tissue, paracancerous tissue, and cancer surface, and 9 species overlap among the other three groups were observed, suggesting that the controlateral normal mucosa, saliva, and tongue coat had similar microbial structure in their co-occurrence networks. These findings were consistent with the results shown above.

Diagnostic Performance of the Oral Microbiome in Discriminating OSCC

To assess the association between the microbial community and the clinical index of OSCC, tumor samples were grouped by tumor size (1: T1, 2: T2, 3: T3, 4: T4), grade (1: highly differentiated, 2: moderately differentiated, 3: poorly differentiated), stage (1: T1 N0 M0, 2: T2 N0 M0, 3: T1-2 N1 M0 and T3 N0-1 M0, 4: T1-3 N2 M0 and T4a N0-2 M0), and metastasis (1: metastasis, 2: no metastasis) using the TNM classification of the American Joint Committee on Cancer (AJCC Cancer Staging Manual, Eighth Edition). MaAsLin2 analysis was conducted to identify bacterial differences between groups. ROC curve analysis was performed to evaluate whether the relative abundances of specific microorganisms reflected any clinical characteristics. As presented in **Figures 5A, B**, the ROC curve was constructed to assess the diagnostic ability of selected bacterials for OSCC metastasis. The AUC reached 0.823 at the genus level, indicating a good level of diagnostic performance of the genera *Lautropia*, *Asteroleplasma*, *Parvimonas*, *Peptostreptococcus*, *Pyramidobacter*, *Roseburia*, and *Propionibacterium* to predict tumor metastasis. The species *Parvimonas micra*, *Prevotella pallens*, *Propionibacterium acnes*, *Pyramidobacter piscolens*, *Luteimonas marina*, and *Peptostreptococcus stomatis* also correlated significantly with metastasis (AUC = 0.776; **Figures 5C, D**). However, the associations between bacterial populations and other clinicopathological characteristics (tumor size, grade, and stage) were poor (**Supplementary Figure 3**).

Prediction of Microbiome Phenotype and Functions

BugBase was used to predict and compare the microbial phenotype across the six sample locations. As shown in **Supplementary Figure 4**, tumor tissue was characterized by the highest abundance of anaerobes, while the highest abundance of aerobic, gram-negative bacteria, biofilm formation, potential pathogenicity, and stress tolerance were found in the paracancerous tissue. Tumor and paracancerous tissues both showed a low abundance of mobile elements. Upon comparing tumor tissue and paracancerous tissue, tumor tissue exhibited a greater abundance of gram-positive bacteria, anaerobes, and facultative anaerobes than paracancerous tissue, while gram-negative bacteria, aerobic, biofilm formation, potential pathogenicity, and stress tolerance were more frequent in the paracancerous tissue (all $p < 0.05$; **Figure 6A**).

Tax4Fun2 analysis was used to predict and compare changes in microbial function and metabolism pathways between the two groups (**Figure 6B**). Functions related to nucleotide metabolism, including amino sugar and nucleotide sugar metabolism, purine, and pyrimidine metabolism, as well as functions related to mRNA translation including ribosome and aminoacyl tRNA biosynthesis, were significantly enriched in tumor tissue ($P < 0.05$). Several metabolic pathways related to biosynthesis, energy supply, such as biosynthesis of amino acids, carbon fixation pathways, carbon metabolism, fructose and mannose metabolism, pyruvate metabolism, glycolysis/glucogenesis, and ABC transporters were also more abundant in tumor tissue ($P < 0.05$), While biofilm formation, fatty acid biosynthesis, metabolism and degradation were decreased.

DISCUSSION

The oral microbiome plays an essential role both in the stability and balance of oral microecology and host defense. Once homeostasis is disturbed, an imbalance of microbial flora contributes to oral diseases such as dental caries, periodontitis, and oral mucosal diseases, and systemic diseases, such as cardiovascular disease, diabetes, rheumatoid arthritis, Alzheimer's disease, and head and neck cancers (Sampaio-Maia et al., 2016; Long et al., 2017; Kilian, 2018; Sudhakara et al., 2018; Sureda et al., 2020; Radaic and Kapila, 2021). There is much evidence that the colonization, translocation, and imbalance of oral microflora play key roles in OSCC, providing potential biomarkers for the occurrence, development, and prognosis of OSCC (Wang and Ganly, 2014; Sun et al., 2020). However, at present, differences in oral microbiome across multiple oral niches in OSCC patients have not been truly investigated.

In the present study, samples were collected from 65 patients with OSCC, and 16S rDNA sequencing was used to characterize the microbial profile in tumor tissue, paracancerous tissue, cancer surface, contralateral normal mucosa, saliva, and tongue coat to evaluate associations between the oral microbiome and OSCC. Significant differences in microbial composition and function were found between the six different oral niches. The diversity and uniformity of tumor tissue were found to be higher than that of other niches, as indicated by the Shannon and Simpson diversity indices, consistent with previous findings

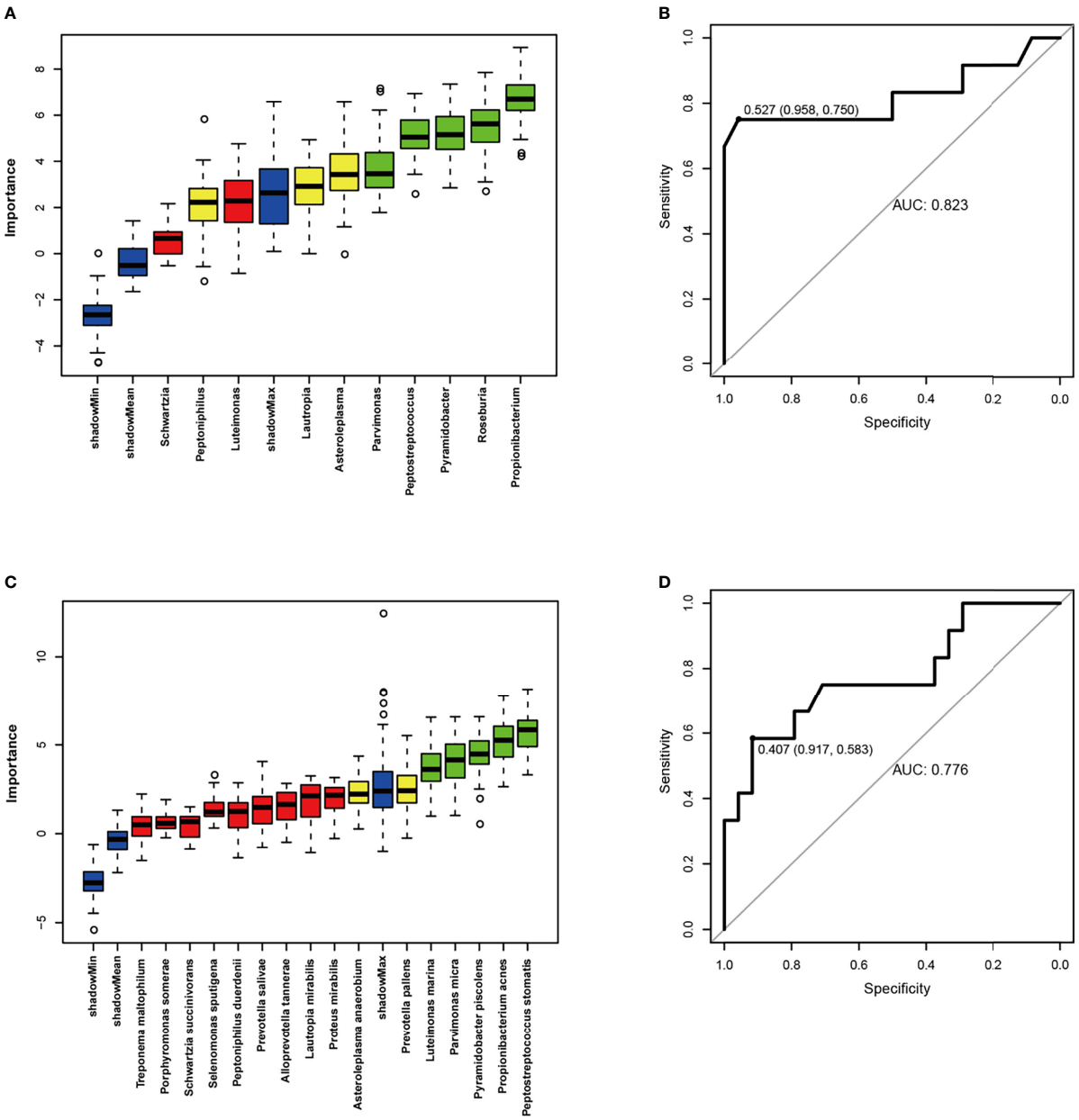

FIGURE 5 | ROC curve analyses were performed to evaluate the diagnostic performance of oral microbiome for OSCC metastasis. **(A, C)** Boruta algorithm was used for feature selection and to assess the importance of variables. **(B, D)** ROC curves were constructed to predict diagnostic power of microbiome for tumor metastasis. It suggested that higher abundance of Lautropia, Asteroleplasma, Parvimonas, Peptostreptococcus, Pyramidobacter, Roseburia and Propionibacterium in the tumor tissue appeared to be associated with higher rates of tumor metastases.

(Zhao et al., 2017; Yang et al., 2018; Su et al., 2021). However, some contradictory results have also been reported, such as decreases in the diversity of bacterial communities in tumor samples (Pushalkar et al., 2012; Schmidt et al., 2014; Wang et al., 2017; Sarkar et al., 2021).

Previous studies have shown *Proteobacteria*, *Firmicutes*, *Bacteroidetes*, *Fusobacteria*, and *Actinobacteria* to be the dominant phyla (Schmidt et al., 2014; Guerrero-Preston et al., 2016; Al-Hebshi et al., 2017b; Wang et al., 2017; Sarkar et al., 2021), in support of our findings. The *Firmicutes* have been reported to be the most abundant phylum in the oral microbiome (Schmidt et al., 2014; Guerrero-Preston et al., 2016; Perera et al., 2018; Sarkar et al., 2021). In this study, *Firmicutes* was the most abundant phylum in contralateral normal mucosa and saliva, and the microflora of the two niches was similar at the phylum, genus, and species levels.

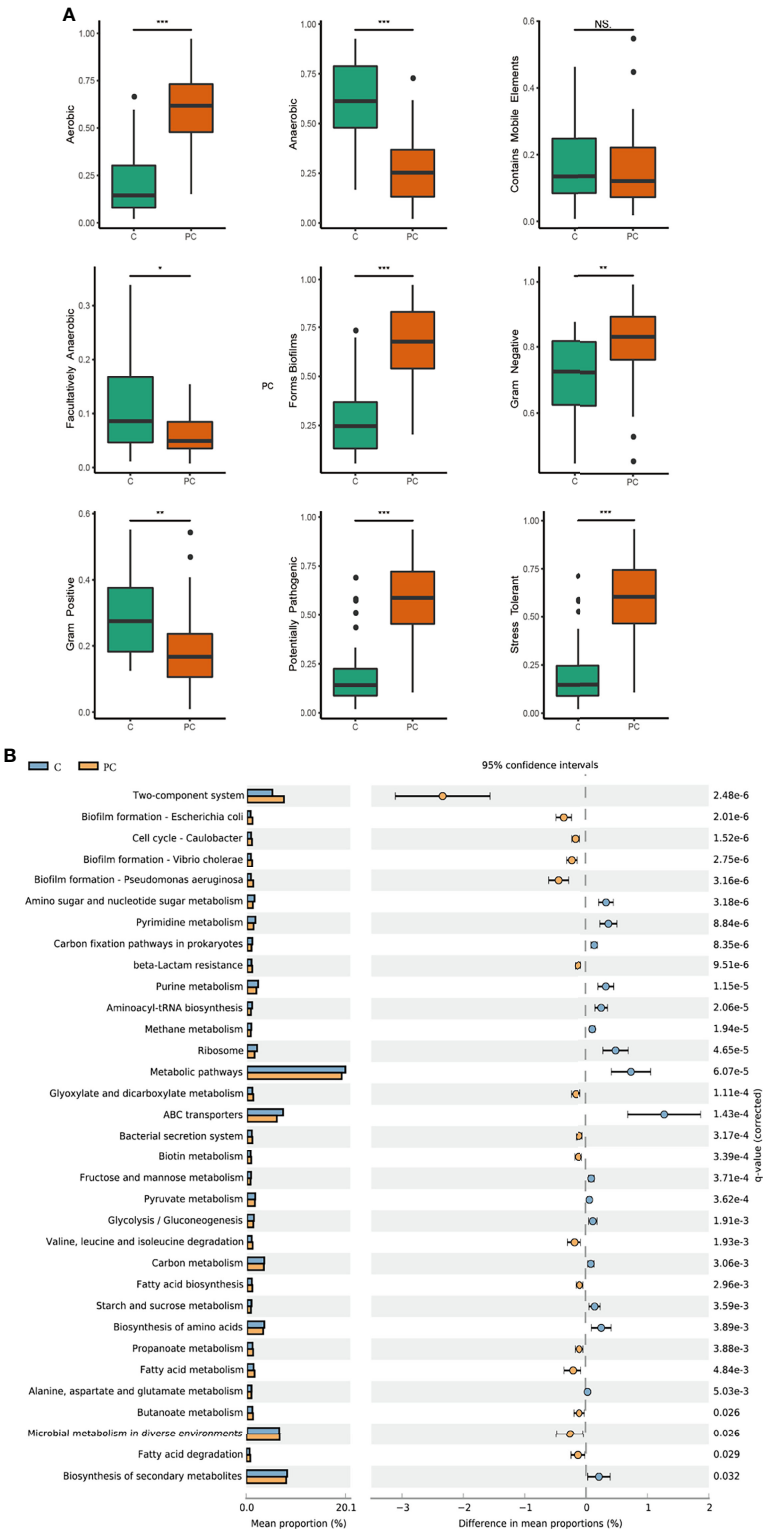

FIGURE 6 | Prediction of microbiome phenotypes and functions. **(A)** Phenotypes prediction was conducted by BugBase analysis, including gram-positive, gram-negative, biofilm forming, stress tolerance, potential pathogenicity, aerobic, anaerobic, facultatively aerobic and mobile elements. **(B)** Microbial functional profile was predicted by Tax4Fun2 based on the KEGG pathway, and statistically analyzed by STAMP. KEGG pathways with significant abundance difference ($P < 0.05$) are shown. C, tumor tissue; PC, paracancerous tissue. ns, no significance; *$P < 0.05$, **$P < 0.005$, ***$P < 0.001$.

Upon comparing tumor tissue and paracancerous tissue, the tumor tissue demonstrated greater populations of *Fusobacterium*, *Prevotella*, *Porphyromonas*, *Campylobacter*, *Aggregatibacter*, *Treponema*, and *Peptostreptococcus*, and lower populations of *Stenotrophomonas*, *Neisseria*, *Sphingomonas*, and *Veillonella*. Most of the genera significantly enriched in tumor tissue samples were those that have been associated with periodontal diseases, in agreement with previous studies (Zhao et al., 2017; Li et al., 2020; Kavarthapu and Gurumoorthy, 2021). Periodontitis-associated bacteria promote the production of pro-inflammatory mediators, such as interleukin, TNF-α, and matrix metalloproteinase, which are released into the oral microenvironment, causing chronic inflammation, and promoting tumor cell migration and invasion (Champagne et al., 2003; Tezal et al., 2009; Schmidt et al., 2014; Li et al., 2020). Fusobacterium, a normal component of the oral microbiome, coexists with other bacteria in dental plaque, forming a bridge between early and late colonizers (Zhao et al., 2017). The virulence factors produced by Fusobacterium, such as adhesins, LPS, and RadD, have been associated with aberrant immune responses, chronic infection, modulating oral carcinogenesis, and promoting cancer progression (Gholizadeh et al., 2017; De Andrade, et al., 2019). Aggregatibacter has been associated with invasive periodontitis (Ando et al., 2012) and can induce inflammation through cytolethal distendin toxin (CDT), leukotoxin and lipopolysaccharide (LPS) (Herbert et al., 2016). Further, the abundance of *Neisseria*, *Veillonella*, *Rothia*, and *Streptococcus* had been reported to decrease significantly in tumor tissue, which may be related to a decrease in the health of the oral cavity (Pushalkar et al., 2012; Zhao et al., 2017; Al-Hebshi et al., 2017b; Sun et al., 2020).

At the species level, the relative abundances of *Porphyromonas endodontalis*, *Campylobacter gracilis*, *Peptostreptococcus stomatis*, *Prevotella intermedia*, *Eubacterium vuril subsp schtika*, and *Parvimonas micra* in tumor tissue increased in comparison to those in paracancerous tissue. Notably, these florae are all anaerobes or facultative anaerobes. The phenotype prediction also showed that tumor samples exhibited the highest abundances of anaerobes. Tumor cells live in an environment that is comparatively hypoxic and of a lower pH in comparison to healthy tissue, which may be due to the increased metabolic rate of tumor cells combined with an insufficient local blood supply, causing most of the bacteria that are found thriving in tumor tissue to be anaerobes. *Porphyromonas Endodontalis*, a newly discovered periodontal pathogen, was observed to be highly abundant in cancerous tissue (Tezal et al., 2009; Pérez-Chaparro et al., 2014; Gonçalves et al., 2016). *Parvimonas micra* was also reported to be enriched in OSCC tumor lesions and be associated with tumor stages. (Al-Hebshi et al., 2017a; Yang et al., 2018).

We used SparCC analysis to illustrate the microbial network. In tumor tissues, the key species was Clostridium disporicum. Clostridium disporicum was first isolated from rat intestinal flora in 1987 (Horn, 1987). Otherwise, Clostridia are an important component of the human intestinal anaerobic flora, so the predisposing factors of clostridial infections are commonly associated with malignancy or antibiotherapy (Mallozzi et al., 2010). As a common conditional pathogen, Clostridium can colonize to colonic epithelial cells and produce carcinogenic substances to promote tumorigenesis.

ROC curve analysis is typically used to evaluate the discrimination ability and diagnostic efficacy of a predictive model. In this study, the ROC model containing *Lautropia*, *Asteroleplasma*, *Parvimonas*, *Peptostreptococcus*, *Pyramidobacter, Roseburia*, and *Propionibacterium* provided a good level of prediction accuracy for OSCC metastasis, with a statistically significant diagnostic accuracy of 82.3%, suggestive of a significant correlation with the metastasis of OSCC. OSCC is prone to early transfer to the regional lymph nodes, so the tumor metastasis trend is an important predictor of survival outcomes in OSCC patients. Mager et al. found that high abundance of several bacterials in salivary may be diagnostic indicators of OSCC (Mager et al., 2005). Wei et al. proved that salivary metabolomics (Valine, lactic acid, and phenylalanine) had the potential for detection of OSCC (Wei et al., 2011). Furthermore, two other studies have demonstrated good diagnostic power of oral microbiome for the OSCC (Zhao et al., 2017; Li et al., 2020). The above studies compare OSCC patients to healthy control individuals, while our research performed a comparison between patients with tumor metastasis and patients without lymph nodes and other organ metastases, drawing the conclusion of good diagnostic ability of oral microbiome for OSCC metastases. Our study has some limitations in samples and methodology, further research is needed to confirm the present results.

Finally, Tax4Fun2 was used to predict the functional profile based on 16S rDNA gene sequences, furthering the understanding of the significance of the oral microbiome. Nucleotide metabolism is an important pathway providing purine and pyrimidine molecules for DNA replication and RNA biogenesis (Siddiqui and Ceppi, 2020), and mRNA translation is a critical process of gene expression and protein synthesis. The current study showed that functions related to nucleotide metabolism and mRNA translation, such as amino sugar and nucleotide sugar metabolism, purine and pyrimidine synthesis, ribosome and aminoacyl tRNA biosynthesis, and the functions related to biosynthesis and energy supply were significantly enriched in OSCC samples, likely reflecting the enhanced fundamental requirements for bacterial life in the OSCC habitat and specific adaptation to distinct micro-ecological environment. The variations of bacterial metabolic pathways in tumor tissues indicated a contribution of the oral microbiome to creating the tumor microenvironment through the biosynthesis of secondary metabolites (Zhao et al., 2017; Li et al., 2020).

In summary, the present article reports a comprehensive comparison of the microbiome across different oral niches in patients with OSCC, and these findings reveal differences in the characteristics of the oral microflora. The human oral microbiome has been demonstrated to be site-specific (Tanner et al., 2006), and the present study further elucidates species similarities and differences among microbial communities in different oral niches. Periodontitis-related flora and anaerobes were shown to be significantly enriched in tumor tissue. Further, the microorganisms in tumor tissue might be potential indicators of the development and metastasis of OSCC. This study provides

evidence that the dynamic balance between the resident oral microflora and the host is altered in OSCC, which may be the key mechanism by which oral symbiotic bacteria promote or prevent the occurrence of oral cancer. This study had some limitations. Firstly, the taxonomic accuracy of 16S rDNA was limited (Zhao et al., 2017; Johnson et al., 2019). Recent studies have shown that although more than 99% of the sequencing analyses can be correctly classified at the genus level, many bacteria are misclassified (Winand et al., 2019). Further, many bacteria have not yet been sequenced or discovered. Also, the exact pathogenesis of this phenomenon is still to be clarified and it is not currently possible to determine with sufficient certainty, based on these data, whether the observed bacterial changes contribute to the carcinogenesis or progression of OSCC.

DATA AVAILABILITY STATEMENT

The original contributions presented in the study are publicly available. This data can be found here: [http://www.ncbi.nlm.nih.gov/bioproject/866676 /PRJNA866676].The sequencing data generated in this study are submitted to the Sequence Read Archive of the National Center for Biotechnology Information database (accession number: PRJNA866676).

ETHICS STATEMENT

The studies involving human participants were reviewed and approved by Ethics Committee of Qilu Hospital of Shandong University. The patients/participants provided their written informed consent to participate in this study.

AUTHOR CONTRIBUTIONS

FN: Conceptualization, Investigation, Writing-original draft. LW: Conceptualization, Investigation, Methodology, Software, Writing-review & editing. YH: Conceptualization, Investigation,Writing-review & editing. PY: Conceptualization, Supervision, Writing-review & editing. PG: Conceptualization, Investigation,Writing-review & editing. QF: Conceptualization, Formal analysis, Investigation, Visualization, Supervision, Writing-review & editing. CY: Formal analysis, Data curation, Supervision, Project administration. All authors contributed to the article and approved the submitted version.

FUNDING

This work was supported by the National Natural Science Foundation of China (No. 81702684). National Natural Science Foundation of China (No. 82071122), The Taishan Young Scholars of Shandong Province (tsqn 201909180), Oral Microbiome Innovation Team of Shandong Province (No. 2020KJK001), The National High-level Young Scientist Project Foundation (2019), Excellent Young Scientist Foundation of Shandong Province (No. ZR202102230369) and periodontitis microbiome innovation team of Jinan City (2021GXRC021).

SUPPLEMENTARY MATERIAL

The Supplementary Material for this article can be found online at: https://www.frontiersin.org/articles/10.3389/fcimb.2022.905653/full#supplementary-material

REFERENCES

Al-Hebshi, N. N., Alharbi, F. A., Mahri, M., and Chen, T. (2017a). Differences in the Bacteriome of Smokeless Tobacco Products With Different Oral Carcinogenicity: Compositional and Predicted Functional Analysis. *Genes (Basel)* 8 (4), 106. doi: 10.3390/genes8040106

Al-Hebshi, N. N., Nasher, A. T., Maryoud, M. Y., Homeida, H. E., Chen, T., Idris, A. M., et al. (2017b). Inflammatory Bacteriome Featuring Fusobacterium Nucleatum and Pseudomonas Aeruginosa Identified in Association With Oral Squamous Cell Carcinoma. *Sci. Rep.* 7 (1), 1834. doi: 10.1038/s41598-017-02079-3

Ando, E. S., De-Gennaro, L. A., Faveri, M., Feres, M., DiRienzo, J. M., and Mayer, M. P. (2012). Immune Response to Cytolethal Distending Toxin of Aggregatibacter Actinomycetemcomitans in Periodontitis Patients. *J. Periodontal. Res.* 45 (4), 471–480. doi: 10.1111/j.1600-0765.2009.01260.x

Basu, S., Kumbier, K., Brown, J. B., and Yu, B. (2018). Iterative Random Forests to Discover Predictive and Stable High-Order Interactions. *Proc. Natl. Acad. Sci. U. S. A.* 115 (8), 1943–1948. doi: 10.1073/pnas.1711236115

Bolyen, E., Rideout, J. R., Dillon, M. R., Bokulich, N. A., Abnet, C. C., Al-Ghalith, G. A., et al. (2019). Reproducible, Interactive, Scalable and Extensible Microbiome Data Science Using QIIME 2. *Nat. Biotechnol.* 37 (8), 852–857. doi: 10.1038/s41587-019-0209-9

Brennan, C. A., and Garrett, W. S. (2019). Fusobacterium Nucleatum-Symbiont, Opportunist and Oncobacterium. *Nat. Rev. Microbiol.* 17 (3), 156–166. doi: 10.1038/s41579-018-0129-6

Champagne, C. M. E., Buchanan, W., Reddy, M. S., Preisser, J. S., Beck, J. D., and Offenbacher, S. (2003). Potential for Gingival Crevice Fluid Measures as Predictors of Risk for Periodontal Diseases. *Periodontol. 2000* 31, 167–180. doi: 10.1034/j.1600-0757.2003.03110.x

Chattopadhyay, I., Verma, M., and Panda, M. (2019). Role of Oral Microbiome Signatures in Diagnosis and Prognosis of Oral Cancer. *Technol. Cancer Res. Treat.* 18, 1533033819867354. doi: 10.1177/1533033819867354

Chi, A. C., Day, T. A., and Neville, B. W. (2015). Oral Cavity and Oropharyngeal Squamous Cell Carcinoma–an Update. *CA Cancer J. Clin.* 65 (5), 401–421. doi: 10.3322/caac.21293

Choi, S. W., Moon, E. K., Park, J. Y., Jung, K. W., Oh, C. M., Kong, H. J., et al. (2014). Trends in the Incidence of and Survival Rates for Oral Cavity Cancer in the Korean Population. *Oral. Dis.* 20 (8), 773–779. doi: 10.1111/odi.12251

De Andrade, K. Q., Almeida-da-Silva, C. L. C., and Coutinho-Silva, R. (2019). Immunological Pathways Triggered by Porphyromonas Gingivalis and Fusobacterium Nucleatum: Therapeutic Possibilities? *Mediators Inflamm.* 2019, 7241312. doi: 10.1155/2019/7241312

Edgar, R. C. (2010). Search and Clustering Orders of Magnitude Faster Than BLAST. *Bioinformatics* 26 (19), 460–461. doi: 10.1093/bioinformatics/btq461

Friedman, J., and Alm, E. J. (2012). Inferring Correlation Networks From Genomic Survey Data. *PloS Comput. Biol.* 8 (9), e1002687. doi: 10.1371/journal.pcbi.1002687

Ganly, I., Yang, L., Giese, R. A., Hao, Y., Nossa, C. W., Morris, L. G. T., et al. (2019). Periodontal Pathogens Are a Risk Factor of Oral Cavity Squamous Cell Carcinoma, Independent of Tobacco and Alcohol and Human Papillomavirus. *Int. J. Cancer* 145 (3), 775–784. doi: 10.1002/ijc.32152

Gholizadeh, P., de Eslami, H., and Kafil, H. S. (2017). Carcinogenesis Mechanisms of Fusobacterium Nucleatum. *BioMed. Pharmacother.* 89, 918–925. doi: 10.1016/j.biopha.2017.02.102

Gonçalves, C., Soares, G. M., Faveri, M., Pérez-Chaparro, P. J., Lobão, E., Figueiredo, L. C., et al. (2016). Association of Three Putative Periodontal Pathogens With Chronic Periodontitis in Brazilian Subjects. *J. Appl. Oral. Sci.* 24 (2), 181–185. doi: 10.1590/1678-775720150445

Guerrero-Preston, R., Godoy-Vitorino, F., Jedlicka, A., Rodríguez-Hilario, A., González, H., Bondy, J., et al. (2016). 16s rRNA Amplicon Sequencing Identifies Microbiota Associated With Oral Cancer, Human Papilloma Virus Infection and Surgical Treatment. *Oncotarget* 7 (32), 51320–51334. doi: 10.18632/oncotarget.9710

Herbert, B. A., Novince, C. M., and Kirkwood, K. L. (2016). Aggregatibacter Actinomycetemcomitans, a Potent Immunoregulator of the Periodontal Host Defense System and Alveolar Bone Homeostasis. *Mol. Oral. Microbiol.* 31 (3), 207–227. doi: 10.1111/omi.12119

Hooper, S. J., Crean, S. J., Fardy, M. J., Lewis, M. A. O., Spratt, D. A., Wade, W. G., et al. (2007). A Molecular Analysis of the Bacteria Present Within Oral Squamous Cell Carcinoma. *J. Med. Microbiol.* 56 (Pt 12), 1651–1659. doi: 10.1099/jmm.0.46918-0

Horn, N. (1987). Clostridium-Disporicum Sp-Nov, a Saccharolytic Species Able to Form 2 Spores Per Cell, Isolated From a Rat Cecum. *Int. J. Syst. Bacteriol.* 37 (4), 398–401. doi: 10.1099/00207713-37-4-398

Johnson, J. S., Spakowicz, D. J., Hong, B. Y., Petersen, L. M., Demkowicz, P., Chen, L., et al. (2019). Evaluation of 16S rRNA Gene Sequencing for Species and Strain-Level Microbiome Analysis. *Nat. Commun.* 10 (1), 5029. doi: 10.1038/s41467-019-13036-1

Kanehisa, M., and Goto, S. (2000). KEGG: Kyoto Encyclopedia of Genes and Genomes. *Nucleic Acids Res.* 28 (1), 27–30. doi: 10.1093/nar/28.1.27

Kavarthapu, A., and Gurumoorthy, K. (2021). Linking Chronic Periodontitis and Oral Cancer: A Review. *Oral. Oncol.* 121, 105375. doi: 10.1016/j.oraloncology.2021.105375

Kilian, M. (2018). The Oral Microbiome - Friend or Foe? *Eur. J. Oral. Sci.* 126 Suppl 1, 5–12. doi: 10.1111/eos.12527

Li, Y., Tan, X., Zhao, X., Xu, Z., Dai, W., Duan, W., et al. (2020). Composition and Function of Oral Microbiome Between Gingival Squamous Cell Carcinoma and Periodontitis. *Oral. Oncol.* 107, 104710. doi: 10.1016/j.oraloncology.2020.104710

Long, J., Cai, Q., Steinwandel, M., Hargreaves, M. K., Bordenstein, S. R., Blot, W. J., et al. (2017). Association of Oral Microbiome With Type 2 Diabetes Risk. *J. Periodontal. Res.* 52 (3), 636–643. doi: 10.1111/jre.12432

Mager, D. L., Haffajee, A. D., Devlin, P. M., Norris, C. M., Posner, M. R., and Goodson, J. M. (2005). The Salivary Microbiota as a Diagnostic Indicator of Oral Cancer: A Descriptive, non-Randomized Study of Cancer-Free and Oral Squamous Cell Carcinoma Subjects. *J. Transl. Med.* 3, 27. doi: 10.1186/1479-5876-3-27

Mager, D. L., Ximenez-Fyvie, L. A., Haffajee, A. D., and Socransky, S. S. (2003). Distribution of Selected Bacterial Species on Intraoral Surfaces. *J. Clin. Periodontol.* 30 (7), 644–654. doi: 10.1034/j.1600-051x.2003.00376.x

Mallozzi, M., Viswanathan, V. K., and Vedantam, G. (2010). Spore-Forming Bacilli and Clostridia in Human Disease. *Future Microbiol.* 5 (7), 1109–1123. doi: 10.2217/fmb.10.60

Mascitti, M., Togni, L., Troiano, G., Caponio, V. C. A., Gissi, D. B., Montebugnoli, L., et al. (2019). Beyond Head and Neck Cancer: The Relationship Between Oral Microbiota and Tumour Development in Distant Organs. *Front. Cell Infect. Microbiol.* 9, 232. doi: 10.3389/fcimb.2019.00232

McInnes, P., and Cutting, M. (2010). *Manual of Procedures for Human Microbiome Project: Core Microbiome Sampling, Protocol A, HMP Protocol No. 07–001, Version 11. 2010*. Available at: https://hmpdacc.org/hmp/doc/HMP_MOP_Version12_0_072910.pdf.

Minarovits, J. (2021). Anaerobic Bacterial Communities Associated With Oral Carcinoma: Intratumoral, Surface-Biofilm and Salivary Microbiota. *Anaerobe* 68, 102300. doi: 10.1016/j.anaerobe.2020.102300

Patel, M. A., Blackford, A. L., Rettig, E. M., Richmon, J. D., Eisele, D. W., and Fakhry, C. (2016). Rising Population of Survivors of Oral Squamous Cell Cancer in the United States. *Cancer* 122 (9), 1380–1387. doi: 10.1002/cncr.29921

Perera, M., Al-Hebshi, N. N., Perera, I., Ipe, D., Ulett, G. C., Speicher, D. J., et al. (2018). Inflammatory Bacteriome and Oral Squamous Cell Carcinoma. *J. Dent. Res.* 97 (6), 725–732. doi: 10.1177/0022034518767118

Peres, M. A., Macpherson, L. M. D., Weyant, R. J., Daly, B., Venturelli, R., Mathur, M. R., et al. (2019). Oral Diseases: A Global Public Health Challenge. *Lancet* 2394 (10194), 249–260. doi: 10.1016/S0140-6736(19)31146-8

Pérez-Chaparro, P. J., Gonçalves, C., Figueiredo, L. C., Faveri, M., Lobão, E., Tamashiro, N., et al. (2014). Newly Identified Pathogens Associated With Periodontitis: A Systematic Review. *J. Dent. Res.* 93 (9), 846–858. doi: 10.1177/0022034514542468

Pushalkar, S., Ji, X., Li, Y., Estilo, C., Yegnanarayana, R., Singh, B., et al. (2012). Comparison of Oral Microbiota in Tumor and non-Tumor Tissues of Patients With Oral Squamous Cell Carcinoma. *BMC Microbiol.* 12, 144. doi: 10.1186/1471-2180-12-144

Radaic, A., and Kapila, Y. L. (2021). The Oralome and Its Dysbiosis: New Insights Into Oral Microbiome-Host Interactions. *Comput. Struct. Biotechnol. J.* 19, 1335–1360. doi: 10.1016/j.csbj.2021.02.010

Rai, A. K., Panda, M., Das, A. K., Rahman, T., Das, R., Das, K., et al. (2021). Dysbiosis of Salivary Microbiome and Cytokines Influence Oral Squamous Cell Carcinoma Through Inflammation. *Arch. Microbiol.* 203 (1), 137–152. doi: 10.1007/s00203-020-02011-w

Sampaio-Maia, B., Caldas, I. M., Pereira, M. L., Pérez-Mongiovi, D., and Araujo, R. (2016). The Oral Microbiome in Health and Its Implication in Oral and Systemic Diseases. *Adv. Appl. Microbiol.* 97, 171–210. doi: 10.1016/bs.aambs.2016.08.002

Sarkar, P., Malik, S., Laha, S., Das, S., Bunk, S., Ray, J. G., et al. (2021). Dysbiosis of Oral Microbiota During Oral Squamous Cell Carcinoma Development. *Front. Oncol.* 11. doi: 10.3389/fonc.2021.614448

Schmidt, B. L., Kuczynski, J., Bhattacharya, A., Huey, B., Corby, P. M., Queiroz, E. L., et al. (2014). Changes in Abundance of Oral Microbiota Associated With Oral Cancer. *PloS One* 9 (6), e98741. doi: 10.1371/journal.pone.0098741

Siddiqui, A., and Ceppi, P. (2020). A non-Proliferative Role of Pyrimidine Metabolism in Cancer. *Mol. Metab.* 35, 100962. doi: 10.1016/j.molmet.2020.02.005

Siegel, R. L., Miller, K. D., and Jemal, A. (2020). Cancer Statistic. *CA Cancer J. Clin.* 70 (1), 7–30. doi: 10.3322/caac.21590

Su, S. C., Chang, L. C., Huang, H. D., Peng, C. Y., Chuang, C., Chen, Y. T., et al. (2021). Oral Microbial Dysbiosis and Its Performance in Predicting Oral Cancer. *Carcinogenesis* 42 (1), 127–135. doi: 10.1093/carcin/bgaa062

Sudhakara, P., Gupta, A., Bhardwaj, A., and Wilson, A. (2018). Oral Dysbiotic Communities and Their Implications in Systemic Diseases. *Dent. J. (Basel)* 6 (2), 10. doi: 10.3390/dj6020010

Sun, J., Tang, Q., Yu, S., Xie, M., Xie, Y., Chen, G., et al. (2020). Role of the Oral Microbiota in Cancer Evolution and Progression. *Cancer Med.* 9 (17), 6306–6321. doi: 10.1002/cam4.3206

Sureda, A., Daglia, M., Argüelles Castilla, S., Sanadgol, N., Fazel Nabavi, S., Khan, H., et al. (2020). Oral Microbiota and Alzheimer's Disease: Do All Roads Lead to Rome? *Pharmacol. Res.* 151, 104582. doi: 10.1016/j.phrs.2019.104582

Tanner, A. C., Paster, B. J., Lu, S. C., Kanasi, E., Kent, R.Jr, Van Dyke, T., et al. (2006). Subgingival and Tongue Microbiota During Early Periodontitis. *J. Dent. Res.* 85 (4), 318–323. doi: 10.1177/154405910608500407

Tezal, M., Sullivan, M. A., Hyland, A., Marshall, J. R., Stoler, D., Reid, M. E., et al. (2009). Chronic Periodontitis and the Incidence of Head and Neck Squamous Cell Carcinoma. *Cancer Epidemiol. Biomarkers Prev.* 18 (9), 2406–2412. doi: 10.1158/1055-9965.EPI-09-0334

van Dijk, B. A., Brands, M. T., Geurts, S. M., Merkx, M. A. , and Roodenburg, J. L. (2016). Trends in Oral Cavity Cancer Incidence, Mortality, Survival and Treatment in the Netherlands. *Int. J. Cancer.* 2139 (3), 574–583. doi: 10.1002/ijc.30107

Verma, D., Garg, P. K., and Dubey, A. K. (2018). Insights Into the Human Oral Microbiome. *Arch. Microbiol.* 200 (4), 525–540. doi: 10.1007/s00203-018-1505-3

Wang, H., Funchain, P., Bebek, G., Altemus, J., Zhang, H., Niazi, F., et al. (2017). Microbiomic Differences in Tumor and Paired-Normal Tissue in Head and Neck Squamous Cell Carcinomas. *Genome Med.* 9 (1), 14. doi: 10.1186/s13073-017-0405-5

Wang, L., and Ganly, I. (2014). The Oral Microbiome and Oral Cancer. *Clin. Lab. Med.* 34 (4), 711–719. doi: 10.1016/j.cll.2014.08.004

Watts, S. C., Ritchie, S. C., Inouye, M., and Holt, K. E. (2019). FastSpar: Rapid and Scalable Correlation Estimation for Compositional Data. *Bioinformatics* 35 (6), 1064–1066. doi: 10.1093/bioinformatics/bty734

Wei, J., Xie, G., Zhou, Z., Shi, P., Qiu, Y., Zheng, X., et al. (2011). Salivary Metabolite Signatures of Oral Cancer and Leukoplakia. *Int. J. Cancer* 129 (9), 2207–2217. doi: 10.1002/ijc.25881

Winand, R., Bogaerts, B., Hoffman, S., Lefevre, L., Delvoye, M., Braekel, J. V., et al. (2019). Targeting the 16S rRNA Gene for Bacterial Identification in Complex

Mixed Samples: Comparative Evaluation of Second (Illumina) and Third (Oxford Nanopore Technologies) Generation Sequencing Technologies. *Int. J. Mol. Sci.* 21 (1), 298. doi: 10.3390/ijms21010298

Yang, C. Y., Yeh, Y. M., Yu, H. Y., Chin, C. Y., Hsu, C. W., Liu, H., et al. (2018). Oral Microbiota Community Dynamics Associated With Oral Squamous Cell Carcinoma Staging. *Front. Microbiol.* 9. doi: 10.3389/fmicb.2018.00862

Zhao, H., Chu, M., Huang, Z., Yang, X., Ran, S., Hu, B., et al. (2017). Variations in Oral Microbiota Associated With Oral Cancer. *Sci. Rep.* 7 (1), 11773. doi: 10.1038/s41598-017-11779-9

Conflict of Interest: The authors declare that the research was conducted in the absence of any commercial or financial relationships that could be construed as a potential conflict of interest.

Publisher's Note: All claims expressed in this article are solely those of the authors and do not necessarily represent those of their affiliated organizations, or those of the publisher, the editors and the reviewers. Any product that may be evaluated in this article, or claim that may be made by its manufacturer, is not guaranteed or endorsed by the publisher.

frontiers | Frontiers in Cellular and Infection Microbiology

TYPE Review
PUBLISHED 16 August 2022
DOI 10.3389/fcimb.2022.953277

OPEN ACCESS

EDITED BY
Zheng Zhang,
Nankai University, China

REVIEWED BY
Shu Deng,
Boston University, United States
Houxuan Li,
Nanjing University, China

*CORRESPONDENCE
Jinlin Song
songjinlin@hospital.cqmu.edu.cn

SPECIALTY SECTION
This article was submitted to Microbiome in Health and Disease, a section of the journal Frontiers in Cellular and Infection Microbiology

RECEIVED 26 May 2022
ACCEPTED 18 July 2022
PUBLISHED 16 August 2022

CITATION
Xu X, Zhang T, Xia X, Yin Y, Yang S, Ai D, Qin H, Zhou M and Song J (2022) Pyroptosis in periodontitis: From the intricate interaction with apoptosis, NETosis, and necroptosis to the therapeutic prospects. *Front. Cell. Infect. Microbiol.* 12:953277. doi: 10.3389/fcimb.2022.953277

Pyroptosis in periodontitis: From the intricate interaction with apoptosis, NETosis, and necroptosis to the therapeutic prospects

Xiaohui Xu[1,2,3], Tingwei Zhang[1,2,3], Xuyun Xia[4], Yuanyuan Yin[1,2,3], Sihan Yang[1,2,3], Dongqing Ai[1,2,3], Han Qin[1,2,3], Mengjiao Zhou[1,2,3] and Jinlin Song[1,2,3]*

[1]College of Stomatology, Chongqing Medical University, Chongqing, China, [2]Chongqing Key Laboratory of Oral Diseases and Biomedical Sciences, Chongqing, China, [3]Chongqing Municipal Key Laboratory of Oral Biomedical Engineering of Higher Education, Chongqing, China, [4]Department of Endocrinology, The Second Affiliated Hospital, Chongqing Medical University, Chongqing, China

Periodontitis is highly prevalent worldwide. It is characterized by periodontal attachment and alveolar bone destruction, which not only leads to tooth loss but also results in the exacerbation of systematic diseases. As such, periodontitis has a significant negative impact on the daily lives of patients. Detailed exploration of the molecular mechanisms underlying the physiopathology of periodontitis may contribute to the development of new therapeutic strategies for periodontitis and the associated systematic diseases. Pyroptosis, as one of the inflammatory programmed cell death pathways, is implicated in the pathogenesis of periodontitis. Progress in the field of pyroptosis has greatly enhanced our understanding of its role in inflammatory diseases. This review first summarizes the mechanisms underlying the activation of pyroptosis in periodontitis and the pathological role of pyroptosis in the progression of periodontitis. Then, the crosstalk between pyroptosis with apoptosis, necroptosis, and NETosis in periodontitis is discussed. Moreover, pyroptosis, as a novel link that connects periodontitis with systemic disease, is also reviewed. Finally, the current challenges associated with pyroptosis as a potential therapeutic target for periodontitis are highlighted.

KEYWORDS

pyroptosis, periodontitis, programmed cell death, diabetes, cardiovascular diseases, rheumatoid arthritis

Introduction

Pyroptosis has been demonstrated to participate in the pathophysiological processes of various inflammatory diseases, such as coronavirus disease—2019, colitis, rheumatoid arthritis, Crohn's disease, and neuroinflammatory injury (Xu et al., 2019; Wu et al., 2020; Cai et al., 2021; Tan et al., 2021; Vora et al., 2021). Pyroptosis is categorized as inflammatory programmed cell death that is mainly dependent on caspases and gasdermins (GSDMs). The canonical pyroptosis pathway is initiated by the activation of the NOD-like receptor (NLR) family pyrin domain containing 3 (NLRP3), followed by caspase-1-mediated cleavage and activation of GSDMD, pro-interleukin (IL)-1β, and pro-IL-18. Mature GSDMD (N-terminal fragment of GSDMD) ultimately assembles on the plasma membrane and forms pore-like structures, allowing water to enter cells and enabling the excretion of cellular contents and mature inflammatory factors (Yu et al., 2021). This determines the distinct morphological characteristics of pyroptosis compared to other forms of programmed cell death. Recent studies on pyroptosis have reported that apoptosis-associated caspase-3 and 8 can also mediate the cleavage of GSDMs, thus mediating the activation of pyroptosis (Sarhan et al., 2018; Jiang et al., 2020). This highlights the crosstalk between pyroptosis and apoptosis. According to the existent proofs of pyroptosis in infectious diseases, appropriate pyroptosis activation is beneficial in defending and clearing foreign pathogens, while aberrant activation can cause uncontrolled inflammatory responses and tissue damage. Hence, there are two sides to pyroptosis in the pathophysiological processes of periodontitis, with the potential to be either beneficial or detrimental to the host's defense and periodontal tissue regeneration.

Periodontitis is initiated by infection with pathogenic microorganisms; inadequate treatment results in long-term plaque accumulation, leading to a sustained inflammatory response and irreversible loss of periodontal tissues. Genetics, treatments, and self-performed oral hygiene all affect the prognosis of periodontitis (Kinane et al., 2017). Among the reported mechanisms, various programmed cell death pathways have been reported to be involved in the progression of periodontitis. To date, more than ten kinds of programmed cell death pathways have been identified, and studies have addressed their roles in the pathogenesis of periodontitis. While apoptosis is well studied in periodontitis, there is still a lack of an in-depth investigation of pyroptosis and its relation to apoptosis, necroptosis, and NETosis in this field. Pyroptosis was reported to be associated with an extensive inflammatory reaction in periodontitis. Clinical studies of apical periodontitis (AP) have shown that the level of periodontal pyroptosis correlates positively with disease severity (Cheng et al., 2018). Furthermore, an increased level of pyroptosis in periodontal tissue leads to overactive immune responses and promotes the secretion of active inflammatory factors (IL-1β, IL-18), further contributing to the overactivation of inflammatory signaling pathways. This, in turn, leads to reduced bone formation ability via the suppression of osteoblast activity and enhanced bone resorption via the upregulation of the proliferation and activity of osteoclasts (Li et al., 2021). Ultimately, this results in the exacerbation of the destruction of periodontal tissue and the suppression of its regeneration (Li et al., 2021). The exact mechanisms will be discussed below.

Recent studies have broadened our understanding of the role of pyroptosis in periodontitis. However, there remains a significant gap in comprehending the specific molecular mechanisms of pyroptosis in periodontitis, and the favorable aspect of pyroptosis in periodontitis, regarding its role in clearing pathogens, also requires further verification. This review summarizes the most recent contributions to our understanding of the potential mechanisms underlying the role of pyroptosis in the pathogenesis and development of periodontitis. Moreover, the crosstalk between pyroptosis and apoptosis, necroptosis, and NETosis is discussed. Based on this review, it is hypothesized that pyroptosis might be a novel target that connects periodontitis with systemic disease. Finally, the recent progress and challenges in the translation of pyroptosis research into therapeutic targets are summarized to reveal the new therapeutic options applicable to periodontitis.

Mechanisms of pyroptosis activation in periodontitis

Pyroptosis is initiated by canonical and noncanonical activation of inflammasomes. In the canonical pathway, pathogen-associated molecular patterns (PAMPs) or damage-associated molecular patterns (DAMPs) bind to the major histocompatibility complex or pattern recognition receptors (PRRs), which leads to the increased transcription and translation of inflammasome constituents, and also promotes the activation of inflammasomes by oligomerization and recruitment of the components of the inflammasomes (Rathinam and Fitzgerald, 2016). Inflammasomes are heterologous oligomeric protein complexes usually comprised of NLRs or absent in melanoma 2 (AIM2)-like receptors (ALRs), apoptosis-associated speck-like proteins containing a caspase recruitment domain (ASC), and pro-caspase-1 (Li et al., 2021). Among the 23 identified NLRs in humans, only a few of them participate in the formation of inflammasomes; they include NLRP3, NLRP1, NLRP6, and NLRC4. NLRs usually possess a leucine-rich repeat (LRR) domain at the C-terminal, a nucleotide-binding domain (NBD) or a nucleotide-binding and oligomerization (NACHT) domain in the central region, and a pyrin domain (PYD) at the N terminal of the NLRP or a caspase recruitment domain (CARD) at the N terminal of the

NLRC (Swanson et al., 2019; Li et al., 2021; Yu et al., 2021). Following the activation of inflammasomes, the PYD in the NLRP, such as NLRP3, assembles pro-caspase-1 (full-length) by indirectly binding to the ASC (containing a CARD at the C-terminal and a PYD at the N-terminal) of the inflammasome via the homotypic interaction between PYD–PYD and CARD–CARD. However, the CARD in NLRP1 and NLRC4 can promote the recruitment of pro-caspase-1 by directly binding to their CARD domains (Kay et al., 2020; Taabazuing et al., 2020; Sundaram and Kanneganti, 2021). Once bound to inflammasomes, there is the promotion of the dimerization and autoproteolysis of pro-caspase-1, followed by the release of central and small catalytic domains, p20 and p10 (Guo et al., 2015; Huang et al., 2021; Li et al., 2021).

Unlike in the canonical pathway, in the noncanonical pathway, caspase-4/5 in humans and caspase-11 in mice function as both sensor and effector molecules of lipopolysaccharide (LPS)-induced pyroptosis. After the recognition of LPS, caspase-4/5/11 dimerization and autoproteolysis occur, releasing the p10 and p20 domains (Kayagaki et al., 2015; Downs et al., 2020). Recent advances in this field have indicated that several guanylate binding proteins (GBPs) are involved in caspase-4 signaling induced by LPS (Fisch et al., 2020; Kutsch et al., 2020; Santos et al., 2020; Wandel et al., 2020); however, this requires further investigation in periodontitis. The active caspases in the canonical and noncanonical pathways ultimately proteolytically cleave pro-IL-1β and pro-IL-18 into their biologically active forms. Although caspase-4/5/11 cannot directly cleave pro-IL-1β and pro-IL-18, they can promote the maturation and secretion of IL-1β and IL-18 by activating the NLRP3/caspase-1 pathway (Yu et al., 2021). Simultaneously, the active caspase-1/4/5/11 cleaves the GSDMD protein, the key effector protein of pyroptosis, to form active N- and C-terminal kinase portions. The N-terminal of GSDMD binds to phosphatidylserine, phosphatidic acid, and phosphatidylinositol on the cell membrane, promoting oligomerization and resulting in the formation of pore-like structures on the cells. Changes in membrane permeability lead to cell swelling and membrane rupture, which facilitate the active forms of inflammatory factors to pass through the membrane pores. Moreover, new evidence indicates that the GSDMD pore conduit is predominantly negatively charged, thus favoring the passage of positively charged and neutral cargo, such as the mature forms of IL-1β and IL-18 (Xia et al., 2021).

As mentioned above, GSDMD is the most studied member of the GSDM family, and it mediates both the canonical and noncanonical pathways. GSDMA, -B, -C, and -E, as well as autosomal recessive deafness-59 (DFNB59), are less studied and require further investigation. Aside from DFNB59, all GSDMs have a pore-forming domain at the N-terminal, an autoinhibitory domain at the C-terminal, and a loop domain that links the N- and C-terminal domains (Julien and Wells, 2017; Kovacs and Miao, 2017; Xia et al., 2020). Except for DFNB59, they were proved to be involved in the activation of pyroptosis. Restricted reports showed that GSDME can be cleaved by caspase-3, which specifically generates an N-terminal fragment of GSDME, thus promoting pyroptosis (Wang et al., 2017; Jiang et al., 2020). Moreover, GSDMC was reported to be cleaved by caspase-8, specifically with TNFα treatment, generating an N-terminal fragment of GSDMC, thereby inducing pyroptosis (Hou et al., 2020; Zhang et al., 2021). Caspase-8 has also been reported to cleave GSDMD to induce pyroptosis (Orning et al., 2018; Sarhan et al., 2018; Demarco et al., 2020). These results also indicated that GSDME and GSDMC might be two points linking pyroptosis with apoptosis. This will be discussed below. Aside from caspases, granzyme A has been reported to cleave GSDMB in lymphocytes (Zhou et al., 2020), and granzyme B was reported to directly cleave GSDME in tumor cells (Zhang et al., 2020), ultimately contributing to tumor suppression by invoking pyroptosis. In addition, a recent study reported that neutrophil-specific serine protease-neutrophil elastase (ELANE) can also cleave GSDMD at the N terminal to promote pyroptosis, thereby mediating its biological effects (Kambara et al., 2018). However, non-caspases-dependent cleavage of GSMDs was not clarified in periodontitis. Therefore, detailed molecular and biological investigations need to be conducted to shed light on it.

Accumulating evidence has shown that pyroptosis participates in the pathophysiological process of periodontitis (Bullon et al., 2018; Zhou et al., 2020; Li et al., 2021). Continuous pathogenic microorganism infection is the initiating factor in periodontitis, including bacterial, fungal, viral, and mycoplasma infections. Toll-like receptor 4 (TLR4) is the most characterized pattern recognition receptor during periodontitis and has been largely argued for its crucial role in the LPS-mediated pyroptosis pathway. Basic studies using TLR4 knockout mice models have documented that TLR4 is involved in periodontitis and peri-implantitis initiated by P. gingivalis (Lin et al., 2014; Deng et al., 2020). Recent advances documented that after recognizing and binding to the lipid A portion of LPS by TLR4 particularly, the myeloid differetial protien-2 mediates the binding of LPS with TLR4, followed by initiating the homotypic interaction of TLR4's intracellular toll/interleukin-1 receptor domain with adaptors, including myeloid differentiation factor88 (MyD88) and TIR domain-containing adapter protein inducing IFN-Beta (TRIF). Consecutively, MyD88 binds to interleukin-1 receptor-associated kinase (IRAK) 1 and 2, which facilitates the assembly of TRAF6 and provokes TAK1-mediated phosphorylation and activation of IκB kinases α/β (IKKα/β) (Ciesielska et al., 2021), ultimately leading to nuclear translocation of NF-kB. This step is essential for the transcription of NLRP3, pro-IL-1β, and pro-IL-18, the priming step for the activation of NLRP3 inflammasome (Ciesielska et al., 2021). In the TRIF-dependent pathway, TRAF3 and TRAF6 were involved in the activation of the MAPK and ERK1/2 pathways, which also contributed to cytokine production (Ciesielska et al., 2021). The activation of NLRP3

was demonstrated to be associated with posttranslational modification, which was supported by NLRP3 deubiquitination by BRCC3 or phosphorylation by JNK1, promoting the activation of the NLRP3 inflammasome (Py et al., 2013; Song et al., 2017). In addition, ion flux, mitochondrial damage, ROS and mitochondrial DNA, and lysosomal disruption were also documented to be involved in NLRP3 activation (Huang et al., 2021). However, the exact underlying mechanisms are still obscure. In addition to recruiting and activating inflammasomes in the canonical pyroptosis pathway, downstream molecular TRIF initiates the activation of IRF3/7 and the induction of type I interferon release in parallel. This is followed by IFNAR1/2-dependent activation of JAK/STAT signaling to initiate pro-caspase-11 expression, thus participating in the noncanonical pyroptosis pathway (Gurung et al., 2012; Rathinam et al., 2012; Zamyatina and Heine, 2020). These findings extend our understanding of LPS and TLR4 in pyroptosis. However, these results have not been verified in periodontitis. Pyroptosis was demonstrated to arise in human gingival fibroblasts (HGFs), macrophages, oral epithelial cells, human periodontal ligament fibroblasts (HPDLFs), human periodontal ligament stem cells (HPDLSCs), and osteoblasts during periodontitis (Ziauddin et al., 2018; Zhuang et al., 2019; Chen et al., 2021; Lei et al., 2021; Li et al., 2021; Zhao et al., 2021). The human gingival epithelium (HGEs) is considered the first line of periodontal defense, protecting the periodontal tissue against various harmful pathogens. Streptococcus sanguinis and oral anaerobic bacteria-produced butyrate can destroy the epithelial barrier through the activation of pyroptosis by upregulating caspase-3/GSDME and caspase-1, respectively (Liu et al., 2019; White et al., 2020). HGFs are the most abundant cells in the periodontal tissue; activation of the pyroptosis pathway in gingival fibroblasts contributes to the exacerbation of inflammation and the destruction of periodontal tissues. Porphyromonas gingivalis (P. gingivalis) and LPS are reported to induce pyroptosis in HGFs by activating the NLRP3/NLRP6/caspase-1/GSDMD pathway (Liu et al., 2018; Huang et al., 2020; Yang et al., 2021). Moreover, caspase-4/GSDMD, which belongs to the noncanonical pathway, can also be activated in HGFs in response to the Treponema pallidum surface protein Tp92 (Jun et al., 2018). Macrophages are key mediators of the inflammatory response in the innate immune system and are involved in defense against pathogen invasion by recognizing the byproducts of pathogens and other endogenous factors. Nonetheless, overactivation of microphages results in an extended inflammatory response and tissue damage (Shapouri-Moghaddam et al., 2018). In addition, macrophages are remarkable plastic cells that can be phenotypically polarized to classically activated or inflammatory (M1) and alternatively activated or anti-inflammatory (M2) forms. While M2 can be induced by IL-4 and IL-13, which is followed by the production of anti-inflammatory factors IL-10 and TGF-β, M1 is triggered by recognizing IFN-γ, TNF-α, or LPS with TLRs and IL-1R, and this is followed by the production of pro-inflammatory cytokines TNF-α, IL-1α, IL-1β, IL-6, IL-12, and IL-23 (Murray, 2017; Locati et al., 2020). Cytokine production during this process was activated NF-κB signaling dependent (Murray, 2017; Locati et al., 2020). These results showed that M1 polarization shares the same initiated signaling pathways with pyroptosis. Concomitant with these findings, M1 macrophages showed increased caspase-1 expression (Xia et al., 2022), and polarization to M1 can be prevented by caspase-1 suppression (Li et al., 2019). So, we speculate that in response to infection, M1 polarization occurs in the early stage, while accumulating inflammatory factors produced by M1 contribute to pyroptosis activation. Given that M2 macrophages have scavenger receptors, they might participate in the phagocytosis of cells undergoing pyroptosis, thus restricting the amplification of inflammation. However, the interaction between macrophage polarization and pyroptosis has never been investigated in periodontitis; gene knockout of pyroptosis-related caspases will help us understand this topic. Limited evidence in periodontitis revealed that P. gingivalis, Mycoplasma salivarium, Treponema denticola surface protein Td92, E. faecalis, and LPS can induce pyroptosis in macrophages through the NLRP3/caspase-1/GSDMD pathway, contributing to the pathogenesis and development of periodontitis (Jun et al., 2012; Sugiyama et al., 2016; Li et al., 2019; Li et al., 2020; Ran et al., 2021). Moreover, pyroptosis induced by the cyclic stretch, dental calculus, and outer membrane vesicles of P. gingivalis in macrophages can also promote periodontitis (Fleetwood et al., 2017; Ziauddin et al., 2018; Zhuang et al., 2019).

Table 1 presents a summary of the current research on the role of pathogens and their byproducts in the induction of pyroptosis in periodontal tissue, providing an update on the comprehensive understanding of the possible effects of pyroptosis on periodontal diseases. As displayed in Table 1, studies restricted their focus on caspase-1/GSDMD, the role of caspases, GSDMs, granzymes, and ELANE, which, beyond caspase-1/GSDMD, remain to be fully elucidated in periodontitis. Also, the favorable aspect of pyroptosis in macrophages, which might contribute to the clearance of periodontal pathogens, needs to be clarified.

Advances in the field have led to a more detailed understanding of how pyroptosis is regulated. Recent studies have shown that Ninjurin-1 mediates the breakdown of the plasma membrane to smaller pieces after pyroptosis induced by GSDMD (Kayagaki et al., 2021), thus amplifying inflammation and helping clear pathogens. The Ragulator-Rag complex of mTORC1 is reported to be necessary for GSDMD pore-forming activity in macrophages (Evavold et al., 2021). Posttranslational modification of GSDMs also contributes to the regulation of pyroptosis. For example, it has been reported that the Shigella ubiquitin ligase IpaH7.8 mediates the ubiquitylation of N-terminal PFD in human GSDMD and GSDMB and promotes their degradation in immune cells to prevent pyroptosis, enabling infection (Hansen et al., 2021;

TABLE 1 Reported periodontal pathogenic factors in the activation of pyroptosis-related caspases and gasdermins.

Tissue and/or cells	Pyroptosis inducers	Inflammasome	Caspases	Gasdermins	Reference
THP-1	*Mycoplasma salivarium*	NLRP3	Caspase-1	N/A	Sugiyama et al., 2016
	T. denticola surface protein Td92	NLRP3	Caspase-1	N/A	Jun et al., 2012
	LPS from *E. coli*	NLRP3	Caspase-1/4	GSDMD	Li et al., 2020
	E. faecalis	NLRP3	Caspase-1	GSDMD	Ran et al., 2021
U937	*P. gingivalis*	NLRP3	Caspase-1/11	GSDMD	Li et al., 2019
XS106	*Mycoplasma salivarium*	NLRP3	Caspase-1	N/A	Sugiyama et al., 2016
HPDLCs	Cyclic stretch	NLRP1 and NLRP3	Caspase-1/5	GSDMD	Zhao et al., 2016; Zhuang et al., 2019
	P. gingivalis and LPS	NLRP3	Caspase-4	GSDMD	Chen et al., 2021
HGEs	Butyrate	N/A	Caspase-3/1/5	GSDME	Liu et al., 2019
HGFs	*T. denticola* surface protein Tp92	N/A	Caspase-4	GSDMD	Jun et al., 2018
	LPS from *E. coli*	NLRP3	Caspase-1	GSDMD	Huang et al., 2020
	Combination of hypoxia and LPS from *P. gingivalis*	NLRP3	Caspase-1	GSDMD	Yang et al., 2021
	P. gingivalis	NLRP6	Caspase-1	GSDMD	Liu et al., 2018
	LPS from *P. gingivalis*	NLRP3	Caspase-1/4/5	GSDMD	Li et al., 2021
Human macrophages from blood	*A. actinomycetemcomitans* leukotoxin	N/A	Caspase-1	N/A	Kelk et al., 2011
HSC-2; HOMK107; Immortalized mouse macrophages	Dental calculus	NLRP3	Caspase-1	N/A	Ziauddin et al., 2018
RAW 264.7 co-cultured with HPDLSCs	Hyperglycemia	NLRC4	Caspase-1	GSDMD	Zhao et al., 2021
RAW 264.7; Mice gingival tissue	High glucose, diabetes, and LPS from *P. gingivalis*	AIM2 and NLRP3	Caspase-1	GSDMD	Nie et al., 2021; Zhou et al., 2020
Murine bone-marrow-derived macrophages; Human monocyte-derived macrophages	*P. gingivalis* and its outer membrane vesicles	NLRP3	Caspase-1	N/A	Fleetwood et al., 2017
Oral epithelial cell	*Streptococcus sanguinis*	N/A	Caspase-1/3/7	N/A	White et al., 2020
MG63 cells	LPS from *E. coli*	NLRP3	Caspase-1	GSDMD	Liu et al., 2020
HPDLFs	LPS from *P. gingivalis* and *E. coli*	NLRP3	Caspase-1	N/A	Cheng et al., 2018

XS106, murine epidermal-derived Langerhans cell line; THP-1, human acute monocytic leukemia cell line; HPDLCs, human periodontal ligament stem cells; HSC-2, human oral squamous carcinoma cells; HOMK107, human primary oral epithelial cells; HGFs, human gingival fibroblasts; RAW 264.7, murine macrophage line; MG63, human osteosarcoma MG63 cell line; U937, human myelomonocytic cell line.

Luchetti et al., 2021). In addition, succination at C192 of the N terminal of GSDMD reduces its binding to caspase-1, thus blocking its processing and oligomerization and preventing pyroptosis-induced cell death (Humphries et al., 2020). Moreover, chemotherapy drugs were reported to promote pyroptosis by palmitoylation of GSDME (Hu et al., 2020). However, these newly discovered regulation mechanisms have not been verified in periodontitis.

Despite accumulating achievements in this field recently, few studies have focused on the basic molecular mechanism of pyroptosis in periodontitis and the potential favorable aspects of pyroptosis in periodontitis, and whether the recently discovered regulation mechanisms also participate in the process of periodontitis are still unknown.

Role of pyroptosis-regulated cell death mechanisms in periodontitis

Pyroptosis in periodontal tissue has been demonstrated to induce inflammation, resulting in periodontal tissue damage (Table 1). Pyroptosis-related inflammasomes, caspases, and cytokines have been proven to be tightly associated with inflammatory diseases and play important roles in pathogen defense, bone resorption, and regeneration of various tissues. Among all the pyroptosis-related inflammasomes and caspases, NLRP3 and caspase-1 are the most comprehensively characterized members in periodontitis. One study found that caspase-1 deficiency suppressed the secretion of inflammation factors from macrophages and alleviated bone resorption in

periodontal tissue during periodontitis (Rocha et al., 2020). These authors also found that NLRP3 deficiency did not contribute to this process (Rocha et al., 2020). However, this is inconsistent with the findings of (Zang et al., 2020), which indicated that aged mice lacking NLRP3 showed better bone mass, and inhibition of the activation of NLRP3 with MCC950 significantly suppressed alveolar bone loss (Zang et al., 2020). In line with this result, Chen also found that in mice with ligature-induced periodontitis, NLRP3 deficiency decreased osteoclast precursors and suppressed osteoclast differentiation and alveolar bone destruction (Chen et al., 2021). These contradictory results might be attributed to the different ages of the studied mice; however, this hypothesis requires clarification in future studies.

The activation of inflammasomes and caspases ultimately leads to the maturation and secretion of inflammatory factors; the active forms of IL-1β and IL-18 are the direct byproducts of this process. IL-1β is considered to be the most important factor contributing to periodontal tissue damage. It is expressed in macrophages, dendritic cells, GFs, PDLCs, and osteoblasts. IL-1β was markedly increased in the saliva of patients with periodontitis and gingivitis, as compared to that of healthy individuals (Lira-Junior et al., 2021). Evidence shows that elevated IL-1β levels caused by pyroptosis play a direct role in the pathophysiological process of periodontitis (Cheng et al., 2020). Previous studies have reported that elevated IL-1β enhanced extracellular matrix degradation and bone resorption by directly upregulating collagenolytic enzymes and matrix metalloproteinases (MMPs) in periodontal tissues (Panagakos et al., 1994; Polzer et al., 2010; Schett et al., 2016). IL-1β was also found to upregulate receptor activator for NF-kB ligand (RANKL) expression and promote osteoclast genesis directly, thus promoting inflammatory bone loss (Bloemen et al., 2011; Huynh et al., 2017). In line with this, IL-1β was also proved to promote inflammatory cell infiltration toward alveolar bone in experimental periodontitis (Graves et al., 1998), thus further aggravating alveolar bone loss.

IL-1β certainly activates inflammatory pathways and triggers the release of other inflammatory factors from various cell types, amplifying the inflammatory pathway signals and mediating the amplification of the inflammatory damage caused by pyroptosis. For example, it stimulated chondrocytes to synthesize IL-8, TNF-α, and IL-6 (Guerne et al., 1990; Lotz et al., 1992; Xu et al., 2021), promoted the expression of IL-6 and TNF-α in human retinal microvascular endothelial cells (Giblin et al., 2021), and facilitated the secretion of IL-1a, IL-8, and IL-18 from fibroblast-like synoviocytes (Kim et al., 2021). More importantly, IL-1β was evidenced to promote the secretion of C-C motif chemokine ligand (CCL) 20 and C-X-C motif chemokine ligand (CXCL) 10 from HPDLSCs (Long et al., 2001; Zhu et al., 2012; Hosokawa et al., 2015); IL-2, IL-6, IL-8, IL-23, interferon (IFN)-γ, IL-13, and TNF-α from HPDLFs (Abidi et al., 2020); and prostaglandin E2 (PGE2), IL-6, and IL-8 from HGFs (Ono et al., 2011). These elevated inflammatory factors in periodontal tissue ultimately lead to increased inflammation in periodontitis. However, IL-1β was reported to have dual roles in the osteogenesis of periodontal ligament stem cells (PDLSCs), where low doses of active IL-1β can promote the osteogenesis of PDLSCs through the BMP/Smad pathway, while higher doses of IL-1β can inhibit osteogenesis through the activation of NF-κB and MAPK signaling (Mao et al., 2016). This needs to be verified in pyroptosis-mediated periodontitis, which is usually a severe inflammatory condition. Besides, IL-1β is also reported to upregulate apoptotic signaling pathways (Guadagno et al., 2015; Liang et al., 2018; Wang et al., 2019; Kang et al., 2021), autophagy (Romagnoli et al., 2018), and oxidative stress and is thus involved in tissue damage through inflammatory independent pathways (Zhu et al., 2015; Wang et al., 2021).

IL-18 belongs to the IL-1 family. Its roles in viral, bacterial, parasitic, and fungal infections have been comprehensively studied. Polymorphism of the IL-18 gene was demonstrated to be associated with periodontitis (Shan et al., 2020). In one study, RANKL and periodontal bone loss were proved to be evoked in IL-18 transgenic mice (Yoshinaka et al., 2014). Studies have also reported that IL-18 stimulation promotes proinflammatory cytokine production in periodontal ligament cells, including IFN-γ, IL-2, and TNFα (Vecchie et al., 2021). When infected with P. gingivalis, neutralization of IL-18 inhibited the release of cytokines, chemokines, and MMPs, i.e., IL-1β, IL-6, IL-8, and MMP-1/8/9. This also contributes to decreasing the recruitment of inflammatory cells into periodontal tissues and to less alveolar bone resorption (Zhang et al., 2021). In addition, IL-18 is reported to promote the secretion of matrix metalloproteinases in HPDLFs by activating NF-kB signaling (Wang et al., 2019). Previous studies have indicated that IL-18 blockade is a promising therapeutic target for rheumatic diseases and infantile-onset macrophage activation syndrome (Vecchie et al., 2021). Given its role in regulating the inflammation damage associated with periodontitis, IL-18 blockade may also be an option for the treatment of periodontitis. Further detailed studies are warranted to investigate the exact role of IL-18 in periodontitis.

Taken together, the literature shows that an increased level of pyroptosis in periodontitis can promote the secretion of active inflammatory factors (IL-1β, IL-18), thus amplifying the inflammation response, leading to an overactive immune response; this ultimately decreases bone formation, enhances bone resorption by upregulation of RANKL, exacerbates the destruction of periodontal tissue, and suppresses its regeneration (Figure 1). Although persistent localized pyroptosis could enhance periodontal tissue disruption and pathogen dissemination, pyroptosis has also been found to limit pathogen replication, enhance innate and adaptive immune responses, and improve host survival in other tissues (Jorgensen et al., 2016), as a recent study found that GSDMD deficiency diminished neutrophil-killing responses against Escherichia coli infection (Kambara

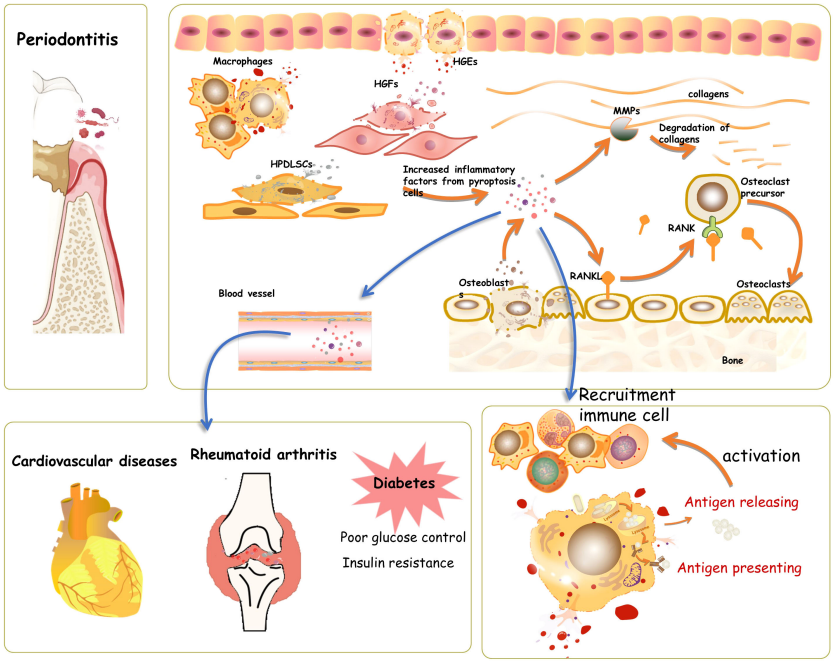

FIGURE 1
Pyroptosis in periodontal tissue. During the process of periodontitis, pyroptosis takes place in human gingival epithelial cells (HGEs), human gingival fibroblasts (HGFs), osteoblasts, and human periodontal ligament stem cells. The induced pyroptosis involves the activation and recruitment of immune cells, thus helping clear and prevent the spread of pathogens. However, the hyperactive and long-lasting pyroptosis would accelerate the process of periodontitis by increasing cell death and elevating inflammatory factors, which mediate the activation of oxygen species and matrix metalloproteinases, further causing connective tissue damage in periodontal tissue directly. The cascade amplification of the inflammatory response during pyroptosis might also contribute to the aggravation of systematic diseases, such as cardiovascular disease, diabetes, and rheumatoid arthritis.

et al., 2018). However, whether this favorable aspect of pyroptosis can help clear pathogens in periodontal tissue has yet to be addressed experimentally.

Pyroptosis in the relationship between periodontitis and systemic disease

Emerging evidence demonstrates that pyroptosis might be involved in the bidirectional relationship between periodontitis and systemic diseases, such as diabetes, cardiovascular diseases, and rheumatoid arthritis (Jain et al., 2021). These relationships are further summarized below.

Diabetes

The association between diabetes and periodontitis has been thoroughly investigated (Jain et al., 2021; Pirih et al., 2021). Diabetes is characterized by chronic subclinical inflammation, which is directly involved in the pathogenesis of diabetes-associated periodontitis (Pirih et al., 2021). In addition, diabetes induces increased advanced glycation end-products (AGEs) (Yu et al., 2012; Zizzi et al., 2013; Mei et al., 2019), oxidative stress (Tothova and Celec, 2017; Buranasin et al., 2018), an unbalanced periodontal microbiome (Shi et al., 2020; Sun et al., 2020; Balmasova et al., 2021), and immune dysfunction (Lazenby and Crook, 2010; Zhu and Nikolajczyk, 2014), which also contribute to the progression of periodontitis. Recently, considerable attention has been directed to pyroptosis caused by diabetes and its role in diabetes complications. The induction of pyroptosis in human retinal microvascular endothelial cells through the AGEs/P2X7R/NLRP3/GSDMD pathway was found to contribute to the progression of diabetic retinopathy (Yang et al., 2020). (Chai et al., 2021) reported that intermittent high glucose induces pyroptosis of cardiomyocytes through NLRP3/caspase-1/GSDMD (Chai et al., 2021). Moreover, AGEs produced by high-glucose induced pyroptosis in human kidney-2 cells through AGEs/NLRP3/GSDMD were found to accelerate the kidney damage caused by diabetes (Li et al., 2020). Hyperglycemia also leads to an increase in NLRP3 in diabetic muscle cells, further upregulating the pyroptosis pathway in muscle cells (Aluganti Narasimhulu and Singla, 2021). There is

also accumulating evidence indicating that pyroptosis mediates the adverse outcomes of diabetes-associated periodontitis. (Nie et al., 2021) reported that hyperglycemia triggers gingival destruction and impairment of macrophage function, including inflammatory cytokine secretion, phagocytosis, chemotaxis, and immune responses (Nie et al., 2021). In line with this, (Zhao et al., 2021) also reported that hyperglycemia promotes GSDMD-dependent pyroptosis of macrophages through NLRC4 phosphorylation, thus activating NF-κB signaling in HGFs and further aggravating periodontitis (Zhao et al., 2021). Diabetes also inhibits the proliferation and differentiation of osteoblasts in alveolar bone by activating the caspase-1/GSDMD/IL-1β pathway (Yang et al., 2020). Given the evidence suggesting that pyroptosis mediates the progression of diabetes-induced periodontitis, pyroptosis may serve as a new therapeutic target for diabetes-associated periodontitis. However, more comprehensive research on pyroptosis in diabetes-associated periodontitis is warranted to fully understand its mechanism.

Periodontitis also participates in the pathological process of diabetes, as has been reviewed by others (Lalla and Papapanou, 2011; Preshaw et al., 2012; Polak and Shapira, 2018; Pirih et al., 2021). Increased circulating levels of different inflammatory cytokines are associated with poor glucose control and insulin resistance (Polak and Shapira, 2018). IL-1β, a byproduct of pyroptosis, has been suggested to link periodontitis and systemic disorders (Zhu et al., 2015); however, this has not been validated in diabetes-associated periodontitis. Therefore, the exact mechanisms by which periodontitis-induced pyroptosis affects the progression of diabetes are largely unknown. Both in vivo and in vitro studies are needed to address this issue.

Cardiovascular diseases

Cardiomyocytes, macrophages, vascular smooth muscle cells, endothelial cells, and fibroblasts in the cardiovascular system can undergo pyroptosis, resulting in the progression of cardiovascular diseases (Fidler et al., 2021; Jan et al., 2021; Yao et al., 2021; Zhou et al., 2021). This was also evidenced by alleviated cardiac damage in NLRP3 knockout mice (Busch et al., 2021). Therefore, NLRP3-mediated pyroptosis has been considered a candidate for cardiovascular disease treatment.

Periodontitis has been suggested to be the source of inflammation resulting in cardiovascular diseases. However, patients with periodontitis and cardiovascular diseases often suffer from diabetes and are tobacco users, which can also increase systemic inflammation, making it challenging to prove that periodontitis is the direct source of inflammation resulting in cardiovascular disease. Nonetheless, periodontal pathogenic bacteria, such as P. gingivalis, have been confirmed to be present in atherosclerotic plaques (Haraszthy et al., 2000; Pavlic et al., 2021). The colonized periodontal pathogens in the cardiovascular system were suggested to come from transient bacteremia caused by dental procedures, such as daily tooth care, tooth extraction, scaling, and periodontal probing. This also contributes to periodontal bacteria entering the circulation and inducing low-grade inflammation. Moreover, bacterial metabolic products, such as endotoxins and gingipains, can also trigger systemic inflammatory responses, and some of them have been shown to induce pyroptosis in other tissues (Naderi and Merchant, 2020; Jain et al., 2021). However, whether pyroptosis participates in periodontitis-associated cardiovascular diseases remains largely unknown.

Rheumatoid arthritis

Studies have reported that periodontitis-related pathogens and their byproducts can disturb the immune balance. Invasive P. gingivalis promotes the occurrence and development of collagen-induced arthritis in mice through the inhibition of the process of B-cell differentiation into B10 cells (Zhou et al., 2021). In addition, P. gingivalis can produce peptidyl-arginine deiminase, thus increasing the formation of anticyclic citrullinated peptide. Moreover, P. gingivalis–induced gingipain mediates the degradation of fibrinogen and alpha-enolase, which provides more substrates for citrullination (Wegner et al., 2010; Quirke et al., 2014). Pyroptosis was reported to participate in elevated inflammation in rheumatoid arthritis (Li et al., 2019; Wu et al., 2020). Thus, we speculate that pyroptosis might be involved in the pathophysiology of periodontitis-associated rheumatoid arthritis. However, this requires further clarification.

Crosstalk between pyroptosis and other forms of programmed cell death

Pyroptosis and apoptosis

Pyroptosis was traditionally conceived to have a distinct morphology and undergo distinct pathways from apoptosis; nonetheless, this has been challenged with more recent evidence showing connections between pyroptosis and apoptosis. Apoptosis was the first characterized form of programmed cell death and can be classified as either extrinsic or intrinsic apoptosis. Caspase-3 has traditionally been regarded as a critical effector of apoptosis-induced cell death in intrinsic apoptosis. Recent advances have indicated that caspase-3/GSDME might be a switch between apoptosis and pyroptosis (Jiang et al., 2020). A study by (Jiang et al., 2020) reported that in coral, GSDME is cleaved by caspase-3 at two tetrapeptide motifs, 238DATD241 and 254DEPD257, yielding two active isoforms of

the N-terminal domain of GSDME that are capable of inducing pyroptosis (Jiang et al., 2020). (Rogers et al., 2017) reported that during apoptosis in 293T cells, caspase-3 cleaves the 267DMPD270 domain of GSDME, which targets the plasma membrane to induce pyroptosis (Rogers et al., 2017). In peri-implantitis and periodontitis, this signal pathway has been found to mediate TNF-α- and butyrate-triggered pyroptosis in human gingival epithelial cells, respectively (Liu et al., 2019; Chen et al., 2021). The relationship between pyroptosis and apoptosis was also verified by the finding that exposure to cadmium, an apoptosis trigger, can evoke the caspase-1 mediated pyroptosis pathway (Wei et al., 2020). Caspase-8, the initiator of extrinsic apoptosis, has also been found to be involved in the pyroptosis signaling pathway (Sarhan et al., 2018; Fritsch et al., 2019; Zhang et al., 2021). (Sarhan et al., 2018) reported that caspase-8 mediated pyroptosis during Yersinia infection in macrophages by directly binding to GSDMD, driving the cleavage of GSDMD (Orning et al., 2018; Sarhan et al., 2018). In addition, caspase-8 has been found to mediate the cleavage of GSDMC after α-ketoglutarate treatment in Hela cells, thus promoting pyroptosis (Zhang et al., 2021). Furthermore, caspase-8 was found to stimulate caspase-3-dependent GSDME cleavage, further facilitating pyroptosis (Li et al., 2021). These results indicate that caspase-8 is another molecular switch beyond caspase-3 that controls apoptosis and pyroptosis (Fritsch et al., 2019). The roles of granzyme A and B in apoptosis have been thoroughly studied (Martinvalet et al., 2005; Velotti et al., 2020). Recently, it has been discovered that they are also able to directly cleave GSDMs, as discussed above, further confirming the connection between apoptosis and pyroptosis.

In turn, the upstream signals of pyroptosis have also been reported to evoke apoptosis pathways. Oligomerization of the initiating proteins, such as AIM2 and NLRP3, was found to promote apoptosis through the recruitment of caspase-8 by ASC, thereby initiating apoptosis (Sagulenko et al., 2013). During pyroptosis, activated caspase-1 can bidirectionally lead to the activation of caspase-3/8/9-related apoptosis (Tsuchiya et al., 2019). More recently, the N-terminal of GSDME was found to permeabilize the mitochondrial membrane, releasing cytochrome c and thus activating apoptosis through the intrinsic apoptosis pathway (Yang et al., 2020). However, the role of pyroptosis-dependent secondary apoptosis in periodontitis is unclear.

In sum, these results confirm the presence of a bidirectional relationship between pyroptosis and apoptosis and further suggest that pyroptosis tends to be concurrent with apoptosis (Xi et al., 2016; Doitsh et al., 2017) (Figure 2). However, cells or tissues are usually dominated by one programmed death pathway in response to a certain trigger, and this can be attributed to the expression levels of GSDMs and certain caspases. Deficiency of pyroptosis-associated caspases or GSDMs switches pyroptosis to apoptosis; for example, deficiency of GSDMD reverts the cell-death morphology to apoptosis upon the activation of caspase-1 or caspase-8 (Pierini et al., 2012; Sarhan et al., 2018; Tsuchiya et al., 2019; Jiang et al., 2020; Zhang et al., 2020). A sufficient amount of substrates for pyroptosis contributes to the initiation of pyroptosis (Wang and Kanneganti, 2021). In addition, the cell type has also been suggested to influence the undergoing form of programmed death (Yang et al., 2020). This requires further clarification in various periodontal cell types.

Caspase-1/4/5/11/3/8 levels have all been reported to be increased in periodontitis (Hirasawa and Kurita-Ochiai, 2018; Jun et al., 2018; Liu et al., 2018). Elevated expression and activity of caspase-3 and caspase-8 certainly participate in aggravating the progression of periodontitis through the apoptosis pathway (Alikhani et al., 2004; Hirasawa and Kurita-Ochiai, 2018; Aral et al., 2019). However, no studies analyzed apoptosis–pyroptosis interactions during this process, and whether pyroptosis can be activated simultaneously and participate in the progression of periodontitis is unclear. Given the accumulating evidence of a connection between apoptosis and pyroptosis, we speculate that the interaction between the two might contribute to the pathophysiology of periodontitis. The role of the bidirectional relationship between pyroptosis and apoptosis in periodontitis needs to be investigated in more detailed mechanistic studies.

Pyroptosis and necroptosis

Necroptosis is another well-defined form of programmed cell death. It is initiated by the activation of tumor necrosis factor receptor (TNFR), death receptor, TLR, or type I interferon receptor (IFNAR). This is followed by the formation of complex I on the membrane, which contains TNFR-associated death domain (TRADD), Fas-associated death domain (FADD), TNFR-associated factors (TRAFs), receptor-interacting protein 1(RIPK1), and cellular inhibitor of apoptosis protein 1 and 2. Then, there is the recruitment of RIPK3 and the formation of the RIP complex, leading to the phosphorylation and activation of mixed lineage kinase domain-like (MLKL). Activated MLKL mediates pore formation, which facilitates the release of inflammatory factors and cellular components, ultimately resulting in the collapse of the membrane (Frank and Vince, 2019; Yuan et al., 2019; Bertheloot et al., 2021). This process has already been summarized in detail. As alluded to above, necroptosis occurs through a discriminate pathway compared with pyroptosis. In addition, there are also distinct morphologies: cells that undergo necroptosis usually exhibit loose cellular detachment and exaggerated cellular swelling due to the ion-selective MLKL pores (Frank and Vince, 2019). Nonetheless, they still interact with each other, as the previously defined receptors for initiating necroptosis have also been demonstrated to be involved in pyroptosis pathways (Frank and Vince, 2019). Triggers such as P. gingivalis and LPS have been identified to induce both pyroptosis and necroptosis

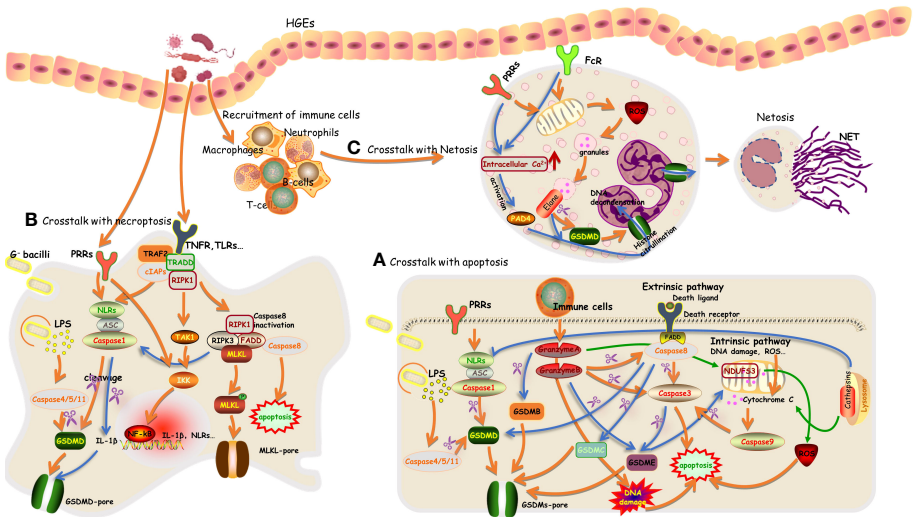

FIGURE 2
An overview of the crosstalk between pyroptosis with apoptosis, necroptosis, and NETosis in periodontal tissue **(A–C)**.

in periodontitis (Ke et al., 2016; Geng et al., 2022; Yang et al., 2022). More recently, RIPK1, RIPK3, and MLKL have been identified to be involved in the mediation of the activation of NLRP3/caspase 1, which might contribute to the activation of pyroptosis during periodontitis (Conos et al., 2017; Speir and Lawlor, 2021). These results suggest the simultaneous existence of these two forms of death in periodontal tissue. Unlike apoptosis, which is immunologically silent, the excessive activation of pyroptosis and necroptosis consequently elicits a destructive immune response that participates in the process of periodontitis. The complex interaction of these pathways in periodontitis is largely unknown, and the primary inflammatory programmed death pathway in distinct periodontal cells has yet to be deciphered. Understanding this topic will provide us with new opportunities for potential clinical treatments of periodontitis.

Pyroptosis and NETosis

There is growing evidence indicating neutrophils as crucial regulators in periodontitis. In response to pathogens, the recruited neutrophils exert their host defense effects by releasing cytotoxic factors and enzymes, phagocytosing pathogens, and discharging neutrophil extracellular traps (NETs) during NETosis (Hajishengallis, 2020). NETosis is initiated by the activation of neutrophils and, simultaneously, changes in intracellular calcium concentration, the elevation of reactive oxygen species, and the activation of kinase signaling cascades contributing to the formation of NETs (Thiam et al., 2020). NETs are intercellular chromatins decorated with activated protease (such as elastase and myeloperoxidase), acting as scaffolds to trap and obliterate pathogens. The release of intracellular contents, including DNA, histones, and proteins, during NETosis, contributes to the autoimmune response, which directs research on NETosis mainly to the field of autoimmune diseases. Limited evidence in periodontitis showed that periodontal pathogens F. nucleatum, Aggregatibacter actinomycetemcomitans, and P. gingivalis contribute to the activation of NETosis (Hirschfeld et al., 2016; Alyami et al., 2019; Bryzek et al., 2019). P. gingivalis–induced NETosis was gingipains dependent, and gingipains in turn mediated the proteolysis of components of NETs (Bryzek et al., 2019). This might lead to the amplification of the accumulation of NETs during periodontitis and further aggravate tissue damage caused by neutrophils. These NETosis-invoked pathogens have also been reported to trigger pyroptosis in other types of cells in periodontal tissues. The key factors that influence neutrophils to undergo NETosis, pyroptosis, or phagocytose when responding to identical triggers and pathogens remain unclear. In essence, whether neutrophils can undergo pyroptosis is still controversial (Sollberger, 2022). The large amount of neutrophil proteases and the low expression level of caspases and inflammasomes determine the priority for NETosis in neutrophils. In addition, this was also evidenced by neutrophil protease-mediated activation of GSDMD, and activated inflammasomes and GSDMD tend to participate in the release of chromatin in a feed-forward loop to promote NETosis instead of inducing pyroptosis (Chen et al., 2018; Sollberger et al., 2018). Researchers also failed to detect pyroptosis morphologies during this process. This has been summarized in Figure 2. However, these were not explored in periodontitis.

Pyroptosis, apoptosis, and necroptosis are interconnected

The recent progress in the research on cell death advanced our understanding of the extensive and intricate crosstalk between different cell death signaling cascades. Caspase-8 was proposed as a master regulator of apoptosis, necroptosis, and pyroptosis. Signal transduction via LPS binding to TLRs results in the activation of caspase-8, RIPK1, and RIPK3, thus contributing to the activation of necroptosis. During this process, mammalian inhibitor of apoptosis (IAP) proteins, including X-linked IAP (XIAP), cellular IAP1, and IAP2 (cIAP1/2), can bind caspase-8, caspase-3, and caspase-7 directly and inhibit their apoptotic caspase activity; this depends on the BIR domains in IAPs (Silke and Meier, 2013; Bertheloot et al., 2021). The combined loss of XIAP and cIAP1/2 enhanced the caspase-8-mediated apoptotic pathway and cleavage of pro-IL-1β. In parallel, RIPK3-mediated necroptosis and activation of NLRP3/IL-1β were also enhanced (Tenev et al., 2011; Moulin et al., 2012; Lawlor et al., 2015). Furthermore, tumor necrosis factor-related apoptosis-inducing ligand decoy receptors, survivin and XIAP, have been suggested to suppress the apoptosis of inflammatory cells in periodontitis and are thus associated with a prolonged lifespan of inflammatory cells (Lucas et al., 2010). Caspase-8 deficiency failed to suppress the maturation of IL-1β but enhanced the recruitment of RIPK1, followed by phosphorylation of RIPK3, and ultimately contributed to MLKL-mediated necroptosis and the activation of NLRP3/IL-1β in pyroptosis (Fritsch et al., 2019). Notably, RIPK1 is required to limit RIPK3 and caspase-8 mediated cell death; this was evidenced by mice with Ripk1 deficiency dying soon after birth due to uncontrolled cell death depending on caspase-8, RIPK3 (Rickard et al., 2014; Samir et al., 2020), or RIPK3 mediated activation of NLRP3/IL-1β. However, whether activated NLRP3/IL-1β was involved in the activation of pyroptosis was not clear. Presumably, this depended on the cellular substrate content and the specific type of cell and tissue. c-FLIP is also identified as a checkpoint to control the activation of caspase-8. c-FLIP was upregulated in LPS-primed macrophages. The elevated short isoform of c-FILP inhibited caspase-8-dependent apoptosis by disrupting pro-caspase-8 oligomer assembly (Speir and Lawlor, 2021). Correspondingly, NLRP3/IL-1β and necroptosis signaling were evoked. Contradictorily, the caspase-8-cFLIP (long isoform) complex is required for the inhibition of both apoptosis and necroptosis to suppress cell death (Van Opdenbosch et al., 2017). These results indicate the intricate connection between cell death pathways and imply that different periodontal cell types could undergo distinct cell death pathways during periodontitis. However, these need to be clarified in future explorations.

PANoptosis, another newly recognized proinflammatory programmed cell death pathway, is executed by the PANoptosome, which contains molecules involved in the pyroptotic, apoptotic, and necroptotic pathways. This new definition of cell death highlights the crosstalk and concurrence of these three pathways. The PANoptosome was regarded as a platform that acts as a sensor and executor during infection; it was initially shown to consist of NLRP3, NLRC4, AIM2, ASC, TNFR1, RIPK1, RIPK3, MLKL, caspase-1/3/7/8, and GSDMD (Samir et al., 2020). Recently, ZBP1 was recognized as an apical sensor by recruiting RIPK3 and caspase-8 during IAV infection. This was evidenced by ZBP1 deficiency completely abolishing IAV-induced PANoptosis (Zheng and Kanneganti, 2020). Caspase-6 was proved to facilitate the interactions between RIPK3 and ZBP1 in this process (Zheng et al., 2020). These results extend our understanding of the participating molecules. However, Sendai virus and respiratory syncytial virus were demonstrated to trigger PANoptosis through ZBP1-independent pathways, implying different PANoptosome components in response to specific microbes (Place et al., 2021). Hitherto, no study has focused on this topic with regard to periodontitis. Considering the critical role of PANoptosis in defending and restricting pathogens, exploring it in periodontal disease might be helpful in the development of new treatment strategies in this field.

Pyroptosis: A new therapeutic opportunity for periodontitis

Appropriate pyroptosis plays a key role in the clearance of pathogens by removing intracellular replication niches and enhancing the host's defense responses (Bergsbaken et al., 2009; Jorgensen et al., 2016; Hansen et al., 2021). The adequate release of cytokines is critical for immune activity, contributing to tissue angiogenesis and repair. However, overactivation of pyroptosis can result in a massive inflammatory response, leading to aggravation of damage to tissues and organs; moreover, long-term exposure to an inflammatory environment can also increase the risk of diabetes, cancers, and so on (Schroder et al., 2010; Hou et al., 2021). Studies have reported elevated levels of pyroptosis in periodontitis, and pharmacological inhibition of pyroptosis prevents the progression of periodontitis. For example, the caspase-1 inhibitor vx-765 was found to suppress bone loss and inhibit the expression of inflammatory factors (IL-1β, MCP-1, IL-6, and IL-8) in an experimental AP rat model (Cheng et al., 2018). Another caspase-1 inhibitor, Z-YVAD-FMK, was found to suppress gingivitis caused by LPS (Li et al., 2021). In addition, the NLRP3 inhibitor MCC950 restored the osteogenic function of MG63 cells under LPS stimulation (Liu et al., 2020). Also, the pan-caspase inhibitor Z-VAD-FMK and the caspase-4 inhibitor Z-LEVD-FMK have been found to alleviate inflammation in PDLSCs exposed to P. gingivalis (Chen et al., 2021). Knockdown of GSDMD has been found to alleviate P. gingivalis–related inflammation in HGFs (Zhao et al., 2021). These results showed

that pharmacological inhibition of canonical or noncanonical pyroptosis pathways or gene knockout of pyroptosis-associated molecules results in significantly reduced alveolar bone loss and periodontal tissue inflammation and damage. Given the elevated pyroptosis level in periodontal tissue during periodontitis and its role in the pathological progression of periodontitis, treatments targeting pyroptosis will provide another effective way to cope with periodontitis. However, at present, the available inhibitors of pyroptosis generally act on caspases and inflammasomes, which also participate in other forms of programmed death; to date, there is still a lack of direct and specific pyroptosis inhibitors. Moreover, the role of pyroptosis in periodontitis is only just beginning to be understood; further studies of the signaling pathways involved in pyroptosis should be performed to provide new directions for the treatment of periodontitis.

Summary

The last decade has witnessed tremendous progress in pyroptosis research with an improved understanding of the role of pyroptosis in inflammatory diseases, cancers, and metabolic and autoimmune diseases. This review has provided a brief overview of the mechanisms of pyroptosis in periodontitis and the most recent research on the mechanisms of pyroptosis in relation to apoptosis. A large number of studies have revealed the critical role of pyroptosis-mediated activation of inflammation in periodontitis; however, as discussed above, the existing studies typically only explored the most characterized pyroptosis pathways. The physiological roles of GSDMs other than GSDMD in periodontitis remain poorly understood. Moreover, knowledge of posttranslational modification and molecular interactions between GSDMs in periodontitis remains incomplete. Therefore, it is critical to continue performing detailed investigations to gain extensive knowledge of pyroptosis in periodontitis. In light of the clear evidence that periodontitis causes systemic inflammation and increases the risk of systemic chronic comorbidities, it can be speculated that pyroptosis may link periodontitis with systemic disease. In this regard, future studies should address the mechanisms of pyroptosis in the connection between periodontitis and systemic diseases. This will facilitate the establishment of pyroptosis-targeted adjunctive treatments, thus contributing to reducing systemic inflammation and promoting systemic health. Crosstalk between pyroptosis and apoptosis, NETosis, and necroptosis has been investigated in various cells and tissues. Caspase-3/8 are considered the switch between apoptosis and pyroptosis, and deficiency in pyroptotic substrates contributes to the switch from apoptosis to pyroptosis. Notably, it seems that pyroptosis is usually concurrent with apoptosis, NETosis, and necroptosis in periodontal tissues during periodontitis. However, these conclusions have not been verified, and it remains unclear which is the primary type of programmed cell death in periodontal tissues during periodontitis. Understanding this topic will help us develop more precise therapeutic methods.

With respect to infectious disease, pyroptosis participates in the clearance of pathogens and enhances the host's defense responses. On the other hand, long-lasting pyroptosis leads to inflammatory damage in periodontal tissue. While many studies have reported that elevated pyroptosis contributes to the pathophysiological progression of periodontitis, there is limited research exploring the favorable aspect of pyroptosis in the clearance of periodontal pathogens. This proves a challenge for the application of pyroptosis inhibitors in periodontitis. The exploration of the molecules that directly target pyroptosis and the design of experiments to help understand the dual role of pyroptosis in periodontitis will shed light on novel therapeutic opportunities. Overall, it is crucial that pyroptosis be further explored in detail, with the expectation that basic research will translate to clinical practice prevention strategies.

Author contributions

XHX conceived the structure of the manuscript and wrote the manuscript. XYX, DA, YY, SY, MZ, and HQ collected the materials. TZ and JS reviewed and edited the manuscript. All authors read and approved the final manuscript.

Funding

This work was financially supported by funding from the National Natural Science Foundation of China (Grant No. 82101014; 81771082; 31971282), China postdoctoral Science Foundation (Grant No. 2021M700628), Natural Science Foundation of Chongqing (Grant No. cstc2021jcyj-bsh0005), and the Chongqing Graduate Tutor Team (2019) (Grant No. dstd201903).

Conflict of interest

The authors declare that the research was conducted in the absence of any commercial or financial relationships that could be construed as a potential conflict of interest.

Publisher's note

References

Abidi, A. H., Alghamdi, S. S., Dabbous, M. K., Tipton, D. A., Mustafa, S. M., and Moore, B. M. (2020). Cannabinoid type-2 receptor agonist, inverse agonist, and anandamide regulation of inflammatory responses in IL-1beta stimulated primary human Periodontal ligament fibroblasts. *J. Periodontal Res.* 55 (5), 762–783. doi: 10.1111/jre.12765

Alikhani, M., Alikhani, Z., and Graves, D. T. (2004). Apoptotic effects of LPS on fibroblasts are indirectly mediated through TNFR1. *J. Dental Res.* 83 (9), 671–676. doi: 10.1177/154405910408300903

Aluganti Narasimhulu, C., and Singla, D. K. (2021). Amelioration of diabetes-induced inflammation mediated pyroptosis, sarcopenia, and adverse muscle remodelling by bone morphogenetic protein-7. *J. Cachexia Sarcopenia Muscle* 12 (2), 403–420. doi: 10.1002/jcsm.12662

Alyami, H. M., Finoti, L. S., Teixeira, H. S., Aljefri, A., Kinane, D. F., and Benakanakere, M. R. (2019). Role of NOD1/NOD2 receptors in fusobacterium nucleatum mediated NETosis. *Microbial Pathogenesis* 131, 53–64. doi: 10.1016/j.micpath.2019.03.036

Aral, K., Aral, C. A., and Kapila, Y. (2019). The role of caspase-8, caspase-9, and apoptosis inducing factor in Periodontal disease. *J. Periodontol.* 90 (3), 288–294. doi: 10.1002/JPER.17-0716

Balmasova, I. P., Olekhnovich, E. I., Klimina, K. M., Korenkova, A. A., Vakhitova, M. T., Babaev, E. A., et al. (2021). Drift of the subgingival Periodontal microbiome during chronic periodontitis in type 2 diabetes mellitus patients. *Pathogens* 10 (5), 504–520. doi: 10.3390/pathogens10050504

Bergsbaken, T., Fink, S. L., and Cookson, B. T. (2009). Pyroptosis: Host cell death and inflammation. *Nat. Rev. Microbiol.* 7 (2), 99–109. doi: 10.1038/nrmicro2070

Bertheloot, D., Latz, E., and Franklin, B. S. (2021). Necroptosis, pyroptosis and apoptosis: An intricate game of cell death. *Cell. Mol. Immunol.* 18 (5), 1106–1121. doi: 10.1038/s41423-020-00630-3

Bloemen, V., Schoenmaker, T., de Vries, T. J., and Everts, V. (2011). IL-1beta favors osteoclastogenesis *via* supporting human Periodontal ligament fibroblasts. *J. Cell. Biochem.* 112 (7), 1890–1897. doi: 10.1002/jcb.23109

Bryzek, D., Ciaston, I., Dobosz, E., Gasiorek, A., Makarska, A., Sarna, M., et al. (2019). Triggering NETosis *via* protease-activated receptor (PAR)-2 signaling as a mechanism of hijacking neutrophils function for pathogen benefits. *PLoS Pathog.* 15 (5), e1007773. doi: 10.1371/journal.ppat.1007773

Bullon, P., Pavillard, L. E., and de la Torre-Torres, R. (2018). Inflammasome and oral diseases. *Experientia Supplementum* 108, 153–176. doi: 10.1007/978-3-319-89390-7_7

Buranasin, P., Mizutani, K., Iwasaki, K., Pawaputanon Na Mahasarakham, C., Kido, D., Takeda, K., et al. (2018). High glucose-induced oxidative stress impairs proliferation and migration of human gingival fibroblasts. *PLoS One* 13 (8), e0201855. doi: 10.1371/journal.pone.0201855

Busch, K., Kny, M., Huang, N., Klassert, T. E., Stock, M., Hahn, A., et al. (2021). Inhibition of the NLRP3/IL-1beta axis protects against sepsis-induced cardiomyopathy. *J. Cachexia Sarcopenia Muscle* 12 (6), 1653–1668. doi: 10.1002/jcsm.12763.

Cai, X., Zhang, Z. Y., Yuan, J. T., Ocansey, D. K. W., Tu, Q., Zhang, X., et al. (2021). hucMSC-derived exosomes attenuate colitis by regulating macrophage pyroptosis *via* the miR-378a-5p/NLRP3 axis. *Stem Cell Res. Ther.* 12 (1), 416. doi: 10.1186/s13287-021-02492-6

Chai, Q., Meng, Z., Lu, D., Zhang, Z., Liu, M., and Wu, W. (2021). Intermittent high glucose induces pyroptosis of rat H9C2 cardiomyocytes *via* sodium-glucose cotransporter 1. *Mol. Cell. Biochem.* 476 (6), 2479–2489. doi: 10.1007/s11010-021-04104-6

Cheng, R., Feng, Y., Zhang, R., Liu, W., Lei, L., and Hu, T. (2018). The extent of pyroptosis varies in different stages of apical periodontitis. *Biochim. Biophys. Acta Mol. basis Dis.* 1864 (1), 226–237. doi: 10.1016/j.bbadis.2017.10.025

Cheng, R., Wu, Z., Li, M., Shao, M., and Hu, T. (2020). Interleukin-1beta is a potential therapeutic target for periodontitis: A narrative review. *Int. J. Oral. Sci.* 12 (1), 2. doi: 10.1038/s41368-019-0068-8

Chen, C., Jiang, Z., Jiang, Q., Dai, W., Shao, Q., Chen, Q., et al. (2021). Caspase-3 and gasdermin e detection in peri-implantitis. *Biochim. Biophys. Acta Mol. basis Dis.* 1867 (11), 166217. doi: 10.1016/j.bbadis.2021.166217

Chen, Q., Liu, X., Wang, D., Zheng, J., Chen, L., Xie, Q., et al. (2021). Periodontal inflammation-triggered by Periodontal ligament stem cell pyroptosis exacerbates periodontitis. *Front. Cell Dev. Biol.* 9, 663037. doi: 10.3389/fcell.2021.663037

Chen, K. W., Monteleone, M., Boucher, D., Sollberger, G., Ramnath, D., Condon, N. D., et al. (2018). Noncanonical inflammasome signaling elicits gasdermin d-dependent neutrophil extracellular traps. *Sci. Immunol.* 3 (26), eaar6676. doi: 10.1038/s41368-019-0068-8.

Chen, Y., Yang, Q., Lv, C., Chen, Y., Zhao, W., Li, W., et al. (2021). NLRP3 regulates alveolar bone loss in ligature-induced periodontitis by promoting osteoclastic differentiation. *Cell Proliferation* 54 (2), e12973. doi: 10.1111/cpr.12973

Ciesielska, A., Matyjek, M., and Kwiatkowska, K. (2021). TLR4 and CD14 trafficking and its influence on LPS-induced pro-inflammatory signaling. *Cell Mol. Life Sci.* 78 (4), 1233–1261. doi: 10.1007/s00018-020-03656-y

Conos, S. A., Chen, K. W., De Nardo, D., Hara, H., Whitehead, L., Nunez, G., et al. (2017). Active MLKL triggers the NLRP3 inflammasome in a cell-intrinsic manner. *Proc. Natl. Acad. Sci. USA* 114 (6), E961–E9E9. doi: 10.1073/pnas.1613305114

Demarco, B., Grayczyk, J. P., Bjanes, E., Le Roy, D., Tonnus, W., Assenmacher, C. A., et al. (2020). Caspase-8-dependent gasdermin d cleavage promotes antimicrobial defense but confers susceptibility to TNF-induced lethality. *Sci. Adv.* 6 (47), eabc3465. doi: 10.1126/sciadv.abc3465.

Deng, S., Hu, Y., Zhou, J., Wang, Y., Wang, Y., Li, S., et al. (2020). TLR4 mediates alveolar bone resorption in experimental peri-implantitis through regulation of CD45(+) cell infiltration, RANKL/OPG ratio, and inflammatory cytokine production. *J. Periodontol.* 91 (5), 671–682. doi: 10.1002/JPER.18-0748

Doitsh, G., Galloway, N. L., Geng, X., Yang, Z., Monroe, K. M., Zepeda, O., et al. (2017). Corrigendum: Cell death by pyroptosis drives CD4 T-cell depletion in HIV-1 infection. *Nature* 544 (7648), 124. doi: 10.1038/nature22066

Downs, K. P., Nguyen, H., Dorfleutner, A., and Stehlik, C. (2020). An overview of the non-canonical inflammasome. *Mol. Aspects Med.* 76, 100924. doi: 10.1016/j.mam.2020.100924

Evavold, C. L., Hafner-Bratkovic, I., Devant, P., D'Andrea, J. M., Ngwa, E. M., Borsic, E., et al. (2021). Control of gasdermin d oligomerization and pyroptosis by the ragulator-Rag-mTORC1 pathway. *Cell* 184 (17), 4495–511.e19. doi: 10.1016/j.cell.2021.06.028

Fidler, T. P., Xue, C., Yalcinkaya, M., Hardaway, B., Abramowicz, S., Xiao, T., et al. (2021). The AIM2 inflammasome exacerbates atherosclerosis in clonal haematopoiesis. *Nature* 592 (7853), 296–301. doi: 10.1038/s41586-021-03341-5.

Fisch, D., Clough, B., Domart, M. C., Encheva, V., Bando, H., Snijders, A. P., et al. (2020). Human GBP1 differentially targets salmonella and toxoplasma to license recognition of microbial ligands and caspase-mediated death. *Cell Rep.* 32 (6), 108008. doi: 10.1016/j.celrep.2020.108008

Fleetwood, A. J., Lee, M. K. S., Singleton, W., Achuthan, A., Lee, M. C., O'Brien-Simpson, N. M., et al. (2017). Metabolic remodeling, inflammasome activation, and pyroptosis in macrophages stimulated by porphyromonas gingivalis and its outer membrane vesicles. *Front. Cell. Infection Microbiol.* 7, 351. doi: 10.3389/fcimb.2017.00351

Frank, D., and Vince, J. E. (2019). Pyroptosis versus necroptosis: similarities, differences, and crosstalk. *Cell Death Differentiation* 26 (1), 99–114. doi: 10.1038/s41418-018-0212-6

Fritsch, M., Gunther, S. D., Schwarzer, R., Albert, M. C., Schorn, F., Werthenbach, J. P., et al. (2019). Caspase-8 is the molecular switch for apoptosis, necroptosis and pyroptosis. *Nature* 575 (7784), 683–687. doi: 10.1038/s41586-019-1770-6

Geng, F., Liu, J., Yin, C., Zhang, S., Pan, Y., and Sun, H. (2022). Porphyromonas gingivalis lipopolysaccharide induced RIPK3/MLKL-mediated necroptosis of oral epithelial cells and the further regulation in macrophage activation. *J. Oral. Microbiol.* 14 (1), 2041790. doi: 10.1080/20002297.2022.2041790

Giblin, M. J., Smith, T. E., Winkler, G., Pendergrass, H. A., Kim, M. J., Capozzi, M. E., et al. (2021). Nuclear factor of activated T-cells (NFAT) regulation of IL-1beta-induced retinal vascular inflammation. *Biochim. Biophys. Acta Mol. basis Dis.* 1867 (12), 166238. doi: 10.1016/j.bbadis.2021.166238

Graves, D. T., Delima, A. J., Assuma, R., Amar, S., Oates, T., and Cochran, D. (1998). Interleukin-1 and tumor necrosis factor antagonists inhibit the progression of inflammatory cell infiltration toward alveolar bone in experimental periodontitis. *J. Periodontol.* 69 (12), 1419–1425. doi: 10.1902/jop.1998.69.12.1419

Guadagno, J., Swan, P., Shaikh, R., and Cregan, S. P. (2015). Microglia-derived IL-1beta triggers p53-mediated cell cycle arrest and apoptosis in neural precursor cells. *Cell Death Dis.* 6, e1779. doi: 10.1038/cddis.2015.151

Guerne, P. A., Carson, D. A., and Lotz, M. (1990). IL-6 production by human articular chondrocytes. modulation of its synthesis by cytokines, growth factors, and hormones *in vitro*. *J. Immunol.* 144 (2), 499–505.

Guo, H., Callaway, J. B., and Ting, J. P. (2015). Inflammasomes: Mechanism of action, role in disease, and therapeutics. *Nat. Med.* 21 (7), 677–687. doi: 10.1038/nm.3893

Gurung, P., Malireddi, R. K., Anand, P. K., Demon, D., Vande Walle, L., Liu, Z., et al. (2012). Toll or interleukin-1 receptor (TIR) domain-containing adaptor inducing interferon-beta (TRIF)-mediated caspase-11 protease production

integrates toll-like receptor 4 (TLR4) protein- and Nlrp3 inflammasome-mediated host defense against enteropathogens. *J. Biol. Chem.* 287 (41), 34474–34483. doi: 10.1074/jbc.M112.401406

Hajishengallis, G. (2020). New developments in neutrophil biology and periodontitis. *Periodontol 2000* 82 (1), 78–92. doi: 10.1111/prd.12313

Hansen, J. M., de Jong, M. F., Wu, Q., Zhang, L. S., Heisler, D. B., Alto, L. T., et al. (2021). Pathogenic ubiquitination of GSDMB inhibits NK cell bactericidal functions. *Cell* 184 (12), 3178–3191.e18. doi: 10.1016/j.cell.2021.04.036

Haraszthy, V. I., Zambon, J. J., Trevisan, M., Zeid, M., and Genco, R. J. (2000). Identification of Periodontal pathogens in atheromatous plaques. *J. Periodontol.* 71 (10), 1554–1560. doi: 10.1902/jop.2000.71.10.1554

Hirasawa, M., and Kurita-Ochiai, T. (2018). Porphyromonas gingivalis induces apoptosis and autophagy *via* ER stress in human umbilical vein endothelial cells. *Mediators Inflammation* 2018, 1967506. doi: 10.1155/2018/1967506

Hirschfeld, J., Roberts, H. M., Chapple, I. L., Parcina, M., Jepsen, S., Johansson, A., et al. (2016). Effects of aggregatibacter actinomycetemcomitans leukotoxin on neutrophil migration and extracellular trap formation. *J. Oral. Microbiol.* 8, 33070. doi: 10.3402/jom.v8.33070

Hosokawa, Y., Hosokawa, I., Shindo, S., Ozaki, K., and Matsuo, T. (2015). Calcitriol suppressed inflammatory reactions in IL-1beta-Stimulated human Periodontal ligament cells. *Inflammation* 38 (6), 2252–2258. doi: 10.1007/s10753-015-0209-y

Hou, J., Hsu, J. M., and Hung, M. C. (2021). Molecular mechanisms and functions of pyroptosis in inflammation and antitumor immunity. *Mol. Cell* 81 (22), 4579–4590. doi: 10.1016/j.molcel.2021.09.003

Hou, J., Zhao, R., Xia, W., Chang, C. W., You, Y., Hsu, J. M., et al. (2020). PD-L1-mediated gasdermin c expression switches apoptosis to pyroptosis in cancer cells and facilitates tumour necrosis. *Nat. Cell Biol.* 22 (10), 1264–1275. doi: 10.1038/s41556-020-0575-z

Huang, Y., Xu, W., and Zhou, R. (2021). NLRP3 inflammasome activation and cell death. *Cell. Mol. Immunol.* 18 (9), 2114–2127. doi: 10.1038/s41423-021-00740-6

Huang, C., Zhang, C., Yang, P., Chao, R., Yue, Z., Li, C., et al. (2020). Eldecalcitol inhibits LPS-induced NLRP3 inflammasome-dependent pyroptosis in human gingival fibroblasts by activating the Nrf2/HO-1 signaling pathway. *Drug design Dev. Ther.* 14, 4901–4913. doi: 10.2147/DDDT.S269223

Hu, L., Chen, M., Chen, X., Zhao, C., Fang, Z., Wang, H., et al. (2020). Chemotherapy-induced pyroptosis is mediated by BAK/BAX-caspase-3-GSDME pathway and inhibited by 2-bromopalmitate. *Cell Death Dis.* 11 (4), 281. doi: 10.1038/s41419-020-2476-2

Humphries, F., Shmuel-Galia, L., Ketelut-Carneiro, N., Li, S., Wang, B., Nemmara, V. V., et al. (2020). Succination inactivates gasdermin d and blocks pyroptosis. *Science* 369 (6511), 1633–1637. doi: 10.1126/science.abb9818

Huynh, N. C., Everts, V., Pavasant, P., and Ampornaramveth, R. S. (2017). Interleukin-1beta induces human cementoblasts to support osteoclastogenesis. *Int. J. Oral. Sci.* 9 (12), e5. doi: 10.1038/ijos.2017.45

Jain, P., Hassan, N., Khatoon, K., Mirza, M. A., Naseef, P. P., Kuruniyan, M. S., et al. (2021). Periodontitis and systemic disorder-an overview of relation and novel treatment modalities. *Pharmaceutics* 13 (8), 1175. doi: 10.3390/pharmaceutics13081175

Jan, M., Cueto, R., Jiang, X., Lu, L., Sardy, J., Xiong, X., et al. (2021). Molecular processes mediating hyperhomocysteinemia-induced metabolic reprogramming, redox regulation and growth inhibition in endothelial cells. *Redox Biol.* 45, 102018. doi: 10.1016/j.redox.2021.102018

Jiang, M., Qi, L., Li, L., and Li, Y. (2020). The caspase-3/GSDME signal pathway as a switch between apoptosis and pyroptosis in cancer. *Cell Death Discovery* 6, 112. doi: 10.1038/s41420-020-00349-0

Jiang, S., Zhou, Z., Sun, Y., Zhang, T., and Sun, L. (2020). Coral gasdermin triggers pyroptosis. *Sci. Immunol.* 5 (54), 112. doi: 10.1126/sciimmunol.abd2591.

Jorgensen, I., Zhang, Y., Krantz, B. A., and Miao, E. A. (2016). Pyroptosis triggers pore-induced intracellular traps (PITs) that capture bacteria and lead to their clearance by efferocytosis. *J. Exp. Med.* 213 (10), 2113–2128. doi: 10.1084/jem.20151613

Julien, O., and Wells, J. A. (2017). Caspases and their substrates. *Cell Death Differentiation* 24 (8), 1380–1389. doi: 10.1038/cdd.2017.44

Jun, H. K., Jung, Y. J., Ji, S., An, S. J., and Choi, B. K. (2018). Caspase-4 activation by a bacterial surface protein is mediated by cathepsin G in human gingival fibroblasts. *Cell Death Differentiation* 25 (2), 380–391. doi: 10.1038/cdd.2017.167

Jun, H. K., Lee, S. H., Lee, H. R., and Choi, B. K. (2012). Integrin alpha5beta1 activates the NLRP3 inflammasome by direct interaction with a bacterial surface protein. *Immunity* 36 (5), 755–768. doi: 10.1016/j.immuni.2012.05.002

Kambara, H., Liu, F., Zhang, X., Liu, P., Bajrami, B., Teng, Y., et al. (2018). Gasdermin d exerts anti-inflammatory effects by promoting neutrophil death. *Cell Rep.* 22 (11), 2924–2936. doi: 10.1016/j.celrep.2018.02.067

Kang, T., Huang, H., Mandrup-Poulsen, T., and Larsen, M. R. (2021). Divalent metal transporter 1 knock-down modulates IL-1beta mediated pancreatic beta-cell pro-apoptotic signaling pathways through the autophagic machinery. *Int. J. Mol. Sci.* 22 (15), 8013. doi: 10.3390/ijms22158013.

Kayagaki, N., Kornfeld, O. S., Lee, B. L., Stowe, I. B., O'Rourke, K., Li, Q., et al. (2021). NINJ1 mediates plasma membrane rupture during lytic cell death. *Nature* 591 (7848), 131–136. doi: 10.1038/s41586-021-03218-7

Kayagaki, N., Stowe, I. B., Lee, B. L., O'Rourke, K., Anderson, K., Warming, S., et al. (2015). Caspase-11 cleaves gasdermin d for non-canonical inflammasome signalling. *Nature* 526 (7575), 666–671. doi: 10.1038/nature15541

Kay, C., Wang, R., Kirkby, M., and Man, S. M. (2020). Molecular mechanisms activating the NAIP-NLRC4 inflammasome: Implications in infectious disease, autoinflammation, and cancer. *Immunol. Rev.* 297 (1), 67–82. doi: 10.1111/imr.12906

Ke, X., Lei, L., Li, H., Li, H., and Yan, F. (2016). Manipulation of necroptosis by porphyromonas gingivalis in periodontitis development. *Mol. Immunol.* 77, 8–13. doi: 10.1016/j.molimm.2016.07.010

Kelk, P., Abd, H., Claesson, R., Sandstrom, G., Sjostedt, A., and Johansson, A. (2011). Cellular and molecular response of human macrophages exposed to aggregatibacter actinomycetemcomitans leukotoxin. *Cell Death Dis.* 2, e126. doi: 10.1038/cddis.2011.6

Kim, M., Sur, B., Villa, T., Nah, S. Y., and Oh, S. (2021). Inhibitory activity of gintonin on inflammation in human IL-1beta-stimulated fibroblast-like synoviocytes and collagen-induced arthritis in mice. *J. Ginseng Res.* 45 (4), 510–518. doi: 10.1016/j.jgr.2020.12.001

Kinane, D. F., Stathopoulou, P. G., and Papapanou, P. N. (2017). Periodontal diseases. *Nat. Rev. Dis. Primers* 3, 17038. doi: 10.1038/nrdp.2017.38

Kovacs, S. B., and Miao, E. A. (2017). Gasdermins: Effectors of pyroptosis. *Trends Cell Biol.* 27 (9), 673–684. doi: 10.1016/j.tcb.2017.05.005

Kutsch, M., Sistemich, L., Lesser, C. F., Goldberg, M. B., Herrmann, C., and Coers, J. (2020). Direct binding of polymeric GBP1 to LPS disrupts bacterial cell envelope functions. *EMBO J.* 39 (13), e104926. doi: 10.15252/embj.2020104926

Lalla, E., and Papapanou, P. N. (2011). Diabetes mellitus and periodontitis: A tale of two common interrelated diseases. *Nat. Rev. Endocrinol.* 7 (12), 738–748. doi: 10.1038/nrendo.2011.106

Lawlor, K. E., Khan, N., Mildenhall, A., Gerlic, M., Croker, B. A., D'Cruz, A. A., et al. (2015). RIPK3 promotes cell death and NLRP3 inflammasome activation in the absence of MLKL. *Nat. Commun.* 6, 6282. doi: 10.1038/ncomms7282

Lazenby, M. G., and Crook, M. A. (2010). The innate immune system and diabetes mellitus: The relevance of periodontitis? a hypothesis. *Clin. Sci.* 119 (10), 423–429. doi: 10.1042/CS20100098

Lei, L., Sun, J., Han, J., Jiang, X., Wang, Z., and Chen, L. (2021). Interleukin-17 induces pyroptosis in osteoblasts through the NLRP3 inflammasome pathway in vitro. *Int. Immunopharmacol.* 96, 107781. doi: 10.1016/j.intimp.2021.107781

Liang, S., Lv, Z. T., Zhang, J. M., Wang, Y. T., Dong, Y. H., Wang, Z. G., et al. (2018). Necrostatin-1 attenuates trauma-induced mouse osteoarthritis and IL-1beta induced apoptosis *via* HMGB1/TLR4/SDF-1 in primary mouse chondrocytes. *Front. Pharmacol.* 9, 1378. doi: 10.3389/fphar.2018.01378

Li, Y. Y., Cai, Q., Li, B. S., Qiao, S. W., Jiang, J. Y., Wang, D., et al. (2021). The effect of porphyromonas gingivalis lipopolysaccharide on the pyroptosis of gingival fibroblasts. *Inflammation* 44 (3), 846–858. doi: 10.1007/s10753-020-01379-7

Li, Q., Dai, Z., Cao, Y., and Wang, L. (2019). Caspase-1 inhibition mediates neuroprotection in experimental stroke by polarizing M2 microglia/macrophage and suppressing NF-kappaB activation. *Biochem. Biophys. Res. Commun.* 513 (2), 479–485. doi: 10.1016/j.bbrc.2019.03.202

Li, Y., Ling, J., and Jiang, Q. (2021). Inflammasomes in alveolar bone loss. *Front. Immunol.* 12, 691013. doi: 10.3389/fimmu.2021.691013

Li, J., Mao, H., Pan, Y., Li, H., and Lei, L. (2020). Cyclin-dependent kinase 9 inhibition suppresses necroptosis and pyroptosis in the progress of endotoxemia. *Inflammation* 43 (6), 2061–2074. doi: 10.1007/s10753-020-01274-1

Lin, J., Bi, L., Yu, X., Kawai, T., Taubman, M. A., Shen, B., et al. (2014). Porphyromonas gingivalis exacerbates ligature-induced, RANKL-dependent alveolar bone resorption *via* differential regulation of toll-like receptor 2 (TLR2) and TLR4. *Infect. Immun.* 82 (10), 4127–4134. doi: 10.1128/IAI.02084-14

Lira-Junior, R., Bissett, S. M., Preshaw, P. M., Taylor, J. J., and Bostrom, E. A. (2021). Levels of myeloid-related proteins in saliva for screening and monitoring of Periodontal disease. *J. Clin. Periodontol.* 48 (11), 1430–1440. doi: 10.1111/jcpe.13534

Li, Y., Shen, Y., Jin, K., Wen, Z., Cao, W., Wu, B., et al. (2019). The DNA repair nuclease MRE11A functions as a mitochondrial protector and prevents T cell pyroptosis and tissue inflammation. *Cell Metab.* 30 (3), 477–492.e6. doi: 10.1016/j.cmet.2019.06.016

Li, L., Song, D., Qi, L., Jiang, M., Wu, Y., Gan, J., et al. (2021). Photodynamic therapy induces human esophageal carcinoma cell pyroptosis by targeting the

PKM2/caspase-8/caspase-3/GSDME axis. *Cancer Lett.* 520, 143–159. doi: 10.1016/j.canlet.2021.07.014

Liu, S., Du, J., Li, D., Yang, P., Kou, Y., Li, C., et al. (2020). Oxidative stress induced pyroptosis leads to osteogenic dysfunction of MG63 cells. *J. Mol. Histol.* 51 (3), 221–232. doi: 10.1007/s10735-020-09874-9

Liu, W., Liu, J., Wang, W., Wang, Y., and Ouyang, X. (2018). NLRP6 induces pyroptosis by activation of caspase-1 in gingival fibroblasts. *J. Dental Res.* 97 (12), 1391–1398. doi: 10.1177/0022034518775036

Liu, J., Wang, Y., Meng, H., Yu, J., Lu, H., Li, W., et al. (2019). Butyrate rather than LPS subverts gingival epithelial homeostasis by downregulation of intercellular junctions and triggering pyroptosis. *J. Clin. Periodontol.* 46 (9), 894–907. doi: 10.1111/jcpe.13162

Li, C., Yin, W., Yu, N., Zhang, D., Zhao, H., Liu, J., et al. (2019). miR-155 promotes macrophage pyroptosis induced by porphyromonas gingivalis through regulating the NLRP3 inflammasome. *Oral. Dis.* 25 (8), 2030–2039. doi: 10.1111/odi.13198

Li, N., Zhao, T., Cao, Y., Zhang, H., Peng, L., Wang, Y., et al. (2020). Tangshen formula attenuates diabetic kidney injury by imparting anti-pyroptotic effects *via* the TXNIP-NLRP3-GSDMD axis. *Front. Pharmacol.* 11, 623489. doi: 10.3389/fphar.2020.623489

Locati, M., Curtale, G., and Mantovani, A. (2020). Diversity, mechanisms, and significance of macrophage plasticity. *Annu. Rev. Pathol.* 15, 123–147. doi: 10.1146/annurev-pathmechdis-012418-012718

Long, P., Hu, J., Piesco, N., Buckley, M., and Agarwal, S. (2001). Low magnitude of tensile strain inhibits IL-1beta-dependent induction of pro-inflammatory cytokines and induces synthesis of IL-10 in human Periodontal ligament cells in vitro. *J. Dental Res.* 80 (5), 1416–1420. doi: 10.1177/00220345010800050601

Lotz, M., Terkeltaub, R., and Villiger, P. M. (1992). Cartilage and joint inflammation. regulation of IL-8 expression by human articular chondrocytes. *J. Immunol.* 148 (2), 466–473.

Lucas, H., Bartold, P. M., Dharmapatni, A. A., Holding, C. A., and Haynes, D. R. (2010). Inhibition of apoptosis in periodontitis. *J. Dental Res.* 89 (1), 29–33. doi: 10.1177/0022034509350708

Luchetti, G., Roncaioli, J. L., Chavez, R. A., Schubert, A. F., Kofoed, E. M., Reja, R., et al. (2021). Shigella ubiquitin ligase IpaH7.8 targets gasdermin d for degradation to prevent pyroptosis and enable infection. *Cell Host Microbe* 29 (10), 1521–1530. doi: 10.1016/j.chom.2021.08.010.

Mao, C. Y., Wang, Y. G., Zhang, X., Zheng, X. Y., Tang, T. T., and Lu, E. Y. (2016). Double-edged-sword effect of IL-1beta on the osteogenesis of Periodontal ligament stem cells *via* crosstalk between the NF-kappaB, MAPK and BMP/Smad signaling pathways. *Cell Death Dis.* 7, e2296. doi: 10.1038/cddis.2016.204

Martinvalet, D., Zhu, P., and Lieberman, J. (2005). Granzyme a induces caspase-independent mitochondrial damage, a required first step for apoptosis. *Immunity* 22 (3), 355–370. doi: 10.1016/j.immuni.2005.02.004

Mei, Y. M., Li, L., Wang, X. Q., Zhang, M., Zhu, L. F., Fu, Y. W., et al. (2019). AGEs induces apoptosis and autophagy *via* reactive oxygen species in human Periodontal ligament cells. *J. Cell. Biochem.* 121 (8-9), 3764–3779. doi: 10.1002/jcb.29499.

Moulin, M., Anderton, H., Voss, A. K., Thomas, T., Wong, W. W., Bankovacki, A., et al. (2012). IAPs limit activation of RIP kinases by TNF receptor 1 during development. *EMBO J.* 31 (7), 1679–1691. doi: 10.1038/emboj.2012.18

Murray, P. J. (2017). Macrophage polarization. *Annu. Rev. Physiol.* 79, 541–566. doi: 10.1146/annurev-physiol-022516-034339

Naderi, S., and Merchant, A. T. (2020). The association between periodontitis and cardiovascular disease: An update. *Curr. Atheroscl. Rep.* 22 (10), 52. doi: 10.1007/s11883-020-00878-0

Nie, L., Zhao, P., Yue, Z., Zhang, P., Ji, N., Chen, Q., et al. (2021). Diabetes induces macrophage dysfunction through cytoplasmic dsDNA/AIM2 associated pyroptosis. *J. Leukocyte Biol.* 110 (3), 497–510. doi: 10.1002/JLB.3MA0321-745R

Ono, M., Kantoh, K., Ueki, J., Shimada, A., Wakabayashi, H., Matsuta, T., et al. (2011). Quest for anti-inflammatory substances using IL-1beta-stimulated gingival fibroblasts. *In Vivo* 25 (5), 763–768.

Orning, P., Weng, D., Starheim, K., Ratner, D., Best, Z., Lee, B., et al. (2018). Pathogen blockade of TAK1 triggers caspase-8-dependent cleavage of gasdermin d and cell death. *Science* 362 (6418), 1064–1069. doi: 10.1126/science.aau2818.

Panagakos, F. S., Jandinski, J. J., Feder, L., and Kumar, S. (1994). Effects of plasminogen and interleukin-1 beta on bone resorption in vitro. *Biochimie* 76 (5), 394–397. doi: 10.1016/0300-9084(94)90114-7

Pavlic, V., Peric, D., Kalezic, I. S., Madi, M., Bhat, S. G., Brkic, Z., et al. (2021). Identification of periopathogens in atheromatous plaques obtained from carotid and coronary arteries. *BioMed. Res. Int.* 2021, 9986375. doi: 10.1155/2021/9986375

Pierini, R., Juruj, C., Perret, M., Jones, C. L., Mangeot, P., Weiss, D. S., et al. (2012). AIM2/ASC triggers caspase-8-dependent apoptosis in francisella-infected caspase-1-deficient macrophages. *Cell Death Differentiation* 19 (10), 1709–1721. doi: 10.1038/cdd.2012.51

Pirih, F. Q., Monajemzadeh, S., Singh, N., Sinacola, R. S., Shin, J. M., Chen, T., et al. (2021). Association between metabolic syndrome and periodontitis: The role of lipids, inflammatory cytokines, altered host response, and the microbiome. *Periodontol 2000* 87 (1), 50–75. doi: 10.1111/prd.12379

Place, D. E., Lee, S., and Kanneganti, T. D. (2021). PANoptosis in microbial infection. *Curr. Opin. Microbiol.* 59, 42–49. doi: 10.1016/j.mib.2020.07.012

Polak, D., and Shapira, L. (2018). An update on the evidence for pathogenic mechanisms that may link periodontitis and diabetes. *J. Clin. Periodontol.* 45 (2), 150–166. doi: 10.1111/jcpe.12803

Polzer, K., Joosten, L., Gasser, J., Distler, J. H., Ruiz, G., Baum, W., et al. (2010). Interleukin-1 is essential for systemic inflammatory bone loss. *Ann. Rheumatic Dis.* 69 (1), 284–290. doi: 10.1136/ard.2008.104786

Preshaw, P. M., Alba, A. L., Herrera, D., Jepsen, S., Konstantinidis, A., Makrilakis, K., et al. (2012). Periodontitis and diabetes: A two-way relationship. *Diabetologia* 55 (1), 21–31. doi: 10.1007/s00125-011-2342-y

Py, B. F., Kim, M. S., Vakifahmetoglu-Norberg, H., and Yuan, J. (2013). Deubiquitination of NLRP3 by BRCC3 critically regulates inflammasome activity. *Mol. Cell* 49 (2), 331–338. doi: 10.1016/j.molcel.2012.11.009

Quirke, A. M., Lugli, E. B., Wegner, N., Hamilton, B. C., Charles, P., Chowdhury, M., et al. (2014). Heightened immune response to autocitrullinated porphyromonas gingivalis peptidylarginine deiminase: A potential mechanism for breaching immunologic tolerance in rheumatoid arthritis. *Ann. rheumatic Dis.* 73 (1), 263–269. doi: 10.1136/annrheumdis-2012-202726

Ran, S., Huang, J., Liu, B., Gu, S., Jiang, W., and Liang, J. (2021). Enterococcus faecalis activates NLRP3 inflammasomes leading to increased interleukin-1 beta secretion and pyroptosis of THP-1 macrophages. *Microbial Pathogenesis* 154, 104761. doi: 10.1016/j.micpath.2021.104761

Rathinam, V. A., and Fitzgerald, K. A. (2016). Inflammasome complexes: Emerging mechanisms and effector functions. *Cell* 165 (4), 792–800. doi: 10.1016/j.cell.2016.03.046

Rathinam, V. A., Vanaja, S. K., Waggoner, L., Sokolovska, A., Becker, C., Stuart, L. M., et al. (2012). TRIF licenses caspase-11-dependent NLRP3 inflammasome activation by gram-negative bacteria. *Cell* 150 (3), 606–619. doi: 10.1016/j.cell.2012.07.007

Rickard, J. A., O'Donnell, J. A., Evans, J. M., Lalaoui, N., Poh, A. R., Rogers, T., et al. (2014). RIPK1 regulates RIPK3-MLKL-driven systemic inflammation and emergency hematopoiesis. *Cell* 157 (5), 1175–1188. doi: 10.1016/j.cell.2014.04.019

Rocha, F. R. G., Delitto, A. E., de Souza, J. A. C., Gonzalez-Maldonado, L. A., Wallet, S. M., and Rossa Junior, C. (2020). Relevance of caspase-1 and Nlrp3 inflammasome on inflammatory bone resorption in a murine model of periodontitis. *Sci. Rep.* 10 (1), 7823. doi: 10.1038/s41598-020-64685-y

Rogers, C., Fernandes-Alnemri, T., Mayes, L., Alnemri, D., Cingolani, G., and Alnemri, E. S. (2017). Cleavage of DFNA5 by caspase-3 during apoptosis mediates progression to secondary necrotic/pyroptotic cell death. *Nat. Commun.* 8, 14128. doi: 10.1038/ncomms14128

Romagnoli, A., Petruccioli, E., Palucci, I., Camassa, S., Carata, E., Petrone, L., et al. (2018). Clinical isolates of the modern mycobacterium tuberculosis lineage 4 evade host defense in human macrophages through eluding IL-1beta-induced autophagy. *Cell Death Dis.* 9 (6), 624. doi: 10.1038/s41419-018-0640-8

Sagulenko, V., Thygesen, S. J., Sester, D. P., Idris, A., Cridland, J. A., Vajjhala, P. R., et al. (2013). AIM2 and NLRP3 inflammasomes activate both apoptotic and pyroptotic death pathways *via* ASC. *Cell Death Differentiation* 20 (9), 1149–1160. doi: 10.1038/cdd.2013.37

Samir, P., Malireddi, R. K. S., and Kanneganti, T. D. (2020). The PANoptosome: A deadly protein complex driving pyroptosis, apoptosis, and necroptosis (PANoptosis). *Front. Cell. Infection Microbiol.* 10, 238. doi: 10.3389/fcimb.2020.00238

Santos, J. C., Boucher, D., Schneider, L. K., Demarco, B., Dilucca, M., Shkarina, K., et al. (2020). Human GBP1 binds LPS to initiate assembly of a caspase-4 activating platform on cytosolic bacteria. *Nat. Commun.* 11 (1), 3276. doi: 10.1038/s41467-020-16889-z

Sarhan, J., Liu, B. C., Muendlein, H. I., Li, P., Nilson, R., Tang, A. Y., et al. (2018). Caspase-8 induces cleavage of gasdermin d to elicit pyroptosis during yersinia infection. *Proc. Natl. Acad. Sci. USA* 115 (46), E10888–E10E97. doi: 10.1073/pnas.1809548115

Schett, G., Dayer, J. M., and Manger, B. (2016). Interleukin-1 function and role in rheumatic disease. *Nat. Rev. Rheumatol.* 12 (1), 14–24. doi: 10.1038/nrrheum.2016.166

Schroder, K., Zhou, R., and Tschopp, J. (2010). The NLRP3 inflammasome: A sensor for metabolic danger? *Science* 327 (5963), 296–300. doi: 10.1126/science.1184003.

Shan, C., Ma, T., Wang, T. T., Wu, L., Abasijiang, A., and Zhao, J. (2022). Association of polymorphism in IL-18 gene with periodontitis in uyghur adults in

xinjiang and evidence from six case-control studies with a comprehensive analysis. *Immunol. investigations* 51 (3), 511–530. doi: 10.1080/08820139.2020.1841222.

Shapouri-Moghaddam, A., Mohammadian, S., Vazini, H., Taghadosi, M., Esmaeili, S. A., Mardani, F., et al. (2018). Macrophage plasticity, polarization, and function in health and disease. *J. Cell. Physiol.* 233 (9), 6425–6440. doi: 10.1002/jcp.26429

Shi, B., Lux, R., Klokkevold, P., Chang, M., Barnard, E., Haake, S., et al. (2020). The subgingival microbiome associated with periodontitis in type 2 diabetes mellitus. *ISME J.* 14 (2), 519–530. doi: 10.1038/s41396-019-0544-3

Silke, J., and Meier, P. (2013). Inhibitor of apoptosis (IAP) proteins-modulators of cell death and inflammation. *Cold Spring Harbor Perspect. Biol.* 5 (2), a008730. doi: 10.1101/cshperspect.a008730

Sollberger, G. (2022). Approaching neutrophil pyroptosis. *J. Mol. Biol.* 434 (4), 167335. doi: 10.1016/j.jmb.2021.167335

Sollberger, G., Choidas, A., Burn, G. L., Habenberger, P., Di Lucrezia, R., Kordes, S., et al. (2018). Gasdermin d plays a vital role in the generation of neutrophil extracellular traps. *Sci. Immunol.* 3 (26), eaar6689. doi: 10.1126/sciimmunol

Song, N., Liu, Z. S., Xue, W., Bai, Z. F., Wang, Q. Y., Dai, J., et al. (2017). NLRP3 phosphorylation is an essential priming event for inflammasome activation. *Mol. Cell* 68 (1), 1851–97.e6. doi: 10.1016/j.molcel.2017.08.017

Speir, M., and Lawlor, K. E. (2021). RIP-roaring inflammation: RIPK1 and RIPK3 driven NLRP3 inflammasome activation and autoinflammatory disease. *Semin. Cell Dev. Biol.* 109, 114–124. doi: 10.1016/j.semcdb.2020.07.011

Sugiyama, M., Saeki, A., Hasebe, A., Kamesaki, R., Yoshida, Y., Kitagawa, Y., et al. (2016). Activation of inflammasomes in dendritic cells and macrophages by mycoplasma salivarium. *Mol. Oral. Microbiol.* 31 (3), 259–269. doi: 10.1111/omi.12117

Sundaram, B., and Kanneganti, T. D. (2021). Advances in understanding activation and function of the NLRC4 inflammasome. *Int. J. Mol. Sci.* 22 (3), 1048. doi: 10.3390/ijms22031048

Sun, X., Li, M., Xia, L., Fang, Z., Yu, S., Gao, J., et al. (2020). Alteration of salivary microbiome in periodontitis with or without type-2 diabetes mellitus and metformin treatment. *Sci. Rep.* 10 (1), 15363. doi: 10.1038/s41598-020-72035-1

Swanson, K. V., Deng, M., and Ting, J. P. (2019). The NLRP3 inflammasome: molecular activation and regulation to therapeutics. *Nat. Rev. Immunol.* 19 (8), 477–489. doi: 10.1038/s41577-019-0165-0

Taabazuing, C. Y., Griswold, A. R., and Bachovchin, D. A. (2020). The NLRP1 and CARD8 inflammasomes. *Immunol. Rev.* 297 (1), 13–25. doi: 10.1111/imr.12884

Tan, G., Huang, C., Chen, J., Chen, B., and Zhi, F. (2021). Gasdermin-e-mediated pyroptosis participates in the pathogenesis of crohn's disease by promoting intestinal inflammation. *Cell Rep.* 35 (11), 109265. doi: 10.1016/j.celrep.2021.109265

Tenev, T., Bianchi, K., Darding, M., Broemer, M., Langlais, C., Wallberg, F., et al. (2011). The ripoptosome, a signaling platform that assembles in response to genotoxic stress and loss of IAPs. *Mol. Cell* 43 (3), 432–448. doi: 10.1016/j.molcel.2011.06.006

Thiam, H. R., Wong, S. L., Wagner, D. D., and Waterman, C. M. (2020). Cellular mechanisms of NETosis. *Annu. Rev. Cell Dev. Biol.* 36, 191–218. doi: 10.1146/annurev-cellbio-020520-111016

Tothova, L., and Celec, P. (2017). Oxidative stress and antioxidants in the diagnosis and therapy of periodontitis. *Front. Physiol.* 8, 1055. doi: 10.3389/fphys.2017.01055

Tsuchiya, K., Nakajima, S., Hosojima, S., Thi Nguyen, D., Hattori, T., Manh Le, T., et al. (2019). Caspase-1 initiates apoptosis in the absence of gasdermin d. *Nat. Commun.* 10 (1), 2091. doi: 10.1038/s41467-019-09753-2

Van Opdenbosch, N., Van Gorp, H., Verdonckt, M., Saavedra, P. H. V., de Vasconcelos, N. M., Goncalves, A., et al. (2017). Caspase-1 engagement and TLR-induced c-FLIP expression suppress ASC/Caspase-8-Dependent apoptosis by inflammasome sensors NLRP1b and NLRC4. *Cell Rep.* 21 (12), 3427–3444. doi: 10.1016/j.celrep.2017.11.088

Vecchie, A., Bonaventura, A., Toldo, S., Dagna, L., Dinarello, C. A., and Abbate, A. (2021). IL-18 and infections: Is there a role for targeted therapies? *J. Cell. Physiol.* 236 (3), 1638–1657. doi: 10.1002/jcp.30008

Velotti, F., Barchetta, I., Cimini, F. A., and Cavallo, M. G. (2020). Granzyme b in inflammatory diseases: Apoptosis, inflammation, extracellular matrix remodeling, epithelial-to-Mesenchymal transition and fibrosis. *Front. Immunol.* 11, 587581. doi: 10.3389/fimmu.2020.587581

Vora, S. M., Lieberman, J., and Wu, H. (2021). Inflammasome activation at the crux of severe COVID-19. *Nat. Rev. Immunol* 21 (11), 694–703. doi: 10.1038/s41577-021-00588-x

Wandel, M. P., Kim, B. H., Park, E. S., Boyle, K. B., Nayak, K., Lagrange, B., et al. (2020). Guanylate-binding proteins convert cytosolic bacteria into caspase-4 signaling platforms. *Nat. Immunol.* 21 (8), 880–891. doi: 10.1038/s41590-020-0697-2

Wang, Y., Gao, W., Shi, X., Ding, J., Liu, W., He, H., et al. (2017). Chemotherapy drugs induce pyroptosis through caspase-3 cleavage of a gasdermin. *Nature* 547 (7661), 99–103. doi: 10.1038/nature22393

Wang, F., Guan, M., Wei, L., and Yan, H. (2019). IL18 promotes the secretion of matrix metalloproteinases in human Periodontal ligament fibroblasts by activating NFkappaB signaling. *Mol. Med. Rep.* 19 (1), 703–710. doi: 10.3892/mmr.2018.9697

Wang, B. W., Jiang, Y., Yao, Z. L., Chen, P. S., Yu, B., and Wang, S. N. (2019). Aucubin protects chondrocytes against IL-1beta-Induced apoptosis *In vitro* and inhibits osteoarthritis in mice model. *Drug Design Dev. Ther.* 13, 3529–3538. doi: 10.2147/DDDT.S210220

Wang, Y., and Kanneganti, T. D. (2021). From pyroptosis, apoptosis and necroptosis to PANoptosis: A mechanistic compendium of programmed cell death pathways. *Comput. Struct. Biotechnol. J.* 19, 4641–4657. doi: 10.1016/j.csbj.2021.07.038

Wang, J., Luo, X., Cai, S., Sun, J., Wang, S., and Wei, X. (2021). Blocking HOTAIR protects human chondrocytes against IL-1beta-induced cell apoptosis, ECM degradation, inflammatory response and oxidative stress *via* regulating miR-222-3p/ADAM10 axis. *Int. Immunopharmacol.* 98, 107903. doi: 10.1016/j.intimp.2021.107903

Wegner, N., Wait, R., Sroka, A., Eick, S., Nguyen, K. A., Lundberg, K., et al. (2010). Peptidylarginine deiminase from porphyromonas gingivalis citrullinates human fibrinogen and alpha-enolase: implications for autoimmunity in rheumatoid arthritis. *Arthritis Rheumatism* 62 (9), 2662–2672. doi: 10.1002/art.27552

Wei, Z., Nie, G., Yang, F., Pi, S., Wang, C., Cao, H., et al. (2020). Inhibition of ROS/NLRP3/Caspase-1 mediated pyroptosis attenuates cadmium-induced apoptosis in duck renal tubular epithelial cells. *Environ. Pollut.* 273, 115919. doi: 10.1016/j.envpol.2020.115919

White, T., Alimova, Y., Alves, V. T. E., Emecen-Huja, P., Al-Sabbagh, M., Villasante, A., et al. (2020). Oral commensal bacteria differentially modulate epithelial cell death. *Arch. Oral. Biol.* 120, 104926. doi: 10.1016/j.archoralbio.2020.104926

Wu, X. Y., Li, K. T., Yang, H. X., Yang, B., Lu, X., Zhao, L. D., et al. (2020). Complement C1q synergizes with PTX3 in promoting NLRP3 inflammasome over-activation and pyroptosis in rheumatoid arthritis. *J. Autoimmun.* 106, 102336. doi: 10.1016/j.jaut.2019.102336

Xia, S., Hollingsworth, L., and Wu, H. (2020). Mechanism and regulation of gasdermin-mediated cell death. *Cold Spring Harbor Perspect. Biol.* 12 (3), a036400. doi: 10.1101/cshperspect.a036400

Xia, W., Lu, Z., Chen, W., Zhou, J., and Zhao, Y. (2022). Excess fatty acids induce pancreatic acinar cell pyroptosis through macrophage M1 polarization. *BMC Gastroenterol.* 22 (1), 72. doi: 10.1186/s12876-022-02146-8

Xia, S., Zhang, Z., Magupalli, V. G., Pablo, J. L., Dong, Y., Vora, S. M., et al. (2021). Gasdermin d pore structure reveals preferential release of mature interleukin-1. *Nature* 593 (7860), 607–611. doi: 10.1038/s41586-021-03478-3

Xi, H., Zhang, Y., Xu, Y., Yang, W. Y., Jiang, X., Sha, X., et al. (2016). Caspase-1 inflammasome activation mediates homocysteine-induced pyrop-apoptosis in endothelial cells. *Circ. Res.* 118 (10), 1525–1539. doi: 10.1161/CIRCRESAHA.116.308501

Xu, Z., Ke, T., Zhang, Y., Guo, L., Chen, F., and He, W. (2021). Danshensu inhibits the IL-1beta-induced inflammatory response in chondrocytes and osteoarthritis possibly *via* suppressing NF-kappaB signaling pathway. *Mol. Med.* 27 (1), 80. doi: 10.1186/s10020-021-00329-9.

Xu, P., Zhang, X., Liu, Q., Xie, Y., Shi, X., Chen, J., et al. (2019). Microglial TREM-1 receptor mediates neuroinflammatory injury *via* interaction with SYK in experimental ischemic stroke. *Cell Death Dis.* 10 (8), 555. doi: 10.1038/s41419-019-1777-9

Yang, W., Liu, S., Li, Y., Wang, Y., Deng, Y., Sun, W., et al. (2020). Pyridoxine induces monocyte-macrophages death as specific treatment of acute myeloid leukemia. *Cancer Lett.* 492, 96–105. doi: 10.1016/j.canlet.2020.08.018

Yang, L., Liu, J., Shan, Q., Geng, G., and Shao, P. (2020). High glucose inhibits proliferation and differentiation of osteoblast in alveolar bone by inducing pyroptosis. *Biochem. Biophys. Res. Commun.* 522 (2), 471–478. doi: 10.1016/j.bbrc.2019.11.080

Yang, K., Liu, J., Zhang, X., Ren, Z., Gao, L., Wang, Y., et al. (2020). H3 relaxin alleviates migration, apoptosis and pyroptosis through P2X7R-mediated nucleotide binding oligomerization domain-like receptor protein 3 inflammasome activation in retinopathy induced by hyperglycemia. *Front. Pharmacol.* 11, 603689. doi: 10.3389/fphar.2020.603689

Yang, Y., Wang, L., Zhang, H., and Luo, L. (2022). Mixed lineage kinase domain-like pseudokinase-mediated necroptosis aggravates periodontitis progression. *J. Mol. Med. (Berl)* 100 (1), 77–86. doi: 10.1007/s00109-021-02126-7

Yang, K., Xu, S., Zhao, H., Liu, L., Lv, X., Hu, F., et al. (2021). Hypoxia and porphyromonas gingivalis-lipopolysaccharide synergistically induce NLRP3 inflammasome activation in human gingival fibroblasts. *Int. Immunopharmacol.* 94, 107456. doi: 10.1016/j.intimp.2021.107456

Yao, F., Jin, Z., Lv, X., Zheng, Z., Gao, H., Deng, Y., et al. (2021). Hydroxytyrosol acetate inhibits vascular endothelial cell pyroptosis *via* the HDAC11 signaling pathway in atherosclerosis. *Front. Pharmacol.* 12, 656272. doi: 10.3389/fphar.2021.656272

Yoshinaka, K., Shoji, N., Nishioka, T., Sugawara, Y., Hoshino, T., Sugawara, S., et al. (2014). Increased interleukin-18 in the gingival tissues evokes chronic periodontitis after bacterial infection. *Tohoku J. Exp. Med.* 232 (3), 215–222. doi: 10.1620/tjem.232.215

Yuan, J., Amin, P., and Ofengeim, D. (2019). Necroptosis and RIPK1-mediated neuroinflammation in CNS diseases. *Nat. Rev. Neurosci.* 20 (1), 19–33. doi: 10.1038/s41583-018-0093-1

Yu, S., Li, H., Ma, Y., and Fu, Y. (2012). Matrix metalloproteinase-1 of gingival fibroblasts influenced by advanced glycation end products (AGEs) and their association with receptor for AGEs and nuclear factor-kappaB in gingival connective tissue. *J. Periodontol.* 83 (1), 119–126. doi: 10.1902/jop.2011.100754

Yu, P., Zhang, X., Liu, N., Tang, L., Peng, C., and Chen, X. (2021). Pyroptosis: mechanisms and diseases. *Signal Transduction Targeted Ther.* 6 (1), 128. doi: 10.1038/s41392-021-00507-5

Zamyatina, A., and Heine, H. (2020). Lipopolysaccharide recognition in the crossroads of TLR4 and caspase-4/11 mediated inflammatory pathways. *Front. Immunol.* 11, 585146. doi: 10.3389/fimmu.2020.585146

Zang, Y., Song, J. H., Oh, S. H., Kim, J. W., Lee, M. N., Piao, X., et al. (2020). Targeting NLRP3 inflammasome reduces age-related experimental alveolar bone loss. *J. Dental Res.* 99 (11), 1287–1295. doi: 10.1177/0022034520933533

Zhang, Y., Kuang, W., Li, D., Li, Y., Feng, Y., Lyu, X., et al. (2021). Natural killer-like b cells secreting interleukin-18 induces a proinflammatory response in periodontitis. *Front. Immunol.* 12, 641562. doi: 10.3389/fimmu.2021.641562

Zhang, X., Zhang, P., An, L., Sun, N., Peng, L., Tang, W., et al. (2020). Miltirone induces cell death in hepatocellular carcinoma cell through GSDME-dependent pyroptosis. *Acta Pharm. Sin. B* 10 (8), 1397–1413. doi: 10.1016/j.apsb.2020.06.015

Zhang, Z., Zhang, Y., Xia, S., Kong, Q., Li, S., Liu, X., et al. (2020). Gasdermin e suppresses tumour growth by activating anti-tumour immunity. *Nature* 579 (7799), 415–420. doi: 10.1038/s41586-020-2071-9

Zhang, J. Y., Zhou, B., Sun, R. Y., Ai, Y. L., Cheng, K., Li, F. N., et al. (2021). The metabolite alpha-KG induces GSDMC-dependent pyroptosis through death receptor 6-activated caspase-8. *Cell Res.* 31 (9), 980–997. doi: 10.1038/s41422-021-00506-9

Zhao, D., Wu, Y., Zhuang, J., Xu, C., and Zhang, F. (2016). Activation of NLRP1 and NLRP3 inflammasomes contributed to cyclic stretch-induced pyroptosis and release of IL-1beta in human Periodontal ligament cells. *Oncotarget* 7 (42), 68292–68302. doi: 10.18632/oncotarget.11944

Zhao, P., Yue, Z., Nie, L., Zhao, Z., Wang, Q., Chen, J., et al. (2021). Hyperglycaemia-associated macrophage pyroptosis accelerates Periodontal inflamm-aging. *J. Clin. Periodontol.* 48 (10), 1379–1392. doi: 10.1111/jcpe.13517

Zheng, M., and Kanneganti, T. D. (2020). The regulation of the ZBP1-NLRP3 inflammasome and its implications in pyroptosis, apoptosis, and necroptosis (PANoptosis). *Immunol. Rev.* 297 (1), 26–38. doi: 10.1111/imr.12909

Zheng, M., Karki, R., Vogel, P., and Kanneganti, T. D. (2020). Caspase-6 is a key regulator of innate immunity, inflammasome activation, and host defense. *Cell* 181 (3), 674–687.e13. doi: 10.1016/j.cell.2020.03.040

Zhou, Z., He, H., Wang, K., Shi, X., Wang, Y., Su, Y., et al. (2020). Granzyme a from cytotoxic lymphocytes cleaves GSDMB to trigger pyroptosis in target cells. *Science* 368 (6494), eaaz7548. doi: 10.1126/science.aaz7548

Zhou, Y., Li, T., Chen, Z., Huang, J., Qin, Z., and Li, L. (2021). Overexpression of lncRNA TUG1 alleviates NLRP3 inflammasome-mediated cardiomyocyte pyroptosis through targeting the miR-186-5p/XIAP axis in coronary microembolization-induced myocardial damage. *Front. Immunol.* 12, 637598. doi: 10.3389/fimmu.2021.637598

Zhou, X., Wang, Q., Nie, L., Zhang, P., Zhao, P., Yuan, Q., et al. (2020). Metformin ameliorates the NLPP3 inflammasome mediated pyroptosis by inhibiting the expression of NEK7 in diabetic periodontitis. *Arch. Oral. Biol.* 116, 104763. doi: 10.1016/j.archoralbio.2020.104763

Zhou, N., Zou, F., Cheng, X., Huang, Y., Zou, H., Niu, Q., et al. (2021). Porphyromonas gingivalis induces periodontitis, causes immune imbalance, and promotes rheumatoid arthritis. *J. Leukocyte Biol.* 110 (3), 461–473. doi: 10.1002/JLB.3MA0121-045R

Zhuang, J., Wang, Y., Qu, F., Wu, Y., Zhao, D., and Xu, C. (2019). Gasdermin-d played a critical role in the cyclic stretch-induced inflammatory reaction in human Periodontal ligament cells. *Inflammation* 42 (2), 548–558. doi: 10.1007/s10753-018-0912-6

Zhu, H., Lin, X., Zheng, P., and Chen, H. (2015). Inflammatory cytokine levels in patients with periodontitis and/or coronary heart disease. *Int. J. Clin. Exp. Pathol.* 8 (2), 2214–2220.

Zhu, M., and Nikolajczyk, B. S. (2014). Immune cells link obesity-associated type 2 diabetes and periodontitis. *J. Dental Res.* 93 (4), 346–352. doi: 10.1177/0022034513518943

Zhu, X., Wang, K., Zhang, K., Tan, X., Wu, Z., Sun, S., et al. (2015). Tetramethylpyrazine protects retinal capillary endothelial cells (TR-iBRB2) against IL-1beta-Induced Nitrative/Oxidative stress. *Int. J. Mol. Sci.* 16 (9), 21775–21790. doi: 10.3390/ijms160921775

Zhu, L., Wu, Y., Wei, H., Yang, S., Zhan, N., Xing, X., et al. (2012). Up-regulation of IL-23 p19 expression in human Periodontal ligament fibroblasts by IL-1beta *via* concurrent activation of the NF-kappaB and MAPKs/AP-1 pathways. *Cytokine* 60 (1), 171–178. doi: 10.1016/j.cyto.2012.05.016

Ziauddin, S. M., Yoshimura, A., Montenegro Raudales, J. L., Ozaki, Y., Higuchi, K., Ukai, T., et al. (2018). Crystalline structure of pulverized dental calculus induces cell death in oral epithelial cells. *J. Periodontal Res.* 53 (3), 353–361. doi: 10.1111/jre.12520

Zizzi, A., Tirabassi, G., Aspriello, S. D., Piemontese, M., Rubini, C., and Lucarini, G. (2013). Gingival advanced glycation end-products in diabetes mellitus-associated chronic periodontitis: An immunohistochemical study. *J. Periodontal Res.* 48 (3), 293–301. doi: 10.1111/jre.12007

10.3389/fcimb.2022.953277

Glossary

GSDMs	Gasdermins
NLRP3	NLR family pyrin domain containing 3
PAMPs	pathogen-associated molecular patterns
AP	apical periodontitis
IL	interleukin
DAMPs	damage-associated molecular patterns
MHC	major histocompatibility complex
NLRs	NOD-like receptors
ALRs	absent in melanoma 2 (AIM2)-like receptors
ASC	apoptosis-associated speck-like proteins containing a caspase recruitment domain
LRR	leucine-rich repeat domain
NBD	nucleotide-binding domain
NACHT	nucleotide-binding and oligomerization domain
PYD	pyrin domain
CARD	caspase recruitment domain
GBPs	guanylate binding proteins
DFNB59	autosomal recessive deafness-59
ELANE	neutrophil-specific serine protease-neutrophil elastase
HGFs	human gingival fibroblasts
HPDLFs	human periodontal ligament fibroblasts
HPDLSCs	human periodontal ligament stem cells
HGEs	human gingival epithelium
MMPs	matrix metalloproteinases
CCL	C-C motif chemokine ligand
CXCL	C-X-C motif chemokine ligand
IFN	interferon
PGE2	prostaglandin E2
AGEs	advanced glycation end-products.

frontiers | Frontiers in Cellular and Infection Microbiology

TYPE Original Research
PUBLISHED 29 August 2022
DOI 10.3389/fcimb.2022.937725

OPEN ACCESS

EDITED BY
Zheng Zhang,
Nankai University, China

REVIEWED BY
Almagul Kushugulova,
Nazarbayev University, Kazakhstan
Yuichiro Noiri,
Niigata University, Japan

*CORRESPONDENCE
WanQi Lv
lvwanqi_kq@fudan.edu.cn

†These authors have contributed equally to this work

SPECIALTY SECTION
This article was submitted to Microbiome in Health and Disease, a section of the journal Frontiers in Cellular and Infection Microbiology

RECEIVED 06 May 2022
ACCEPTED 29 July 2022
PUBLISHED 29 August 2022

CITATION
Chen S, Niu C and Lv W (2022) Multi-omics insights reveal the remodeling of gut mycobiome with *P. gingivalis*. *Front. Cell. Infect. Microbiol.* 12:937725. doi: 10.3389/fcimb.2022.937725

Multi-omics insights reveal the remodeling of gut mycobiome with *P. gingivalis*

Si Chen[1,2†], ChenGuang Niu[3,4†] and WanQi Lv[2*]

[1]Department of Oral Implantology, Shanghai Stomatological Hospital and School of Stomatology, Fudan University, Shanghai, China, [2]Shanghai Key Laboratory of Craniomaxillofacial Development and Diseases, Fudan University, Shanghai, China, [3]Department of Endodontics, Shanghai Ninth People's Hospital, Shanghai Jiao Tong University School of Medicine, College of Stomatology, Shanghai Jiao Tong University, Shanghai, China, [4]National Clinical Research Center for Oral Diseases, National Center for Stomatology, Shanghai Key Laboratory of Stomatology, Shanghai, China

As a keystone periodontal pathogen, *Porphyromonas gingivalis* (*P. gingivalis*) was suggested to be involved in the progression of systemic diseases by altering the intestinal microecology. However, studies concerning gut microbiome have focused entirely on the bacterial component, while the fungal community (gut mycobiome) has been overlooked. In this study, we aimed to characterize the alteration of gut mycobiome profile with *P. gingivalis* administration using mice fecal samples. Metagenomic analysis showed a distinct composition pattern of mycobiome and significant difference of beta diversity between control and the *P. gingivalis* group. Some fungal species were differentially characterized with *P. gingivalis* administration, among which *Pyricularia pennisetigena* and *Alternaria alternata* showed positive correlation with *P. gingivalis*. KEGG functional analyses revealed that three pathways, namely, "pentose and glucuronate interconversions", "metabolic pathways", and "two-component system", were statistically enriched with *P. gingivalis* administration. Moreover, the alteration of gut mycobiome was also closely related with serum metabolites, especially lipid and tryptophan metabolic pathways. Taken together, this study demonstrated the alteration of fungal composition and function with *P. gingivalis* administration for the first time, and investigated the fungi–bacterial interaction and fungi–metabolite interaction preliminarily, providing a whole insight into gut mycobiome remodeling with oral pathobiont through multi-omics analyses.

KEYWORDS

***porphyromonas gingivalis*, gut mycobiome, metagenomics, metabolomics, fungi-bacterial interaction, fungi-metabolite interaction**

Introduction

Periodontitis is the most common oral infection with a wide global prevalence and is characterized by the loss of tooth-supporting tissues (Kinane et al., 2017). The dysbiosis of oral microbial communities has been considered as the main cause of this disease (Curtis et al., 2020). *P. gingivalis*, a Gram-negative anaerobic bacterium, has been strongly implicated as a pathogen in the development of periodontitis. The detection rate of *P. gingivalis* in the periodontitis population ranges from 79% to 90%, which only accounts for 10% to 25% in the healthy population (Igboin et al., 2009). Moreover, the detrimental effects of *P. gingivalis* are not confined to the oral cavity; they can also contribute to systemic disorders, such as type 2 diabetes mellitus, cardiovascular disease, rheumatoid arthritis, and inflammatory bowel disease (IBD) (Hajishengallis and Chavakis, 2021).

The intestine harbors a complex diversity of microorganisms, consisting of bacteria, fungi, viruses, protozoa, and archaea, termed the gut microbiota. Due to the multiple functions revealed in the last decade, the gut microbiota has been recognized as a central regulator of some systemic disorders. Deciphering the mechanisms of host–intestinal microbiota interactions has been defined as a promising therapeutic strategy (Augs et al., 2021). The oral cavity and intestinal tract are linked by a constant flow of ingested food and saliva along the gastrointestinal tract, providing an opportunity for the translocation and colonization of oral microbiota (du Teil Espina et al., 2019; Schmidt et al., 2019). The oral–gut translocation of *P. gingivalis* has been proven in some gastrointestinal diseases, including IBD, colorectal cancer, nonalcoholic fatty liver disease, and other intestinal diseases (Komiya et al., 2019; Park et al., 2021). Recent studies have investigated the alterations of gut microbiota with *P. gingivalis* administration, though most of them are merely concerned about the bacterial microbiota (Nakajima et al., 2015; Ohtsu et al., 2019); the characteristics of other important components of the gut microbiome, such as fungi, remain undefined.

Fungi are an indispensable part of the intestinal microbiome and play a vital role in multiple physiological processes. Shotgun metagenomics suggests that fungi constitute ~0.1% of the human gut microbiome, which is termed the gut mycobiome (Huffnagle and Noverr, 2013). Research using germ-free mice indicated that the gut mycobiome could promote significant alterations in bacterial microbiome ecology and participate in the development of the innate and adaptive immune systems (Van Tilburg et al., 2020). Dysbiosis of the gut mycobiome has been illustrated in some systemic diseases, such as obesity, alcoholic liver disease, IBD, and COVID-19, by regulating the immune system and intestinal permeability (Sokol et al., 2017; Yang et al., 2017; Zuo et al.,2020). Moreover, the interaction between bacteria and fungi shapes the complex ecosystem and maintains intestinal homeostasis. For example, multiomics research based on 1,244 adults implicated that the gut mycobiome is interdependent on bacterial taxonomy and function, in which *Saccharomycetales* spp. interact with gut bacterial diversity to influence insulin resistance. Meanwhile, bacterial function participates in the effects of *Pichia* on blood cholesterol (Shuai et al., 2022).

Despite the emerging evidence of the importance of the gut mycobiome and fungi–bacterial interactions in health and disease, little research has focused on the remodeling of gut mycobiome with *P. gingivalis*. Our previous research demonstrated alterations in the gut bacteriome and serum metabolite profile induced by *P. gingivalis* administration (Dong et al., 2022). In this study, we aimed to demonstrate the alteration of the gut mycobiome with *P. gingivalis* administration, investigate the interaction between the gut mycobiome and bacteriome, especially *P. gingivalis*, and further explore the correlation of the gut mycobiome and serum metabolites preliminarily.

Methods

P. gingivalis cultivation

P. gingivalis strain ATCC33277 was obtained from ATCC, cultured in a brain–heart infusion (BD Bioscience, Franklin Lakes, NJ) consisting of 0.5% yeast extract (BD Bioscience), 10 mg/L hemin (Wako Chemicals, Osaka, Japan), and 1 mg/L 2-methyl-1,4-naphthoquinone (Tokyokasei, Tokyo, Japan) and incubated under anaerobic conditions (80% N_2, 10% CO_2, and 10% H_2) at 37°C. The bacterial suspensions were prepared in phosphate-buffered saline (PBS) without Mg^{2+}/Ca^{2+}, and the optical density (OD) was measured at 600 nm with a standard curve.

Animal experiments

C57BL/6 male mice at 8 weeks of age were obtained from Vital River Laboratory Animal Technology Company (Beijing, China) and group-housed in a specific pathogen-free (SPF) controlled environment with free access to food and water under a strict 12-h light/dark cycle. All animal experiments were approved by the Committee for the Care and Use of Laboratory Animals at Fudan University (Approval number: 202202006S). Sixteen mice were randomly divided into two equal groups. Mice in the *P. gingivalis* group were orally administered with 10^9 CFU *P. gingivalis* twice a week for 6 weeks, and mice in the control group were administered PBS as a control.

Sample collection

All animals were euthanized with carbon dioxide 6 weeks later. The colon contents were collected for metagenomic sequencing at Majorbio Bio-Pharm Technology Co. Ltd. (Shanghai, China). The serum samples were collected for untargeted metabolomics at Majorbio. The detailed information was demonstrated in our previous report (Dong et al., 2022).

Untargeted metabolomics profiling

Untargeted metabolomics profiling of serum samples in the *P. gingivalis* and control groups was performed by Majorbio Bio-Pharm Technology Co. Ltd. (Shanghai, China). Chromatographic separation of the metabolites was performed on a Thermo UHPLC system equipped with an ACQUITY UPLC HSS T3 (100 mm × 2.1 mm i.d., 1.8 μm; Waters, Milford, USA). Mass spectrometry (MS) was performed using a Thermo UHPLC-Q Exactive Mass Spectrometer equipped with an electrospray ionization source operating in either positive or negative ion mode. Data acquisition was performed with the data-dependent acquisition mode. The detection was carried out over a mass range of 70–1,050 m/z. Raw data were imported into Progenesis QI 2.3 for peak detection and alignment. The preprocessing results contained the m/z values and peak intensity. The mass spectra of these metabolic features were identified using accurate masses. And the metabolites were searched and identified, and the main database was the HMDB (http://www.hmdb.ca/), Metlin (https://metlin.scripps.edu/) and Majorbio Database. The variable importance of the projection (VIP) score generated from orthogonal partial least squares discriminate analysis was used to determine the most differentiated metabolites. Metabolites with VIP ≥ 1.0 and *p*-value ≤ 0.05 were defined as significantly changed metabolites. A multivariate statistical analysis was performed using the R package ropls version 1.6.2.

Metagenome taxonomic classification of fungal genomic reads

The DNA extract was fragmented to an average size of approximately 300 bp using Covaris M220 (Gene Company Limited, China) for paired-end library construction. Paired-end sequencing was performed on an Illumina NovaSeq/HiSeq Xten (Illumina Inc., San Diego, CA, USA) at Majorbio Bio-Pharm Technology Co., Ltd. (Shanghai, China) using NovaSeq Reagent Kits/HiSeq X Reagent Kits according to the manufacturer's instructions (www.illumina.com). Reads were aligned to the mouse genome by BWA (http://bio-bwa.sourceforge.net), and any hits associated with the reads and their mates were removed. All predicted genes with 95% sequence identity (90% coverage) were clustered using CD-HIT (http://www.bioinformatics.org/cd-hit/), and the longest sequences from each cluster were selected as representative sequences to construct a nonredundant gene catalog. After quality control, reads were mapped to the representative sequences with 95% identity using SOAPaligner (http://soap.genomics.org.cn/), and the gene abundance in each sample was evaluated. Read counts assigned to the fungal kingdom were then extracted for analysis.

Species and functional annotation

Representative sequences of the nonredundant gene catalog were aligned to the NCBI NR database with an e-value cutoff of 1e-5 using BLASTP (Version 2.2.28+, http://blast.ncbi.nlm.nih.gov/Blast.cgi) for taxonomic annotations. The Kyoto Encyclopedia of Genes and Genomes (KEGG) annotation was conducted using BLASTP (Version 2.2.28+) against the Kyoto Encyclopedia of Genes and Genomes database (http://www.genome.jp/keeg/) with an e-value cutoff of 1e-5.

Supervised integration for interkingdom interactions

To identify the associations between the gut mycobiome and bacteriome or metabolome that were altered in the control and *P. gingivalis* groups, multi-omics datasets were integrated using the DIABLO framework from the mixOmics package in a supervised analysis. Standing for Data Integration Analysis for Biomarker discovery using Latent variable approaches for Omics studies, DIABLO is a novel multiomics framework for the integration of multiple datasets in a supervised analysis (Kong et al., 2022). A signature of 10 bacterial and 10 fungal species was selected for the integration of gut mycobiome and gut bacteriome. For the analysis of gut mycobiome and serum metabolome, the top 10 metabolites ranked with VIP (variable important in projection) value and the top 10 fungi by abundance were included. A design matrix of 0.1 was used to place higher importance on the discrimination of genotypes rather than maximizing the correlation between the two datasets. A signature of 10 bacterial and 10 fungal species was selected for the model. A correlation cutoff of 0.5 was set for the network visualization using Gephi.

Statistical analysis

Alpha diversity was calculated using the Shannon index. The equality of variance was confirmed with Levene's test. Normality

of the data was evaluated using the Shapiro–Wilk test. The significance of genotype was assessed with the Student's *t*-test.

Beta diversity was measured using the principal coordinate analysis (PCoA) with Bray–Curtis distance used to calculate the distance metric. Analysis of similarities (ANOSIM) test was used for the statistical analysis.

Linear discriminant analysis effect size (LEfSe) was used to identify the significant differential fungal biomarkers with a linear discriminant analysis (LDA) score greater than 3.5. The Kruskal–Wallis test was used to detect significant differences in abundance, and the Wilcoxon rank-sum test was used for *post-hoc* comparison. A p-value < 0.05 was considered significant.

For KEGG analysis, Wilcoxon rank-sum test was used for the differential pathways and KEGG orthology (KO), and FDR (false discovery rate) was performed on p-values. Two-tailed p < 0.05 was considered statistically significant. Correlation analysis was constructed to investigate the interaction between fungal species and KEGG pathways, and Spearman coefficient $|r| > 0.5$ and p-value < 0.05 are shown.

To investigate correlations between fungal taxa and Porphyromonadaceae or *P. gingivalis*, correlation networks with Spearman coefficient $|r| > 0.6$ and p-value < 0.05 were set. A heatmap was used to demonstrate the correlations between the 39 differential metabolites and the top 20 species in abundance. The Spearman coefficients represented by R values (range from −0.8 to 0.8) are shown in different colors. A p-value < 0.05 is marked with *, and a p-value < 0.01 is marked with **.

Results

Alterations in gut mycobiome composition with *P. gingivalis* administration

A total of 10,392 microorganisms were detected according to the metagenomic sequencing, among which 0.52% (54/10,392) of the reads aligned to fungal genomes. The alpha diversity analysis measured by the Shannon index demonstrated no significant differences in the richness of fungal communities with *P. gingivalis* administration (t test, p = 0.285, Figure 1A).

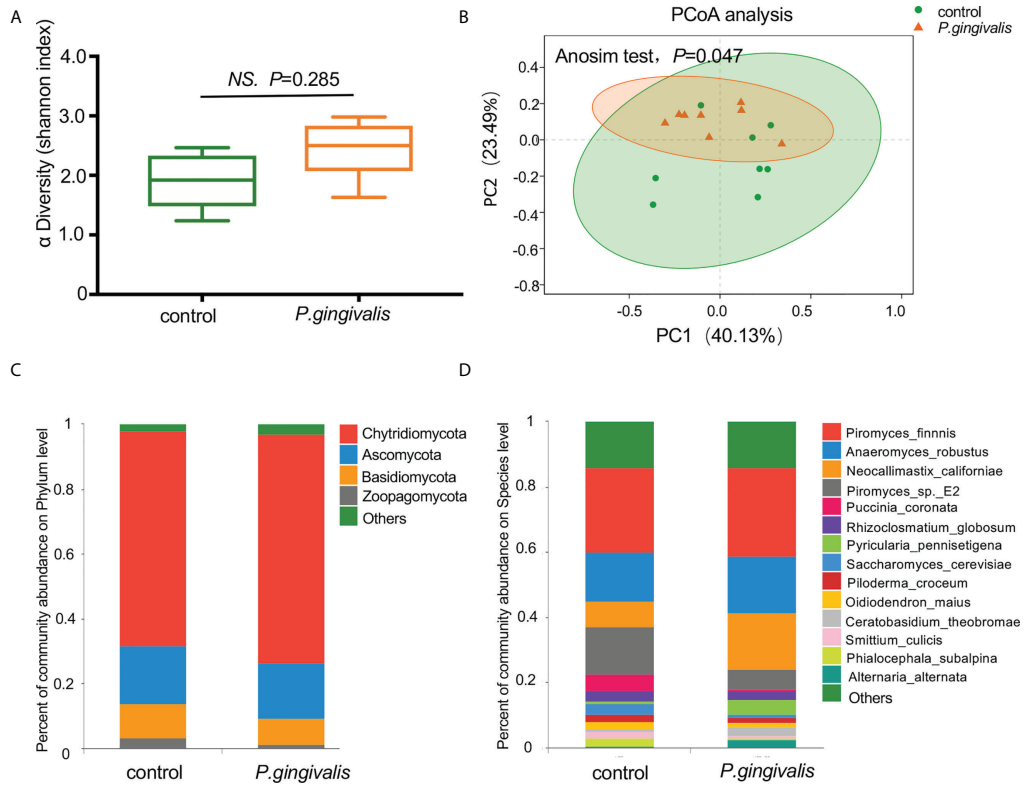

FIGURE 1
Diversity and composition of gut mycobiome with *P. gingivalis* administration in C57BL/6 mice. **(A)** Alpha diversity of fecal mycobiome measured by Shannon index between *P. gingivalis* and control mice (t test, p = 0.285). **(B)** Principal coordinate analysis (PCoA) plots of the gut mycobiome by Bray–Curtis distance between *P. gingivalis* and control mice (ANOSIM test, p = 0.047). **(C)** Mean relative abundances of gut fungi at the phylum level. **(D)** Mean relative abundances of gut fungi at the species level.

The PCoA results measured by Bray–Curtis distance indicated a significant difference in the fungal diversity between the *P. gingivalis* and control groups (ANOSIM test, p = 0.047, Figure 1B). The composition of the gut mycobiome at different levels was then characterized. Chytridiomycota, Ascomycota, Basidiomycota, and Zoopagomycota constituted the main dominant phyla in *P. gingivalis*-treated mice, with mean relative abundances of 70.6%, 17.2%, 7.9%, and 1.4%, respectively. Mice in the control group demonstrated a different gut fungal pattern, consisting of 66.5% of Chytridiomycota, 17.7% of Ascomycota, 10.6% of Basidiomycota, and 3.2% of Zoopagomycota (Figure 1C). In particular, 54 kinds of fungi were detected at the species level (Table S1). *Piromyces finnis* was the most abundant species in both the *P. gingivalis* and control groups, with proportions of 27.1% and 25.9%, respectively, followed by *Anaeromyces robustus* (17.7%) and *Neocallimastix californiae* (17.1%) in the *P. gingivalis* group and *A. robustus* (15.1%) and *Piromyces_sp._E2* (14.7%) in the control group (Figure 1D).

Identification of differential gut fungi with *P. gingivalis* administration

To further identify the gut fungi with significant differences between the *P. gingivalis* and control groups, LEfSe was introduced. The differential taxa at various levels (phylum, class, order, family, genus, and species) based on an LDA score greater than 3.5 were identified (Figure 2A). Specifically, at the species level, *Valsa malicola* was abundant in the control group, while eight other species, namely, *N. californiae*, *Pyricularia pennisetigena*, *Alterbaria alternata*, *Botrytis cinerea*, *Candida glabrata*, *Aspergillus lentulus*, *Ceratobasidium theobromae*, and *Amphiamblys_sp_WSBS2006*, were abundant in the *P. gingivalis* group (Figure 2B). We further characterized the species with significant importance, and 20 of the top important species were listed with *P. gingivalis* administration according to the random forest algorithm (Figure S1). The most important species was *P. pennisetigena*, followed by *V. malicola* and *Amphiamblys_sp_WSBS2006*.

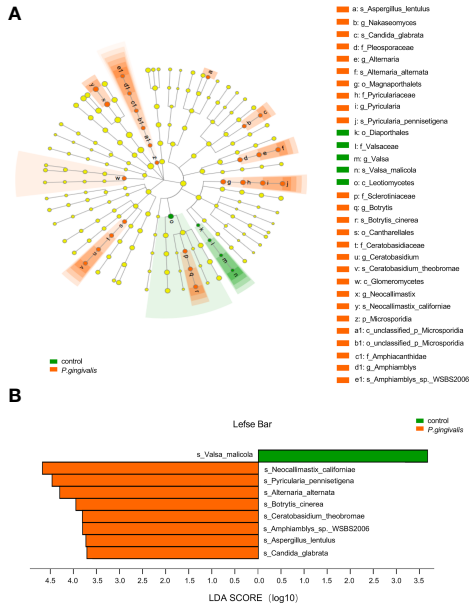

FIGURE 2
Differential gut fungi based on LEfSe between *P. gingivalis* and control groups. The differential fungal taxa are demonstrated based on an LDA score greater than 3.5 and marked by lowercase letters. **(A)** Cladogram of gut fungi at different levels. Each small circle at different taxonomic levels represents a taxon at that level, and the diameter of the circle is proportional to the relative abundance. Node in different color represents different group, and node in yellow represents no significant difference. **(B)** Significant altered gut fungi at the species level in the *P. gingivalis* and control groups. $p < 0.05$ with Wilcoxon rank-sum test followed by Kruskal–Wallis test.

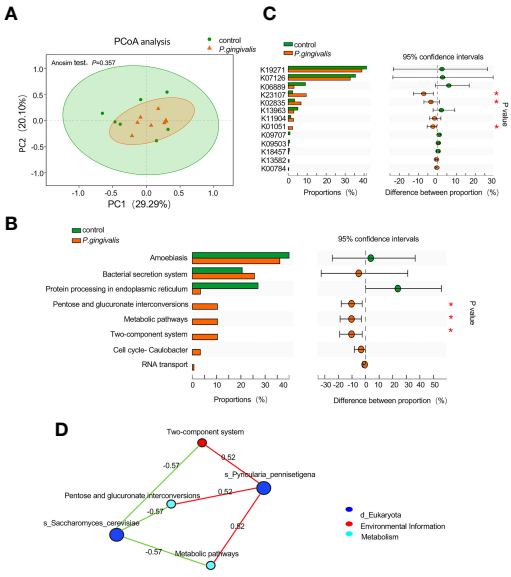

FIGURE 3
Functional alteration of gut mycobiome with *P. gingivalis* administration in C57BL/6 mice. **(A)** Principal coordinate analysis (PCoA) plots of the functional alterations by Bray–Curtis distance between *P. gingivalis* and control mice (ANOSIM test, p = 0.357). **(B)** Altered pathways in response to *P. gingivalis* administration based on the proportion of the abundance of each KEGG pathway. The 95% confidence intervals are presented with differences in the abundance of each pathway (Wilcoxon rank-sum test, *$p < 0.05$). **(C)** Altered KOs in response to *P. gingivalis* administration based on the proportion of KOs. The 95% confidence intervals are presented with differences in the KO abundance (Wilcoxon rank-sum test, *$p < 0.05$). **(D)** Correlation network analysis between functional alterations and differential fungal species. Spearman correlation of >0.5 or <– 0.5 was represented.

Alterations in gut mycobiome function with *P. gingivalis* administration

To investigate the potential biological function arising from alterations of the fungal community, the fungal genes were annotated to KO. The PCoA results based on Bray–Curtis distance showed no remarkable difference in the microbial function between the *P. gingivalis* and control groups (ANOSIM test, $p = 0.357$, Figure 3A). However, "pentose and glucuronate interconversions", "metabolic pathways" and "two-component system" were statistically enriched with *P. gingivalis* administration (Wilcoxon rank-sum test, $p < 0.05$, Figure 3B). K23107, encoding 1-deoxy-D-xylulose 5-phosphate synthase, K02835, encoding peptide chain release factor 1, and K01051, encoding pectinesterase, were increased with *P. gingivalis* administration (Wilcoxon rank-sum test, $p < 0.05$, Figure 3C). Correlation network analysis between significant functional alterations and fungal species showed that *Pyriculari pennisetigena* had positive correlations with "metabolic pathways", "pentose and glucuronate interconversions", and "two-component system" ($r = 0.52$), while *Saccharomyces cerevisiae* demonstrated a negative correlation with the functional alteration ($r = -0.57$) (Figure 3D).

Interactions between the gut mycobiome and bacterial microbiome

To investigate the relationship between mycobiome and bacteriome in the gut, we performed correlation analysis with the highest 10 species in abundance from the bacterial and fungal communities using DIABLO. With a design matrix of 0.1, which was set to maximize the discrimination between the two genotypes, the correlation between the gut fungal dataset and the gut bacterial dataset was still strong ($r = 0.86$) (Figure 4A). Components involved in the analysis were clustered as shown in

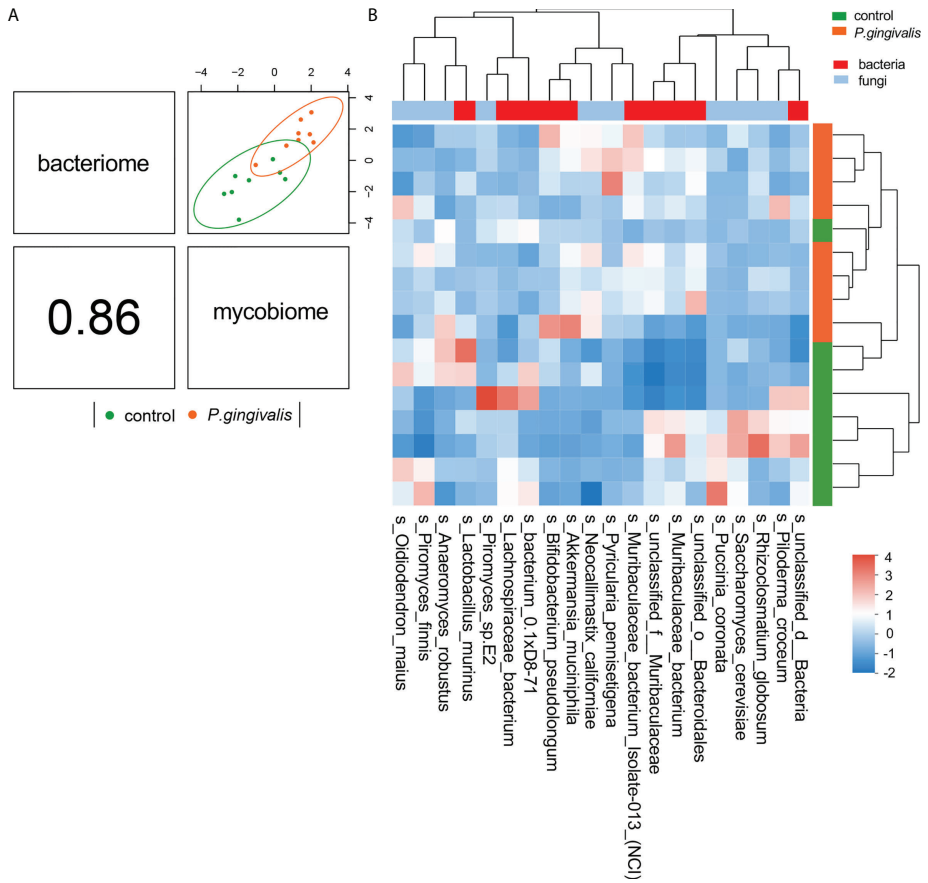

FIGURE 4
Integration of gut bacteriome and mycobiome. **(A)** The gut bacteriomes and mycobiomes were highly concordant with each other ($r = 0.86$) and revealed distinct clustering of samples from control and *P. gingivalis* mice. DIABLO was used for integration of gut bacteriome and mycobiome compositions. **(B)** Clustered heatmap of the abundances of bacterial and fungal species that covary with each other as shown in the column.

Figure 4B. Additionally, correlation analysis was conducted between the abundance of *P. gingivalis* and the fungal mycobiome, and the Spearman coefficient was used to evaluate the correlation. At the family level, Porphyromonadaceae demonstrated a positive correlation with many fungal families, among which Pleosporaceae, Sclerotiniaceae, Pyriculariaceae, and Ceratobasidiaceae all showed positive correlations (r > 0.6) (Figure S2); these fungi are all recognized as pathogens and play important roles in the occurrence and progression of systematic diseases (Mahmoud et al., 2012; Klaubauf et al., 2014; Teifoori et al., 2018; Feng et al., 2021). In particular, two fungal species, *Alternaria alternata* and *P. pennisetigena*, possessed strong positive correlations with *P. gingivalis* (r = 0.82 and r = 0.76, respectively), while *Phialocephala subalpina* possessed a negative correlation (r = −0.71) (Figure 5).

Correlation between the gut mycobiome and the serum metabolome

Microbial metabolites are key factors in host–microbiota crosstalk. Our previous analysis confirmed 39 metabolism-related metabolites with *P. gingivalis* administration with untargeted metabolomics profiling (Dong et al., 2022). To further identify correlations between the fungi species and metabolic features that differed between the two groups, we integrated the two datasets using supervised analysis, and a strong correlation was concluded (r = 0.83) (Figure 6A). The top 10 metabolites by VIP value and the top 10 fungi by abundance were clustered for the analysis (Figure 6B). Correlations between the significantly altered metabolites and the gut mycobiome were further investigated, and R values of Pearson correlation coefficients and P values of significance were used to evaluate the correlations. A total of 20 gut fungi were identified with significant correlations. Notably, *Amphiamblys*, *P. pennisetigena*, and *V. malicola* were significantly correlated with most metabolites and were the top three most important species in the random forest ranking. As a more abundant species with *P. gingivalis* administration, *P. pennisetigena* was positively correlated with lipid metabolism-related metabolites, such as LysoPC, and negatively correlated with indole-3-acetamide, 5-hydroxy-tryptophan, and indoleacetaldehyde (Figure S3). All three metabolites are key actors in tryptophan metabolism, suggesting an interpretation of the gut mycobiome and functional synergism.

Discussion

The current study demonstrates the first evidence of gut fungal dysbiosis with *P. gingivalis* administration. *P. gingivalis* alters the gut fungal composition, which correlates with metabolic pathways and serum metabolites, indicating an interactive relationship between the gut bacteriome and the

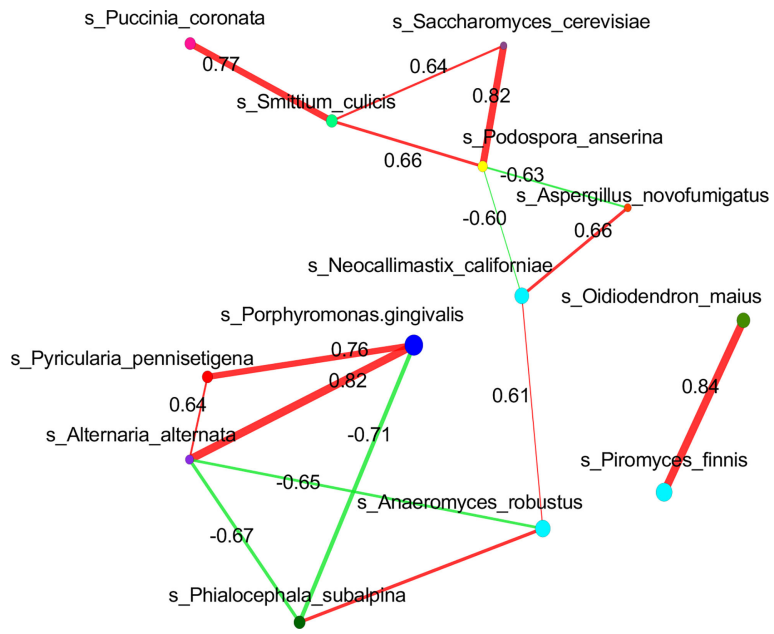

FIGURE 5
Correlation of *P. gingivalis* and gut mycobiome at the species level. Correlation network analysis revealed strong positive and negative correlation associations between *P. gingivalis* and fungal species taxa. Spearman correlation of >0.6 or <−0.6 between fungal species was represented.

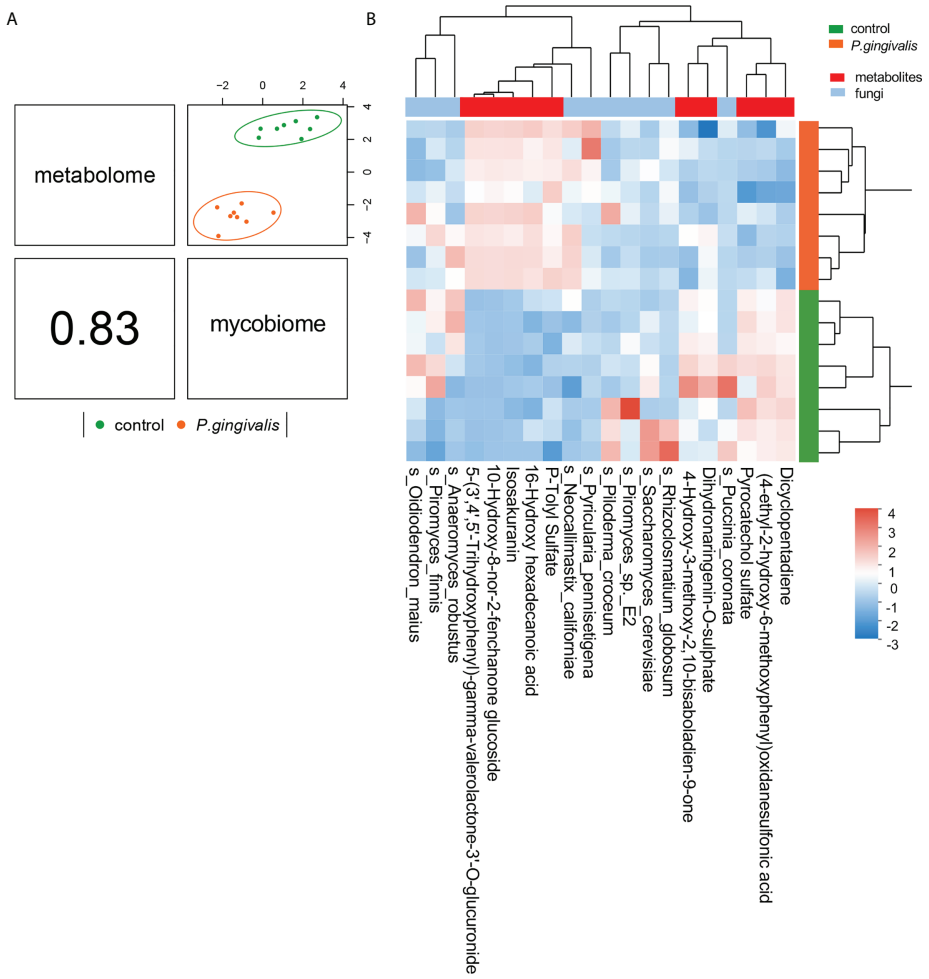

FIGURE 6
Integration of serum metabolome and gut mycobiome. **(A)** The serum metabolome and gut mycobiome were highly concordant with each other (r = 0.83) and revealed distinct clustering of samples from control and *P. gingivalis* mice. DIABLO was used for integration of serum metabolome and gut mycobiome compositions. **(B)** Clustered heatmap of the abundances of serum metabolites and fungal species that covary with each other as shown in the column.

gut mycobiome. Eight species were identified in the fecal samples of *P. gingivalis*-treated mice, among which *P. pennisetigena* ranked first due to its discrepant contribution and correlation with metabolic pathways.

The gut mycobiome accounts for less than 1% of the entire microbiome and has long been considered to be less important than the bacteriome. However, recent studies have confirmed the gut mycobiome as an integral part of the gut ecosystem (Hillman et al., 2017). As a periodontopathic bacterium, *P. gingivalis* plays a key role in the pathogenesis of periodontitis-associated comorbidities. In this study, a remarkable difference was observed in the fungal composition with *P. gingivalis* administration. In particular, *N. californiae*, *P. pennisetigena*, *A. alternata*, *B. cinerea*, *C. glabrata*, *A. lentulus*, and *C. theobromae* were significantly enriched in *P. gingivalis*-treated mice, and most of these fungi have been reported as pathogens in previous research. For example, *A. alternata* is a dematiaceous fungus and can cause cutaneous, even fatal, infection in humans (Sinha et al., 2021). *C. glabrata* can suppress immune responses and adapt to changing environmental conditions through a distinct set of virulence attributes (Bolotin-Fukuhara and Fairhead, 2014; Rasheed et al., 2020). *A. lentulus* is a drug-resistant species and has been identified as a main cause of azole-breakthrough disease (Nematollahi et al., 2021). *C. theobromae* is reported to be the causal agent of vascular streak dieback of cacao (Ali et al., 2019). *N. californiae* has been regarded as a member of the anaerobic gut fungi whose character has not been extensively explored but showed a positive correlation with total volatile fatty acids, including acetate, butyrate, and propionate (Wu et al., 2021).

Bacteria and fungi are in a dynamic balance. Some studies have demonstrated that disturbance of bacterial communities using long-term antibiotic treatments is often associated with fungal overgrowth and is ultimately linked to infectious diseases (Mason et al., 2012; Dollive et al., 2013). Sovran et al. revealed that the detrimental effects of *Candida albicans* and the beneficial effects of *Saccharomyces boulardii* in colitis depend on a specific bacterial environment of the Enterobacteriaceae population within the gut microbiota (Sovran et al., 2018). It has also been shown that commensal anaerobic bacteria—specifically Clostridial, Firmicutes, and Bacteroidetes—are critical in promoting *C. albicans* colonization resistance in mice by activating gut mucosal immune effectors (Fan et al., 2015). In our study, we found that administration of *P. gingivalis* not only changed the composition of intestinal bacteria but also altered the composition and function of intestinal fungi and further showed strong correlations with some gut fungi, illustrating the interaction between bacteria and fungi in health and disease.

Although "pentose and glucuronate interconversions", "metabolic pathways", and "two-component system" were statistically enriched with *P. gingivalis* administration though fungal KEGG annotations, the beta diversity of gut fungal function demonstrated no significant difference between the *P. gingivalis* and control groups, suggesting the potential role of the gut bacteriome. However, co-abundance network analysis revealed the mutual relationships between gut fungi and bacteria. In this study, *A. alternata* and *P. pennisetigena* possessed strong positive associations with *P. gingivalis*, while *P. subalpina* possessed a negative association. Broad associations between the gut mycobiome and the gut bacteriome and intestinal metabolites have been illustrated in recent studies (Shah et al., 2021; Shuai et al., 2022). Our previous research concerning the function of gut bacteria revealed that the "tryptophan metabolism pathway" was significantly altered with *P. gingivalis* administration and that indole and its derivatives were downregulated (Dong et al., 2022). Here, *P. pennisetigena* was shown to positively correlate with lipid metabolism-related metabolites, such as LysoPC, and negatively correlate with indole-3-acetamide, 5-hydroxy-tryptophan, and indoleacetaldehyde, which might be a potential reason for its correlation with the metabolic pathway. Acting as a pathogen for many plants, *P. pennisetigena* was found to be enriched in tuberculosis patients with bacteriologically confirmed infection compared with the negative group (Ding et al., 2021). In conclusion, it is reasonable to speculate that the systemic diseases associated with *P. gingivalis* or periodontitis may be related to the intestinal fungal alterations caused by *P. gingivalis*.

There are some limitations in our study. First, due to the technical difficulty of fungal culture, the correlations between gut fungi and the bacteriome and serum metabolites could not be validated *in vitro*. Moreover, we failed to relate these correlations between *P. gingivalis* and fungi to the phenotype. Many of the fungal species reported are of environmental origin, and their biological relevance in mammals remains unknown. Despite these findings, our study illustrated the remodeling of the gut mycobiome with *P. gingivalis* and further suggested the potential interrelationship between the gut mycobiome and metabolic functions and metabolites.

Data availability statement

The datasets presented in this study can be found in online repositories. The names of the repository/repositories and accession number(s) can be found below: https://www.ncbi.nlm.nih.gov/sra/, PRJNA811648. https://www.ebi.ac.uk/metabolights/, MTBLS4106".

Ethics statement

This study was reviewed and approved by All animal experiments were approved by the Committee for the Care and Use of Laboratory Animals at Fudan University (Approval number: 2022020065).

Author contributions

WL and SC designed the study. SC and CN conducted experiments. WL analyzed the data. WL and SC prepared and revised the manuscript. All the authors contributed to the article and approved the submitted version.

Funding

This study was financially supported by grants from the National Natural Science Foundation of China (82001056) and Shanghai Sailing Program (21YF1439900).

Conflict of interest

The authors declare that the research was conducted in the absence of any commercial or financial relationships that could be construed as a potential conflict of interest.

Publisher's note

All claims expressed in this article are solely those of the authors and do not necessarily represent those of their affiliated

organizations, or those of the publisher, the editors and the reviewers. Any product that may be evaluated in this article, or claim that may be made by its manufacturer, is not guaranteed or endorsed by the publisher.

Supplementary material

The Supplementary Material for this article can be found online at: https://www.frontiersin.org/articles/10.3389/fcimb.2022.937725/full#supplementary-material

SUPPLEMENTARY FIGURE 1
Ranking of fungi species importance with *P. gingivalis* administration. Random forests algorithm was used to rank the importance of fungal species. The abscissa (Mean Decrease in Accuracy) is a measure of species importance, and the larger the value is, the more important the species is. The ordinate is the species in order of importance.

SUPPLEMENTARY FIGURE 2
Correlation of *Porphyromonadaceae and* gut mycobiome at the family level. Correlation network analysis revealed strong positive- and negative-correlation associations between *Porphyromonadaceae* and fungal family taxa. Spearman correlation of > 0.6 or < - 0.6 between fungal family was represented.

SUPPLEMENTARY FIGURE 3
Association of serum metabolites and gut mycobiome. Heatmap of gut mycobiome and serum metabolites with Spearman correlation. Color denotes positive (red) and negative (blue) correlation values. *$P < 0.05$, **$P < 0.01$, ***$P < 0.001$.

SUPPLEMENTARY TABLE 1
Composition of gut fungi at species level both in *P. gingivalis* and control groups.

References

Agus, A., Clement, K., and Sokol, H. (2021). Gut microbiota-derived metabolites as central regulators in metabolic disorder. *Gut.* 70 (6), 1174–1182. doi: 10.1136/gutjnl-2020-323071

Ali, S. S., Asman, A., Shao, J., Firmansyah, A. P., Susilo, A. W., Rosmana, A., et al. (2019). Draft genome sequence of fastidious pathogen ceratobasidium theobromae, which causes vascular-streak dieback in theobroma cacao. *Fungal. Biol. Biotechnol.* 6, 14. doi: 10.1186/s40694-019-0077-6

Bolotin-Fukuhara, M., and Fairhead, C. (2014). Candida glabrata: A deadly companion? *Yeast.* 31 (8), 279–288. doi: 10.1002/yea.3019

Curtis, M. A., Diaz, P. I., and Van Dyke, T. E. (2020). The role of the microbiota in periodontal disease. *Periodontol 2000.* 83 (1), 12–25. doi: 10.1111/prd.12296

Ding, L., Liu, Y., Wu, X., Wu, M., Luo, X., Ouyang, H., et al. (2021). Pathogen metagenomics reveals distinct lung microbiota signatures between bacteriologically confirmed and negative tuberculosis patients. *Front. Cell. Infect. Microbiol.* 11. doi: 10.3389/fcimb.2021.708827

Dollive, S., Chen, Y. Y., Grunberg, S., Bittinger, K., Hoffmann, C., Vandivier, L., et al. (2013). Fungi of the murine gut: Episodic variation and proliferation during antibiotic treatment. *PLoS One* 8 (8), e71806. doi: 10.1371/journal.pone.0071806

Dong, Z. J., Lv, W. Q., Zhang, C. Y., and Chen, S. (2022). Correlation analysis of gut microbiota and serum metabolome with porphyromonas gingivalis-induced metabolic disorders. *Front. Cell. Infect. Microbiol.* 12. doi: 10.3389/fcimb.2022.858902

du Teil Espina, M., Gabarrini, G., Harmsen, H. J. M., Westra, J., van Winkelhoff, A. J., and van Dijl, J. M. (2019). Talk to your gut: The oral-gut microbiome axis and its immunomodulatory role in the etiology of rheumatoid arthritis. *FEMS. Microbiol. Rev.* 43 (1), 1–18. doi: 10.1093/femsre/fuy035

Fan, D., Coughlin, L. A., Neubauer, M. M., Kim, J., Kim, M. S., Zhan, X., et al. (2015). Activation of HIF-1alpha and LL-37 by commensal bacteria inhibits candida albicans colonization. *Nat. Med.* 21 (7), 808–814. doi: 10.1038/nm.3871

Feng, C., Feng, J., Wang, Z., Pedersen, C., Wang, X., Saleem, H., et al. (2021). Identification of the viral determinant of hypovirulence and host range in sclerotiniaceae of a genomovirus reconstructed from the plant metagenome. *J. Virol.* 95 (17), e0026421. doi: 10.1128/JVI.00264-21

Hajishengallis, G., and Chavakis, T. (2021). Local and systemic mechanisms linking periodontal disease and inflammatory comorbidities. *Nat. Rev. Immunol.* 21 (7), 426–440. doi: 10.1038/s41577-020-00488-6

Hillman, E. T., Lu, H., Yao, T., and Nakatsu, C. H. (2017). Microbial ecology along the gastrointestinal tract. *Microbes Environ.* 32 (4), 300–313. doi: 10.1264/jsme2.ME17017

Huffnagle, G. B., and Noverr, M. C. (2013). The emerging world of the fungal microbiome. *Trends. Microbiol.* 21 (7), 334–341. doi: 10.1016/j.tim.2013.04.002

Igboin, C. O., Griffen, A. L., and Leys, E. J. (2018). Porphyromonas gingivalis strain diversity. *J Clin Microbiol* 47 (10), 3073–3081. doi: 10.1128/JCM.00569-09

Kinane, D. F., Stathopoulou, P. G., and Papapanou, P. N. (2017). Periodontal diseases. *Nat. Rev. Dis. Primers.* 3, 17038. doi: 10.1038/nrdp.2017.38

Klaubauf, S., Tharreau, D., Fournier, E., Groenewald, J. Z., Crous, P. W., de Vries, R. P., et al. (2014). Resolving the polyphyletic nature of pyricularia (Pyriculariaceae). *Stud. Mycol.* 79, 85–120. doi: 10.1016/j.simyco.2014.09.004

Komiya, Y., Shimomura, Y., Higurashi, T., Sugi, Y., Arimoto, J., Umezawa, S., et al. (2019). Patients with colorectal cancer have identical strains of fusobacterium nucleatum in their colorectal cancer and oral cavity. *Gut.* 68 (7), 1335–1337. doi: 10.1136/gutjnl-2018-316661

Kong, G., Le Cao, K. A., and Hannan, A. J. (2022). Alterations in the gut fungal community in a mouse model of huntington's disease. *Microbiol. Spectr.* 10 (2), e0219221. doi: 10.1128/spectrum.02192-21

Mahmoud, M. A., Al-Sohaibani, S. A., Abdelbacki, A. M. M., Al-Othman, M. R., Abd El-Aziz, A. R. M., Kasem, K. K., et al. (2012). Molecular characterization of the pathogenic plant fungus rhizoctonia solani (Ceratobasidiaceae) isolated from Egypt based on protein and PCR-RAPD profiles. *Genet. Mol. Res.* 11 (4), 3585–3600. doi: 10.4238/2012

Mason, K. L., Erb Downward, J. R., Mason, K. D., Falkowski, N. R., Eaton, K. A., Kao, J. Y., et al. (2012). Candida albicans and bacterial microbiota interactions in the cecum during recolonization following broad-spectrum antibiotic therapy. *Infect. Immun.* 80 (10), 3371–3380. doi: 10.1128/IAI.00449-12

Nakajima, M., Arimatsu, K., Kato, T., Matsuda, Y., Minagawa, T., Takahashi, N., et al. (2015). Oral administration of p. gingivalis induces dysbiosis of gut microbiota and impaired barrier function leading to dissemination of enterobacteria to the liver. *PLoS. One* 10 (7), e0134234. doi: 10.1371/journal.pone.0134234

Nematollahi, S., Permpalung, N., Zhang, S. X., Morales, M., and Marr, K. A. (2021). Aspergillus lentulus: An under-recognized cause of antifungal drug-resistant aspergillosis. *Open Forum. Infect. Dis.* 8 (8), ofab392. doi: 10.1093/ofid/ofab392

Ohtsu, A., Takeuchi, Y., Katagiri, S., Suda, W., Maekawa, S., Shiba, T., et al. (2019). Influence of porphyromonas gingivalis in gut microbiota of streptozotocin-induced diabetic mice. *Oral. Dis.* 25 (3), 868–880. doi: 10.1111/odi.13044

Park, S. Y., Hwang, B. O., Lim, M., Ok, S. H., Lee, S. K., Chun, K. S., et al. (2021). Oral-gut microbiome axis in gastrointestinal disease and cancer. *Cancers (Basel).* 13 (9), 2124. doi: 10.3390/cancers13092124

Rasheed, M., Battu, A., and Kaur, R. (2020). Host-pathogen interaction in candida glabrata infection: Current knowledge and implications for antifungal therapy. *Expert. Rev. Anti Infect. Ther.* 18 (11), 1093–1103. doi: 10.1080/14787210.2020.1792773

Schmidt, T. S., Hayward, M. R., Coelho, L. P., Li, S. S., Costea, P. I., Voigt, A. Y., et al. (2019). Extensive transmission of microbes along the gastrointestinal tract. *Elife.* 8, e42693. doi: 10.7554/eLife.42693

Shah, S., Locca, A., Dorsett, Y., Cantoni, C., Ghezzi, L., Lin, Q., et al. (2021). Alterations of the gut mycobiome in patients with MS. *EBioMedicine.* 71, 103557. doi: 10.1016/j.ebiom.2021.103557

Shuai, M., Fu, Y., Zhong, H. L., Gou, W., Jiang, Z., Liang, Y., et al. (2022). Mapping the human gut mycobiome in middle-aged and elderly adults: multiomics

insights and implications for host metabolic health. *Gut*. 71 (9), 1812–1820. doi: 10.1136/gutjnl-2021-326298. Gutjnl-2021-326298.

Sinha, P., Singh, M., Sagar, T., Jain, S., and Bains, L. (2021). Cytological clues to alternaria alternata. *Diagn. Cytopathol.* 49 (7), E269–E272. doi: 10.1002/dc.24702

Sokol, H., Leducq, V., Aschard, H., Pham, H. P., Jegou, S., Landman, C., et al. (2017). Fungal microbiota dysbiosis in IBD. *Gut.* 66 (6), 1039–1048. doi: 10.1136/gutjnl-2015-310746

Sovran, B., Planchais, J., Jegou, S., Straube, M., Lamas, B., Natividad, J. M., et al. (2018). Enterobacteriaceae are essential for the modulation of colitis severity by fungi. *Microbiome.* 6 (1), 152. doi: 10.1186/s40168-018-0538-9

Teifoori, F., Shams-Ghahfarokhi, M., Razzaghi-Abyaneh, M., and Martinez, J. (2018). Gene profiling and expression of major allergen alt a 1 in alternaria alternata and related members of the pleosporaceae family. *Rev. Iberoam. Micol.* 36 (2), 66–71. doi: 10.1016/j.riam.2018.01.006

Van Tilburg, B. E., Pettersen, V. K., Gutierrez, M. W., Laforest-Lapointe, I., Jendzjowsky, N. G., Cavin, J. B., et al. (2020). Intestinal fungi are causally implicated in microbiome assembly and immune development in mice. *Nat. Commun.* 11 (1), 2577. doi: 10.1038/s41467-020-16431-1

Wu, X., Huang, S., Huang, J., Peng, P., Liu, Y., Han, B., et al. (2021). Identification of the potential role of the rumen microbiome in milk protein and fat synthesis in dairy cows using metagenomic sequencing. *Anim. (Basel).* 11 (5), 1247. doi: 10.3390/ani11051247

Yang, A. M., Inamine, T., Hochrath, K., Chen, P., Wang, L., Llorente, C., et al. (2017). Intestinal fungi contribute to development of alcoholic liver disease. *J. Clin. Invest.* 127 (7), 2829–2841. doi: 10.1172/JCI90562

Zuo, T., Zhan, H., Zhang, F., Liu, Q., Tso, E. Y. K., Lui, G. C. Y., et al. (2020). Alterations in fecal fungal microbiome of patients with COVID-19 during time of hospitalization until discharge. *Gastroenterology* 159 (4), 1302–1310.e5. doi: 10.1053/j.gastro.2020.06.048

frontiers | Frontiers in Cellular and Infection Microbiology

TYPE Review
PUBLISHED 02 September 2022
DOI 10.3389/fcimb.2022.998313

OPEN ACCESS

EDITED BY
Zuomin Wang,
Capital Medical University, China

REVIEWED BY
Fuhua Yan,
Nanjing University, China
Ashu Sharma,
University at Buffalo, United States

*CORRESPONDENCE
Xiangying Ouyang
kqouyangxy@bjmu.edu.cn
Jiang Lin
kelvinperio@163.com

SPECIALTY SECTION
This article was submitted to Extra-intestinal Microbiome, a section of the journal Frontiers in Cellular and Infection Microbiology

RECEIVED 19 July 2022
ACCEPTED 15 August 2022
PUBLISHED 02 September 2022

CITATION
Li Q, Ouyang X and Lin J (2022) The impact of periodontitis on vascular endothelial dysfunction.
Front. Cell. Infect. Microbiol. 12:998313.
doi: 10.3389/fcimb.2022.998313

The impact of periodontitis on vascular endothelial dysfunction

Qian Li[1], Xiangying Ouyang[2]* and Jiang Lin[1]*

[1]Department of Stomatology, Beijing Tongren Hospital, Capital Medical University, Beijing, China, [2]Department of Periodontology, Peking University School and Hospital of Stomatology, Beijing, China

Periodontitis, an oral inflammatory disease, originates from periodontal microbiota dysbiosis which is associated with the dysregulation of host immunoinflammatory response. This chronic infection is not only harmful to oral health but is also a risk factor for the onset and progress of various vascular diseases, such as hypertension, atherosclerosis, and coronary arterial disease. Vascular endothelial dysfunction is the initial key pathological feature of vascular diseases. Clarifying the association between periodontitis and vascular endothelial dysfunction is undoubtedly a key breakthrough for understanding the potential relationship between periodontitis and vascular diseases. However, there is currently a lack of an updated review of their relationship. Therefore, we aim to focus on the implications of periodontitis in vascular endothelial dysfunction in this review.

KEYWORDS

periodontitis, *Porphyromonas gingivalis*, vascular endothelial cells, vascular endothelial dysfunction, vascular disease

Introduction

Periodontitis is a common inflammatory oral disease associated with periodontal microbiota dysbiosis and host immune response dysregulation (Papapanou et al., 2018). Periodontal dysbiosis signifies the shift from a symbiotic to a dysbiotic microbial community, resulting in the transition from a periodontal healthy state to inflammation (Slazhneva et al., 2020). Moreover, host immunological and genetic mechanisms have been further discerned as contributory factors for periodontitis (Sedghi et al., 2021b). Periodontal infection is not only harmful to oral health but is also linked to a number of systemic diseases. Periodontal medicine, a term defined to discover how periodontal infection affects extraoral health, is therefore considered (Monsarrat et al., 2016; Beck et al., 2019). Over the past decades, great progress has been made in periodontal medicine. Up to date, over 50 systemic diseases are now being researched regarding their relation to periodontal diseases (Loos, 2016; Fi and Wo, 2021).

The role of periodontal inflammation in vascular pathology has been consistently highlighted. Vascular endothelial cells (VECs), a layer of cells lining the lumen of the

blood vessel, play an important role in vascular diseases. They have active metabolism and can secrete various factors to regulate cell migration and adhesion, thrombosis, smooth muscle cell proliferation and migration, and vascular wall inflammation, which are extremely significant for vascular homeostasis (Krüger-Genge et al., 2019; Hennigs et al., 2021). When responding to adverse stimuli, the phenotype of VECs changes to an activated one, i.e., endothelial dysfunction (ED) (Corban et al., 2019; Medina-Leyte et al., 2021). ED has been demonstrated to have initiating and promoting effects on the occurrence and development of vascular diseases, such as atherosclerotic disease, hypercholesterolemia, diabetes, and hypertension (Lyle and Taylor, 2019).

In addition to traditional risk factors, inflammatory diseases, including periodontitis, are closely related to ED development (Paul et al., 2020). A large number of epidemiological studies and clinical evidences have confirmed the correlation between periodontitis and ED. However, a causative link between periodontal infection and endothelial cells and the direct molecular mechanism of periodontitis role in ED remain unclear. This review thus summarizes the possibility of the link between periodontitis and ED.

Periodontitis

Periodontitis is a very common biofilm-associated infection of the periodontium. It is now the sixth most prevalent disease globally, affecting about 50% of the world population (Balta et al., 2021). Despite its high prevalence, periodontitis is not taken seriously enough in the early stage, and most patients seeking treatment are in advanced stages of the disease. Approximately 11% of the world population suffer from severe periodontitis, which is the main reason leading to tooth loss and life quality reduction (Sanz et al., 2020). Periodontitis is characterized by inflammatory destruction of the tooth-supporting tissues, and its clinical features comprise gingival bleeding, periodontal pocket formation, clinical attachment loss, alveolar bone absorption, and even tooth mobility and loss (Slots, 2017; Kwon et al., 2021).

Periodontitis is a microbial-shift disease owing to polymicrobial dysbiosis (Lamont et al., 2018; Sedghi et al., 2021a). During the transition from periodontal homeostasis to dysbiosis, although the affected sites have greater microbial diversity and richness or present no significant difference, these sites exhibit unique microbial community structural characteristics. Specific genera, including *Porphyromonas, Treponema*, *Campylobacter*, *Eubacterium*, and *Tannerella*, have been identified at high levels in periodontitis sites, while other genera, such as *Veillonella, Neisseria, Rothia, Corynebacterium*, and *Actinomyces*, were highly prevalent in the healthy gingival sulcus (Plachokova et al., 2021; Abusleme et al., 2021). The characteristic of the periodontal microbiota is thus an ideal predictor of periodontal status. Nevertheless, the underlying mechanisms keeping the stability of and triggering the change in the microbial community are still not well understood. The inhibitory phenotype of *P. gingivalis*, *Tannerella forsythia* (*T. forsythia*), and *Treponema denticola* (*T. denticola*), namely the red-complex periopathogens, against the host innate response might play a pivotal role during the transition from periodontal health to disease (Xu et al., 2020; Prucsi et al., 2021). Moreover, community-based attack of periodontal pathogens on the host also offers a new possibility for periodontal microbial shift. The inoculation of *Porphyromonas gingivalis* (*P. gingivalis*, a keystone periodontal pathogen) with *T. denticola* (Verma et al., 2010) or *S. gordonii* (Lamont et al., 2010) has led to enhanced periodontal inflammation compared with *P. gingivalis* alone. Further research is still needed to elaborate on the biological mechanism of the dynamic change in the periodontal microorganisms.

More importantly, periodontitis presents a systematic chronic low-grade infection burden. Evidence-based literature has identified that periodontitis is not only a common oral health problem but also a risk factor implicated in multiple systemic cardiovascular diseases, such as hypertension, diabetes, and stroke (Thomas et al., 2015; Priyamvara et al., 2020; Del Pinto et al., 2020). Cardiovascular diseases are the biggest killers of human life and health worldwide, and they also remain the major public health problems in both developed and developing countries (Roth et al., 2020). The risk for cardiovascular disease is increased in periodontitis patients (Gheorghita et al., 2019; Sanz et al., 2020).

Vascular endothelial dysfunction

VECs lining the inner layer of blood vessels are the main regulator of vascular and organ homeostasis. The investigation of the implications of periodontitis in vascular endothelial function is undoubtedly a key breakthrough for the potential relationship between periodontitis and cardiovascular diseases.

The endothelium is in direct contact with blood flow and forms a barrier between blood and underlying tissues. Under quiescent conditions, VECs sense and transduce signals between blood and tissues, regulate the trafficking of cells in blood, and maintain a non-thrombogenic blood vessel surface (Zhu and Lee, 2016; Hennigs et al., 2021). When perturbed, these cells respond rapidly to various stimuli, such as microbial components, cytokines, oxidized low-density lipoproteins, immune complexes, and mechanical damage, to maintain vascular homeostasis (Eelen et al., 2018; Shao et al., 2020). However, exaggerated response of VECs may finally result in ED. The inflammatory reaction is the main characteristic of vascular ED. Vascular inflammation involves the onset of signaling cascades triggered by endothelial signaling, leading to increased production of cytokines, chemokines, and cell adhesion molecules, finally directing the recruitment of

inflammatory cells (Eelen et al., 2018). Additionally, this process is also accompanied by the up-regulation of reactive oxygen species, endothelin, lipid peroxidation, and thrombus regulatory protein and the impaired production of nitric oxide (NO) (Bondareva and Sheikh, 2020).

VEC dysfunction provides favorable conditions for increased endothelial permeability, augmented immune cell adhesion, platelet activation, activation of coagulation and fibrinolytic systems, lipid deposition, vascular vasomotor disorder, proliferation and migration of smooth muscle cells, and deposition of extracellular matrix, finally resulting in vascular diseases, such as hypertension, atherosclerosis, and coronary arterial disease (Favarato, 2018; Corban et al., 2019; Krüger-Genge et al., 2019). The pathologic state of dysfunctional endothelium as an early pathologic change occurring before detectable morphologic changes in the blood vessel wall is thought to be an independent predictor of the risk and prognosis of cardiovascular diseases. For example, ED has been observed in patients with hypertension, dyslipidemia, diabetes mellitus, and inflammatory diseases (Haas et al., 2018). And abnormal vascular endothelial function is a known prognostic indicator in children with familial cardiomyopathies (Tavares et al., 2012). Additionally, ED can also be used to predict future restenosis and major cardiovascular events in acute coronary syndrome patients treated with percutaneous coronary intervention (Yamamoto et al., 2014; Cheng et al., 2018).

Clinical assessment of endothelial function is an important insight into the patient's vascular status. The most widely applied indicators for endothelial function measurement are flow-mediated dilation (FMD) and nitroglycerin-mediated dilation (NMD) of the brachial artery. Both of them are performed by measuring macrovascular endothelial function with brachial artery ultrasound (Ambrosino et al., 2021). In contrast, the application of reactive hyperemia-peripheral arterial tonometry (RH-PAT), evaluating the ratio of blood flow volume of microvascular endothelium before and after blood flow release, offers a simpler assessment approach. However, there is currently no clinical guideline-based recommendation for vascular endothelial function testing, and more work are required to develop such a guideline. In addition to clinical assessment, many laboratory biomarkers can also be applied to ED evaluation. These biomarkers contain vascular cell adhesion molecule-1 (VCAM-1), intercellular cell adhesion molecule-1 (ICAM-1), pentraxin-3, e-selectin, von Willebrand factor-1 (vWF), asymmetrical dimethylarginine (ADMA), angiopoietin-1 (Ang-1), thrombomodulin, endothelial microparticles (EMPs), and endothelial progenitor cells (Balta, 2021). Noteworthily, there are two novel biomarkers: endocan and endoglin. Endoglin is a transmembrane receptor for transforming growth factor β-1 and 3 in VECs (Jeng et al., 2021). The long-form endoglin (L-endoglin) and short-form endoglin (S-endoglin) are two isoforms of endoglin. L-endoglin is undetectable in resting ECs but is highly expressed in ECs at sites of angiogenesis, upon inflammation or ischemic stimuli (Ollauri-Ibáñez et al., 2017). Endocan is a soluble proteoglycan secreted by vascular ECs (Çimen et al., 2016). The expression of endocan in ECs can be upregulated in response to inflammatory triggers, such as lipopolysaccharide and cytokines (Meurer and Weiskirchen, 2020). Both of endoglin and endocan are suggested as possible biomarkers for ED (Leite et al., 2020). However, they are not VECs-specific and can be expressed in other cells like monocytes and bronchi epithelial cells respectively, so more research is necessary to evaluate their predictive value and reproducibility in vascular diseases. In a word, all of the current potential indicators have not been proven to be a causal risk factor for cardiovascular disease, although they are highly associated with worsening vascular endothelial function.

The implication of periodontitis in vascular endothelial function

Epidemiological studies and clinical cohort and case-control evidences have suggested that periodontal treatment can be an effective measure for ED improvement. Additionally, the biological plausibility of periodontitis impact on VECs has been gradually revealed.

The effect of periodontal therapy on vascular endothelial function

Epidemiologic evidences support that people with periodontitis have a higher prevalence of subclinical cardiovascular disease, peripheral artery disease, and coronary events (Sanz et al., 2020). In a large longitudinal population-based study, periodontitis has been significantly associated with high FMD levels (Holtfreter et al., 2013). Moreover, in an update pilot study, increased tooth mobility has been independently correlated with endothelial dysfunction using RH-PAT after adjustment for age and glycosylated hemoglobin (HbA1c) (Fujitani et al., 2020). Ronaldo et al. (Lira-Junior et al., 2014) have evaluated endothelial function in severe chronic periodontitis patients. They have found that severe periodontitis was associated with nailfold and gingival microvascular and endothelial dysfunction. Specifically, there was a decrease in functional capillary density, capillary diameters, red blood cell velocity at rest, endothelium-independent vasodilatation, and post-ischemic peak flow in patients with periodontitis. Other experimental findings have also supported the passive impact of periodontitis on function of vascular endothelium (Brito et al., 2013; Lira-Junior et al., 2014; Parvaneh et al., 2021).

Intensive periodontitis treatment, consisting of oral hygiene education, scaling, and root planing, has been suggested to improve endothelial function by the vast majority of trials. Potential biomarkers linking periodontitis with endothelial dysfunction, including C-reactive protein (CRP), interleukin (IL)-1, ICAM-1, E-selectin, vWF, plasminogen activator inhibitor type-1 (PAT-1), and plasminogen, have been found to be decreased after periodontal treatment (Tonetti et al., 2007; Li et al., 2011b; D'Aiuto et al., 2013; Hansen and Holmstrup, 2022). More than 10 years ago, Tonetti et al. (2007) showed that improved endothelial function paralleled periodontal health 60 and 120 days after periodontal therapy, although ED and an increase in inflammatory factors were observed 24 h after periodontal treatment. The immediate ED might be caused by the acute, transient systemic inflammation after periodontal treatment, and the improved endothelial function ultimately benefits from good oral health after 2 months of therapy. Additionally, the number of missing teeth, an easily accessible clinic marker, has been reported to be correlated with higher coronary artery calcium score (CACS) (Donders et al., 2020). Combining the result of this explorative pilot study with additional clinical information and biomarkers might contribute to the further exploration of the relationship between missing teeth and ED. The result of Matsui et al.'s study is appealing as well. Their result has shown that low frequency and short duration of tooth brushing were associated with an increased odds ratio of a low FMD after conventional risk factors adjustment (Matsui et al., 2017). This conclusion was in line with the findings of Kajikawa (Kajikawa et al., 2014). Their research achievement has well confirmed the passive impact of poor oral health on ED, but more large-scale clinical studies are needed. Furthermore, several clinical trials have confirmed the positive effect of periodontal treatment on endothelial function in groups of periodontitis with other co-morbidities. Endothelial function improvement and inflammatory biomarkers reduction have been observed after periodontal treatment of subjects with both periodontitis and cardiovascular diseases, and this improvement sustained well over half a year after therapy (Teeuw et al., 2014). In addition, EMPs, together with systolic and diastolic blood pressure (BP), have also been found to be markedly reduced by subgingival scaling and root planing (without antihypertensive medication therapy) in prehypertensive patients with periodontitis, and the reduction in EMPs and BP levels has been significantly related to the improvement in pocket depth (Zhou et al., 2017).

There are surely contradictory findings. A study has reported that no significant improvement in vascular endothelial function could be confirmed after periodontal treatment in patients with moderate-to-severe periodontitis (Li et al., 2011a). We suggest two possible reasons for their different results. First, their assessment criterion of periodontitis degree (half-mouth method at three sites per tooth) has been different from that in other studies (full-mouth periodontal recordings), which might be the most potential influence factor. The difference might also be explained by the study population, which has been compromised by the broad age range and even confounding factors, such as smoking, cardiovascular risk factors, diabetes mellitus, and chronic kidney disease. In another 3-month follow-up period, it has also not been shown that nonsurgical periodontal therapy improved FMD in patients with coronary disease (control 1.37% *vs.* test 1.39%) (Saffi et al., 2018). In this study, the selected individuals were suffering from periodontitis and chronic heart disease and even have already been receiving cardiovascular treatments. Regular cardiovascular therapies may explain the absence of significant between-group differences.

Generally, most existing clinical trials have tended to include participants affected by chronic severe generalized periodontitis. However, whether the improvement degree of vascular function by periodontal therapy is influenced by periodontitis severity remains unknown. Furthermore, current understanding of the effect of periodontal therapy on ED is mainly based on patient comparative and treatment clinical studies. More large-scaled and well-designed cohort studies and clinical trials with improved design in multicenter groups are indispensable.

The influence of periodontitis on vascular endothelial function

Periodontitis can contribute to or increase endothelial inflammation. Periodontal pathogens and their noxious stimuli or periodontal cytokines can be detected by receptors on vascular endothelial cells, leading to the activation of an inflammatory cascades. The most well-characterized specialized pattern-recognition receptors (PRRs) are toll-like receptor-2 (TLR-2) and TLR-4, which play a key role in periodontal bacterial recognition (Hajishengallis et al., 2006; Hajishengallis and Lambris, 2011; Chen et al., 2021). Nucleotide-binding leucine-rich repeat receptors (NLRs) and scavenger receptors (SRs) are also involved in ED induced by periodontal infection (Zelkha et al., 2010; Huck et al., 2015; Li et al., 2020). After the recognition of noxious substances from the periodontium, the release of an inflammatory cytokine network is initiated, which can result in a complex proinflammatory and prothrombotic phenotype of endothelial cells. For example, tumor necrosis factor (TNF)-α, IL-1, IL-6, and IL-8 released by periodontal bacteria can invade the endothelial layer (Chhibber-Goel et al., 2016) and promote the expression of chemokines and adhesion molecules, including ICAM-1, VCAM-1, lymphocyte function-associated antigen 1 (LFA-1), P-selectin, and E-selectin (Schenkein and Loos, 2013). These chemokines and adhesion molecules can be induced or increased by lipopolysaccharide (LPS) and endothelial microvesicles (MVs) of *P. gingivalis* as well (An et al., 2014; Bugueno et al., 2020). Moreover, *P. gingivalis* infection can also modulate the production of inflammatory cytokines, such as IL-1, IL-6, TNF-α, myeloperoxidase, and

matrix metalloproteinase 2 (MMP-2)/tissue inhibitor of metalloproteinases 2 (TIMP-2) complex, and chemokines, such as monocyte chemotactic protein-1 (MCP-1), IL-8, and CX3C chemokine ligand 1 (CX3CL1), in VECs (Hashizume et al., 2011; Moura et al., 2017; Pan and Yan, 2019). The release of inflammatory factors further induces the migration and adhesion of leukocytes and monocytes to the intimal layer of the blood vessel. These immune cells can transport periodontal bacteria into the lesion and secrete more inflammatory factors at the same time, ultimately exacerbating endothelial inflammation. Moreover, ICAM-1 can bind to fibrinogen and reduce the expression of actin-associated endothelial tight junction proteins, such as occludin and zonula occludens-1, to increase endothelial layer permeability (Patibandla et al., 2010; Leite et al., 2020). In an *in vitro* model, LPS has also been found to induced caspase-mediated cleavage of adherens junction proteins (Ding et al., 2020). Other studies have ever reported that the gingipains and outer membrane vesicles of *P. gingivalis* mediated increased vascular permeability *via* a mechanism that involves proteolytic cleavage of the platelet endothelial cell adhesion molecule 1 (PECAM-1) (Yun et al., 2005; Farrugia et al., 2020; Zhang et al., 2021)

The increased permeability of the endothelium creates conditions for the coagulation and fibrinolytic systems activation, smooth muscle cells (SMCs) migration into the intima, lipoprotein flux, and foam cell formation. The coagulation and fibrinolytic system includes fibrinogen, vWF, tissue plasminogen activator (tPA), PAI-1, and coagulation factors VII and VIII. They play a vital role in maintaining vascular homeostasis. PAI-1 is one of the best-established fibrinolytic members and risk factors for vascular diseases. *P. gingivalis* infection can significantly reduce PAI-1 levels in human endothelial cells, and the degradation of PAI-1 will induce permeabilization and dysfunction of the vascular endothelial cells *via* the low-density lipoprotein receptor-related protein (Song et al., 2021). Fibrinogen is another important member of the coagulation and fibrinolytic system. Elevated fibrinogen is followed by an increased blood viscosity and shear stress, which, in turn, activate endothelial cells and platelets (Paraskevas et al., 2008; Luyendyk et al., 2018). Periodontitis has been reported to present with higher plasma fibrinogen levels and white blood cell counts than controls (Jayaraman et al., 2021). The increased fibrinogen can further stimulate the production of MCP-1, IL-6, IL-8, TNF-α, MMP-1, and MMP-9 (Patibandla et al., 2010; Luyendyk et al., 2018; Surma and Banach, 2021), and aggravate endothelial inflammation. A vicious pathogenic cycle is thus formed where the damaged coagulation and fibrinolytic system and endothelial inflammation reinforce each other by the positive feedback loop between them.

Periodontitis has also been strongly associated with an increase in the endothelial synthesis of Reactive oxidative stress (ROS) and the reduction in NO bioavailability. ROS is an important factor in causing ED. Excessive ROS accumulation interferes with the nitric oxide (NO) signaling pathway, thereby reducing NO bioavailability and leading to ED and endothelium-dependent relaxation reduction (Garcia and Sessa, 2019). As described by Xie et al. (Xie et al., 2020), increased mitochondrial ROS production has been observed in endothelial cells infected with *P. gingivalis*. Furthermore, salivary NO concentration has been reported as a potential linkage between periodontitis and ED (Moura et al., 2017). The reduced bioavailability of NO can inhibit the expression of adhesion molecules and promote SMCs migration and proliferation (Liccardo et al., 2019; Yang et al., 2022; Suh et al, 2019), further aggravating aberrant function of VECs. Recently, Parvaneh et al. (Parvaneh et al., 2021) established periodontitis in 8-week-old $ApoE^{-/-}$ mice and showed that periodontitis exhibited impaired endothelial-dependent vasorelaxation responses to acetylcholine, which was indicative of NO bioactivity impairment and the onset of ED. Similarly, Campi et al. (Campi et al., 2016) have found that after 7 days of the induction of periodontitis, the vascular response of adult rat aorta was impaired in terms of norepinephrine-induced contraction and acetylcholine-dependent relaxation, and the endothelium-derived NO and cyclooxygenase 2 (COX-2) were involved in the process (Zhou et al., 2019; De Oliveira et al., 2021). Nuclear factor erythroid-derived 2-like 2 (Nrf-2) is a key transcriptional factor protecting cells from oxidative stress and influencing vascular endothelium homeostasis (Kovac et al., 2014). Periodontal infection can lead to impaired vascular relaxation *via* the glycogen synthase kinase 3β (GSK-3β)/tetrahydrobiopterin (BH4)/nitric oxide synthase (eNOS)/Nrf2/NOS pathways (Kovac et al., 2014), which may contribute to a potential new therapeutic strategy for periodontitis-induced ED.

Interestingly, Pereira et al. (Pereira et al., 2011) discovered that no significant changes in endothelium-dependent vasodilation were observed in 18-week-old mice with *P. gingivalis* over 12 weeks. The authors have suggested that the opposing results different from other studies might originate from the older mice used. In 18-week old adult mice, the senescence might begin, and even significant vascular pathology might have already been established (Pereira et al., 2011). However, significant ED has been observed in periodontitis-treated middle-aged (57-week) rats, in which increased nicotinamide adenine dinucleotide phosphate oxidase (NADPH oxidase) and COXs, downregulated eNOS and NO, and endothelium-derived hyperpolarizing factor-mediated vascular relaxation were found (Silva et al., 2021). Interestingly, Brito et al., (2013) have revealed that some systemic inflammatory markers and oxidative stress products returned to basal levels at day 28 after periodontitis establishment in a 10-week rat. This might be a consequence of host resistance to periodontal infection and inflammatory stimuli. Moreover, the activation of the endothelial calcium-activated potassium channel might be the key mediator for the

recovery of VEC impairment (Jr et al., 2018). These findings together make the result of Pereira more comprehensible. And there is also a thought-provoking question that whether there are limitations to applying endothelial-dependent relaxation as a marker of endothelial dysfunction.

The mechanism of periodontitis affecting vascular endothelial dysfunction

The biological pathways by which periodontitis accelerates vascular diseases have not been fully elucidated so far. To date, there are three plausible hypotheses, including the bacteriological, inflammatory, and immunological theories (Hajishengallis, 2015; Febbraio et al., 2022).

The bacteriological hypothesis postulates that the entry of periodontal pathogens into the bloodstream activates endothelial inflammatory response by multiple mechanisms, resulting in ED. The inflammatory theory favors that inflammatory mediators in infected periodontium are released into the systemic circulation, in turn, affecting endothelial function. The ulcerated periodontal pocket epithelium is one of the main accesses whereby periodontal pathogens, noxious products, and inflammatory cytokines enter the blood circulation. The ulcerated periodontal pocket epithelial area in patients with severe periodontitis is about 18–28 cm^2 (Leira et al., 2018). This niche harbors 1×10^8–1×10^{10} bacteria feeding on the inflammatory spoils (Hajishengallis, 2015). Periodontal microorganisms and their noxious products can enter the blood circulation from the ulcerated area during chewing, brushing, or invasive dental therapy (Dyke and Winkelhoff, 2013). Then, they cause chronically sustained systemic infection. This persistent low-level inflammation has detrimental effects on the blood vessel endothelium. However, it is challenging to discriminate the role of bacteria from the inflammatory response in ED. The specific pharmacotherapeutic interventions might shed light on this troublesome matter.

The detection of periodontal pathogens in atheromatous plaques from patients further supports the hypothesis above (Padilla et al., 2010; Rao et al., 2021). Moreover, these pathogens also have been shown to invade and survive in endothelial cells *in vitro* (Velsko et al., 2014; Dorn et al., 1999; Schenkein et al., 2020). Results from mice with periodontitis have further confirmed the systemic dissemination of periodontal bacteria within aortic endothelial cells (Chukkapalli et al., 2014; Velsko et al., 2014; Velsko et al., 2015). The question of how periodontal bacteria exit from ulcerated periodontal epithelium to systemic circulation is currently broadly emphasized and explored. Current evidences have suggested that periodontal bacteria can exploit recirculating monocytes (Suwatanapongched et al., 2010), erythrocytes (Ganuelas et al., 2013), and dendritic cells (Carrion et al., 2012) for dissemination. These cells engulf bacteria and transport them to distal vascular endothelial cells. Fimbriae protein possessing adherence and invasive properties may play a key role in this process, as the fimA-deficient mutant strain of *P. gingivalis* failed to adhere and invade cells (Jotwani and Culter, 2004; Hasegawa and Nagano, 2021). The transmission of *P. gingivalis* among cells can be mediated by membranous projections (Yilmaz et al., 2006) and autophagosomes (Takeuchi et al., 2011). More recently, research has shown that *P. gingivalis* was first encapsulated by early endosomes immediately upon their entry into cells, and then some of them were sorted to late endosomes for degradation, whereas others escaped from cells for further dissemination (Takeuchi et al., 2016). This discovery further reveals the recycling pathways by which intracellular bacteria exit infected cells. With such a dynamic, *P. gingivalis* can control its population in infected cells and allow for persistent infection.

The immunological hypothesis is based on the fact that the host immune response in susceptible individuals favors vascular inflammation. Although microbial plaque is indispensable in vascular pathology related to periodontitis, it is the host immune system that primarily drives the outcome of microbial infection. This is the underlying reason why patients are not equally susceptible and do not respond similarly to the same treatment (Dyke, 2020). There is a phenotype of hyper-inflammatory monocytes when the host is challenged by the periodontal bacteria, which can result in an abnormal release of a high amount of proinflammatory mediators (Jagannathan et al., 2014). People with this phenotype of monocytes have a higher risk of suffering from periodontitis and ED (Gurav, 2014). Noz et al. deepen this theory. They applied trained immunity to describe that monocytes/macrophages build immunological memory after encountering a pathogen, resulting in a persistent hyper-responsive phenotype (Noz et al., 2021). The results of them revealed that *P. gingivalis* can induce trained immunity in human monocytes, in terms of an augmented cytokine production capacity (Noz et al., 2021). These augmented cytokine production can further promote Th1 responses to increase macrophages activation to enhance inflammation in the vessel (Tonetti and Dyke, 2013). And it is worth noting that antibodies produced by adaptive immune cells may be cross-reacting with endothelial cells to enhance inflammation at the same time. For example, the autoimmune reaction against the heat-shock proteins (HSPs) is responsible for periodontitis-related ED. HSPs can activate dendritic cells and natural killer cells and play a major role in MHC-antigen processing and presentation (Bolhassani and Agi, 2019). They are protective and function as chaperones under physiological conditions, and their expression would enhance in response to various physical, chemical and microbial stimuli (Finlayson-Trick et al., 2019). Bacterial HSP60 (GroEL) of periodontopathic bacteria is homologous with the host HSPs and displays a

strong immunogenic nature. The homology between the host HSP60 expressed by the ECs and GroEL in periodontal microorganism is unrecognizable by the host T cells (Ford et al., 2010). Thus, the antibodies directed against the bacterial GroEL cross-reacts with HSP60 on ECs, finally resulting in autoimmune responses that ensue in ED (Lee et al., 2011; Joo et al., 2020). The keystone pathogens are key contributors for the host immune response subversion. For example, *P. gingivalis*, the keystone bacterium, possess virulence factors that can inactivate critical elements of the host response and enhance the proliferation and differentiation of Th-17 cells (Stein, 2015). However, further molecular mechanism exploration is still imperative and is promising for host homeostasis restoration that promote the resolution of inflammation.

Recently, new evidence has suggested that periodontitis can affect systemic health through the oral-intestinal axis, which might be a novel pathway independent of blood circulation (Bao et al., 2022). Whether periodontitis affects vascular endothelial health through this pathway is still unknown. However, there is a study that might be instructive. It detected the trimethylamine-N-oxide (TMAO), a harmful intestinal microbiota-dependent metabolite in periodontitis (Jalandra et al., 2021). In this research, elevated TMAO was presented in patients with stage III-IV periodontitis, and its concentration has been correlated with reduced circulating endothelial progenitor cells (EPCs) and FMD levels (Zhou et al., 2022). These data provide a novel perspective on the possibility of periodontitis affecting endothelial function through the oral-intestinal axis, which deserves deep exploration.

Summary

This review summarizes current insights into the implication of periodontitis in ED (Figure 1). Current evidences suggest that periodontitis is highly associated with ED, which is of considerable importance for the risk and prognosis of cardiovascular diseases. Most of the epidemiological studies and clinical evidences have shown periodontal treatment as an effective measure for ED improvement. But more evidences are necessary for the impact of periodontal therapy on endothelial function in subjects with less widespread and severe periodontitis or with complex systemic conditions. Furthermore, the biological plausibility of periodontitis impact on vascular endothelium is being widely explored and gradually revealed. But much more researches are needed to elaborate the direct causal relationship between them.

To sum up, we still strongly recommend more collaboration between stomatologists and cardiologists in clinical work. Our stomatologists should pay more attention to the systemic health of patients and recommend them to visit cardiologists when necessary. At the same time, it is advocated that our general physicians attach importance to the oral health of patients and suggest them visit their stomatologists for periodontitis screening. If they are diagnosed with periodontitis, periodontal therapy is needed to improve their

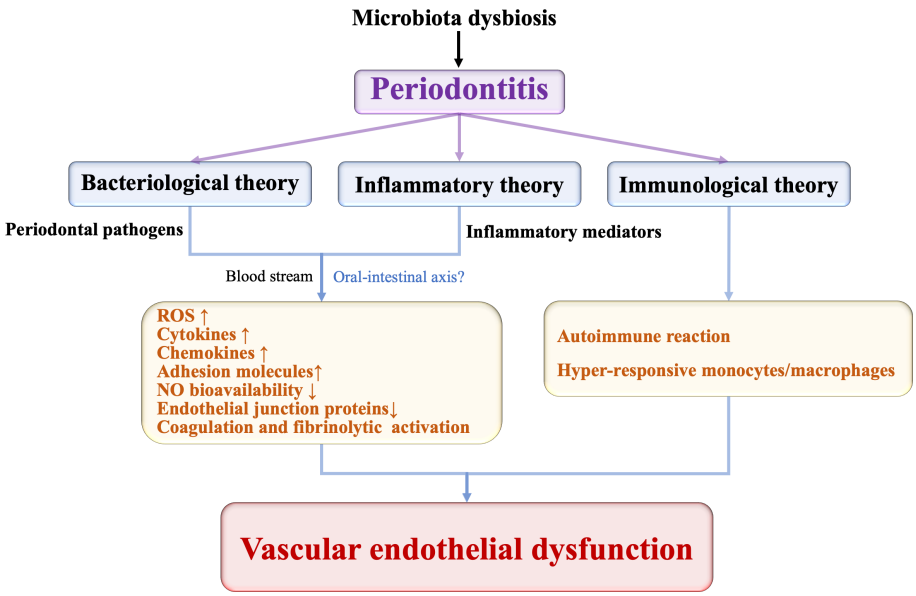

FIGURE 1
The potential pathways periodontitis induces vascular endothelial dysfunction.

vascular endothelial function, thereby reducing the risk for cardiovascular disease events.

Author contributions

QL wrote and edited this paper. XO and JL reviewed and edited the manuscript. All authors contributed to the article and approved the submitted version.

Funding

This present work was supported by the National Natural Science Foundation of China (grant no. 82170957, 81870772), and by the Foundation of Beijing Tongren Hospital, Capital Medical University (grant no. 2021-YJJ-ZZL-047).

Conflict of interest

The authors declare that the research was conducted in the absence of any commercial or financial relationships that could be construed as a potential conflict of interest.

The handling editor ZW declared a shared parent affiliation with the authors QL and JL at the time of review.

Publisher's note

References

Abusleme, L., Hoare, A., Hong, B. Y., and Diaz, P. I. (2021). Microbial signatures of health, gingivitis, and periodontitis. *Periodontol. 2000.* 86, 57–78. doi: 10.1111/prd.12362

Ambrosino, P., Papa, A., Buonauro, A., Mosella, M., Calcaterra, I., Spedicato, G. A., et al. (2021). Clinical assessment of endothelial function in heart failure with preserved ejection fraction: A meta-analysis with meta-regressions. *Eur. J. Clin. Invest.* 51, e13552. doi: 10.1111/eci.13552

An, N., Andrukhov, O., Tang, Y., Falkensammer, F., Bantleon, H. P., Ouyang, X., et al. (2014). Effect of nicotine and porphyromonas gingivalis lipopolysaccharide on endothelial cells *in vitro*. *PLoS. One* 9, e96942. doi: 10.1371/journal.pone.0096942

Balta, S. (2021). Endothelial dysfunction and inflammatory markers of vascular disease. *Curr. Vasc. Pharmacol.* 19, 243–249. doi: 10.2174/1570161118666200421142542

Balta, M. G., Papathanasiou, E., Blix, I. J., and Dyke, T. (2021). Host modulation and treatment of periodontal disease. *J. Dent. Res.* 100, 798–809. doi: 10.1177/0022034521995157

Bao, J., Li, L., Zhang, Y., Wang, M., Chen, F., Ge, S., et al. (2022). Periodontitis may induce gut microbiota dysbiosis *via* salivary microbiota. *Int. J. Oral. Sci.* 14, 32. doi: 10.1038/s41368-022-00183-3

Beck, J. D., Papapanou, P. N., Philips, K. H., and Offenbacher, S. (2019). Periodontal medicine: 100 years of progress. *J. Dent. Res.* 98, 1053–1062. doi: 10.1177/0022034519846113

Bolhassani, A., and Agi, E. (2019). Heat shock proteins in infection. *Clin. Chim. Acta* 498, 90–100. doi: 10.1016/j.cca

Bondareva, O., and Sheikh, B. N. (2020). Vascular homeostasis and inflammation in health and disease-lessons from single cell technologies. *Int. J. Mol. Sci.* 21, 4688. doi: 10.3390/ijms21134688

Brito, L. C., DalBó, S., Striechen, T. M., Farias, J. M., Olchanheski, L. R.Jr., Mendes, R. T., et al. (2013). Experimental periodontitis promotes transient vascular inflammation and endothelial dysfunction. *Arch. Oral. Biol.* 58, 1187–1198. doi: 10.1016/j.archoralbio.2013.03.009

Bugueno, I. M., Zobairi El-Ghazouani, F., Batool, F., El Itawi, H., Anglès-Cano, E., Benkirane-Jessel, N., et al. (2020). Porphyromonas gingivalis triggers the shedding of inflammatory endothelial microvesicles that act as autocrine effectors of endothelial dysfunction. *Sci. Rep.* 10, 1778. doi: 10.1038/s41598-020-58374-z

Campi, P., Herrera, B. S., de Jesus, F. N., Napolitano, M., Teixeira, S. A., Maia-Dantas, A., et al. (2016). Endothelial dysfunction in rats with ligature-induced periodontitis: Participation of nitric oxide and cycloxygenase-2-derived products. *Arch. Oral. Biol.* 63, 66–74. doi: 10.1016/j.archoralbio

Carrion, J., Scisci, E., Miles, B., Sabino, G. J., Zeituni, A. E., Gu, Y., et al. (2012). Microbial carriage state of peripheral blood dendritic cells (DCs) in chronic periodontitis influences DC differentiation, atherogenic potential. *J. Immunol.* 189, 3178–3187. doi: 10.4049/jimmunol.1201053

Cheng, X., He, Y., Fan, H., Liu, T., Pan, W., Wang, K., et al. (2018). Endothelial function as predictor in patients with coronary syndrome treated by percutaneous coronary intervention. *Biosci. Rep.* 38, BSR20180732. doi: 10.1042/BSR20180732

Chen, Y., Wang, X., Ng, C., Tsao, S., and Leung, W. (2021). Toll-like receptors 1/2/4/6 and nucleotide-binding oligomerization domain-like receptor 2 are key damage-associated molecular patterns sensors on periodontal resident cells. *Appl. Sci.* 11, 4724. doi: 10.3390/app11114724

Chhibber-Goel, J., Singhal, V., Bhowmik, D., Vivek, R., Parakh, N., Bhargava, B., et al. (2016). Linkages between oral commensal bacteria and atherosclerotic plaques in coronary artery disease patients. *Npj. Biofilms. Microbiomes.* 2, 7. doi: 10.1038/s41522-016-0009-7

Chukkapalli, S. S., Rivera, M. F., Velsko, I. M., Lee, J. Y., Chen, H., Zheng, D., et al. (2014). Invasion of oral and aortic tissues by oral spirochete treponema denticola in ApoE(-/-) mice causally links periodontal disease and atherosclerosis. *Infect. Immunity.* 82, 1959–1967. doi: 10.1128/IAI.01511-14

Çimen, T., Efe, T. H., Akyel, A., Sunman, H., Algül, E., Şahan, H. F., et al. (2016). Human endothelial cell-specific molecule-1 (Endocan) and coronary artery disease and microvascular angina. *Angiology* 67, 846–853. doi: 10.1177/0003319715625827

Corban, M. T., Lerman, L. O., and Lerman, A. (2019). Endothelial dysfunction. *Arterioscler. Thromb. Vasc. Biol.* 39, 1272–1274. doi: 10.1161/ATVBAHA.119.312836

D'Aiuto, F., Orlandi, M., and Gunsolley, J. C. (2013). Evidence that periodontal treatment improves biomarkers and CVD outcomes. *J. Periodontol.* 84, S85–S105. doi: 10.1902/jop.2013.134007

Del Pinto, R., Pietropaoli, D., Munoz-Aguilera, E., D'Aiuto, F., Czesnikiewicz-Guzik, M., Monaco, A., et al. (2020). Periodontitis and hypertension: Is the association causal? *High. Blood. Press Cardiovasc. Prev.* 27, 281–289. doi: 10.1007/s40292-020-00392-z

De Oliveira, H. T., Couto, G. K., Davel, A. P., Xavier, F. E., and Rossoni, L. V. (2021). Chronic cyclooxygenase-2 inhibition prevents the worsening of hypertension and endothelial dysfunction induced by ouabain in resistance arteries of spontaneously hypertensive rats. *Vasc. Pharmacol.* 139, 106880. doi: 10.1016/j.vph.2021.106880

Ding, L., Li, L. M., Hu, B., Wang, J. L., Lu, Y. B., Zhang, R. Y., et al. (2020). TM4SF19 aggravates LPS-induced attenuation of vascular endothelial cell adherens junctions by suppressing VE-cadherin expression. *Biochem. Biophys. Res. Commun.* 533, 1204–1211. doi: 10.1016/j.bbrc.2020.08.078

Donders, H., Ijzerman, L. M., Soffner, M., Hof, A., and Lange, J. D. (2020). Elevated coronary artery calcium scores are associated with tooth loss. *PLoS. One* 5, e0243232. doi: 10.1371/journal.pone.0243232

Dorn, R. B., Dunn, A. W.Jr., and Progulske-Fox, A. (1999). Invasion of human coronary artery cells by periodontal pathogens. *Infect. Immun.* 67, 5792–5798. doi: 10.1128/IAI.67.11.5792-5798.1999

Dyke, T. (2020). Shifting the paradigm from inhibitors of inflammation to resolvers of inflammation in periodontitis. *J. Periodtol.* 91, S19–S25. doi: 10.1002/JPER.20-0088

Dyke, T. V., and Winkelhoff, A. V. (2013). Infection and inflammatory mechanisms. *J. Clin. Periodontol.* 14, S1–S7. doi: 10.1111/jcpe.12088

Eelen, G., de Zeeuw, P., Treps, L., Harjes, U., Wong, B. W., and Carmeliet, P. (2018). Endothelial cell metabolism. *Physiol. Rev.* 98, 3–58. doi: 10.1152/physrev.00001.2017

Farrugia, C., Stafford, G. P., and Murdoch, C. (2020). Porphyromonas gingivalis outer membrane vesicles increase vascular permeability. *J. Dent. Res.* 99, 1494–1501. doi: 10.1177/0022034520943187

Favarato, D. (2018). "Chapter 34 "Endothelial function and cardiovascular risk factors"," in *Endothelium and cardiovascular diseases*. Eds. P. L. Da Luz, P. Libby, A. C. P. Chagas and F. R. M. Laurindo (London: Academic Press).

Febbraio, M., Roy, C. B., and Levin, L. (2022). Is there a causal link between periodontitis and cardiovascular disease? a concise review of recent findings. *Int. Dent. J.* 72, 37–51. doi: 10.1016/j.identj.2021.07.006

Finlayson-Trick, E., Connors, J., Stadnyk, A., and Limbergen, J. V. (2019). Regulation of antimicrobial pathways by endogenous heat shock proteins in gastrointestinal disorders. *Gastrointest. Disord.* 19, 34–39. doi: 10.3390/gidisord1010005

Fi, C., and Wo, W. (2021). Periodontal disease and systemic diseases: an overview on recent progresses. *J. Biol. Regul. Homeost. Agents.* 35, 1–9.

Ford, P. J., Gemmell, E., Chan, A., Carter, C. L., and Seymour, G. J. (2010). Inflammation, heat shock proteins and periodontal pathogens in atherosclerosis: an immunohistologic study. *Oral. Microbiol. Immunol.* 21, 206–211. doi: 10.1111/j.1399-302X.2006.00276.x

Fujitani, T., Aoyama, N., Hirata, F., and Minabe, M. (2020). Association between periodontitis and vascular endothelial function using noninvasive medical device-a pilot study. *Clin. Exp. Dent. Res.* 6, 576–582. doi: 10.1002/cre2.312

Ganuelas, L. A., Li, N., Yun, P., Hunter, N., and Collyer, C. A. (2013). The lysine gingipain adhesin domains from porphyromonas gingivalis interact with erythrocytes and albumin: Structures correlate to function. *Eur. J. Microbiol. Immunol. (Bp).* 3, 152–162. doi: 10.1556/EuJMI.3.2013.3.2

Garcia, V., and Sessa, W. C. (2019). Endothelial NOS: perspective and recent developments. *Brit. J. Pharmacol.* 176, 189–196. doi: 10.1111/bph.14522

Gheorghita, D., Eördegh, G., Nagy, F., and Antal, M. (2019). Periodontal disease, a risk factor for atherosclerotic cardiovascular disease. *Orv. Hetil.* 160, 419–425. doi: 10.1556/650.2019.31301

Gurav, A. N. (2014). The implication of periodontitis in vascular endothelial dysfunction. *Eur. J. Clin. Invest.* 44, 1000–1009. doi: 10.1111/eci.12322

Haas, E. A., Nishiyama, M., and da Luz, P. L. (2018). "Chapter 48 "Clinical endothelial dysfunction: Prognosis and therapeutic target"," in *Endothelium and cardiovascular diseases*. Eds. P. L. Da Luz, P. Libby, A. C. P. Chagas and F. R. M. Laurindo (London: Academic Press).

Hajishengallis, G. (2015). Periodontitis: from microbial immune subversion to systemic inflammation. *Nat. Rev. Immunol.* 15, 30–44. doi: 10.1038/nri3785

Hajishengallis, G., and Lambris, J. D. (2011). Microbial manipulation of receptor crosstalk in innate immunity. *Nat. Rev. Immunol.* 11, 187–200. doi: 10.1038/nri2918

Hajishengallis, G., Tapping, R. I., Harokopakis, E., Nishiyama, S., Ratti, P., Schifferle, R. E., et al. (2006). Differential interactions of fimbriae and lipopolysaccharide from porphyromonas gingivalis with the toll-like receptor 2-centred pattern recognition apparatus. *Cell. Microbiol.* 8, 1557–1570. doi: 10.1111/j.1462-5822.2006.00730.x

Hansen, P. R., and Holmstrup, P. (2022). Cardiovascular diseases and periodontitis. *Adv. Exp. Med. Biol.* 1373, 261–280. doi: 10.1007/978-3-030-96881-6_14

Hasegawa, Y., and Nagano, K. (2021). Porphyromonas gingivalis FimA and Mfa1 fimbriae: Current insights on localization, function, biogenesis, and genotype. *Jpn. Dent. Sci. Rev.* 57, 190–200. doi: 10.1016/j.jdsr.2021.09.003

Hashizume, T., Kuritaochiai, T., Mikuni, D., Kawanabe, K., Kanamaru, S., and Yamamoto, M. (2011). Effect of porphyromonas gingivalis on human umbilical vein endothelial cells. *Int. J. Med. Sci.* 8, 157–161. doi: 10.5466/ijoms.8.157

Hennigs, J. K., Matuszcak, C., Trepel, M., and Körbelin, J. (2021). Vascular endothelial cells: Heterogeneity and targeting approaches. *Cells* 10, 2712. doi: 10.3390/cells10102712

Holtfreter, B., Empen, K., Gläser, S., Lorbeer, R., Völzke, H., Ewert, R., et al. (2013). Periodontitis is associated with endothelial dysfunction in a general population: a cross-sectional study. *PLoS. One* 8, e84603. doi: 10.1371/journal.pone.0084603

Huck, O., Elkaim, R., Davideau, J. L., and Tenenbaum, H. (2015). Porphyromonas gingivalis-impaired innate immune response *via* NLRP3 proteolysis in endothelial cells. *Innate. Immun.* 21, 65–72. doi: 10.1177/1753425914523459

Jagannathan, R., Lavu, V., and Rao, S. R. (2014). Comparison of the proportion of non-classic (CD14+CD16+) monocytes/macrophages in peripheral blood and gingiva of healthy individuals and patients with chronic periodontitis. *J. Periodontol.* 85, 852–858. doi: 10.1902/jop.2013.120658

Jalandra, R., Dalal, N., Yadav, A. K., Verma, D., Sharma, M., Singh, R., et al. (2021). Emerging role of trimethylamine-n-oxide (TMAO) in colorectal cancer. *Appl. Microbiol. Biotechnol.* 105, 7651–7660. doi: 10.1007/s00253-021-11582-7

Jayaraman, D. R. S., Mahendra, D. J., Mahendra, D. L., and Srinivasan, D. R. S. (2021). Title of the article: Effect of chronicperiodontitis on systemic inflammation -a cross sectional study. *Int. J. Pharmaceut. Res.* 13, 2. doi: 10.31838/ijpr/2021.13.02.105

Jeng, K. S., Sheen, I. S., Lin, S. S., Leu, C. M., and Chang, C. F. (2021). The role of endoglin in hepatocellular carcinoma. *Int. J. Mol. Sci.* 22, 3208. doi: 10.3390/ijms22063208

Joo, J. Y., Cha, G. S., Kim, H. J., Lee, J. Y., and Choi, J. (2020). Atheroprotective nasal immunization with a heat shock protein 60 peptide from porphyromonas gingivalis. *J. Periodontal. Implant. Sci.* 50 (3), 159–170. doi: 10.5051/jpis.2020.50.3.159

Jotwani, R., and Cutler, C. W. (2004) Fimbriated porphyromonas gingivalis is more efficient than fimbria-deficient p. gingivalis in entering human dendritic cells in vitro and induces an inflammatory Th1 effector response. *Infect. Immun.* 72, 1725–3172. doi: 10.1128/IAI.72.3.1725-1732.2004

Jr, L. O., Sordi, R., Oliveira, J. G., Alves, G. F., Mendes, R. T., Santos, F. A., et al. (2018). The role of potassium channels in the endothelial dysfunction induced by periodontitis. *J. Appl. Oral. Sci.* 26, e20180048. doi: 10.1590/1678-7757-2018-0048

Kajikawa, M., Nakashima, A., Maruhashi, T., Iwamoto, Y., Iwamoto, A., Matsumoto, T., et al. (2014). Poor oral health, that is, decreased frequency of tooth brushing, is associated with endothelial dysfunction. *Circ. J.* 78, 950–954. doi: 10.1253/circj.cj-13-1330

Kovac, S., Angelova, P. R., Holmström, K. M., Zhang, Y., Dinkova-Kostova, A. T., and Abramov, A. Y. (2015). Nrf2 regulates ROS production by mitochondria and NADPH oxidase. *Biochim. Biophy. Acta.* 1850, 794–801. doi: 10.1016/j.bbagen.2014.11.021

Krüger-Genge, A., Blocki, A., Franke, R. P., and Jung, F. (2019). Vascular endothelial cell biology: An update. *Int. J. Mol. Sci.* 20, 4411. doi: 10.3390/ijms20184411

Kwon, T., Lamster, I. B., and Levin, L. (2021). Current concepts in the management of periodontitis. *Int. Dent. J.* 71, 462–476. doi: 10.1111/idj.12630

Lamont, R. J., Koo, H., and Hajishengallis, G. (2018). The oral microbiota: dynamic communities and host interactions. *Nat. Rev. Microbiol.* 16, 745–759. doi: 10.1038/s41579-018-0089-x

Lamont, R. J., Verma, R., Bainbridge, B., Demuth, D., and Kesavalu, L (2010). In vivo interaction of p.gingivalis with s.gordonii in periodontal disease. *Iadr Gen. Session.*

Lee, H. R., Jun, H. K., Kim, H. D., Lee, S. H., and Choi, B. K. (2011). Fusobacterium nucleatum GroEL induces risk factors of atherosclerosis in human microvascular endothelial cells and ApoE−/− mice. *Mol. Oral. Microbiol.* 27, 109–123. doi: 10.1111/j.2041-1014.2011.00636.x

Leira, Y., Martín-Lancharro, P., and Blanco, J. (2018). Periodontal inflamed surface area and periodontal case definition classification. *Acta Odontol. Scand.* 76, 195–198. doi: 10.1080/00016357.2017.1401659

Leite, A. R., Borges-Canha, M., Cardoso, R., Neves, J. S., Castro-Ferreira, R., and Leite-Moreira, A. (2020). Novel biomarkers for evaluation of endothelial dysfunction. *Angiology* 71, 397–410. doi: 10.1177/0003319720903586

Liccardo, D., Cannavo, A., Spagnuolo, G., Ferrara, N., Cittadini, A., Rengo, C., et al. (2019). Periodontal disease: A risk factor for diabetes and cardiovascular disease. *Int. J. Mol. Sci.* 20, 1414. doi: 10.3390/ijms20061414

Li, Q., Liu, J., Liu, W., Chu, Y., Zhong, J., Xie, Y., et al. (2020). LOX-1 regulates p. gingivalis-induced monocyte migration and adhesion to human umbilical vein endothelial cells. *Front. Cell. Dev. Biol.* 8. doi: 10.3389/fcell.2020.00596

Lira-Junior, R., Figueredo, C. M., Bouskela, E., and Fischer, R. G. (2014). Severe chronic periodontitis is associated with endothelial and microvascular dysfunctions: a pilot study. *J. Periodontol.* 85, 1648–1657. doi: 10.1902/jop.2014.140189

Li, X., Tse, H., Yiu, K., Li, L., and Jin, L. (2011a). Effect of periodontal treatment on circulating CD34+ cells and peripheral vascular endothelial function: a randomized controlled trial. *J. Clin. Periodontol.* 38, 148–156. doi: 10.1111/j.1600-051X.2010.01651.x

Li, X., Tse, H. F., and Jin, L. J. (2011b). Novel endothelial biomarkers: implications for periodontal disease and CVD. *J. Dent. Res.* 90, 1062–1069. doi: 10.1177/0022034510397194

Loos, B. G. (2016). Periodontal medicine: work in progress! *J. Clin. Periodontol.* 43, 470–471. doi: 10.1111/jcpe.12550

Luyendyk, J. P., Schoenecker, J. G., and Flick, M. J. (2018). The multifaceted role of fibrinogen in tissue injury and inflammation. *Blood* 133, 511–520. doi: 10.1182/blood-2018-07-818211

Lyle, A. N., and Taylor, W. R. (2019). The pathophysiological basis of vascular disease. *Lab. Invest.* 99, 284–289. doi: 10.1038/s41374-019-0192-2

Matsui, S., Kajikawa, M., Maruhashi, T., Iwamoto, Y., Iwamoto, A., Oda, N., et al. (2017). Decreased frequency and duration of tooth brushing is a risk factor for endothelial dysfunction. *Int. J. Cardiol.* 241, 30–34. doi: 10.1016/j.ijcard.2017.03.049

Medina-Leyte, D. J., Zepeda-García, O., Domínguez-Pérez, M., González-Garrido, A., Villarreal-Molina, T., and Jacobo-Albavera, L. (2021). Endothelial dysfunction, inflammation and coronary artery disease: Potential biomarkers and promising therapeutical approaches. *Int. J. Mol. Sci.* 22, 3850. doi: 10.3390/ijms22083850

Meurer, S. K., and Weiskirchen, R. (2020). Endoglin: An 'Accessory' receptor regulating blood cell development and inflammation. *Int. J. Mol. Sci.* 21, 9247. doi: 10.3390/ijms21239247

Monsarrat, P., Blaizot, A., Kémoun, P., Ravaud, P., Nabet, C., Sixou, M., et al. (2016). Clinical research activity in periodontal medicine: a systematic mapping of trial registers. *J. Clin. Periodontol.* 43, 390–400. doi: 10.1111/jcpe.12534

Moura, M. F., Navarro, T. P., Silva, T. A., Cota, L. O. M., and Costa, F. O. (2017). Periodontitis and endothelial dysfunction: Periodontal clinical parameters and the levels of salivary markers IL-1β, TNF-α, MMP2/TIMP2 complex, and nitric oxide. *J. Periodontol.* 88, 778–787. doi: 10.1902/jop.2017.170023

Noz, M. P., Plachokova, A. S., Smeets, E. M. M., Aarntzen, E., Bekkering, S., Vart, P., et al. (2021). An explorative study on monocyte reprogramming in the context of periodontitis *In vitro* and *In vivo*. *Front. Immunol.* 12. doi: 10.3389/fimmu.2021.695227

Ollauri-Ibáñez, C., López-Novoa, J. M., and Pericacho, M. (2017). Endoglin-based biological therapy in the treatment of angiogenesis-dependent pathologies. *Expert. Opin. Biol. Ther.* 17, 1053–1063. doi: 10.1080/14712598.2017.1346607

Padilla, C., Lobos, O., Hubert, E., González, C., and Descouvieres, C. (2010). Periodontal pathogens in atheromatous plaques isolated from patients with chronic periodontitis. *J. Periodontal. Res.* 41, 350–353. doi: 10.1111/j.1600-0765.2006.00882.x

Pan, S. B., and Yan, F. H. (2019). Effects of Porphyromonas gingivalis infection on inflammatory response of human aortic endothelial cells. *Chinese J. Pract. Stomatol.* 12, 6. doi: 10.19538/j.kq.2019.05.007

Papapanou, P. N., Sanz, M., Buduneli, N., Dietrich, T., Feres, M., Fine, D. H., et al. (2018). Periodontitis: Consensus report of workgroup 2 of the 2017 world workshop on the classification of periodontal and peri-implant diseases and conditions. *J. Periodontol.* 89, S173–S182. doi: 10.1002/JPER.17-0721

Paraskevas, K. I., Baker, D. M., Vrentzos, G. E., and Mikhailidis, D. P. (2008). The role of fibrinogen and fibrinolysis in peripheral arterial disease. *Thromb. Res.* 122, 1–12. doi: 10.1016/j.thromres.2007.06.003

Parvaneh, M., Witting, P. K., Ku, J., Moradi, T., Eroglu, E., Freedman, B., et al. (2021). Periodontitis induces endothelial dysfunction in mice. *Sci. Rep.* 11, 14993. doi: 10.1038/s41598-021-94418-8

Patibandla, P. K., Tyagi, N., Dean, W. L., Tyagi, S. C., and Lominadze, D. (2010). Fibrinogen induces alterations of endothelial cell tight junction proteins. *J. Cell. Physiol.* 221, 195–203. doi: 10.1002/jcp.21845

Paul, O., Arora, P., Mayer, M., and Chatterjee, S. (2020). Inflammation in periodontal disease: Possible link to vascular disease. *Front. Physiol.* 11. doi: 10.3389/fphys.2020.609614

Pereira, R. B., Vasquez, E. C., Stefanon, I., and Meyrelles, S. S. (2011). Oral p. gingivalis infection alters the vascular reactivity in healthy and spontaneously atherosclerotic mice. *Lipids. Health Dis.* 10, 80. doi: 10.1186/1476-511X-10-80

Plachokova, A. S., Andreu-Sánchez, S., Noz, M. P., Fu, J., and Riksen, N. P. (2021). Oral microbiome in relation to periodontitis severity and systemic inflammation. *Int. J. Mol. Sci.* 22, 5876. doi: 10.3390/ijms22115876

Priyamvara, A., Dey, A. K., Bandyopadhyay, D., Katikineni, V., Zaghlol, R., Basyal, B., et al. (2020). Periodontal inflammation and the risk of cardiovascular disease. *Curr. Atheroscler. Rep.* 22, 28. doi: 10.1007/s11883-020-00848-6

Prucsi, Z., Płonczyńska, A., Potempa, J., and Sochalska, M. (2021). Uncovering the oral dysbiotic microbiota as masters of neutrophil responses in the pathobiology of periodontitis. *Front. Microbiol.* 12. doi: 10.3389/fmicb.2021.729717

Rao, A., D'Souza, C., Subramanyam, K., Rai, P., and Kumar, B. K. (2021). Molecular analysis shows the presence of periodontal bacterial DNA in atherosclerotic plaques of patients with coronary artery disease. *Indian. Heart. J.* 73, 218–220. doi: 10.1016/j.ihj.2021.01.011

Roth, G. A., Mensah, G. A., Johnson, C. O., Addolorato, G., Ammirati, E., Baddour, L. M., et al. (2020). Global burden of cardiovascular diseases and risk factor 1990-2019: Update from the GBD 2019 study. *J. Am. Coll. Cardiol.* 76, 2982–3021. doi: 10.1016/j.jacc.2020.11.010

Saffi, M. A. L., Rabelo-Silva, E. R., Polanczyk, C. A., Furtado, M. V., Montenegro, M. M., Ribeiro, I. W. J., et al. (2018). Periodontal therapy and endothelial function in coronary artery disease: A randomized controlled trial. *Oral. Dis.* 24, 1349–1357. doi: 10.1111/odi.12909

Sanz, M., Marco Del Castillo, A., Jepsen, S., Gonzalez-Juanatey, J. R., D'Aiuto, F., Bouchard, P., et al. (2020). Periodontitis and cardiovascular diseases: Consensus report. *J. Clin. Periodontol.* 47, 268–288. doi: 10.1111/jcpe.13189

Schenkein, H. A., and Loos, B. G. (2013). Inflammatory mechanisms linking periodontal diseases to cardiovascular diseases. *J. Clin. Periodontol.* 40, S51–S69. doi: 10.1111/jcpe.12060

Schenkein, H. A., Papapanou, P. N., Genco, R., and Sanz, M. (2020). Mechanisms underlying the association between periodontitis and atherosclerotic disease. *Periodontol. 2000.* 83, 90–106. doi: 10.1111/prd.12304

Sedghi, L. M., Bacino, M., and Kapila, Y. L. (2021b). Periodontal disease: The good, the bad, and the unknown. *Front. Cell. Infect. Microbiol.* 11. doi: 10.3389/fcimb.2021.766944

Sedghi, L. M., DiMassa, V., Harrington, A., Lynch, S. V., and Kapila, Y. L. (2021a). The oral microbiome: Role of key organisms and complex networks in oral health and disease. *Periodontol. 2000.* 87, 107–131. doi: 10.1111/prd.12393

Shao, Y., Saredy, J., Yang, W. Y., Sun, Y., Lu, Y., Saaoud, F., et al. (2020). Vascular endothelial cells and innate immunity. *Arterioscler. Thromb. Vasc. Biol.* 40, e138–e152. doi: 10.1161/ATVBAHA.120.314330

Silva, G. C., Costa, E. D., Lemos, V. S., Queiroz-Junior, C. M., and Pereira, L. J. (2021). Experimental periodontal disease triggers coronary endothelial dysfunction in middle-aged rats: Preventive effect of a prebiotic β-glucan. *J. Gerontol. A. Biol. Sci. Med. Sci.* 76, 1398–1406. doi: 10.1093/gerona/glab066

Slazhneva, E. S., Tikhomirova, E. A., and Atrushkevich, V. G. (2020). Periodontopathogens: a new view. systematic review. part 2. *Pediatr. Dent. Dent. Profilaxis.* 20, 160–167. doi: 10.33925/1683-3031-2020-20-2-160-167

Slots, J. (2017). Periodontitis: facts, fallacies and the future. *Periodontol. 2000.* 75, 7–23. doi: 10.1111/prd.12221

Song, L. T., Tada, H., Nishioka, T., Nemoto, E., Imamura, T., Potempa, J., et al. (2021). Porphyromonas gingivalis gingipains-mediated degradation of plasminogen activator inhibitor-1 leads to delayed wound healing responses in human endothelial cells. *J. Innate. Immun.* 14, 306–319. doi: 10.1159/000519737

Stein, S. H. (2015). Maturation of the host response and its impact upon periodontal disease. *SOJ. Immunol.* 3, 1–4. doi: 10.15226/soji/3/3/00129

Suh, J. S., Kim, S., Boström, K. I., Wang, C. Y., Kim, R. H., and Park, N. H. (2019). Periodontitis-induced systemic inflammation exacerbates atherosclerosis partly *via* endothelial–mesenchymal transition in mice. *Int. J. Oral. Sci.* 11, 21. doi: 10.1038/s41368-019-0054-1

Surma, S., and Banach, M. (2021). Fibrinogen and atherosclerotic cardiovascular diseases-review of the literature and clinical studies. *Int. J. Mol. Sci.* 23, 193. doi: 10.3390/ijms23010193

Suwatanapongched, P., Surarit, R., Srisatjaruk, R., and Offenbacher, S. (2010). Survival of porphyromovas gingivalis in human monocyte cell line. *IADR Gen. Session* 2010.

Takeuchi, H., Furuta, N., Morisaki, I., and Amano, A. (2011). Exit of intracellular porphyromonas gingivalis from gingival epithelial cells is mediated by endocytic recycling pathway. *Cell. Microbiol.* 13, 677–691. doi: 10.1111/j.1462-5822.2010.01564.x

Takeuchi, H., Takada, A., Kuboniwa, M., and Amano, A. (2016). Intracellular periodontal pathogen exploits recycling pathway to exit from infected cells. *Cell. Microbiol.* 18, 928–948. doi: 10.1111/cmi.12551

Tavares, A. C., Bocchi, E. A., and Guimarães, G. V. (2012). Endothelial function in pre-pubertal children at risk of developing cardiomyopathy: a new frontier. *Clinics* 67, 273–278. doi: 10.6061/clinics/2012(03)12

Teeuw, W. J., Slot, D. E., Susanto, H., Gerdes, V. E. A., Abbas, F., D'Aiuto, F., et al. (2014). Treatment of periodontitis improves the atherosclerotic profile: a systematic review and meta-analysis. *J. Clin. Periodontal.* 41, 70–79. doi: 10.1111/jcpe.12171

Thomas, R. Z., Loos, B. G., Teeuw, W., Kunnen, A., van Winkelhoff, A. J., and Abbas, F. (2015). [Periodontitis and systemic diseases: from science to clinical practice]. *Ned. Tijdschr. Tandheelkd.* 122, 542–548. doi: 10.5177/ntvt

Tonetti, M. S., D'Aiuto, F., Nibali, L., Donald, A., Storry, C., Parkar, M., et al. (2007). Treatment of periodontitis and endothelial function. *New. Engl. J. Med.* 378, 2450. doi: 10.1056/NEJMx180022

Tonetti, M. S., and Dyke, T. (2013). Periodontitis and atherosclerotic cardiovascular disease: consensus report of the joint EFP/AAP workshop on periodontitis and systemic diseases. *J. Clin. Periodontol.* 40, S24–S29. doi: 10.1111/jcpe.12089

Velsko, I. M., Chukkapalli, S. S., Rivera-Kweh, M. F., Zheng, D., Aukhil, I., Lucas, A. R., et al. (2015). Periodontal pathogens invade gingiva and aortic adventitia and elicit inflammasome activation in αvβ6 integrin-deficient mice. *Infect. Immun.* 83, 4582–4593. doi: 10.1128/IAI.01077-15

Velsko, I. M., Chukkapalli, S. S., Rivera, M. F., Lee, J. Y., Hao, C., Zheng, D., et al. (2014). Active invasion of oral and aortic tissues by porphyromonas gingivalis in mice causally links periodontitis and atherosclerosis. *Plos. One* 9, e97811. doi: 10.1371/journal.pone.0097811

Verma, R. K., Rajapakse, S., Meka, A., Hamrick, C., Pola, S., Bhattacharyya, I., et al. (2010). Porphyromonas gingivalis and treponema denticola mixed microbial infection in a rat model of periodontal disease. *Interdiscip. Perspect. Infect. Dis.* 2010, 605125. doi: 10.1155/2010/605125

Xie, M., Tang, Q., Nie, J., Zhang, C., Zhou, X., Yu, S., et al. (2020). BMAL1-downregulation aggravates porphyromonas gingivalis-induced atherosclerosis by encouraging oxidative stress. *Circ. Res.* 126, e15–e29. doi: 10.1161/CIRCRESAHA.119.315502

Xu, W., Zhou, W., Wang, H., and Liang, S. (2020). Roles of porphyromonas gingivalis and its virulence factors in periodontitis. *Adv. Protein. Chem. Struct. Biol.* 120, 45–84. doi: 10.1016/bs.apcsb.2019.12.001

Yamamoto, M., Hara, H., Moroi, M., Ito, S., and Sugi, K. (2014). Impaired digital reactive hyperemia and the risk of restenosis after primary coronary intervention in patients with acute coronary syndrome. *J. Atheroscler. Thromb.* 21, 957–965. doi: 10.5551/jat.19497

Yang, S., Cheng, R., Xu, X., Zhang, R., Zhao, Y., Shi, X., et al. (2022). Periodontitis exacerbates endothelial dysfunctions partly *via* endothelial-mesenchymal transition in streptozotocin-induced diabetes rats. *J. Periodontal. Res.* 57, 660–669. doi: 10.1111/jre.12994

Yilmaz, O., Verbeke, P., Lamont, R. J., and Ojcius, D. M. (2006). Intercellular spreading of porphyromonas gingivalis infection in primary gingival epithelial cells. *Infect. Immun.* 74, 703–710. doi: 10.1128/IAI.74.1.703-710.2006

Yun, P., Decarlo, A. A., Chapple, C. C., and Hunter, N. (2005). Functional implication of the hydrolysis of platelet endothelial cell adhesion molecule 1 (CD31) by gingipains of porphyromonas gingivalis for the pathology of periodontal disease. *Infect. Immun.* 73, 1386–1398. doi: 10.1128/IAI.73.3.1386-1398.2005

Zelkha, S. A., Freilich, R. W., and Amar, S. (2010). Periodontal innate immune mechanisms relevant to atherosclerosis and obesity. *Periodontol. 2000.* 54, 207–221. doi: 10.1111/j.1600-0757.2010.00358.x

Zhang, C., Chen, H., He, Q., Luo, Y., He, A., Tao, A., et al. (2021). Fibrinogen/AKT/Microfilament axis promotes colitis by enhancing vascular permeability. *Cell. Mol. Gastroenterol. Hepatol.* 11, 683–696. doi: 10.1016/j.jcmgh.2020.10.007

Zhou, J., Chen, S., Ren, J., Zou, H., Liu, Y., Chen, Y., et al. (2022). Association of enhanced circulating trimethylamine n-oxide with vascular endothelial dysfunction in periodontitis patients. *J. Periodontol.* 93, 770–779. doi: 10.1002/JPER.21-0159

Zhou, Q. B., Xia, W. H., Jing, R., Yu, B. B., and Yang, J. Y. (2017). Effect of intensive periodontal therapy on blood pressure and endothelial microparticles in patients with prehypertension and periodontitis: A randomized controlled trial. *J. Periodontol.* 88, 711–722. doi: 10.1902/jop.2017.160447

Zhou, Z. Y., Zhao, W. R., Shi, W. T., Xiao, Y., Ma, Z. L., Xue, J. G., et al. (2019). Endothelial-dependent and independent vascular relaxation effect of tetrahydropalmatine on rat aorta. *Front. Pharmacol.* 10. doi: 10.3389/fphar.2019.00336

Zhu, W., and Lee, S. W. (2016). Surface interactions between two of the main periodontal pathogens: Porphyromonas gingivalis and tannerella forsythia. *J. Periodontal. Implant. Sci.* 46, 2–9. doi: 10.5051/jpis.2016.46.1.2

frontiers | Frontiers in Cellular and Infection Microbiology

TYPE Original Research
PUBLISHED 15 September 2022
DOI 10.3389/fcimb.2022.934298

OPEN ACCESS

EDITED BY
Zheng Zhang,
Nankai University, China

REVIEWED BY
Yuichiro Noiri,
Niigata University, Japan
Maria D'Accolti,
University of Ferrara, Italy

*CORRESPONDENCE
Claudia M. Parra-Giraldo
claudia.parra@javeriana.edu.co

SPECIALTY SECTION
This article was submitted to Microbiome in Health and Disease, a section of the journal Frontiers in Cellular and Infection Microbiology

RECEIVED 02 May 2022
ACCEPTED 10 August 2022
PUBLISHED 15 September 2022

CITATION
Téllez-Corral MA, Herrera-Daza E, Cuervo-Jimenez HK, Arango-Jimenez N, Morales-Vera DZ, Velosa-Porras J, Latorre-Uriza C, Escobar-Arregoces FM, Hidalgo-Martinez P, Cortés ME, Roa-Molina NS, Otero L and Parra-Giraldo CM (2022) Patients with obstructive sleep apnea can favor the predisposing factors of periodontitis by the presence of *P. melaninogenica* and *C. albicans*, increasing the severity of the periodontal disease. *Front. Cell. Infect. Microbiol.* 12:934298. doi: 10.3389/fcimb.2022.934298

Patients with obstructive sleep apnea can favor the predisposing factors of periodontitis by the presence of *P. melaninogenica* and *C. albicans*, increasing the severity of the periodontal disease

Mayra A. Téllez-Corral[1,2,3], Eddy Herrera-Daza[4], Hayde K. Cuervo-Jimenez[2], Natalia Arango-Jimenez[5], Darena Z. Morales-Vera[5], Juliana Velosa-Porras[1], Catalina Latorre-Uriza[1,5], Francina M. Escobar-Arregoces[1,5], Patricia Hidalgo-Martinez[6], Maria E. Cortés[3], Nelly S. Roa-Molina[1], Liliana Otero[1] and Claudia M. Parra-Giraldo[2]*

[1]Centro de Investigaciones Odontológicas, Facultad de Odontología, Pontificia Universidad Javeriana, Bogotá D.C., Colombia, [2]Unidad de Investigación en Proteómica y Micosis Humanas, Facultad de Ciencias, Pontificia Universidad Javeriana, Bogotá D.C., Colombia, [3]Facultade de Odontología, Programa de Pós-graduação em Inovação Tecnológica, Universidade Federal de Minas Gerais, Belo Horizonte, Minas Gerais, Brazil, [4]Departamento de Matemáticas, Facultad de Ciencias, Pontificia Universidad Javeriana, Bogotá D.C., Colombia, [5]Periodoncia, Facultad de Odontología, Pontificia Universidad Javeriana, Bogotá D.C., Colombia, [6]Clínica del Sueño, Hospital Universitario San Ignacio y Facultad de Medicina, Pontificia Universidad Javeriana, Bogotá D.C., Colombia

Objective: The aim of this study was to analyze the cultivable oral microbiota of patients with obstructive sleep apnea (OSA) and its association with the periodontal condition.

Methods: The epidemiology profile of patients and their clinical oral characteristics were determined. The microbiota was collected from saliva, subgingival plaque, and gingival sulcus of 93 patients classified into four groups according to the periodontal and clinical diagnosis: Group 1 (n = 25), healthy patients; Group 2 (n = 17), patients with periodontitis and without OSA; Group 3 (n = 19), patients with OSA and without periodontitis; and Group 4 (n = 32), patients with periodontitis and OSA. Microbiological samples were cultured, classified, characterized macroscopically and microscopically, and identified by MALDI-TOF-MS. The distribution of complexes and categories of microorganisms and correlations were established for inter- and intra-group

of patients and statistically evaluated using the Spearman *r* test (*p*-value <0.5) and a multidimensional grouping analysis.

Result: There was no evidence between the severity of OSA and periodontitis ($p = 0.2813$). However, there is a relationship between the stage of periodontitis and OSA ($p = 0.0157$), with stage III periodontitis being the one with the highest presence in patients with severe OSA (prevalence of 75%; $p = 0.0157$), with more cases in men. The greatest distribution of the complexes and categories was found in oral samples of patients with periodontitis and OSA (Group 4 P-OSA); even *Candida* spp. were more prevalent in these patients. Periodontitis and OSA are associated with comorbidities and oral conditions, and the microorganisms of the orange and red complexes participate in this association. The formation of the dysbiotic biofilm was mainly related to the presence of these complexes in association with *Candida* spp.

Conclusion: Periodontopathogenic bacteria of the orange complex, such as *Prevotella melaninogenica*, and the yeast *Candida albicans*, altered the cultivable oral microbiota of patients with periodontitis and OSA in terms of diversity, possibly increasing the severity of periodontal disease. The link between yeasts and periodontopathogenic bacteria could help explain why people with severe OSA have such a high risk of stage III periodontitis. Antimicrobial approaches for treating periodontitis in individuals with OSA could be investigated *in vitro* using polymicrobial biofilms, according to our findings.

KEYWORDS

cultivable oral microbiota, periodontitis, obstructive sleep apnea, MALDI-TOF-MS, *Candida albicans*

Introduction

Periodontitis is a chronic infectious disease that affects approximately 50% of adults in the world (Genco and Sanz, 2020). This infection is caused by pathogenic microbial communities known as dysbiotic microbiota. The dysbiotic microbiota produce an inflammatory response of the periodontal tissue resulting in the formation of periodontal pockets, progressive loss of periodontal attachment with the destruction of soft and hard supporting periodontal tissues, and loss of teeth (Hajishengallis and Korostoff, 2017).

This dysbiotic microbiota was described by Socransky (Socransky et al., 1998) who identified genera of microorganisms with certain pathogenicity factors that facilitate the colonization of periodontal tissue. In this way, he proposed six microbial complexes present in subgingival plaque recognized by colors: the yellow complex (*Streptococcus* spp.), the blue complex (*Actinomyces* spp.), the purple complex (*Veillonella* spp.), the green complex (*Eikenella* spp., *Capnocytophaga* spp., and *Campylobacter* spp.), the orange complex (*Eubacterium* sp., *Fusobacterium* spp., *Parviomonas* sp., *Prevotella* spp., *Slackia* sp., and *S. constellatus*), and the red complex (*Porphyromonas* sp., *Tanarella* sp., and *Treponema* sp.). The last two complexes are recognized for grouping the bacteria considered periodontal–pathogenic. Therefore, the periodontal–pathogenic dysbiotic microbiota, which is mostly bacterial, is strongly related to periodontitis as a determining factor in the inflammatory reaction of the periodontal tissues that results in systemic inflammatory events. (Lamont et al., 2018), triggering an exacerbated chronic inflammatory response, which is associated with systemic diseases, such as cardiovascular diseases (CVDs) (Bui et al., 2019), diabetes mellitus (Escobar et al., 2014), and obstructive sleep apnea (OSA) (Gamsiz-Isik et al., 2017).

OSA is a sleep-disordered breathing that occurs when the soft tissues around the upper airway collapse, partially or completely obstructing airflow despite the increased ventilatory effort. It is probably the most common sleep respiratory disorder in adults. OSA is more prevalent in men, and it becomes similar in both sexes after menopause (Ruiz et al.,

2016; Hidalgo-Martínez and Lobelo, 2017). In recent years, OSA has been related to periodontitis. Previous studies have shown that people with OSA have a higher risk of severe periodontitis than people without sleep apnea and that periodontitis is more frequent in young adults with mild OSA (Gunaratnam et al., 2009; Seo et al., 2013; Sanders et al., 2015; Cuervo et al., 2016).

Different mechanisms involving genetic, immunological, and microbiological factors (Al-Jewair et al., 2015; Cade et al., 2016; Nizam et al., 2016; Zhang et al., 2021) have been suggested for the cause–effect relationship between OSA and periodontitis. The genetic predisposition, the inflammatory response shared in both diseases (Nizam et al., 2016), and the oral dryness (Seo et al., 2013) have been described among the hypotheses proposed to explain the increase in periodontitis in patients with OSA. Oral dryness decreases the ability of the immune system to respond to infections, alters bone remodeling stimulated by hypoxia, and increases CO_2 levels (Nizam et al., 2016), enabling an environment that allows the colonization of a different polymicrobial and dysbiotic microbiota, in such a way that there may be a synergistic effect among these factors. Consequently, environmental changes in the oral cavity due to the relationship between periodontitis and OSA would allow associations of bacteria and yeasts (Vieira Colombo et al., 2016; Janus et al., 2017), which can form polymicrobial biofilms in the gingival sulcus. An *in vitro* study showed that *Porphyromona gingivalis*' InlJ protein and *Candida albicans*' hyphal protein Als3 facilitate the adhesion between the two microorganisms and cause significant changes in gene expression by *P. gingivalis*, thereby increasing the pathogenic potential of this bacteria (Sztukowska et al., 2018). In addition, a study revealed that *C. albicans* biofilms encourage the growth of anaerobic bacteria by removing the oxygen that is present and creating a hypoxic microenvironment (Fox et al., 2014).

Therefore, the presence of *Candida* spp. could play an important role in the progression of periodontitis due to its ability to colonize gingival tissue in greater proportion (Tamai et al., 2011; Canabarro et al., 2013; Arumugam, 2015). However, some authors still consider that there is little evidence for the association between periodontitis and OSA, the pathophysiological mechanisms, and the cause–effect relationship between both pathologies (Lembo et al., 2021). Then, it is necessary to start with a periodontal clinic analysis of the microbiological aspects present in patients with these pathologies and their relationship with the periodontal condition and the systemic factors that the patients are exposed to.

Proteomic tools such as Matrix-Assisted Laser Desorption/Ionization Time-of-Flight Mass Spectrometry (MALDI-TOF MS) allow the identification of microorganisms from libraries that store the mass spectrum of their cytoplasmic proteins, especially chaperones and ribosomal proteins. This technology allows the quick identification of up to 200 microorganisms as bacteria and yeasts, both aerobic and anaerobic (Barberis et al., 2014; Antezack et al., 2020). In this study we used MALDI-TOF MS to determine the microbial composition of cultivable oral microbiota (yeast and bacteria) in patients with OSA and its association with the periodontal condition.

Materials and methods

Patients/study population

A convenience sample of 93 eligible participants that fulfilled the inclusion criteria (56 women and 37 men aged 30–72 years) were enrolled from the Sleep Clinic of the *Hospital Universitario San Ignacio* and the Sleep Clinic of the Faculty of Dentistry at the *Pontificia Universidad Javeriana-PUJ*, Bogotá, D.C., Colombia with a polysomnographic diagnosis for OSA, and were included in the present study between April 2019 and March 2021. This study was carried out following the Declaration of Helsinki of 1975 revised in 2000 and approved by the Research and Ethics Committee of the Faculty of Dentistry at the *Pontificia Universidad Javeriana-PUJ* (CIEFOUJ 016B). Informed consent was obtained from all patients after the explanation of conditions and before their clinical examination.

The inclusion criteria were as follows: (1) adults over 30 years old; (2) having at least six teeth in their mouth; and (3) having a polysomnographic study done no more than 6 months before. The exclusion criteria were as follows: (1) smoker; (2) diabetic; (3) having taken antibiotics in the last 3 months; (4) no previous periodontal treatment in the last 3 months; (5) treated with continuous positive airway pressure (CPAP) or bilevel positive airway pressure (BPAP); and (6) having received a pharmacological or surgical treatment for OSA.

All patients were diagnosed by a sleep medicine pulmonologist. The apnea–hypopnea index (AHI) described in the polysomnogram was used to determine the presence and severity of OSA. AHI was calculated as the total number of apneas and hypopneas per hour of sleep. The occurrence of OSA was determined with an AHI score >5; mild OSA with an AHI of 5–15; moderate OSA with an AHI of 16–30; and severe OSA with an AHI >30 (Sateia, 2014). To determine the presence of periodontitis, all patients were examined at the clinic of the Faculty of Dentistry of the PUJ. Panoramic x-rays of each patient were taken and then the specialists in periodontics followed the same protocol to make the periodontal diagnosis of periodontitis stages I, II, III, and IV according to the 2017 World Workshop on the Classification of Periodontal and Peri-implant Diseases and Conditions (Caton et al., 2018). Periodontal probing was performed by two calibrated periodontists who used a North Carolina (Hu-Friedy®) probe to determine the insertion level, the gingival margin, and the pocket depth. Data from six points

around the tooth were collected and bleeding with probing was determined. The presence of biofilm was determined with the O'Leary index (O'Leary et al., 1972). Patients were considered periodontally healthy if they did not bleed while probing and had a pocket depth of less than 3 mm.

The demographic data of the participants were recorded in the medical history, including age, sex, and medical records. The participants were assigned to one of four groups according to the severity of their OSA and their periodontal diagnosis, as follows: Group 1 (H), healthy patients: non-periodontitis and non-OSA ($n = 25$); Group 2 (P), periodontitis and non-OSA patients ($n = 17$); Group 3 (OSA), OSA and non-periodontitis patients ($n = 19$); and Group 4 (P-OSA), periodontitis and OSA patients ($n = 32$).

Oral sample collection

There was no periodontal stimulus performed prior to the collection of the samples (probing, prophylaxis, and calculus removal). Three samples (saliva, subgingival plaque, and gingival sulcus) were taken from the oral cavity of patients. First, they were asked to simply spit into polypropylene tubes containing thioglycolate medium (Oxoid®) to collect approximately 1 ml of unstimulated saliva (Nizam et al.,2014). Immediately, the gingival sulcus sample was collected, performing a relative isolation of the area of the tooth of interest with gauze and cotton rolls, and constant drying with cotton swabs to eliminate saliva contamination. In healthy patients, the gingival sulcus sample collection was any area without bleeding, while in patients with periodontitis, this sample was at a site diagnosed with periodontitis. This sample was taken by inserting standardized absorbent papers (Periopapers, Oral Flow®, Plainview, NY), approximately 3 mm for 30 s into the periodontal sulcus, which were then put into PBS to elute the Periopaper content by vortexing for 10 s and subsequently transferred to polypropylene tubes containing thioglycolate medium (Gamsiz-Isik et al., 2017). The supragingival plaque was removed with a sterile curette and gauze before obtaining the subgingival plaque sample, which was collected with a curette and introduced into polypropylene tubes containing thioglycolate medium (Nizam et al., 2016). The samples were stored at 4°C during transportation until arrival at the laboratory to be processed.

Microbial identification by MALDI-TOF-MS

All oral samples were centrifuged at 4,000 ×*g* for 20 min and the pellet was resuspended in 1 ml of thioglycolate medium. A suspension aliquot was cultivated in BBL Columbia Agar™ with 5% sheep blood and another one in Sabouraud agar (Merck®), and incubated at 37°C for 2 and 7 days in anaerobiosis and aerobiosis conditions, respectively. At the end of the incubation time, each type of microbial colony was characterized macroscopically and microscopically and identified by mass spectrometry with MALDI-TOF MS, using the MALDI Biotyper® system (Bruker Daltonics Inc., Billerica, MA). For this procedure, the direct method for extracting proteins from microorganisms in plaque was performed applying a small amount of colony on a plaque of the MALDI in duplicate, allowing it to dry at room temperature. Subsequently, 1 µl of formic acid was added to the colonies allowed to dry and then 1 µl of the matrix solution (alpha-cyano-4-hydroxycinnamic acid) was added to extract proteins, mainly ribosomal ones present in high concentrations, and again allowed to dry at room temperature. Once this procedure was performed, the mass spectra were acquired using MALDI-TOF-MS equipment (Microflex from® Burker Daltonik Inc). The mass spectra were analyzed within a range of 2,000 to 20,000 m/z. The MALDI Biotyper version 3.0 library and the MALDI Biotyper version 3.1 software were used for identification considering the cutoff scores ≥1.5 for the genus level and ≥1.7 for the species level. Finally, once the colonies were identified, they were stored at −70°C in thioglycolate medium with 20% glycerol for further studies.

Statistical analysis

The first part of this research consisted in the characterization and level of the microbiota for each group. Then, the relative abundances of microorganisms were quantified according to Socransky's microbial complexes (Socransky et al., 1998), adding three categories: yeasts (*Candida* spp.), microorganisms of the oral cavity not classified in the complexes (*Lactobacillus* spp.), and other microorganisms neither classified in the complexes nor associated with specific pathologies in the oral cavity (*Staphylococcus* spp., *Rothia* spp., *Cutibacterium* spp., and *Atopobium* spp.). In the second part, tests were carried out to compare the relative abundance of each category of microorganisms for each type of sample (saliva, subgingival plaque, and gingival sulcus) within each group of patients. The comparison of the relative abundances of microorganisms among the different groups of patients was carried out (p-value <0.5). Finally, association tests were performed within each group using the Spearman r test (p-value <0.5) and a multidimensional grouping analysis according to the abundance of microorganisms common among the groups of patients. The tests GraphPad Prism 9.0.2 (GraphPad Software, California, USA), the free software R 4.01 license GPNU (Free Software Foundation, Boston, USA), and XLSTAT statistical and data analysis solution (Addinsoft, New York, USA) were used.

Results

The demographic data, medical history and periodontal parameters of the patients are presented in Table 1. The ratio of women to men was high in all groups, except in the Group 4 (P-OSA), where there was a higher percentage of men. The periodontal clinical parameters showed statistically significant differences between Group 1 (H) and the other groups of patients ($p < 0.05$) in relation to the percentage of teeth with periodontitis and the percentage of biofilm (Table 1).

Regarding the periodontal condition, it was evidenced that 56% of patients in Group 1 (H) had biofilm-induced gingivitis in a reduced periodontium vs. clinical gingival health on an intact periodontium ($p = 0.000419$), followed by stable periodontal disease in a reduced periodontium with a 32% prevalence vs. clinical gingival health on an intact periodontium ($p = 0.03248$). These conditions are considered in healthy patients according to the latest classification of periodontal diseases (Caton et al., 2018). In Group 2 (P), 65% of patients presented stage III periodontitis vs. stage I periodontitis ($p = 0.0012$). In Group 3 (OSA), 79% of patients presented biofilm-induced gingivitis in a reduced periodontium vs. Group 1 ($p = 0.024$). In Group 4 (P-OSA), 81% of the patients presented stage III periodontitis vs. Groups 1 and 3 ($p < 0.0001$). Regarding the diagnosis of OSA according to the degree of severity in Group 3 (OSA), 63% of patients presented mild OSA (mild OSA vs. moderate OSA: $p = 0.006$; mild OSA vs. severe OSA: $p = 0.023$), 16% presented moderate OSA and 21% presented severe OSA, with mild OSA being the most prevalent. However, in Group 4 (P-OSA), 19% of patients had mild OSA, 31% had moderate OSA, and 50% had severe OSA ($p = 0.02$), showing statistically significant differences between Group 3 (OSA) and Group 4 (P-OSA) ($p = 0.04$) (Table 2).

Similarly, when the link between OSA and periodontitis was investigated, it was found that 35% of individuals with periodontitis had mild OSA, 71% had moderate OSA, and 80% had severe OSA. Although the association between OSA and periodontitis did not show statistically significant difference ($p = 0.2813$), the stage III periodontitis was statistically significant with severe OSA ($p = 0.0157$) (Table 3).

Distribution of complexes and categories of microorganisms

A general descriptive analysis of all groups showed that the relative frequency in the presence of the microorganisms for the purple complex, the categories of *Candida* spp., *Lactobacillus* spp., and others, was higher in saliva and the relative frequency of the other complexes was higher in subgingival plaque (Table 4).

The percentages of microorganisms for each complex and category were adjusted to percentages of relative frequency according to the total number of microorganisms identified by complex and category in each group of patients and the total number of microorganisms identified by each group. In this way, the microbial composition inter- and intra-group of patients was analyzed. According to the inter-group analysis (Figure 1, bar graph) there is a greater number of microorganisms distributed in all complexes and categories in Group 4 (P-OSA), highlighting the greater presence of microorganisms of the

TABLE 1 Demographic data and clinical characteristics of the groups of patients.

	Group 1 (H) ($n = 25$)	Group 2(P) ($n = 17$)	Group 3 (OSA) ($n = 19$)	Group 4(P-OSA) ($n = 32$)
Demographic parameters				
Age (years), mean (SD)	46 (14)	41 (10)	50 (13)	49 (11)
Sex (female) (%)	80	76	63	34
Sex (male) (%)	20	24	37	66
Systemic conditions				
HTN (%)	12	18	42	19
HLD (%)	8	6	11	3
HT (%)	8	18	11	19
Clinical parameters				
Teeth present, mean (SD)	26.0 (3.92)	26.8 (2.22)	23.89 (6.29)	25,22 (5.59)
Missing teeth, mean (SD)	5.96 (3.92)	5.23 (2.22)	8.1 (6.29)	6.78 (5.62)
Percentage of teeth with periodontitis, mean (SD)	1.94 (3.57)	43.83 (24) *	1.62 (3.15)	38.48 (21.25) *
Presence of caries (%)	12	18	5	31
Percentage of biofilm, mean (SD)	23 (16)	45.2 (25.95) **	38.6 (20.63) **	40.6 (18.7) **

Group 1 (H) healthy patients, non-periodontitis, and non-OSA; Group 2 (P) periodontitis and non-OSA patients; Group 3 (OSA) OSA and non-periodontitis patients; Group 4 (P-OSA) periodontitis and OSA patients. SD, standard deviation. HTN, arterial hypertension; HLD, hyperlipidemia; HT, hypothyroidism. Significant differences, G1 (S) vs. G2 (P) p ≤ 0.0001*; G1 (S) vs. G4 (PA) p ≤ 0.0001*; G1 (S) vs. G2 (P) **p = 0**.0014**; G1 (S) vs. G3 (P) p = 0.0072**, G1 (S) vs. G4 (P) p = 0.0004**. Multiple **t**-test (multiple comparisons using the Bonferroni–Dunn method).

TABLE 2 Percentage of patients of each group according to periodontal condition and degree of OSA.

	Group 1 (H) (n = 25)	Group 2 (P) (n = 17)	Group 3 (OSA) (n = 19)	Group 4 (P-OSA) (n = 32)	p-value*	p-value‡
	Percentage (%)					
Periodontal condition						
Clinical gingival health on an intact periodontium	4	0	5	0	ns	ns
Biofilm-induced gingivitis	8	0	0	0	ns	ns
Biofilm-induced gingivitis in a reduced periodontium	56*	0	79‡	0	0.000419	0.024
Stable periodontal disease in reduced periodontium	32*	0	16	0	0.03248	ns
Periodontitis Stage I	0	6	0	0	ns	ns
Periodontitis Stage II	0	24	0	16	ns	ns
Periodontitis Stage III	0	65*	0	81‡	0.0012	0.0001
Periodontitis Stage IV	0	6	0	3	ns	ns
Degree of OSA						
Mild OSA	0	0	63*‡	19	0.006	0.023
Moderate OSA	0	0	16	31	ns	ns
Severe AOS	0	0	21	50*‡	0,02	0,04

Group 1 (H): p-value* of Clinical gingival health on an intact periodontium vs. Biofilm-induced gingivitis in a reduced periodontium and Clinical gingival health on an intact periodontium vs. Stable periodontal disease in reduced periodontium. Group 2 (P): p-value* of Periodontitis Stage I vs. Periodontitis Stage III. Group 3 (OSA): p-value* of Mild OSA vs. Moderate OSA; p-value‡ of Mild OSA vs. Severe AOS, and Clinical gingival health on an intact periodontium vs. Biofilm-induced gingivitis in a reduced periodontium. Group 4 (P-OSA): p-value* of Mild OSA vs. Severe AOS; p-value‡ of Moderate OSA vs. Severe AOS, and Periodontitis Stage I vs. Periodontitis Stage III.

TABLE 3 Frequency and percentage of the periodontal condition according to apnea diagnosis.

Periodontal diagnosis	OSA Diagnosis								p-value
	Non-OSA		Mild OSA		Moderate OSA		Severe OSA		
	Fr	%	Fr	%	Fr	%	Fr	%	
Non-periodontitis	25	60	11	65	4	29	4	20	0.2813
Stage I Periodontitis (Mild)	1	2	0	0	0	0	0	0	0.0157
Stage II Periodontitis (Moderate)	3	7	1	6	3	21	1	5	
Stage III Periodontitis (Severe)	12	29	5	29	6	43	15	75	
Stage IV Periodontitis (Advanced)	1	2	0	0	1	7	0	0	
Total	42	100	17	100	14	100	20	100	

Fr: Frequency, %: Percentage; two-way ANOVA, $p < 0.05$.

TABLE 4 Relative frequencies of the distribution of complexes and categories by samples in the groups of patients.

	Yellow complex	Blue complex	Purple complex	Green complex	Orange complex	Red complex	*Candida* spp.	*Lactobacillus* spp.	Other
Saliva	0.32	0.14	**0.54**	0.17	0.28	0.25	**0.50**	**0.71**	**0.54**
Subgingival plaque	**0.44**	**0.50**	0.37	**0.50**	**0.45**	**0.75**	0.42	0.16	0.28
Gingival sulcus	0.24	0.36	0.09	0.33	0.28	0.00	0.08	0.12	0.18

The bold values means Kruskal-Wallis chi-squared p-value < 0.05.

10.3389/fcimb.2022.934298

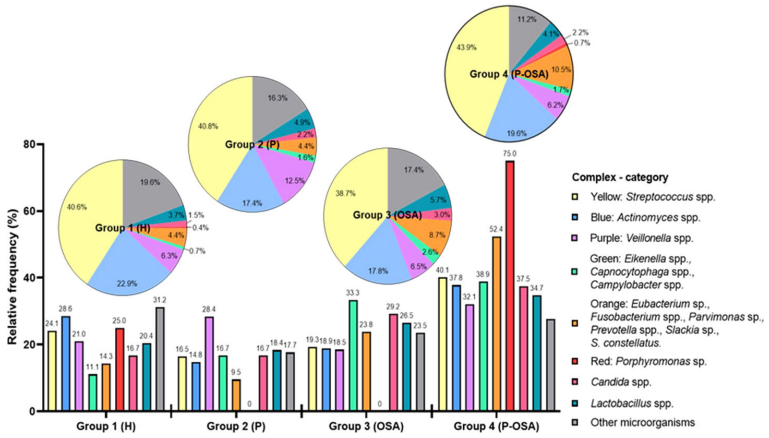

FIGURE 1
Microbial community composition is grouped by complexes or categories. Bars indicate the percentages of the inter-group relative frequencies of the complexes/categories in group patients. Pie charts show the intra-group distribution percentages of complexes/categories in group patients: Group 1 (H) healthy patients, non-periodontitis and non-OSA; Group 2 (P) periodontitis and non-OSA patients; Group 3: (OSA) OSA and non-periodontitis patients; Group 4 (P-OSA) periodontitis and OSA patients.

yellow (40.1%), blue (37.8%), purple (32.1%), green (38.9%), orange (52.4%), and red (75%) complexes as well as *Candida* spp. (37.5%) and *Lactobacillus* spp. (34.7%); on the contrary, other microorganisms had a greater frequency in Group 1 (H) (31.2%). Regarding the intra-group analysis, there was a different composition of complexes and categories. The highest frequency of microorganisms of the yellow complex was found in Group 4 (P-OSA) (43.9%); the blue complex had a higher frequency (22.9%) in Group 1 (H); the purple complex had a higher frequency (12.5%) in Group 2 (P); the green complex (2.6%), *Candida* spp. (3.0%), and *Lactobacillus* spp. (5.7%) had a higher frequency in Group 3 (OSA); the orange (10.5%) and the red (0.7%) complexes had a higher frequency of microorganisms in Group 4 (P-OSA); and, finally, other microorganisms (19.6%) were identified more frequently in Group 1 (H).

Regarding the distribution of the complexes in each sample (saliva, subgingival plaque, and gingival sulcus), it was evident that the greatest distribution of the complexes and categories was found in saliva and gingival sulcus of Group 4 (P-OSA), except for other microorganisms. On the other hand, there was a greater distribution of all complexes in subgingival plaque, except for *Candida* spp. and *Lactobacillus* spp. in this same group of patients. Additionally, this distribution was not group-dependent either in subgingival plaque or in gingival sulcus. The comparison of the distribution for each complex and the categories in the oral samples in the different groups showed no significant differences for yellow and orange complexes ($p = 0.1988$ and $p = 0.3045$, respectively). However, there were significant differences in the distribution of the blue complex between the Group 1 (H) saliva samples and the Group 2 (P) subgingival plaque sample ($p = 0.026$). In addition, there were significant differences ($p = 0.009$) in the distribution of the purple complex between saliva (Group 1, H) and gingival sulcus (Group 4, P-OSA). Also, there were significant differences ($p = 0.017$) in the distribution of *Lactobacillus* spp. between saliva (Group 1, H) and gingival sulcus (Group 4, P-OSA). The distribution of other microorganisms between the saliva (Group 1, H) and gingival sulcus (Group 3, OSA) was statistically significant ($p = 0.019$) (Kruskal–Wallis chi-square method; p-value < 0.05) (Figure 2). Additionally, it was determined that *S. salivarius, S. gordonii, S. oralis, A. odontolyticus, A. naeslundii, V. parvula, E. corrodens, P. micra, F. nucleatum, P. melaninogenica, P. gingivalis, C. albicans, L. paracasei*, and *Staphylococcus* spp. were the most frequent species identified in oral samples from all the groups of subjects (Supplementary Table 1).

Association between medical history and cultivable oral microbiota

This association was established through the analysis of multicomponent matrices to correlate the comorbidities and oral conditions and the complexes and categories of microorganisms present in the four groups of patients evaluated. The association can be positive (+) or negative (−) according to the Spearman correlation range (r_s). R_s values greater than zero in blue tones represent a positive correlation, while r_s values less than zero in reddish tones represent a negative correlation (Figure 3). In Group 1 (H), there was a positive, statistically significant correlation between the percentage of biofilm and the presence of caries ($r_s = 0.44$) and the presence of blue complex ($r_s = 0.34$), green complex ($r_s = 0.34$), and orange complex ($r_s = 0.41$). Also, it is noteworthy that

10.3389/fcimb.2022.934298

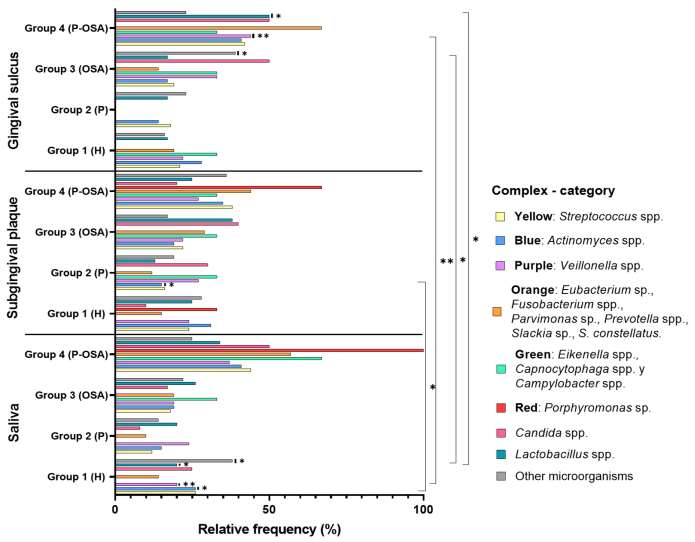

FIGURE 2
Relative frequencies of the complexes/categories in the oral samples by groups of patients. Significant differences between the relative frequencies of the complexes in each group were evaluated using the Kruskal-Wallis chi-square method; *p-value < 0.05, **p-value < 0.01.

the blue and green complexes are correlated with the percentage of biofilm (r_s = 0.54 and 0.37, respectively), in contrast to *Lactobacillus* spp. and the percentage of the biofilm, which showed a negative correlation (r_s = −0.44). Also, there was a positive correlation between the yellow complex and the blue complex (r_s = 0.43) and a negative correlation between the yellow complex and the red complex, with slight statistical significance (r_s = −0.33) (Figure 3A).

In Group 2 (P), there was a positive correlation with statistical significance between age and the presence of caries as with the percentage of biofilm (r_s = 0.51 and 0.45, respectively). In turn, the percentage of biofilm is positively correlated with hypertension, hypothyroidism, and the presence of calculus (r_s = 0.54, 0.50, and 0.59 respectively). Also, the presence of *Candida* spp. was positively correlated with the presence of caries (r_s = 0.62) and the yellow complex (r_s = 0.50). Even though the percentage of teeth with periodontitis, the stage of periodontitis, and the presence of calculus were negatively correlated with the orange complex (r_s = −0.43, −0.52, and −0.50, respectively), they were positively correlated with the green complex and other microorganisms, which likewise presented a positive correlation between them (r_s = 0.65). In addition, there was a positive correlation between the number of teeth absent and the presence of other microorganisms (r_s = 0.43). Other microorganisms have a negative correlation with the presence of *Candida* spp. and the yellow complex (r_s = −0.49 and −0.59, respectively) (Figure 3B).

In Group 3 (OSA), the age of the patients had a positive statistically significant correlation with hypertension and the degree of severity of OSA (r_s = 0.48 and 0.45, respectively). In addition, HTN was positively correlated with severity of OSA (r_s = 0.64), the yellow complex (r_s = 0.38), and the blue complex (r_s = 0.40). When analyzing the percentage of teeth with periodontitis, it was possible to identify a positive correlation with the presence of caries (r_s = 0.50), the severity of OSA (r_s = 0.43), and the presence of *Candida* spp. (r_s = 0.55). The presence of caries and number of decayed teeth were positively correlated with the percentage of biofilm (r_s = 0.39); the yellow (r_s = 0.39), blue (r_s = 0.40), and green r_s = 0.51) complexes; and *Candida* spp. (r_s = 0.48). In turn, the percentage of biofilm correlated positively with the presence of the yellow and blue complexes (r_s = 0.56 and 0.40, respectively). The blue complex was correlated positively with the presence of calculus and the severity of OSA (r_s = 0.45 and 0.48, respectively). When analyzing the relationship between the presence of the complexes, it was evidenced that the yellow complex is positively correlated with *Candida* spp. with a slight statistical significance (r_s = 0.38). A similar correlation was given between the blue and the green complexes (r_s = 0.38), which had a positive correlation with the orange complex (r_s = 0.50). The latter complex was positively correlated with the purple complex (r_s = 0.55), and *Candida* spp. and *Lactobacillus* spp. presented a positive correlation (r_s = 0.41). Other microorganisms presented a negative correlation with the presence of the yellow complex (r_s = −0.43), purple complex (r_s = −0.52), and *Lactobacillus* spp. (r_s = −0.58) (Figure 3C).

In Group 4 (P-OSA), the age of the patients was correlated positively with the HTN (r_s = 0.41), absence of teeth (v = 0.70), the orange complex (r_s = 0.41), and the red complex (r_s = 0.32). Similarly, it was found that HTN has a positive correlation with HLD (r_s = 0.37) and the severity of OSA (r_s = 0.48). The lack of teeth in patients with periodontitis and OSA has been shown to be

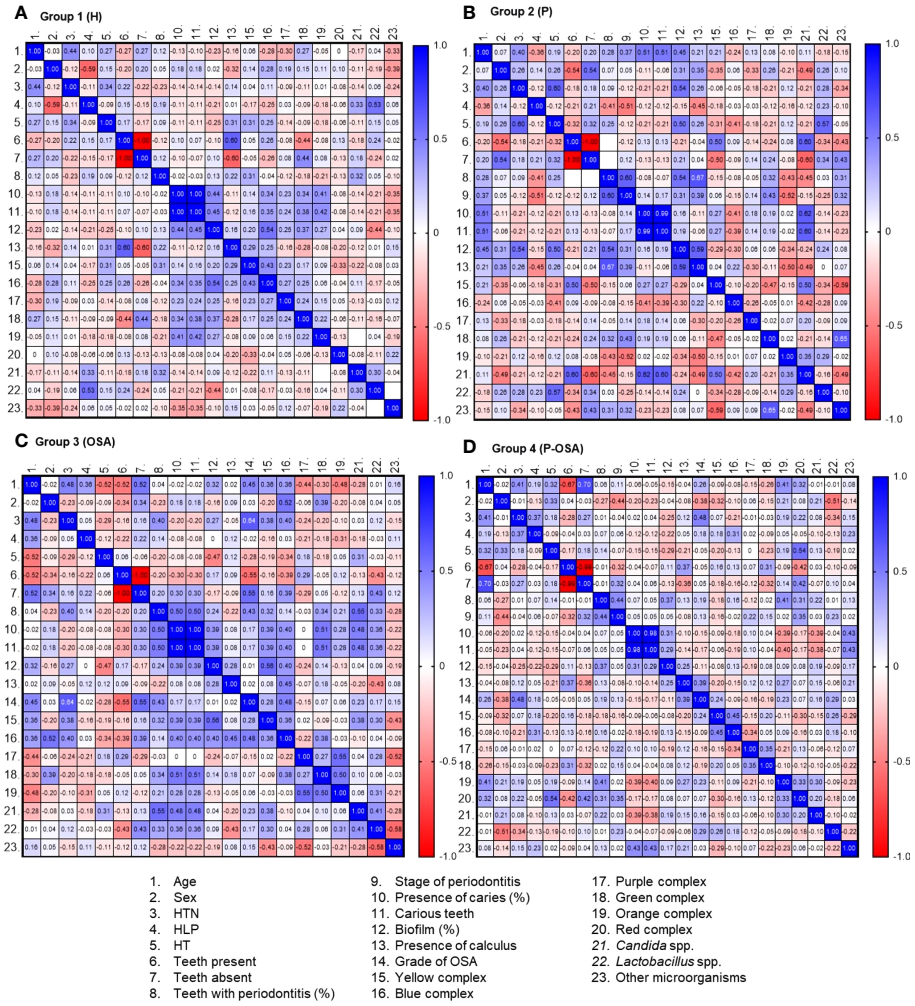

FIGURE 3
Multicomponent matrix for the correlation of clinical factors and complex/categories of microorganisms present in each of the groups of patients evaluated: **(A)** Group 1 (H), n = 25; **(B)** Group 2 (P), n = 17; **(C)** Group 3 (OSA), n = 19; **(D)** Group 4 (P-OSA), n = 32, using the Spearman's rank correlation coefficient rs > 0.30, p<0.05. The blue tones represent a positive correlation and the red tones represent a negative correlation. HTN, arterial hypertension. HLD, hyperlipidemia. HT: hypothyroidism.

strongly connected with periodontitis stage (r_s = 0.32) and the presence of red complex bacteria (r_s = 0.42). On the other hand, the percentage of teeth with periodontitis was correlated with the percentage of biofilm (r_s = 0.37), the presence of the orange complex (r_s = 0.41), and slightly with the red complex (r_s = 0.31). In this group of patients, the presence of calculus was positively correlated with the severity of OSA (r_s = 0.39) and the stage of periodontitis was positively correlated with the presence of the red complex (r_s = 0.35). About the correlation of the presence of the complexes, there was a positive correlation between the yellow and blue complexes (r_s = 0.45), the purple and green complexes (r_s = 0.35), the orange and red complexes (r_s = 0.33), and the orange complex with *Candida* spp. (r_s = 0.30) (Figure 3D).

Prevalence of complexes and categories

Figure 4 presents the percentile plots that indicate the prevalence of the complexes and categories in each group of patients evaluated. This figure indicates that the yellow complex was detected in 27% of the patients of Group 1 (H), who harbored up to 8% of the microorganisms of this complex. In Group 2 (P), it was detected in 18% of the patients, who harbored up to 11% of the microorganisms of this complex. In Group 3 (OSA), it was detected in 21% of the patients, who presented up to 14% of the microorganisms of the complex. In Group 4 (P-OSA), it was detected in 35% of the patients, who presented up to 7% of the microorganisms of the yellow

10.3389/fcimb.2022.934298

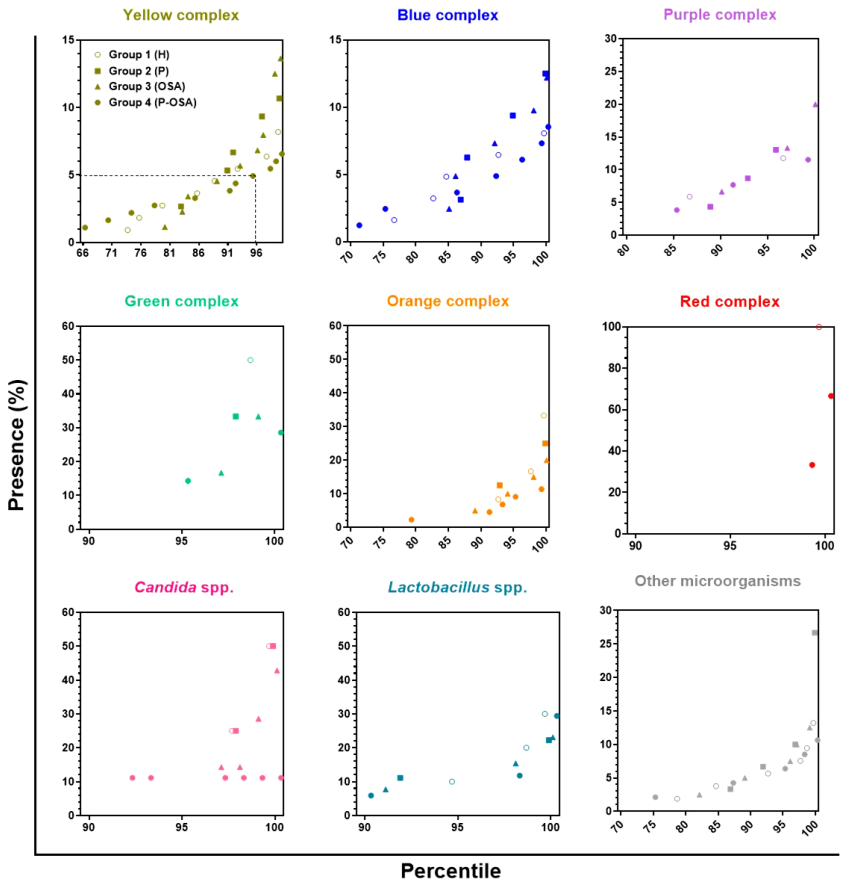

FIGURE 4
Percentile graph of the percentage of presence of complexes/categories in each of the groups of participants evaluated. Each point represents the presence (%) of the complex/category in a patient. The x-axis represents the percentiles, the y-axis the presence (%) of the complexes/categories, and the dotted line in the first panel indicates that 95% of the participants in Group 4 (P-OSA) have less than 5% presence of the yellow complex, on the other hand, 5% of the subjects of this same group exhibit > 5% presence of the yellow complex.

complex. The blue complex was detected in 24% of the patients of Group 1 (H), 14% of the patients of Group 2 (P), 16% of the patients of Group 3 (OSA), and 30% of the patients of Group 4 (P-OSA), who presented up to 8%, 13%, 12%, and 9% of the microorganisms of this complex, respectively. The purple complex was detected in 14%, 12%, 11%, and 16% of the patients of Group 1 (H), Group 2 (P), Group 3 (OSA), and Group 4 (P-OSA), respectively, who presented respectively up to 12%, 13%, 20%, and 11% of the microorganisms of this complex. The green complex was detected in 2%, 3%, 4%, and 6% of the patients of Group 1 (H), Group 2 (P), Group 3 (OSA), and Group 4 (P-OSA), respectively, who presented up to 50%, 33%, 33%, and 29% of the microorganisms of this complex, respectively. The orange complex was detected in 8% of the patients of Group 1 (H) and Group 2 (P), and in 12% and 28% of the patients of Group 3 (OSA) and Group 4 (P-OSA) respectively, who presented up to 33%, 25%, 20%, and 11% of the microorganisms of this complex, respectively. The red complex was detected in 1% of Group 1 (H) and 2% of Group 4 (P-OSA) patients. The category *Candida* spp. was detected in 3% of the patients of Group 1 (H) and Group 2 (P), which housed up to 50% of the yeasts of this category, and on the other hand, this category was detected in 4% of the patients of Group 3 (OSA) and 9% of the patients of Group 4 (P-OSA), which presented up to 42% and 11% of the yeasts of this category, respectively. The category *Lactobacillus* spp. was detected in 6%, 9%, 10%, and 11% of the patients of Group 1 (H), Group 2 (P), Group 3 (OSA), and Group 4 (P-OSA), respectively, who housed up to 30%, 22%, 23%, and 29% of *Lactobacillus* spp., correspondingly. Finally, the category other microorganisms was detected in 22%, 14%, 19%, and 26% of the patients of Group 1 (H), Group 2 (P), Group 3 (OSA), and Group 4 (P-OSA), who presented up to 13%, 27%, 12.5%, and 10.6% of the microorganisms in this category, respectively (Figure 4). All complexes and categories of *Candida* spp., *Lactobacillus* spp., and other microorganisms were more prevalent in Group 4

(P-OSA); however, no statistically significant differences were found.

Multidimensional scaling analysis

To show the differences between the consortia of the most common microorganisms present in each group of patients, we performed a multidimensional scaling (MDS) analysis. This analysis was established according to the dissimilarity (distance matrix) of the microorganisms present in each consortium, through the stress adjustment measure that is based on the differences between the predicted and actual distances and visualized in 3D plots (Figure 5). Six clusters formed the consortiums of microorganisms in both the group of healthy patients (Group 1) and the group of patients with periodontitis (Group 2), which showed the greatest intra-group dissimilarity (Kruskal stress = 0.188 and 0.198, respectively); on the other hand, two clusters formed the consortium of microorganisms in patients with OSA (Group 3) and six clusters formed the consortium of microorganisms in patients with periodontitis and with OSA (Group 4), which showed the smallest intra-group dissimilarity (Kruskal stress = 0.009 and 0.094, respectively).

In Group 3, dimension 3 was defined by *Streptococcus anginosus* (yellow complex) and dimensions 1 and 2 were composed of the rest of the common microorganisms; this means that the presence of *S. anginosus* could be a distinctive marker within the patients of this group, in terms of the most common microorganism found. On the other hand, in Group 4, another microorganism was found as the most common or distinctive marker: *Capnocytophaga ochracea* (green complex), which defined dimension 3 but with a negative modulation, while the positive axis of dimensions 1 and 2 was differentiated by *Actinomyces georgiae* (blue complex), *Prevotella melaninogenica* (orange complex), and *C. albicans*, the three of them forming a cluster, and *Lactobacillus paracasei* predominated in the positive axis of dimension 3.

Discussion

This is the first report regarding the characterization of the oral microbiota in patients with periodontitis associated with

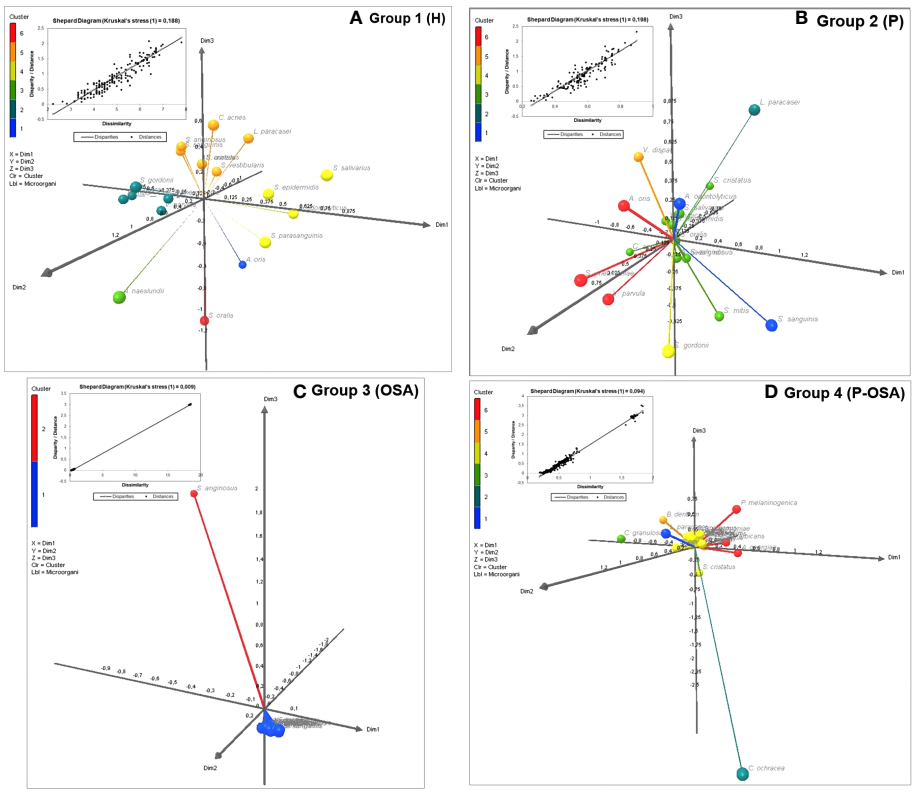

FIGURE 5
Multidimensional Scaling (MDS) based on Proximity Matrices (Euclidean Distance) and Kruskal Stress for the three-dimensional visualization (XLSTAT3DPlot) of the consortia made up of the most common microorganisms by group of patients: **(A)** Group 1 **(H)**; **(B)** Group 2 (P); **(C)** Group 3 (OSA); **(D)** Group 4 (P-OSA).

OSA using MALDI-TOF MS as a tool for rapid identification of oral microorganisms. Additionally, the differences in the oral microbiota between individuals with and without periodontitis, and with and without OSA had not been reported before. The present study showed that there are more cases of stage III periodontitis in patients with severe OSA. Our results are similar to the findings reported by Gamsiz-Isik et al. (2017) and support the hypothesis that there is a higher prevalence of periodontitis in patients with OSA (Gunaratnam et al., 2009; Ahmad et al., 2013; Seo et al., 2013; Cuervo et al., 2016; Gamsiz-Isik et al., 2017; Latorre et al., 2018).

When determining the periodontal parameters of the patients evaluated in this study, a higher percentage of biofilm in patients with periodontitis, with OSA, and with both conditions was detected in opposition to healthy patients ($p < 0.01$). This finding is consistent with the significant relationship between the presence of OSA and the percentage of biofilm reported by Loke et al. (2015) and by Gamsiz-Isik et al. (2017). The evidence suggests that the colonization of a dysbiotic microbiota favored by oral dryness increases CO_2 levels and decreased O_2, and those three are the main factors involved in the pathophysiology of OSA (Nizam et al., 2016), which, in turn, affects bone remodeling in patients with periodontitis.

In the present study, a characterization of the microbiota established in patients with OSA and periodontitis was carried out. It was possible to determine the highest relative frequencies of all of the Socransky's complexes in the subgingival plaque, except the purple one, while the purple complex, *Candida* spp., *Lactobacillus* spp., and other microorganisms presented the highest relative frequencies in saliva. Although it was evidenced that the complexes and categories of microorganisms are present in all the groups evaluated, a greater microbial diversity was demonstrated in the patients with both conditions (OSA and periodontitis). All groups showed different percentages of microorganisms according to the sample evaluated (saliva, subgingival plaque, or gingival sulcus), raising a possible "modulation" of the microorganisms depending on the state of health or disease (Socransky and Haffajee, 2005; Curtis et al., 2020).

The use of the MALDI-TOF MS, which only identifies cultivable microorganisms, was one of the study's limitations. This method might have an impact on the findings and might have omitted the presence of other microorganism species. Additionally, these findings should be validated in further studies with a bigger sample and in other populations.

Despite the limitations in having carried out microbial identification by MALDI-TOF MS, it is important to highlight that our results are comparable to those of prior studies and support the hypothesis that OSA influences the colonization of a potentially infectious dysbiotic microbiota in the oral cavity, as other authors have proposed. Nizam et al. (2016) determined a marked increase in Gram-negative bacteria in dental plaque samples in patients with severe OSA and periodontal disease and also reported Gram-positive bacteria in dental plaque in severe cases of OSA (Nizam et al., 2016), whereas Chen et al. (2021) determined that well-known periodontal pathogen species do not significantly increase their relative abundance in patients with OSA; however, the salivary microbial community structure was altered, affecting the interactions of different bacteria in the pathogenesis process of periodontitis in patients with OSA, along with an increase of *Prevotella* spp. In the present study, we identified the most common microorganisms in patients with both periodontitis and OSA (P-OSA), highlighting the presence of *A. georgiae, P. melaninogenica, L. paracasei , and C. albicans*, as potential distinctive markers for both diseases. These results might explain the presence of periodontitis in patients with OSA.

Concerning the association of clinical factors and the oral microbiota characterized in each group of patients, the relationship between the percentage of biofilm and other oral pathologies such as caries was evidenced, given the presence of microorganisms mainly of the yellow and blue complexes in healthy patients. This finding is consistent with previous reports in the literature (Colombo and Tanner, 2019; Valm, 2019). Despite not fulfilling all the parameters to be classified into the group of periodontitis according to the new classification adopted since 2018 (Caton et al., 2018), the presence of teeth with periodontitis was detected in these patients, and it was related to the bacteria of the yellow complex and *Candida* spp. These data are relevant considering that different authors have reported the colonization of yeasts of the genus *Candida*, especially *C. albicans*, in periodontal pockets of patients with severe chronic periodontitis (Canabarro et al., 2013), and the prevalence of these species was 50% and 60% in patients with aggressive and chronic periodontitis, respectively (Vieira Colombo et al., 2016). These previous results suggest that *C. albicans* plays a role in the progression of conditions such as periodontitis, given its known pathogenic power to invade oral epithelial tissue, form hyphae, secrete proteinases, and interact with commensal streptococci to synergistically promote their virulence (Martin et al., 2011; Xu et al., 2014; Belibasakis et al., 2015; Charalampakis and Belibasakis, 2015; Chevalier et al., 2017; Mombelli, 2018).

In recent decades, there has been an increase in reports demonstrating the bidirectional risk between periodontitis and systemic diseases such as hypertension (Latorre et al., 2018), CVDs (Bui et al., 2019), hypothyroidism, metabolic syndromes (Jaramillo et al., 2017), and diabetes (Zhou et al., 2013; Escobar et al., 2014; Genco and Borgnakke, 2020). In older patients, this risk was confirmed by the correlation of the percentage of biofilm detected in patients of Group 2 (P) with age of patients ($r_s = 0.45$, $p = 0.035$), and with diseases such as hypertension ($r_s = 0.54$, $p = 0.0162$) and hypothyroidism ($r_s = 0.50$, $p = 0.0023$). Additionally, the cases of caries present in this group of subjects were associated with the presence of *Candida* spp. and, in turn, with the bacteria of the yellow complex, contributing to the hypothesis that yeasts of the

genus *Candida* can behave as a primary colonizer in dysbiotic biofilms (Janus et al., 2017). The percentage of teeth with periodontitis was associated with the percentage of biofilm and the presence of calculus. These results confirm that the formation of polymicrobial consortia is one of the main factors contributing to the risk of periodontitis. In Group 2 (P), periodontitis was mainly associated with the presence of green complex bacteria, recognized in mature pathogenic biofilms where environments with low oxygen concentrations are produced (Haffajee et al., 2008). Therefore, these findings support the role of these bacteria as indicators of ecological changes in the subgingival biofilm during the progression of periodontitis (Henne et al., 2014). Likewise, the category of "other microorganisms", in which those that are not usually identified as oral pathogens were grouped, was also associated with periodontitis. These results confirm the prevalence of other potentially pathogenic species of clinical relevance in the oral cavity as was evidenced by Vieira Colombo et al. (2016) who showed the microbiota of the subgingival plaque of individuals with different states of periodontitis, highlighting the presence of bacteria of the genera *Neisseria*, *Peptostreptococus*, *Pseudomonas*, *Clostridium*, and *Enterobacteria*, among others (Vieira Colombo et al., 2016).

OSA is a risk factor for CVDs, as it increases morbidity and mortality in patients with arterial hypertension (HTN), coronary heart disease, atrial fibrillation, and heart failure (Zhou et al., 2013; Genco and Borgnakke, 2020). The results of our study showed that the severity of OSA in Group 3 was associated with hypertension and with the percentage of teeth with periodontitis. Thus, it is necessary to emphasize that the presence of teeth with periodontitis in this group is correlated with the severity of OSA, caries, and the presence of *Candida* spp., establishing a possible association between the infectious processes in the periodontium and the presence of microorganisms such as *Candida* spp. that are different from the usual periodontopathogens.

The cause–effect relationship between periodontitis and OSA, however, is not fully understood. Several mechanisms have been proposed, involving genetic, immunological, and microbiological factors (Nizam et al., 2014; Al-Jewair et al., 2015). Our findings suggest that there is an association between risk factors such as HTN, HLD, and HT and patient age, which supports the previously reported bidirectional relationship of both diseases (Gunaratnam et al., 2009; Keller et al., 2013; Seo et al., 2013; Sanders et al., 2015; Cuervo et al., 2016; Latorre et al., 2018). Additionally, it was evident that the bacteria of the orange complex participate in this association, together with the red complex, which, in turn, was associated with the loss of teeth and the stage of periodontitis. In the same way, both complexes were associated with the formation of the dysbiotic biofilm (Lamont and Hajishengallis, 2015). While it is true that the presence of bacteria considered periodontopathogenic was associated with the presence of periodontitis in patients with OSA, it is important to note that the presence of *Candida* spp. was more prevalent in patients with periodontitis, and in addition, these yeasts were mainly associated with the bacteria of the orange complex. Then, we propose a new hypothesis: in the presence of both diseases, these opportunistic microorganisms may have a behavior that allows the colonization of periodontopathogenic bacteria. It has been demonstrated through *in vitro* studies that yeasts such as *C. albicans* modulate the microenvironment, causing anoxic conditions, favoring the growth of strictly anaerobic bacteria, and synergistically promoting the formation of dysbiotic biofilms (Diaz et al., 2012; Fox et al., 2014; Sztukowska et al., 2018).

Even if OSA can favor the predisposing factors of periodontitis by the presence of *P. melaninogenica* and *C. albicans* increasing the severity of the periodontal disease, questions arise as to whether the inhibition of these microorganisms can control the pathogenicity of biofilm associated with the conditions evaluated. These findings suggest that antimicrobial strategies for treating periodontitis in patients with OSA can be tested *in vitro* using polymicrobial biofilms.

Conclusions

- *Men had a higher prevalence of stage III periodontitis and severe OSA.
- *There was a greater diversity of microorganisms in the oral samples evaluated from the patients with periodontitis and OSA, and the differences in the percentages of the presence of each complex and category were notorious.
- *The association between periodontitis and OSA was evidenced by sharing risk factors such as comorbidities and bacteria of the orange and red complexes associated with yeasts such as *Candida* spp.
- *Periodontal disease in patients showed positive and similar correlations among yellow, blue, orange, green, and purple bacteria complexes, *P. melaninogenica*, *C. albicans*, and the different oral microenvironments, indicating that the presence of *P. melaninogenica* and *C. albicans* should be considered in the prevention and treatment of this disease.

Data availability statement

The raw data supporting the conclusions of this article will be made available by the authors, without undue reservation.

Ethics statement

This study was reviewed and approved by Comite de etica, Facultad de Odontologia, Pontificia Universidad Javeriana. The patients/participants provided their written informed consent to participate in this study.

Author contributions

MT-C, LO, and CP-G conceived and designed the study. MT-C and EH-D performed the statistical analysis. MT-C and HC-J performed the microbial identification. NA-J and DM-V conducted the periodontal examinations. CL-U and FE-A performed and supervised periodontal examinations. JV-P contributed to data analysis. PH-M practiced medical checks and the polysomnographic study. MT-C wrote the manuscript and prepared the tables and figures. MC, NR-M, LO, and CP-G reviewed and edited the manuscript. All authors contributed to the article and approved the submitted version.

Funding

Pontificia Universidad Javeriana-sede Bogotá financial support to the project "Characterization of the microbiota associated with obstructive sleep apnea in patients with periodontitis" (project number 008398).

Acknowledgments

We thank the *Pontificia Universidad Javeriana-sede Bogotá* for the financial support to the project "Characterization of the microbiota associated with obstructive sleep apnea in patients with periodontitis" (project number 008144), and we greatly appreciate the support given by the Training Agreement for postgraduate studies of professors of the *Pontificia Universidad Javeriana* for their doctoral training. We also thank all the participants who were part of this project as patient donors of the oral samples.

Conflict of interest

The authors declare that the research was conducted in the absence of any commercial or financial relationships that could be construed as a potential conflict of interest.

Publisher's note

All claims expressed in this article are solely those of the authors and do not necessarily represent those of their affiliated organizations, or those of the publisher, the editors and the reviewers. Any product that may be evaluated in this article, or claim that may be made by its manufacturer, is not guaranteed or endorsed by the publisher.

Supplementary material

The Supplementary Material for this article can be found online at: https://www.frontiersin.org/articles/10.3389/fcimb.2022.934298/full#supplementary-material

References

Ahmad N. E., Sanders A. E., Sheats R., Brame J. L., Essick G. K. (2013). Obstructive sleep apnea in association with periodontitis: a case-control study. *J. Dental Hygiene* 87 (4), 188–199.

Al-Jewair T. S., Al-Jasser R., Almas K. (2015). Periodontitis and obstructive sleep apnea's bidirectional relationship: a systematic review and meta-analysis. *Sleep Breath* 19 (4), 1111–1120. doi: 10.1007/s11325-015-1160-8

Antezack A., Chaudet H., Tissot-Dupont H., Brouqui P., Monnet-Corti V. (2020). Rapid diagnosis of periodontitis, a feasibility study using MALDI-TOF mass spectrometry. *PloS One* 15 (3), 1–14. doi: 10.1371/journal.pone.0230334

Arumugam M. (2015). A comparative evaluation of subgingival occurrence of candida species in chronic periodontitis and peri-implantitis : A clinical and microbiological study. *Int. J. Clinic Implant Dentis* 1 (December), 95–100. doi: 10.5005/jp-journals-10004-1041

Barberis C., Almuzara M., Join-Lambert O., Ramírez M. S., Famiglietti A., Vay C. (2014). Comparison of the bruker MALDI-TOF mass spectrometry system and conventional phenotypic methods for identification of gram-positive rods. *PloS One* 9 (9), 1–6. doi: 10.1371/journal.pone.0106303

Belibasakis G., Charalampakis G., Bostanci N., Stadlinge B. (2015). "Peri-implant infections of oral biofilm etiology," in *Biofilm-based healthcare-associated infections*. (Cham: Springer) 69–84.

Bui F. Q., Almeida-da-Silva C. L. C., Huynh B., Trinh A., Liu J., Woodward J., et al. (2019). Association between periodontal pathogens and systemic disease. *Biomed. J.* 42 (1), 27–35. doi: 10.1016/j.bj.2018.12.001

Cade B. E., Chen H., Stilp A. M., Gleason K. J., Sofer T., Ancoli-israel S., et al. (2016). Genetic associations with obstructive sleep apnea traits in Hispanic/Latino americans. *Am. J. Respir. Crit. Care Med.* 194 (7), 886–897. doi: 10.1164/rccm.201512-2431OC

Canabarro A., Valle C., Farias M. R., Santos F. B., Lazera M., Wanke B. (2013). Association of subgingival colonization of candida albicans and other yeasts with severity of chronic periodontitis. *J. Periodontal Res.* 48 (4), 428–432. doi: 10.1111/jre.12022

Caton G., Armitage G., Berglundh T., Chapple I. L. C., Jepsen S., Kornman S., et al. (2018). A new classification scheme for periodontal and peri-implant diseases and conditions – introduction and key changes from the 1999 classification. *J. Clin. Periodontol.* 45 (March), S1–S8. doi: 10.1111/jcpe.12935

Charalampakis G., Belibasakis G. N. (2015). Microbiome of peri-implant infections: Lessons from conventional, molecular and metagenomic analyses. *Virulence* 6 (3), 183–187. doi: 10.4161/21505594.2014.980661

Chen Y., Chen X. C., Huang X., Duan Y., Gao H., Gao X., et al. (2021). Analysis of salivary microbiome and its association with periodontitis in patients with

obstructive sleep apnea. *Front. Cell. Inf. Microbiol.* 11 (December), 1–17. doi: 10.3389/fcimb.2021.752475

Chevalier M., Ranque S., Prêcheur I. (2017). Oral fungal-bacterial biofilm models *in vitro*: a review. *Med. Mycol.* 56 (6), 653–667. doi: 10.1093/mmy/myx111

Colombo A. P. V., Tanner A. C. R. (2019). The role of bacterial biofilms in dental caries and periodontal and peri-implant diseases: A historical perspective. *J. Dental Res.* 98 (4), 373–385. doi: 10.1177/0022034519830686

Cuervo A., Martínez M. C., Sosa G., Hernández M., Latorre C., Escobar F., et al. (2016). Condición periodontal de pacientes con apnea obstructiva del sueño. *Universitas Odontol.* 33 (June), 1–34. doi: 10.11144/Javeriana.uo35-74.cppa

Curtis M. A., Diaz P. I., Van Dyke T. E. (2020). The role of the microbiota in periodontal disease. *Periodontol. 2000* 83 (1), 14–25. doi: 10.1111/prd.12296

Diaz P. I., Xie Z., Sobue T., Thompson A., Biyikoglu B., Ricker A., et al. (2012). Synergistic interaction between candida albicans and commensal oral streptococci in a novel *in vitro* mucosal model. *Infect. Immun.* 80 (2), 620–632. doi: 10.1128/IAI.05896-11

Escobar F., Latorre C., Velosa J., Ferro M. B., Ruiz A., Arregoces F. E., et al. (2014). Relation between ultra-sensitive c-reactive protein, diabetes and periodontal disease in patients with and without myocardial infarction. *Arquivos Brasileiros Endocrinol. Metabol.* 58 (4), 362–368. doi: 10.1590/0004-2730000002899

Fox E. P., Cowley E. S., Nobile C. J., Hartooni N., Newman D. K., Johnson A. D. (2014). Anaerobic bacteria grow within candida albicans biofilms and induce biofilm formation in suspension cultures. *Curr. Biol.* 24 (20), 2411–2416. doi: 10.1016/j.cub.2014.08.057

Gamsiz-Isik H., Kiyan E., Bingol Z., Baser U., Ademoglu E., Yalcin F. (2017). Does obstructive sleep apnea increase the risk for periodontal disease? a case-control study. *J. Periodontol.* 88 (5), 443–449. doi: 10.1902/jop.2016.160365

Genco R. J., Borgnakke W. S. (2020). Diabetes as a potential risk for periodontitis : association studies. *Periodontol. 2000* 83, 40–45. doi: 10.1111/prd.12270

Genco R. J., Sanz M. (2020). Clinical and public health implications of periodontal and systemic diseases : An overview. *Periodontol. 2000* 83, 7–13. doi: 10.1111/prd.12344

Gunaratnam K., Taylor B., Curtis B., Cistulli P. (2009). Obstructive sleep apnoea and periodontitis: a novel association? *Sleep Breathing* 13 (3), 233–239. doi: 10.1007/s11325-008-0244-0

Haffajee A. D., Socransky S. S., Patel M. R., Song X. (2008). Microbial complexes in supragingival plaque. *Oral. Microbiol. Immunol.* 23 (3), 196–205. doi: 10.1111/j.1399-302X.2007.00411.x

Hajishengallis G., Korostoff J. M. (2017). Revisiting the page & Schroeder model: the good, the bad and the unknowns in the periodontal host response 40 years later. *Periodontol. 2000* 75 (1), 116–151. doi: 10.1111/prd.12181

Henne K., Fuchs F., Kruth S., Horz H. P., Conrads G. (2014). Shifts in campylobacter species abundance may reflect general microbial community shifts in periodontitis progression. *J. Oral. Microbiol.* 6 (1), 6–11. doi: 10.3402/jom.v6.25874

Hidalgo-Martínez P., Lobelo R. (2017). Epidemiología mundial, latinoamericana y colombiana y mortalidad del síndrome de apnea-hipopnea obstructiva del sueño (SAHOS). *Rev. la Facultad Med.* 65 (1Sup), 17–20. doi: 10.15446/revfacmed.v65n1Sup.59565

Janus M. M., Crielaard W., Volgenant C. M. C., der Veen M. H., Brandt B. W., Krom B. P. (2017). Candida albicans alters the bacterial microbiome of early *in vitro* oral biofilms. *J. Oral. Microbiol.* 9 (1), 1–10. doi: 10.1080/20002297.2016.1270613

Jaramillo A., Contreras A., Lafaurie G. I., Duque A., Ardila C. M., Duarte S., et al. (2017). Association of metabolic syndrome and chronic periodontitis in colombians. *Clin. Oral. Investigations* 21 (5), 1537–1544. doi: 10.1007/s00784-016-1942-9

Keller J. J., Wu C.-S., Chen Y.-H., Lin H.-C. (2013). Association between obstructive sleep apnoea and chronic periodontitis: a population-based study. *J. Clin. Periodontol.* 40 (2), 111–117. doi: 10.1111/jcpe.12036

Lamont R. J., Hajishengallis G. (2015). "Polymicrobial synergy and dysbiosis in inflammatory disease," in *Trends in molecular medicine*. (Elsevier). 21, 172–183. doi: 10.1016/j.molmed.2014.11.004

Lamont R. J., Koo H., Hajishengallis G. (2018). The oral microbiota: dynamic communities and host interactions. *Nat. Rev. Microbiol.* 16, 745–759. doi: 10.17235/reed.20188.4947/2017

Latorre C., Escobar F., Velosa J., Rubiano D., Hidalgo-Martinez P., Otero L. (2018). Association between obstructive sleep apnea and comorbidities with periodontal disease in adults. *J. Indian Soc. Periodontol.* 22 (3), 215–220. doi: 10.4103/jisp.jisp_38_18

Lembo D., Caroccia F., Lopes C., Moscagiuri F., Sinjari B., D'Attilio M. (2021). Obstructive sleep apnea and periodontal disease: A systematic review. *Med. (Lithuania)* 57 (6), 1–12. doi: 10.3390/medicina57060640

Loke W., Girvan T., Ingmundson P., Verrett R., Schoolfield J., Mealey B. L. (2015). Investigating the association between obstructive sleep apnea and periodontitis. *J. Periodontol.* 86 (2), 232–243. doi: 10.1902/jop.2014.140229

Martin R., Wächtler B., Schaller M., Wilson D., Hube B. (2011). Host-pathogen interactions and virulence-associated genes during candida albicans oral infections. *Int. J. Med. Microbiol.* 301 (5), 417–422. doi: 10.1016/j.ijmm.2011.04.009

Mombelli A. (2018). Microbial colonization of the periodontal pocket and its significance for periodontal therapy. *Periodontol. 2000* 76 (1), 85–96. doi: 10.1111/prd.12147

Nizam N., Basoglu O. K., Tasbakan M. S., Holtho A. (2014). Do salivary and serum collagenases have a role in an association between obstructive sleep apnea syndrome and periodontal disease ? a preliminary case – control study. *Arch. Oral. Biol.* 60, 134–143. doi: 10.1016/j.archoralbio.2014.09.006

Nizam N., Basoglu O. K., Tasbakan M. S., Nalbantsoy A., Buduneli N. (2014). Salivary cytokines and the association between obstructive sleep apnea syndrome and periodontal disease. *J. Periodontol.* 85 (7), e251–e258. doi: 10.1902/jop.2014.130579

Nizam N., Tasbakan M. S., Basoglu O. K., Lappin D. F., Buduneli N. (2016). Is there an association between obstructive sleep apnea syndrome and periodontal inflammation? *Clin. Oral. Investigations* 20 (4), 659–668. doi: 10.1007/s00784-015-1544-y

O'Leary T. J., Drake R. B., Naylor J. E. (1972). The plaque control record. *J. Periodontol.* 43 (1), 38. doi: 10.1902/jop.1972.43.1.38

Ruiz A., Rendón M., Hidalgo P., Cañón M., Otero L., Panqueva O., et al. (2016). Prevalence of sleep complaints in Colombia at different altitudes. *Sleep Sci.* 9 (2), 100–105. doi: 10.1016/J.SLSCI.2016.05.008

Sanders A. E., Essick G. K., Beck J. D., Cai J., Beaver S., Finlayson T. L., et al. (2015). Periodontitis and sleep disordered breathing in the Hispanic community health Study/Study of latinos. *Sleep* 38 (8), 1195–1203. doi: 10.5665/sleep.4890

Sateia M. J. (2014). International classification of sleep disorders-third edition highlights and modifications. *CHEST* 146 (5), 1387–1394. doi: 10.1378/chest.14-0970

Seo W. H., Cho E. R., Thomas R. J., An S. Y., Ryu J. J., Kim H., et al. (2013). The association between periodontitis and obstructive sleep apnea: A preliminary study. *J. Periodontal Res.* 48 (4), 500–506. doi: 10.1111/jre.12032

Socransky S. S., Haffajee A. D. (2005). Periodontal microbial ecology. *Periodontol. 2000* 38 (1), 135–187. doi: 10.1111/j.1600-0757.2005.00107.x

Socransky S. S., Haffajee A. D., Cugini M. A., Smith C., Kent R. L. (1998). Microbial complexes in subgingival plaque. *J. Clin. Periodontol.* 25 (2), 134–144. doi: 10.1111/j.1600-051X.1998.tb02419.x

Sztukowska M. N., Dutton L. C., Delaney C., Ramsdale M., Ramage G., Jenkinson H. F., et al. (2018). Community development between porphyromonas gingivalis and candida albicans mediated by InlJ and Als3. *MBio* 9 (2), 1–16. doi: 10.1128/mBio.00202-18

Tamai R., Sugamata M., Kiyoura Y. (2011). Candida albicans enhances invasion of human gingival epithelial cells and gingival fibroblasts by porphyromonas gingivalis. *Microbial. Pathogen.* 51 (4), 250–254. doi: 10.1016/j.micpath.2011.06.009

Valm A. M. (2019). The structure of dental plaque microbial communities in the transition from health to dental caries and periodontal disease. *J. Mol. Biol.* 431 (16), 2957–2969. doi: 10.1016/j.jmb.2019.05.016

Vieira Colombo A. P., Magalhães C. B., Hartenbach F. A. R. R., Martins do Souto R., Maciel da Silva-Boghossian C. (2016). Periodontal-disease-associated biofilm: A reservoir for pathogens of medical importance. *Microbial. Pathogen.* 94, 27–34. doi: 10.1016/j.micpath.2015.09.009

Xu H., Sobue T., Thompson A., Xie Z., Poon K., Ricker A., et al. (2014). Streptococcal co-infection augments candida pathogenicity by amplifying the mucosal inflammatory response. *Cell. Microbiol.* 16 (2), 214–231. doi: 10.1111/cmi.12216

Zhang X., Wang S., Xu H., Yi H., Guan J., Yin S. (2021). Metabolomics and microbiome profiling as biomarkers in obstructive sleep apnoea: A comprehensive review. *Eur. Respir. Rev.* 30 (160), 200220. doi: 10.1183/16000617.0220-2020

Zhou M., Rong R., Munro D., Zhu C., Gao X., Zhang Q., et al. (2013). Investigation of the effect of type 2 diabetes mellitus on subgingival plaque microbiota by high-throughput 16S rDNA pyrosequencing. *PloS One* 8 (4), e61516. doi: 10.1371/journal.pone.0061516

frontiers | Frontiers in Cellular and Infection Microbiology

TYPE Original Research
PUBLISHED 10 October 2022
DOI 10.3389/fcimb.2022.998693

OPEN ACCESS

EDITED BY
Zuomin Wang,
Capital Medical University, China

REVIEWED BY
Leng Wu,
Huazhong University of Science and Technology, China
Fuhua Yan,
Nanjing University, China
E. Xiao,
Peking University, China

*CORRESPONDENCE
Xiaoling Deng
xiaolingdeng@xmu.edu.cn

†These authors have contributed equally to this work and share first authorship

SPECIALTY SECTION
This article was submitted to Extra-intestinal Microbiome, a section of the journal Frontiers in Cellular and Infection Microbiology

RECEIVED 20 July 2022
ACCEPTED 20 September 2022
PUBLISHED 10 October 2022

CITATION
Xu M, Huang J, Zhu F, Shen K, Liu F and Deng X (2022) FOXO1 inhibits FSL-1 regulation of integrin β6 by blocking STAT3 binding to the integrin β6 gene promoter.
Front. Cell. Infect. Microbiol. 12:998693.
doi: 10.3389/fcimb.2022.998693

FOXO1 inhibits FSL-1 regulation of integrin β6 by blocking STAT3 binding to the integrin β6 gene promoter

Mingyan Xu[1,2,3†], Jie Huang[4†], Feixiang Zhu[4], Kailun Shen[1], Fan Liu[4] and Xiaoling Deng[4*]

[1]Xiamen Key Laboratory of Stomatological Disease Diagnosis and Treatment, Department of Implantology, Stomatological Hospital of Xiamen Medical College, Xiamen, China, [2]Engineering Research Center of Fujian University for Stomatological Biomaterials, Department of Stomatology, Xiamen Medical College, Xiamen, China, [3]School of Stomatology, Fujian Medical University, Fuzhou, China, [4]Department of Basic Medical Science, School of Medicine, Xiamen University, Xiamen, China

Integrin β6 (ITGB6), an epithelial-specific receptor, is downregulated in the gingival epithelium of periodontitis and is associated with inflammation response and periodontitis development. However, the transcriptional regulatory mechanism of ITGB6 downregulation in the human gingival epithelium remains unclear. Fibroblast-stimulating lipopeptide-1 (FSL-1), an oral biofilm component, promotes an epithelial cell-driven proinflammatory response in periodontitis partially by suppressing ITGB6 expression. The aim of the current study was to investigate the transcriptional regulatory mechanism of ITGB6 inhibition by FSL-1 in human epithelial cells (HaCaT and primary human gingival epithelial cells), and to delineate the transcriptional mechanism of ITGB6 suppression in periodontitis. We found that FSL-1 inhibited ITGB6 transcription through increasing forkhead box protein O1 (FOXO1) expression and inhibiting signal transducer and activator of transcription 3 (STAT3) activation. Furthermore, FOXO1 bound to STAT3 directly, leading to decreased STAT3 phosphorylation induced by FSL-1. Consequently, the binding of phosphorylated STAT3 to the ITGB6 promoter was decreased, and ITGB6 transcription was therefore downregulated following FSL-1 stimulation. The reciprocal action of STAT3 and FOXO1 on ITGB6 downregulation was also confirmed by the immunostaining of the inflammatory epithelium associated with periodontitis. Our findings suggest that the interaction of FOXO1–STAT3 may be a useful signal target for the treatment of periodontitis.

KEYWORDS

FOXO1, FSL-1, ITGB6, STAT3, Periodontitis

Introduction

Periodontitis is a chronic non-communicable disease affecting approximately 47% of US adults (Teles et al., 2022) and increasing the risk of developing chronic diseases (Zemedikun et al., 2021). Deep periodontal pockets between the gingiva and teeth, inflammation, and bone loss are characteristic of periodontitis. Periodontal microbial insults and associated proinflammatory cascades have been proposed to contribute to the pathogenesis of systemic diseases, such as Alzheimer's disease, diabetes (Kocher et al., 2018), cardiovascular disease (Sanz et al., 2020), respiratory disease (Gomes-Filho et al., 2020), chronic renal disease (Hickey et al., 2020), and oral cancer (Teles et al., 2022).

Integrin β6 (ITGB6) is an epithelial-specific receptor that is absent from normal healthy epidermis and oral mucosa (Breuss et al., 1993), but is constitutively expressed in the healthy gingival epithelium (Meecham and Marshall, 2020). However previous research has shown that gingival epithelial cells (GECs) with reduced ITGB6 expression exhibit an enhanced inflammatory response (Bi et al., 2017). Moreover, the absence of ITGB6 was linked to the initiation and progression of periodontitis in a mouse model (Ghannad et al., 2008). In addition, patients with ITGB6 mutations can develop severe periodontal disease (Ansar et al., 2016). Therefore, repression of ITGB6 may play a key role in acute inflammation and periodontitis development.

Dysbiotic bacterial dental plaque biofilms are considered the main cause of periodontitis and ITGB6 suppression (Bi et al., 2019). ITGB6 expression is transcriptionally regulated. We previously identified several transcriptional binding sites for transcription factors, such as signal transducer and activator of transcription (STAT) and forkhead box-O (FOXO) in the core promoter of ITGB6 (Xu et al., 2015). However, the regulatory mechanisms underlying the repression of ITGB6 expression by oral biofilm components in periodontitis remain unexplored.

The transcription factor family FOXO includes four members: FOXO1, 3, 4, and 6 (van der Vos and Coffer, 2008; Maiese et al., 2009). FOXO proteins are increasingly considered to be unique cellular targets that regulate several cellular processes, including cell differentiation, immune status, apoptosis, and inflammation (Maiese et al., 2009). FOXO1 has been linked to the development of periodontitis. FOXO1 mediates the inflammatory effect of prostaglandins (Pg) in GECs, as FOXO1 silencing attenuates Pg-induced production and secretion of IL-1β (Wang et al., 2015). The FOXO1 signaling axis can regulate periodontal bacteria–epithelial interactions, immune-inflammatory responses, bone remodeling, and wound healing (Ren et al., 2021).

Fibroblast-stimulating lipopeptide-1 (FSL-1) is a diacylated lipopeptide mimicking the 44 kDa lipoprotein of *Mycoplasma salivarium* and is suspected to play an etiological role in periodontal diseases (Shibata et al., 2000). Inflammatory cytokines such as monocyte chemotactic protein (MCP)-1, MMP-9, IL-6, tumor necrosis factor (TNF)-α, and IL-8 can be induced by FSL-1 in monocytes/macrophages (Ahmad et al., 2014). Studies have confirmed that biofilm components and FSL-1 can downregulate ITGB6 expression in the pocket epithelium, thus, promoting an epithelial cell-driven proinflammatory response in periodontal disease (Li et al., 2013; Bi et al., 2017). However, the transcriptional regulatory mechanism of ITGB6 inhibition by FSL-1 in the human gingival epithelium remains unclear.

In the present study, we investigated the transcriptional regulatory mechanism of ITGB6 inhibition by FSL-1 in human epithelial cells (HaCaT and primary human GECs) and delineated the transcriptional mechanism of ITGB6 suppression in periodontitis. We identified that the FOXO1–STAT3 interaction may potentially contribute to FSL-1-suppressed ITGB6 expression in the gingival epithelium of periodontitis.

Materials and methods

Cell culture and FSL-1 treatment

The human keratinocyte cell line HaCaT was purchased from the Kunming Cell Bank of the Chinese Academy of Sciences. HaCaT cells were maintained in Dulbecco's modified Eagle's medium (Gibco) supplemented with 10% fetal bovine serum (Gibco) and 1% penicillin–streptomycin at 37°C in a cell incubator containing 5% CO_2. Primary human GECs were grown from explants of gingival biopsies obtained from healthy volunteers with no gingival inflammation, as described previously (Kedjarune et al., 2001). Primary GECs were maintained in keratinocytes (K)-SFM medium (Gibco) supplemented with human keratinocytes growth supplement, 1% antibiotics, and 10 μM Y-27632 (Sigma-Aldrich, Shanghai, China). When the GECs reached 80% confluence, subculturing was performed *via* trypsin digestion. A third generation of cells was used in the experiment. Primary cells within six generations were used in this study. HaCaT and GECs were stimulated with FSL-1 (Abcam, Shanghai, China) for indicated times at 37°C. Cells were harvested for detection of ITGB6 mRNA and protein levels.

Reverse transcription quantitative polymerase chain reaction (RT-qPCR)

Total RNA was extracted from HaCaT cells and GECs using a generic RNA extraction kit (Dongsheng Biotechnology, Hangzhou, China). Reverse transcription into cDNA was performed according to the instructions of the TaKaRa PrimeScript™ RT Reagent KIT (Takara, Dalian, China). The

RT- qPCR assay was performed in ABI 7500 (Applied Biosystems, USA) using SYBR Green. The obtained data were analyzed using a comparison threshold cycle ($2^{-\Delta\Delta Ct}$) to indicate relative mRNA expression, and GAPDH was used as an internal control. The following primers were used for PCR: ITGB6 forward, 5′- GCAAGCTGCTGTGTGTAAGGAA-3′; ITGB6 reverse, 5′-CTTGGGTTACAGCGAAGATCAA-3′; FOXO3 forward, 5′- GCGTGCCCTACTTCAAGGATAAG-3′; FOXO3 reverse, 5′-GACCCGCATGAATCGACTAATG-3′; STAT3 forward, 5′- GAGCTGCACCTGATCACCTT-3′; STAT3 reverse, 5′-CTACCTGGGTCAGCTTCAGG-3′; FOXO1 forward, 5′- GTTGCTGACTTCTGACTCT-3′; FOXO1 reverse, 5′-GCTGCCATAGGTTGACAT-3′; GAPDH forward, 5′- CATCACCATCTTCCAGGAG-3′; and GAPDH reverse, 5′-AGGCTGTTGTCATACTTCTC-3′.

Western blotting

The cells were collected in a 1.5-mL centrifuge tube and placed in ice. RIPA buffer (70–100 μL) was added to the samples, and the tubes incubated for 30 min for cell lysis. Subsequently, the cells were further lysed using ultrasound. The supernatant was then centrifuged in a low-temperature centrifuge at 12000 RPM for 15 min. The supernatant was collected in a new centrifuge tube and the protein concentration was determined using the BCA method. Polyacrylamide gel was prepared according to the size of the target protein. After sodium dodecyl sulfate–polyacrylamide gel electrophoresis, the target protein was transferred to a PVDF membrane. The membrane was placed in 5% milk or bovine serum albumin for 1 h to block non-specific sites. After washing and the corresponding primary antibody was incubated at 4°C overnight. Then, the membrane was rinsed with 1×PBS-0.1% Tween three times, and mouse or rabbit secondary antibodies with corresponding primary antibody properties were incubated at room temperature for 1 h. Enhanced chemiluminescence solution was used to develop the protein bands, and the image was used to quantitatively analyze the optical density of the protein bands.

Cell transfection

When the cell density was approximately 70%, a mixture containing the transfection reagent and plasmid was prepared according to the lipofectamine manufacturer's instructions. After incubating for 15 min, the medium containing the plasmid–liposome complex was gently mixed with the cell supernatant. Transfected cells were collected for subsequent experiments 48 h after incubation at 37°C in a humidified 5% CO_2 atmosphere.

Human tissue and immunohistochemistry

Gingival tissue samples without gingival inflammation (healthy control group, n = 5) and gingival tissue samples with periodontal disease (deep pocket > 5mm) (Inflammation group, n = 5) were selected from routine oral care patients undergoing orthodontic treatment or periodontitis tooth extraction in the Stomatological Hospital of Xiamen Medical College. This study was approved by the Ethics Committee of the Stomatological Hospital of Xiamen Medical College (HS20200908001), and informed consent was obtained from each patient. Tissues were fixed with 4% formaldehyde at 4°C for 24 h, dehydrated, and embedded in paraffin wax. The embedded specimens were cut into 5-μm tissue slices and baked for 2 h in an oven at 65°C. Immunohistochemistry was performed as described previously (Xu et al., 2009). Primary antibodies against ITGB6 2746294 (Millipore, Billerica, MA, USA), pSTAT3 (Y705; Cell Signaling Technology, Danvers, MA,USA), and pFOXO1 (ab76055; Abcam, Cambridge, MA, USA) were used. The staining intensity in each section was measured using the cell counting function of the Image-Pro® Plus software.

Double luciferase reporter gene assay

A double luciferase reporter assay kit was used to detect the effect of FOXO1 and STAT3 plasmids on the ITGB6 gene promoter. The passive lysis buffer (PLB, 20 μL) was added to the cells plated in 96-well plate. After 15 min, 20 μL of PLB lysate was transferred into a 1.5-mL centrifuge tube. First, 20 μL of the LAR solution was added to the tube to determine the firefly luciferase value. The Renilla luciferase value was obtained by immediately adding 20 μL of STOP&Glo buffer. The firefly luciferase/Renilla luciferase intensity ratio was calculated for each group.

Chromatin immunoprecipitation

The chromatin immunoprecipitation (ChIP) assay was performed using a ChIP kit (Cell Signaling Technology, Danvers, MA, USA). Cells were cultured to a density of 70%–80% (10-cm dish) collected after drug stimulation. Crosslinking was performed with 1% formaldehyde. After fixation, 10× glycine units were added to terminate the cross-linking process. After three times of washing with PBS, the sample was collected in a 1.5-mL centrifuge tube, and 1 μL of 100 mM PMSF and 1 μL of PIC were added. The sample was resuspended in 1 mL of ChIP-lysis

buffer. Ultrasound treatment was performed 30 min after ice lysis to concentrate chromatin DNA fragments of 500–1000 bp. The sample was centrifuged at 12000 RPM at 4 °C for 10 min, and the supernatant was collected in a new centrifuge tube. After the DNA fragments were separated and purified, chromatin fragmentation was observed using 12% agarose gel electrophoresis. The number of immunoprecipitation (IP) and Ig G groups was calculated according to the concentration. Proteins were captured *via* immunoprecipitation using the corresponding primary antibody or control IgG and incubated overnight at 4°C. Further collection and purification of chromatin fragments was performed, followed by protein unlinking at 65°C. The precipitated DNA fragments were analyzed using PCR.

Coimmunoprecipitation

Three groups of cells (IP-FOXO1 group, IP-STAT3 group, and IgG control group) were prepared using two 10-cm discs in each group. HaCaT cells were washed twice with pre-cooled PBS and then collected in a 1.5-mL centrifuge tube with a pre-cooled cell scraper. Subsequently, 1 mL of mild IP cracking solution was added, sloshed slowly for 15 min, and left to crack on ice for 1 h. After centrifugation at 14000 RPM for 15 min at 4°C, the supernatant was collected in a new centrifuge tube, 100 μL was removed from each set as input, and its concentration was determined using the BCA method. Each input group was supplemented with 25 μL of 5× loading buffer. This was boiled for 10 min and store at −20°C. After cleaning the protein A agarose twice with pre-cooled PBS, the protein A agarose with concentration of 50% was prepared. Protein A agarose (100 μL) was added to each centrifuge tube and incubated for 2 h in a suspension apparatus at 4°C. The IP group was incubated with the corresponding antibodies, and protein A agarose and incubated overnight under continuous rotation at 4°C. After centrifugation, the supernatant was carefully removed. Another 1 mL of IP lysate was added and washed three times for 3 min each, followed by centrifugation at 4°C at 3000 RPM for 3 min. After the last washing, 30 μL of 2× loading buffer was boiled and centrifuged to remove the precipitate, and the supernatant was collected as the protein sample of the IP group. Proteins released from the complex components were examined *via* SDS-PAGE and western blotting.

Statistical analysis

The significance of differences between groups was determined using an unpaired two-tailed Student's *t*-test and ANOVA using GraphPad Prism software (version 7.0). All experiments were independently repeated at least three times, and the differences were considered significant when $^{*}P < 0.05$, $^{**}P < 0.01$, and $^{***}P < 0.001$.

Results

Lipopeptide FSL-1 downregulates ITGB6 expression in epithelial cells

To elucidate the mechanism underlying ITGB6 downregulation in periodontitis, oral biofilm component FSL-1 was used as the stimulus.

As 100ng/mL FSL-1 has been reported to significantly inhibit ITGB6 expression in human GECs (Bi et al., 2017), we chose this concentration to investigate the mechanism of ITGB6 downregulation in epithelial cells. Epithelial HaCaT and GECs were exposed to FSL-1 (100 ng/mL) for the indicated times (0.5–2 h). ITGB6 mRNA and protein levels were detected using RT-qPCR and western blotting, respectively. The results showed that FSL-1 significantly downregulated ITGB6 mRNA expression in a time-dependent manner in both HaCaT and GECs (Figures 1A, B), with a 50% reduction in HaCaT and 30% reduction in GECs after 2 h of stimulation. FSL-1 also significantly attenuated ITGB6 protein production after 0.5–2 h of stimulation in HaCaT and GECs (Figures 1C, D). These results indicate that FSL-1 can reduce ITGB6 transcriptional expression in both the human epithelial cell line and primary derived GECs.

FOXO1 and STAT3 binding sites are located in ITGB6 promoter

As ITGB6 expression is transcriptionally regulated and the transcription factors FOXO1 and STAT3 are involved in the inflammatory response, we hypothesized that FOXO1 and STAT3 are involved in ITGB6 transcription in epithelial cells. Sequence analysis predicted several putative transcription factor FOXO1 and STAT3 binding sites in the −289 to −150 region of the ITGB6 promoter (Figure 2A). Overexpression of FOXO1 or STAT3 significantly upregulated the activity of the pGL2-B6(−421/+208) construct but had no effect on the activity of the pGL2-B6(−150/+208) construct, suggesting that the region between −421 and −150 bp upstream of the translational start codon may contain binding sites for the transcription factors FOXO1 and STAT3 (Figures 2B, C). To determine whether cellular FOXO1 and STAT3 can bind to the ITGB6 promoter, a ChIP assay was performed and assayed using PCR targeting the −421 to −150 region of the ITGB6 promoter. ChIP with an antibody against FOXO1 and STAT3 resulted in marked enrichment of the ITGB6 promoter DNA compared to the control IgG (Figures 2D, E). These results suggest that FOXO1 and STAT3 could bind to the region located at positions −421 to −150 of the human ITGB6 promoter *in vivo* and may be involved in human ITGB6 promoter transcriptional activity.

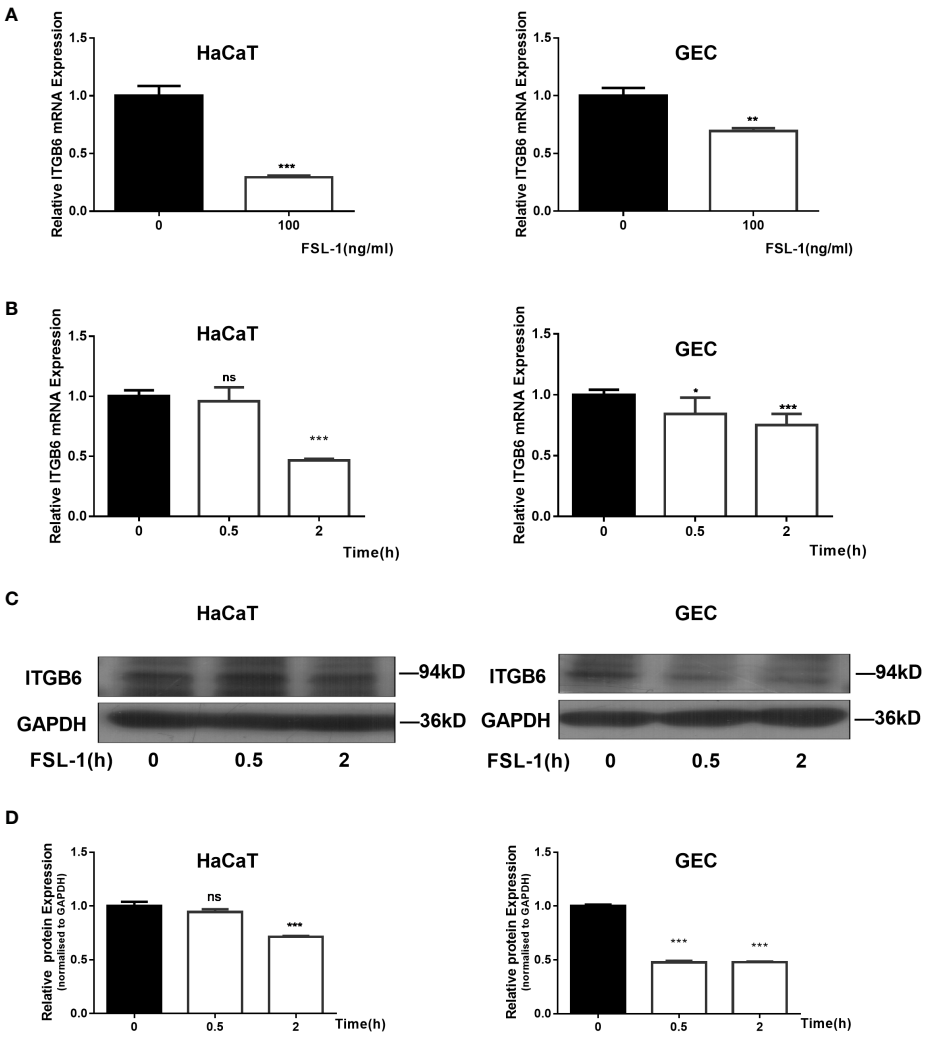

FIGURE 1
Suppression of ITGB6 by FSL-1 in human epithelial cells. **(A)** HaCaT (Left) or GECs (Right) were treated with 100 ng/mL FSL-1 for 2 h. *ITGB6* mRNA were then extracted, and the mRNA levels were measured by qRT-PCR. **(B)** HaCaT (Left) or GECs (Right) were treated with 100 ng/ml FSL-1 for indicated times, and the *ITGB6* mRNA expression levels were detected by qRT-PCR. **(C)** HaCaT or GECs were treated with 100 ng/mL FSL-1 for indicated times and the protein levels were assessed using western blotting. **(D)** Densitometric analysis was used to quantify protein bands. Data are presented as mean ± SEM from triplicates. no significance (ns), *P < 0.05, **P < 0.01, ***P < 0.001, comparison with time zero medium control cells.

FOXO1 is involved in FSL-1-mediated ITGB6 downregulation

To explore whether FOXO1 is involved in FSL-1-decreased ITGB6 expression in HaCaT and GECs, we first examined the effect of FSL-1 on FOXO1 expression using western blotting. As shown in Figure 3, FSL-1 significantly upregulated FOXO1 (Figures 3A, B) protein levels in a time-dependent manner in both HaCaT and GECs. Furthermore, overexpression of FOXO1 significantly decreased the expression level of mRNA (about 40%, $P < 0.01$) and protein of ITGB6 (Figures 3C–E). In addition, the FSL-1 inhibitor AS1842856 significantly reversed the expression of mRNA (about 20%, $P < 0.05$) and ITGB6 protein (Figures 3F–H), which was inhibited by FSL-1. These results indicated that FOXO1 is involved in the downregulation of ITGB6 expression.

Next, a ChIP assay was performed to further clarify whether FOXO1 mediates the effect of FSL-1 on ITGB6 transcription *via* increased binding to the ITGB6 promoter *in vivo*. HaCaT cells were treated with FSL-1 (100 ng/mL) for 1–2 h, and whole-cell chromatin was extracted. As shown in Figure 3I, no increase in the binding of FOXO1 to the ITGB6 promoter was detected after FSL-1 stimulation, suggesting that FOXO1 involvement in ITGB6 downregulation was not mediated by increased binding to the ITGB6 promoter site.

10.3389/fcimb.2022.998693

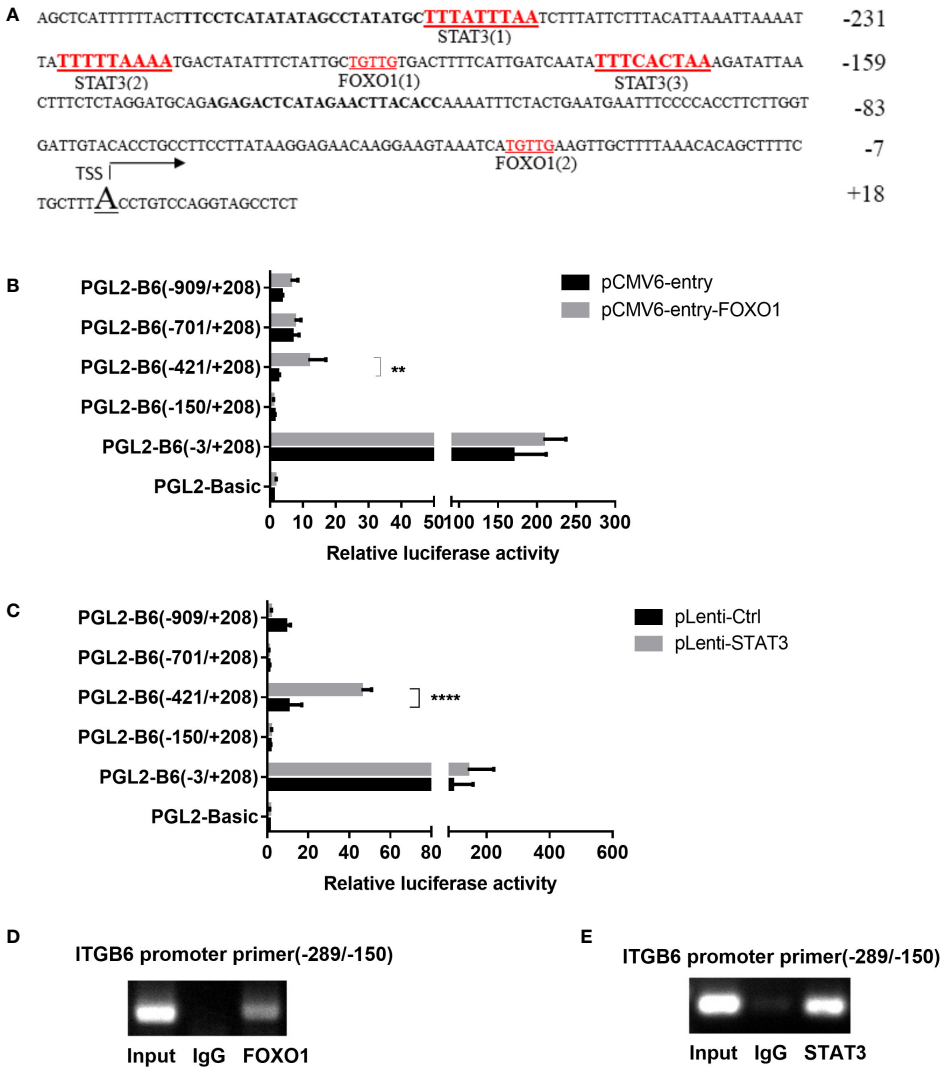

FIGURE 2
FOXO1 and STAT3 binding sites located at the ITGB6 promoter. **(A)** Potential binding sites at the ITGB6 promoter were predicted by the JASPER database. All numbers presented are relative to the TSS of the human *ITGB6* gene. There are three latent STAT3 binding sites and two FOXO1 binding sites between −26 and +18 of the *ITGB6* promoter. **(B, C)** Effect of FOXO1 **(B)** and STAT3 **(C)** overexpression on *ITGB6* promoter activity in HaCaT. Luciferase reporter constructs containing various lengths of the *ITGB6* promoter, or the empty plasmid pGL2-basic, were co-transfected with pRL-TK and with either FOXO1 or STAT3-overexpressing plasmid into HaCaT cells. Luciferase activity was measured at 48 h after transfection. The luciferase value of the pGL2-basic was set to a value of one. Relative promoter activities are presented on the right (mean ± SEM, at least three independent experiments) and were analyzed using one-way ANOVA. **(D, E)** Measurement of FOXO1 and STAT3 binding to the ITGB6 promoter. ChIP assay was performed using anti-FOXO1 antibody **(D)**, anti-STAT3 antibody **(E)**, or IgG as a control in HaCaT cells. Input and immunoprecipitated DNA was then amplified by PCR using primer pairs covering FOXO1 and STAT3 binding sites from −289 to −150 bp. The associated *ITGB6* promoter DNA was amplified using PCR and resolved using agarose electrophoresis. **P < 0.01 and ****P < 0.0001.

STAT3 suppression is involved in ITGB6 downregulation by FSL-1

To explore the role of STAT3 in FSL-1-decreased ITGB6 transcription, we first examined the effect of STAT3 on ITGB6 expression in HaCaT and GECs. As shown in Figure 4, STAT3 overexpression increased the expression levels of ITGB6 mRNA and protein in both HaCaT and GECs (Figures 4A, B). These results indicated that STAT3 may be involved in the upregulation of ITGB6 expression.

Next, we examined the effect of FSL-1 on STAT3 activation using western blotting. As shown in Figure 4, FSL-1 significantly decreased STAT3 phosphorylation in both cell lines from 0.5 h onwards (Figure 4C). Furthermore, the ChIP assay results

10.3389/fcimb.2022.998693

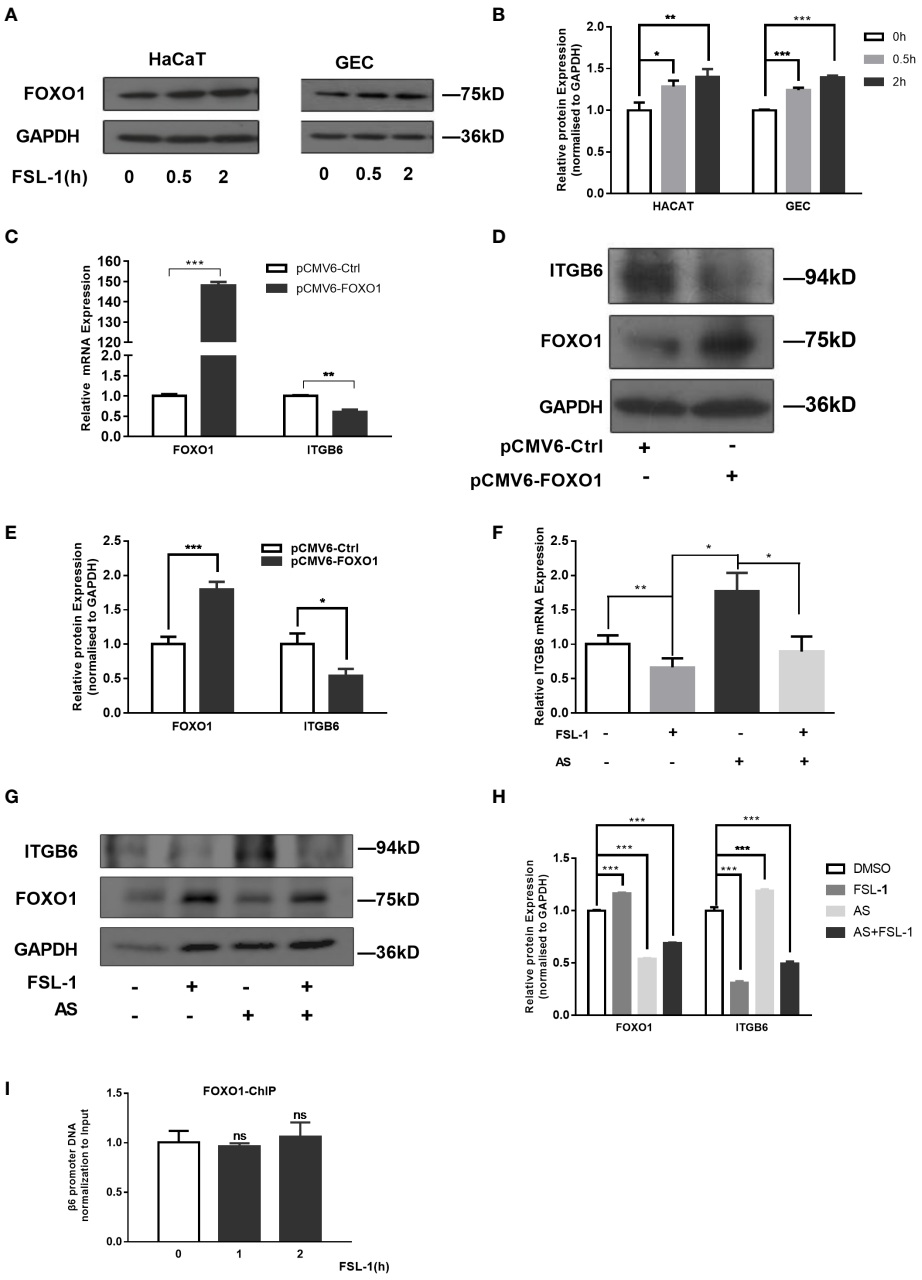

FIGURE 3
FOXO1 is involved in ITGB6 suppression by FSL-1 in HaCaT and GECs. Serum-starved HaCaT and GECs were treated with FSL-1 (100 ng/mL) for 0.5–2 h, and the total FoxO1 **(A)** protein expression levels were analyzed using western blotting. Protein loading was verified using GAPDH. **(B)** Densitometric analysis was used to quantify protein bands. Data are presented as mean ± SEM from triplicates, comparised with time zero medium control cells **(C)** HaCaT cells were transfected with pCMV6-Ctrl or pCMV6-FOXO1 for 48 h. Total RNA was extracted, and the mRNA expression of *ITGB6* was detected by RT-qPCR. Data are shown as the mean ± SEM of triplicates and comparisoned with the pCMV6-Ctrl group. **(D)** Protein expression levels were analyzed using Western blotting. Protein loading was verified using GAPDH. **(E)** Densitometric analysis was used to quantify protein bands. Data are presented as mean ± SEM from triplicates and compared with pCMV6-Ctrl group. The effect of the FSL-1 inhibitor AS1842856 (AS) on the expression level of *ITGB6* mRNA **(F)** and protein **(G)**. HaCaT cells were exposed to FSL-1 (100 ng/mL) for 2 h with or without pre-incubation with AS (1 μM) for 0.5 h. Final concentrations of DMSO were kept constant for all treatment conditions. *ITGB6* mRNA levels were determined using qRT-PCR. Data are shown as mean ± SEM of triplicates. Protein levels of ITGB6, FOXO1, and GAPDH (loading control) were measured using western blotting. The blots are representative of three independent experiments with similar results **(G)**. **(H)** Densitometric analysis was used to quantify protein bands. Data are presented as mean ± SEM from triplicates. **(I)** Measurement of FOXO1 binding to ITGB6 promoter. HaCaT cells were treated with FSL-1 at the indicated times, and the binding of FOXO1 to the *ITGB6* promoter was detected by ChIP assay. The associated *ITGB6* promoter DNA was measured using qPCR. The results were normalized to the input control. Data are shown as mean ± SEM of triplicates. no significance (ns), compared to the time zero. *P < 0.05, **P < 0.01, ***P < 0.001.

showed that FSL-1 stimulation inhibited the binding of phosphorylated STAT3 to the ITGB6 promoter site from 1 h onwards (Figure 4D). Overall, these results suggest that inhibition of phosphorylated STAT3 binding to the ITGB6 promoter is involved in the FSL-1-mediated ITGB6 transcriptional downregulation.

Transcription factor FOXO1 interacts with STAT3 to mediate the effect of FSL-1 on ITGB6 downregulation

As FOXO1 negatively regulates leptin-induced pro-opiomelanocortin (POMC) transcription through its direct interaction with STAT3 (Ma et al., 2015), we speculated that FOXO1 may mediate the negative effect of FSL-1 on ITGB6 expression *via* interaction with STAT3. To test this possibility, we first performed co-immunoprecipitation experiments to assess the interaction between FOXO1 and STAT3, and the results confirmed the interaction between FOXO1 and STAT3 (Figure 5A).

Moreover, FOXO1 overexpression attenuated STAT3 phosphorylation. In addition, incubation with FSL-1 after FOXO1 overexpression further downregulated STAT3 phosphorylation levels, suggesting a synergistic effect on STAT3 phosphorylation level by FSL-1 incubation and FOXO1 overexpression (Figure 5B). Next, we performed a ChIP assay to determine the effect of FOXO1 overexpression on the binding of phosphorylated STAT3 (p-STAT3) to the ITGB6 promoter. The results (Figure 5C) showed that FOXO1 overexpression significantly inhibited the binding of p-STAT3 to the ITGB6 promoter.

Thus far, the *in vitro* data strongly suggest that transcription factor FOXO1 is involved in regulating the effect of FSL-1 on ITGB6 downregulation by inhibiting STAT3 activation and reducing the binding of p-STAT3 to the ITGB6 promoter region.

To confirm the role of FOXO1 and STAT3 and its relation to ITGB6 expression *in vivo*, we performed immunohistochemistry to detect the expression of ITGB6, FOXO1, and STAT3 using sequencing slices from healthy human gingival tissue and gingival epithelium of patients with periodontitis. First, we confirmed the reduction of ITGB6 expression level in periodontitis samples as compared with that in the healthy controls (Figures 6A, B). As shown in Figures 6E, F, p-STAT3 was expressed in the nucleus of healthy gingival epithelium but was minimally detected in inflammatory tissue. On the contrary, FOXO1 was strongly detected in the inflammatory epithelium, both in the nucleus and cytoplasm, and was weakly detected in healthy gingival epithelium (Figures 6C, D). These results suggest that FOXO1 interacts with STAT3 and may be involved in the downregulation of ITGB6 in the inflammatory epithelium associated with periodontitis.

Discussion

The presence of ITGB6 is essential for periodontal health, as its low expression in the gingival epithelium is related to the development of periodontal diseases (Ghannad et al., 2008). Although previous research has confirmed that periodontal bacteria or pathogens may cause ITGB6 repression in periodontitis (Bi et al., 2017), limited work has been performed to further investigate the transcriptional mechanism of ITGB6 downregulation in periodontitis. In the present study, we found that the interaction of the transcription factors FOXO1 and STAT3 mediated periodontitis-related lipopeptide FSL-1-induced ITGB6 downregulation in human epithelial cells. While EGFR–ERK signaling pathways have previously been implicated in ITGB6 suppression in periodontal inflammation (Bi et al., 2019), the critical involvement of the transcription factors FOXO1 and STAT3 in ITGB6 suppression by oral bacterial biofilm components is a novel finding.

It is generally accepted that gene expression is critically governed by various transcription factors in a cell- and stimulus-specific manner. However, the composition of periodontal bacteria or pathogens that cause periodontitis is complex, and it is difficult to determine the effect of these pathogens on ITGB6 expression. Therefore, we selected a single microbial biofilm component, FSL-1, to study ITGB6 transcriptional regulation. FSL-1 is the N-terminal lipopeptide of the cell membrane lipoprotein LP44 produced by the common oral bacterium *M. salivarium*, which preferentially inhabits the gingival sulci and is suspected to play an etiological role in periodontal diseases (Shibata et al., 2000). Our results showed that FSL-1 could suppress ITGB6 expression in both commercial epithelial cell lines and primary GECs, which is consistent with the results of a previous study (Bi et al., 2017). Moreover, the effect of FSL-1 on ITGB6 suppression is similar to that of oral bacterial biofilm extracts (Bi et al., 2017). FSL-1 was then used as a stimulator to investigate the transcriptional regulation mechanism of ITGB6 suppression associated with periodontitis in the current study.

Accumulating evidence indicates that FOXO1 activity can be induced by periodontal pathogens and plays a crucial role in periodontal homeostasis and disease (Ren et al., 2021). Wang et al. showed that FOXO1 accumulates in the nucleus of *Porphyromonas gingivalis*-infected cells (Wang et al., 2015) and is involved in gene expression related to cell death, barrier function, differentiation, and inflammation (Li et al., 2013). In our study, we verified that FSL-1 significantly upregulated the expression of FOXO1. In addition, upregulation of FOXO1 downregulated ITGB6 expression, whereas blocking FOXO1 expression inhibited the downregulation of ITGB6 by FSL-1. These results indicated the involvement of FOXO1 in FSL-1-induced ITGB6 downregulation. Transcription factors normally regulate gene expression by binding to the target gene promoter.

10.3389/fcimb.2022.998693

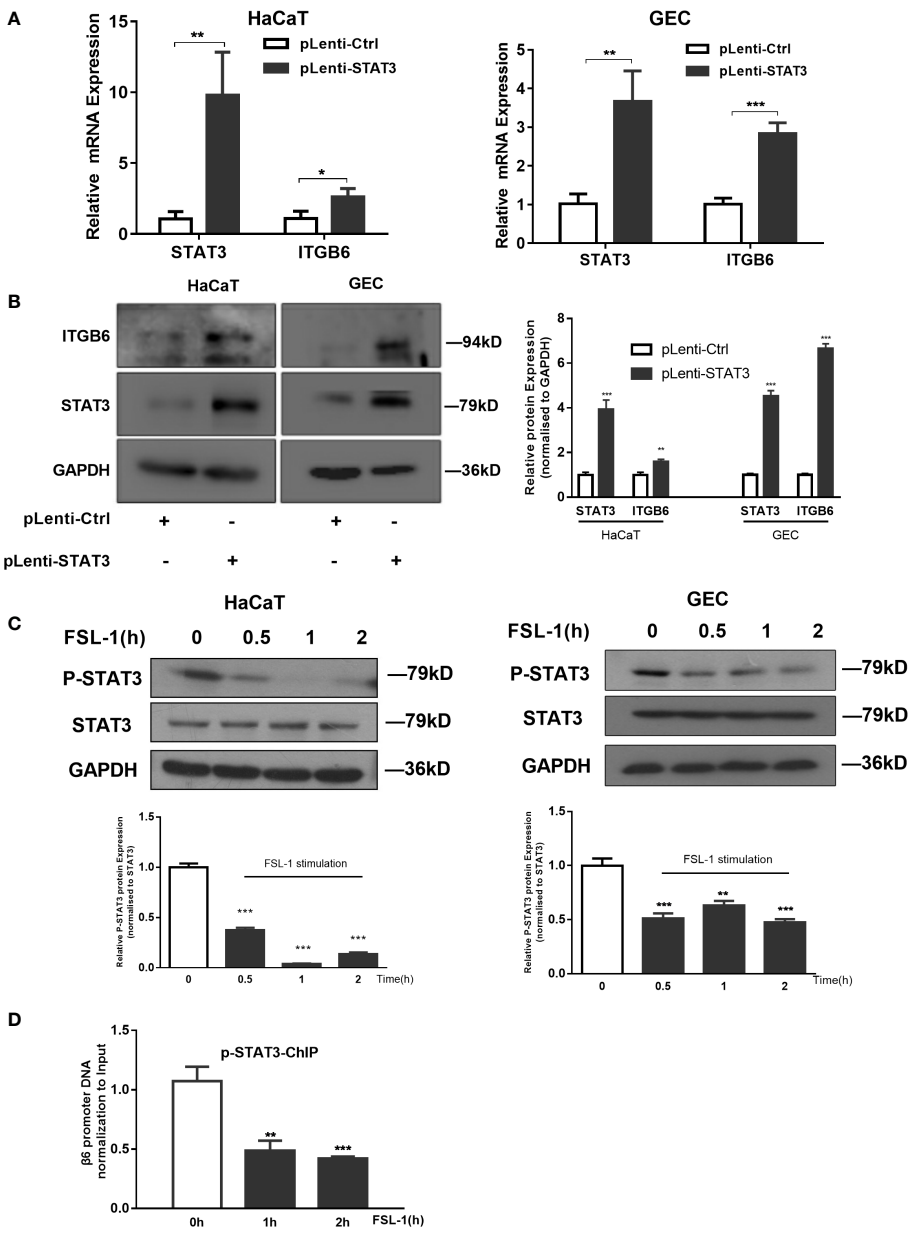

FIGURE 4
STAT3 suppression is involved in FSL-1 mediated ITGB6 downregulation. **(A, B)** STAT3 is involved in ITGB6 transcriptional regulation in HaCaT and GECs. Serum-starved HaCaT and GECs were transfected with the control vectors pLenti-Ctrl or pLenti-STAT3 for 48 h. The mRNA expression of STAT3 and ITGB6 was measured by qRT-PCR **(A)** Data are presented as mean ± SEM from triplicates and compared with pLenti-Ctrl. The protein expression of ITGB6 and STAT3 in HaCaT and GECs was measured using western blotting (left). Densitometric analysis was used to quantify protein bands (right). Data are presented as mean ± SEM from triplicates and compared with pLenti-Ctrl group. **(C)** FSL-1 inhibits STAT3 activation in HaCaT and GECs. Serum-starved HaCaT and GECs were treated with FSL-1 (100 ng/mL) for the indicated times (0.5–2 h). Whole-cell extracts were prepared for western blot analysis of phosphorylated STAT3, STAT3, and GAPDH (loading control). Densitometric analysis was used to quantify protein bands (lower panel). Data are presented as mean ± SEM from triplicates and compared with time zero group. **(D)** FSL-1 inhibited phosphorylated STAT3 binding to the *ITGB6* promoter. HaCaT cells were treated with FSL-1 (100 ng/mL) for the indicated times (1–2 h), and the binding of STAT3 to the *ITGB6* promoter was detected using ChIP assay. The associated *ITGB6* promoter DNA was amplified using qPCR. Data are shown as the mean ± SEM of triplicate experiments and comparison with time zero medium control cells. *P < 0.05, **P < 0.01, ***P < 0.001.

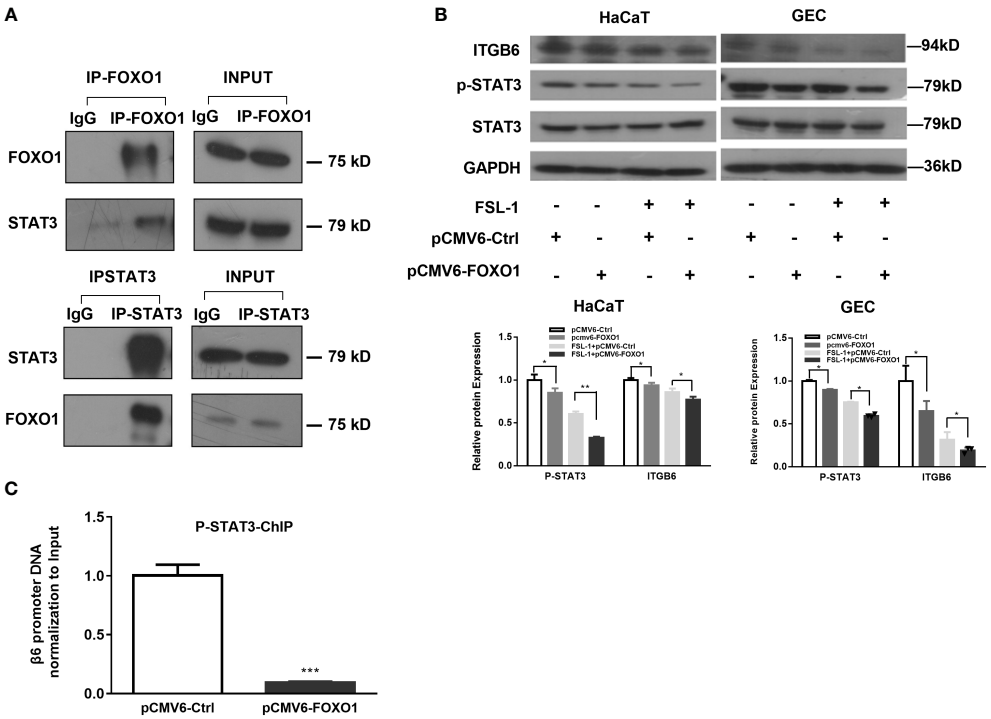

FIGURE 5
FOXO1-inhibited STAT3 activation is involved in FSL-1-mediated ITGB6 downregulation. **(A)** The interaction of STAT3 and FOXO1 was detected *via* co-immunoprecipitation in HaCaT cells. Cell lysate was incubated with FOXO1, STAT3 antibodies or control IgG. The corresponding interacting protein was then detected by western blotting using antibody against STAT3, FOXO1, or IgG. Cell lysate (5%) was used as input positive control. **(B)** Overexpression of FOXO1 inhibited STAT3 activation and ITGB6 expression. HaCaT cells were transfected with pCMV6-Ctrl or pCMV6-FOXO1 plasmids for 24 h before treatment with or without FSL-1 (100 ng/mL) for 2 h. The protein expression of FOXO1, STAT3, p-STAT3, and ITGB6 was analyzed using western blotting. **(C)** FOXO1 overexpression inhibited phosphorated STAT3 binding to the ITGB6 promoter. HaCaT cells were transfected with pCMV6-Ctrl or pCMV6-FOXO1 plasmids for 24 h. The binding of phosphorated STAT3 to the ITGB6 promoter was detected by ChIP assay. The associated ITGB6 promoter DNA was amplified by qPCR using primers covering the potential STAT3-binding sites from −289/−150 of ITGB6 promoter. The input was 5% of the total cell lysate. Data are shown as mean ± SEM of triplicates and compared, V6-Ctrl group. *P < 0.05, **P < 0.01, ***P < 0.001.

However, FOXO1 binding to the ITGB6 promoter did not increase upon FSL-1 stimulation. This suggested that FSL-1-induced FOXO1 expression may indirectly regulate ITGB6 transcription *via* a different mechanism such as protein–protein interaction. Previous studies have confirmed that FOXO1 may regulate the expression of target genes without directly binding to DNA. A FOXO1 mutant that lacks DNA-binding activity can regulate target gene expression (Ramaswamy et al., 2002). In addition, FOXO1 can regulate target gene transcription through direct interaction with other transcription factors, such as STAT3 (Yang et al., 2009; Oh et al., 2012; Ma et al., 2015; Zhang et al., 2021). STAT3 is a critical transcription factor in inflammatory responses and induces the expression of a large array of inflammatory mediators (Hillmer et al., 2016). We previously reported that the promoter region of the human ITGB6 gene contains STAT3 binding sites, and the basal rate of ITGB6 expression in oral squamous cell carcinoma cells is primarily defined by STAT3 (Xu et al., 2015). Therefore, we speculated that the reciprocal action of STAT3 and FOXO1 might regulate FSL-1-induced ITGB6 downregulation.

Being a pivotal inflammatory transcription factor, STAT3 activation has been shown to mediate the biological effects of several oral proinflammatory factors such as *P. gingivalis* (Ma et al., 2021) and LPS (Zhang et al., 2021). However, it is still unclear whether STAT3 plays a role in FSL-1-induced cellular effects in periodontitis. Our results demonstrated for the first time that FSL-1 stimulation reduced STAT3 phosphorylation levels in both HaCaT and GECs. FSL-1 stimulation also inhibits the binding of phospho-STAT3 to the ITGB6 promoter. These results indicate that FSL-1 downregulates ITGB6 expression in GECs by inhibiting STAT3 activation and binding to the ITGB6 promoter.

We also determined how FOXO1 interfered with STAT3 to regulate ITGB6 suppression by FSL-1. First, our co-IP experiments confirmed the direct interaction of FOXO1 with STAT3. Next, overexpression of FOXO1 further attenuated STAT3 activation and its binding to the ITGB6 promoter. These results are

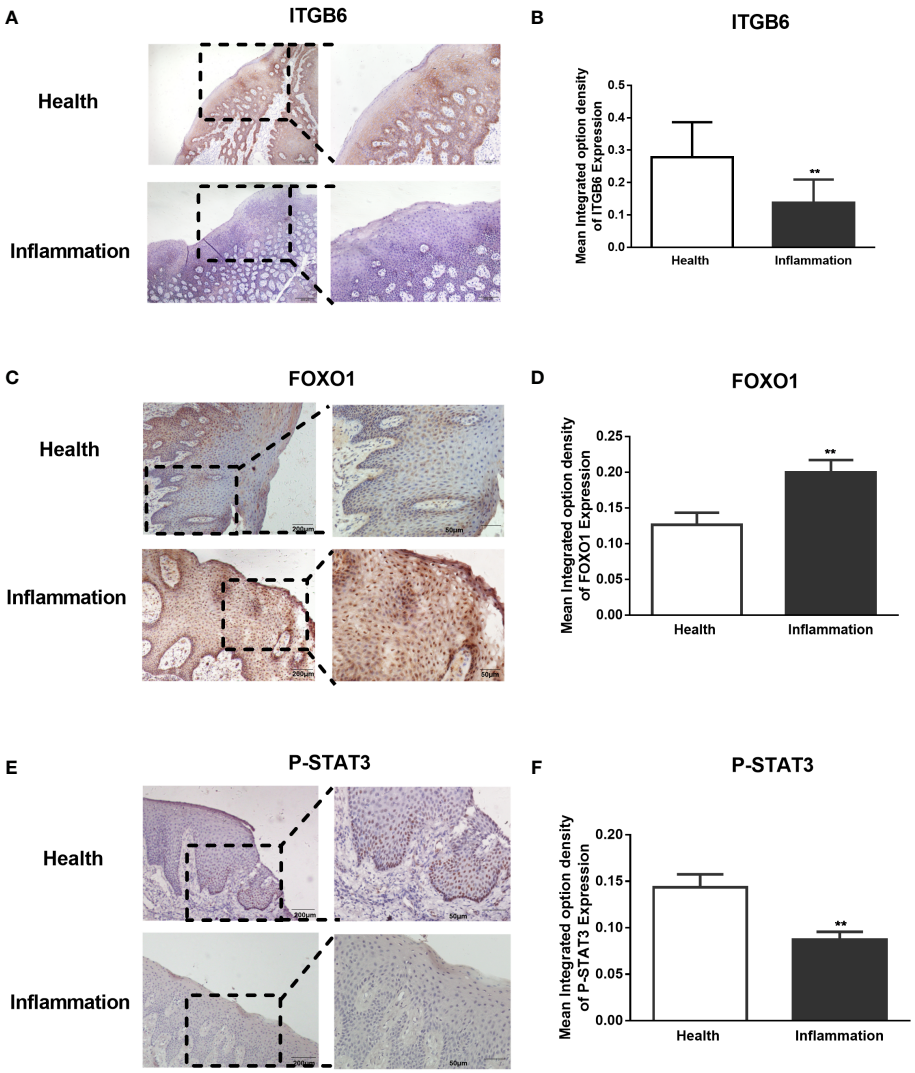

FIGURE 6
Expression of ITGB6, FoxO1, and phosphorated STAT3 in human gingival epithelium. Paraffin-embedded human gingival epithelia were obtained from patients who had undergone tooth extraction for periodontitis treatment (n = 5) or orthodontic treatment as healthy controls (n=5). Immunohistochemistry for ITGB6, phosphorated STAT3, and FOXO1 was performed. Representative sections of healthy gingival epithelium showing strong staining of ITGB6 in the cytosol **(A)** and phosphorylated STAT3 in the nucleus **(E)**, whereas both molecules were barely expressed in periodontal disease specimens. In contrast, a representative section of inflammatory gingival epithelium showed strong staining of FOXO1 in both the nucleus and cytoplasm, whereas minor staining was detected in healthy gingival epithelium **(C)**. **(A)** Low power scale bar: 200 μm. High power scale bar: 100 μm. **(C–E)** Low power scale bar: 200 μm. High power scale bar: 50 μm. **(B, D, F)** Quantitative statistics of immunostaining were analyzed using Image Pro-Plus 6.0. The average integrated optical density (IOD) of both healthy and inflamed tissues was analyzed. Five regions of the epithelial tissue were randomly selected for the average value. Data are shown as the mean ± SEM of triplicate experiments and compared to healthy gingival epithelium. **P < 0.01.

consistent with the notion that FOXO1 inhibits STAT3 activity by preventing STAT3 from interacting with the ITGB6 promoter DNA. Furthermore, the reciprocal action of STAT3 and FOXO1 on ITGB6 downregulation was also confirmed by the immunostaining of the inflammatory epithelium associated with periodontitis. Together, these data support our proposed model of a potential mechanism of how FSL-1-induced FOXO1 inhibits ITGB6 transcription regulation; with increasing amount of FOXO1 expression, FOXO1 binds to phospho-STAT3 in the nucleus, prevents STAT3 from interacting with the ITGB6 promoter, and consequently, inhibits ITGB6 transcription (Figure 7).

In conclusion, the current study demonstrates that FOXO1 is involved in FSL-1-mediated ITGB6 downregulation in HaCaT and GECs. The FOXO1 inhibitory effect on ITGB6 expression was a consequence of its interaction with STAT3 rather than binding to the ITGB6 promoter site. FOXO1 attenuated STAT3 activation and

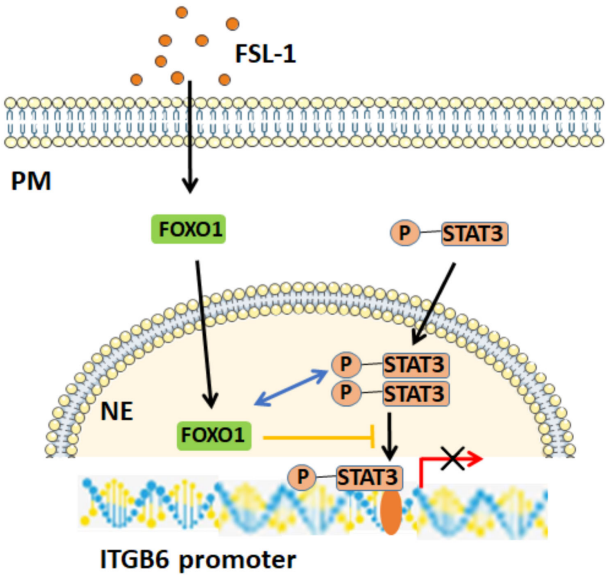

FIGURE 7
Potential mechanism of FOXO1-mediated FSL-1-induced ITGB6 downregulation. FSL-1 increases FOXO1 expression, and FOXO1 interacts with p-STAT3 in the nucleus, prevents the binding of p-STAT3 to the ITGB6 promoter, and consequently inhibits STAT3-mediated ITGB6 transcriptional expression. *PM*, plasma membrane; *NE*, nuclear envelope.

binding to the ITGB6 promoter, which resulted in FSL-1-induced downregulation of ITGB6. Therefore, the interaction of FOXO1 and STAT3 may contribute to periodontitis progression by inhibiting ITGB6 expression. Targeting the FOXO1–STAT3 signaling axis may be an effective method for treating periodontal diseases.

Data availability statement

The raw data supporting the conclusions of this article will be made available by the authors, without undue reservation.

Ethics statement

The studies involving human participants were reviewed and approved by the Ethics Committee of the Stomatological Hospital of Xiamen Medical College (HS20200908001). The patients/participants provided their written informed consent to participate in this study.

Author contributions

MX contributed to conception, analysis, and interpretation, drafted and critically revised the manuscript; JH and FZ, contributed to data acquisition, analysis, and interpretation the manuscript; KS and FL contributed to conception and critically revised the manuscript; XD contributed to conception and design, and drafted the manuscript. All authors gave final approval and agreed to be accountable for all aspects of the work.

Funding

This work was supported by National Natural Science Foundation of China (NO. 82071128, 82270988, 81771079), the Fujian Provincial Health Technology Project (2020-CXB055) and the Xiamen Health Commission project (2022D006).

Acknowledgments

We would like to thank Editage (www.editage.cn) for English language editing.

Conflict of interest

The authors declare that the research was conducted in the absence of any commercial or financial relationships that could be construed as a potential conflict of interest.

Publisher's note

References

Ahmad, R., Shihab, P. K., Jasem, S., and Behbehani, K. (2014). FSL-1 induces MMP-9 production through TLR-2 and NF-kappaB/AP-1 signaling pathways in monocytic THP-1 cells. *Cell Physiol. Biochem.* 34, 929–942. doi: 10.1159/000366310

Ansar, M., Jan, A., Santos-Cortez, R. L., Wang, X., Suliman, M., Acharya, A., et al. (2016). Expansion of the spectrum of ITGB6-related disorders to adolescent alopecia, dentogingival abnormalities and intellectual disability. *Eur. J. Hum. genetics: EJHG* 24, 1223–1227. doi: 10.1038/ejhg.2015.260

Bi, J., Dai, J., Koivisto, L., Larjava, M., Bi, L., Hakkinen, L., et al. (2019). Inflammasome and cytokine expression profiling in experimental periodontitis in the integrin beta6 null mouse. *Cytokine* 114, 135–142. doi: 10.1016/j.cyto.2018.11.011

Bi, J., Koivisto, L., Dai, J., Zhuang, D., Jiang, G., Larjava, M., et al. (2019). Epidermal growth factor receptor signaling suppresses alphavbeta6 integrin and promotes periodontal inflammation and bone loss. *J. Cell Sci.* 133 (5), jcs236588. doi: 10.1242/jcs.236588.

Bi, J., Koivisto, L., Pang, A., Li, M., Jiang, G., Aurora, S., et al. (2017). Suppression of alphavbeta6 integrin expression by polymicrobial oral biofilms in gingival epithelial cells. *Sci. Rep.* 7, 4411. doi: 10.1038/s41598-017-03619-7

Breuss, J. M., Gillett, N., Lu, L., Sheppard, D., and Pytela, R. (1993). Restricted distribution of integrin beta 6 mRNA in primate epithelial tissues. *J. Histochem Cytochem* 41, 1521–1527. doi: 10.1177/41.10.8245410

Ghannad, F., Nica, D., Fulle, M. I., Grenier, D., Putnins, E. E., Johnston, S., et al. (2008). Absence of alphavbeta6 integrin is linked to initiation and progression of periodontal disease. *Am. J. Pathol.* 172, 1271–1286. doi: 10.2353/ajpath.2008.071068

Gomes-Filho, I. S., Cruz, S. S. D., Trindade, S. C., Passos-Soares, J. S., Carvalho-Filho, P. C., Figueiredo, A., et al. (2020). Periodontitis and respiratory diseases: A systematic review with meta-analysis. *Oral. Dis.* 26, 439–446. doi: 10.1111/odi.13228

Hickey, N. A., Shalamanova, L., Whitehead, K. A., Dempsey-Hibbert, N., van der Gast, C., and Taylor, R. L. (2020). Exploring the putative interactions between chronic kidney disease and chronic periodontitis. *Crit. Rev. Microbiol.* 46, 61–77. doi: 10.1080/1040841X.2020.1724872

Hillmer, E. J., Zhang, H., Li, H. S., and Watowich, S. S. (2016). STAT3 signaling in immunity. *Cytokine Growth Factor Rev.* 31, 1–15. doi: 10.1016/j.cytogfr.2016.05.001

Kedjarune, U., Pongprerachok, S., Arpornmaeklong, P., and Ungkusonmongkhon, K. (2001). Culturing primary human gingival epithelial cells: comparison of two isolation techniques. *J. Craniomaxillofac Surg.* 29, 224–231. doi: 10.1054/jcms.2001.0229

Kocher, T., Konig, J., Borgnakke, W. S., Pink, C., and Meisel, P. (2018). Periodontal complications of hyperglycemia/diabetes mellitus: Epidemiologic complexity and clinical challenge. *Periodontol* 2000 78, 59–97. doi: 10.1111/prd.12235

Li, S., Dong, G., Moschidis, A., Ortiz, J., Benakanakere, M. R., Kinane, D. F., et al. (2013). P. gingivalis modulates keratinocytes through FOXO transcription factors. *PloS One* 8, e78541. doi: 10.1371/journal.pone.0078541

Ma, W., Fuentes, G., Shi, X., Verma, C., Radda, G. K., and Han, W. (2015). FoxO1 negatively regulates leptin-induced POMC transcription through its direct interaction with STAT3. *Biochem. J.* 466, 291–298. doi: 10.1042/BJ20141109

Maiese, K., Chong, Z. Z., Hou, J., and Shang, Y. C. (2009). The "O" class: crafting clinical care with FoxO transcription factors. *Adv. Exp. Med. Biol.* 665, 242–260. doi: 10.1007/978-1-4419-1599-3_18

Ma, L., Liu, H., Wang, X., Jiang, C., Yao, S., Guo, Y., et al. (2021). CXXC5 orchestrates Stat3/Erk/Akt signaling networks to modulate p. *gingivalis-elicited autophagy cementoblasts Biochim. Biophys. Acta Mol. Cell Res.* 1868, 118923. doi: 10.1016/j.bbamcr.2020.118923

Meecham, A., and Marshall, J. F. (2020). The ITGB6 gene: its role in experimental and clinical biology. *Gene: X* 5, 100023. doi: 10.1016/j.gene.2019.100023

Oh, H. M., Yu, C. R., Dambuza, I., Marrero, B., and Egwuagu, C. E. (2012). STAT3 protein interacts with class O forkhead transcription factors in the cytoplasm and regulates nuclear/cytoplasmic localization of FoxO1 and FoxO3a proteins in CD4(+) T cells. *J. Biol. Chem.* 287, 30436–30443. doi: 10.1074/jbc.M112.359661

Ramaswamy, S., Nakamura, N., Sansal, I., Bergeron, L., and Sellers, W. R. (2002). A novel mechanism of gene regulation and tumor suppression by the transcription factor FKHR. *Cancer Cell* 2, 81–91. doi: 10.1016/S1535-6108(02)00086-7

Ren, L., Yang, J., Wang, J., Zhou, X., and Liu, C. (2021). The roles of FOXO1 in periodontal homeostasis and disease. *J. Immunol. Res.* 2021, 5557095. doi: 10.1155/2021/5557095

Sanz, M., Marco Del Castillo, A., Jepsen, S., Gonzalez-Juanatey, J. R., D'Aiuto, F., Bouchard, P., et al. (2020). Periodontitis and cardiovascular diseases: Consensus report. *J. Clin. Periodontol* 47, 268–288. doi: 10.1111/jcpe.13189

Shibata, K., Hasebe, A., Into, T., Yamada, M., and Watanabe, T. (2000). The n-terminal lipopeptide of a 44-kDa membrane-bound lipoprotein of mycoplasma salivarium is responsible for the expression of intercellular adhesion molecule-1 on the cell surface of normal human gingival fibroblasts. *J. Immunol.* 165, 6538–6544. doi: 10.4049/jimmunol.165.11.6538

Teles, F., Collman, R. G., Mominkhan, D., and Wang, Y. (2022). Viruses, periodontitis, and comorbidities. *Periodontol* 2000 89, 190–206. doi: 10.1111/prd.12435

van der Vos, K. E., and Coffer, P. J. (2008). FOXO-binding partners: it takes two to tango. *Oncogene* 27, 2289–2299. doi: 10.1038/onc.2008.22

Wang, Q., Sztukowska, M., Ojo, A., Scott, D. A., Wang, H., and Lamont, R. J. (2015). FOXO responses to porphyromonas gingivalis in epithelial cells. *Cell. Microbiol.* 17, 1605–1617. doi: 10.1111/cmi.12459

Xu, M., Chen, X., Yin, H., Yin, L., Liu, F., Fu, Y., et al. (2015). Cloning and characterization of the human integrin beta6 gene promoter. *PloS One* 10, e0121439. doi: 10.1371/journal.pone.0121439

Xu, M. Y., Porte, J., Knox, A. J., Weinreb, P. H., Maher, T. M., Violette, S. M., et al. (2009). Lysophosphatidic acid induces {alpha}v{beta}6 integrin-mediated TGF-{beta} activation *via* the LPA2 receptor and the small G protein g{alpha}q. *Am. J. Pathol.* 174, 1264–1279. doi: 10.2353/ajpath.2009.080160

Yang, G., Lim, C. Y., Li, C., Xiao, X., Radda, G. K., Li, C., et al. (2009). FoxO1 inhibits leptin regulation of pro-opiomelanocortin promoter activity by blocking STAT3 interaction with specificity protein 1. *J. Biol. Chem.* 284, 3719–3727. doi: 10.1074/jbc.M804965200

Zemedikun, D. T., Chandan, J. S., Raindi, D., Rajgor, A. D., Gokhale, K. M., Thomas, T., et al. (2021). Burden of chronic diseases associated with periodontal diseases: a retrospective cohort study using UK primary care data. *BMJ Open* 11, e048296. doi: 10.1136/bmjopen-2020-048296

Zhang, W., Bai, S. S., Zhang, Q., Shi, R. L., Wang, H. C., Liu, Y. C., et al. (2021). Physalin b reduces abeta secretion through down-regulation of BACE1 expression by activating FoxO1 and inhibiting STAT3 phosphorylation. *Chin. J. Nat. Med.* 19, 732–740. doi: 10.1016/S1875-5364(21)60090-0

Zhang, X., Zhang, X., Qiu, C., Shen, H., Zhang, H., He, Z., et al. (2021). The imbalance of Th17/Treg *via* STAT3 activation modulates cognitive impairment in p. gingivalis LPS-induced periodontitis mice. *J. Leukoc. Biol.* 110, 511–524. doi: 10.1002/JLB.3MA0521-742RRR

frontiers | Frontiers in Cellular and Infection Microbiology

TYPE Original Research
PUBLISHED 10 October 2022
DOI 10.3389/fcimb.2022.998600

OPEN ACCESS

EDITED BY
Zuomin Wang,
Capital Medical University, China

REVIEWED BY
Hong Yu,
Medical University of South Carolina, United States
Lang Lei,
Nanjing University, China
Xiaoping Lin,
ShengJing Hospital of China Medical University, China

*CORRESPONDENCE
Yu Cai
jessonjesson@hotmail.com
Qingxian Luan
kqluanqx@163.com

†These authors have contributed equally to this work

SPECIALTY SECTION
This article was submitted to Extra-intestinal Microbiome, a section of the journal Frontiers in Cellular and Infection Microbiology

RECEIVED 20 July 2022
ACCEPTED 16 September 2022
PUBLISHED 10 October 2022

CITATION
Kang N, Zhang Y, Xue F, Duan J, Chen F, Cai Y and Luan Q (2022) Periodontitis induced by *Porphyromonas gingivalis* drives impaired glucose metabolism in mice. *Front. Cell. Infect. Microbiol.* 12:998600.
doi: 10.3389/fcimb.2022.998600

Periodontitis induced by *Porphyromonas gingivalis* drives impaired glucose metabolism in mice

Ni Kang[1,2†], Yong Zhang[3†], Fei Xue[3], Jinyu Duan[3], Fan Chen[4], Yu Cai[1,2*] and Qingxian Luan[1*]

[1]Department of Periodontology, Peking University School and Hospital of Stomatology and National Center of Stomatology and National Clinical Research Center for Oral Diseases and National Engineering Research Center of Oral Biomaterials and Digital Medical Devices and Beijing Key Laboratory of Digital Stomatology and Research Center of Engineering and Technology for Computerized Dentistry Ministry of Health and National Medical Products Administration (NMPA) Key Laboratory for Dental Materials, Beijing, China, [2]Central Laboratory, Peking University School and Hospital of Stomatology and National Center of Stomatology and National Clinical Research Center for Oral Diseases and National Engineering Research Center of Oral Biomaterials and Digital Medical Devices and Beijing Key Laboratory of Digital Stomatology and Research Center of Engineering and Technology for Computerized Dentistry Ministry of Health and National Medical Products Administration (NMPA) Key Laboratory for Dental Materials, Beijing, China, [3]First Clinical Division, Peking University School and Hospital of Stomatology and National Center of Stomatology and National Clinical Research Center for Oral Diseases and National Engineering Research Center of Oral Biomaterials and Digital Medical Devices and Beijing Key Laboratory of Digital Stomatology and Research Center of Engineering and Technology for Computerized Dentistry Ministry of Health and National Medical Products Administration (NMPA) Key Laboratory for Dental Materials, Beijing, China, [4]Department of Stomatology, People's Hospital of Peking University, Beijing, China

Periodontitis has been demonstrated to be bidirectionally associated with diabetes and has been recognized as a complication of diabetes. As a periodontal pathogen, *Porphyromonas gingivalis* is a possible pathogen linking periodontal disease and systemic diseases. It has also been found to be involved in the occurrence and development of diabetes. In this study, 6-week-old male C57BL/6 mice were orally administered the *P. gingivalis* strain ATCC381 for 22 weeks. Histological analysis of the gingival tissue and quantified analysis of alveolar bone loss were performed to evaluate periodontal destruction. Body weight, fasting glucose, glucose tolerance test (GTT), and insulin tolerance test (ITT) were used to evaluate glucose metabolism disorder. We then analyzed the expression profiles of inflammatory cytokines and chemokines in gingival tissue, the liver, and adipose tissue, as well as in serum. The results showed that mice in the *P. gingivalis*-administered group developed apparent gingival inflammation and more alveolar bone loss compared to the control group. After 22 weeks of *P. gingivalis* infection, significant differences were observed at 30 and 60 min for the GTT and at 15 min for the ITT. *P. gingivalis*-administered mice showed an increase in the mRNA expression levels of the pro-inflammatory cytokines (TNF-α, IL-6, IL-17, and IL-23) and chemokines (CCL2, CCL8, and CXCL10) in the gingiva and serum. The expression levels of the glucose metabolism-related genes were also changed in the liver and adipose tissue. Our results

indicate that oral administration of *P. gingivalis* can induce changes in the inflammatory cytokines and chemokines in the gingiva and blood, can lead to alveolar bone loss and to inflammatory changes in the liver and adipose tissues, and can promote glucose metabolism disorder in mice.

KEYWORDS

periodontitis, *Porphyromonas gingivalis* (*P. gingivalis*), glucose metabolism, inflammation, alveolar bone loss

Introduction

Periodontitis is a chronic infectious disease caused by a dental plaque microbiome. It features connective tissue destruction and alveolar bone loss. A series of studies have demonstrated that periodontitis not only causes tooth loss but also contributes to the progress of systemic diseases; it has also been recognized as a complication of diabetes (Cullinan and Seymour, 2013). It has been established that diabetes has bidirectional positive associations with periodontitis and that high prevalence and severe periodontitis in diabetes mellitus patients may influence glycemic control (Nascimento et al., 2018; Sthr et al., 2021). The underlying mechanisms linking periodontitis and diabetes have been considered to be pro-inflammatory cytokines derived from gingival lesions [tumor necrosis factor alpha (TNF-α), interleukin 6 (IL-6), and IL-17]. These are chronically overexpressed in advanced periodontitis and can be released into the blood to affect other organs and exacerbate metabolic diseases (Kashiwagi et al., 2021); however, several reports have shown that the levels of serum TNF-α and other pro-inflammatory cytokines in periodontitis patients are not elevated compared with those of healthy subjects (Yamazaki et al., 2005). Thus, the pathogenic mechanisms of periodontitis affecting diabetes remain to be elucidated.

Recent studies have shown that *Porphyromonas gingivalis*, a major pathogenic bacterium in periodontitis, is a possible pathogen linking periodontal disease to other systemic diseases (Darveau et al., 2012). It has been found to participate in the occurrence and development of insulin resistance (Makiura et al., 2008; Aemaimanan et al., 2013; Arimatsu et al., 2014; Bhat et al., 2014). The levels of HbA1c have been shown to be related to the number of red complex bacteria, including *P. gingivalis*, in periodontal tissues (Aemaimanan et al., 2013). *P. gingivalis* infection increased systemic inflammation, especially in adipose tissue, through the induction of IL-6, which can induce insulin resistance (Pradhan et al., 2001). Oral administration of *P. gingivalis* has also been observed to elicit endotoxemia and induce insulin resistance in mice (Arimatsu et al., 2014).

To demonstrate the causal role of periodontal disease as a risk factor for diabetes, we orally administered *P. gingivalis* to mice. Alveolar bone loss levels were evaluated and glucose metabolism was measured. Inflammatory mediators and the expression levels of glucose metabolism-related genes were also investigated. We report the observation of a causal role for *P. gingivalis*, a periodontitis-related pathogen, in the progress of diabetes and metabolic disorders. We have shown that oral administration of *P. gingivalis* has an impact on serum inflammatory cytokines, chemokines, and the expression levels of glucose-related genes in liver and adipose tissue, resulting in metabolic disorders. Our results also confirm that *P. gingivalis* can aggravate impaired glucose metabolism. This may enhance our knowledge of the mechanistic relationship between periodontitis and the clinical features of diabetes.

Materials and methods

Ethics statement

All animal experimental procedures in this study were approved by the Animal Welfare Ethics of Peking University Biomedical Ethics Committee (LA2018142).

Mice

Twelve 4-week-old C57BL/6 male mice, weighing nearly 20 g (Vital River Inc., Beijing, China) were purchased and group-housed (six mice per cage) in a specific pathogen-free environment. The mice were fed regular chow and sterile water until the commencement of infection at 6 weeks of age. During the observation period, body weight and food intake were monitored every other week.

Bacterial cultures

The *P. gingivalis* strain ATCC381 was cultured on anaerobic basal agar plates (Oxoid, Oxoid Ltd., Hampshire, England) enriched with 5% sheep blood and incubated under anaerobic

conditions (80% N_2, 10% CO_2, and 10% H_2) for 3–5 days at 37°C. Cultures were then inoculated into brain heart infusion broth (Oxoid, Oxoid Ltd., Hampshire, England), supplemented with 5 μg/ml hemin and 0.4 μg/ml menadione (Sigma-Aldrich, St. Louis, MO, USA), and grown for 2 days based on a calibration curve of optical density measured at 600 nm *versus* the viable cell count in colony forming units (CFU) per milliliter, corresponding to 10^9 CFU/ml. The cultured cells were then centrifuged at 8,000 × *g* for 20 min at 4°C and suspended in phosphate-buffered saline (PBS) with 2% carboxymethylcellulose (CMC) (Sigma-Aldrich, St. Louis, MO, USA) for oral administration to increase viscosity.

Induction of diabetes and periodontitis in mice

Twelve mice were randomly divided into two groups: the control group and the *P.gingivalis*-administered group. *P. gingivalis* and CMC were administered orally through a plastic tube, with 10^8 CFU *P. gingivalis* in 100 μl PBS mixed with 2% CMC (for the *P. gingivalis*-administered group) or only 100 μl PBS mixed with 2% CMC (for the control group) every 2 days for 22 weeks. The mice were then sacrificed after anesthetization. The blood, gingiva, liver, adipose tissue, and maxilla samples were excised and harvested for the following experiments.

Tissue collection and preparation

Blood samples were collected *via* infraorbital puncture. Serum was isolated by centrifugation at 10,000 rpm for 5 min at 4°C. The gingiva, liver, and the epididymal white adipose tissues were collected from each mouse and were rapidly removed from the mice, placed into a liquid nitrogen box, and kept at −80°C until analyzed, or fixed by 10% formalin for histological staining. Mouse maxillae were harvested and fixed in 4% paraformaldehyde at 4°C overnight, and then transferred to a 70% ethanol solution. Horizontal bone loss around the maxillary molars was examined using micro-CT.

Glucose and insulin tolerance tests

Glucose tolerance test (GTT) and insulin tolerance test (ITT) were performed. For the GTT, the fasting glucose levels were measured following overnight (12 h) fasting. Thereafter, the mice were injected intraperitoneally with 1.5 g of glucose (Solarbio, Beijing, China) per kilogram of body weight. Blood samples were collected through the tail tip vein at 30, 60, and 90 min after injection. For the ITT, following 4 h of fasting, the mice were injected intraperitoneally with 2 U of insulin (Actrapid MC, Novo Nordisk, Bagsværd, Denmark) per kilogram of body weight. Blood samples were collected through the tail vein at 15, 30, 45, and 60 min after injection. The glucose levels were determined using a glucometer (Sinocare, Hunan, China).

Quantification of maxillary alveolar bone resorption

Micro-CT imaging of the mouse hemi-maxillae, free of soft tissues, was performed using a CT scanner (Inveon MM Gantry-STD 3121, Siemens, Munich, Germany) for the purpose of generating three-dimensional models. The parameters were as follows: 360° rotation, 360 projections, 1,500-ms exposure time, 60-kV source voltage, 220-μA beam current, 8.82-μm effective pixel size, and 18-μm isotropic resolution. Acquisitions were reconstructed with a filtered back-projection algorithm, matrix size of 1,024 × 1,024 × 448, using Inveon Acquisition Workplace software (COBRA, Siemens, Berlin, Germany). The images were rotated and adjusted from M1 to M3 and then analyzed by an examiner (NK) blinded to the experimental groups. Inveon Research Workplace software (COBRA, Siemens, Berlin, Germany) was used to measure the distance from the cemento-enamel junction (CEJ) to the alveolar bone crest (ABC) at six points: 1) mesiobuccal and 2) distobuccal regions of the first maxillary molar; 3) mesiobuccal and 4) distobuccal regions of the second maxillary molar; and 5) mesiobuccal and 6) distobuccal regions of the third maxillary molar. Measurements were taken for the purpose of evaluating the levels of alveolar bone loss (ABL). Prior to the observation, the intraclass correlation for the evaluation of bone loss measurements was calculated. The same examiner evaluated the same tooth points on different days, and the intraclass correction coefficient (ICC) was 0.89.

Serum cytokine, chemokine, and receptor levels

Serum samples were isolated from the blood after euthanasia. Commercially available ELISA kits were used to determine the serum concentrations of cytokines (TNF-α, IL-6, IL-17, and IL-23) (RayBiotech Inc., Norcross, GA, USA), chemokines and receptor chemokines [C–C motif ligand 2 (CCL2), C–C motif receptor 2 (CCR2), CCL3, CCL8, C–X–C motif ligand 10 (CXCL10), and CCL20] (Mei Mian, Jiangsu, China), and developmental endothelial locus-1 (Del-1) (Signalway Antibody Co., Ltd., Pearland, TX, USA) according to the manufacturers' protocols.

RNA isolation and quantitative real-time PCR analysis

Total RNAs from the gingiva, liver, and adipose tissue were extracted using an RNeasy Mini kit (Qiagen, Valencia, CA, USA) according to the manufacturer's instructions. Total RNA was

quantified by measuring the absorbance at 260–280 nm. Subsequently, aliquots of RNA were reverse transcribed to complementary DNA (cDNA) using a Primescript RT Master Mix Kit (Takara Bio, Shiga, Japan). Quantitative real-time PCR analysis was performed using an Applied Biosystems 7500 Fast Real-time PCR System (Life Technology, Carlsbad, CA, USA) in accordance with the manufacturer's protocol. Briefly, the reactions were carried in a 10-μl mixture of 2× SYBR Green (Takara Bio, Shiga, Japan), each primed at 100 nM and 30 ng of reverse-transcribed RNA. The PCR program consisted of a 30-s incubation at 95°C, followed by 40 cycles at 95°C for 5 s and 60°C for 34 s. A dissociation curve analysis was then performed to confirm specificity. Each gene was tested in triplicate. The relative level of messenger RNA (mRNA) for each target mRNA was determined using the $2^{-\Delta\Delta Ct}$ method. The relative quantities were normalized to glyceraldehyde 3-phosphate dehydrogenase (*GAPDH*) mRNA and represented in fold changes relative to those from control group mice. The sequences of the primers are provided in Table 1.

Statistical analysis

All results are presented as the mean ± standard deviation (SD). Data between two groups were analyzed using unpaired two-tailed Student's *t*-test. Multiple comparisons were analyzed with one-way analysis of variance (ANOVA) followed by Tukey–Kramer multiple tests using SPSS 20.0 statistical software (SPSS Inc., IBM, Chicago, IL, USA) and GraphPad Prism v8.0.2 (GraphPad Software, San Diego, CA, USA). $P < 0.05$ was considered to indicate statistical significance.

Results

P. gingivalis administration had no significant effect on animal body weight

There was no significant difference in body weight from the baseline of the experiment after treatment with *P. gingivalis* for 22 weeks. In addition, there was no significant difference in body weight or food intake between the *P. gingivalis*-administered group and the control group (Figure 1).

P. gingivalis Administration induced alveolar bone loss

We showed *via* hematoxylin–eosin (H&E) staining that inflammatory cells infiltrated the periodontal tissue of mice (Figure 2A), and apparent gingival inflammation was observed after oral *P. gingivalis* infection. Mice in the *P. gingivalis*-administered group exhibited significantly more alveolar bone loss compared to those in the control group (Figure 2B). Quantification of bone resorption indicated a statistical increase

TABLE 1 Primer sequences used for real-time PCR.

Gene	Forward	Reverse
GAPDH	AGGTTGTCTCCTGCGACTTCA	CTGTTGCTGTAGCCGTATTCATTG
TNF-α	AGGCGGTGCCTATGTCTCAG	GCCATTTGGGAACTTCTCATC
IL-6	TAGCTACCTGGAGTACATGAAGAACA	TGGTCCTTAGCCACTCCTTCTG
IL-17	CCTCAGACTACCTCAACCGTTC	ACTGAGCTTCCCAGATCACAGAG
IL-23	GAGCAACTTCACACCTCCCTACTA	TGCCACTGCTGACTAGAACTCA
Del-1	CTTGGTAGCAGCCTGGCTTT	GCCTTCTGGACACTCACAGG
CCL2	GCATCCACGTGTTGGCTCA	CTCCAGCCTACTCATTGGGATCA
CCL8	CGCAGTGCTTCTTTGCCTG	TCTGGCCCAGTCAGCTTCTC
CXCL10	AGAACGGTGCGCTGCAC	CCTATGGCCCTGGGTCTCA
CCR2	ATCCACGGCATACTATCAACATC	CAAGGCTCACCATCATCGTAG
CCL20	TTTTGGGATGGAATTGGACAC	TGCAGGTGAAGCCTTCAACC
CCL3	CCACTGCCCTTGCTGTTCTT	GCAAAGGCTGCTGG-TTTCAA
G6pc	CAGCAAGGTAGATCCGGGA	AAAAAGCCAACGTATGGATTCCG
Saa	GTAATTGGGGTCTTTGCC	TTCTGCTCCCTGCTCCTG
Pck1	AAGTGCCTGCACTCTGTGG	CAGGCCCAGTTGTTGACC
Pparα	GTCATCACAGACACCCTC	TATTCGACACTCGATGTTCAG
Irs1	CTTCTCAGACGTGCGCAAGG	GTTGATGTTGAAACAGCTCTC
Fitm2	ATGGAGCACCTGGAGCGC	TCATTTCTTGTAAGTATCTCGCTTCAAAG
Angptl4	CCAACGCCACCCACTTAC	CTCGGTTCCCTGTGATGC
C1qtnf9	CCTGCACACCAAGGACAGTTAC	TGTCACCTGCATCCACACTTC
Sirt1	TTCACATTGCATGTGTGTGG	TAGCCTGCGTAGTGTTGGTG

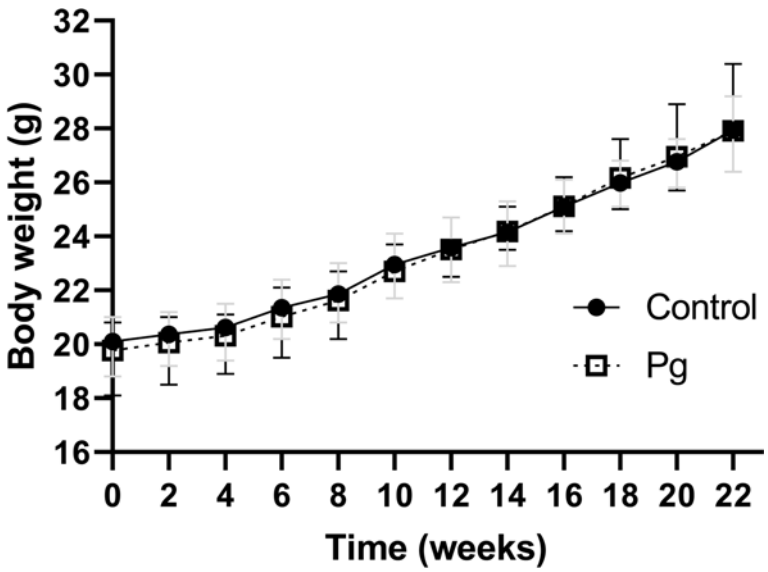

FIGURE 1
Effects of the oral administration of *Porphyromonas gingivalis* on body weight. Body changes during the experimental period in the control group (N = 6) and the *P. gingivalis*-administered group (N = 6) were measured. All data for each time point are expressed as the mean ± SEM.

at all six points in the *P. gingivalis*-administered group compared to the control group (the sum of the six points; 0.18 ± 0.07 mm *vs.* 0.25 ± 0.09 mm for the control and *P. gingivalis*, respectively, $p < 0.01$) (Figure 2C). Based on these data, we conclude that repeated oral administration of *P. gingivalis* can induce alveolar bone resorption.

P. gingivalis administration induced an inflammatory response in gingival tissue

To examine the inflammatory mediators in periodontitis induced by *P. gingivalis*, the expression levels of the genes in the gingiva from the two groups of mice were determined using real-time PCR. The *P. gingivalis*-administered group showed an increase in the mRNA expression levels of the pro-inflammatory cytokines (TNF-α, IL-6, IL-17, and IL-23; $p < 0.05$) and chemokines (CCL2, CCL8 and CXCL10; $p < 0.05$). We also observed a decrease in the mRNA expression levels of the anti-inflammatory mediator (Del-1; $p < 0.05$). However, there was no significant difference in the gingival gene expressions of CCR2, CCL3, and CCL20 between the two groups (Figure 3).

P. gingivalis administration induced impaired glucose metabolism

To explore the effect of oral administration of *P. gingivalis* on the glucose metabolism of mice, we performed fasting GTT and ITT at baseline, 11 weeks, and at 22 weeks of oral *P. gingivalis* administration. As shown in Figure 4A, at baseline, there were no significant differences in the fasting glucose levels and the GTT and ITT results between the control group and the experimental group. At 11 and 22 weeks after *P. gingivalis* infection, the fasting glucose levels showed no significant difference between these two groups. Although the effect of *P. gingivalis* infection was relatively weak, at 11 weeks after *P. gingivalis* administration, a significant difference was observed at 30 min for the GTT. At 22 weeks after *P. gingivalis* infection, in the *P. gingivalis*-administered group, significant differences were observed at 30 and 60 min for the GTT and at 15 min for the ITT. An overall effect was evident, as shown in Figures 4B, C.

P. gingivalis administration induced an inflammation- and glucose metabolism-related gene response in the liver

We compared the gene expression profiles of live tissue samples from mice in the *P. gingivalis*-administered group and the control group. Oral administration of *P. gingivalis* led to increased mRNA expressions of the pro-inflammatory cytokines TNF-α and IL-6 and the expression levels of genes related to glucose metabolism [negative regulation effect genes: glucose 6 phosphatase (*G6pc*), serum amyloid A (*Saa*), and phosphoenolpyruvate carboxykinase 1 (*Pck1*)]. The mRNA expressions of peroxisome proliferator activated

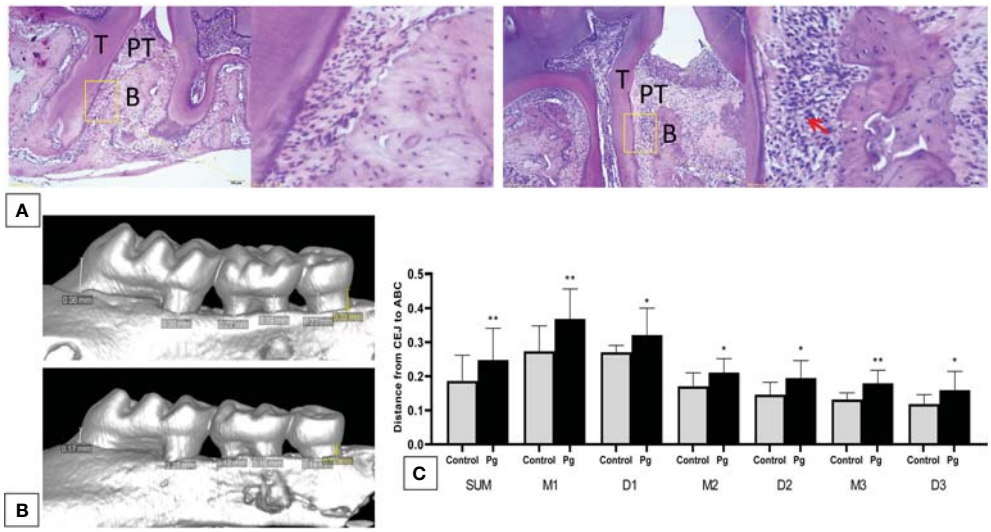

FIGURE 2
Oral administration of *Porphyromonas gingivalis* for 22 weeks induced periodontitis. **(A)** Histological examination of the hemi-maxillae (*T*, tooth; *PT*, periodontal tissue; *B*, alveolar bone) stained with hematoxylin–eosin (H&E). Apparent losses of periodontal attachment and alveolar bone resorption. The *arrow* shows inflammatory cells that have infiltrated the periodontal tissue. **(B)** Buccal side maxillary alveolar bone loss measured from the cemento-enamel junction (CEJ) to the alveolar bone crest (ABC) at six points—*1*) mesiobuccal and *2*) distobuccal regions for the first maxillary molar; *3*) mesiobuccal and *4*) distobuccal regions for the second maxillary molar; and *5*) mesiobuccal and *6*) distobuccal regions for the third maxillary molar—in mice from the *P. gingivalis*-administered group and the control group. **(C)** comparison of the six CEJ–ABC linear distances (*SUM*, the sum of six points; *M1*, mesiobuccal for the first maxillary molar; *D1*, distobuccal for the first maxillary molar; *M2*, mesiobuccal for the second maxillary molar; *D2*, distobuccal for the second maxillary molar; *M3*, mesiobuccal for the third maxillary molar; *D3*, distobuccal for the third maxillary molar). $*p < 0.05$, $**p < 0.01$. $N = 6$. Data are expressed as the mean ± SEM.

receptor alpha (*Ppara*) and insulin receptor substrate (*Irs1*), which positively regulate glucose metabolism, were downregulated in the *P. gingivalis*-administered group (Figure 5A). There was no significant difference in the expression of fat storage-inducing transmembrane protein 2 (*Fitm2*) between these two groups.

P. gingivalis administration induced an inflammation- and glucose metabolism-related gene response in adipose tissue

TNF-α and IL-6 are known to be pro-inflammatory and are adipocytokines that are expressed in adipocytes to modulate

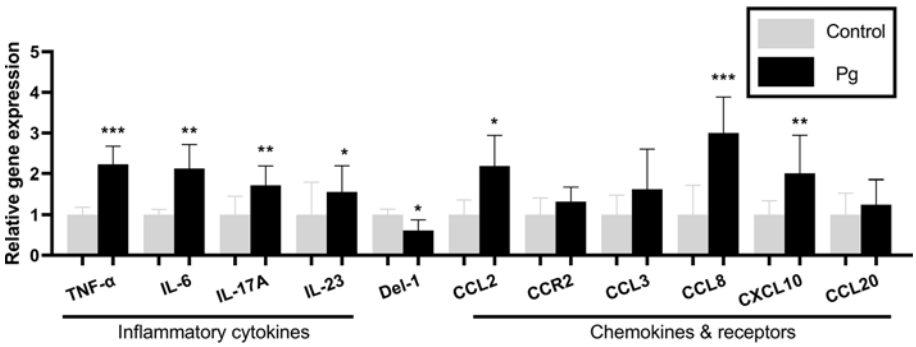

FIGURE 3
Effects of the oral administration of *Porphyromonas gingivalis* on the gene expressions of inflammatory cytokines and chemokines in the gingiva of mice in the *P. gingivalis*-administered group and the control group. The relative mRNA expressions of the genes of interest were normalized to the relative quantity of glyceraldehyde 3-phosphate dehydrogenase (*GAPDH*) mRNA. $*p < 0.05$, $**p < 0.01$, $***p < 0.001$. $N = 6$. Data are expressed as the mean ± SEM.

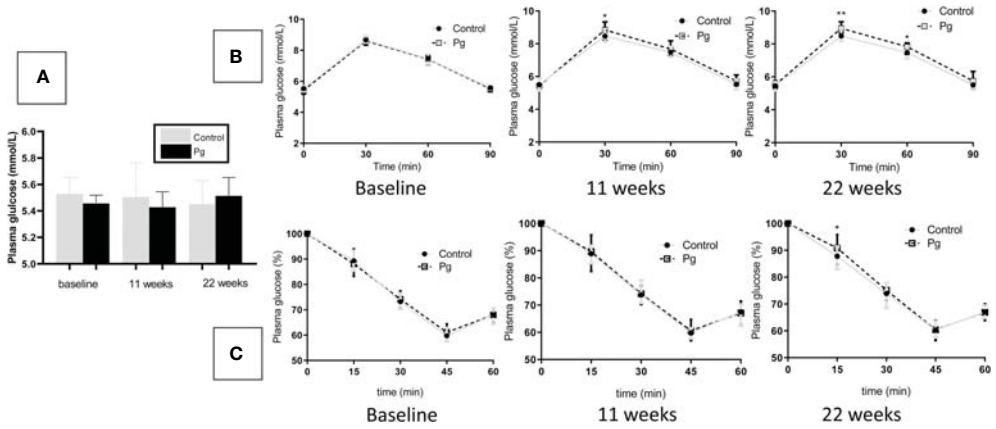

FIGURE 4
Effects of the oral administration of *Porphyromonas gingivalis* on fasting glucose, glucose tolerance, and insulin sensitivity. **(A)** Fasting glucose levels between the *P. gingivalis*-administered group and the control group at baseline, 11 weeks, and at 22 weeks after *P. gingivalis* infection. **(B)** Plasma glucose levels during an intraperitoneal glucose tolerance test (GTT) following overnight (12 h) fasting at baseline, 11 weeks, and at 22 weeks after *P. gingivalis* infection. **(C)** Plasma glucose levels during an intraperitoneal insulin tolerance test (ITT) following 4 h of fasting at baseline, 11 weeks, and at 22 weeks after *P. gingivalis* infection. $*p < 0.05$, $**p < 0.01$. $N = 6$. Data are expressed as the mean ± SEM.

glucose metabolism by suppressing insulin signals (Pradhan et al., 2001). The mRNA expressions of *TNF-α*, *IL-6*, and angiopoietin-like 4 (*Angptl4*), which are involved in insulin resistance (Watanabe et al., 2008; Trayhurn and Alomar, 2015), were shown to be higher in the adipose tissue of mice from the *P. gingivalis*-administered group. Conversely, the *Irs1* gene, which improves insulin sensitivity (Copps and White, 2012), was downregulated in the *P. gingivalis*-administered group. There was no significant difference in the expressions of c1q/tnf-related protein 9 (*C1qtnf9*) and sirtuin type 1 (*Sirt1*) between the two groups (Figure 5B).

P. gingivalis administration increased serum cytokine and chemokine levels

We compared the levels of inflammatory cytokines and chemokines in serum between the *P. gingivalis*-administered group and the control group. As shown in Figure 6, *P. gingivalis* infection increased the serum levels of the pro-inflammatory cytokines TNF-α, IL-6, IL-17A, and IL-23 and the chemokines CCL2, CCL8, and CXCL10. The serum level of the potential anti-inflammatory mediator Del-1 was decreased in the *P. gingivalis*-administered group compared to the control group. Similar to the results of the gingival mRNA gene expression levels, there was no significant difference in serum CCR2, CCL3, and CCL20 between the two groups.

Discussion

Periodontitis is believed to be bidirectionally related to diabetes. Clinical investigations have confirmed that periodontitis increases the severity of diabetes (Kuo et al., 2008; Genco et al., 2020; Genco and Borgnakke, 2020) and that periodontal treatment can improve glycemic control in diabetes patients (Lalla et al., 2006; D'Aiuto et al., 2018). However, the mutually promotional relationship between periodontitis and diabetes is still not fully understood.

Numerous studies have explored the role of periodontitis in the incidence of diabetes in animal investigations and have shown that oral administration of periodontal bacteria diminished glucose tolerance and insulin sensitivity in mice (Arimatsu et al., 2014; Komazaki et al., 2017). In this study, after oral *P. gingivalis* infection, the levels of fasting glucose showed no significant difference compared to those in the control group. However, after GTT, mice in the *P. gingivalis* group showed high blood glucose levels 30 min after glucose injection at 11 weeks after *P. gingivalis* infection. Furthermore, the mice in this group displayed high blood glucose 30 and 60 min after glucose injection at 22 weeks after *P. gingivalis* infection. After ITT, the mice in the *P. gingivalis* group showed high blood glucose 15 min after insulin injection at 22 weeks after *P. gingivalis* infection. Although these effects were relatively modest, we confirmed that mice could develop impaired glucose metabolism after repeated oral administration of *P. gingivalis* (Sasaki et al., 2018; Seyama

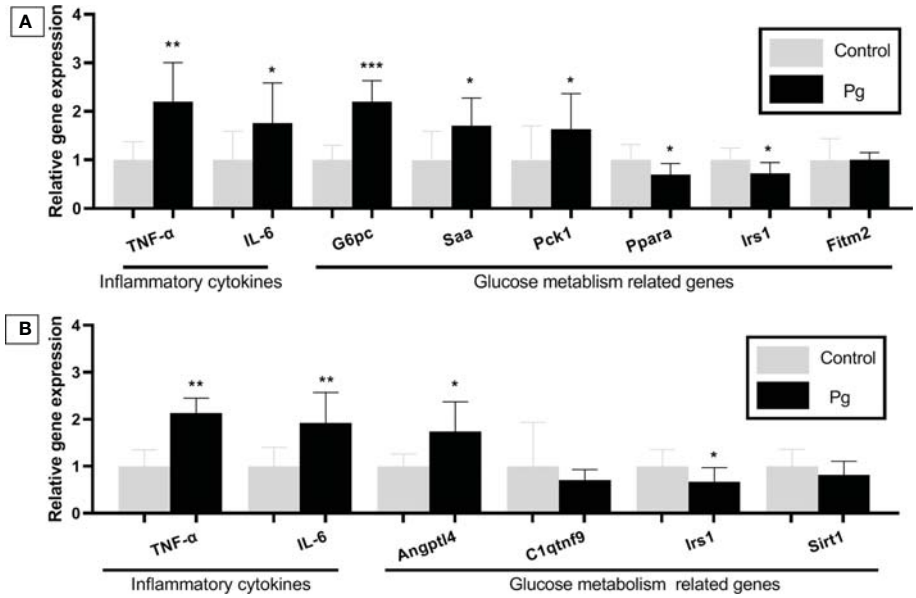

FIGURE 5
Effects of the oral administration of *Porphyromonas gingivalis* on the gene expression of inflammatory cytokines and the expression of the glucose metabolism-related genes in the liver **(A)** and adipose tissue **(B)** of mice in the *P. gingivalis*-administered group and the control group. The relative mRNA expressions of the genes of interest were normalized to the relative quantity of glyceraldehyde 3-phosphate dehydrogenase (*GAPDH*) mRNA. **p* < 0.05, ***p* < 0.01, ****p* < 0.001. *N* = 6. Data are expressed as the mean ± SEM.

et al., 2020; Tian et al., 2020). However, some researchers have shown inconsistent or contradictory results. The study by Mahamed et al. (2005) showed that periodontitis is not associated with the onset and severity of diabetes after oral administration of *P. gingivalis*. The studies of Li et al. (2013); Wang et al. (2016); Ahn et al. (2021), and Ohtsu et al. (2019) showed no significant difference in glucose metabolism between *P. gingivalis*-infected and sham-infected mice. These discrepancies might be due to differences in the procedures of oral infection and the measures of glucose metabolism. Our study administered *P. gingivalis* infection every 2 days for 22 weeks, Li et al. carried out *P. gingivalis* infection in three batches during the experimental period and three times at 2-day intervals per batch, and Ahn and Ohtsu administered *P. gingivalis* infection only for 6 or 5 weeks and calculated the fasting glucose levels without performing GTT or ITT.

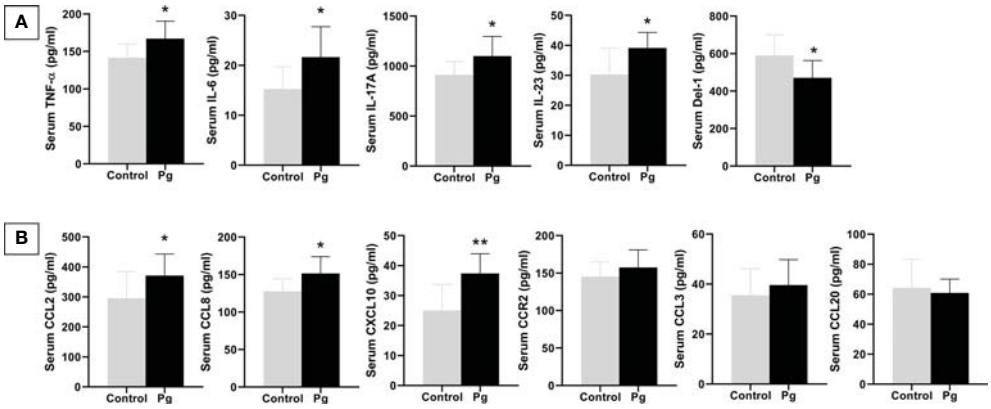

FIGURE 6
Effects of the oral administration of *Porphyromonas gingivalis* on serum inflammatory cytokines **(A)** and chemokines **(B)** between mice in the *P. gingivalis*-administered group and the control group determined by ELISA. **p* < 0.05, ***p* < 0.01. *N* = 6. Data are expressed as the mean ± SEM.

In previous studies, TNF-α and IL-6 had been proven to be pro-inflammatory cytokines in periodontal tissues (Kurgan and Kantarci, 2018). Moreover, they are also recognized as adipocytokines with fairly negative impacts on insulin signaling (Pradhan et al., 2001); the combination of TNF-α and IL-6 had an impact on progressive pancreatic β-cell loss during the progression of diabetes (Watanabe et al., 2008; Ilievski et al., 2017). In this study, we compared the gingival and serum levels of TNF-α and IL-6 between the *P. gingivalis* administration and control groups and found that the gingival mRNA expression levels of *TNF-α* and *IL-6* were upregulated after *P. gingivalis* infection and that their serum levels were also significantly increased. These results reveal that oral *P. gingivalis* infection induced an increase in gingival and serum TNF-α and IL-6. This had harmful effects on insulin sensitivity and was attributable to the progression of impaired glucose metabolism.

Low-grade inflammation is considered the common systemic effect of periodontitis (Preshaw et al., 2012; Hajishengallis and Chavakis, 2021b). IL-17 and IL-23 are pro-inflammatory cytokines that can cause dysbiosis in bacterial communities and are associated with leukocyte adhesion (Abusleme and Moutsopoulos, 2017). IL-17 and Del-1 have exhibited an antagonistic relationship in inflammatory effects (Saxena et al., 2020; Hajishengallis and Chavakis, 2021a). In addition, they have been observed to play a critical role in the loss of pancreatic B cells and have been shown to have pro-diabetic effects (Mensah-Brown et al., 2006; Marwaha et al., 2014). In the present study, we observed an upregulated mRNA expression of *IL-17* and a downregulated mRNA expression of *Del-1* in the gingiva. Similar changes were observed in the serum levels of IL-17 and IL-23, which were increased, and the potential anti-inflammatory mediator Del-1, which was decreased in the *P. gingivalis* group compared to the control group.

Chemokines have also been observed to be involved in the pathogenesis of insulin resistance and diabetes (Esser et al., 2014). IL-17 can increase the expression and the production of CCL2 and CXCL10 to enhance its pro-inflammatory effect (Matsui and Yoshida, 2016). CCL2 (Elmarakby and Sullivan, 2012; Ota, 2013), CCL8 (Sarkar et al., 2012), and CXCL10 (Antonelli et al., 2014; Hueso et al., 2018; Moreno et al., 2022) have also been demonstrated to play a role in the development of diabetes. Along with the elevation of IL-17, the gingival mRNA expressions of *CCL2*, *CCL8*, and *CXCL10* were upregulated. Similar alterations were seen in serum, CCL2, CCL8, and CXCL10 were increased in the *P. gingivalis* group compared to the control group. All of these results provide evidence that elevated chemokine levels induced by IL-17 after *P. gingivalis* infection may be related to the progression of glucose metabolism disorder.

The liver is crucial for maintaining normal glucose homeostasis and regulating glycogen synthesis and degradation, glycolysis, and gluconeogenesis, depending on the fasting and postprandial states. Accompanied by changes of the cytokines and chemokines in the gingiva and serum, the expressions of *TNF-α* and *IL-6* were upregulated in the livers of mice in the *P. gingivalis* group. In addition, the expression levels of the glucose metabolism-related genes *G6pc* (Bruni et al., 1999; Pound et al., 2013), *Saa* (Leinonen et al., 2003; Han et al., 2007; Sjöholm et al., 2009), and *Pck*1 (Choi et al., 2008; Yuan et al., 2019), which can influence gluconeogenesis, were upregulated in the livers of mice in the *P. gingivalis* group. The expression levels of the genes *Ppara* (Srinivasan et al., 2004; Maciejewska-Skrendo et al., 2019) and *Irs1* (Dong et al., 2006; Copps and White, 2012; Takatani et al., 2021), which have been reported to improve insulin sensitivity, were downregulated in the livers of *P. gingivalis*-administered mice. Adipose tissue also plays an important role in mediating glucose metabolism and insulin sensitivity through various molecules, including the adipocytokines TNF-α and IL-6, which possess strong, naturally pro-inflammatory traits that negatively impact insulin signaling. In the present study, the expression levels of *TNF-α* and *IL-6* were significantly upregulated in the adipose tissue from the *P. gingivalis*-administered group. Additionally, an upregulated expression of the pro-inflammatory gene *Angptl*4 (Trayhurn and Alomar, 2015), which is supposed to increase insulin resistance, was observed; on the other hand, *Irs1* (Copps and White, 2012), a gene that improves insulin sensitivity, was downregulated. Taken together, these results indicate that the oral administration of *P. gingivalis* has harmful effects on the inflammatory response and on insulin sensitivity. Although the effect was not robust, continuous deterioration of these cytokines and chemokines could have significant negative effects on both glucose tolerance and insulin sensitivity. The above results confirm that the proposed mechanism for periodontitis-induced diabetes is the increase of the expressions of the inflammatory cytokines and chemokines produced in periodontal lesions.

One limitation of our study is that the symptoms of impaired glucose metabolism were mild. Therefore, further investigations using an increased dosage of bacterial infection, shorter intervals of bacterial incubation, or combined treatment with molar ligation might be targeted for future study.

In the present study, we demonstrated that the oral administration of *P. gingivalis* induced alveolar bone loss and inflammatory changes in the liver and adipose tissues, which also induced impaired glucose metabolism after GTT and ITT. These changes were considered to be attributable to the changes in the levels of the inflammatory cytokines (TNF-α, IL-6, IL-17, and IL-23), chemokines (CCL2, CCL8, and CXCL10), and another mediator (Del-1) in the gingiva and blood. They provide further insight into the role of *P. gingivalis*-mediated inflammatory cytokines and chemokines in the development of diabetes. However, it remains to be elucidated whether a causal relationship exists between periodontitis and impaired glucose metabolism. Further investigations are needed to examine whether other oral periodontal pathogens have similar effects on glucose metabolism.

Data availability statement

The original contributions presented in the study are included in the article/supplementary material. Further inquiries can be directed to the corresponding authors.

Ethics statement

This study was reviewed and approved by the Animal Welfare Ethics of Peking University Biomedical Ethics Committee.

Author contributions

NK and YZ contributed equally to the conception, experimentation, and preparation of the manuscript and figures. FX, JD, and FC participated in the experimentation and preparation of the manuscript, including text and figures. YC and QL provided supervision and wrote and edited the manuscript. All authors contributed to the article and approved the submitted version.

Funding

This study was supported by the National Natural Science Foundation of China (project no. 81800978). The funder had no role in the design of the study, collection, analysis or interpretation of the data, or in writing the manuscript.

Conflict of interest

The authors declare that the research was conducted in the absence of any commercial or financial relationships that could be construed as a potential conflict of interest.

Publisher's note

All claims expressed in this article are solely those of the authors and do not necessarily represent those of their affiliated organizations, or those of the publisher, the editors and the reviewers. Any product that may be evaluated in this article, or claim that may be made by its manufacturer, is not guaranteed or endorsed by the publisher.

References

Abusleme, L., and Moutsopoulos, N. M. (2017). IL-17: overview and role in oral immunity and microbiome. *Oral. Dis.* 23, 854–865. doi: 10.1111/odi.12598

Aemaimanan, P., Amimanan, P., and Taweechaisupapong, S. (2013). Quantification of key periodontal pathogens in insulin-dependent type 2 diabetic and non-diabetic patients with generalized chronic periodontitis. *Anaerobe* 22, 64–68. doi: 10.1016/j.anaerobe.2013.06.010

Ahn, J. S., Yang, J. W., Oh, S. J., Shin, Y. Y., Kang, M. J., Park, H. R., et al. (2021). Porphyromonas gingivalis exacerbates the progression of fatty liver disease *via* CD36-PPARgamma pathway. *BMB Rep.* 54, 323–328. doi: 10.5483/BMBRep.2021.54.6.050

Antonelli, A., Ferrari, S. M., Corrado, A., Ferrannini, E., and Fallahi, P. (2014). CXCR3, CXCL10 and type 1 diabetes. *Cytokine Growth Factor Rev.* 25, 57–65. doi: 10.1016/j.cytogfr.2014.01.006

Arimatsu, K., Yamada, H., Miyazawa, H., Minagawa, T., Nakajima, M., Ryder, M. I., et al. (2014). Oral pathobiont induces systemic inflammation and metabolic changes associated with alteration of gut microbiota. *Sci. Rep.* 4, 4828. doi: 10.1038/srep04828

Bhat, U. G., Ilievski, V., Unterman, T. G., and Watanabe, K. (2014). Porphyromonas gingivalis lipopolysaccharide upregulates insulin secretion from pancreatic beta cell line MIN6. *J. Periodontol.* 85, 1629–1636. doi: 10.1902/jop.2014.140070

Bruni, N., Rajas, F., Montano, S., Chevalier-Porst, F., and Mithieux, G. (1999). Enzymatic characterization of four new mutations in the glucose-6 phosphatase (G6PC) gene which cause glycogen storage disease type 1a. *Ann. Hum. Genet.* 63, 141–146. doi: 10.1046/j.1469-1809.1999.6320141.x

Choi, M. S., Jung, U. J., Yeo, J., Kim, M. J., and Lee, M. K. (2008). Genistein and daidzein prevent diabetes onset by elevating insulin level and altering hepatic gluconeogenic and lipogenic enzyme activities in non-obese diabetic (NOD) mice. *Diabetes Metab. Res. Rev.* 24, 74–81. doi: 10.1002/dmrr.780

Copps, K. D., and White, M. F. (2012). Regulation of insulin sensitivity by serine/threonine phosphorylation of insulin receptor substrate proteins IRS1 and IRS2. *Diabetologia* 55, 2565–2582. doi: 10.1007/s00125-012-2644-8

Cullinan, M. P., and Seymour, G. J. (2013). Periodontal disease and systemic illness: will the evidence ever be enough? *Periodontol. 2000* 62, 271–286. doi: 10.1111/prd.12007

D'Aiuto, F., Gkranias, N., Bhowruth, D., Khan, T., Orlandi, M., Suvan, J., et al. (2018). Systemic effects of periodontitis treatment in patients with type 2 diabetes: a 12 month, single-centre, investigator-masked, randomised trial. *Lancet Diabetes Endocrinol.* 6, 954–965. doi: 10.1016/S2213-8587(18)30038-X

Darveau, R. P., Hajishengallis, G., and Curtis, M. A. (2012). Porphyromonas gingivalis as a potential community activist for disease. *J. Dent. Res.* 91, 816–820. doi: 10.1177/0022034512453589

Dong, X., Park, S., Lin, X., Copps, K., and White, M. F. (2006). Irs1 and Irs2 signaling is essential for glucose homeostastis and systemic growth. *J. Clin. Invest.* 116, 101–114. doi: 10.1172/JCI25735

Elmarakby, A. A., and Sullivan, J. C. (2012). Relationship between oxidative stress and inflammatory cytokines in diabetic nephropathy. *Cardiovasc. Ther.* 30, 49–59. doi: 10.1111/j.1755-5922.2010.00218.x

Esser, N., Legrand-Poels, S., Piette, J., Scheen, A. J., and Paquot, N. (2014). Inflammation as a link between obesity, metabolic syndrome and type 2 diabetes. *Diabetes Res. Clin. Pract.* 105, 141–150. doi: 10.1016/j.diabres.2014.04.006

Genco, R. J., and Borgnakke, W. S. (2020). Diabetes as a potential risk for periodontitis: association studies. *Periodontol. 2000* 83, 40–45. doi: 10.1111/prd.12270

Genco, R. J., Graziani, F., and Hasturk, H. (2020). Effects of periodontal disease on glycemic control, complications, and incidence of diabetes mellitus. *Periodontol. 2000* 83, 59–65. doi: 10.1111/prd.12271

Hajishengallis, G., and Chavakis, T. (2021a). DEL-1: a potential therapeutic target in inflammatory and autoimmune disease? *Expert Rev. Clin. Immunol.* 17, 549–552. doi: 10.1080/1744666X.2021.1915771

Hajishengallis, G., and Chavakis, T. (2021b). Local and systemic mechanisms linking periodontal disease and inflammatory comorbidities. *Nat. Rev. Immunol.* 21, 426–440. doi: 10.1038/s41577-020-00488-6

Han, C. Y., Subramanian, S., Chan, C. K., Omer, M., Chiba, T., Wight, T. N., et al. (2007). Adipocyte-derived serum amyloid A3 and hyaluronan play a role in monocyte recruitment and adhesion. *Diabetes* 56, 2260–2273. doi: 10.2337/db07-0218

Hueso, L., Ortega, R., Selles, F., Wu-Xiong, N. Y., Ortega, J., Civera, M., et al. (2018). Upregulation of angiostatic chemokines IP-10/CXCL10 and I-TAC/CXCL11 in human obesity and their implication for adipose tissue angiogenesis. *Int. J. Obes.* 42, 1406–1417. doi: 10.1038/s41366-018-0102-5

Ilievski, V., Bhat, U. G., Suleiman-Ata, S., Bauer, B. A., Toth, P. T., Olson, S. T., et al. (2017). Oral application of a periodontal pathogen impacts SerpinE1 expression and pancreatic islet architecture in prediabetes. *J. Periodontal Res.* 52, 1032–1041. doi: 10.1111/jre.12474

Kashiwagi, Y., Aburaya, S., Sugiyama, N., Narukawa, Y., Sakamoto, Y., Takahashi, M., et al. (2021). Porphyromonas gingivalis induces entero-hepatic metabolic derangements with alteration of gut microbiota in a type 2 diabetes mouse model. *Sci. Rep.* 11, 18398. doi: 10.1038/s41598-021-97868-2

Komazaki, R., Katagiri, S., Takahashi, H., Maekawa, S., Shiba, T., Takeuchi, Y., et al. (2017). Periodontal pathogenic bacteria, aggregatibacter actinomycetemcomitans affect non-alcoholic fatty liver disease by altering gut microbiota and glucose metabolism. *Sci. Rep.* 7, 13950. doi: 10.1038/s41598-017-14260-9

Kuo, L. C., Polson, A. M., and Kang, T. (2008). Associations between periodontal diseases and systemic diseases: a review of the inter-relationships and interactions with diabetes, respiratory diseases, cardiovascular diseases and osteoporosis. *Public Health* 122, 417–433. doi: 10.1016/j.puhe.2007.07.004

Kurgan, S., and Kantarci, A. (2018). Molecular basis for immunohistochemical and inflammatory changes during progression of gingivitis to periodontitis. *Periodontol. 2000* 76, 51–67. doi: 10.1111/prd.12146

Lalla, E., Cheng, B., Lal, S., Tucker, S., Greenberg, E., Goland, R., et al. (2006). Periodontal changes in children and adolescents with diabetes: a case-control study. *Diabetes Care* 29, 295–299. doi: 10.2337/diacare.29.02.06.dc05-1355

Leinonen, E., Hurt-Camejo, E., Wiklund, O., Hultén, L. M., Hiukka, A., and Taskinen, M. R. (2003). Insulin resistance and adiposity correlate with acute-phase reaction and soluble cell adhesion molecules in type 2 diabetes. *Atherosclerosis* 166, 387–394. doi: 10.1016/s0021-9150(02)00371-4

Li, H., Yang, H., Ding, Y., Aprecio, R., Zhang, W., Wang, Q., et al. (2013). Experimental periodontitis induced by porphyromonas gingivalis does not alter the onset or severity of diabetes in mice. *J. Periodontal Res.* 48, 582–590. doi: 10.1111/jre.12041

Maciejewska-Skrendo, A., Buryta, M., Czarny, W., Król, P., Spieszny, M., Stastny, P., et al. (2019). The polymorphisms of the peroxisome-proliferator activated receptors' Alfa gene modify the aerobic training induced changes of cholesterol and glucose. *J. Clin. Med.* 8, 1043. doi: 10.3390/jcm8071043

Mahamed, D. A., Marleau, A., Alnaeeli, M., Singh, B., Zhang, X., Penninger, J. M., et al. (2005). G(-) anaerobes-reactive CD4+ T-cells trigger RANKL-mediated enhanced alveolar bone loss in diabetic NOD mice. *Diabetes* 54, 1477–1486. doi: 10.2337/diabetes.54.5.1477

Makiura, N., Ojima, M., Kou, Y., Furuta, N., Okahashi, N., Shizukuishi, S., et al. (2008). Relationship of porphyromonas gingivalis with glycemic level in patients with type 2 diabetes following periodontal treatment. *Oral. Microbiol. Immunol.* 23, 348–351. doi: 10.1111/j.1399-302X.2007.00426.x

Marwaha, A. K., Tan, S., and Dutz, J. P. (2014). Targeting the IL-17/IFN-gamma axis as a potential new clinical therapy for type 1 diabetes. *Clin. Immunol.* 154, 84–89. doi: 10.1016/j.clim.2014.06.006

Matsui, T., and Yoshida, Y. (2016). Reduction of the expression and production of adhesion molecules and chemokines by brain endothelial cells in response to tumor necrosis factor-α and interleukin-17 in hypothermia. *Clin. Exp. Neuroimmunol.* 7, 174–182. doi: 10.1111/cen3.12298

Mensah-Brown, E. P., Shahin, A., Al-Shamisi, M., Wei, X., and Lukic, M. L. (2006). IL-23 leads to diabetes induction after subdiabetogenic treatment with multiple low doses of streptozotocin. *Eur. J. Immunol.* 36, 216–223. doi: 10.1002/eji.200535325

Moreno, B., Hueso, L., Ortega, R., Benito, E., Martínez-Hervas, S., Peiro, M., et al. (2022). Association of chemokines IP-10/CXCL10 and I-TAC/CXCL11 with insulin resistance and enhance leukocyte endothelial arrest in obesity. *Microvascular Res.* 139, 1042–1054. doi: 10.1016/j.mvr.2021.104254

Nascimento, G. G., Leite, Fábio R.M., Vestergaard, P., Scheutz, F., and López, R. (2018). Does diabetes increase the risk of periodontitis? a systematic review and meta-regression analysis of longitudinal prospective studies. *Acta Diabetologica* 55, 653–667. doi: 10.1016/j.mvr.2021.104254

Ohtsu, A., Takeuchi, Y., Katagiri, S., Suda, W., Maekawa, S., Shiba, T., et al. (2019). Influence of porphyromonas gingivalis in gut microbiota of streptozotocin-induced diabetic mice. *Oral. Dis.* 25, 868–880. doi: 10.1111/odi.13044

Ota, T. (2013). Chemokine systems link obesity to insulin resistance. *Diabetes Metab. J.* 37, 165–172. doi: 10.4093/dmj.2013.37.3.165

Pound, L. D., Oeser, J. K., O'Brien, T. P., Wang, Y., Faulman, C. J., Dadi, P. K., et al. (2013). G6PC2: a negative regulator of basal glucose-stimulated insulin secretion. *Diabetes* 62, 1547–1556. doi: 10.2337/db12-1067

Pradhan, A. D., Manson, J. E., Rifai, N., Buring, J. E., and Ridker, P. M. (2001). C-reactive protein, interleukin 6, and risk of developing type 2 diabetes mellitus. *JAMA* 286, 327–334. doi: 10.1001/jama.286.3.327

Preshaw, P. M., Alba, A. L., Herrera, D., Jepsen, S., Konstantinidis, A., Makrilakis, K., et al. (2012). Periodontitis and diabetes: a two-way relationship. *Diabetologia* 55, 21–31. doi: 10.1007/s00125-011-2342-y

Sarkar, S. A., Lee, C. E., Victorino, F., Nguyen, T. T., Walters, J. A., Burrack, A., et al (2012) Expression and regulation of chemokines in murine and human type 1 diabetes. *Diabetes* 61, 436–446. doi: 10.2337/db11-0853

Sasaki, N., Katagiri, S., Komazaki, R., Watanabe, K., Maekawa, S., Shiba, T., et al. (2018). Endotoxemia by porphyromonas gingivalis injection aggravates non-alcoholic fatty liver disease, disrupts Glucose/Lipid metabolism, and alters gut microbiota in mice. *Front. Microbiol.* 9. doi: 10.3389/fmicb.2018.02470

Saxena, S., Venugopal, R., Chandrayan Rao, R., Yuwanati, M. B., Awasthi, H., and Jain, M. (2020). Association of chronic periodontitis and type 2 diabetes mellitus with salivary del-1 and IL-17 levels. *J. Oral. Biol. Craniofac Res.* 10, 529–534. doi: 10.1016/j.jobcr.2020.08.013

Seyama, M., Yoshida, K., Yoshida, K., Fujiwara, N., Ono, K., Eguchi, T., et al. (2020). Outer membrane vesicles of porphyromonas gingivalis attenuate insulin sensitivity by delivering gingipains to the liver. *Biochim. Biophys. Acta Mol. Basis Dis.* 1866, 165731. doi: 10.1016/j.bbadis.2020.165731

Sjöholm, K., Lundgren, M., Olsson, M., and Eriksson, J. W. (2009) Association of serum amyloid a levels with adipocyte size and serum levels of adipokines: differences between men and women *Cytokine* 48, 260–266. doi: 10.1016/j.cyto.2009.08.005

Srinivasan, S., Hatley, M. E., Reilly, K. B., Danziger, E. C., and Hedrick, C. C. (2004). Modulation of PPARalpha expression and inflammatory interleukin-6 production by chronic glucose increases monocyte/endothelial adhesion. *Arterioscler. Thromb. Vasc. Biol.* 24, 851–857. doi: 10.1161/01.ATV.zhq0504.2260

Sthr, J., Barbaresko, J., Neuenschwander, M., and Schlesinger, S. (2021). Bidirectional association between periodontal disease and diabetes mellitus: a systematic review and meta-analysis of cohort studies. *Sci. Rep.* 11, 13686. doi: 10.1038/s41598-021-93062-6

Takatani, T., Shirakawa, J., Shibue, K., Gupta, M. K., and Kulkarni, R. N. (2021). Insulin receptor substrate 1 (IRS1), but not IRS2, plays a dominant role in regulating pancreatic alpha cell function in mice. *J. Biol. Chem.* 296, 100646. doi: 10.1016/j.jbc.2021.100646

Tian, J., Liu, C., Zheng, X., Jia, X., Peng, X., Yang, R., et al. (2020). Porphyromonas gingivalis induces insulin resistance by increasing BCAA levels in mice. *J. Dent. Res.* 99, 839–846. doi: 10.1177/0022034520911037

Trayhurn, P., and Alomar, S. Y. (2015). Oxygen deprivation and the cellular response to hypoxia in adipocytes - perspectives on white and brown adipose tissues in obesity. *Front. Endocrinol. (Lausanne)* 6. doi: 10.3389/fendo.2015.00019

Wang, Q., Zhang, P., Aprecio, R., Zhang, D., Li, H., Ji, N., et al. (2016). Comparison of experimental diabetic periodontitis induced by porphyromonas gingivalis in mice. *J. Diabetes Res.* 2016, 4840203. doi: 10.1155/2016/4840203

Watanabe, K., Petro, B. J., Shlimon, A. E., and Unterman, T. G. (2008). Effect of periodontitis on insulin resistance and the onset of type 2 diabetes mellitus in zucker diabetic fatty rats. *J. Periodontol.* 79, 1208–1216. doi: 10.1902/jop.2008.070605

Yamazaki, K., Honda, T., Oda, T., Ueki-Maruyama, K., Nakajima, T., and Yoshie H. Seymour, G. J. (2005). Effect of periodontal treatment on the c-reactive protein and proinflammatory cytokine levels in Japanese periodontitis patients. *J. Periodontal Res.* 40, 53–58. doi: 10.1111/j.1600-0765.2004.00772.x

Yuan, X., Dong, D., Li, Z., and Wu, B. (2019). Rev-erbα activation down-regulates hepatic Pck1 enzyme to lower plasma glucose in mice. *Pharmacol. Res.* 141, 310–318. doi: 10.1016/j.phrs.2019.01.010

frontiers | Frontiers in Cellular and Infection Microbiology

TYPE Original Research
PUBLISHED 02 November 2022
DOI 10.3389/fcimb.2022.1012316

OPEN ACCESS

EDITED BY
Zuomin Wang,
Capital Medical University, China

REVIEWED BY
Qing Xian Luan,
Peking University, China
Dongmei Zhang Zhang,
China Medical University, China

*CORRESPONDENCE
Daonan Shen
shendaonan@126.com
Yafei Wu
yfw1110@163.com

SPECIALTY SECTION
This article was submitted to Extra-intestinal Microbiome, a section of the journal Frontiers in Cellular and Infection Microbiology

RECEIVED 05 August 2022
ACCEPTED 12 October 2022
PUBLISHED 02 November 2022

CITATION
Zou R, Zhao L, Shen D and Wu Y (2022) TrkA serves as a virulence modulator in *Porphyromonas gingivalis* by maintaining heme acquisition and pathogenesis. *Front. Cell. Infect. Microbiol.* 12:1012316. doi: 10.3389/fcimb.2022.1012316

TrkA serves as a virulence modulator in *Porphyromonas gingivalis* by maintaining heme acquisition and pathogenesis

Renjie Zou, Lei Zhao, Daonan Shen* and Yafei Wu*

State Key Laboratory of Oral Diseases, National Clinical Research Center for Oral Diseases, West China Hospital of Stomatology, Department of Periodontics, Sichuan University, Chengdu, China

Periodontitis is an inflammatory disease of the supporting tissues of the teeth, with polymicrobial infection serving as the major pathogenic factor. As a periodontitis-related keystone pathogen, *Porphyromonas gingivalis* can orchestrate polymicrobial biofilm skewing into dysbiosis. Some metatranscriptomic studies have suggested that modulation of potassium ion uptake might serve as a signal enhancing microbiota nososymbiocity and periodontitis progression. Although the relationship between potassium transport and virulence has been elucidated in some bacteria, less is mentioned about the periodontitis-related pathogen. Herein, we centered on the virulence modulation potential of TrkA, the potassium uptake regulatory protein of *P. gingivalis*, and uncovered TrkA as the modulator in the heme acquisition process and in maintaining optimal pathogenicity in an experimental murine model of periodontitis. Hemagglutination and hemolytic activities were attenuated in the case of *trkA* gene loss, and the entire transcriptomic profiling revealed that the *trkA* gene can control the expression of genes in relation to electron transport chain activity and translation, as well as some transcriptional factors, including *cdhR*, the regulator of the heme uptake system hmuYR. Collectively, these results link the heme acquisition process to the potassium transporter, providing new insights into the role of potassium ion in *P. gingivalis* pathogenesis.

KEYWORDS

potassium ion uptake regulatory protein, *Porphyromonas gingivalis*, high-throughput sequencing, heme acquisition, pathogenicity

Introduction

Porphyromonas gingivalis is a gram-negative bacteria considered as the keystone pathogen of periodontitis. While coinhabiting with various microorganisms in the subgingival pocket, it can orchestrate the whole virulence of the community, named nososymbiocity, regardless of its relative minor biomass (Hajishengallis et al., 2011).

Equipped with miscellaneous virulence factors including but not limited to gingipains, fimbriae, and untypical lipopolysaccharide, *P. gingivalis* can subvert the host response by paralyzing the function of complement and immune cells while accentuating the hyperinflammatory state, such that more pathobionts will multiply synergistically for nutrition acquisition and persistence in the inflammatory environment which certainly creates a skewing to dysbiosis of subgingival flora (Hajishengallis et al., 2012).

Microbial dysbiosis is the initial factor of periodontitis. Following longitudinal monitoring of periodontal attachment level, Socransky and his colleagues put forward a model of periodontitis in which attachment loss undergoes acute bursts for short periods randomly in individual sites (Socransky et al., 1984). Some clinical trials have attempted to associate periodontitis progression with dysbiosis features, whereas most studies reported an overlap in the constitution of the microbial community during different phases of progression (Teles et al., 2008; Byrne et al., 2009). Remarkably, a recent omics study on metatranscriptomic analysis of subgingival plaque biofilm suggested a link of cobalamin biosynthesis, proteolysis, and potassium transport activity to periodontitis progression (Yost et al., 2015). Subsequent research confirmed that potassium ion was associated with enhanced virulence of the plaque community *in vitro* (Yost et al., 2017). As the keystone pathogen of periodontitis, it is thus of interest to determine what function alterations and underlying mechanisms of *P. gingivalis* would be brought about when the level of potassium ion or corresponding transporter activity was manipulated.

The virulence potential of potassium cation and transporter has been investigated in some pathogens in the field of environmental cues and host cell colonization. Potassium transporter is indispensable for *Salmonella enterica* serovar Typhimurium to express type III secretion (T3SS) and conduct swift intestinal invasion (Liu et al., 2013). The secretion of virulent factors by T3SS can be also affected by a high concentration of intracellular potassium ion (Tandhavanant et al., 2018). The studies on the inactivation of the potassium uptake system in *Vibrio vulnificus* (Carda-Dieguez et al., 2018), *Francisella tularensis* (Alkhuder et al., 2010), and *Mycobacterium tuberculosis* (MacGilvary et al., 2019) have also highlighted the link with host defense resistance and colonization. Beyond bacteria, potassium still works as the signal for the parasite *Plasmodium* spp. egress from the host cells and bunyavirus genome release during endosomal trafficking (Moraes et al., 2017; Hover et al., 2018). Those phenomena mark potassium ion as an extensive signal for bacteria to show virulence.

While the impact of disruptive potassium homeostasis on bacterial pathological roles is beginning to be elucidated, little is known about *P. gingivalis* as well as the underlying effect of potassium in linking *P. gingivalis* to periodontitis. Herein, we attempted to decipher the role of TrkA, the regulatory subunit of the potassium uptake system Trk in *P. gingivalis* W83. To achieve that, the *trkA* mutant was constructed, and we undertook sequential investigations. Finally, our data associated the function of the *trkA* gene with the heme acquisition process as well as virulence in the murine experimental periodontitis model, which laid the basis for elucidating the role of potassium ion in periodontitis progression.

Material and methods

Bacterial culture

Porphyromonas gingivalis W83 strains were cultured in an anaerobic chamber at 37°C in tryptic soy broth (TSB) medium supplemented with 5 μg/ml of heme and 1 μg/ml of menadione. For the culture of its isogenic *trkA* mutants and complemented strains, erythromycin or tetracycline at a concentration of 10 or 0.6 μg/ml was added to the medium. *Escherichia coli* strains S17-1 were cultivated aerobically at 37°C and 200 rpm in Luria–Bertani medium added with 50 μg/ml of carbenicillin or 5 μg/ml of tetracycline whenever applicable.

Mutant construction and complementation

For the construction of Δ*trkA* mutants, *ermF* cassette was first amplified and fused with the upstream and downstream sequences of the *trkA* gene using overlap extension PCR. The primers applied in the former procedure are shown in Table S1. The recombinant DNA fragments obtained were purified, sequenced, and subsequently electroporated into electrocompetent *P. gingivalis* cells. After a 10-day anaerobic incubation on TSB plates supplemented with erythromycin, the positive clones were selected and confirmed through colony PCR analysis.

To generate the complemented Δ*trkA*/*trkA* strain, operon analysis was conducted to confirm the *trkA* operon structure such that recombinant pT-COW (kindly donated by Prof. Richard J. Lamont) can be generated by incorporating the encoding sequence and the promoter region of the *trkA* gene. Then, the constructs were transformed into Δ*trkA*/*trkA* cells by being conjugated with *E. coli* S17-1 carrying recombinant pT-COW. Positive transconjugants were selected with erythromycin, gentamicin, and tetracycline.

Transcriptomic sequencing and bioinformatic analysis

The total RNAs of three biological replicates were extracted from the cells using TRIzol reagent according to the

manufacturer's instructions (Invitrogen, Carlsbad, USA), and genomic DNAs were removed by DNase (TaKaRa, Kusatsu, Japan). After depleting ribosomal RNA, RNA-seq transcriptome library was prepared using the TruSeq™ RNA sample preparation kit (Illumina, San Diego, USA). Then, the paired-end RNA-seq sequencing library was sequenced with the Illumina HiSeq×TEN (2 × 150 bp read length). Reads were mapped to the reference genome of *P. gingivalis* W83 (Acuna-Amador et al., 2018). Normalized read counts based on transcripts per million mapped reads (TPM) for the gene expression level were calculated.

All bioinformatic analyses were performed using the online platform of Majorbio Cloud Platform (http://www.majorbio.com). Specifically, trimmed read counts were used to determine differential gene expression *via* DESeq2 packages. Data processed in the form of $\log_2$ fold change expression with adjusted *p*-values were obtained. Then, the threshold of 1.0 for $\log_2$ fold change expression and adjusted *p*-values of less than 0.05 were used to determine differentially expressed genes. For gene ontology (GO) enrichment analysis, GOATOOLS (https://github.com/tanghaibao/GOatools) was used to identify statistically significantly enriched GO terms using Fisher's exact test with the adjusted *p*-values of less than 0.05.

Hemagglutination assay

The hemagglutination activity of *P. gingivalis* W83 was analyzed in reference to what was previously described (Fujise et al., 2017). Briefly, *P. gingivalis* W83 growing to the mid-log phase was collected and spun at 8,000 rpm for 10 min. The pellets were washed and diluted to a final OD_{600} of 1 in phosphate-buffered saline (PBS). A 2-fold diluted bacteria suspension was equally mixed with 1% sheep erythrocytes in a round-bottom 96-well plate. After incubation at 4°C for 4 h, the hemagglutination titers were compared among WT, Δ*trkA*, and Δ*trkA*/*trkA*.

Hemolytic activity

Hemolysis assay of *P. gingivalis* W83 was conducted as previously mentioned (Vanterpool et al., 2004). Bacteria cultured in sTSB medium were harvested by centrifugation (3,000*g* for 10 min). The pellets were collected, washed, and resuspended again in PBS to the final OD_{600} of 1.5. After incubation with an equivalent volume of 1% sheep erythrocytes for 3 h at 37°C, the samples were spun at 1,300*g* for 5 min in a Heraeus Multifuge X1R centrifuge at room temperature. The optical absorbance of the supernatant at 405 nm was determined by spectrometry. The erythrocytes were used alone as the negative control. After normalized by the negative control and bacterial amount, the ratio of OD_{405} of the treatment groups to WT was calculated to determine relative hemolytic activity.

Gingipain activity

N-Benzoyl-DL-arginine-*p*-nitroaniline hydrochloride (Macklin, Shanghai, China) and N-(p-Tosyl)-Gly-Pro-Lys 4-nitroanilide acetate salt (Sigma-Aldrich, St. Louis, USA) were utilized as the substrate for testing the arginine (Rgp)-dependent and lysine (Kgp)-dependent gingipain activity of *P. gingivalis* W83 WT, Δ*trkA*, and Δ*trkA*/*trkA* (Fujise et al., 2017). Briefly, the mid-log phase culture of *P. gingivalis* W83 was collected and centrifuged at 8,000*g* for 10 min at 4°C. The resulting pellets were then washed and resuspended in 10 mM of HEPES/NaOH as the whole cells. To prepare the reaction buffer, 0.2 mM of substrate, 50 mM of Tris–HCl (pH 8.0), and 10 mM of DTT were added. Reactions were proceeded by adding 4 µl of bacterial suspension of whole cells at 37°C for 30 min and terminated using acetate acid (50%). The release of *p*-nitroanilide from the substrate was then determined by spectrometry at 450 nm. The gingipain activity measurements of *P. gingivalis* WT, Δ*trkA*, and Δ*trkA*/*trkA* were normalized by bacterial density at 600 nm in HEPES/NaOH buffer.

Membrane potential determination

$DiOC_2(3)$ was used to demonstrate the alteration of bacterial membrane potential. When encountering intracellular less-negative electrical membrane potential, such fluorochrome tended to self-polymerase accompanied by its emission wavelength shifting from green to red fluorescence. To test the membrane potential, bacteria growing to the mid-log phase were harvested and processed in EDTA (10 mM) for 5 min to allow the dye to penetrate the inner membrane (Hudson et al., 2020). The bacteria were then spun to collect the pellets and resuspended in sTSB mimicking the same culture condition. After incubation with $DiOC_2(3)$ (30 µM) for 30 min, the red/green fluorescence ratios of *P. gingivalis* WT, Δ*trkA*, and Δ*trkA*/*trkA* were normalized to those of WT treated with 0.5% DMSO and 5 µM of CCCP, each alone. The formula used is as follows:

$$\mathrm{Fluor}_{\mathrm{normalized}} = \left(\mathrm{Fluor}_{\mathrm{sample}} - \mathrm{Fluor}_{\mathrm{CCCP}}\right)/\left(\mathrm{Fluor}_{\mathrm{CCCP}} - \mathrm{Fluor}_{\mathrm{DMSO}}\right)$$

$\mathrm{Fluor}_{\mathrm{sample}}$ represents the red/green fluorescence ratio of the samples, while $\mathrm{Fluor}_{\mathrm{CCCP}}$ and $\mathrm{Fluor}_{\mathrm{DMSO}}$ represent the positive and negative controls (Zhang et al., 2020).

Identification of heme-bound ability to *Porphyromonas gingivalis* cells

Porphyromonas gingivalis WT, Δ*trkA*, and Δ*trkA*/*trkA* were grown in the sTSB medium to OD_{600} of 0.8–1.2. Cultures were then centrifuged (9,000*g* for 10 min), washed, and resuspended in PBS to

the adjusted OD_{600} of 1.0. The bacterial suspension (800 µl) was then mixed with 200 µl of 50 µM heme. After incubation at 37°C for 1 h, the samples were centrifuged and decreased optical density was determined at 380 nm (Liu et al., 2006). The heme diluted in 800 µl of PBS was used as the negative control.

qRT-PCR

Total RNA was extracted from *P. gingivalis* WT, Δ*trkA*, and Δ*trkA*/*trkA* using RNAiso Plus (TaKaRa, Kusatsu, Japan) and transcribed into cDNA by PrimeScript™ RT reagent kit with gDNA Eraser (TaKaRa, Kusatsu, Japan). qRT-PCR was performed on the QuantStudio 6 Flex (Applied Biosystems, Carlsbad , USA) using TB Green® Premix Ex Taq™ II (TaKaRa, Kusatsu, Japan). The 16S rRNA gene was used as the endogenous control, and relative expression counts were calculated. All primers used are listed in Table S1.

Virulence assay *in vivo*

Virulence *in vivo* of *P. gingivalis* WT and Δ*trkA* was compared in terms of murine alveolar bone loss. Briefly, 6-week-old female mice were obtained from the Ensiweier Laboratory and fed with a standard diet. All experiments involving animals were approved by the Ethics Committee of West China Hospital of Stomatology. *Porphyromonas gingivalis* WT and Δ*trkA* strains of 10^{10} CFUs were resuspended in 100 µl of PBS buffer containing 2% carboxymethylcellulose (CMC) and orally inoculated into randomly assigned mice with a 2-day interval for 12 days (Shen et al., 2020). As for the blank control group, an equivalent volume of PBS only with 2% CMC was used. Forty-two days after the last bacteria inoculation, mice were euthanized and maxillary bones were then scanned by microcomputed tomography (Hiscan XM). Bone volume fraction, trabecular thickness, trabecular number, and trabecular separation were measured with the help of the software Hiscan Analyzer. Bone resorption was analyzed by measuring the distance from the cementoenamel junction to the alveolar bone crest at 14 sites of three molars.

Statistical analysis

Statistical analysis was conducted using GraphPad Prism software version 7.0. Unpaired two-tailed *t*-tests were performed to analyze the differences between the two groups. For data from two groups with no homogeneity of variance, Welch's *t*-test was carried out instead. Ordinary one-way analysis of variance (ANOVA) was used to measure the differences of more than two groups, while Tukey's test was added for further multiple comparisons. Data are presented as mean ± standard deviation (mean ± SD). Statistical significance was set at $p< 0.05$.

Results

Role of the *trkA* gene in the transcriptomic level

To comprehensively investigate how the *trkA* gene functioned in *P. gingivalis*, we compared the transcriptomic difference between wild-type and Δ*trkA* strains by applying bulk RNA sequencing. Principal component analysis showed apparent separation between the wild-type and Δ*trkA* strain groups (Figure 1A). To figure out which genes contributed to such difference, we curated a list of differentially expressed genes with a threshold of $\log_2$ fold change ≥1 and adjusted *p*-value<0.05 (Tables S2, S3). As shown in Figure 1B, the top 5 differentially expressed genes with the lowest adjusted *p*-value were noted among 129 upregulated and 86 downregulated genes. Differential expression of some genes and subsets was verified by qRT-PCR (Figure 1C).

We then mapped differentially expressed genes to the GO database for enrichment analysis (Figure 1D), since almost 72% of those genes were annotated in the database. It was accordingly found that downregulated genes were mainly enriched during translation, sodium ion transport, oxidoreductase activity, and electron transport chain (ETC) (Figure 1F). The regulated genes mapped to sodium ion transport were *nqrABCDEF*, considered as the putative complex I of ETC (Meuric et al., 2010). Additionally, another candidate gene encoding complex I, *rnfABCDGE*, was also downregulated together with the complex II regulon, *frdAB*, and *sdhC*. The latter protein complex was reckoned as the final electron receptor during anaerobic respiration (Spinelli et al., 2021), converting fumarate to succinate for further fermentation, hence associated with putative alteration of metabolic profile. For upregulated genes, there was an overrepresentation of GO terms related to DNA binding, methylation, and transferase activity of transferring one-carbon groups (Figure 1E). Of note, *cdhR* was the most upregulated gene among a series of DNA-binding and transcriptional factors. Such gene encoding protein acted as an upstream regulator of heme uptake regulon *hmuYR* (Wu et al., 2009), indicating a putative modification of the heme acquisition process after deleting *trkA*.

trkA knockout strain exhibits reduced hemagglutination ability

Since hemagglutination plays a critical role in heme acquisition and virulence, we began by measuring the hemagglutinate ability of *P. gingivalis* after deleting the gene *trkA*. As shown in Figure 2A, the Δ*trkA* strain displayed hemagglutination titers one to two dilutions lower than the wild-type strain. We further compared the transcript level of protein containing the heme-binding domain (HA2). qRT-

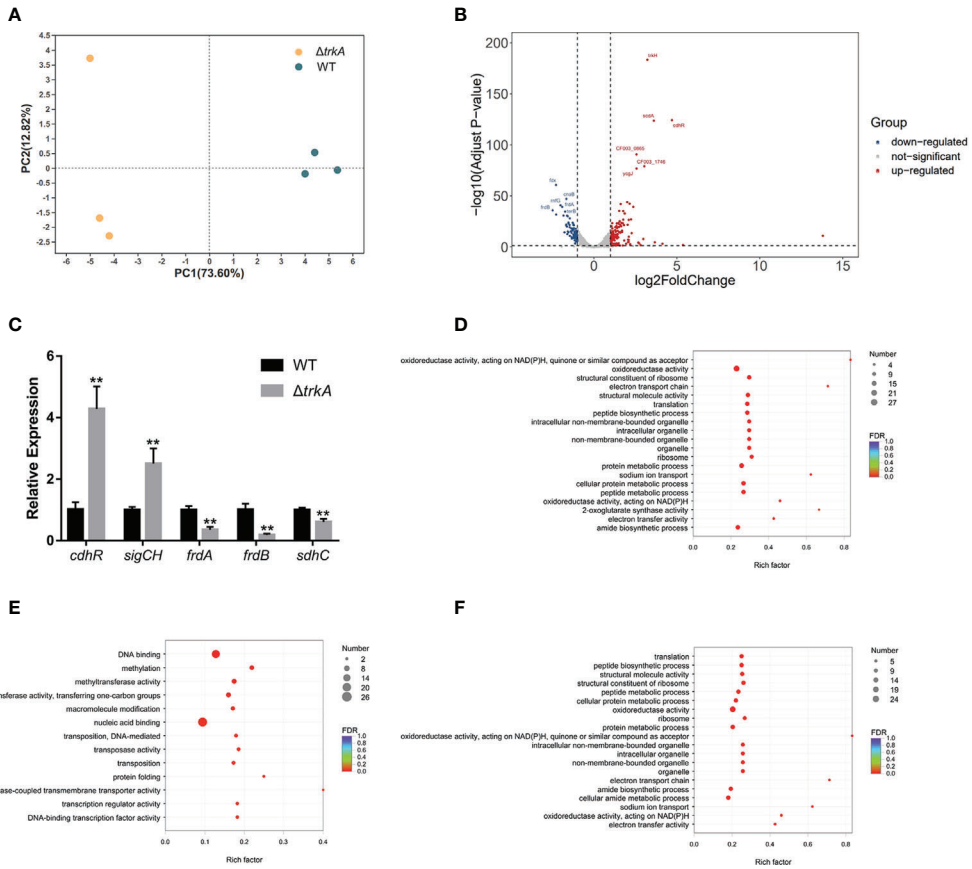

FIGURE 1
Transcriptional profiling of *Porphyromonas gingivalis* Δ*trkA* versus the wild-type (WT) strain. **(A)** Principal component analysis of *P. gingivalis* Δ*trkA* versus the WT strain shows a clear divergence. **(B)** Volcano plot of differentially expressed genes. **(C)** qRT-PCR analysis of a subset of differentially expressed genes detected by RNA sequencing. Gene ontology enrichment analysis of **(D)** differentially expressed genes, **(E)** upregulated genes, and **(F)** downregulated genes in the *P. gingivalis* Δ*trkA* strain. Data are presented as means ± SD, normalized to 16S rRNA and compared to WT ($2^{-\Delta\Delta CT}$). $N = 3$, $^{**}p < 0.01$.

PCR analysis showed that the mRNA level of the *hagA* gene encoding hemagglutinin was decreased, while complementation of *trkA* rescued *hagA* expression. The expression of other genes encoding proteins with adhesion domains such as *rgpA*, *kgp*, and *hbp35* was unaffected (Figure 2B). Thus, downregulated *hagA* might be the determinant of reduced hemagglutination activity in Δ*trkA* strains, indicating the correlated function between the *hagA* and *trkA* genes.

The *trkA* knockout strain displays membrane potential-related hemolysis activity alteration

Porphyromonas gingivalis releases free heme sources from hemoglobulin-contained erythrocytes much more efficiently than from albumin and hemopexin when residing in the inflammatory pocket (Shizukuishi et al., 1995), such that hemolysis works as the main pathway during the heme acquisition process. To test whether there was an alteration of hemolysis after deleting *trkA*, we compared the hemolytic activity of the wild-type, Δ*trkA*, and Δ*trkA*/*trkA* strains by calculating the released amount of hemoglobulin into the supernatant during incubation with erythrocytes. As shown in Figure 3A, the relative activity of the Δ*trkA* strain group showed an apparent downward tendency to approximately 64% of that in the wild-type and Δ*trkA*/*trkA* strain groups. Gingipain activity was later assessed, as it accounts for 85% of the extracellular proteolytic activity of *P. gingivalis* and is responsible for hemolysis (Potempa et al., 2003; Li et al., 2010). However, there was no difference in arginine- and lysine-specific gingipain activity among *P. gingivalis* WT, Δ*trkA*, and Δ*trkA*/*trkA* strains (Figures 3E, F).

Notably, the relative hemolytic activity of the Δ*trkA* strain could be augmented when adding a certain concentration of potassium ion, the extent to which there was no statistically significant difference between the Δ*trkA* strain in the medium

(80 mM of potassium ion) and the wild type cultured without extra potassium added (p = 0.9935) (Figure 3B). Thus, there is a certain relationship between hemolytic activity and *trkA* as well as extracellular potassium. Considering that the *trkA* gene, encoding the potassium transport regulatory protein, can control the influx and efflux of potassium across the membrane (Cao et al., 2013), we subsequently measured the status of membrane potential in response to *trkA* deleted and variant extracellular potassium ion. It was found that the *P. gingivalis* Δ*trkA* strain exhibited more hyperpolarized membrane potential (Figure 3C), in line with our hypothesis that less potassium influx was permitted in the case of *trkA* loss and, thus, more negative membrane potential could be displayed. Similar to the alteration of extracellular potassium-related hemolytic activity, the extent of hyperpolarization was gradually attenuated as the extracellular potassium concentration increased (Figure 3D). Accordingly, the hyperpolarization of membrane potential could partially explain the diminished hemolytic activity.

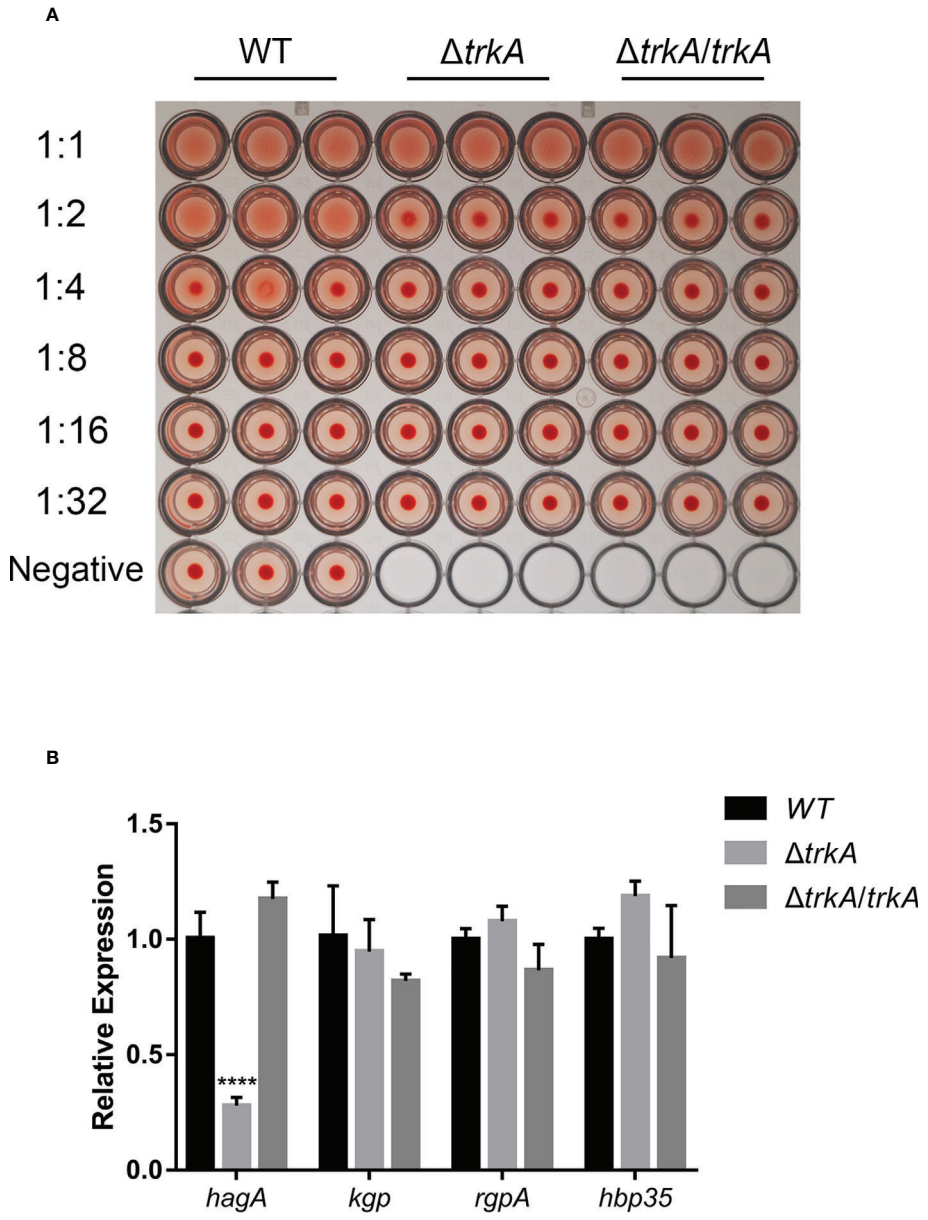

FIGURE 2
trkA deletion attenuates hemagglutination activity of *Porphyromonas gingivalis*. **(A)** Hemagglutination activity of *P. gingivalis* WT, Δ*trkA*, and Δ*trkA*/*trkA* strains. **(B)** qRT-PCR analysis of *hagA*, *kgp*, *rgpA*, and *hbp35* mRNA expression in *P. gingivalis* WT, Δ*trkA*, and Δ*trkA*/*trkA* strains. Data are presented as means ± SD, normalized to 16S rRNA and compared to WT ($2^{-\Delta\Delta CT}$). N = 3, ****p< 0.001.

10.3389/fcimb.2022.1012316

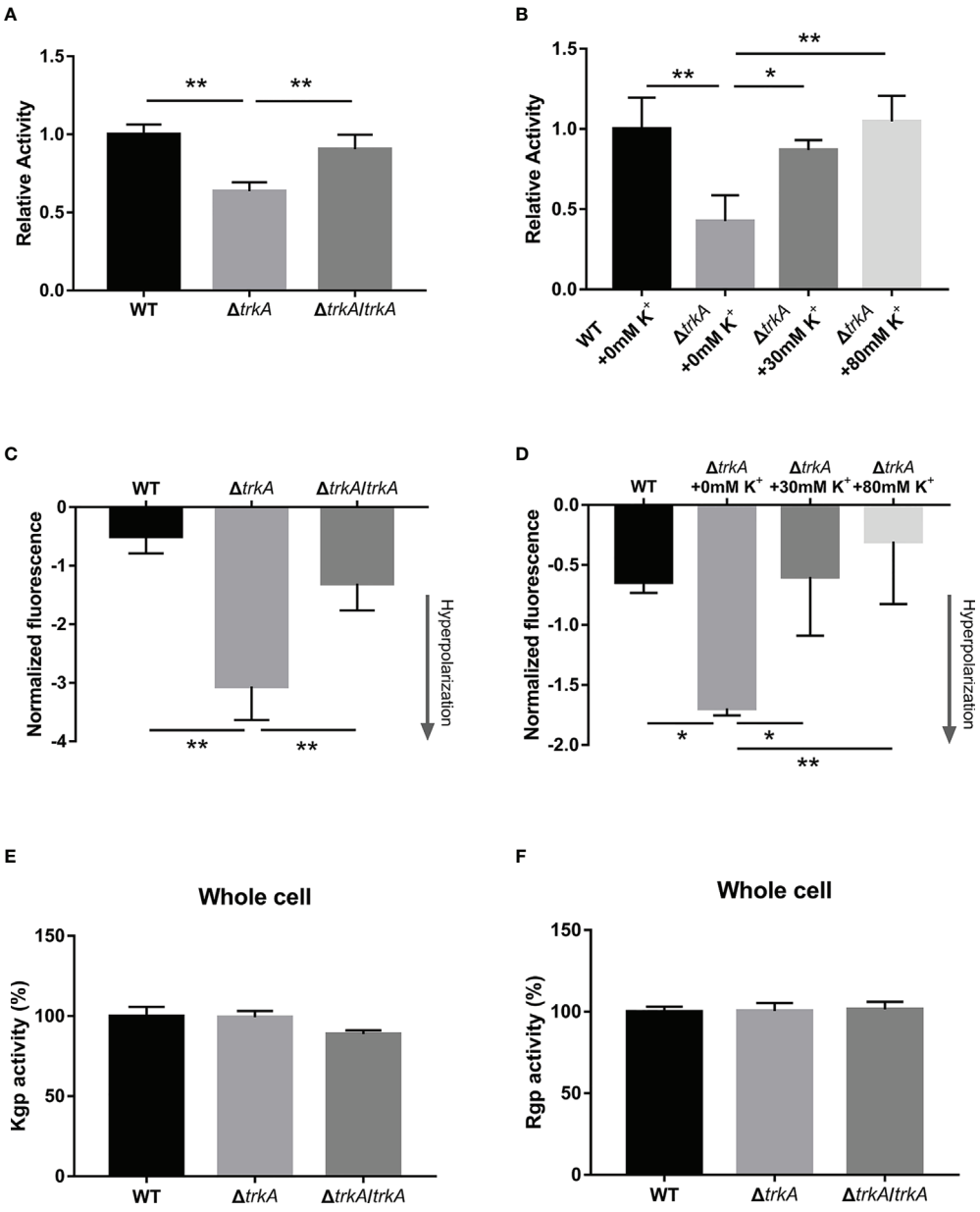

FIGURE 3
Loss of *trkA* leads to membrane potential-related hemolysis activity alteration. **(A, B)** Hemolytic assay, **(C, D)** membrane potential determination, and **(E, F)** Kgp and Rgp activities of *Porphyromonas gingivalis* WT, Δ*trkA*, and Δ*trkA*/*trkA* strains. $N = 3$, $^{*}p < 0.05$, $^{**}p < 0.01$.

Loss of *trkA* exerts no effect on heme-bound capacity but is related to gene transcripts

Heme liberated from hemoglobulin would adhere to the bacterial surface and be transferred across the outer membrane into the cells. Therefore, we ulteriorly estimated the effect of *trkA* on the heme-bound capacity in *P. gingivalis*. The heme-bound assay depicted that there was no apparent difference among the wild-type, Δ*trkA*, and Δ*trkA*/*trkA* strains (Figure 4A). Such phenotype result was not in congruency with related transcriptomic alteration. As is uncovered of the highly upregulated expression of the *cdhR* gene, encoding the transcriptional regulator of *hmuYR*, in transcriptomic analysis, we further tested the implication on *hmuYR* transcripts after deleting *trkA*. In accordance with upregulated *cdhR*, the mRNA level of *hmuYR* was increased (Figure 4B). Additionally, the expression of other genes encoding the heme transporter

complex was unaffected, and there was exclusion of compensation effect (Figure 4C). Thus, the paradox between transcripts and phenotype awaits further investigation.

In vivo pathogenicity determination of *Porphyromonas gingivalis* Δ*trkA* strain

The pathogenicity of the *P. gingivalis* Δ*trkA* strain was evaluated by measuring murine alveolar bone resorption after oral inoculation for a period. As shown in the three-dimensional reconstruction of bone through micro-CT (Figure 5), mice inoculated with the *P. gingivalis* wild-type strain exhibited reduced bone loss level compared with the control group treated with 2% CMC. Deletion of *trkA* displayed alleviated bone resorption. Additionally, the mutant strain showed abated levels of bone volume fraction (BV/TV), trabecular number (Tb.N), and trabecular separation (Tb.Sp) compared with the wild-type strain group (Figure S1). Thus, *trkA* can control the optimal virulence of *P. gingivalis* to mediate oral infection.

Discussion

Potassium accounts for the most abundant inorganic cation in the cytoplasm, and its uptake is crucial for multiple basic cellular activities (Epstein, 2003; Beagle and Lockless, 2021; Do and Gries, 2021). Apart from the physiological functions of osmotic and pH homeostasis, the putative pathological roles of potassium ion uptake systems have been successively well-reported in various bacteria species, whereas few are hitherto investigated in periodontal-related pathogens, such as *P. gingivalis*. According to retrieval from the KEGG database, *trkA* and *trkH* are genes involved in potassium transport in *P. gingivalis*. TrkA of *Vibrio parahaemolyticus* has been reported to change its conformation from tetramer to dimer when binding to nucleotides such as ATP in the regulation of the opening frequency of the TrkH ion channel and, thus, works as a regulator of cation flux and then impacts other biological processes (Zhang et al., 2020). The TrkA protein from *P. gingivalis* shares 47% similar matches to *V. parahaemolyticus*, while the ARG98 residue responsible for binding to γ-phosphate of ATP (Cao et al., 2013) is conserved in both species based on the NCBI Protein BLAST. It is then plausible that the TrkA protein might act in a similar way as observed in *V. parahaemolyticus*. In this study, we initially reported a correlation between the gene-encoding potassium transport regulatory protein TrkA and the heme acquisition pathway, especially in the hemagglutination and hemolysis process of *P. gingivalis*, demonstrating the role of the *trkA* gene in maintaining optimal virulence during murine oral infection.

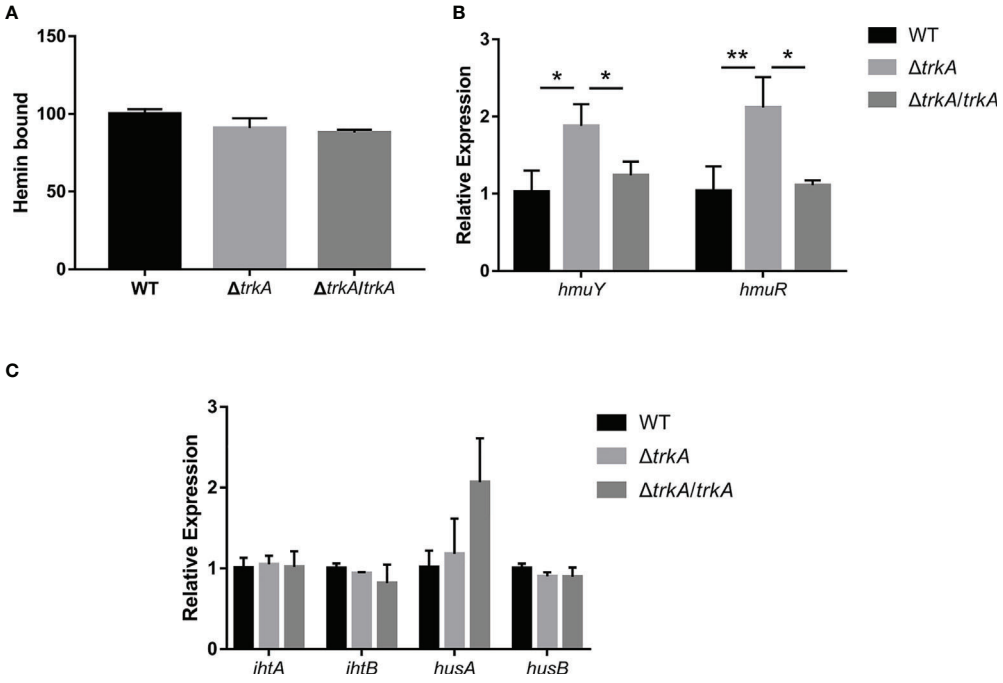

FIGURE 4
Heme-bound capacity of *Porphyromonas gingivalis* is not altered except for the corresponding transcripts. **(A)** Heme-bound assay. qRT-PCR of **(B)** *hmuYR* and **(C)** *ihtAB* and *husAB* mRNA expression of *P. gingivalis* WT, Δ*trkA*, and Δ*trkA*/*trkA* strains. Data are presented as means ± SD, normalized to 16S rRNA and compared to WT ($2^{-\Delta\Delta CT}$). $N = 3$, $^{*}p < 0.05$, $^{**}p < 0.01$.

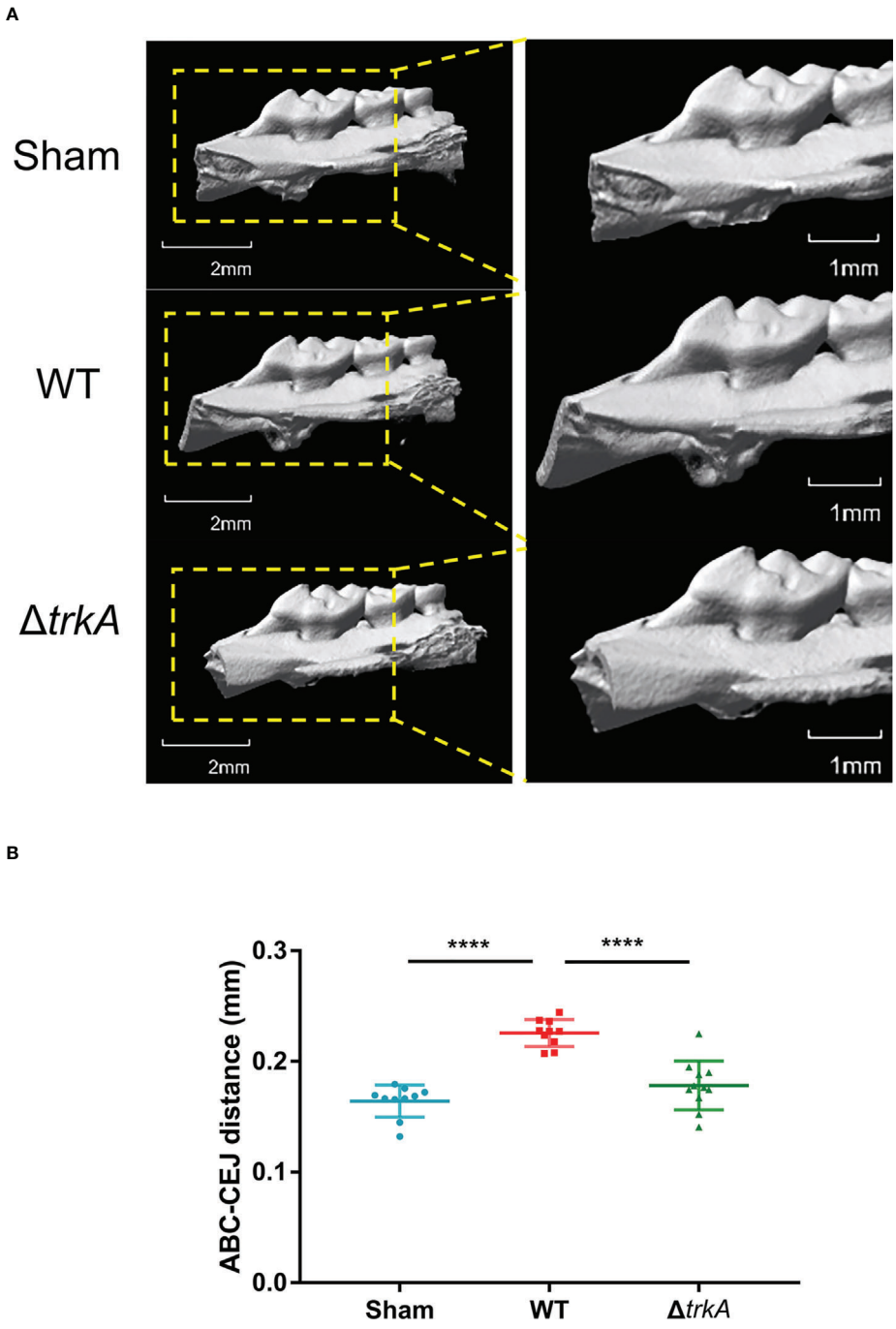

FIGURE 5
trkA is required for the virulence of *Porphyromonas gingivalis in vivo*. Micro-CT analysis of alveolar bone loss in mice following infection with *P. gingivalis* wild-type and Δ*trkA* strains. The group treated with CMC (sham) worked as a control. **(A)** Three-dimensional micro-CT reconstruction of the alveolar bone and **(B)** analysis of bone resorption. All data of the distance between ABC and CEJ in 14 sites of the first, second, and third molars were measured and presented as mean ± SD. ABC, alveolar bone crest; CEJ, cementoenamel junction. *N* = 10 or 11, ****$p < 0.001$.

The heme acquisition process is an indispensable way for *P. gingivalis* to multiply and exhibit pathogenicity. It has been demonstrated that *P. gingivalis* displayed a changeable growth rate in the influence of heme concentration in the culture medium (Marsh et al., 1994) and enhanced virulence *in vivo* in a heme dose-dependent manner (McKee et al., 1986). Elementally, heme accumulates onto the cell surface of *P. gingivalis* in a μ-oxo bisheme form to catalyze excess H_2O_2

released by activated neutrophils (Smalley et al., 2000). Meanwhile, ferrous ions liberated from heme can be utilized and integrated into an iron–sulfur cluster involving ETC and energy metabolism (Olczak et al., 2005). Moreover, increased heme added into the culture would also bring about energy metabolism conversion in relation to more metabolites such as succinate, propionate, and butyrate, thus augmenting the virulence *in vivo* (McKee et al., 1986).

Porphyromonas gingivalis mainly takes erythrocytes as the source for heme utilization. Physiologically, heme from free hemoglobulin as a result of cell lysis is rapidly liberated and scavenged by albumin and hemopexin which display higher affinity. Therefore, *P. gingivalis* would proactively undergo the procedure in the acquisition of heme through adherence to erythrocytes, hemolysis, heme uptake, and storage (Smalley and Olczak, 2017). In the isogenic Δ*trkA* strain, we observed alleviated hemagglutinate and hemolytic activity along with downregulated *hagA* expression and membrane potential alteration, which indicated that the basic steps of the heme acquisition process were impaired. Interestingly, we detected a distinct downregulation of the *hagA* gene, which is considered as the main attribute to adherence to erythrocytes (Han et al., 1996) and to stabilize the porUV sortase structure of type IX secretion system for the normal secretion of proteins like gingipains (Saiki and Konishi, 2014). The mechanism of *hagA* regulation by *trkA* is unclear. It was reported that the ferric uptake regulation protein homolog (PgFur) positively controlled *hagA* expression (Ciuraszkiewicz et al., 2014). Another mechanism involving the regulation of *hagA* expression is the two-component system haeSR regulon which was determined to bind to the upstream sequence of the *hagA* gene according to the ChIP-Seq experiment (Scott et al., 2013). *haeSR* and *PgFur* were both unaffected pursuant to our RNA-seq data, which indicated the downstream role of TrkA in the HaeSR– and PgFur–hagA regulatory axis, or there might be another candidate independent signaling. So far, further study is needed to elucidate the relation between the *trkA* and *hagA* genes.

In the control of cation flux, TrkA and its associated protein TrkH can impact the membrane potential. In line with multiple studies (Gries et al., 2013; Cholo et al., 2015), our result showed a more hyperpolarized membrane potential and potassium-related repolarization in the isogenic Δ*trkA* strain, supporting the hypothesis of the important role of TrkA in regulating potassium flux into the cytoplasm and causing a less hostile and negative intracellular environment. Earlier experiments have elucidated that various factors would contribute to the alteration of hemolytic activity, including magnesium, calcium, protease inhibitors, and metabolic inhibitors. Notably, one of them, CCCP, also brings about the depolarization of the membrane potential (Chu et al., 1991). Thus, a certain membrane potential is crucial for *P. gingivalis* to maintain optimal hemolytic activity. It is of much concern that membrane potential could give rise to multiple impacts on bacteria, including cell growth (Stratford et al., 2019), antibiotic resistance (Gries et al., 2013), and biofilm formation (Prindle et al., 2015). Those alterations were also recognized in the isogenic Δ*trkA* strain (data not shown) with retarded growth and tiny single colony formation, which needs further analysis.

The diminished heme acquisition process would possibly induce lower virulence *in vivo*, in accordance with what we detected in the murine model of experimental periodontitis. To have a comprehensive understanding of function disorder and supplement extra information on the mechanisms underlying virulence changing caused by *trkA* deletion in *P. gingivalis*, we performed transcriptomic analysis between the wild-type and isogenic Δ*trkA* strains. Following enrichment analysis and retrieval for individual genes, genes encoding ETC were mostly downregulated. As the pathway involving energy metabolism, ETC has been deduced of giving way to substrate level phosphorylation during anaerobic respiration in *P. gingivalis* by providing succinate and facilitating the formation of the high-energy compound butyryl-CoA through the ferredoxin and butyryl-CoA dehydrogenase/electron transfer flavoprotein (Bcd/EtfAB) complex (Meuric et al., 2010). As such, we hypothesized that the downregulation of genes encoding complexes I and II would disrupt the output of metabolites like butyrate and acetate, which might partly affect the holistic virulence of *P. gingivalis*. Of note, *cdhR* was the most upregulated gene and linked to the heme uptake process. As a transcriptional regulator, it is believed to control *hmuYR* expression (Wu et al., 2009), in agreement with the transcript result in our study. However, the phenotype comparison was not congruent with the mRNA level. We inferred that such paradox would be ascribed to a weak protein biosynthesis. Deletion of the potassium transporter can give rise to a decreased level of intracellular potassium ion (Durand et al., 2016), which has been elucidated to be involved in ribosome assembling and functions. Structurally, potassium has been reported to maintain mRNA within the decoding center during the elongation state of translation and to stabilize tRNA, rRNA, and subunits of the ribosome (Rozov et al., 2019), and loss of potassium can lead to absent poly-Phe polymerization activity *in vitro* (Naslund and Hultin, 1970). Furthermore, the potential alteration of posttranslational modification and subcellular localization remains obscure. Accordingly, more investigations such as on the protein concentration of whole cells, membrane part, and cytosol need to be further determined. In that regard, the upregulated expression of *cdhR* might be a negative feedback to impaired heme uptake process in the case of insufficient potassium influx of the Δ*trkA* strain. Additionally, *cdhR* was also reported to control *P. gingivalis* microcolony formation on the substratum of *Streptococcus gordonii*. The initial attachment to *S. gordonii* will lead to a sequence of protein tyrosine (de) phosphorylation which gives rise to phosphorylation of CdhR along with increased nososymbiocity (Lamont et al., 2018). Although we observed a high level of *cdhR* mRNA, the protein

level and posttranscriptional modification were not determined heretofore.

Collectively, we focus for the first time on the *trkA* effect on *P. gingivalis* W83, as it belongs to the virulent strains of *P. gingivalis* according to the murine subcutaneous soft tissue abscess model analysis (Slots and Rams, 1993). The potential function variance of *trkA* in other strains of *P. gingivalis* such as ATCC33277, HG66, and TDC60 needs further study. Moreover, it remains elusive what attributes in the *P. gingivalis* Δ*trkA* strain account for the reduced pathogenicity. More investigations need to be made such as comparison in terms of single or multiple species biofilm formation and *in-vitro* analysis of metabolic profile as well as under various stresses like intracellular survival to understand the regulatory mechanism of TrkA.

Data availability statement

The datasets presented in this study can be found in online repositories. The names of the repository/repositories and accession number(s) can be found below: NCBI, GSE210663.

Ethics statement

The animal study was reviewed and approved by the Ethics Committee of West China Hospital of Stomatology, Sichuan University.

Author contributions

RZ contributed to the study conceptualization, data acquisition, analysis, interpretation, and writing of the original draft. LZ contributed to the study design and interpretation. DS and YW contributed to the study conceptualization, design, interpretation, and critical revision of the manuscript. All authors approved the final version of the manuscript and accounted for all aspects of the work.

Funding

This study was supported by the National Natural Science Foundation of China (grant number 82170970).

Conflict of interest

The authors declare that the research was conducted in the absence of any commercial or financial relationships that could be construed as a potential conflict of interest.

Publisher's note

All claims expressed in this article are solely those of the authors and do not necessarily represent those of their affiliated organizations, or those of the publisher, the editors and the reviewers. Any product that may be evaluated in this article, or claim that may be made by its manufacturer, is not guaranteed or endorsed by the publisher.

Supplementary material

The Supplementary Material for this article can be found online at: https://www.frontiersin.org/articles/10.3389/fcimb.2022.1012316/full#supplementary-material

References

Acuna-Amador, L., Primot, A., Cadieu, E., Roulet, A., and Barloy-Hubler, F. (2018). Genomic repeats, misassembly and reannotation: a case study with long-read resequencing of porphyromonas gingivalis reference strains. *BMC Genomics* 19 (1), 54. doi: 10.1186/s12864-017-4429-4

Alkhuder, K., Meibom, K. L., Dubail, I., Dupuis, M., and Charbit, A. (2010). Identification of trkH, encoding a potassium uptake protein required for francisella tularensis systemic dissemination in mice. *PloS One* 5 (1), e8966. doi: 10.1371/journal.pone.0008966

Beagle, S. D., and Lockless, S. W. (2021). Unappreciated roles for k(+) channels in bacterial physiology. *Trends Microbiol.* 29 (10), 942–950. doi: 10.1016/j.tim.2020.11.005

Byrne, S. J., Dashper, S. G., Darby, I. B., Adams, G. G., Hoffmann, B., and Reynolds, E. C. (2009). Progression of chronic periodontitis can be predicted by the levels of porphyromonas gingivalis and treponema denticola in subgingival plaque. *Oral. Microbiol. Immunol.* 24 (6), 469–477. doi: 10.1111/j.1399-302X.2009.00544.x

Cao, Y., Pan, Y., Huang, H., Jin, X., Levin, E. J., Kloss, B., et al. (2013). Gating of the TrkH ion channel by its associated RCK protein TrkA. *Nature* 496 (7445), 317–322. doi: 10.1038/nature12056

Carda-Dieguez, M., Silva-Hernandez, F. X., Hubbard, T. P., Chao, M. C., Waldor, M. K., and Amaro, C. (2018). Comprehensive identification of vibrio vulnificus genes required for growth in human serum. *Virulence* 9 (1), 981–993. doi: 10.1080/21505594.2018.1455464

Cholo, M. C., van Rensburg, E. J., Osman, A. G., and Anderson, R. (2015). Expression of the genes encoding the trk and kdp potassium transport systems of mycobacterium tuberculosis during growth *In vitro*. *BioMed. Res. Int.* 2015, 608682. doi: 10.1155/2015/608682

Chu, L., Bramanti, T. E., Ebersole, J. L., and Holt, S. C. (1991). Hemolytic activity in the periodontopathogen porphyromonas gingivalis: kinetics of enzyme release and localization. *Infect. Immun.* 59 (6), 1932–1940. doi: 10.1128/iai.59.6.1932-1940.1991

Ciuraszkiewicz, J., Smiga, M., Mackiewicz, P., Gmiterek, A., Bielecki, M., Olczak, M., et al. (2014). Fur homolog regulates porphyromonas gingivalis virulence under low-iron/heme conditions through a complex regulatory network. *Mol. Oral. Microbiol.* 29 (6), 333–353. doi: 10.1111/omi.12077

Do, E. A., and Gries, C. M. (2021). Beyond homeostasis: Potassium and pathogenesis during bacterial infections. *Infect. Immun.* 89 (7), e0076620. doi: 10.1128/IAI.00766-20

Durand, A., Sinha, A. K., Dard-Dascot, C., and Michel, B. (2016). Mutations affecting potassium import restore the viability of the escherichia coli DNA polymerase III holD mutant. *PloS Genet*. 12 (6), e1006114. doi: 10.1371/journal.pgen.1006114

Epstein, W. (2003). The roles and regulation of potassium in bacteria. *Prog. Nucleic Acid Res. Mol. Biol.* 75, 293–320. doi: 10.1016/s0079-6603(03)75008-9

Fujise, K., Kikuchi, Y., Kokubu, E., Okamoto-Shibayama, K., and Ishihara, K. (2017). Effect of extracytoplasmic function sigma factors on autoaggregation, hemagglutination, and cell surface properties of porphyromonas gingivalis. *PloS One* 12 (9), e0185027. doi: 10.1371/journal.pone.0185027

Gries, C. M., Bose, J. L., Nuxoll, A. S., Fey, P. D., and Bayles, K. W. (2013). The ktr potassium transport system in staphylococcus aureus and its role in cell physiology, antimicrobial resistance and pathogenesis. *Mol. Microbiol.* 89 (4), 760–773. doi: 10.1111/mmi.12312

Hajishengallis, G., Darveau, R. P., and Curtis, M. A. (2012). The keystone-pathogen hypothesis. *Nat. Rev. Microbiol.* 10 (10), 717–725. doi: 10.1038/nrmicro2873

Hajishengallis, G., Liang, S., Payne, M. A., Hashim, A., Jotwani, R., Eskan, M. A., et al. (2011). Low-abundance biofilm species orchestrates inflammatory periodontal disease through the commensal microbiota and complement. *Cell Host Microbe* 10 (5), 497–506. doi: 10.1016/j.chom.2011.10.006

Han, N., Whitlock, J., and Progulske-Fox, A. (1996). The hemagglutinin gene a (hagA) of porphyromonas gingivalis 381 contains four large, contiguous, direct repeats. *Infect. Immun.* 64 (10), 4000–4007. doi: 10.1128/iai.64.10.4000-4007.1996

Hover, S., Foster, B., Fontana, J., Kohl, A., Goldstein, S. A. N., Barr, J. N., et al. (2018). Bunyavirus requirement for endosomal k+ reveals new roles of cellular ion channels during infection. *PloS Pathog.* 14 (1), e1006845. doi: 10.1371/journal.ppat.1006845

Hudson, M. A., Siegele, D. A., and Lockless, S. W. (2020). Use of a fluorescence-based assay to measure escherichia coli membrane potential changes in high throughput. *Antimicrob. Agents Chemother.* 64 (9), e00910–20. doi: 10.1128/AAC.00910-20

Lamont, R. J., Koo, H., and Hajishengallis, G. (2018). The oral microbiota: dynamic communities and host interactions. *Nat. Rev. Microbiol.* 16 (12), 745–759. doi: 10.1038/s41579-018-0089-x

Liu, Y., Ho, K. K., Su, J., Gong, H., Chang, A. C., and Lu, S. (2013). Potassium transport of salmonella is important for type III secretion and pathogenesis. *Microbiol. (Reading)* 159 (Pt 8), 1705–1719. doi: 10.1099/mic.0.068700-0

Liu, X., Olczak, T., Guo, H. C., Dixon, D. W., and Genco, C. A. (2006). Identification of amino acid residues involved in heme binding and hemoprotein utilization in the porphyromonas gingivalis heme receptor HmuR. *Infect. Immun.* 74 (2), 1222–1232. doi: 10.1128/IAI.74.2.1222-1232.2006

Li, N., Yun, P., Nadkarni, M. A., Ghadikolaee, N. B., Nguyen, K. A., Lee, M., et al. (2010). Structure determination and analysis of a haemolytic gingipain adhesin domain from porphyromonas gingivalis. *Mol. Microbiol.* 76 (4), 861–873. doi: 10.1111/j.1365-2958.2010.07123.x

MacGilvary, N. J., Kevorkian, Y. L., and Tan, S. (2019). Potassium response and homeostasis in mycobacterium tuberculosis modulates environmental adaptation and is important for host colonization. *PloS Pathog.* 15 (2), e1007591. doi: 10.1371/journal.ppat.1007591

Marsh, P. D., McDermid, A. S., McKee, A. S., and Baskerville, A. (1994). The effect of growth rate and haemin on the virulence and proteolytic activity of porphyromonas gingivalis W50. *Microbiol. (Reading)* 140 (Pt 4), 861–865. doi: 10.1099/00221287-140-4-861

McKee, A. S., McDermid, A. S., Baskerville, A., Dowsett, A. B., Ellwood, D. C., and Marsh, P. D. (1986). Effect of hemin on the physiology and virulence of bacteroides gingivalis W50. *Infect. Immun.* 52 (2), 349–355. doi: 10.1128/iai.52.2.349-355.1986

Meuric, V., Rouillon, A., Chandad, F., and Bonnaure-Mallet, M. (2010). Putative respiratory chain of porphyromonas gingivalis. *Future Microbiol.* 5 (5), 717–734. doi: 10.2217/fmb.10.32

Moraes, M. S., Budu, A., Singh, M. K., Borges-Pereira, L., Levano-Garcia, J., Curra, C., et al. (2017). Plasmodium falciparum GPCR-like receptor SR25 mediates extracellular k(+) sensing coupled to Ca(2+) signaling and stress survival. *Sci. Rep.* 7 (1), 9545. doi: 10.1038/s41598-017-09959-8

Naslund, P. H., and Hultin, T. (1970). Effects of potassium deficiency on mammalian ribosomes. *Biochim. Biophys. Acta* 204 (1), 237–247. doi: 10.1016/0005-2787(70)90507-1

Olczak, T., Simpson, W., Liu, X., and Genco, C. A. (2005). Iron and heme utilization in porphyromonas gingivalis. *FEMS Microbiol. Rev.* 29 (1), 119–144. doi: 10.1016/j.femsre.2004.09.001

Potempa, J., Sroka, A., Imamura, T., and Travis, J. (2003). Gingipains, the major cysteine proteinases and virulence factors of porphyromonas gingivalis: structure, function and assembly of multidomain protein complexes. *Curr. Protein Pept. Sci.* 4 (6), 397–407. doi: 10.2174/1389203033487036

Prindle, A., Liu, J., Asally, M., Ly, S., Garcia-Ojalvo, J., and Suel, G. M. (2015). Ion channels enable electrical communication in bacterial communities. *Nature* 527 (7576), 59–63. doi: 10.1038/nature15709

Rozov, A., Khusainov, I., El Omari, K., Duman, R., Mykhaylyk, V. , Yusupov, M., et al. (2019). Importance of potassium ions for ribosome structure and function revealed by long-wavelength X-ray diffraction. *Nat. Commun.* 10 (1), 2519. doi: 10.1038/s41467-019-10409-4

Saiki, K., and Konishi, K. (2014). Porphyromonas gingivalis c-terminal signal peptidase PG0026 and HagA interact with outer membrane protein PG27/LptO. *Mol. Oral. Microbiol.* 29 (1), 32–44. doi: 10.1111/omi.12043

Scott, J. C., Klein, B. A., Duran-Pinedo, A., Hu, L., and Duncan, M. J. (2013). A two-component system regulates hemin acquisition in porphyromonas gingivalis. *PloS One* 8 (9), e73351. doi: 10.1371/journal.pone.0073351

Shen, D., Perpich, J. D., Stocke, K. S., Yakoumatos, L., Fitzsimonds, Z. R., Liu, C., et al. (2020). Role of the RprY response regulator in p. gingivalis community development and virulence. *Mol. Oral. Microbiol.* 35 (6), 231–239. doi: 10.1111/omi.12311

Shizukuishi, S., Tazaki, K., Inoshita, E., Kataoka, K., Hanioka, T., and Amano, A. (1995). Effect of concentration of compounds containing iron on the growth of porphyromonas gingivalis. *FEMS Microbiol. Lett.* 131 (3), 313–317. doi: 10.1111/j.1574-6968.1995.tb07793.x

Slots, J., and Rams, E. T. (1993). *Pathogenicity* (Boca Raton, FL: CRC Press Inc).

Smalley, J. W., Birss, A. J., and Silver, J. (2000). The periodontal pathogen porphyromonas gingivalis harnesses the chemistry of the mu-oxo bishaem of iron protoporphyrin IX to protect against hydrogen peroxide. *FEMS Microbiol. Lett.* 183 (1), 159–164. doi: 10.1111/j.1574-6968.2000.tb08951.x

Smalley, J. W., and Olczak, T. (2017). Heme acquisition mechanisms of porphyromonas gingivalis - strategies used in a polymicrobial community in a heme-limited host environment. *Mol. Oral. Microbiol.* 32 (1), 1–23. doi: 10.1111/omi.12149

Socransky, S. S., Haffajee, A. D., Goodson, J. M., and Lindhe, J. (1984). New concepts of destructive periodontal disease. *J. Clin. Periodontol* 11 (1), 21–32. doi: 10.1111/j.1600-051x.1984.tb01305.x

Spinelli, J. B., Rosen, P. C., Sprenger, H. G., Puszynska, A. M., Mann, J. L., Roessler, J. M., et al. (2021). Fumarate is a terminal electron acceptor in the mammalian electron transport chain. *Science* 374 (6572), 1227–1237. doi: 10.1126/science.abi7495

Stratford, J. P., Edwards, C. L. A., Ghanshyam, M. J., Malyshev, D., Delise, M. A., Hayashi, Y., et al. (2019). Electrically induced bacterial membrane-potential dynamics correspond to cellular proliferation capacity. *Proc. Natl. Acad. Sci. U.S.A.* 116 (19), 9552–9557. doi: 10.1073/pnas.1901788116

Tandhavanant, S., Matsuda, S., Hiyoshi, H., Iida, T., and Kodama, T. (2018). Vibrio parahaemolyticus senses intracellular k(+) to translocate type III secretion system 2 effectors effectively. *mBio* 9 (4), e01366–18. doi: 10.1128/mBio.01366-18

Teles, R. P., Patel, M., Socransky, S. S., and Haffajee, A. D. (2008). Disease progression in periodontally healthy and maintenance subjects. *J. Periodontol* 79 (5), 784–794. doi: 10.1902/jop.2008.070485

Vanterpool, E., Roy, F., and Fletcher, H. M. (2004). The vimE gene downstream of vimA is independently expressed and is involved in modulating proteolytic activity in porphyromonas gingivalis W83. *Infect. Immun.* 72 (10), 5555–5564. doi: 10.1128/IAI.72.10.5555-5564.2004

Wu, J., Lin, X., and Xie, H. (2009). Regulation of hemin binding proteins by a novel transcriptional activator in porphyromonas gingivalis. *J. Bacteriol* 191 (1), 115–122. doi: 10.1128/JB.00841-08

Yost, S., Duran-Pinedo, A. E., Krishnan, K., and Frias-Lopez, J. (2017). Potassium is a key signal in host-microbiome dysbiosis in periodontitis. *PloS Pathog.* 13 (6), e1006457. doi: 10.1371/journal.ppat.1006457

Yost, S., Duran-Pinedo, A. E., Teles, R., Krishnan, K., and Frias-Lopez, J. (2015). Functional signatures of oral dysbiosis during periodontitis progression revealed by microbial metatranscriptome analysis. *Genome Med.* 7 (1), 27. doi: 10.1186/s13073-015-0153-3

Zhang, H., Pan, Y., Hu, L., Hudson, M. A., Hofstetter, K. S., Xu, Z., et al. (2020). TrkA undergoes a tetramer-to-dimer conversion to open TrkH which enables changes in membrane potential. *Nat. Commun.* 11 (1), 547. doi: 10.1038/s41467-019-14240-9

frontiers | Frontiers in Cellular and Infection Microbiology

TYPE Original Research
PUBLISHED 17 November 2022
DOI 10.3389/fcimb.2022.1016523

OPEN ACCESS

EDITED BY
Zuomin Wang,
Capital Medical University, China

REVIEWED BY
Gena D. Tribble,
University of Texas Health Science Center at Houston, United States
Yan Zhou,
Sun Yat-sen University, China
Ruijie Huang,
Sichuan University, China

*CORRESPONDENCE
Jin Zhao
zhaojin@xjmu.edu.cn

†These authors have contributed equally to this work

SPECIALTY SECTION
This article was submitted to Extra-intestinal Microbiome, a section of the journal Frontiers in Cellular and Infection Microbiology

RECEIVED 11 August 2022
ACCEPTED 20 October 2022
PUBLISHED 17 November 2022

CITATION
Zhang Y, Wu Z, Li L, Wang X, Fan W and Zhao J (2022) Characterizing the supragingival microbiome of healthy pregnant women.
Front. Cell. Infect. Microbiol. 12:1016523.
doi: 10.3389/fcimb.2022.1016523

Characterizing the supragingival microbiome of healthy pregnant women

Yangyang Zhang[1,2†], Zeyu Wu[1,2†], Ling Li[3], Xiaohe Wang[1,2], Wenxian Fan[1,2] and Jin Zhao[1,2*]

[1]Department of Cariology and Endodontics, The First Affiliated Hospital of Xinjiang Medical University (The Affiliated Stomatology Hospital of Xinjiang Medical University), Urumqi, China, [2]Stomatology Disease Institute of Xinjiang Uyghur Autonomous Region, Xinjiang Medical University, Urumqi, China, [3]Department of Obstetrics and Gynecology, The First Affiliated Hospital of Xinjiang Medical University, Urumqi, China

The ecological characteristics and changes of the supragingival plaque microbial community during pregnancy are poorly understood. This study compared the microbial community characteristics of supragingival plaque in pregnant and non-pregnant women, with the aim of identifying specific microbial lineages and genera that may be associated with pregnancy. Thirty pregnant women were randomly selected from the First Affiliated Hospital of Xinjiang Medical University and divided into groups based on pregnancy trimester: first trimester (group P1, n=10, ≤12 weeks), second trimester (group P2, n=10, 13–27 weeks), and third trimester (group P3, n=10, 28–40 weeks). Ten healthy non-pregnant women (group N) were enrolled as the control group. Supragingival plaque samples of all subjects were collected and oral microbial composition was surveyed using a 16S rRNA gene sequencing approach. Statistical analysis was performed using a nonparametric test. The Chao 1 index of P3 was significantly lower compared with that of N, P1, and P2 (P<0.05). The Simpson indices of P2 and P3 were significantly higher than that of N (P<0.05). The Shannon index of P2 was significantly higher compared with that of N (P<0.05). Principal coordinate analysis (PCoA) showed different clustering according to the pregnancy status. Linear discriminant analysis effect size (LEfSe) revealed that the microbial species in group N that were significantly different from those of other groups were concentrated in the genus *Neisseria*. Species in P1 that were significantly different from those of other groups were concentrated in the genus *Tannerella*, while those in P2 and P3 were concentrated in the genus *Leptotrichia*. A total of 172 functional pathways were predicted for the bacterial communities in this study using PICRUSt2. Principal Component Analysis (PCA) showed that most predicted functional pathways clustered together in N and P1 and in P2 and P3. LEfSe analysis revealed that 11 pathways played a discriminatory role in the four groups. This work suggests a potential role of pregnancy in the formation of supragingival plaque microbiota and indicates that physiological changes

during pregnancy may convert supragingival plaque into entities that could cause harm, which may be a risk factor for maternal health. Furthermore, findings from the study provide a basis for etiological studies of pregnancy-associated oral ecological disorders.

KEYWORDS

supragingival plaque, diversity, 16S rRNA gene sequencing, pregnancy, functional pathway

Introduction

A broad microbiome consisting of bacteria, viruses, phages, and fungi is present in almost every part of the body (Proal et al., 2017), and the oral cavity is one of the five major habitats of human microbes (Human Microbiome Project, 2012). The oral microbiome is an essential part of the human microbiome (Human Microbiome Project, 2012) and the expanded Human Oral Microbiome Database (eHOMD) includes 775 oral microbial species (Escapa et al., 2018). Oral microbiota interact with the host microenvironment in a complex way to maintain the dynamic balance of oral microecology. Smoking (Al Bataineh et al., 2022), circadian rhythm disorders (Chellappa et al., 2022), poor dietary habits (Chen et al., 2022; Santonocito et al., 2022), obesity (Hudek Turkovic et al., 2022), hormones (Ye and Kapila, 2021), oral hygiene (Harding et al., 2017; Sedghi et al., 2021), and other factors can alter this balance, and imbalance of human oral microecology is closely related to local and systemic diseases of the oral cavity. This includes oral diseases such as caries (AlEraky et al., 2021; Pitts et al., 2021), periodontal disease (Chen et al., 2018; Usui et al., 2021), and oral cancer (McIlvanna et al., 2021; Stasiewicz and Karpiński, 2021) as well as systemic diseases such as diabetes (Zhang et al., 2021a), cardiovascular disease (Deraz et al., 2022), rheumatoid arthritis (Kroese et al., 2021), inflammatory bowel disease (Read et al., 2021), colorectal cancer (Yu et al., 2022), and premature birth (Vander Haar et al., 2022; Yang et al., 2022). Oral microbiology can therefore be used as an approach to explore the biomarkers of oral diseases and related systemic diseases. However, to characterize changes in the oral microbiome during disease, it is necessary to understand the species composition and functional genetic metabolic pathways of the oral microbiome in healthy populations.

Adverse pregnancy outcomes include preterm birth, stillbirth, low birth weight, pre-eclampsia, and so on, and affect more than 20% of newborns globally each year (Ye and Kapila, 2021). Adverse pregnancy outcomes can directly lead to infant/fetal death or congenital disabilities and may also be associated with the development of chronic diseases in adulthood, placing a heavy economic burden on families and society (Rogers and Velten, 2011; Chen et al., 2012). However, half of the causes of adverse pregnancy outcomes remain unknown (Ye and Kapila, 2021). Intrauterine infections play a major role in adverse pregnancy outcomes (Ye and Kapila, 2021). Intrauterine placental bacterial infection most likely originates from upstream infection by lower genital tract bacteria and bloodstream infection by oral bacteria (Han Y and Wang, 2013; Vornhagen et al., 2016). Women undergo changes in their oral microecological environment during pregnancy owing to hormonal and immunological alterations (Ye and Kapila, 2021). Such changes increase the susceptibility of pregnant women to oral diseases like periodontal disease and gingivitis (Saadaoui et al., 2021). Previous studies have indicated that periodontal disease is a significant risk factor for the development of adverse pregnancy outcomes (Daalderop et al., 2018; Bobetsis et al., 2020). Two different mechanisms have been proposed to explain how periodontal disease affects pregnancy outcome. The first mechanism is that oral microorganisms directly invade the fetoplacental unit (Saadaoui et al., 2021; Xu and Han, 2022), while the second mechanism is that oral microbes produce inflammatory mediators that affect the fetoplacental unit (Xu and Han, 2022). In both cases, microorganisms or inflammatory mediators entering the fetoplacental unit can cause an inflammatory response, which, in turn, can affect fetal development, lead to spontaneous abortion, or trigger preterm labor and delivery (Saadaoui et al., 2021). Therefore, studies of the oral microbiome during pregnancy are necessary to improve prediction and interventions of adverse pregnancy outcomes.

Current findings regarding the differences in oral microbial composition between pregnant and non-pregnant women and the dynamics of the oral microbiome during pregnancy are inconsistent. Numerous studies have reported significant differences in oral microbiome composition between pregnant and non-pregnant women (Fujiwara et al., 2017; Lin et al., 2018; Balan et al., 2021; Zhang et al., 2021b), but a few studies concluded that there are no differences in oral microbiome composition between pregnant and non-pregnant women

(Machado et al., 2012). Furthermore, there are reports suggesting that the oral microbial composition of pregnant women changes significantly (Borgo et al., 2014; Fujiwara et al., 2017; Lin et al., 2018), while other studies indicate that the oral microbial composition of pregnant women remains stable (Carrillo-de-Albornoz et al., 2010; Bisanz et al., 2015; DiGiulio et al., 2015). Hence, the composition and structural transformation of the oral microbiota during pregnancy remains poorly understood.

In this study, high-throughput 16S rRNA gene sequencing was used to compare the microbial community characteristics of supragingival plaque in 30 pregnant and 10 non-pregnant women, with the aim of identifying specific microbial lineages and genera that may be associated with pregnancy. Functional pathways of the microbial communities were also predicted. These findings may provide a broader understanding of pregnancy-associated oral microecological dysbiosis.

Materials and methods

Ethics statement

This study was approved by the Research and Ethics Committee of the First Affiliated Hospital of Xinjiang Medical University, China (file no. K202203-27) and was conducted according to the Declaration of Helsinki. All participants were fully informed about the study and provided written consent to participate.

Participants

Forty subjects were recruited from November 2020 to February 2021 [sample size was referenced from previous studies (Bik et al., 2010; Lin et al., 2018; Balan et al., 2021)] and comprised 30 healthy pregnant women recruited from the obstetrics department of the First Affiliated Hospital of Xinjiang Medical University (Xinjiang, China) and a control group of 10 healthy non-pregnant women (group N). The pregnant women were divided into three groups (10 subjects per group) based on pregnancy trimester: first trimester (group P1, ≤12 weeks), second trimester (group P2, 13–27 weeks), and third trimester (group P3, 28–40 weeks). The inclusion criteria for the pregnant group were: (1) 20–35 years of age; (2) 28 natural teeth; (3) good oral health; (4) <42 weeks of gestation; and (5) good systemic health. The recruitment criteria for non-pregnant women were: (1) 20–35 years of age; (2) 28 natural teeth; (3) good oral health; and (4) good systemic health. Pregnant and non-pregnant women who met one of the following criteria were excluded: (1) systemic disease; (2) clinically diagnosable untreated oral lesions; (3) use of antibiotics within the past 3 months; and (4) smoking or alcohol consumption habits.

Demographic information was obtained through a self-reported questionnaire. Referring to the standards in the WHO Basic Methods for Oral Health Surveys, 5th edition (World Health Organization, 2013), a comprehensive oral health examination was performed on each subject by a professionally trained dentist under natural light, and the number of caries, missing teeth, and fillings (DMFT), plaque index (PLI), and gingival index (GI) were recorded by an assistant. Dental caries were recorded according to WHO criteria (World Health Organization, 2013), and prevalence of caries was expressed by the number of decayed, missing, and filled teeth (DMFT index).

Oral hygiene status was assessed using the PLI. Patients rinsed their mouth with water, then used a cotton swab or small cotton ball dipped in 2% neutral red solution and applied it to the tooth surface near the gingival margin, then rinsed again and checked the stained area of the tooth surface. The PLI is recorded as six levels, and the scoring criteria are: 0=No plaque on the tooth surface; 1=Scattered spot plaque on the gingival margin of the tooth neck; 2=Wide band of continuous narrow plaque on the tooth neck not more than 1 mm; 3=Area covered by plaque on the tooth neck more than 1 mm, but less than 1/3 of the tooth surface; 4=Area covered by plaque at least 1/3 of the tooth surface, but not more than 2/3; 5=Area covered by plaque 2/3 of the tooth surface or more.

Gingival health status was assessed using the GI. A periodontal probe was placed in the gingival margin at the opening of the gingival sulcus and gently slid along the gingival margin, only slightly touching the gingival tissue. Four levels of gingival tissue are scored: 0=Healthy gums; 1=Mild gingival inflammation: gums with mild color change and edema, no bleeding on probing; 2=Moderate gingival inflammation: gums with red color, edema, and bleeding on probing; 3=Severe gingival inflammation: gums with marked redness, swelling or ulceration, and a tendency to bleed spontaneously. A score of 0 is normal gums, while 1, 2, and 3 correspond to mild, moderate, and severe gingivitis, respectively.

Sample collection

Supragingival plaque samples were taken from six index teeth from each woman according to the methods recommended by the Manual of Procedures for Human Microbiome Project (Mcinnes PCMA, 2010). All subjects did not brush their teeth on the morning of the sampling and did not eat or rinse lightly for 2 hours prior to sampling. Sampling was performed by a professionally trained dentist in a simple dental chair used for oral examination. The six index teeth included two molars (#3 and #19), two premolars (#12 and #28), and two incisors (#9 and #25). The areas to be sampled were separated with a cotton roll and dried with a gentle stream of air from an air-water syringe. All supragingival plaque was removed from the surfaces of the selected index teeth using a Gracey spatula. The tip of the spatula was then dipped into 500 μL phosphate-buffered saline (PBS) in

a 2-mL Eppendorf tube for 4–5 s and the face of the curette was wiped on the inside edge of the collection tube. The same procedure can be used immediately Sampling of the locus again. If a subject had little plaque, the arch counterparts to the index molar and premolar teeth were also be sampled. The lid of the Eppendorf tube was closed, and the tube was shaken for 4–5 seconds to maximize dispersion of the specimen in the fluid. Dental plaque samples collected from each participant were immediately frozen, transferred to the microbiology laboratory, and stored at −80°C until use.

DNA extraction

Total bacterial genomic DNA was extracted using a PowerMax Soil DNA Isolation Kit (MOBIO, Carlsbad, CA, USA) following the manufacturer's protocol. The concentration of DNA was measured using a NanoDrop2000 instrument (Thermo Fisher Scientific, USA).

Deep amplicon sequencing

The V3–V4 region of bacterial 16S rRNA genes were amplified by polymerase chain reaction (PCR) using the primer pair 338F/806R. Reactions were performed in triplicate in a volume of 25.0 μL each. PCR conditions were an initial denaturation at 95°C for 5 min, followed by 25 cycles of denaturation at 95°C for 45 s, annealing at 55°C for 50 s, and extension at 72°C for 45 s, and then a final incubation at 72°C for 10 min. The amplification results were confirmed by 1% agarose gel electrophoresis. PCR amplicons were then individually purified using Agencourt AMPure XP (Beckman Coulter, USA) and pooled in equal amounts. Sequencing libraries were generated using the NEB Next Ultra II DNA Library Preparation Kit (New England Biolabs, USA) according to the manufacturer's instructions. Illumina sequencing was performed by Beijing Allwegene Technology Co. Ltd. (Beijing, China) using the paired-end method and the Illumina MiSeq PE300 platform. Sequencing data have been uploaded to the NCBI (National Center for Biotechnology Information) sequence read archive (BioProject no. PRJNA826664).

Bioinformatic analysis

The raw sequencing data were screened to remove sequences shorter than 230 bp and low-quality tags. According to the UCHIME algorithm process, all arrangements were then examined and assigned taxonomically with a 97.0% bootstrap truncation rate based on 16S rRNA gene combinations from the Human Oral Microbiome Database (HOMD, version 15.2). High-quality representative sequences were aligned and clustered into operational taxonomic units (OTUs) with a threshold similarity of 97.0%. The Ribosome Database Project (RDP) classification tool assigned all sequences to different taxonomic groups. The relative abundance of individual taxa within each community was estimated by comparing the number of sequences assigned to a particular taxon with the number of sequences obtained for that sample. The community structure was statistically analyzed at the taxonomic level of the phylum, genus, and species. The top clades and top genera were listed. Alpha-diversity analysis was performed using QIIME (v1.8.0), including Chao1, Simpson, and Shannon indices. For beta-diversity analysis, a heat map-based distance matrix using weighted uniFrac and unweighted uniFrac distances was employed. Differences in microbial community composition were analyzed using principal coordinate analysis (PCoA) (Lozupone et al., 2007). PCoA and bacterial taxonomic analysis were calculated and plotted in R v3.5.2 software. Microbial community composition was visualized using Sankey diagrams, which are flow diagrams in which the arrow width is proportional to the quantity (e.g. gene expression) to depict changes over time or hierarchy between nodes (Platzer et al., 2018). Linear discriminant analysis (LDA) effect size (LEfSe) was employed to identify the taxa most likely to explain the differences between groups. LEfSe uses a nonparametric Kruskal–Wallis rank sum test to assess different features with significantly different abundance between assigned taxa and performs LDA to estimate the effect size of each sequence variant, as reported by Segata et al. (2011). The LDA scores ranked the different taxa and are displayed on the LEfSe bars according to their effect sizes. For LEfSe analysis, data were first converted to log10 before the non-parametric Kruskal–Wallis rank sum test. A significant alpha level of 0.05 and an effect size threshold of three times larger differences were used to display the results in this study. Co-occurrence networks of the 50 most abundant genera were analyzed using Mothur and visualized *via* Gephi (https://gephi.org/). Spearman's correlation coefficients were also calculated. Network edges were set using genera for which the ρ-value was >0.6 and significant (P<0.05). To predict metabolic pathways, a phylogenetic survey of the community was performed from the sequencing data by reconstructing the unobserved state (PICRUSt2), as shown previously (Douglas et al., 2020). Fastq sequence files for each sample were processed using QIIME2. Representative sequences were used as input files for the PICRUSt2 analysis pipeline. Metabolic pathways were assigned based on the Kyoto Encyclopedia of Genes and Genomes (KEGG) Ortholog (KO) database. Read abundance data for all predicted pathways were converted to relative abundance and subjected to LEfSe analysis by the Galaxy server (https://huttenhower.sph.harvard.edu/galaxy/) using an LDA score of 3.0 as the threshold level to identify pathway taxa most likely to explain intergroup differences.

Statistical analysis

Results were expressed as median and interquartile range. The Kruskal–Wallis test was used to compare differences in

general clinical characteristics of study subjects between groups and differences in oral microbial communities. SPSS (version 27.0) software was used for statistical analysis. Results were considered statistically significant when the probability value (*P*) was <0.05.

Results

Clinical characteristics of participants

A total of 40 women—30 pregnant women and 10 non-pregnant women–were recruited for this study. The characteristics of the study population are illustrated in Table 1 and Table S1 in Additional File 1. No statistical differences were found between the groups regarding age, race, and oral status characteristics (Kruskal–Wallis test, $P>0.05$). However, body mass index was higher in the second- and third-trimester groups compared with that in the non-pregnant control group (Kruskal–Wallis test, $P<0.001$).

Bacterial diversity of supragingival microbiota

Illumina MiSeq sequencing produced 2909243 raw sequences, and after pre-processing, 2531486 usable, high-quality reads, with an average of 63287 ± 29723 sequences per sample, remained in the dataset (Additional File 1: Table S1, Additional File 2: Figure S1A). The average sequence length ranged from 400 to 440 bp (Additional File 1: Table S3, Additional File 2: Figure S1B). After removing the low-credibility OTUs, the taxonomic assignment of the sequences resulted in the identification of a total of 1335 OTUs in the supragingival microbiota. The number of OTUs in N, P1, P2, and P3 groups were 1339, 1440, 1096, and 869, respectively (Figure 1A). At this sequencing depth, the Shannon–Wiener curves for all samples have reached a plateau (Additional File 2: Figure S2), indicating that this sequencing depth is sufficient to capture the full range of microbial diversity.

The Chao 1 index reflects community species richness, while the Simpson and Shannon indices reflect microbial diversity

TABLE 1 Demographic, medical, and oral status characteristics of study subjects.

Categories		Pregnant (n=30)			Non-Pregnant (n=10)	*P*-value
		1st trimester (n=10)	2nd trimester (n=10)	3rd trimester (n=10)		
Age (years)		28.50 (32.00, 25.75)	29.50 (32.25, 26.50)	28.50 (32.25, 27.75)	27.50 (33.00, 24.75)	0.90
Ethnicity	Han nationality	9	10	9	9	0.79
	Minority nationalities	1	0	1	1	
Education	<High school completion	6	5	3	4	0.58
	≥High school completion	4	5	7	6	
BMI		23.17 (24.17, 21.36)	23.43 (24.25, 23.22)	24.36 (24.52, 22.84)	21.38 (21.76, 20.60)	<0.001
Smoking status	Never smoked	9	10	10	9	0.56
	Former smoker	1	0	0	1	
	Current smoker	0	0	0	0	
Alcohol consumption	Abstainer	10	9	9	9	0.79
	Non-current	0	1	1	1	
	Current	0	0	0	0	
Sweet consumption	Once/day	9	8	7	9	0.75
	more than once/day	1	2	3	1	
	None	10	10	9	10	
Tooth brushing	Twice/day	9	9	10	9	0.79
	Once/day	1	1	0	1	
	Less than once/day	0	0	0	0	
Flossing habit	Once or more/day	1	3	2	3	0.67
	Less than once/day	9	7	8	7	
DMFT		1.00 (2.00, 0.75)	2.00 (2.00, 0.75)	1.00 (2.25, 0.75)	0.50 (2.00, 0.00)	0.59
PLI		1.00 (1.25, 1.00)	1.00 (2.00, 0.00)	1.00 (1.25, 0.00)	1.00 (2.00, 1.00)	0.81
GI		1.00 (1.00, 0.00)	0.00 (1.00, 0.00)	0.00 (1.00, 0.00)	1.00 (1.00, 0.00)	0.67

BMI, body mass index (kg/m^2); DMFT, decayed, missing, filled teeth number; PLI, plaque index; GI, gingival index.

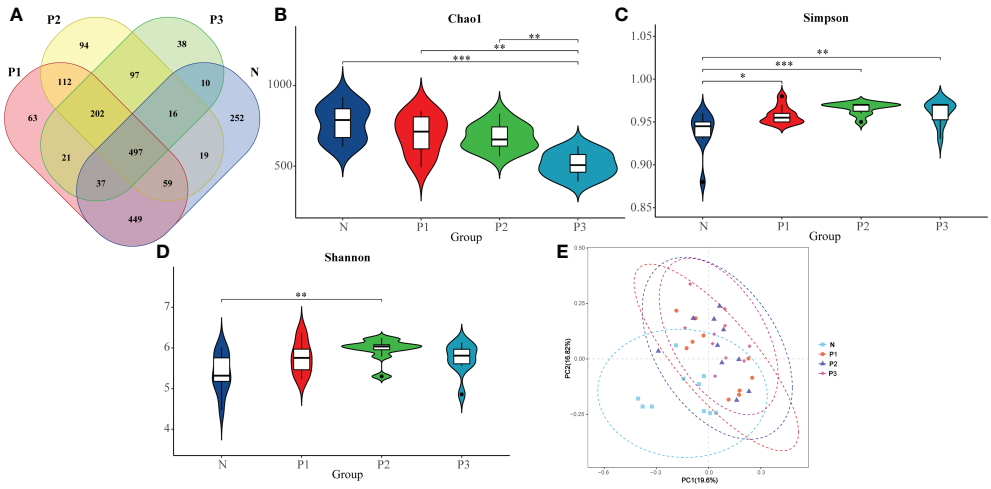

FIGURE 1
(A) Differences in number of OTUs among microbiota from N, P1, P2, and P3. **(B)** The comparison of Chao 1 index in N, P1, P2, and P3. **(C)** The comparison of Simpson index in N, P1, P2, and P3. **(D)** The comparison of Shannon index in N, P1, P2, and P3. **(E)** PCoA analysis revealing the bacterial communities in N, P1, P2, and P3. * P<0.05, ** P<0.01, *** P<0.001.

(Hill et al., 2003). Kruskal–Wallis nonparametric tests and pairwise comparisons were conducted for the alpha-diversity indices of N, P1, P2, and P3. From The Chao 1, Simpson, and Shannon indices of these four groups were significantly different (Table 2). After pairwise comparison, the Chao 1 index of P3 was lower compared with those of N, P1, and P2, and the differences were statistically significant (P<0.05), indicating that the species richness of the oral microbial community decreased during late pregnancy (Additional File 1: Tables S4, S5 and Figure 1B). The Simpson indices of P2 and P3 were higher compared with those of N and P1, and the differences were statistically significant (P<0.05), indicating that the microbial diversity of the oral microbial community decreased in mid- and late pregnancy (Additional File 1: Tables S4, S5 and Figure 1C). The Shannon index of P2 was higher compared with that of N, and the difference was statistically significant (P<0.05), indicating that the microbial diversity of the oral microbial community increased in the middle of pregnancy (Additional File 1: Tables S4, S5 and Figure 1D). It can be concluded that pregnancy may lead to a decrease in species richness of the

TABLE 2 Alpha-diversity indices of N, P1, P2, and P3.

Group		Chao 1	Simpson	Shannon
N		786.22 (867.61, 664.54)	0.95 (0.95, 0.93)	5.32 (5.82, 5.10)
P1		714.14 (826.80, 578.63)	0.96 (0.96, 0.95)	5.76 (6.08, 5.40)
P2		665.75 (746.40, 618.13)	0.97 (0.97, 0.96)	6.04 (6.11, 5.91)
P3		506.12 (582.77, 448.90)	0.97 (0.97, 0.95)	5.81 (6.01, 5.58)
P-value	All groups	<0.001 (**)	0.002 (*)	0.023 (*)
	N-P1	1	0.283	0.714
	N-P2	1	0.001 (*)	0.012 (*)
	N-P3	<0.001 (**)	0.022 (*)	0.661
	P1-P2	1	0.583	0.770
	P1-P3	0.011 (*)	1	1
	P2-P3	0.026 (*)	1	0.829

Each value is the median and interquartile range. *indicates significant differences (P<0.05); **indicates extremely significant differences between groups (P<0.001).

oral microbial community. However, the results of the two indicators reflecting microbial diversity were inconsistent, possibly influenced by species evenness.

A heatmap of beta-diversity index was used to measure the dissimilarity coefficient between samples. Weighted and unweighted UniFrac distances were used to indicate the close proximity of the bacterial communities in the four groups. A lower number represents greater similarity in bacterial microbiota between samples in the heatmap. The heatmaps (Additional File 2: Figures S3A, B) show that the communities of N and P1 are closer together, suggesting that the two groups are more similar, while the distance between the communities of N and P2 and P3 is larger, suggesting that the communities of N and P2 and P3 are more different. These findings suggest that the microbial community of supragingival plaque may have changed during mid- and late-pregnancy.

In addition, the differences in microbial community composition of N, P1, P2, and P3 were analyzed by PCoA (Figure 1E), and PC1 and PC2 accounted for 19.60% and 16.82% of the total variation, respectively. The PCoA plot revealed that the microbial community composition of N was different from those of the other three groups and the differences were statistically significant (PERMANOVA, pseudo-F=2.4218, *P*=0.001). This suggests that pregnancy may have an effect on the composition of oral microbial communities.

Community structure of supragingival microbiota

To characterize the bacterial distribution, the supragingival plaque microbiota of N, P1, P2, and P3 were analyzed in terms of relative taxonomic abundance. A total of 15 phyla, 32 classes, 53 orders, 98 families, 194 genera, and 503 species were detected. Bar graphs show the top 15 phyla in each of the four groups (Additional File 1: Table S6 and Figure 2A). Four phyla—Fusobacteria, Bacteroidetes, Firmicutes, and Proteobacteria—were the most abundant, accounting for 91.56%, 91.07%, 92.18%, and 89.64% of the total OTUs in each of the N, P1, P2, and P3 groups, respectively. The top 20 genera in each of the four groups are depicted in bar charts (Additional File 1: Table S7 and Figure 2B). *Leptotrichia* was the most abundant genus in the pregnancy group, followed by *Fusobacterium*, *Prevotella*, and *Streptococcus*, together accounting for 50.82%, 51.85%, and 53.22% in P1, P2, and P3, respectively. *Streptococcus* was the most abundant genus in the non-pregnancy group, followed by

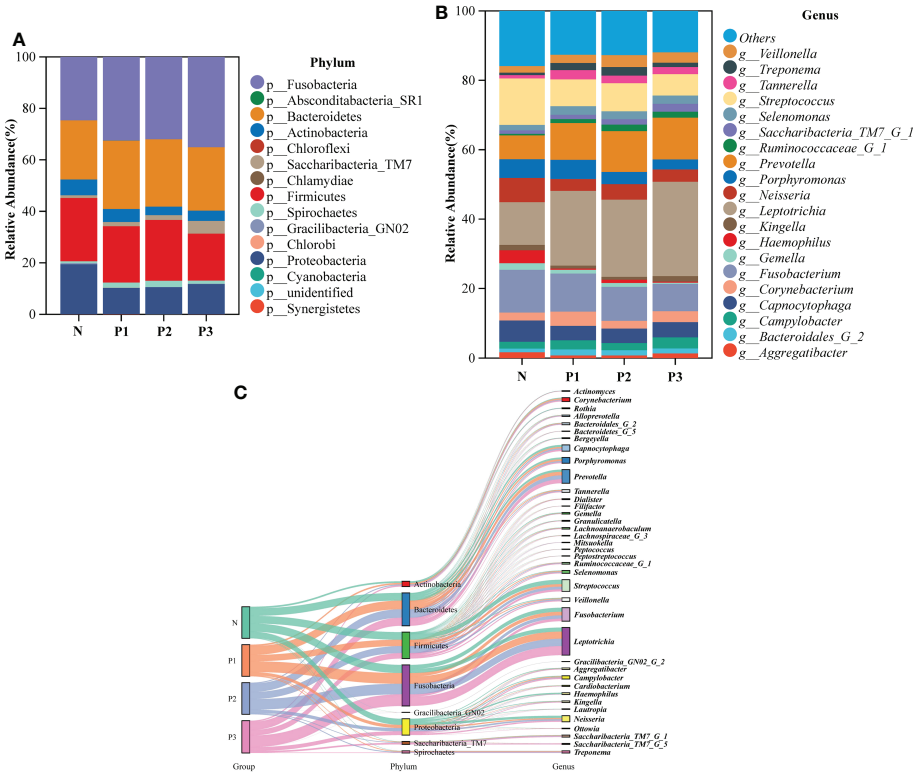

FIGURE 2
(A) The bacterial structure comparison in N, P1, P2, and P3 at the phylum level. **(B)** The bacterial structure comparison in the four groups at the genus level. **(C)** Sankey analysis of the bacterial structure comparison in the four groups at phylum and genus levels.

Fusobacterium, *Leptotrichia*, and *Neisseria*, which together accounted for 45.00% of the total OTUs in N group. Relative abundance at the phylum and genus levels could also be visualized by the Sankey diagram (Figure 2C), which showed results similar to those in Figures 2A, B. Collectively, these results suggest that the oral microbial community composition in the pregnant and non-pregnant groups was essentially the same at the phylum level but differed at the genus level.

The LEfSe method was used to identify the distinguishing phylotype that most likely explained the differences between N, P1, P2, and P3. LDA was combined with effect size measures for assessing the effect sizes of taxa (Figure 3A). A circular clade plot was created to show taxa with different abundances (Figure 3B). Species in group N that differed significantly from those of the other groups were concentrated in the genus *Neisseria*. In P1, the species that differed significantly from those of the other groups were concentrated in the genus *Tannerella*. In P2 and P3, the species that differed significantly from those of the other groups were concentrated in the genus *Leptotrichia*. (Additional File 1: Table S8 and Figures 3A, B).

Network analysis was performed to recognize interactions among genera in different groups. The top 20 genera for each group in the relative abundance ranking were selected from the four groups. Genera that met the threshold of Spearman's correlation coefficient of $\rho > 0.6$ and $P<0.05$ are shown in the networks (Additional File 1: Table S9 and Figure 4). The modularity, node, edge, and graph density for group N were 0.30, 19, 40, and 0.30, respectively. *Streptococcus*, *Fusobacterium*, *Leptotrichia*, and *Neisseria* were present in greater relative abundance in N, compared with the other genera in the network, with *Streptococcus* and *Fusobacterium* showing negative correlation. The modularity, node, edge, and graph densities were 0.38, 19, 29, and 0.17 for P1; 0.56, 18, 25, and 0.163 for P2; and 0.63, 17, 15, and 0.11 for P3. In P1, P2, and P3, *Leptotrichia*, *Fusobacterium*, and *Prevotella* were present in greater relative abundance, compared with the other genera in the networks, and *Leptotrichia* was negatively correlated with *Fusobacterium* and *Prevotella*. These analyses suggest that group N may have a more complex network topology, and the network topology of N differs from that of the three pregnancy groups (Additional File 1: Table S9, Additional File 2: Figure S4).

Predicted metabolic functions of supragingival microbiota

Functional pathways for the bacterial communities of N, P1, P2, and P3 were predicted using PICRUSt2 (Additional File 1: Table S10). Level 1 functional pathways that differed significantly among the four groups included metabolism, genetic information processing, and human diseases. The abundance of predicted functions related to metabolic pathways and genetic information processing was high in all four groups, accounting for 93.93%, 93.73%, 93.63%, and 93.76% of all level 1 predicted functions in N, P1, P2, and P3 groups, respectively (Figure 5A). Level 2 functional pathways that differed significantly among the four groups included metabolism of other amino acids, energy metabolism, lipid metabolism, xenobiotics biodegradation and metabolism, nucleotide metabolism, replication and repair, translation, and cell growth and death. The abundance of predicted functions related to metabolism of cofactors and vitamins, carbohydrate metabolism, amino acid metabolism, and metabolism of terpenoids and polyketides was high in all four groups, accounting for 48.01%, 48.28%, 48.51%, and 48.94% of all level 2 predicted functions in N, P1, P2, and P3 groups, respectively. (Figure 5B). PICRUSt2 predicted 172 level 3 functional pathways by comparison with KEGG immediate relatives (Additional File 1: Table S10, Additional File 2: Figure S4).

PCA demonstrated that most of the N and P1 predictive function pathways clustered together, and that the P2 and P3

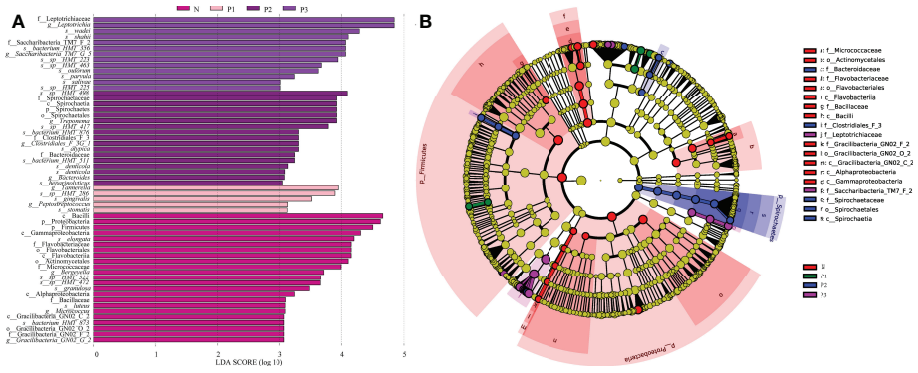

FIGURE 3
(A) Significantly enriched bacterial taxa in the different groups as determined by LEfSe analysis (LDA sore >3). **(B)** LEfSe taxonomic cladogram. The size of each node represents the relative abundance of the species. (p, phylum; c, class; o, order; f, family; g, genus; s, species).

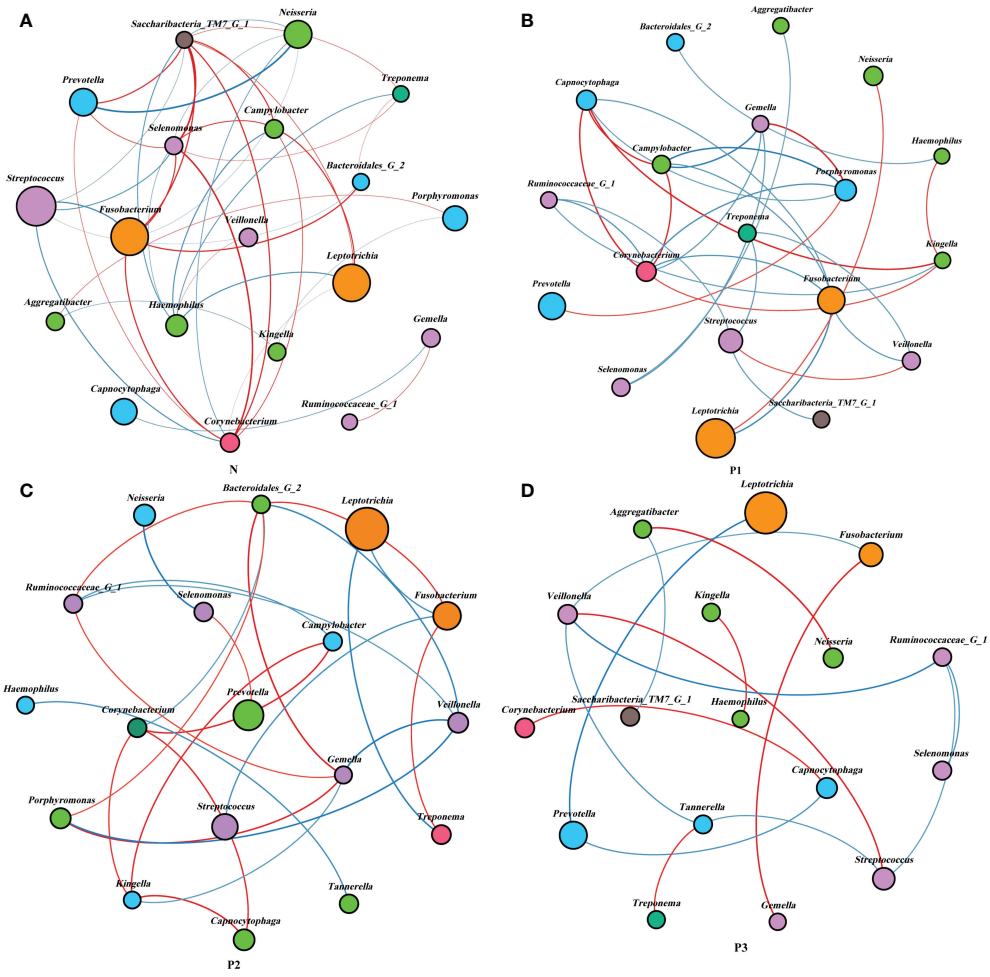

FIGURE 4
Network analysis between bacterial taxa in the four groups. Network analysis revealed the 20 most abundant genera (|SpearmanCoef>0.6 and *P*<0.05). Bacterial interactions in N **(A)**, P1 **(B)**, P2 **(C)**, and P3 **(D)** are depicted. The size of the nodes is proportional to the genus abundance. Node color corresponds to the phylum classification. Edge colors indicate positive (red) and negative (blue) correlations.

predictive function pathways clustered together (Figure 6A). Changes in oral microbial predictive functional pathways occurred during mid- and late-pregnancy, and these changes may be related to pregnancy. Data for predicted functional pathways were converted to relative abundance and differences between groups are shown in Figure 6B. LEfSe analysis showed that 11 pathways played a discriminatory role in the four studied groups (Figure 6B). Functional pathways in the bacterial community of N that were clearly distinguished from those of the other groups included polyketide sugar unit biosynthesis, cyanoamino acid metabolism, primary bile acid biosynthesis, and betalain biosynthesis. The functional pathway that clearly distinguishes the P1 bacterial community from those of the other three groups is the biosynthesis of type II polyketide backbone. The functional pathway that clearly distinguishes P2 from the other groups is monoterpenoid biosynthesis, and the functional pathways that clearly distinguish the bacterial community of P3 from those of the other three groups include chagas disease (American trypanosomiasis) and biosynthesis of ansamycins.

Discussion

Adverse pregnancy outcomes affect more than 20% of newborns worldwide each year (Ye and Kapila, 2021), imposing a heavy economic burden on families and society (Rogers and Velten, 2011; Chen et al., 2012). However, half of the causes are still unknown (Ye and Kapila, 2021). Intrauterine infections play a major role in adverse pregnancy outcomes. In addition to upstream infection by bacteria from the lower genital tract, intrauterine placental bacterial infections may also arise from bloodstream infection by oral bacteria (Han Y and Wang, 2013;

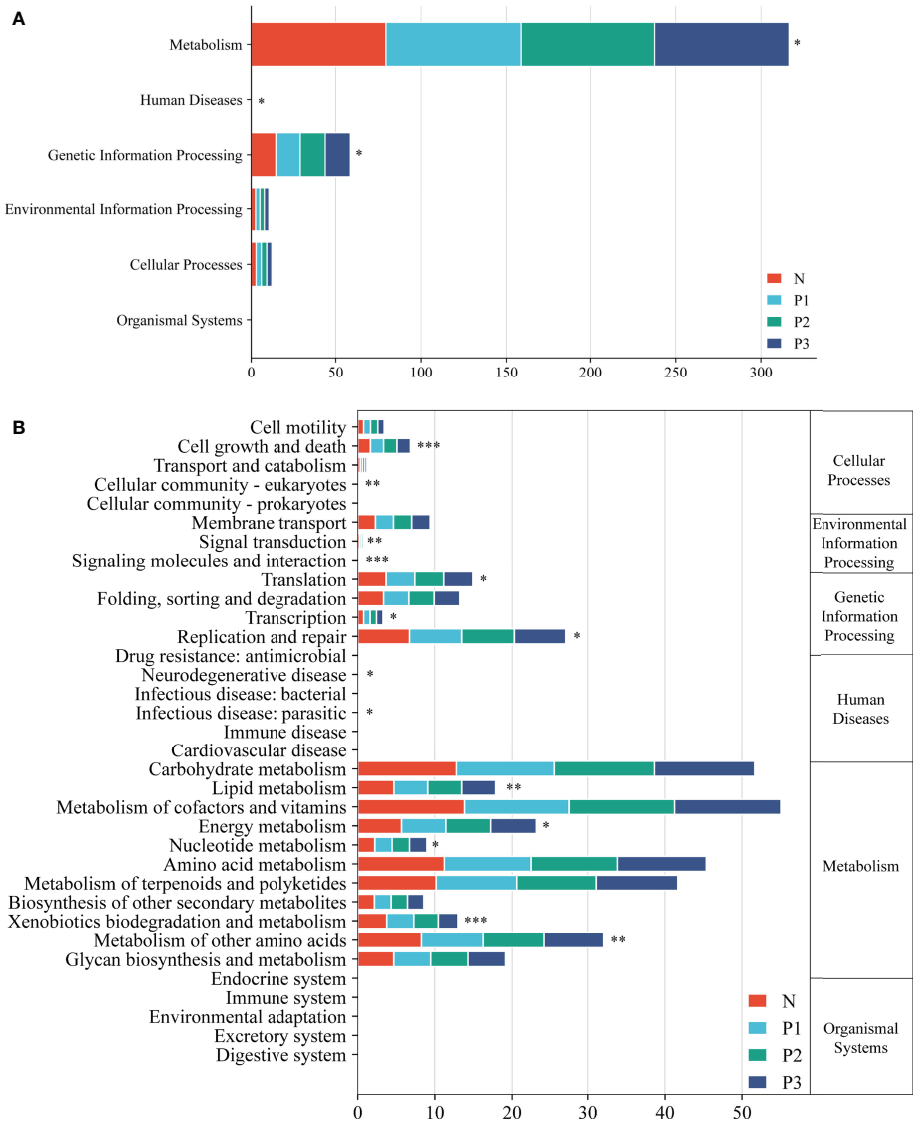

FIGURE 5
Level 1 **(A)** and level 2 **(B)** KEGG pathways in the four groups. Asterisks indicate significant differences; * $P<0.05$, ** $P<0.01$, *** $P<0.001$.

Vornhagen et al., 2016). Therefore, studies of the oral microbiome during pregnancy are necessary to better predict and intervene in adverse pregnancy outcomes.

Advances in sequencing technology are rapidly changing the experimental landscape of microbial ecology (Kozich et al., 2013). High-throughput sequencing technologies provide an efficient and effective method for studying the composition and structure of bacterial communities associated with health and disease. The current study was conducted using Illumina MiSeq sequencing, and the supragingival plaque microbiota of pregnant and non-pregnant women exhibited significant differences in community structure and composition.

The groups of subjects in this study were not statistically different in terms of age, race, and oral status characteristics ($P>0.05$). However, BMI was higher in the second and third trimester groups compared with the non-pregnant control group (Kruskal–Wallis test, $P<0.001$). Currently, there is no agreement on the effect of elevated BMI on oral microbiology without reaching obesity levels. One study showed higher numbers of red complexes (*Porphyromonas gingivalis*, *Treponema denticola*, and *Tannellera forsythia*) in non-diabetic patients with a high BMI or waist circumference (Matsushita et al., 2015). In contrast, another study showed no statistical effect on the composition of the salivary bacterial profile based on the extreme degree of fractional

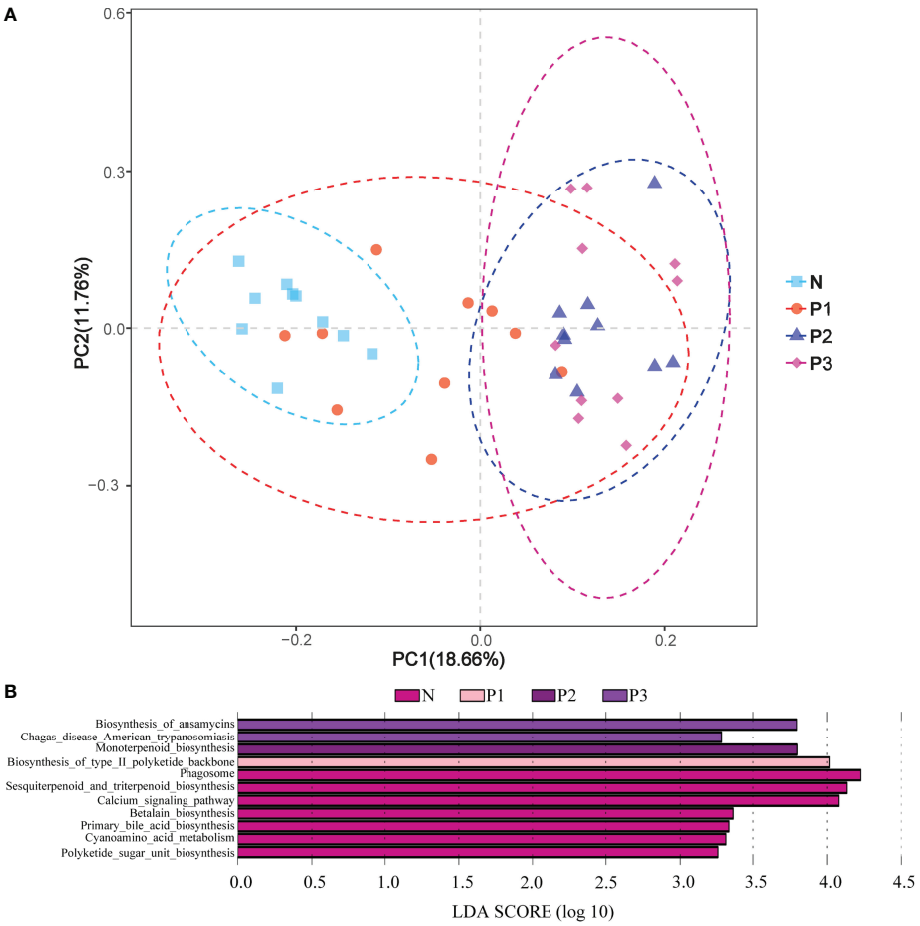

FIGURE 6
(A) PCA plots to assess beta diversity among the KEGG level 3 predicted microbial metabolic functions in the four studied groups. **(B)** Linear discriminant analysis (LDA) of the KEGG level 3 predicted microbial metabolic functions in the four groups. The length of the histogram represents the LDA score.

stratification of parameters such as age, sex, alcohol consumption, BMI, and dietary intake (Belstrøm et al., 2014). Consequently, the effect of BMI on the results of the present study is unclear. Follow-up studies should aim to select women with similar BMIs to exclude the possible effects of BMI on the results.

Both Simpson's index and Shannon's index are indicators of microbial diversity (Hill et al., 2003; Kim et al., 2017). However, in the present study, these two diversity indices reflected inconsistent results. The reason for this contradictory result may be that these two diversity indices were influenced by species evenness (Hill et al., 2003; Kim et al., 2017). Most studies only use the Shannon index as a community diversity indicator, thus the following discussion focuses on the trend of the Shannon index. Previous studies have mostly reported an increase in oral microbial diversity in pregnant women compared with non-pregnant women (Fujiwara et al., 2017; Lin et al., 2018; Balan et al., 2021). Among these studies, Balan et al. found significantly higher alpha diversity in the subgingival plaque microbial community of a pregnant group compared with that of a non-pregnant group (Balan et al., 2021). Fujiwara et al. concluded that the total number of culturable microorganisms in subgingival plaque was substantially higher in early pregnancy compared with that in non-pregnant women (Fujiwara et al., 2017). These two studies used subgingival plaque samples, while the present study used supragingival plaque samples. However, although the samples were different, we demonstrated from different perspectives that oral microbial diversity changed during pregnancy. Lin et al. found that supragingival plaque microbial diversity was higher in pregnancy compared with that in non-pregnancy, with the Shannon index significantly higher in late pregnancy compared with that in the non-pregnancy group (Lin et al., 2018). These results have some similarity with the results of the present study. The samples used in that study were the same as those in the present study, both being supragingival plaque. The changes in Shannon index were essentially the same in both studies, both showing a higher oral microbial diversity in pregnancy compared with that in non-pregnancy, except that it was the late pregnancy Shannon

index that was significantly higher in the study of Lin et al., whereas in the present study, it was the mid-pregnancy Shannon index that was significantly higher compared with that the non-pregnancy group (Table 2 and Figure 1B). Our results are consistent with those of previous studies, which indicate a trend toward increased oral microbial diversity during pregnancy. This elevated trend is also congruent with the hormonal surge of progesterone and estradiol during pregnancy (Wu et al., 2015). However, a few studies found no significant difference in oral bacterial diversity between pregnant and non-pregnant groups. Machado et al. showed that the bacteria most commonly associated with periodontal disease did not differ in subgingival plaque between pregnant and non-pregnant women (Machado et al., 2012). Differences in samples and study methods might explain the difference in results from Machado et al. compared with those of both the present study and other studies. Since the current findings are from studies with small sample sizes, the results need to be validated in future studies with large sample sizes.

The composition of the microbiome is closely related to the disease state (Willis and Gabaldón, 2020). Significant increases in circulating levels of estrogen and progesterone are thought to have a significant effect on the periodontium throughout pregnancy (Wu et al., 2015). Therefore, it can be hypothesized that pregnancy may create a nutritional environment more favorable for certain sensitive microbial strains. A total of 15 phyla, 32 classes, 53 orders, 98 families, 194 genera, and 503 species were detected in all specimens. The predominant phyla were Fusobacteria, Bacteroidetes, Firmicutes, and Proteobacteria, which is similar to the findings of previous studies (Dewhirst et al., 2010; Lin et al., 2018). The current study showed that, at the phylum level, most of the prevalent bacteria were essentially the same in the four groups, but different relative abundances were observed among groups. At the genus level, the dominant genera differed slightly between the pregnant and non-pregnant groups. *Leptotrichia* was the most abundant genus in the pregnancy group, followed by *Fusobacterium*, *Prevotella*, and *Streptococcus*, together accounting for 50.82%, 51.85%, and 53.22% of the total OTUs in P1, P2, and P3, respectively. *Streptococcus* was the most abundant genus in the non-pregnancy group, followed by *Fusobacterium*, *Leptotrichia*, and *Neisseria*, which together accounted for 45.00% of the total OTUs in N group. As shown in the community structure bar charts and Sankey plot, the pregnant and non-pregnant groups exhibited different community structures, suggesting that pregnancy status may significantly affect bacterial composition.

In the current study, LEfSe analysis was used to identify bacterial species in each group that were significantly different from those of other groups (Additional File 1: Table S8 and Figures 2C, D). The species in group N that differed significantly from those of other groups were mainly concentrated in the genus *Neisseria*. The species in group P1 that differed significantly from those in the other groups were mainly concentrated in the genus *Tannerella*. The species in groups P2 and P3 that differed significantly from those in the other groups were concentrated in the genus *Leptotrichia*. Species of the genus *Neisseria* usually colonize the nasopharynx without causing any significant pathological changes and can be considered a normal part of the respiratory microbiome, causing serious disease only when meningococci leave their usual ecological niche (Seifert, 2019). *Tannerella forsythia* is a periodontopathogenic bacterium that, together with *Porphyromonas gingivalis* and *Treponema denticola*, constitutes the "red complex", which is a multibacterial pathogenic complex in periodontitis (Mysak et al., 2014). *Tannerella forsythia* is also one of the species most associated with halitosis and has even been associated with some systemic diseases, such as Alzheimer's disease (Singhrao et al., 2015) and esophageal cancer (Peters et al., 2017). Members of the genus *Leptotrichia* are non-motile pathogenic bacteria found predominantly in the oral cavity and other parts of the body (Eribe and Olsen, 2017; Hou et al., 2018). All species of the genus *Leptotrichia* ferment carbohydrates and produce lactic acid, which may be associated with dental caries (Eribe and Olsen, 2017; Hou et al., 2018). It follows that pathogenic microorganisms associated with periodontitis, dental caries, and systemic diseases may increase in the mouth of healthy individuals as pregnancy progresses. This suggests that we must pay attention to oral hygiene care during pregnancy.

Network analysis was used to explore the potential relevance of the supragingival plaque microbiota detected in the current study. The modularity, node, edge, and graph density of group N were 0.30, 19, 40, and 0.30, respectively. *Streptococcus*, *Fusobacterium*, *Leptotrichia*, and *Neisseria* were present greater relative abundance in N, compared with other genera in the network, with *Streptococcus* and *Fusobacterium* showing negative correlation. This is consistent with the results of a previous study (Lin et al., 2018). The non-pregnant group showed more complex and convergent relationships among bacterial genera compared with those of the pregnant groups, suggesting that some microbial relationships may be disrupted and lead to dysbiosis of oral ecology during pregnancy.

The functional pathways of the oral microbial community were also predicted in the current study. PCA analysis showed that most predicted functional pathways of groups N and P1 clustered together, while those of P2 and P3 clustered together (Figure 3A). This indicates that changes in oral microbial predictive functional pathways occurred during mid- and late-pregnancy and that these changes may be related to pregnancy. LEfSe analysis also identified 11 functional pathways that were significantly different in the four groups. However, given the limitations of PICRUSt2 (Zhang et al., 2022), the analysis of predicted oral microbiota function only provided some preliminary results. Functional changes in the oral microbiota should be confirmed by combining metabolomics and macrogenomics in the future.

This study provides a preliminary assessment of the supragingival plaque microbiota and its relationship to healthy pregnant women. However, there are limitations to the study. Firstly, experimental procedures are needed to determine how pregnancy and sex hormones affect the microorganisms

involved. In addition, the number of study subjects in each group was limited and the samples from the three trimesters were not from the same group of women. In future studies, the number of study subjects should be increased and oral samples should be collected from the same group of women in all three trimesters to improve the credibility of the conclusions.

Conclusion

This study characterized the microbiota of supragingival plaque in pregnant and non-pregnant women and improved understanding of the ecological and microbial shifts associated with pregnancy. Findings from the study suggest that pregnancy has a potential role in shaping the supragingival plaque microbiota and that physiological changes during pregnancy may transform supragingival plaque into entities that may cause harm, which may be a risk factor for maternal health.

Data availability statement

The datasets presented in this study can be found in online repositories. The names of the repository/repositories and accession number(s) can be found in the article/Supplementary Material.

Ethics statement

The studies involving human participants were reviewed and approved by Research and Ethics Committee of the First Affiliated Hospital of Xinjiang Medical University. The patients/participants provided their written informed consent to participate in this study.

Author contributions

Conceived and designed the study: JZ, YZ, and ZW; Participated in investigation: YZ and WF; Performed formal analysis: YZ, ZW, and WF; Collected the resources: YZ, LL, XW, and WF; Curated the data: YZ, LL, XW, and WF; Wrote the manuscript: YZ and LL; Supervised the study: JZ, YZ, and ZW. All authors read and approved the final version of the manuscript.

Acknowledgments

This work was financially supported by the Natural Science Foundation of Xinjiang Uygur Autonomous Region (No. 2018D01C183), Xinjiang Uygur Autonomous Region Postgraduate Scientific Research Innovation Project (No. XJ2022G164) and the National Natural Science Foundation of China (No. 81760194). We appreciate all pregnant and non-pregnant individuals for participating in the research.

Conflict of interest

The authors declare that the research was conducted in the absence of any commercial or financial relationships that could be construed as a potential conflict of interest.

Publisher's note

All claims expressed in this article are solely those of the authors and do not necessarily represent those of their affiliated organizations, or those of the publisher, the editors and the reviewers. Any product that may be evaluated in this article, or claim that may be made by its manufacturer, is not guaranteed or endorsed by the publisher.

Supplementary material

The Supplementary Material for this article can be found online at: https://www.frontiersin.org/articles/10.3389/fcimb.2022.1016523/full#supplementary-material

References

Al Bataineh, M. T., Kunstner, A., Dash, N. R., Abdulsalam, R. M., Al-Kayyali, R., Adi, M. B., et al. (2022). Altered composition of the oral microbiota in depression among cigarette smokers: A pilot study. *Front. Psychiatry* 13, 902433. doi: 10.3389/fpsyt.2022.902433

AlEraky, D. M., Madi, M., El Tantawi, M., AlHumaid, J., Fita, S., AbdulAzeez, S., et al. (2021). Predominance of non-streptococcus mutans bacteria in dental biofilm and its relation to caries progression. *Saudi J. Biol. Sci.* 28 (12), 7390–7395. doi: 10.1016/j.sjbs.2021.08.052

Balan, P., Brandt, B. W., Chong, Y. S., Crielaard, W., Wong, M. L., Lopez, V., et al. (2021). Subgingival microbiota during healthy pregnancy and pregnancy gingivitis. *JDR Clin. Trans. Res.* 6 (3), 343–351. doi: 10.1177/2380084420948779

Belstrøm, D., Holmstrup, P., Nielsen, C. H., Kirkby, N., Twetman, S., Heitmann, B. L., et al. (2014). Bacterial profiles of saliva in relation to diet, lifestyle factors, and socioeconomic status. *J. Oral. Microbiol.* 6, 23609. doi: 10.3402/jom.v6.23609

Bik, E. M., Long, C. D., Armitage, G. C., Loomer, P., Emerson, J., Mongodin, E. F., et al. (2010). Bacterial diversity in the oral cavity of 10 healthy individuals. *ISME J.* 4 (8), 962–974. doi: 10.1038/ismej.2010.30

Bisanz, J. E., Enos, M. K., PrayGod, G., Seney, S., Macklaim, J. M., Chilton, S., et al. (2015). Microbiota at multiple body sites during pregnancy in a rural Tanzanian population and effects of moringa-supplemented probiotic yogurt. *Appl. Environ. Microbiol.* 81 (15), 4965–4975. doi: 10.1128/AEM.00780-15

Bobetsis, Y. A., Graziani, F., Gursoy, M., and Madianos, P. N. (2020). Periodontal disease and adverse pregnancy outcomes. *Periodontol. 2000* 83 (1), 154–174. doi: 10.1111/prd.12294

Borgo, P. V., Rodrigues, V. A., Feitosa, A. C., Xavier, K. C., and Avila-Campos, M. J. (2014). Association between periodontal condition and subgingival microbiota in women during pregnancy: A longitudinal study. *J. Appl. Oral. Sci.* 22 (6), 528–533. doi: 10.1590/1678-775720140164

Carrillo-de-Albornoz, A., Figuero, E., Herrera, D., and Bascones-Martínez, A. (2010). Gingival changes during pregnancy: II. influence of hormonal variations on the subgingival biofilm. *J. Clin. Periodontol.* 37 (3), 230–240. doi: 10.1111/j.1600-051X.2009.01514.x

Chellappa, S. L., Engen, P. A., Naqib, A., Qian, J., Vujovic, N., Rahman, N., et al. (2022). Proof-of-principle demonstration of endogenous circadian system and circadian misalignment effects on human oral microbiota. *FASEB J.* 36 (1), e22043. doi: 10.1096/fj.202101153R

Chen, W. P., Chang, S. H., Tang, C. Y., Liou, M. L., Tsai, S. J., and Lin, Y. L. (2018). Composition analysis and feature selection of the oral microbiota associated with periodontal disease. *BioMed. Res. Int.* 2018, 3130607. doi: 10.1155/2018/3130607

Chen, X., Hu, X., Fang, J., Sun, X., Zhu, F., Sun, Y., et al. (2022). Association of oral microbiota profile with sugar-sweetened beverages consumption in school-aged children. *Int. J. Food Sci. Nutr.* 73 (1), 82–92. doi: 10.1080/09637486.2021.1913102

Chen, W., Srinivasan, S. R., Yao, L., Li, S., Dasmahapatra, P., Fernandez, C., et al. (2012). Low birth weight is associated with higher blood pressure variability from childhood to young adulthood: the bogalusa heart study. *Am. J. Epidemiol.* 176 Suppl 7, S99–105. doi: 10.1093/aje/kws298

Daalderop, L. A., Wieland, B. V., Tomsin, K., Reyes, L., Kramer, B. W., Vanterpool, S. F., et al. (2018). Periodontal disease and pregnancy outcomes: Overview of systematic reviews. *JDR Clin. Trans. Res.* 3 (1), 10–27. doi: 10.1177/2380084417731097

Deraz, O., Range, H., Boutouyrie, P., Chatzopoulou, E., Asselin, A., Guibout, C., et al. (2022). Oral condition and incident coronary heart disease: A clustering analysis. *J. Dent. Res.* 101 (5), 526–533. doi: 10.1177/00220345211052507

Dewhirst, F. E., Chen, T., Izard, J., Paster, B. J., Tanner, A. C., Yu, W. H., et al. (2010). The human oral microbiome. *J. Bacteriol.* 192 (19), 5002–5017. doi: 10.1128/JB.00542-10

DiGiulio, D. B., Callahan, B. J., McMurdie, P. J., Costello, E. K., Lyell, D. J., Robaczewska, A., et al. (2015). Temporal and spatial variation of the human microbiota during pregnancy. *Proc. Natl. Acad. Sci. U.S.A.* 112 (35), 11060–11065. doi: 10.1073/pnas.1502875112

Douglas, G. M., Maffei, V. J., Zaneveld, J. R., Yurgel, S. N., Brown, J. R., Taylor, C. M., et al. (2020). PICRUSt2 for prediction of metagenome functions. *Nat. Biotechnol.* 38 (6), 685–688. doi: 10.1038/s41587-020-0548-6

Eribe, E. R. K., and Olsen, I. (2017). Leptotrichia species in human infections II. *J. Oral. Microbiol.* 9 (1), 1368848. doi: 10.1080/20002297.2017.1368848

Escapa, I. F., Chen, T., Huang, Y., Gajare, P., Dewhirst, F. E., and Lemon, K. P. (2018). New insights into human nostril microbiome from the expanded human oral microbiome database (eHOMD): A resource for the microbiome of the human aerodigestive tract. *mSystems* 3 (6), e00187–e00118. doi: 10.1128/mSystems.00187-18

Fujiwara, N., Tsuruda, K., Iwamoto, Y., Kato, F., Odaki, T., Yamane, N., et al. (2017). Significant increase of oral bacteria in the early pregnancy period in Japanese women. *J. Investig. Clin. Dent.* 8 (1), 1–8. doi: 10.1111/jicd.12189

Han Y, W., and Wang, X. (2013). Mobile microbiome: Oral bacteria in extra-oral infections and inflammation. *J. Dent. Res.* 92 (6), 485–491. doi: 10.1177/0022034513487559

Harding, A., Gonder, U., Robinson, S. J., Crean, S., Singhrao, S. K., et al. (2017). Exploring the association between alzheimer's disease, oral health, microbial endocrinology and nutrition. *Front. Aging Neurosci.* 9, 398. doi: 10.3389/fnagi.2017.00398

Hill, T. C., Walsh, K. A., Harris, J. A., and Moffett, B. F. (2003). Using ecological diversity measures with bacterial communities. *FEMS Microbiol. Ecol.* 43 (1), 1–11. doi: 10.1111/j.1574-6941.2003.tb01040.x

Hou, H., Chen, Z., Tian, L., et al, Sun, Z. (2018). Leptotrichia trevisanii bacteremia in a woman with systemic lupus erythematosus receiving high-dose chemotherapy. *BMC Infect. Dis.* 18 (1), 661. doi: 10.1186/s12879-018-3495-9

Hudek Turkovic, A., Matovinovic, M., Zuna, K., Škara, L., Kazazić, S., Bačun-Družina, V., et al. (2022). Association of vitamins d, B9 and B12 with obesity-related diseases and oral microbiota composition in obese women in Croatia. *Food Technol. Biotechnol.* 60 (2), 135–144. doi: 10.17113/ftb.60.02.22.7478

Human Microbiome Project, C. (2012). Structure, function and diversity of the healthy human microbiome. *Nature* 486 (7402), 207–214. doi: 10.1038/nature11234

Kim, B. R., Shin, J., Guevarra, R., Lee, J. H., Kim, D. W., Seol, K. H., et al. (2017). Deciphering diversity indices for a better understanding of microbial communities. *J. Microbiol. Biotechnol.* 27 (12), 2089–2093. doi: 10.4014/jmb.1709.09027

Kozich, J. J., Westcott, S. L., Baxter, N. T., Highlander, S. K., and Schloss, P. D. (2013). Development of a dual-index sequencing strategy and curation pipeline for analyzing amplicon sequence data on the MiSeq illumina sequencing platform. *Appl. Environ. Microbiol.* 79 (17), 5112–5120. doi: 10.1128/AEM.01043-13

Kroese, J. M., Brandt, B. W., Buijs, M. J., Crielaard, W., Lobbezoo, F., Loos, B. G., et al. (2021). Differences in the oral microbiome in patients with early rheumatoid arthritis and individuals at risk of rheumatoid arthritis compared to healthy individuals. *Arthritis Rheumatol.* 73 (11), 1986–1993. doi: 10.1002/art.41780

Lin, W., Jiang, W., Hu, X., Gao, L., Ai, D., Pan, H., et al. (2018). Ecological shifts of supragingival microbiota in association with pregnancy. *Front. Cell Infect. Microbiol.* 8, 24. doi: 10.3389/fcimb.2018.00024

Lozupone, C. A., Hamady, M., Kelley, S. T., and Knight, R. (2007). Quantitative and qualitative beta diversity measures lead to different insights into factors that structure microbial communities. *Appl. Environ. Microbiol.* 73 (5), 1576–1585. doi: 10.1128/AEM.01996-06

Machado, F. C., Cesar, D. E., Assis, A. V., Diniz, C. G., and Ribeiro, R. A. (2012). Detection and enumeration of periodontopathogenic bacteria in subgingival biofilm of pregnant women. *Braz. Oral. Res.* 26 (5), 443–449. doi: 10.1590/S1806-83242012000500011

Matsushita, K., Hamaguchi, M., Hashimoto, M., Yamazaki, M., Yamazaki, T., Asai, K., et al. (2015). The novel association between red complex of oral microbe and body mass index in healthy Japanese: A population based cross-sectional study. *J. Clin. Biochem. Nutr.* 57 (2), 135–139. doi: 10.3164/jcbn.15-19

McIlvanna, E., Linden, G. J., Craig, S. G., Lundy, F. T., and James, J. A. (2021). *Fusobacterium nucleatum* and oral cancer: A critical review. *BMC Cancer* 21 (1), 1212. doi: 10.1186/s12885-021-08903-4

Mcinnes PCMA (2010). *Core microbiome sampling protocol a HMP protocol # 07–001* (Bethesda: NIH Manual of Procedures).

Mysak, J., Podzimek, S., Sommerova, P., Lyuya-Mi, Y., Bartova, J., Janatova, T., et al. (2014). *Porphyromonas gingivalis*: Major periodontopathic pathogen overview. *J. Immunol. Res.* 2014, 476068. doi: 10.1155/2014/476068

Peters, B. A., Wu, J., Pei, Z., Yang, L., Purdue, M. P., Freedman, N. D., et al. (2017). Oral microbiome composition reflects prospective risk for esophageal cancers. *Cancer Res.* 77 (23), 6777–6787. doi: 10.1158/0008-5472.CAN-17-1296

Pitts, N. B., Twetman, S., Fisher, J., and Marsh, P. D. (2021). Understanding dental caries as a non-communicable disease. *Br. Dent. J.* 231 (12), 749–753. doi: 10.1038/s41415-021-3775-4

Platzer, A., Polzin, J., Rembart, K., Han, P. P., Rauer, D., and Nussbaumer, T. (2018). BioSankey: Visualization of microbial communities over time. *J. Integr. Bioinform.* 15 (4), 20170063. doi: 10.1515/jib-2017-0063

Proal, A. D., Lindseth, I. A., and Marshall, T. G. (2017). Microbe-microbe and host-microbe interactions drive microbiome dysbiosis and inflammatory processes. *Discovery Med.* 23 (124), 51–60. Available at: https://www.discoverymedicine.com/Amy-D-Proal/2017/01/microbe-microbe-and-host-microbe-interactions-drive-microbiome-dysbiosis-and-inflammatory-processes/.

Read, E., Curtis M, A., and Neves, J. F. (2021). The role of oral bacteria in inflammatory bowel disease. *Nat. Rev. Gastroenterol. Hepatol.* 18 (10), 731–742. doi: 10.1038/s41575-021-00488-4

Rogers L, K., and Velten, M. (2011). Maternal inflammation, growth retardation, and preterm birth: Insights into adult cardiovascular disease. *Life Sci.* 89 (13-14), 417–421. doi: 10.1016/j.lfs.2011.07.017

Saadaoui, M., Singh, P., and Al Khodor, S. (2021). Oral microbiome and pregnancy: A bidirectional relationship. *J. Reprod. Immunol.* 145, 103293. doi: 10.1016/j.jri.2021.103293

Santonocito, S., Giudice, A., Polizzi, A., Troiano, G., Merlo, E. M., Sclafani, R., et al. (2022). A cross-talk between diet and the oral microbiome: Balance of nutrition on inflammation and immune system's response during periodontitis. *Nutrients* 14 (12), 2426. doi: 10.3390/nu14122426

Sedghi, L., DiMassa, V., Harrington, A., and Kapila, Y. L. (2021). The oral microbiome: Role of key organisms and complex networks in oral health and disease. *Periodontol. 2000* 87 (1), 107–131. doi: 10.1111/prd.12393

Segata, N., Izard, J., Waldron, L., Gevers, D., Miropolsky, L., Garrett, W. S., et al. (2011). Metagenomic biomarker discovery and explanation. *Genome Biol.* 12 (6), R60. doi: 10.1186/gb-2011-12-6-r60

Seifert, H. S. (2019). Location, location, location-commensalism, damage and evolution of the pathogenic neisseria. *J. Mol. Biol.* 431 (16), 3010–3014. doi: 10.1016/j.jmb.2019.04.007

Singhrao, S. K., Harding, A., Poole, S., Kesavalu, L., and Crean, S. (2015). *Porphyromonas gingivalis* periodontal infection and its putative links with alzheimer's disease. *Mediators Inflamm.* 2015, 137357. doi: 10.1155/2015/137357

Stasiewicz, M., and Karpiński, T. M. (2021). The oral microbiota and its role in carcinogenesis *Semin. Cancer Biol* 86 (Pt 3), 633–642. doi: 10.1016/j.semcancer.2021.11.002

Usui, M., Onizuka, S., Sato, T., Kokabu, S., Ariyoshi, W., and Nakashima, K. (2021). Mechanism of alveolar bone destruction in periodontitis - periodontal bacteria and inflammation. *Jpn. Dent. Sci. Rev.* 57, 201–208. doi: 10.1016/j.jdsr.2021.09.005

Vander Haar, E. L., Wu, G., Gyamfi-Bannerman, C., Thomas, C., Wapner, R. J., Reddy, U. M., et al. (2022). Microbial analysis of umbilical cord blood reveals novel pathogens associated with stillbirth and early preterm birth. *mBio* 13 (5), e0203622. doi: 10.1128/mbio.02036-22

Vornhagen, J., Quach, P., Boldenow, E., Merillat, S., Whidbey, C., Ngo, L. Y., et al. (2016). Bacterial hyaluronidase promotes ascending GBS infection and preterm birth. *mBio* 7 (3), e00781–e00716. doi: 10.1128/mBio.00781-16

Willis, J. R., and Gabaldón, T. (2020). The human oral microbiome in health and disease: From sequences to ecosystems. *Microorganisms* 8 (2), 308. doi: 10.3390/microorganisms8020308

World Health Organization (2013). *Oral health surveys: Basic methods. 5th edition* (Geneva: WHO), 125 p.

Wu, M., Chen, S. W., and Jiang, S. Y. (2015). Relationship between gingival inflammation and pregnancy. *Mediators Inflamm.* 2015, 623427. doi: 10.1155/2015/623427

Xu, B., and Han, Y. W. (2022). Oral bacteria, oral health, and adverse pregnancy outcomes. *Periodontol. 2000* 89 (1), 181–189. doi: 10.1111/prd.12436

Yang, I., Claussen, H., Arthur, R. A., Hertzberg, V. S., Geurs, N., and Corwin, E. J. (2022). Subgingival microbiome in pregnancy and a potential relationship to early term birth. *Front. Cell Infect. Microbiol.* 12, 873683. doi: 10.3389/fcimb.2022.873683

Ye, C., and Kapila, Y. (2021). Oral microbiome shifts during pregnancy and adverse pregnancy outcomes: Hormonal and immunologic changes at play. *Periodontol. 2000* 87 (1), 276–281. doi: 10.1111/prd.12386

Yu, T. C., Zhou Y, L., and Fang, J. Y. (2022). Oral pathogen in the pathogenesis of colorectal cancer. *J. Gastroenterol. Hepatol.* 37 (2), 273–279. doi: 10.1111/jgh.15743

Zhang, S., Huang, J., Wang, Q., You, M., and Xia, X. (2022). Changes in the host gut microbiota during parasitization by parasitic wasp cotesia vestalis. *Insects* 13 (9), 760. doi: 10.3390/insects13090760

Zhang, X., Wang, P., Ma, L., Guo, R., Zhang, Y., and Wang, P. (2021a). Differences in the oral and intestinal microbiotas in pregnant women varying in periodontitis and gestational diabetes mellitus conditions. *J. Oral. Microbiol.* 13 (1), 1883382. doi: 10.1080/20002297.2021.1883382

Zhang, X., Wang, M., Wang, X., Qu, H., Zhang, R., Gu, J., et al. (2021b). Relationship between periodontitis and microangiopathy in type 2 diabetes mellitus: A meta-analysis. *J. Periodontal. Res.* 56 (6), 1019–1027. doi: 10.1111/jre.12916

frontiers | Frontiers in Cellular and Infection Microbiology

TYPE Original Research
PUBLISHED 30 November 2022
DOI 10.3389/fcimb.2022.1013920

OPEN ACCESS

EDITED BY
Zuomin Wang,
Capital Medical University, China

REVIEWED BY
Zhengwei Huang,
Shanghai Jiao Tong University, China
Rui Ma,
Shanghai Jiao Tong University, China

*CORRESPONDENCE
Lei Cheng
chenglei@scu.edu.cn
Yue Ma
Gordonrozen@qq.com

†These authors have contributed equally to this work

SPECIALTY SECTION
This article was submitted to Extra-intestinal Microbiome, a section of the journal Frontiers in Cellular and Infection Microbiology

RECEIVED 08 August 2022
ACCEPTED 12 October 2022
PUBLISHED 30 November 2022

CITATION
Hao Y, Zeng Z, Peng X, Ai P, Han Q, Ren B, Li M, Wang H, Zhou X, Zhou X, Ma Y and Cheng L (2022) The human oral – nasopharynx microbiome as a risk screening tool for nasopharyngeal carcinoma. *Front. Cell. Infect. Microbiol.* 12:1013920. doi: 10.3389/fcimb.2022.1013920

The human oral – nasopharynx microbiome as a risk screening tool for nasopharyngeal carcinoma

Yu Hao[1,2†], Zhi Zeng[3†], Xian Peng[1], Ping Ai[4], Qi Han[1,5], Biao Ren[1], Mingyun Li[1], Haohao Wang[1,2], Xinxuan Zhou[1], Xuedong Zhou[1,2], Yue Ma[6*] and Lei Cheng[1,2*]

[1]State Key Laboratory of Oral Diseases & West China Hospital of Stomatology & National Clinical Research Center for Oral Diseases, Sichuan University, Chengdu, China, [2]Department of Operative Dentistry and Endodontics, West China School of Stomatology, Sichuan University, Chengdu, China, [3]Head & Neck Oncology Ward, Cancer Center, West China Hospital, Sichuan University, Chengdu, China, [4]Division of Radiotherapy, Cancer Center, West China Hospital, Sichuan University, Chengdu, China, [5]Department of Oral Pathology, West China School of Stomatology, Sichuan University, Chengdu, China, [6]West China School of Public Health and West China Fourth Hospital, Sichuan University, Chengdu, China

Nasopharyngeal carcinoma (NPC) is a common head and neck cancer with a poor prognosis. There is an urgent need to develop a simple and convenient screening tool for early detection and risk screening of NPC. 139 microbial samples were collected from 40 healthy people and 39 patients with nasopharyngeal biopsy. A total of 40 and 39 oral, eight and 27 nasal cavity, nine and 16 nasopharyngeal microbial samples were collected from the two sets of individuals. A risk screening tool for NPC was established by 16S rDNA sequencing and random forest. Patients with nasopharyngeal biopsy had significantly lower nasal cavity and nasopharynx microbial diversities than healthy people. The beta diversity of the oral microbiome was significantly different between the two groups. The NPC screening tools based on nasopharyngeal and oral microbiomes have 88% and 77.2% accuracies, respectively. The nasopharyngeal biopsy patients had significantly higher *Granulicatella* abundance in their oral cavity and lower *Pseudomonas* and *Acinetobacter* in the nasopharynx than healthy people. This study established microbiome-based non-invasive, simple, no radiation, and low-cost NPC screening tools. Individuals at a high risk of NPC should be advised to seek further examination, which might improve the early detection of NPC and save public health costs.

KEYWORDS

nasopharyngeal carcinoma, screening, microbiome, 16S rDNA sequencing, random forest

Introduction

Nasopharyngeal carcinoma (NPC) is an aggressive malignant tumor of the head and neck mucosal epithelium. In 2018, 129,100 new NPC cases were reported worldwide (Ferlay et al., 2019), with over 70% of the cases in Southeast Asia (Chen et al., 2019). Severe NPC symptoms include headache, nasal bleeding, nasal congestion, hearing loss, and neck mass. Given that these symptoms are unspecific, NPC misdiagnosis is a common phenomenon (Kamran et al., 2015). Consequently, 80% of clinically confirmed NPC patients have locally advanced or distant metastases, all with poor prognoses (Chan et al., 2017; Lee H. M. et al., 2019). The 5-year survival rate of stage I and IV NPC are 90% and 60%, respectively (Li et al., 2014). Early diagnosis and treatment are vital for a good NPC prognosis, underscoring the need for early screening of NPC (Lee A.W.M. et al., 2019).

Clinical NPC diagnosis involves biopsy and imaging examinations, including endoscopy, Magnetic Resonance Imaging (MRI), Computed Tomography (CT), and ultrasound. Nasopharyngeal endoscopy examines the lesion range, and a biopsy is taken using forceps. MRI, CT, and ultrasound show nasopharyngeal lesions, invasion, and metastasis (King et al., 2011; Gao et al., 2014). However, these methods are expensive, require experienced personnel and expose patients to ion radiation. Presently, conventional NPC diagnosis methods are inaccurate for early screening. Thus, there is an urgent need for non-invasive, simple, and low-cost NPC screening tools.

Numerous factors, including genetics, dietary habits of preserved food, and Epstein-Barr virus (EBV) infection, have been implicated in the development of NPC (Tsao et al., 2017; Lee H. M. et al., 2019). Persistent nasopharyngeal mucosal inflammation and certain medications increase the risk of NPC (Xiao et al., 2018; Zhang et al., 2019). Recently, there has been increasing interest in the association between the microbiome and NPC. A retrospective study showed that poor oral hygiene, including infrequent brushing and frequent dental caries, increases the risk of NPC (Turkoz, 2011; Liu et al., 2016). Another study showed that the relative abundance of *Firmicutes* and *Streptococcus* was lower in the saliva of NPC patients than in healthy controls (Xu et al., 2014). The cytolethal distending toxin of *Aggregatibacter actinomycetemcomitans*, oral pathogenic bacteria, reactivates EBV and triggers DNA destruction. Thus, co-infection with bacteria and viruses can cause EBV-induced epithelial malignancy, including NPC (Frisan et al., 2018). A case-control study of 499 NPC patients and 495 healthy controls found that oral microbiome richness was significantly low in NPC patients ($P < 0.001$). The study revealed *Granulicatella adiacens*, a possible disease-related species (Debelius et al., 2020). These case studies suggest an aberrant oral microbial composition in NPC patients. However, the NPC screening tools of the oral microbiome are lacking.

This study analyzed the microbiome of the oral and nasal cavities, and the nasopharynx from people with high NPC risk, requiring a nasopharyngeal biopsy and healthy controls. The NPC risk screening tool was established based on the16S rDNA sequencing and the random forest.

Materials and methods

Ethics statement and subjects

The experimental protocol of this study was approved by the ethics committee approved the (Approval number: WCHSIRB-D-2018-101). Previous studies (Xiao et al., 2018; Zhang et al., 2019) revealed that persistent nasopharyngeal mucosal inflammation increases the risk of NPC development, and a nasopharyngeal biopsy of such patients should be further analyzed for a definitive diagnosis. The inclusion criteria included: patients needing a nasopharyngeal biopsy and healthy people confirmed by nasopharyngeal fiberscope, aged 20-70 years old, and provided informed consent before sample collection.

The exclusion criteria were: antibiotics use within three months; a history of dental treatment within six months; less than 20 natural teeth; over six DMFT (decayed, missing, or filled teeth); severe oral disease (periodontal diseases, oral fungal infection, and oral cancer); pregnant or nursing women; a family history of cancer; and having smoked over 100 cigarettes in a lifetime (Yu et al., 2017).

Sample collection

As in a previous study (Hao et al., 2021), the participants included 40 healthy people and 39 patients with nasopharyngeal biopsy who were advised not to eat, drink, or chew gum 30 min before sampling. A 5 mL of saliva from each study participant was collected in a sterile centrifuge tube. After centrifugation (2600×g, 10min), the saliva was stored in a 2 mL cryogenic tube and immediately frozen at −80°C.

Nasopharyngeal microbiome were collected by nasopharyngeal swabs from nine healthy individuals and 17 patients with nasopharyngeal biopsies. The sterile nasopharyngeal swab was dipped in sterile saline and wrapped in a sterile infusion tube, passed through the nasal cavity into the nasopharynx. While in the nasopharynx, the swab was extended and rotated through 360° to dip in nasopharyngeal secretions. The swab was then withdrawn into the infusion tube, which was removed altogether. The swab tip was cut off with sterile scissors, stored in a cryogenic tube, and immediately frozen at −80°C. The microbiome of the nasal cavity was collected from eight healthy people and 27 patients with nasopharyngeal biopsy. Two swabs dipped in sterile saline were used to collect the microbiome in the left and right noses. The swabs

were rotated and wiped the anterior nostril mucosa. The swab tip was cut off with sterile scissors, stored in a cryogenic tube, and immediately frozen at −80°C (Luna et al., 2018).

Illumina MiSeq sequencing

The collected microbiome samples above were used for DNA extraction, amplification, and 16S rDNA sequencing (Wang et al., 2016; Yin et al., 2016). Microbial DNA was extracted using the E.Z.N.A.® soil DNA Kit (Omega Bio-Tek, USA) following the manufacturer's protocol. The V4-V5 target regions of the bacterial 16S rRNA gene were amplified *via* polymerase chain reaction (PCR) with barcoded primers 515 F (5′-GTGCCAGCMGCCGCGG-3′) and 907R (5′−CCGTCAA TTCMTTTRAGTTT-3′) (Wu et al., 2020).

Majorbio Bio-Pharm Technology Co., Ltd. (Shanghai, China) purified and pooled amplicons in equimolar amounts and sequenced paired-end (2 x 300bp) on the Illumina MiSeq platform (Illumina, CA, USA) following standard protocols. Raw reads were deposited to the National Center for Biotechnology Information(NCBI) Sequence Read Archive (SRA) database (Accession Number: PRJNA722880).

Processing of sequencing data

Majorbio Bio-pharm Technology Co., Ltd. quality-filtered raw FASTQ files using Trimmomatic software and merged files using the FLASH software following the standard criteria. Operational taxonomic units(OTUs) were clustered with a 97% similarity cutoff using UPARSE Version 7.1 (http://drive5.com/uparse/) with a novel 'greedy' algorithm that simultaneously performs chimera filtering and OTU clustering. The taxonomy of each 16S rRNA gene sequence was analyzed using the Ribosomal Database Project(RPD) Classifier algorithm (http://rdp.cme.msu.edu/) against the Silva database using a 70% confidence threshold (Cole et al., 2005; Dewhirst et al., 2010) (Table S4, Figure S3).

Statistical analysis

The states of nasopharynx were divided into healthy or tissue need biopsy according to the nasopharyngeal fiberscope. Then the nasopharyngeal biopsy group was further divided into cancer and inflammation groups based on pathological analysis (Table S3). Thus, the study participants were classified into healthy, inflammation, and cancer groups according to the states of the nasopharynx. The healthy and inflammation groups were integrated into non-cancer group, while the inflammation and cancer groups were integrated into the nasopharyngeal biopsy group.

The microbiome composition, alpha and beta diversity based on the genus level was established using the mother software (version.1.30.2.). Shannon indices were tested using the Wilcoxon rank-sum test, and the Principal Coordinates Analysis(PCoA) was performed based on the Bray_curtis distance methods. The differences among groups were determined using Analysis of Similarity (ANOSIM). Differences with $P<0.05$ were considered statistically significant. The R>0 was considered that there is a significant difference between the two sampling units.

Random Forest is a robust machine learning algorithm by combining the output of multiple decision trees to obtain a single outcome that could handle both classification and regression problems (Breiman, 2001). The random forest classifier and screened model establishment based on the high dimensional 16S rDNA sequencing data. One to three nasal and nasopharynx oral samples were used to establish the screening model considering the microbial community diversity from the different sample sources. The error rates of the training and verification sets were calculated. The optimal n_{tree}value for establishing the random forest models with low and stable error rates were determined using multiple iterations. Repeated cross-validations with 80% training and 20% testing sets evaluated the model external accuracy. The weight, known as variable importance, was originally defined in the random forest using a measure involving surrogate variables, and it was calculated by randomly permuting a variable (Ishwaran, 2007). The weights of characteristic variables were calculated to correlate genus and outcomes according to the established optimal models.

Results

Characteristics and exploratory analysis of microbiome

The characteristics analysis was performed among the three microbiome habitats (oral, nasal and nasopharyngeal). The Shannon index of alpha diversity (Figure S1A) showed that the oral microbiome was the most diverse ($P<0.001$). PCoA analysis (Figure S1B) showed that the beta diversity of the oral, nasal, and nasopharyngeal microbiome was significantly different ($P<0.05$, R=0.9627). The Venn graph (Figure S1C) of species composition illustrated 599 common OTUs in the three groups, accounting for 25.72-37.94% of the total microbiome. The microbial community composition in the nasal cavity and nasopharynx was similar between the two groups. However, the oral microbial composition was different between the two groups (Figure S1D).

The Figure 1 shows the alpha diversity between healthy and biopsy groups. The oral microbiome of patients with nasopharyngeal biopsy and healthy counterparts were not

significantly different (Figure 1A). As for nasal and nasopharyngeal microbiome (Figures 1B, C), the Shannon indices of patients with nasopharyngeal biopsy were significantly lower than healthy counterparts (P<0.05, P<0.01).

The PCoA based on Bray_curtis distance revealed that there was a significant difference in the beta diversity of oral microbiome between nasopharyngeal biopsy patients and healthy counterparts (R>0; P<0.05) (Figure 2A). However, there was no significant difference in the composition of the nasal cavity and nasopharyngeal microbiome between nasopharyngeal biopsy patients and healthy counterparts (Figures 2B, C).

The similarity of microbial composition among groups was determined using ANOSIM (Table 1). The oral microbiome showed a significant difference between the healthy and the nasopharyngeal biopsy groups (R>0; P<0.05). The diversity of the nasopharyngeal microbiome was significantly different of the healthy vs. cancer, and healthy vs. inflammation groups (R>0; P<0.05). However, the microbial composition in the oral, nasal cavity and nasopharynx was not significantly different between the inflammation and the cancer groups (P>0.05).

Figure 3A shows the species differences in the oral microbiome on genus level. The relative abundance of *Granulicatella* genus was higher in the patients with nasopharyngeal biopsy than in healthy group (P < 0.001), but the *Porphyromonas* and *Haemophilus* were relatively less abundant (P < 0.05). There was no significant difference in the dominant microbial species in the nasal cavity between nasopharyngeal biopsy group and healthy counterparts (Figure 3B). Considering the nasopharynx, the relative abundances of *Pseudomonas* and *Acinetobacter* in the healthy counterparts were significantly higher than in patients with nasopharyngeal biopsy (P < 0.001, Figure 3C).

NPC risk screening model based on oral or nasopharyngeal microbiome

The NPC risk screening models were established *via* random forests using the microbial sequencing data. The accuracy of the models are shown in Table 2. The accuracy of models based on different microbial combinations were approximately 80%. The accuracy of the risk screening model based on the microbiome from one habitat (the oral microbiome) was 77.22%. The Area Under Curve(AUC), sensitivity, and specificity of the model were 80.96%, 0.7692, and 0.775, respectively. For the risk screening model based on the nasopharyngeal microbiome, the accuracy was 88%. The AUC, sensitivity, and specificity of the model were 83.33%, 0.875, and 0.8889, respectively.

The external performance of the model was evaluated using repeated cross-validations. For each model, 80% random samples were used for model training and 20% samples for validating the external test sets. The average external accuracy of all random forests provided an estimate of the model applied in external populations. The average accuracy of the model was stable in a 5000 times validation. Based on the oral microbiome, the average accuracy rate of the screening model was 75.08%, and the median accuracy rate was 75%. The nasopharyngeal microbiome had an 85.22% average accuracy rate of the screening model and an 80% median accuracy rate.

The weights of characteristic variables were calculated following the above-built models. Considering the oral microbial model, the most important genera in weight value were *Graulicatella*, *Prevotella*, *Rhodococcus*, and *Haemophilus* (Table S1). *Granulicatella* ranked first and fourth, suggesting that this genus is a key biomarker of the oral microbiome. For the nasopharyngeal microbial model, *Candidatus solibacter*, *Pseudomonas*, *Bradyrhizobium*, and *Reyranella* were the most

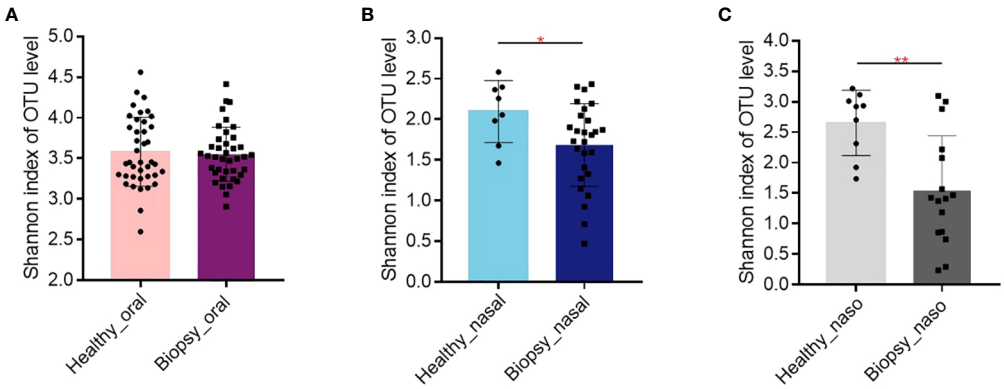

FIGURE 1
Alpha diversity of Shannon index. **(A)** The Shannon index of oral microbiome between patients with nasopharyngeal biopsy and healthy counterparts. **(B)** The Shannon index of nasal microbiome between patients with nasopharyngeal biopsy and healthy counterparts. **(C)** The Shannon index of nasopharyngeal microbiome between patients with nasopharyngeal biopsy and healthy counterparts. Oral represents oral microbiome, nasal represents nasal microbiome, naso represents nasopharyngeal microbiome. "*" represented P<0.05, "**" represented P<0.01.

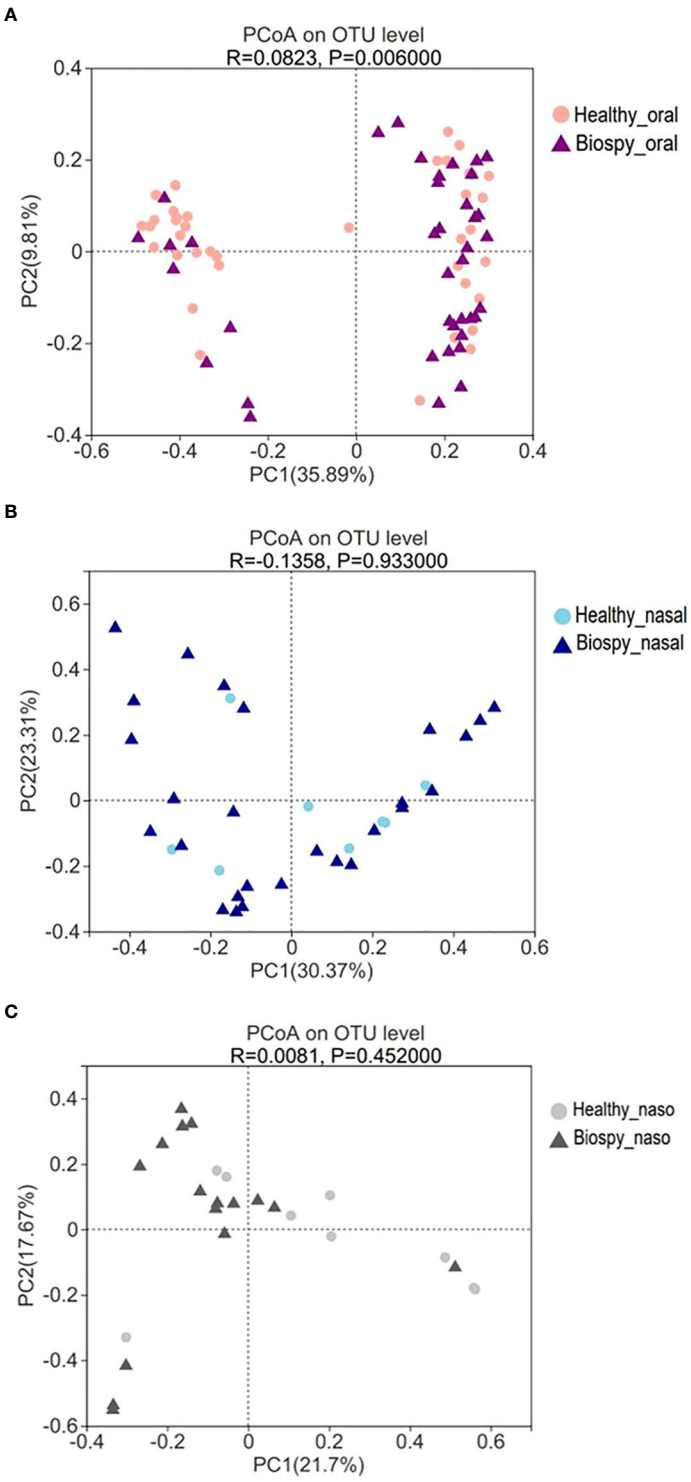

FIGURE 2
Beta diversity of PCoA analysis. **(A)** The PCoA analysis of oral microbiome between patients with nasopharyngeal biopsy and healthy counterparts. **(B)** The PCoA analysis of nasal microbiome between patients with nasopharyngeal biopsy and healthy counterparts. **(C)** The PCoA analysis of nasopharyngeal microbiome between patients with nasopharyngeal biopsy and healthy counterparts. Oral represents oral microbiome, nasal represents nasal microbiome, naso represents nasopharyngeal microbiome.

TABLE 1 Analysis of similarity among groups.

Microbiome	Groups	R value	P value
Oral	Hea vs. Bio	0.0823	0.006
	Can vs. non-Can	-0.0168	0.732
	Hea vs. Can	0.0015	0.405
	Hea vs. Inf	-0.0083	0.481
	Inf vs. Can	-0.0456	0.7
Nasal Cavity	Hea vs. Bio	-0.1358	0.933
	Can vs. non-Can	0.0767	0.066
	Hea vs. Can	-0.0612	0.705
	Hea vs. Inf	-0.077	0.839
	Inf vs. Can	0.0369	0.211
Nasopharynx	Hea vs. Bio	0.0081	0.452
	Can vs. non-Can	0.1041	0.131
	Hea vs. Can	0.1877	0.029
	Hea vs. Inf	0.2832	0.003
	Inf vs. Can	0.0611	0.239

Hea represented the healthy group, Bio represented nasopharyngeal biopsy group, Can represented the cancer group, Non-can represented the non-cancer group, Inf represented the inflammation group.

important genera, ranked by the front of weight value (Table S2). Genus *Pseudomonas* ranked the second, third, and seventh, suggesting it is a key biomarker of the nasopharyngeal microbiome.

Discussion

Many recent studies revealed the close relationship between the microbiome and neoplasm (Flemer et al., 2018; Yang et al., 2018; Li et al., 2020). In some studies, the specific microbiome composition was used as a biomarker to evaluate the risk of cancers and establishing diagnostic models (Lim et al., 2018; Ren et al., 2018; Sze and Schloss, 2018; Zhou et al., 2021). The microbiome capability to serve as disease biomarkers varied with the specificity of the microbial composition at the disease and anatomical site (Nejman et al., 2020). This study established for the first time the NPC risk screening models using the oral and nasopharyngeal microbiomes. The accuracy rates of nasopharyngeal and oral microbiomes were 88% and 77.2%, respectively. This model can preliminarily screen the NPC high-risk group through a non-invasive microbial sample detection. For the high-risk group with detected NPC, invasive nasopharyngeal fiberscope and biopsy can be applied for further examination, a conducive strategy for early NPC detection.

The 16S rDNA sequencing showed that the alpha diversity of the oral microbiome displayed no significant difference between healthy and biopsy samples (Figure 1A), whereas the beta diversity was significantly different (Figure 2A). The Shannon index of oral microbiome was differed from that of previous study, which might due to different clustering methods and grouping (Debelius et al., 2020). The different beta-diversity suggested that the development of NPC shaped different microbiome in the oral cavity. Besides, there was no significant difference in the oral, nasal cavity, and nasopharynx microbial composition betwwen the inflammation and cancer groups (Table 1, $P>0.05$). The dominant species of the inflammation group were more similar to cancer than the healthy group (Figure S2). Studies revealed that persistent nasopharyngeal mucosal inflammation increases the risk of NPC (Xiao et al., 2018; Zhang et al., 2019). Inflammation produces reactive oxygen and nitrogen, which damage DNA and cause stem cell mutations, damage biological macromolecules, and induce cell dysfunction, promoting NPC occurrence and development (Murata, 2018). Thus, the inflammation group was a likely NPC high-risk group that needed further examination.

Traditional analysis methods for establishing the risk screening tools based on the microbial community suffer numerous limitations and challenges for the multi-dimensionally complex microbial sequencing data (Quince et al., 2009; Hu et al., 2013). Random forests are effective tool in prediction which can effectively analyze large and noisy datasets with small samples and build classification models (Caruana and Niculescu-Mizil, 2006;Teng et al., 2015; Zhu et al., 2017). Random forests models do not overfit because of the law of large numbers. Following the right kind of randomness makes them accurate classifiers. (Breiman, 2001; Doupe et al., 2019). The performances of random forests vary among diseases (Teng et al., 2015; Ren et al., 2018; Zhou et al., 2021). This study established the NPC risk screening tools using a non-invasive approach based on microbial sample detection for the first time.

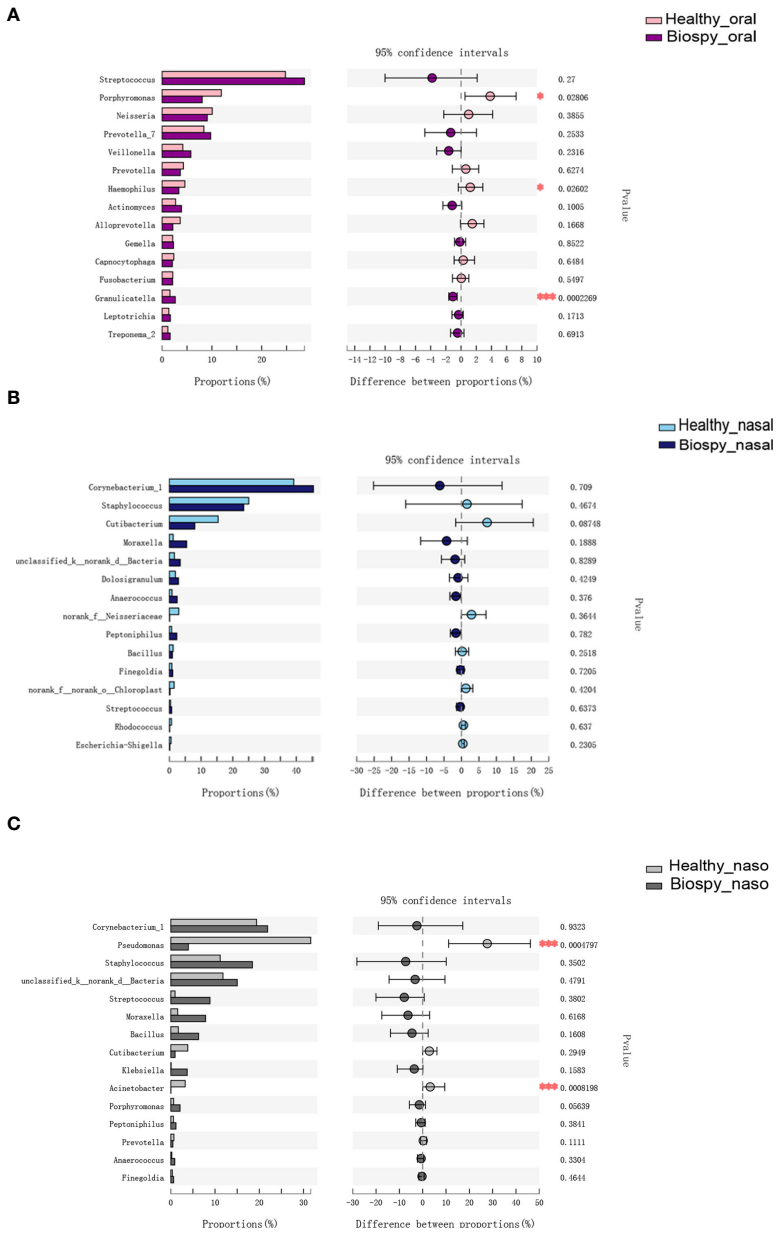

FIGURE 3
Genus level analysis of species differences. **(A)** Differences in the dominant species composition of oral microbiome between patients with nasopharyngeal biopsy and healthy counterparts. **(B)** Differences in the dominant species composition of nasal cavity microbiome between patients with nasopharyngeal biopsy and healthy counterparts. **(C)** Differences in the dominant species composition of nasopharyngeal microbiome between patients with nasopharyngeal biopsy and healthy counterparts. Oral represents oral microbiome, nasal represents nasal microbiome, naso represents nasopharyngeal microbiome. "*" represented P<0.05, "***" represented P<0.001.

Risk screening tools based on different sample sources showed different performances (Table 2). The oral or nasopharyngeal microbiome showed good screening capability with balanced sensitivity and specificity based on the microbiome from one habitat. The oral microbiome tool identified approximately 77% of the NPC high-risk population that needed further examination. The nasopharyngeal microbiome tool identified approximately 88% of the NPC high-risk population requiring further examination. Although the specificity of the EBV serology test was 97.12%, which is very high compared with the commonly used screening tool, its positive predictive value was only 4.41%, even in the high prevalence areas (Li et al., 2018). The positive predictive value of the microbiome-based screening tools of the oral and

TABLE 2 Accuracy rates of NPC risk screening models.

Microbial Samples	Accuracy rate	AUC	Sensitivity	Specificity
139 samples (oral+nasal+nasopharyngeal)	79.86%	0.85	0.8537	0.7193
114 samples (oral+nasal)	78.95%	0.82	0.8636	0.6875
104 samples (oral+nasopharyngeal)	78.85%	0.85	0.7818	0.7959
60 samples (nasal+nasopharyngeal)	83.33%	0.83	0.9535	0.5294
79 samples (oral)	77.22%	0.81	0.7692	0.775
35 samples (nasal)	82.86%	0.66	1	0.25
25 samples (nasopharyngeal)	88%	0.83	0.875	0.8889

nasopharyngeal microbiome was 76.9% and 93.3% respectively. The highest sensitivity with a 0% false-negative rate was for the nasal microbiome, conducive for initial NPC screening to avoid missed diagnosis. Similarly, screening tools based on the combination of nasal and other habitats showed higher sensitivities. Meanwhile, higher specificities were registered, and more than half of patients were misdiagnosed. A previous study (Zhou et al., 2021) revealed that more samples improve the performance of the screening tools, especially the nasopharyngeal samples.

Following the weight values order of characteristic variables, the id ranked first, suggesting that the microbiome composition varied among individuals (Zhu et al., 2020). Besides, the weights of characteristic variables provided potential NPC biomarkers. In the oral microbial model, the genus *Granulicatella* ranked first and fourth (Table S1), showing higher relative abundance ($P < 0.001$) in the oral habitat of patients with nasopharyngeal biopsy, consistent with Debelius et al. findings, which suggested that the oral *Granulicatella adiacens* variant from an individual was significantly associated with microbial community structure and may be a way by which NPC status shaped the oral microbiome. (Debelius et al., 2020). The oral microbiome produced carcinogenic metabolites such as nitrosamines. *Granulicatella adiacens* mentions genes related to nitrate and nitrite reduction (Hyde et al., 2014). Carcinogens such as nitrosamines, produced by chemical reactions of nitrates and nitrites, can initiate and stimulate cancer progression through various mechanism including inflammation, DNA damage, oxidative stress, cytotoxicity, and subsequent regenerative proliferation *via* apoptosis (Song et al., 2015; Fishbein et al., 2021).

In the nasopharyngeal microbial model, genus *Pseudomonas* ranked the second, third and seventh among the weight values order (Table S2). The relative abundance of *Pseudomonas* and *Acinetobacter* significantly decreased in the patients with nasopharyngeal biopsy ($P < 0.001$, Figure 3C). Similar microbial changes have been observed in the gut microbiome of patients with colorectal cancer (Yang et al., 2019). *Acinetobacter* and *Pseudomonas* are opportunistic pathogens associated with nosocomial infection (Mwangi et al., 2019). However, the abundance of *Pseudomonas* and *Acinetobacter* was significantly low in the NPC high-risk group. It was illustrated that *Acinetobacter* species play a significant immunomodulatory and anti-inflammatory role in the skin microbiome (Fyhrquist et al., 2014). The high cytotoxic potential of *Pseudomonas* exotoxin A (PE) can generate anti-tumor immunotoxins for targeting tumor-associated antigens (Wolf and Elsasser-Beile, 2009). The *Pseudomonas aeruginosa* exopolysaccharides demonstrated anti-tumor activity against HT-29 colorectal cancer cells (Tahmourespour et al., 2020), while *Pseudomonas aeruginosa* L-asparaginase showed strong anti-tumor activity against HeLa cells (Fatima et al., 2019). Besides, *Pseudomonas fluorescens* lectin (PFL) inhibited neovascularization in a dose-dependent manner and downregulated the integrin and epidermal growth factor receptor, inhibiting *in vitro* and *in vivo* tumor growth (Sato et al., 2016; Sato et al., 2019). Altogether, the abovementioned potential biomarkers provide the preliminary basis for further studying the NPC-microbiome relationship.

The nasopharynx has a higher proportion of potentially pathogenic microorganisms than the nasal cavity (De Boeck et al., 2017). The nasopharyngeal microbiome was *in situ* of NPC, from which the model accuracy reached 88%. Although the nasopharyngeal microbiome sampling causes discomfort, the recent popularity of COVID-19 detection using the nasopharyngeal swab (Seo et al., 2020) has improved sampling acceptability. Thus, the nasopharyngeal microbiome can be used for NPC risk screening.

Saliva can be collected non-invasively and easily. The inorganic components, antioxidants, hormones, antibodies, and antigens in the saliva are biomarkers for diagnosing various oral and systemic diseases (Ngamchuea et al., 2017; Gerner et al., 2019). Specific microbiome changes in saliva are potential diagnostic biomarkers for head and neck cancers, including oral and hypopharyngeal cancers (Lim et al., 2018; Panda et al., 2020). Additionally, the oral microbiome predicts early childhood caries with 81% accuracy (Teng et al., 2015) and also predicts the oral mucositis progression after NPC radiotherapy (Zhu et al., 2017). In this study, the oral microbiome accuracy rate for NPC risk screening reached

77.2%. There is need to establish a non-invasive and convenient oral microbial sampling model to screen various diseases in a large population simultaneously. Therefore, this model has a high prospect of clinical application and could be applied in other regions with high disease incidence.

Conclusion

This study established a non-invasive and low-cost NPC risk screening model based on the oral and nasopharyngeal microbiome. The present study demonstrated characteristic microbial diversities varied from different nasopharynx status in the oral and nasopharyngeal microbiome. Future studies with a larger cohort from the different regions are needed to validate and promote the efficacy of oral microbiome-based NPC screening. Generally, we developed an accurate model with specific microbial markers for early screening of the risk of NPC, which guides further confirmatory examination to achieve early diagnosis and early therapy for NPC.

Data availability statement

The datasets presented in this study can be found in online repositories. The names of the repository/repositories and accession number(s) can be found below: https://www.ncbi.nlm.nih.gov/, PRJNA722880.

Ethics statement

The studies involving human participants were reviewed and approved by the institutional review board of the West China Hospital Stomatology of Sichuan University (Approval number: WCHSIRB-D-2018-101). The patients/participants provided their written informed consent to participate in this study.

Author contributions

YH: Validation, methodology, data curation, writing— original draft, and writing— review and editing. ZZ: Methodology, data curation, and writing— original draft. XP: Methodology, data curation. PA: Methodology and data curation. QH: Methodology and data curation. BR: Supervision. ML: Supervision. HW: Supervision. XXZ: Formal analysis and supervision. XDZ: Conceptualization, methodology. YM: Conceptualization, methodology, formal analysis, writing—review and editing. LC: Conceptualization, methodology, writing— review and editing, and funding acquisition. All authors contributed to the article and approved the submitted version.

Funding

This study was supported by the National Natural Science Foundation of China, (81870759, 82071106, LC), Innovative Research Team Program of Sichuan Province (LC), Research Funding from West China School/Hospital of Stomatology Sichuan University RCDWJS2021-19.

Acknowledgments

Thanks to all the volunteers who participated in this experiment. Thanks to the doctors and technologists from the Department of Otolaryngology-Head and Neck Surgery of West China Hospital of Sichuan University for their professional support.

Conflict of interest

The authors declare that the research was conducted in the absence of any commercial or financial relationships that could be construed as a potential conflict of interest.

Publisher's note

All claims expressed in this article are solely those of the authors and do not necessarily represent those of their affiliated organizations, or those of the publisher, the editors and the reviewers. Any product that may be evaluated in this article, or claim that may be made by its manufacturer, is not guaranteed or endorsed by the publisher.

Supplementary material

The Supplementary Material for this article can be found online at: https://www.frontiersin.org/articles/10.3389/fcimb.2022.1013920/full#supplementary-material

SUPPLEMENTARY TABLE 1
Weight values order of characteristic variables in oral microbiome.

SUPPLEMENTARY TABLE 2
Weight values order of characteristic variables in nasopharyngeal microbiome.

SUPPLEMENTARY TABLE 3
The samples information of each group of subjects.

SUPPLEMENTARY TABLE 4
The Sequencing information statistics.

SUPPLEMENTARY FIGURE 1
The diversities of oral, nasal and nasopharyngeal microbiome. **(A)** Shannon index on OTU level of oral, nasal and nasopharyngeal

microbiome. **(B)** Venn graph of oral, nasal and nasopharyngeal microbiome. **(C)** PCoA based on bray_curtis distance of oral, nasal and nasopharyngeal microbiome. **(D)** Community barplot analysis on genus level of oral, nasal and nasopharyngeal microbiome. KQ represents oral microbiome, BQ represents nasal microbiome, BY represents nasopharyngeal microbiome.

SUPPLEMENTARY FIGURE 2

Genus level analysis of species differences. **(A)** Differences in the dominant species composition of oral microbiome among cancer group, inflammation group and healthy counterparts. **(B)** Differences in the dominant species composition of nasal cavity microbiome among cancer group, inflammation group and healthy counterparts. **(C)** Differences in the dominant species composition of nasopharyngeal microbiome among cancer group, inflammation group and healthy counterparts. oral represents oral microbiome, nasal represents nasal microbiome, naso represents nasopharyngeal microbiome.

SUPPLEMENTARY FIGURE 3

The Rarefaction Curve based on Shannon indexes.

References

Breiman, L. (2001). Random forests. *Mach. Learn.* 45, 5–32. doi: 10.1023/A:1010933404324

Caruana, R., and Niculescu-Mizil, A. (2006). An empirical comparison of supervised learning algorithms. *Proc. 23rd. Int. Conf. Mach. Learn. C.*, 161–168. doi: 10.1145/1143844.1143865

Chan, K. C. A., Woo, J. K. S., King, A., Zee, B. C. Y., Lam, W. K. J., Chan, S. L., et al. (2017). Analysis of plasma Epstein-Barr virus DNA to screen for nasopharyngeal cancer. *N. Engl. J. Med.* 377, 513–522. doi: 10.1056/NEJMoa1701717

Chen, Y. P., Chan, A. T. C., Le, Q. T., Blanchard, P., Sun, Y., and Jun Ma, M. (2019). Nasopharyngeal carcinoma. *Lancet* 394, 64–80. doi: 10.1016/S0140-6736(19)30956-0

Cole, J. R., Chai, B., Farris, R. J., Wang, Q., Kulam, S. A., Mcgarrell, D. M., et al. (2005). The ribosomal database project (RDP-II): sequences and tools for high-throughput rRNA analysis. *Nucleic Acids Res.* 33, D294–D296. doi: 10.1093/nar/gki038

Debelius, J. W., Huang, T., Cai, Y., Ploner, A., Barrett, D., Zhou, X., et al. (2020). Subspecies niche speacialization in the oral microbiome is associated with nasopharyngeal carcinoma risk. *mSystems* 5, e00065–e00020. doi: 10.1128/mSystems.00065-20

De Boeck, I., Wittouck, S., Wuyts, S., Oerlemans, E. F. M., Van Den Broek, M. F. L., Vandenheuvel, D., et al. (2017). Comparing the healthy nose and nasopharynx microbiota reveals continuity as well as niche-specificity. *Front. Microbiol.* 29, 2372. doi: 10.3389/fmicb.2017.02372

Dewhirst, F. E., Chen, T., Izard, J., Paster, B. J., Tanner, A. C., Yu, W. H., et al. (2010). The human oral microbiome. *J. Bacteriol.* 192, 5002–5017. doi: 10.1128/JB.00542-10

Doupe, P., Faghmous, J., and Basu, S. (2019). Machine learning for health services researchers. *Value. Health* 22, 808–815. doi: 10.1016/j.jval.2019.02.012

Fatima, N., Khan, Mm, and Ia, K. (2019). L-asparaginase produced from soil isolates of pseudomonas aeruginosa shows potent anti-cancer activity on HeLa cells. *Saudi. J. Biol. Sci.* 26, 1146–1153. doi: 10.1016/j.sjbs.2019.05.001

Ferlay, J., Colombet, M., Soerjomataram, I., Mathers, C., Parkin, D. M., Piñeros, M., et al. (2019). Estimating the global cancer incidence and mortality in 2018: GLOBOCAN sources and methods. *Int. J. Cancer* 144, 1941–1953. doi: 10.1002/ijc.31937

Fishbein, A., Hammock, B. D., Serhan, C. N., and Panigrahy, D. (2021). Carcinogenesis: Failure of resolution of inflammation? *Pharmacol. Ther.* 218, 107670. doi: 10.1016/j.pharmthera.2020.107670

Flemer, B., Warren, Rd, Barrett, Mp, Cisek, K., Das, A., Jeffery, Ib, et al. (2018). The oral microbiota in colorectal cancer is distinctive and predictive. *Gut* 67, 1454–1463. doi: 10.1136/gutjnl-2017-314814

Frisan, T., Nagy, N., Chioureas, D., Terol, M., Grasso, F., and Mg, M. (2018). A bacterial genotoxin causes virus reactivation and genomic instability in Epstein-Barr virus infected epithelial cells pointing to a role of co-infection in viral oncogenesis. *Int. J. Cancer* 144, 98–109. doi: 10.1002/ijc.31652

Fyhrquist, N., Ruokolainen, L., Suomalainen, A., Lehtimaki, S., Veckman, V., Vendelin, J., et al. (2014). Acinetobacter species in the skin microbiota protect against allergic sensitization and inflammation. *J. Allergy Clin. Immunol.* 134, 1301–1309.e1311. doi: 10.1016/j.jaci.2014.07.059

Gao, Y., Liu, Jj, Zhu, Sy, and Yi, X. (2014). The diagnostic accuracy of ultrasonography versus endoscopy for primary nasopharyngeal carcinoma. *PloS One* 9, e90412. doi: 10.1371/journal.pone.0090412

Gerner, C., Costigliola, V., and Golubnitschaja, O. (2019). Multiomic patterns in body fluids: Technological challenge with a great potential to implement the advanced paradigm of 3p medicine. *Mass. Spectrom. Rev.* 39 (5-6), 442-451. doi: 10.1002/mas.21612

Hao, Y., Tang, C., Du, Q., Zhou, X., Peng, X., and L, C. (2021). Comparative analysis of oral microbiome from zang and han populations living at different altitudes. *Arch. Oral. Biol.* 121, 104986. doi: 10.1016/j.archoralbio.2020.104986

Hu, Y. J., Wang, Q., Jiang, Y. T., Ma, R., Xia, W. W., Tang, Z. S., et al. (2013). Characterization of oral bacterial diversity of irradiated patients by high-throughput sequencing. *Int. J. Oral. Sci.* 5, 21–25. doi: 10.1038/ijos.2013.15

Hyde, E. R., Andrade, F., Vaksman, Z., Parthasarathy, K., Jiang, H., Parthasarathy, D. K., et al. (2014). Metagenomic analysis of nitrate-reducing bacteria in the oral cavity: implications for nitric oxide homeostasis. *PloS One* 9, e88645. doi: 10.1371/journal.pone.0088645

Ishwaran, H. (2007). Variable importance in binary regression trees and forests. *Electronic. J. Stat* 1, 519–537. doi: 10.1214/07-EJS039

Kamran, S. C., Riaz, N., and N, L. (2015). Nasopharyngeal carcinoma. *Surg. Oncol. Clin. N. Am.* 24, 547–561. doi: 10.1016/j.soc.2015.03.008

King, A. D., Vlantis, A. C., Bhatia, K. S., Zee, B. C., Woo, J. K., Tse, G. M., et al. (2011). Primary nasopharyngeal carcinoma diagnostic accuracy of MR imaging versus that of endoscopyand endoscopic biopsy. *Radiology* 258, 531–537. doi: 10.1148/radiol.10101241

Lee, A. W. M., Ng, W. T., Chan, J. Y. W., Corry, J., Mäkitie, A., Mendenhall, W. M., et al. (2019). Management of locally recurrent nasopharyngeal carcinoma. *Cancer Treat Rev.* 79, 101890. doi: 10.1016/j.ctrv.2019.101890

Lee, H. M., Okuda, Ks, González, Fe, and Patel, V. (2019). Current perspectives on nasopharyngeal carcinoma. *Adv. Exp. Med. Biol.* 1164, 11–34. doi: 10.1007/978-3-030-22254-3_2

Li, T., Guo, X., Ji, M., Li, F., Wang, H., Cheng, W., et al. (2018). Establishment and validation of a two-step screening scheme for improved performance of serological screening of nasopharyngeal carcinoma. *Cancer Med.* 7, 1458–1467. doi: 10.1002/cam4.1345

Li, Q., Hu, Y., Zhou, X., Liu, S., Han, Q., and Cheng, L. (2020). Role of oral bacteria in the development of oral squamous cell carcinoma. *Cancers (Basel).* 12, 2797-2814. doi: 10.3390/cancers12102797

Lim, Y., Fukuma, N., Totsika, M., Kenny, L., Morrison, M., and Punyadeera, C. (2018). The performance of an oral microbiome biomarker panel in predicting oral cavity and oropharyngeal cancers. *Front. Cell Infect. Microbiol.* 8, 267. doi: 10.3389/fcimb.2018.00267

Liu, Z., Chang, E. T., Liu, Q., Cai, Y., Zhang, Z., Chen, G., et al. (2016). Oral hygiene and risk of nasopharyngeal carcinoma-a population-based case-control study in China. *Cancer Epidemiol. Biomarkers Prev.* 25, 1201–1207. doi: 10.1158/1055-9965.EPI-16-0149

Li, J., Zou, X., Wu, Y. L., Guo, J. C., Yun, J. P., Xu, M., et al. (2014). A comparison between the sixth and seventh editions of the UICC/AJCC staging system for nasopharyngeal carcinoma in a Chinese cohort. *PloS One* 9, e116261. doi: 10.1371/journal.pone.0116261

Luna, P. N., Hasegawa, K., Ajami, N. J., Espinola, J. A., Henke, D. M., Petrosino, J. F., et al. (2018). The association between anterior nares and nasopharyngeal microbiota in infants hospitalized for bronchiolitis. *Microbiome* 6, 2. doi: 10.1186/s40168-017-0385-0

Murata, M. (2018). Inflammation and cancer. *Environ. Health Prev. Med.* 23, 50. doi: 10.1186/s12199-018-0740-1

Mwangi, J., Yin, Y., Wang, G., Yang, M., Li, Y., Zhang, Z., et al. (2019) The antimicrobial peptide ZY4 combats multidrug-resistant pseudomonas aeruginosa and acinetobacter baumannii infection. *Proc. Natl. Acad. Sci. U. S. A.* 116 (52), 26516-26522. doi: 10.1073/pnas.1909585117

Nejman, D., Livyatan, I., Fuks, G., Gavert, N., Zwang, Y., Geller, Lt, et al. (2020). The human tumor microbiome is composed of tumor type–specific intracellular bacteria. *Science* 368, 973-980. doi: 10.1126/science.aay9189

Ngamchuea, K., Chaisiwamongkhol, K., Batchelor-Mcauley, C., and Compton, R. G. (2017). Chemical analysis in saliva and the search for salivary biomarkers - a tutorial review. *Analyst* 143, 81–99. doi: 10.1039/C7AN01571B

Panda, M., Rai, A. K., Rahman, T., Das, A., Das, R., Sarma, A., et al. (2020). Alterations of salivary microbial community associated with oropharyngeal and hypopharyngeal squamous cell carcinoma patients. *Arch. Microbiol.* 202, 785–805. doi: 10.1007/s00203-019-01790-1

Quince, C., Lanzen, A., Curtis, T. P., Davenport, R. J., Hall, N., Head, I. M., et al. (2009). Accurate determination of microbial diversity from 454 pyrosequencing data. *Nat. Methods* 6, 639–641. doi: 10.1038/nmeth.1361

Ren, Z., Li, A., Jiang, J., Zhou, L., Yu, Z., Lu, H., et al. (2018). Gut microbiome analysis as a tool towards targeted non-invasive biomarkers for early hepatocellular carcinoma. *Gut* 68, 1014–1023. doi: 10.1136/gutjnl-2017-315084

Sato, Y., Kubo, T., Morimoto, K., Yanagihara, K., and Seyama, T. (2016). High mannose-binding pseudomonas fluorescens lectin (PFL) downregulates cell surface integrin/EGFR and induces autophagy in gastric cancer cells. *BMC Cancer* 16, 63. doi: 10.1186/s12885-016-2099-2

Sato, Y., Matsubara, K., Kubo, T., Sunayama, H., Hatori, Y., Morimoto, K., et al. (2019). High mannose binding lectin (PFL) from pseudomonas fluorescens down-regulates cancer-associated integrins and immune checkpoint ligand B7-H4. *Cancers (Basel).* 11, 604. doi: 10.3390/cancers11050604

Seo, G., Lee, G., Kim, M. J., Baek, S.-H., Choi, M., Ku, K. B., et al. (2020). Rapid detection of COVID-19 causative virus (SARS-CoV-2) in human nasopharyngeal swab specimens using field-effect transistor-based biosensor. *ACS Nano.* 14, 5135–5142. doi: 10.1021/acsnano.0c02823

Song, P., Wu, L., and Guan, W. (2015). Dietary nitrates, nitrites, and nitrosamines intake and the risk of gastric cancer: A meta-analysis. *Nutrients* 7, 9872–9895. doi: 10.3390/nu7125505

Sze, M. A., and Schloss, P. D. (2018). Leveraging existing 16S rRNA gene surveys to identify reproducible biomarkers in individuals with colorectal tumors. *MBio* 9, e00630-18. doi: 10.1128/mBio.00630-18

Tahmourespour, A., Ahmadi, A., and M, F. (2020). The anti-tumor activity of exopolysaccharides from pseudomonas strains against HT-29 colorectal cancer cell line. *Int. J. Biol. Macromol.* 149, 1072–1076. doi: 10.1016/j.ijbiomac.2020.01.268

Teng, F., Yang, F., Huang, S., Bo, C., Xu, Z. Z., Amir, A., et al. (2015). Prediction of early childhood caries *via* spatial-temporal variations of oral microbiota. *Cell Host Microbe* 18, 296–306. doi: 10.1016/j.chom.2015.08.005

Tsao, S. W., Tsang, C. M., and Lo, K. W. (2017). Epstein-Barr Virus infection and nasopharyngeal carcinoma. *Philos. Trans. R. Soc. Lond. B. Biol. Sci.* 372, 20160270-20160284. doi: 10.1098/rstb.2016.0270

Turkoz, F. P. (2011). Risk factors of nasopharyngeal carcinoma in Turkey - an epidemiological survey of the Anatolian society of medical oncology. *Asian Pacific. J. Cancer Prev.* 12, 3017.

Wang, A. H., Li, M., Li, C. Q., Kou, G. J., Zuo, X. L., and Li, Y. Q. (2016). Human colorectal mucosal microbiota correlates with its host niche physiology revealed by endomicroscopy. *Sci. Rep.* 6, 21952. doi: 10.1038/srep21952

Wolf, P., and Elsasser-Beile, U. (2009). Pseudomonas exotoxin a: from virulence factor to anti-cancer agent. *Int. J. Med. Microbiol.* 299, 161–176. doi: 10.1016/j.ijmm.2008.08.003

Wu, H., Ma, Y., Peng, X., Qiu, W., Kong, L., Ren, B., et al. (2020). Antibiotic-induced dysbiosis of the rat oral and gut microbiota and resistance to salmonella. *Arch. Oral. Biol.* 114, 104730. doi: 10.1016/j.archoralbio.2020.104730

Xiao, X., Zhang, Z., Chang, E. T., Liu, Z., Liu, Q., Cai, Y., et al. (2018). Medical history, medication use, and risk of nasopharyngeal carcinoma. *Am. J. Epidemiol.* 187, 2117–2125. doi: 10.1093/aje/kwy095

Xu, Y., Teng, F., Huang, S., Lin, Z., Yuan, X., Zeng, X., et al. (2014). Changes of saliva microbiota in nasopharyngeal carcinoma patients under chemoradiation therapy. *Arch. Oral. Biol.* 59, 176–186. doi: 10.1016/j.archoralbio.2013.10.011

Yang, J., Mcdowell, A., Kim, E. K., Seo, H., Lee, W. H., Moon, C. M., et al. (2019). Development of a colorectal cancer diagnostic model and dietary risk assessment through gut microbiome analysis. *Exp. Mol. Med.* 51, 1–15. doi: 10.1038/s12276-019-0313-4

Yang, J., Mu, X., Wang, Y., Zhu, D., Zhang, J., Liang, C., et al. (2018). Dysbiosis of the salivary microbiome is associated with non-smoking female lung cancer and correlated with immunocytochemistry markers. *Front. Oncol.* 8, 520. doi: 10.3389/fonc.2018.00520

Yin, X., Gu, X., Yin, T., Wen, H., Gao, X., and Zheng, X. (2016). Study of enteropathogenic bacteria in children with acute diarrhoea aged from 7 to 10 years in xuzhou, China. *Microb. Pathogen.* 91, 41–45. doi: 10.1016/j.micpath.2015.11.027

Yu, G., Phillips, S., Gail, M. H., Goedert, Jj, Humphrys, M. S., Ravel, J., et al. (2017). The effect of cigarette smoking on the oral and nasal microbiota. *Microbiome* 5, 3. doi: 10.1186/s40168-016-0226-6

Zhang, W., Guo, Q., Liu, G., Zheng, F., Chen, J., Huang, D., et al. (2019). NKILA represses nasopharyngeal carcinoma carcinogenesis and metastasis by NF-κB pathway inhibition. *PloS Genet.* 15, e1008325. doi: 10.1371/journal.pgen.1008325

Zhou, X., Hao, Y., Peng, X., Li, B., Han, Q., Ren, B., et al. (2021). The clinical potential of oral microbiota as a screening tool for oral squamous cell carcinomas. *Front. Cell Infect. Microbiol.* 11, 728933. doi: 10.3389/fcimb.2021.728933

Zhu, X. X., Yang, X. J., Chao, Y. L., Zheng, H. M., Sheng, H. F., Liu, H. Y., et al. (2017). The potential effect of oral microbiota in the prediction of mucositis during radiotherapy for nasopharyngeal carcinoma. *EBioMedicine* 18, 23–31. doi: 10.1016/j.ebiom.2017.02.002

Zhu, C., Yuan, C., Wei, F. Q., Sun, X. Y., and Zheng, S. G. (2020). Intraindividual variation and personal specificity of salivary microbiota. *J. Dent. Res.* 99, 1062–1071. doi: 10.1177/0022034520917155

frontiers | Frontiers in Cellular and Infection Microbiology

TYPE Original Research
PUBLISHED 07 March 2023
DOI 10.3389/fcimb.2023.1104343

OPEN ACCESS

EDITED BY
Zheng Zhang,
Nankai University, China

REVIEWED BY
Minquan Du,
Wuhan University, China
Wang Pengcheng,
Beijing Chaoyang Hospital, Capital Medical University, China

*CORRESPONDENCE
Jun Luo
500210@hospital.cqmu.edu.cn
Zhi Zhou
500119@hospital.cqmu.edu.cn

SPECIALTY SECTION
This article was submitted to Microbiome in Health and Disease, a section of the journal Frontiers in Cellular and Infection Microbiology

RECEIVED 21 November 2022
ACCEPTED 17 February 2023
PUBLISHED 07 March 2023

CITATION
Yang Z, Cai T, Li Y, Jiang D, Luo J and Zhou Z (2023) Effects of topical fluoride application on oral microbiota in young children with severe dental caries. *Front. Cell. Infect. Microbiol.* 13:1104343. doi: 10.3389/fcimb.2023.1104343

Effects of topical fluoride application on oral microbiota in young children with severe dental caries

Zhengyan Yang[1,2,3], Ting Cai[1,2], Yueheng Li[1,2,3], Dan Jiang[2], Jun Luo[1,2]* and Zhi Zhou[1,2]*

[1]Department of Preventive Dentistry, Stomatological Hospital of Chongqing Medical University, Chongqing, China, [2]Chongqing Key Laboratory of Oral Biomedical Engineering of Higher Education, Department of Preventive Dentistry, Chongqing, China, [3]Chongqing Key Laboratory of Oral Diseases and Biomedical Sciences, Chongqing, China

While the effect of fluoride on severe early childhood caries (S-ECC) is clear, knowledge of how it influences the oral microbiota and the consequential effects on oral health is limited. In this cohort study, we investigated the changes introduced in the oral ecosystem before and after using fluoride varnish in 54- to 66-month-old individuals (n=90: 18 children were sampled at 5 different time points). 16S rDNA was amplified from bacterial samples using polymerase chain reaction, and high-throughput sequencing was performed using Illumina MiSeq platforms. Many pronounced microbial changes were related to the effects of fluoride varnishing. The health-associated *Bacteroides* and *Uncultured_bacterium_f_Enterobacteriaceae* were enriched in the saliva microbiome following treatment with fluoride varnishing. Co-occurrence network analysis of the dominant genera showed that different groups clearly showed different bacterial correlations. The PICRUSt algorithm was used to predict the function of the microbial communities from saliva samples. The results showed that starch and sucrose metabolism was greater after fluoride use. BugBase was used to determine phenotypes present in microbial community samples. The results showed that *Haemophilus* and *Neisseria* (phylum *Proteobacteria*) was greater before fluoride use. We conclude that the changes in oral microbiology play a role in fluoride prevention of S-ECC.

KEYWORDS

microbial community, fluoride, dental caries, high-throughput sequencing, saliva

Introduction

Dental caries is a chronic infectious disease resulting from many factors. Its causes are complex and diverse, but its formation is mainly due to the acid production of bacteria in the mouth, which leads to the dissolution and destruction of dental hard tissue (Vos et al., 2012). Currently, most experts think that dental caries is defined as a dysbiosis rather than a

chronic infectious disease. ECC (Early childhood caries) is one of the most common chronic childhood diseases globally, affecting up to 73% of socioeconomically disadvantaged children (2018). The 4th National Oral Health Surgery in mainland China in 2018 (Xiao et al., 2019) revealed that in the past decade, the prevalence of dental caries in young children in China was high, and the prevalence rate showed an upwards trend. The prevalence rate of dental caries in 5-year-old children was 71.9%, and the treatment of ECC, especially S-ECC, is complicated and difficult, with invasive and costly specialist treatment in the hospital under general anesthesia being the only option. Severe early childhood caries (S-ECC) occurred in children younger than three years old, those with one or more cavitated, missing, or filled smooth surfaces in primary maxillary anterior teeth from the ages of three to five, or those with a decayed, missing, or filled surface score ≥4 (age three), ≥5 (age four), or ≥6 (age five) (Losso et al., 2009). In this context, there is interest in simple treatments to halt the progress of cavities after tooth decay onset. Fluoride is recognized as effective in preventing caries. In many developed countries, the general decline in the incidence rate of caries has been largely attributed to the use of fluoride (Clark et al., 2020). From its physical and chemical mechanisms, the role of fluoride lies in the replacement reaction between fluoride ions and hydroxyapatite in the process of enamel mineralization. The formation of fluorapatite improves the hardness and acid resistance of enamel, which can reduce the formation of plaque (Takeuchi et al., 1996) and the incidence of caries.

Since Marsh (1994) proposed the ecological plaque hypothesis, further studies have found that due to changes in the oral environment, such as changes in sugar intake, diet or pH, the relatively balanced bacterial composition in biofilms can change significantly. The ecological balance of plaque is broken, leading to the occurrence of caries, and the occurrence and development of caries is the result of the imbalance of the microbial community. Research has also begun on the effects of fluoride on oral microbes. Studies have reported that long-term use of fluoride may cause changes in the flora (Yasuda et al., 2017). Fluoride can inhibit the growth of a variety of oral microorganisms, such as *Streptococcus sialis, Lactobacillus, Porphyromonas gingivalis, Streptococcus sanguis, Streptococcus mutans, and Candida albicans*, and different types of microorganisms have different sensitivities to fluoride (Kulik et al., 2015; Thomas et al., 2017; Maden et al., 2018). In addition, some studies have found that fluoride toothpaste can affect oral plaque biofilm. After treatment with fluoride toothpaste, the growth of *Streptococcus mutans* and *Porphyromonas gingivalis* was inhibited, while the number of *Streptococcus sanguis* increased (Cheng et al., 2017). Yasuda et al. (2017) established an animal model by simulating the fluoride-containing environment in which humans live. Through 16S rRNA gene amplification and genome sequencing, it was verified that fluoride interference has a selective effect on the composition of the oral microbial community in mice.

Previous studies have also found that fluorinated compounds inhibit bacterial growth by inhibiting the enzyme enolase, which catalyzes the conversion of 2-phosphoglycerate to phosphoenolpyruvate (the last step of anaerobic glycolysis), thereby improving oral health. Therefore, fluorinated compounds are crucial to microbial energy acquisition and growth (Marquis, 1995; Qin et al., 2006). However, how fluoride affects the whole oral microbiome and the changes in the oral microbiome after fluoride use have not been fully studied. This study mainly investigated how fluoride affects the microbial community in S-ECC saliva and its changes over time through Illumina MiSeq sequencing technology to better understand the microbial etiology of fluoride use.

Materials and methods

Subject selection

Patients with S-ECC were recruited from the same kindergarten in Yubei District of Chongqing, China. The inclusion criteria of subjects were as follows: (i) age from 54-66 months, (ii) no bad eating habits, (iii) no other bacterial infectious oral disease such as gingivitis or periodontitis, (iv) no antibiotic use within 2 months, (v) no partial denture and appliance, (vi) never having seen a dentist, and (vii) no systemic disease. All of the participants underwent a comprehensive oral examination, which included a professional assessment from a specialized dentist based on the standards of the World Health Organization "Oral health surveys: basic methods–5th ed (World Health Organization, 2013)." In accordance with the timing of local fluoride varnish use (10 ml fluoride varnish containing 50 mg/ml NaF, Colgate-Palmolive UK For our study, participants received fluoride varnish treatment only at the first time. Before treatment, participants were instructed to brush their teeth, rinse their mouth, and remove any food debris. Dental surfaces were then dried and treated with fluoride using a small brush. Approximately 0.25 mL of fluoride was applied per participant, with emphasis on the grooves and adjacent surfaces.To maximize fluoride adherence, participants were advised to avoid drinking and rinsing for 30 minutes post-treatment. They were also told not to consume hard foods for four hours and to refrain from brushing their teeth that night. These measures ensured optimal fluoride absorption and efficacy. All the participants needed to collect saliva sample at 5 time points: HFB (Prefluoride saliva samples for subjects with high caries), HF1(Saliva samples taken 1 day after fluoride application in subjects with high caries), HF3(Saliva samples taken 3 days after fluoride application in subjects with high caries), HF7 (Saliva samples taken 7 days after fluoride application in subjects with high caries), and HF14 (Saliva samples taken 14 days after fluoride application in subjects with high caries). During this observation period, all the participants were provided with the same toothbrush and toothpaste without fluoride, and they were also forbidden to use mouth rinse, dental floss and so on containing fluoride. These participants' parents or grandparents were sufficiently informed about the aims of the research and provided written informed consent according to the recommendations of the Ethics Committee of the Stomatological Hospital of Chongqing Medical University (CQHS-REC-2018(LSNO.22)).

Sample collection

All of the participants were required to avoid eating, drinking, and brushing their teeth 2 hours before taking samples and then rinsed their mouths with sterile water. Unstimulated saliva was collected, transferred to sterile 1.5 mL microcentrifuge tubes, and frozen at -80°C until further processing.

DNA extraction, PCR amplification and Illumina MiSeq sequencing

Based on the manufacturer's protocol, microbial DNA was extracted from all the specimens by the PowerSoil® DNA Isolation Kit. Primers 338F (5′-ACTCCTACGGGAGGCAGCAG-3′) and 806R (5′-GGACTACHVGGGTWTCTAAT-3′) were used to amplify the V3-V4 hypervariable regions of the bacterial 16S rRNA gene using PCR on the Veriti 96-Well Thermal Cycler (GeneAmp 9902, ABI, USA). Target area PCR was conducted with the following program: initial denaturation at 98°C for 2 mins, 30 cycles of denaturation at 98°C for 30 s, annealing at 50° C for 30 s, and elongation at 72°C for 60 s, and a final extension at 72°C for 5 mins, followed by storage at 4°C. Target area PCR was performed in triplicate with a 30 μL mixture containing 15 μL KOD FX Neo Buffer, 6 μL dNTPs (2 mM each), 0.9 μL Vn F (10 μM)/Vn R (10 μM), 0.6 μL KOD FX Neo and 50 ng ± 20% template DNA. Finally, ddH2O was used to fill to a 30 μL volume. Solexa PCR was conducted with the following program: initial denaturation at 98°C for 30 s, 10 cycles of denaturation at 98°C for 10 s, annealing at 65°C for 30 s, and elongation at 72°C for 60 s, and a final extension at 72° C for 5 mins.

Solexa PCR was performed in triplicate with a 20 μL mixture containing 5 μL target area PCR products, 10 μL of 2×Q5 HF MM, and 2.5 μL MPPI-a (2 μM)/MPPI-b (2 μM). The final PCR products were extracted from a 1.8% agarose gel under a voltage of 120 V. After 40 mins, column purification was performed by using an OMEGA DNA purification column. The PCR products were purified, quantified, and homogenized to form a sequencing library. The built libraries were first subjected to library quality inspection, and the qualified libraries were sequenced by Illumina NovaSeq 6000 PE250.

Processing of sequencing data

Primary FastQ files were divided into multiple files for processing and quality-filtered by Trimmomatic (Edgar Robert, 2013). The following standards were used for sequence combination: (i) Reads containing any site with an average quality score <20 over a 50 bp sliding window were removed. (ii) The primers must be perfectly matched, allowing the mismatch of two nucleotides, and reads with ambiguous bases were removed. (iii) Sequences with an overlap longer than 10 bp were merged based on their overlapping sequence (Jiang et al., 2019).

By USEARCH (Bolger et al., 2014) (version 10.0), operational taxonomic units (OTUs) were clustered with a 97% similarity cut-off. Additionally, chimeric sequences were recognized and deleted by UCHIME (version 8.1) (Edgar et al., 2011). By comparing the RDP Classifier algorithm (Wang et al., 2007) (version 2.2, http://sourceforge.net/projects/rdpclassifier/) against the Silva (Quast et al., 2012) 16S rRNA (Release128, http://www.arb-silva.de) database, the taxonomy of each 16S rRNA gene sequence was analyzed based on an 80% confidence threshold.

Bioinformatics and statistical analysis

Bioinformatics analysis was conducted using QIIME. The alpha diversity indices of Shannon, Simpson, Chao, ACE and PD_whole_tree were calculated at 97% identity by Mothur (Schloss et al., 2009) version v.1.30. Beta diversity analysis was performed by principal coordinate analysis (PCoA) based on Bray-Curtis distances at the OTU level. A hierarchical clustering analysis based on weighted UniFrac distances was also conducted (Lozupone et al., 2007). Analysis of similarities (ANOSIM) was performed using the vegan package in the R language and drawn with Python; unweighted UniFrac distances were used to compare different groups. STAMP v2.1.3 with Welsh's t test ($p < 0.05$) and Kruskal-Wallis were used to compare the relative abundance of predominant bacteria between different groups. A P value of <0.05 was considered to be statistically significant. A Venn diagram was used to define the core microbiome at the species level using Mothur (Schloss et al., 2009). Linear discriminant analysis of effect size (LEfSe) was conducted to define the biomarkers of the groups. The threshold on the logarithmic LDA score for distinguishing features was set to 3 (Segata et al., 2011). Receiver operating characteristic (ROC) curve analysis was performed on the Tutools platform (https://www.cloudtutu.com), a free online data analysis website. Co-occurrence analysis among the genera was performed with Python, and co-occurrence analysis of the 80 richest genera of each group was performed at the same time. The phylogenetic investigation of communities by reconstruction of unobserved states (PICRUSt2) program was used to predict 16S rRNA-based data from high-throughput sequencing and to further analyze the composition and differential Kyoto Encyclopedia of Genes and Genomes (KEGG) metabolic pathways in the context of IMG microbial genome data. STAMP v2.1.3 with Welsh's t test ($p < 0.05$) was used to compare the pathways between different groups. BugBase normalized the OTU by the predicted 16S copy number and then predicted the microbial phenotype (Ward et al., 2017) using the provided precomputed files. Differences were considered significant when $P < 0.05$ and extremely significant when $P < 0.01$. SPSS 25.0 software (SPSS Inc., Chicago, IL, USA) was used for statistical analysis. The raw data will be made available by the authors without undue reservation to any qualified researcher.

10.3389/fcimb.2023.1104343

TABLE 1 The (HFB) participants' caries status (decayed teeth).

Samples	Age (months)	Sex	dmft	dmfs
AHDB	54	Female	8	17
AHPB	55	Female	13	48
BHDB	60	Female	8	27
BHPB	57	Male	18	56
CHDB	62	Male	16	51
CHPB	64	female	8	20
DHDB	63	female	8	18
DHPB	58	female	12	21
EHDB	59	male	12	20
EHPB	63	male	8	20
FHDB	66	male	10	27
FHPB	66	male	12	25
GHDB	57	male	9	29
GHPB	58	female	8	28
HHDB	58	female	8	25
HHPB	60	female	8	17
IHDB	61	female	10	31
IHPB	63	male	8	25

Results

Sequence information

A total of 18 preschool children were enrolled in this study at the end of the follow-up period (Table 1). The mean age at baseline for preschool children was 60.2 months. After Illumina MiSeq sequencing, 6,320,730 effective sequences were acquired from 90 saliva samples, with an average of 70,230 sequences per sample. The average length of the sequences was 423 bp. Ninety-seven percent qualified sequences were clustered, and 2,731 (Appendix 1) operational taxonomic units (OTUs) were obtained. Good's coverage of the generated OTUs reached 99.9%. In the rarefaction curve, each curve first rose sharply and then flattened out with an increase in the number of sequences, indicating that the sequencing quantity was sufficient to cover all species in the samples (Figure 1A). There was a high evenness of saliva microbial composition in the samples, as seen in the rank abundance curve (Figure 1B).

Alpha and beta diversity analysis based on 16S rRNA sequencing

The Shannon, Simpson, Chao, ACE and PD_ whole_tree alpha diversity was calculated to analyze the diversity and abundance of all samples. Student's t test was performed to compare the saliva samples among the five groups (HFB, HF1, HF3, HF7, and HF14).

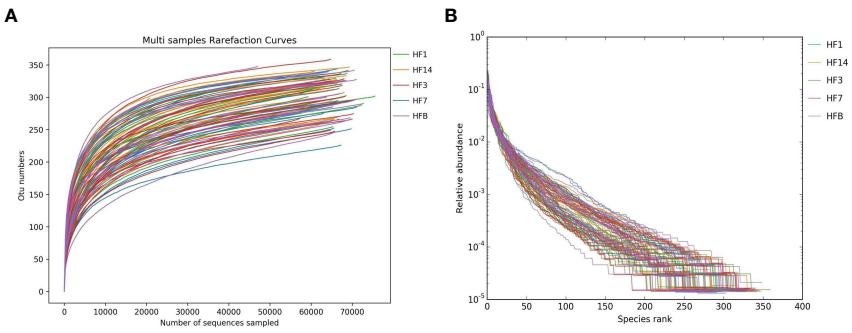

FIGURE 1
Alpha diversity analysis of saliva microorganisms. Rarefaction curve **(A)** and rank abundance curve **(B)** of saliva floral of samples.

10.3389/fcimb.2023.1104343

TABLE 2 Alpha diversity indices of different groups.

Group	Shannon	Simpson	Chao1	ACE	PD_whole_tree
HFB	5.43 ± 0.12	0.95 ± 0.004	338.46 ± 5.53	333.53 ± 4.46	19.64 ± 0.34
HF1	5.41 ± 0.11	0.95 ± 0.004	347.22 ± 2.98	340.99 ± 3.89	19.92 ± 0.25
HF3	5.20 ± 0.98	0.94 ± 0.003	330.90 ± 5.60*	326.44 ± 5.79*	19.44 ± 0.38
HF7	5.27 ± 0.10	0.95 ± 0.004	331.57 ± 6.27*	326.43 ± 6.19	19.28 ± 0.42
HF14	5.32 ± 0.07	0.95 ± 0.003	336.89 ± 4.51	333.82 ± 4.16	19.79 ± 0.31

*Compared with the HF1 group, $P<0.05$.

Table 2 and Figure 2 show that the difference between HF1 and HF3 is statistically significant for ACE and Chao1, the difference between HF1 and HF7 is statistically significant for Chao1, and the other groups are not statistically significant for the other diversity indices. The Chao1 and Ace indices measure the species abundance, that is, the number of species. The results of this study showed that only the difference between HF1 and HF3 and HF7 was statistically significant but when compared with HFB, the difference has no statistically significant, indicating that the diversity and richness of the bacterial communities across the five groups were basically similar. Only in terms of species richness, with the use of local fluoride, did the species richness first increase and then decrease until it returned to a level close to that before the use of fluoride. PCoA and ANOSIM were used to evaluate the similarity in the microbial community structure among the five groups (Figure 3). PCoA and ANOSIM results showed that there was no significant difference in bacterial composition among the five groups. This finding suggested that children's oral microbial community structure was similar before and after topical fluoride application.

Bacterial community structure

OTUs were distributed among 16 phyla, 26 classes, 56 orders, 93 families, 173 genera, and 218 species. The phylogenetic trees of the 68 most abundant genera were constructed, in which the taxonomic composition and abundance can be observed (Figure 4). The top abundant phyla were *Firmicutes* (37.6%), *Bacteroidetes* (22.7%), *Proteobacteria* (16.6%), *Actinobacteria* (10.9%), *Fusobacteria* (8.7%), Patescibacteria (1.7%), Epsilonbacteraeota (1.1%), Cyanobacteria (3.7%), Acidobacteria (1.5%) and Spirochaetes (1.5%), together comprising 98.2% of the total sequences (Figure 5A). The most abundant genera were *Streptococcus* (16.4%), *Veillonella* (12.2%), *Prevotella_7* (10.7%), *Neisseria* (10.2%), *Leptotrichia* (5.6%), Rothia (5.3%), *Actinomyces* (4.2%), *Prevotella* (3.2%), *Fusobacterium* (2.9%), and Alloprevotella (2.5%), accounting for 73.2% of the total (Figure 5B). The predominant bacteria were largely consistent among the five groups, but different relative abundances could be observed. Figure 5C represents a heatmap showing the relative abundances

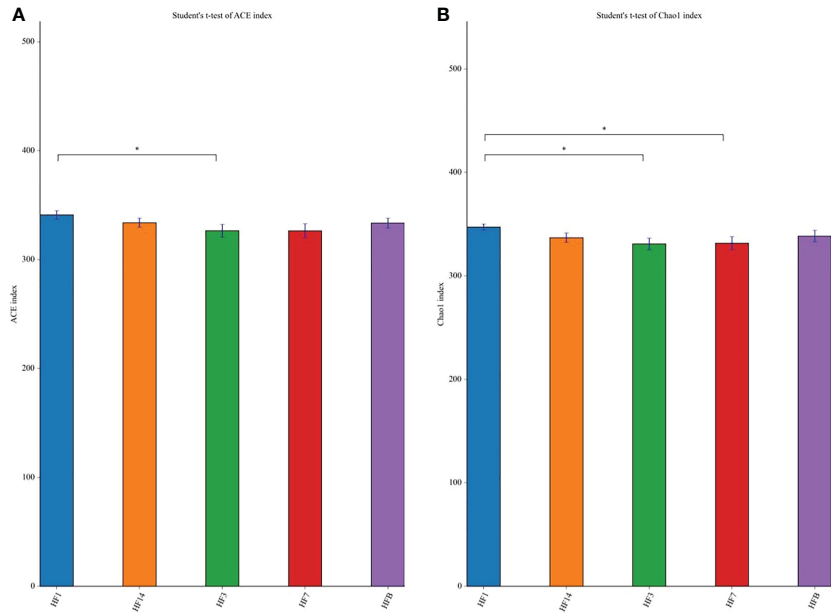

FIGURE 2
The significance of the difference in the Ace index **(A)** and Chao1 **(B)** index between each group. The significant differences were evaluated by t test (*P < 0.05, the asterisk indicates statistical significance).

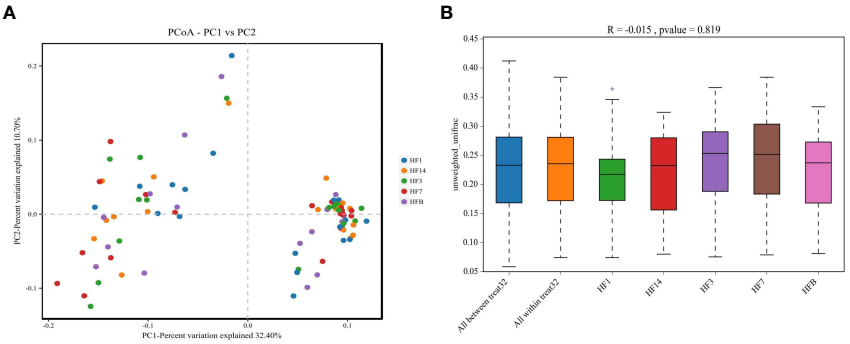

FIGURE 3
PCoA based on Bray-Curtis distances at the OTU level at 97% identity. Each sample is represented by a dot. Circles in different colors represent different groups. PC1 explained 32.4% of the variation observed, and PC2 explained 10.7% of the variation observed **(A)**. ANOSIM was based on unweighted UniFrac distances between the five groups (P=0.819) **(B)**.

of these predominant genera in each sample, as well as the cluster trees of the genera and samples. The microbial compositions of each group were not obviously separated, consistent with the results of beta diversity and ANOSIM based on 16S rRNA sequencing.

A Venn diagram was made to define the core microbiome, which was detected in most individuals at the species level. We identified 217 species in the HF1 group and 218 species in the other groups (Figure 6). Among them, 217 species were shared, occupying 99.5% of all the species detected, and 1 species (*uncultured_bacterium_g_Comamonas*) was unique to the HF1 group, indicating a stable composition of the microbiome in each group.

Similarities and dissimilarities in bacterial compositions

Kruskal-Wallis analysis (Figure 7) of the 5 groups of samples at the genus level showed that *Oscillibacter, Bacteroides, Helicobacter, and uncultured_ bacterium_ f_ Enterobacteriaceae* had the highest relative abundance in the HF14 group; *Turicibacter* had the highest relative abundance in the HFB group; and *Comamonas* had the highest relative abundance in the HF7 group. The relative abundance of *uncultured_ bacterium_ f_ Xanthobacteraceae* in the HF1 group was the highest, and the difference was statistically significant ($P<0.05$). STAMP difference analysis was performed between the HFB group and the other four groups of samples at the genus level. The results showed that compared with the HFB group, the relative abundance of *Helicobacter* and *Oscillibacter* in the HF14 group was higher. The relative abundance of *[Eubacterium]_nodatum_group* and *uncultured_bacterium_o_Bacteroidales* in the HF3 group was higher, and the relative abundance of *Candidatus_Saccharimonas* and *Solobacterium* in the HF1 group was higher. Compared with all groups after local fluoride use, the relative abundance of *Helicobacter, uncultured_bacterium_f_Saccharimonadaceae, Peptostreptococcus* and *[Eubacterium]_nodatum_group* was higher, and the above differences were statistically significant ($P <$ 0.05) (Figure 8). No significant difference was found between the HFB group and HF7 group at the genus level.

LEfSe was used to explain the characteristics of differences among groups HFB, HF1, HF3, HF7, and HF14. Figure 9 shows a branching diagram of potential biomarkers representing different groups. At the genus level, *Bacteroides* was remarkably enriched in the HF14 group. At the species level, the relative abundance of *uncultured_bacterium_g_Bacteroides* was higher in the HF14 group (LEfSe LDA = 3, $P < 0.05$). This result indicated that the higher relative abundance of *Bacteroides* may be related to the local application of fluoride.

The abscissa of the ROC curve model is the false-positive rate, and the ordinate is the true positive rate, which can simultaneously reflect the sensitivity, specificity and accuracy of the results. AUC is the area under the ROC curve, and the AUC value is usually between 0.5 and 1; it is generally believed that the AUC has a certain diagnostic value in the range of 0.7-0.9. At the genus level, ROC curve analysis was performed on the differential species screened by LEfSe, STAMP and Kruskal-Wallis, and the AUC was calculated to assess changes in microbial diversity after fluoride use. As shown in Figure 10, the differences between *Bacteroides* (AUC=0.787), *Turicibacter* (AUC=0.719) and *uncultured_bacterium_f_Enterobacteriaceae* (AUC=0.809) can be used as biomarkers to speculate the changes in microbial diversity after fluoride use.

Network analysis and function prediction

Co-occurrence analysis was performed to recognize interactions among genera in different groups. The top 80 genera with high relative abundance were found to have complex interactions in each group (Figure 11). Different groups clearly showed different bacterial correlations, and there were 7, 3, 8, 13 and 13 negative correlations in the HFB, HF1, HF3, HF7, and HF14 groups, respectively. In the HFB group, *Bacteroides* had a positive correlation with *Faecalibacterium, Megamonas, Prevotella_9, uncultured_bacterium_f_Enterobacteriaceae,*

10.3389/fcimb.2023.1104343

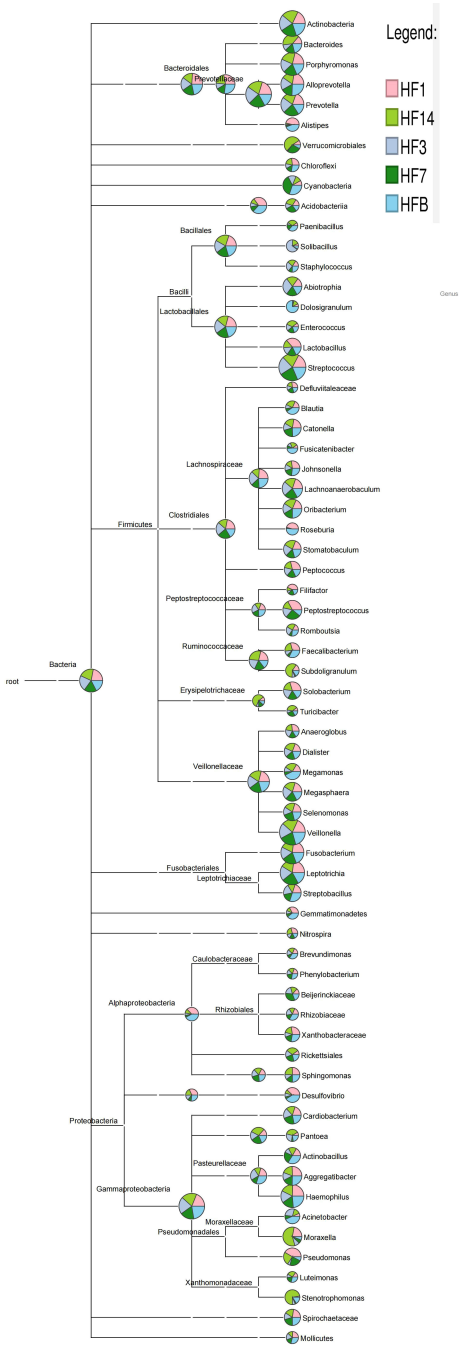

FIGURE 4
Phylogenetic tree of the 68 most abundant genera. Each branch represents a taxon, the length shows the phylogenetic distances between two taxa, and different colors represent different phyla. The bar plot on the right side shows the relative abundance of each genus in the five groups.

Pseudomonas and *Ammopiptanthus_mongolicus* and a negative correlation with *uncultured_bacterium_o_Lactobacillales* and *Abiotrophia*. In the HF1 group, *Bacteroides* had a positive correlation with *Prevotella_9, Megamonas, Faecalibacterium, Sphingomonas, Pseudomonas* and *Ammopiptanthus_mongolicus*. In the HF3 group, *Bacteroides* had a positive correlation with *Escherichia-Shigella, Faecalibacterium, Pseudomonas, Megamonas, Ammopiptanthus_mongolicus, Prevotella_9, uncultured_bacterium_f_Enterobacteriaceae* and *Clostridium_sensu_stricto_1*. In the HF7 group, *Bacteroides* had a positive correlation with *Lachnospiraceae_NK4A136_group, Akkermansia and uncultured_bacterium_f_Muribaculaceae*. In the HF14 group, *Bacteroides* had a positive correlation with *Helicobacter and Akkermansia*. Compared to that in the HFB group, *Bacteroides* in the HF1, HF3, HF7 and HF14 groups only exhibited a positive correlation.

PICRUSt2 was used to help understand the function of microbial communities in saliva samples. A bar graph (Figure 12A) showed that the saliva samples from the five groups had similar KEGG maps, suggesting that the function of microbiota in the five groups was similar. However, STAMP analysis showed that there was a difference in the function of microbiota between each group. Compared with HFB in class 3, there was a higher relative abundance of neomycin, kanamycin and gentamicin biosynthesis and *Vibrio cholerae* infection in the HF14 and HF3 groups; a higher relative abundance of sulfur metabolism in the HFB group; a higher relative abundance of insulin resistance, starch and sucrose metabolism, and cell cycle - Caulobacter in the HF1 group; and a higher relative abundance of proximal tubule bicarbonate reclamation and longevity regulating pathway in the HFB group ($P < 0.05$) (Figure 12B).

BugBase was used to determine phenotypes present in microbiota samples. The nine phenotypes included aerobic, anaerobic, contain_mobile_elements, facultative_anaerobic, forms_biofilms, gram_negative, gram_positive, potentially_pathogenic, and stress_tolerant. We performed pairwise comparisons of five samples using Mann-Whitney-Wilcoxon tests, and differences in the proportion of forms_biofilms bacteria were noted between the HFB group and HF7 groups (P=0.037<0.05), with the HFB group predicted to have significantly more forms_biofilms bacteria than the HF7 group (Figure 13). BugBase attributes differences in the relative abundance of predicted forms_biofilms bacteria to the higher proportion of *Haemophilus* and *Neisseria* (phylum *Proteobacteria)* in the HFB group.

Discussion

Stomatologists have paid increasing attention to the prevention and intervention of ECC, and the main preventive service is the topical application of fluoride varnish every 3 to 6 months. Our study group has demonstrated the effectiveness of fluoride in ECC prevention (Wang, 2019), but the microbial mechanism of dental caries prevention was not investigated. Microbiota are considered biomarkers for disease detection and management (Claesson et al., 2017; Kashyap et al., 2017). High-throughput techniques provide an effective way to study changes in the composition and structure of bacterial communities. In this study, we collected saliva samples at different times before and after fluoride treatment to study the changes in microbial populations, and the results helped us to have a comprehensive understanding of the impact of fluoride on the S-

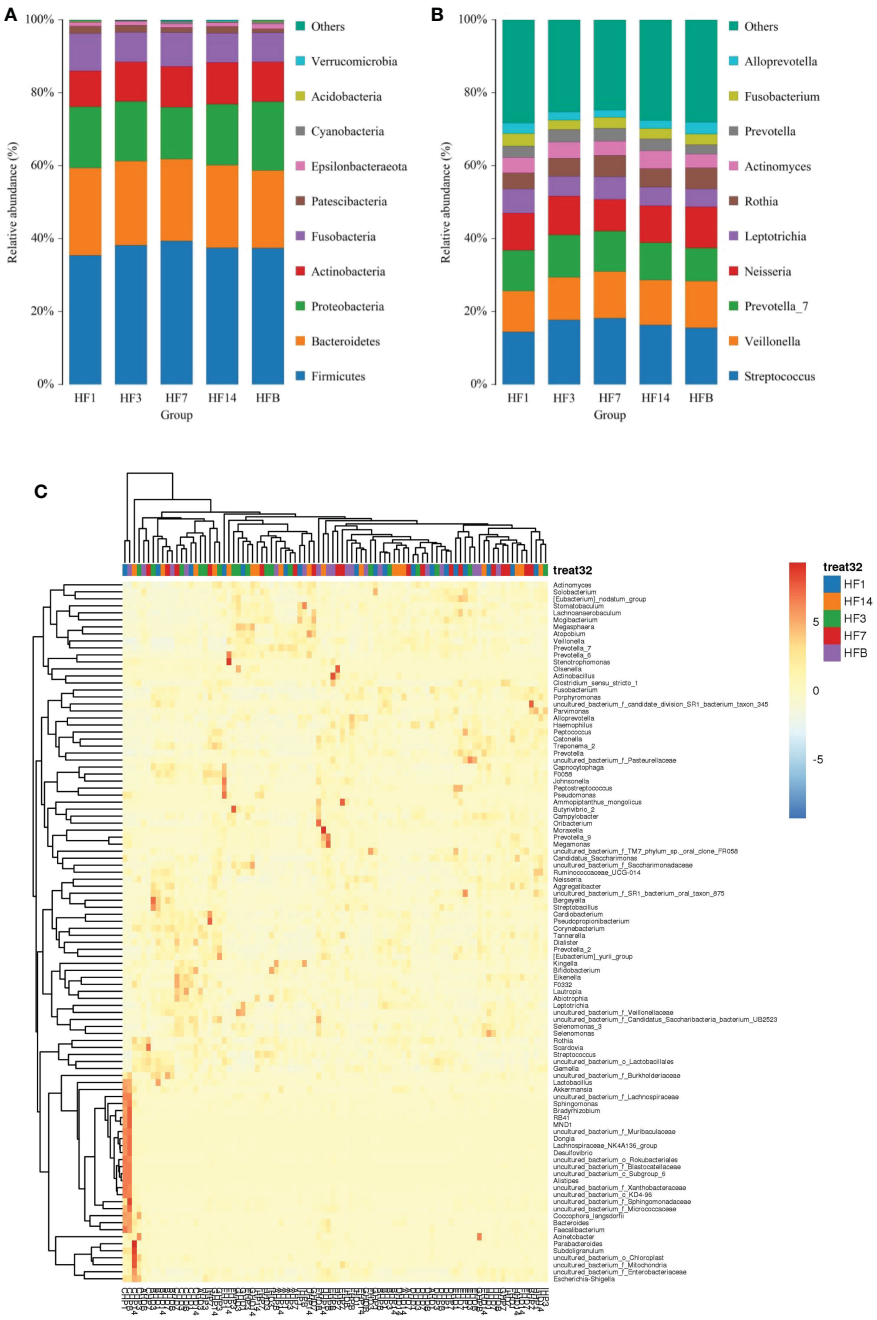

FIGURE 5
The distributions of the predominant bacteria. **(A)** Results at the phylum level. **(B)** Results at the genus level. The predominant taxa (relative abundance >2% on average) are shown. **(C)** Heatmap analysis. Each column represents a sample, and each row represents a genus. The cluster trees of genera and samples are shown on the left and upper sides, respectively. Different colors represent different relative abundances.

ECC oral microbiome, which may provide a theoretical basis for the clinical application of fluoride in S-ECC.

In this study, the alpha diversity index showed that the diversity and richness of bacterial communities in each time period before and after fluoride application were relatively stable and that species richness first increased, then decreased after fluoride use, and finally became comparable to prefluoride levels. As previous studies described, fluoride increased the diversity and richness of intestinal microflora in mice and silkworm 734 (Guannan et al., 2015; Fu et al., 2019; Liu et al., 2019) but decreased it in children with dental fluorosis, silkworm T6, and broiler chickens (Guannan et al., 2015; Luo et al., 2016; Wu, 2019). In conclusion, we speculate that the use of fluoride will affect oral microbial richness, that the post-use time of fluoride will also affect species richness and that the mechanism of the relationship between fluoride and the oral microbiota is related to the time after fluoride use.

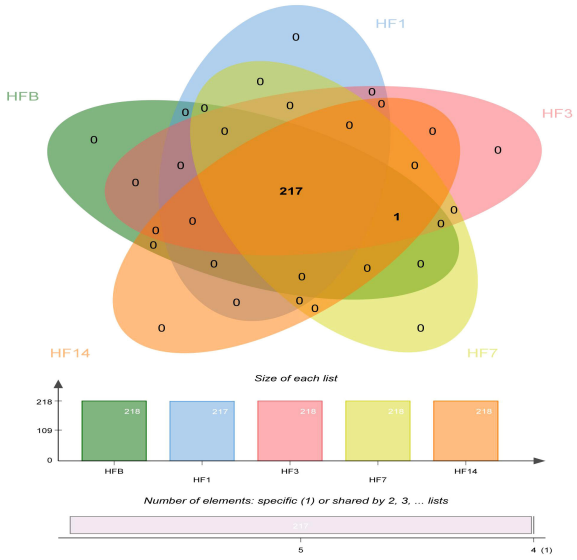

FIGURE 6
Venn diagram at the species level. Different colors represent different groups. The overlaps represent the common taxa between groups, and the nonoverlapping portions represent unique taxa in each group.

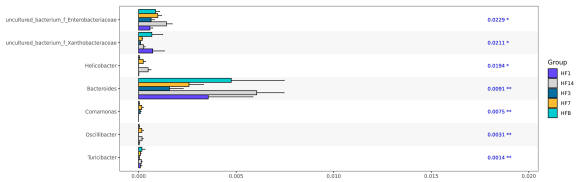

FIGURE 7
Kruskal-Wallis test bar plot at the genus level of five groups. (*P < 0.05, **P<0.01; the asterisk indicates statistical significance).

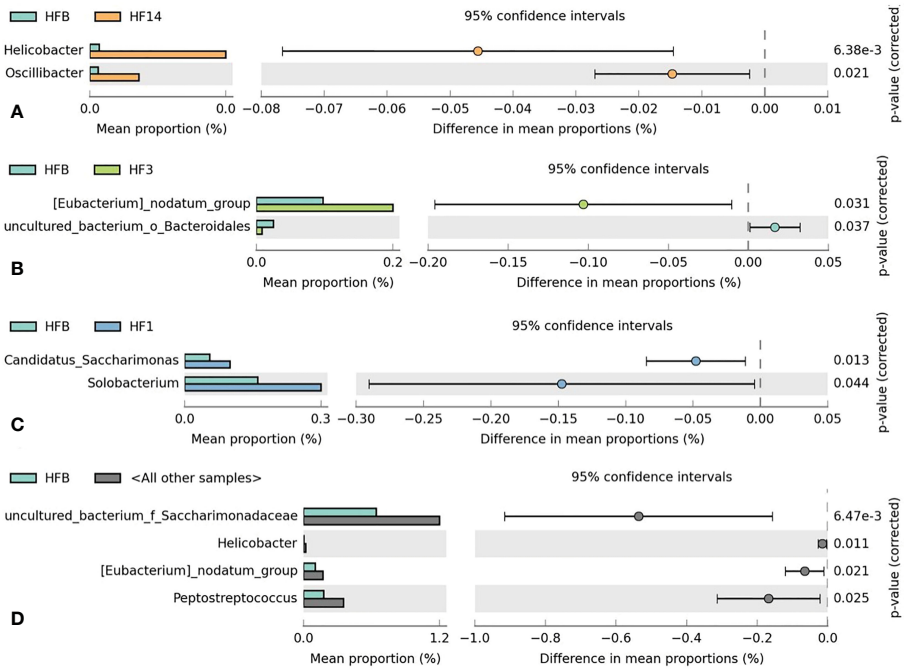

FIGURE 8
Welch's t test bar plot at the genus level. **(A)** Results of the HFB and HF14 groups. **(B)** Results of the HFB and HF3 groups. **(C)** Results of the HFB and HF1 groups. **(D)** Results of the HFB and all other samples. Only the results that were significantly different (P < 0.05) are shown.

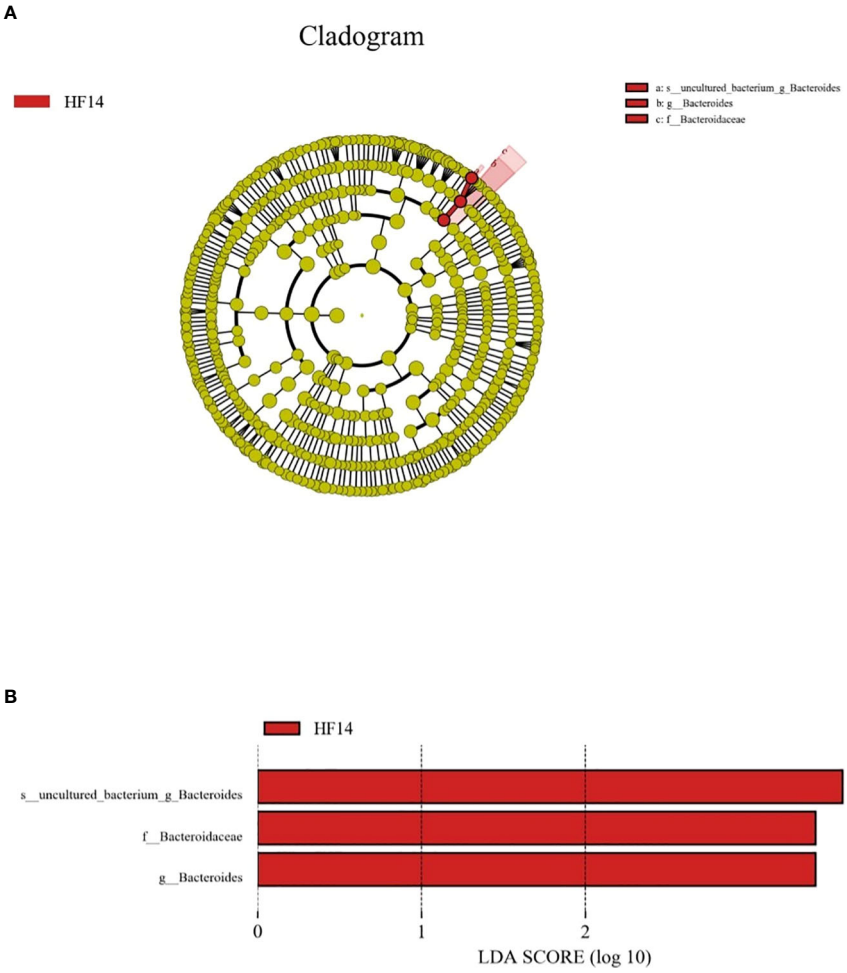

FIGURE 9
The potential biomarkers were defined by LEfSe. **(A)** Cladogram for taxonomic representation of significant differences between the five groups. The colored nodes from the inner to the outer circles represent taxa from the phylum to the genus level. The significantly different taxa are signified by different colors representing the five groups. **(B)** Histogram of the LDA scores for differentially abundant features among the groups. The threshold on the logarithmic LDA score for discriminative features was set to 3.0.

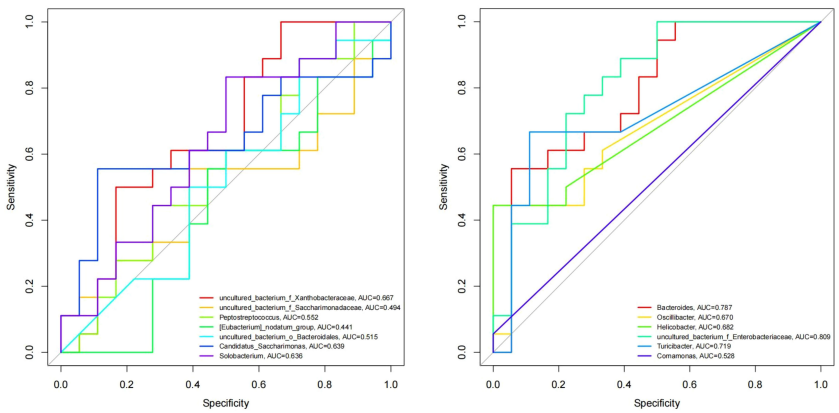

FIGURE 10
ROC curve model of differentially abundant genera. Different colored lines represent different genera.

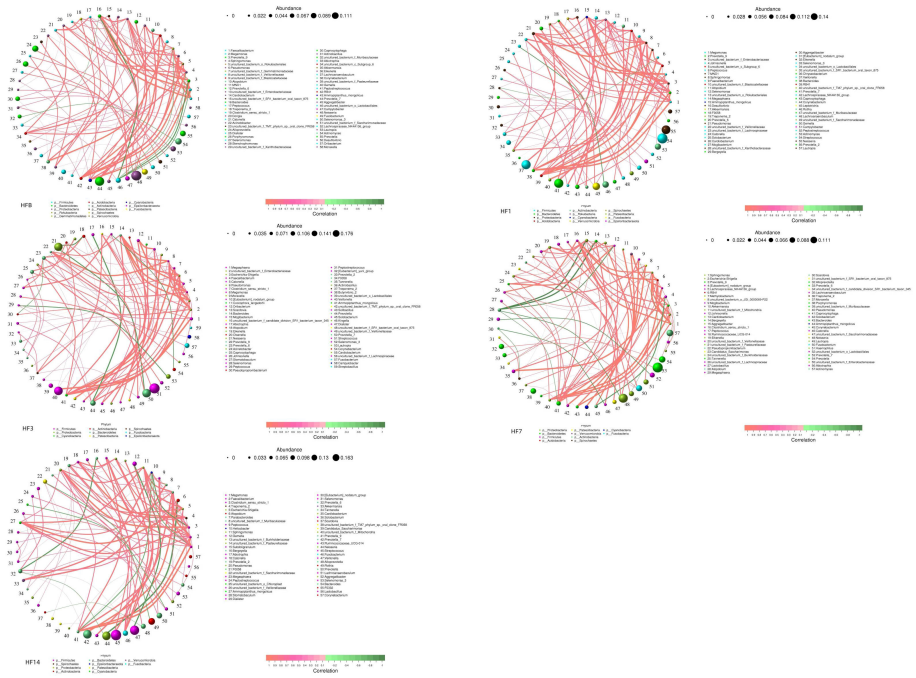

FIGURE 11
Network analysis showing the interactions between genera (|SpearmanCoef| > 0.1 and P < 0.05). Bacterial interactions of the five different groups (the 80 richest genera). The size of the node is proportional to the genera abundance. Node color corresponds to phylum taxonomic classification. Edge color represents positive (red) and negative (green) correlations.

From the community graph, the community structure of the groups was similar before and after fluoride use, indicating that the use of fluoride may not have a significant effect on the bacterial composition, and its main effect appears to be on the demineralization and remineralization processes in the oral cavity, which is similar to a previous study (Koopman et al., 2015). At the genus level, the most prevalent bacteria in the five groups were largely uniform but varied in relative abundance. The differences *in Bacteroides, Turicibacter* and *uncultured_bacterium_f_Enterobacteriaceae* among the five groups could be used as markers of microbial diversity changes following presumed fluoride use. The relative abundance of *Uncultured_bacterium_f_Enterobacteriaceae*, belonging to *Proteobacteria*, was higher in the HF14 group. *Proteobacteria* is a phylum generally associated with health, but *Turicibacte* belongs to *Firmicutes*, a phylum that consists of major cariogenic pathogens. This species was higher in the HFB group, which indicates that the use of local fluoride can reduce *Firmicutes*. Previous studies have reported comparative oral microbiome profiles between healthy individuals and patients with dental caries. Healthy individuals, especially children, had higher levels of *Proteobacteria* and *Bacteroidetes* and lower levels of *Firmicutes* in the oral microbiome (Bik et al., 2010; Chen et al., 2017). *Bacteroides* belongs to *Bacteroidetes*. A study (Wang et al., 2022) found that its change trend in the salivary microflora in children with caries was opposite that of *Firmicutes*, which was consistent with the results of this study. Hence, overall, active dental caries in children is likely to be associated with higher *Firmicutes* and lower *Proteobacteria* and *Bacteroidetes*. The findings of the present study provide new evidence that fluoride use could not only reduce cariogenic bacteria but also enrich the healthier microbiome in treated children.

Network analysis showed the potential correlation of oral microbiota. In this study, the analysis of different groups of microbiota clearly showed the different relationships among oral microbiota, and their relationships gradually changed from complex to simple to complex with time, which indicated that the use of fluoride led to ecological changes in oral microbiota. By analyzing the relationships between *Bacteroides* and other genera in the five groups, it can be concluded that the relationship between *Bacteroides* and other genera changed from complex to simple with the change in local fluoride usage time, and after fluoride usage, their relationships all became positively correlated. The phylum to which *Bacteroides* belongs is a health-related phylum, which indicates that with the change in local fluoride usage time, the microbial population in the oral cavity gradually tends to be healthy.

In this study, the functional analysis of salivary microbial communities before and after the use of local fluoride in children with high caries found that the starch and sucrose metabolism difference was statistically significant when carbohydrate metabolism was annotated to Class 3, and starch and sucrose metabolism was enriched in the HF1 groups, indicating that its

10.3389/fcimb.2023.1104343

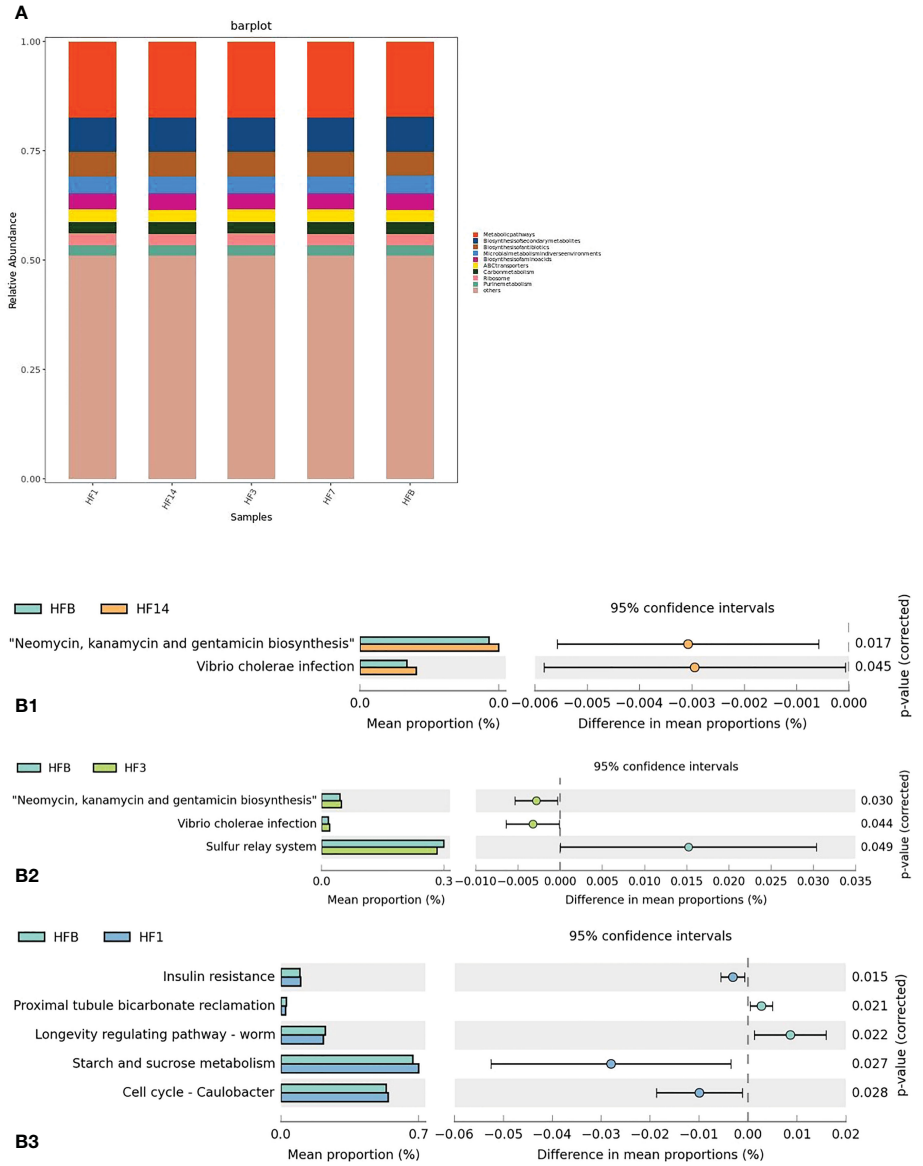

FIGURE 12
Function prediction by PICRUSt. **(A)** The compositions of KEGG functions in the five groups (in class 3). **(B)** Welch's t test bar plot of the KEGG results. (B1) Results of the HFB and HF14 groups in Class 3. (B2) Results of the HFB and HF3 groups in Class 3. (B3) Results of the HFB and HF1 groups in Class 3. Only the results that were significantly different (P < 0.05) are shown.

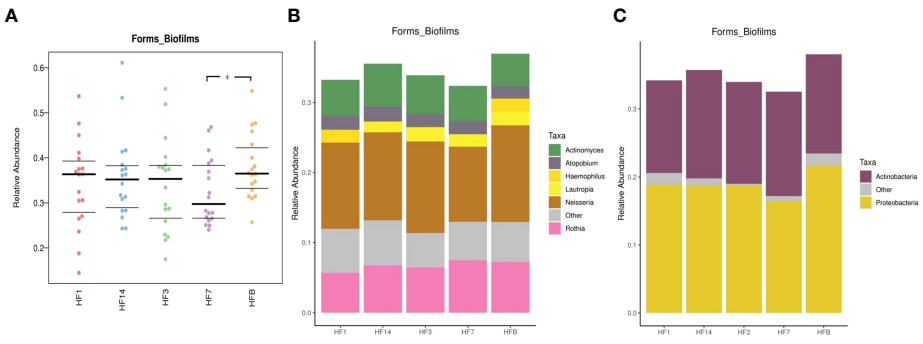

FIGURE 13
(A) BugBase was used to predict the proportion of forms_biofilm bacteria within the microbiomes of each group (n=18, * represents a significant difference, P=0.037<0.05); **(B)** the corresponding OTU contribution plots of the relative abundance of genera possessing each phenotype are also shown; **(C)** the corresponding OTU contribution plots of the relative abundance of phyla possessing each phenotype are also shown.

changes helped to improve the oral microecology of children with high caries and move it towards a healthy oral microecology. The comparative analysis of the high-caries and healthy groups conducted by Liu (2021) found that carbohydrate metabolism (carbohydrate metabolism) was enriched in the healthy group. Wang et al. (2019) found that the functional difference between children with high caries and no caries was mainly reflected in carbohydrate metabolism, and our study found similar results. BugBase phenotype prediction follows pairwise comparisons between HF14 and HFB groups regarding forms_biofilms, with higher relative abundance of *Haemophilus* and *Neisseria* reflected in the HFB group than in the HF7 group, suggesting that *Haemophilus* and *Neisseria* may decrease at 7 days after local fluoride use. Johansson et al. reported that the oral microbiomes of individuals with high caries levels are dominated by *Streptococcus*, *Alloprevotella*, *Leptotrichia*, *Neisseria*, *Prevotella*, and *Porphyromonas*, while caries-free microbiomes are dominated by *Gemella* (Johansson et al., 2016). This is consistent with the results of this study, but there are also studies suggesting that (Liu, 2021) *Haemophilus* and *Neisseria* generally have high relative abundance in children in the healthy group. This study has shown that health-related *Bacteroides* increased after topical fluoride use at Day 14, but no statistically significant differences were found in colonies before and after topical fluoride use at Day 7, suggesting that different genera belonging to the same phylum level may show different changes and that the same genus also shows different changes in different individuals; thus, the oral microbial diversity is in a state of complex dynamic changes, and there are individual differences.

The main limitation of this study is the relatively small sample size, so an increase in the sample size in the future is encouraged. This study explored the effect of fluoride on the microbial diversity of oral saliva. However, there are many environmental conditions affecting microbial diversity in oral saliva, such as temperature, pH, salinity, redox potential, and the acquisition of oxygen or nutrients, so other environmental impact factors need to be strictly controlled to increase the accuracy and reliability of the results. In addition, the concentration of fluoride in saliva after fluoride varnish application is also a factor that affects the results. Eakle et al. (Eakle et al., 2004) found that the maximum fluoride levels in saliva with varnish remained above baseline levels for a longer duration, but further research is needed.

Conclusion

The present study found that certain bacterial phylotypes of the saliva microbiome were significantly modulated by the local use of fluoride in S-ECC. It was observed that health-associated genera such as *Bacteroides* and *Uncultured_bacterium_f_Enterobacteriaceae* were enriched in the saliva microbiome following treatment with fluoride-containing material. The new findings highlight the need for a better understanding of the oral microbiome in the etiopathology of caries in children and evaluating the efficacy of dental treatments such as fluoride-containing materials, which will provide more favorable evidence for the use of fluoride in caries prevention and therapy in severe early childhood caries.

Data availability statement

The datasets presented in this study can be found in online repositories. The names of the repository/repositories and accession number(s) can be found in the article/Supplementary Material.

Ethics statement

The studies involving human participants were reviewed and approved by the Ethics Committee of the Stomatological Hospital of Chongqing Medical University(CQHS-REC-2018(LSNO.22). Written informed consent to participate in this study was provided by the participants' legal guardian/next of kin.

Author contributions

ZY, TC, and YL contributed to research design, data acquisition, data analysis and interpretation, and drafted and critically revised manuscript. DJ contributed to data interpretation and critically revised the manuscript. ZZ and JL contributed to conception and design and critically revised the manuscript. All authors agreed to be accountable for all aspects of this work. All authors contributed to the article and approved the submitted version.

Funding

This study was supported by the Natural Science Foundation Project of Chongqing, No. CSTC2019jcyj-msxmX0191; Science Project of Chongqing Municipal Health Commission, No. 2021MSXM31, and the Program for Innovation Team Building at Institutions of Higher Education in Chongqing in 2016, No. CXTDG201602006; The First Batch of Key Disciplines On Public Health in Chongqing.

Conflict of interest

The authors declare that the research was conducted in the absence of any commercial or financial relationships that could be construed as a potential conflict of interest.

Publisher's note

Supplementary material

The Supplementary Material for this article can be found online at: https://www.frontiersin.org/articles/10.3389/fcimb.2023.1104343/full#supplementary-material

References

Bik, E. M., Long, C. D., Armitage, G. C., Loomer, P., Emerson, J., Mongodin, E. F., et al. (2010). Bacterial diversity in the oral cavity of 10 healthy individuals. *ISME J.* 4, 962–974. doi: 10.1038/ismej.2010.30

Bolger, A. M., Lohse, M., and Usadel, B. (2014). Trimmomatic: A flexible trimmer for illumina sequence data. *Bioinformatics* 30 (15), 2114–2120. doi: 10.1093/bioinformatics/btu170

Chen, T., Shi, Y., Wang, X., Wang, X., Meng, F., Yang, S., et al. (2017). High-throughput sequencing analyses of oral microbial diversity in healthy people and patients with dental caries and periodontal disease. *Mol. Med. Rep.* 16, 127–132. doi: 10.3892/mmr.2017.6593

Cheng, X., Liu, J., Li, J., Zhou, X., Wang, L., Liu, J., et al. (2017). Comparative effect of a stannous fluoride toothpaste and a sodium fluoride toothpaste on a multispecies biofilm. *Arch. Oral. Biol.* 74, 5–11. doi: 10.1016/j.archoralbio.2016.10.030

Claesson, M. J., Clooney, A. G., and O'Toole, P. W. (2017). A clinician's guide to microbiome analysis. *Nat. Rev. Gastroenterol. Hepatol.* 14 (10), 585–595. doi: 10.1038/nrgastro.2017.97

Clark, M. B., Keels, M.A., and Slayton, R.L.. (2020). Fluoride use in caries prevention in the primary care setting. *Pediatrics* 146 (6):e2020034637. doi: 10.1542/peds.2020-034637

Eakle, W. S., Featherstone, J. D., Weintraub, J. A., Shain, S. G., and Gansky, S. A. (2004). Salivary fluoride levels following application of fluoride varnish or fluoride rinse. *Community Dent. Oral. Epidemiol.* 32 (6), 462–469. doi: 10.1111/j.1600-0528.2004.00185.x

Edgar, R. C., Haas, B. J., Clemente, J. C., Quince, C., and Knight, R. (2011). UCHIME improves sensitivity and speed of chimera detection. *Bioinformatics* 27 (16), 2194–2200. doi: 10.1093/bioinformatics/btr381

Edgar Robert, C. (2013). UPARSE: highly accurate OTU sequences from microbial amplicon reads. *Nat. Methods* 10 (10), 996–998. doi: 10.1038/nmeth.2604

Fu, R., Niu, R., Li, R., Yue, B., Zhang, X., Cao, Q., et al. (2019). Fluoride-induced alteration in the diversity and composition of bacterial microbiota in mice colon. *Biol. Trace Elem Res.* 196, 537–544. doi: 10.1007/s12011-019-01942-w

Guannan, L., Xuejuan, X., Sendegeya, P., Huanhuan, Z., Yaohang, L., and Yong, Z. (2015). Effect of fluoride on gut microflora of silkworm. *Acta Microbiologica Sin.* 55 (7), 926–934. doi: 10.13343/j.cnki.wsxb.20140450

Jiang, Q., Liu, J., Chen, L., Gan, N., and Yang, D. (2019). The oral microbiome in the elderly with dental caries and health. *Front. Cell Infect. Microbiol.* 8, 442. doi: 10.3389/fcimb.2018.00442

Johansson, I., Witkowska, E., Kaveh, B., Lif Holgerson, P., and Tanner, A. C. R. (2016). The microbiome in populations with a low and high prevalence of caries. *J. Dent. Res.* 95, 80–86. doi: 10.1177/0022034515609554

Kashyap, P. C., Chia, N., Nelson, H., Segal, E., and Elinav, E. (2017). Microbiome at the frontier of personalized medicine. *Mayo Clin. Proc.* 92 (12), 1855–1864. doi: 10.1016/j.mayocp.2017.10.004

Koopman, J. E., van der Kaaij, N. C., Buijs, M. J., Elyassi, Y., van der Veen, M. H., Crielaard, W., et al. (2015). The effect of fixed orthodontic appliances and fluoride mouthwash on the oral microbiome of adolescents - a randomized controlled clinical trial. *PloS One* 10 (9), e0137318. doi: 10.1371/journal.pone.0137318

Kulik, E. M., Waltimo, T., Weiger, R., Schweizer, I., Lenkeit, K., Filipuzzi-Jenny, E., et al. (2015). Development of resistance of mutans streptococci and porphyromonas gingivalis to chlorhexidine digluconate and amine fluoride/stannous fluoride-containing mouthrinses, *in vitro*. *Clin. Oral. Investigations* 19 (6), 1547–1553. doi: 10.1007/s00784-014-1379-y

Liu, M.-j. (2021). *Metagenomic study of supragingival plaque microorganisms in deciduous dental caries of 5-year-old children in qingdao* (Qingdao: Qingdao University).

Liu, J., Wang, H. W., Lin, L., Miao, C. Y., Zhang, Y., and Zhou, B. H. (2019). Intestinal barrier damage involved in intestinal microflora changes in fluoride-induced mice. *Chemosphere* 234, 409–418. doi: 10.1016/j.chemosphere.2019.06.080

Losso, E. M., Tavares, M. C., Silva, J. Y., and Urban, C. A. (2009). Severe early childhood caries:an integral approach. *J. Pediatr(Rio J)* 85, 295–300. doi: 10.1590/S0021-75572009000400005

Lozupone, C. A., Hamady, M., Kelley, S. T., and Knight, R. (2007). Quantitative and qualitative beta diversity measures lead to different insights into factors that structure microbial communities. *Appl. Environ. Microbiol.* 73, 1576–1585. doi: 10.1128/AEM.01996-06

Luo, Q., Cui, H., Peng, X., Fang, J., Zuo, Z., Deng, J., et al. (2016). Dietary high fluorine alters intestinal microbiota in broiler chickens. *Biol. Trace Elem Res.* 173 (2), 483–491. doi: 10.1007/s12011-016-0672-9

Maden, E. A., Altun, C., Ozmen, B., and Basak, F.. (2018). Antimicrobial effect of toothpastes containing fluoride, xylitol, or xylitol-probiotic on salivary streptococcus mutans and lactobacillus in children. *Nigerian J. Clin. Pract.* 21 (2), 134–138. doi: 10.4103/njcp.njcp_320_16

Marquis, R. E. (1995). Antimicrobial actions of fluoride for oral bacteria. *Can. J. Microbiol.* 41, 955–964. doi: 10.1139/m95-133

Marsh, P. D. (1994). Microbial ecology of dental plaque and its significance in health and disease. *Adv. Dent. Res.* 8, 263–271. doi: 10.1177/08959374940080022001

Qin, J., Chai, G., Brewer, J. M., Lovelace, L. L., and Lebioda, L. (2006). Fluoride inhibition of enolase: crystal structure and thermodynamics. *Biochemistry* 45, 793–800. doi: 10.1021/bi051558s

Quast, C., Pruesse, E., Yilmaz, P., Gerken, J., Schweer, T., Yarza, P., et al. (2012). The SILVA ribosomal RNA gene database project: Improved data processing and web-based tools. *Nucleic Acids Res.* 41 (Database issue), D590-596. doi: 10.1093/nar/gks1219

Schloss, P. D., Westcott, S. L., Ryabin, T., Hall, J. R., Hartmann, M., Hollister, E. B., et al. (2009). Introducing mothur:Open-source,platform-independent,community-supported software for describing and comparing microbial communities. *Appl. Environ. Microbiol.* 75 (23), 7537–7541. doi: 10.1128/AEM.01541-09

Segata, N., Izard, J., Waldron, L., Gevers, D., Miropolsky, L., Garrett, W. S., et al. (2011). Metagenomic biomarker discovery and explanation. *Genome Biol.* 12, 60R. doi: 10.1186/gb-2011-12-6-r60

Takeuchi, K., Nakagaki, H., Toyama, Y., Kimata, N., Ito, F., Robinson, C., et al. (1996). Fluoride concentrations and distribution in premolars of children from low and optimal fluoride areas. *Caries Res.* 30 (1), 76–82. doi: 10.1159/000262140

Thomas, A., Thakur, S., and Habib, R. (2017). Comparison of antimicrobial efficacy of green tea, garlic with lime, and sodium fluoride mouth rinses against streptococcus mutans, lactobacilli species, and candida albicans in children: A randomized double-blind controlled clinical trial. *Int. J. Clin. Pediatr. Dentistry* 10 (3), 234–239. doi: 10.5005/jp-journals-10005-1442

Vos, T., Flaxman, A. D., Naghavi, M., Lozano, R., Michaud, C., Ezzati, M., et al. (2012). Years lived with disability (YLDs) for 1 160 sequelae of 289 diseases and injuries 1990–2010: a systematic analysis for the global burden of disease study 2010. *Lancet* 380 (9859), 2163–2196. doi: 10.1016/S0140-6736(12)61729-2

Wang, J.-x. (2019). *The cost-effctiveness analysis of topical fluoride application program for pre-school children over two years* (Chongqing: Chongqing Medical University).

Wang, Q., Garrity, G. M., Tiedje, J. M., and Cole, J. R. (2007). Naive Bayesian classifier for rapid assignment of rRNA sequences into the new bacterial taxonomy. *Appl. Environ. Microbiol.* 73 (16), 5261–5267. doi: 10.1128/AEM.00062-07

Wang, X., Feng, X. P., and Li, Z. X.(2018). *The fourth national oral health epidemiological survey report* (Beijing: People's Medical Publishing House) 1-34.

Wang, Y., Wang, S., Wu, C., Chen, X., Duan, Z., Xu, Q., et al. (2019). Oral microbiome alterations associated with early childhood caries highlight the importance of carbohydrate metabolic activities. *mSystems* 4 (6), e00450–e00419. doi: 10.1128/mSystems.00450-19

Wang, Y., Zhang, J., Ling, Z.-x., and Deng, S.-l. (2022). Dynamic microbial shifts and functional analysis of saliva microbial communities with caries children. *J. Sichuan Univ. (Med. Sci.)* 53 (2), 242–249. doi: 10.12182/20220360103

Ward, T., Larson, J., Meulemans, J., Hillmann, B., Lynch, J., Sidiropoulos, D., et al. (2017). BugBase predicts organism level microbiome phenotypes. *bioRxiv*. doi: 10.1101/133462

Wu, H. (2019). *Study on the characteristics of gut microbiota for children with dental fluorosis in drinking water-born endemic fluorosis areas* (Zhengzhou University).

Xiao, J., Alkhers, N., Kopycka-Kedzierawski, D. T., Billings, R. J., Wu, T. T., Castillo, D. A., et al. (2019). Prenatal oral health care and early childhood caries prevention: a systematic review and meta-analysis. *Caries Res.* 53 (4), 411–421. doi: 10.1159/000495187

Yasuda, K., Hsu, T., Gallini, C. A., Mclver, L. J., Schwager, E., Shi, A., et al. (2017). Fluoride depletes acidogenic taxa in oral but not gut microbial communities in mice. *mSystems* 2 (4), e00047–e00017. doi: 10.1128/mSystems.00047-17

Frontiers in
Cellular and Infection Microbiology

Investigates how microorganisms interact with their hosts

Explores bacteria, fungi, parasites, viruses, endosymbionts, prions and all microbial pathogens as well as the microbiota and its effect on health and disease in various hosts.

Discover the latest Research Topics

See more →

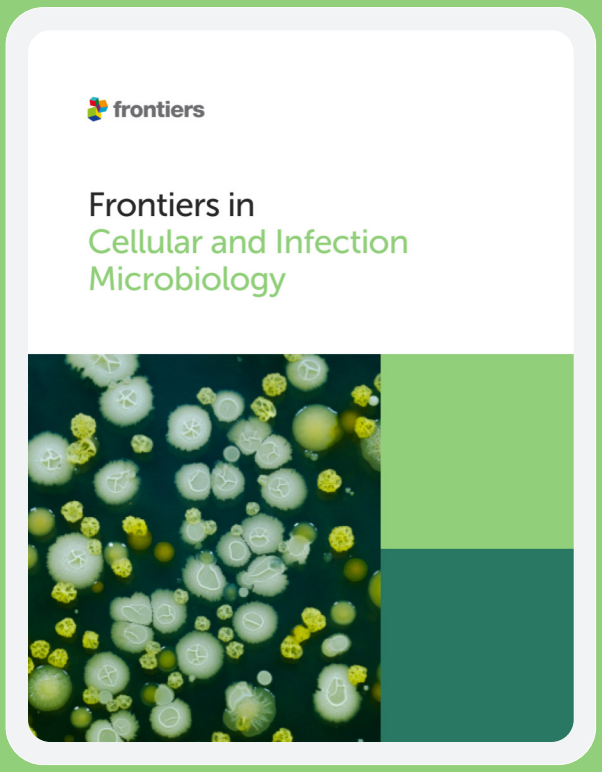

Frontiers

Avenue du Tribunal-Fédéral 34
1005 Lausanne, Switzerland
frontiersin.org

Contact us

+41 (0)21 510 17 00
frontiersin.org/about/contact